Landolt-Börnstein
Numerical Data and Functional Relationships in Science and Technology
New Series / Editor in Chief: W. Martienssen

Group IV: Physical Chemistry
Volume 19

Thermodynamic Properties of Inorganic Materials
compiled by SGTE

Subvolume B
Binary Systems
Phase Diagrams, Phase Transition Data,
Integral and Partial Quantities of Alloys

Part 5
Binary Systems Supplement 1

Editor
Lehrstuhl für Werkstoffchemie,
Rheinisch-Westfälische Technische Hochschule Aachen

Authors
Scientific Group Thermodata Europe (SGTE)

Springer

ISSN 1615-2018 (Physical Chemistry)

ISBN 978-3-540-45279-9 Springer Berlin Heidelberg New York

Library of Congress Cataloging in Publication Data
Zahlenwerte und Funktionen aus Naturwissenschaften und Technik, Neue Serie
Editor in Chief: W. Martienssen
Vol. IV/19B5: Editor: Lehrstuhl für Werkstoffchemie, Rheinisch-Westfälische Technische Hochschule Aachen
At head of title: Landolt-Börnstein. Added t.p.: Numerical data and functional relationships in science and technology.
Tables chiefly in English.
Intended to supersede the Physikalisch-chemische Tabellen by H. Landolt and R. Börnstein of which the 6th ed. began publication in 1950 under title: Zahlenwerte und Funktionen aus Physik, Chemie, Astronomie, Geophysik und Technik.
Vols. published after v. 1 of group I have imprint: Berlin, New York, Springer-Verlag
Includes bibliographies.
1. Physics--Tables. 2. Chemistry--Tables. 3. Engineering--Tables.
I. Börnstein, R. (Richard), 1852-1913. II. Landolt, H. (Hans), 1831-1910.
III. Physikalisch-chemische Tabellen. IV. Title: Numerical data and functional relationships in science and technology.
QC61.23 502'.12 62-53136

Springer is a member of Springer Science+Business Media
springeronline.com

Printed in Germany

Cover layout: Erich Kirchner, Heidelberg
Typesetting: Authors and SciCaster - Wissen kompakt (Dr. Christian Meier), Darmstadt
Printing and Binding: AZ Druck, Kempten

SPIN: 1187 3921 63/3020 - 5 4 3 2 1 0 – Printed on acid-free paper

Editors

P. Franke and D. Neuschütz
Lehrstuhl für Werkstoffchemie
Rheinisch-Westfälische Technische Hochschule Aachen
D-52056 Aachen, Germany
http://www.mch.rwth-aachen.de/

Authors

Scientific Group Thermodata Europe (SGTE)
Chairman: A.T. Dinsdale
6, rue du Tour de l'Eau
F-38400 Saint Martin d'Hères, France
http://www.sgte.org/

Member Organisations of SGTE:

The present series of books is the result of a collective work carried out during many years by many individuals. Since a complete list of all contributors is an impossible task, only a contact person is mentioned under each member organisation.

Forschungszentrum Jülich GmbH
Institute for Energy Research
IEF- 2: Materials Microstructure and Properties
T. Markus
D-52425 Jülich, Germany
http://www.fz-juelich.de/

GTT Technologies
Gesellschaft für Technische Thermochemie und -physik mbH
K. Hack
Kaiserstraße 100
D-52134 Herzogenrath, Germany
http://www.gtt-technologies.de/

Institut National Polytechnique de Grenoble
Laboratoire de Thermodynamique et Physico-Chimie Métallurgiques
C. Bernard
Domaine Universitaire, B.P. 75
F-38402 Saint Martin d'Hères, France
http://www.inpg.fr/ltpcm/

Arcelor Research
Process Engineering Department
J. Lehmann
Voie Romaine - BP 30320
F-57283 Maizières-lès-Metz, France

Max-Planck-Institut für Metallforschung und
Institut für Nichtmetallische Anorganische Materialien der Universität Stuttgart
Pulvermetallurgisches Laboratorium
M. Zinkevich
Heisenbergstraße 3
D-70569 Stuttgart, Germany
http://www.mf-mpg.de/

National Physical Laboratory
NPL Materials Centre
A.T. Dinsdale
Queens Road, Teddington, Middlesex, United Kingdom, TW11 0LW
http://www.npl.co.uk/mtdata

Rheinisch-Westfälische Technische Hochschule Aachen
Lehrstuhl für Werkstoffchemie
E. Münstermann
D-52056 Aachen, Germany
http://www.mch.rwth-aachen.de/

Royal Institute of Technology
Department of Materials Science and Engineering
J. Ågren
S-10044 Stockholm, Sweden
http://www.met.kth.se/tc/

THERMFACT LTD.LTEE
A.D. Pelton
447 Berwick Mont Royal H3R1Z8
Québec, Canada
http://www.crct.polymtl.ca/

Thermo-Calc Software AB
B. Sundman
Stockholm Technology Park
Björnnäsvägen 21
S-113 47 Stockholm, Sweden
http://www.thermocalc.se/

THERMODATA
B. Cheynet
6, rue du Tour de l'Eau
F-38400 Saint Martin d'Hères, France
http://thermodata.online.fr/

The Spencer Group
P.J. Spencer
P.O. Box 393
Trumansburg, New York 14886, USA
http://www.spencergroupintl.com/

The reviews in the present volume of selected binary systems have been prepared by:

P.-Y. Chevalier, E. Fischer, P. Franke, K. Hack and T. Jantzen.

In preparing the data for publication in this series, the editors have been assisted particularly by:

A.T. Dinsdale (Data Manager for Elements), I. Ansara (Data Manager for Pure Substances), B. Sundman (Data Manager for Solutions), S.G. Fries (Solution Database Coordinator) and A. Hovmark (SGTEbin software).

Landolt-Börnstein

Editorial Office
Gagernstr. 8, D-64283 Darmstadt, Germany
fax: +49 (6151) 171760
e-mail: redaktion.landolt-boernstein@springer.com

Internet
http://www.landolt-boernstein.com

Dedication to Ibrahim Ansara

This series of volumes, presenting thermodynamic properties of binary alloys, is dedicated to the memory of Ibrahim Ansara – better known to his friends as Himo. Himo was a member of SGTE from the time of its origin as a CNRS research project in 1967, through the time of its constitution as a European, non-profit-making company under French law in 1979, until his sudden, unexpected death in 2001.

Through all those years, Himo missed scarcely a single SGTE meeting and his continual cheerfulness and enthusiasm, as well as his scientific understanding, were an inspiration to his colleagues both in their joint work of SGTE database development as well as in their individual research projects in their home laboratories. He was a friend to everyone in SGTE, and it is the spirit of friendship and warmth that he promoted that has been largely responsible for the continued close collaboration and achievements of this diverse international group as a whole.

It is very appropriate to dedicate the Landolt-Börnstein handbooks on binary alloy systems to Himo. In the preparation of the previous volumes on pure substances, Himo made substantial contributions both as database manager and as advisor. The present series of volumes on binary alloys has benefited considerably from his contributions to the review and selection of available assessments during the initial stages of the work. It is a sad coincidence that it was during a meeting to prepare the first of these volumes that Himo died.

Philip Spencer

Preface

Thermodynamic data, in conjunction with appropriate software for calculation of complex chemical equilibria, are finding wide application in many areas of materials design and development. In particular, the last 25 years have seen enormous advances in the thermodynamic modelling of alloy solution phases, whereby a knowledge of the underlying crystallographic structure of each phase is fundamental to a reliable representation of the thermodynamic properties and phase equilibria of a particular system of interest. With the aid of thermodynamic calculations, considerable time and costs can and are being saved in producing a material of the required composition and phase constitution required for a particular application.

SGTE has been at the forefront in providing critically assessed thermodynamic data for alloy systems and has provided guidelines for the modelling of alloy phases of different types. Major advantages of the SGTE data are their self-consistency, the fact that they are produced with careful attention to a well-defined quality procedure and that the expertise of SGTE members in various areas of inorganic chemistry and materials science allows review of the numbers by highly qualified scientists in the fields concerned.

Following the publication of a first set of four volumes of SGTE compiled thermodynamic properties of inorganic substances, which dealt with pure substances (Subvolume A), this second set of four volumes presents selected thermodynamic data for binary alloy systems (Subvolume B). The possibility to continue to ternary and multi-component systems is also foreseen. The data in the latter would be so presented as to correspond to potential application themes (steels, light alloys, nickel-base alloys, etc.). The fundamental equations used in evaluating the data are given in the introduction to the volumes and the models used in representing the data are also described.

Each book in this binary alloys series is accompanied by a CD, which allows computer calculation of a range of solution properties for selected temperature and phase composition ranges for the systems presented in that particular volume. Graphical representations, including the calculated phase diagram for each system, are also possible. Information on more comprehensive software, allowing complex equilibrium calculations involving both pure substances and solution phases of different types (e.g. slags, salt systems, aqueous solutions, etc.), can be obtained from SGTE members. A list of the SGTE membership is presented in the cover pages of this volume.

Very many scientists, in addition to those currently participating in SGTE activities, have contributed to the development of the SGTE databases. Their names have become too numerous to list and we respectfully ask them to accept this acknowledgement of their efforts. However, special recognition is given here to the late Himo Ansara, who was SGTE Pure Substances Database manager from the beginning and who made major contributions to these binary alloy volumes. His dedicated work and friendship were an inspiration to all of his colleagues. We remember him with deep affection and gratitude.

Dr. P.J. Spencer
Chairman of SGTE, 1992 – 2002

Ithaca, April 2002

Content

IV/19 Thermodynamic Properties of Inorganic Materials

Subvolume B Binary Systems

Phase Diagrams, Phase Transition Data,
Integral and Partial Quantities of Alloys

Part 5 Binary Systems Supplement 1

CD-ROM: Software for the calculation of phase diagrams and thermodynamic data of binary systems

Survey of volume IV/19

Thermodynamic Properties of Inorganic Materials compiled by SGTE

Pure Substances	Subvolume A
Elements and Compounds from AgBr to Ba_3N_2	Part 1
Compounds from BeBr<g> to $ZrCl_2$<g>	Part 2
Compounds from $CoCl_3$ to Ge_3N_4<g>	Part 3
Compounds from HgH<g> to ZnTe<g>	Part 4
Binary Systems	**Subvolume B**
Elements and Binary Systems from Ag-Al to Au-Tl	Part 1
Binary Systems from B-C to Cr-Zr	Part 2
Binary Systems from Cs-K to Mg-Zr	Part 3
Binary Systems from Mn-Mo to Y-Zr	Part 4
Binary Systems Supplement 1	**Part 5**
Ternary and Multicomponent Systems	
(application oriented, i.e. Light Alloys, Solders, Steels,...)	

Introduction

The first 4 volumes of this series, under the general heading Thermodynamic Properties of Inorganic Materials, presents SGTE-compiled thermodynamic data for pure substances, including the elements in their stable states. The series now continues with a further 4 volumes of SGTE selected and compiled data – this time for binary alloy systems. For thermodynamic calculations involving alloy solution phases, Gibbs energies of the pure elements in different stable and metastable states are required. Such data have been compiled on behalf of SGTE by Dinsdale [91Din] and have recently been updated [02Din]. The values have found wide use internationally as the basis for thermodynamic assessments of higher order systems.

As with the pure element values, the binary alloy descriptions contained in the present 4-volume series are not only complete in themselves, but also extend the basis for thermodynamic assessments and calculations relating to multicomponent alloys.

Members of SGTE have played a principle role in promoting the concept of "computational thermochemistry" as a time and cost-saving basis for guiding materials development and processing in many different areas of technology. At the same time, through organisation of workshops and participation in CODATA Task Groups, SGTE members have contributed significantly to the broader international effort to unify thermodynamic data and assessment methods.

The SGTE data can be obtained via members and their agents world-wide for use with commercially available software developed by some of the members, to enable users to undertake calculations of complex chemical equilibria efficiently and reliably.

The SGTE Member organisations are:

Canada: – THERMFACT LTD.LTEE

France:
– Institut National Polytechnique (LTPCM), Grenoble
– Association THERMODATA, Grenoble
– Arcelor Research, Maizières-lès-Metz

Germany:
– Rheinisch-Westfälische Technische Hochschule (MCh), Aachen
– GTT-Technologies, Herzogenrath
– MPI für Metallforschung (PML), Stuttgart
– Forschungszentrum Jülich GmbH (IEF-2), Jülich

Sweden:
– Royal Institute of Technology (MSE), Stockholm
– Thermo-Calc Software AB, Stockholm

United Kingdom: – National Physical Laboratory (MATC), Teddington

USA: – The Spencer Group

Assessment and selection procedures

The assessments of the binary alloy systems presented in this 4-volume series have all been made using the so-called "CALPHAD method" [98Sau]. This method results in an optimised parametric description of the Gibbs energies of the phases of the system when taking into account the crystallographic structure of the phases and all the experimental thermodynamic and phase boundary data available. The thermodynamic parameters provide a consistent analytical description of the phase diagram, chemical potentials, enthalpies of mixing, heat capacities, etc.

As an example, the relations between the Gibbs energy curves and the phase diagram for the Bi-Sn system are demonstrated in Figs. 1 and 2, respectively. In Fig. 1 the Gibbs energy curves for the phases in the Bi-Sn system are given as a function of the mole fraction of Sn, x_{Sn}, at $T = 450$ K. At fixed pressure, temperature and composition, the equilibrium of the system is determined by the state with the lowest Gibbs energy. All equilibrium states are located on the convex hull of the set of G-curves which is constructed by applying double-tangents to the curves. The tangent points denote the boundaries between one- and two-phase regions. In Fig. 2, these points are marked on the selected isotherm of $T = 450$ K. If this construction is repeated for other temperatures the complete phase diagram of the system is obtained.

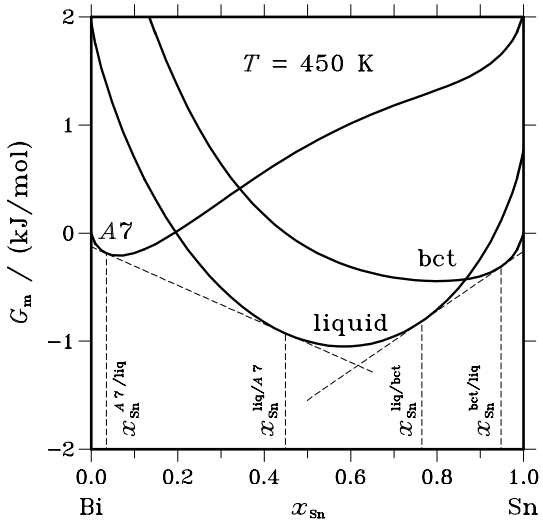

Fig. 1. Gibbs energy functions for the phases in the Bi-Sn system at 450 K.

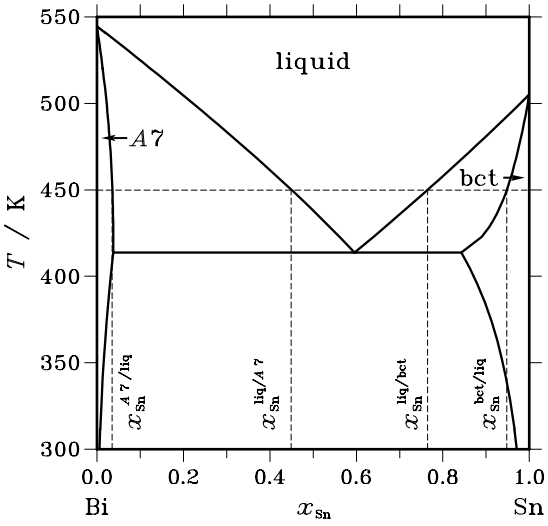

Fig. 2. Phase diagram for the system Bi-Sn.

If several published assessments are available for a particular system, selection has been made following an analysis of how well the available experimental data are reproduced by the description. Compatibility of the modelling used with respect to assembly of a data set for higher order systems has also been taken into account.

There are many different phases present in binary systems and, in order to combine their thermodynamic descriptions in higher order systems, it is important to know their crystal structures as well as the solubilities of alloyed elements in them. In these volumes, the naming of phases has been carried out as consistently as possible so as to facilitate identification of the same phase appearing in different binary systems.

The main characteristics of each system are presented in individual reports which generally include

- the calculated phase diagram
- an abstract summarising the main features of the system
- a summary of the various stable and metastable phases defined in the system together with crystallographic information, the phase name used in the database and the thermodynamic model used, including the occupation of the sublattices
- a table of the invariant reactions
- tables and diagrams with integral quantities
- tables and diagrams with partial quantities
- plots of calculated thermodynamic functions

Criteria for selection of binary alloy assessments

In order to qualify for selection, the following information was reviewed:

- phase diagram
- thermodynamic information
- documentation
- models used for solution phases
- models used for stoichiometric phases
- feasibility of extrapolation
- compatibility with SGTE unary data

Thermodynamic Modelling

Elements

The Gibbs energy of the pure element i, ${}^\circ G_i^\phi(T)$, referred to the enthalpy for its stable state ϕ at 298.15 K, ${}^\circ H_i^\phi(298.15\ \mathrm{K})$, is denoted by GHSER$_i$. This quantity is described as a function of temperature by the following equation:

$$\begin{aligned} \mathrm{GHSER}_i &= {}^\circ G_i^\phi(T) - {}^\circ H_i^\phi(298.15\ \mathrm{K}) \\ &= a + b\,T + c\,T\cdot \ln T + d\,T^2 + e\,T^3 + f\,T^{-1} + g\,T^7 + h\,T^{-9} \end{aligned} \quad (1)$$

A number of temperature ranges may be used. The first and second derivatives of this quantity with respect to temperature are related to the absolute entropy and heat capacity of the compound at the same temperature. Experimental values for heat capacities can thus be directly used in the optimisation and will be related to the coefficients c, d, e, f, g and h.

For elements which have a magnetic ordering, e.g. Co, Cr, Fe, Ni and Mn, the term GHSER is referred to a para-magnetic state. An additional term is thus added to the molar Gibbs energy of the magnetic phase. For elements as well as for solutions, this term is equal to:

$$G^{\mathrm{mag}} = RT\ln(\beta+1)f(\tau) \quad (2)$$

where τ is T/T^* , T^* being the critical temperature for magnetic ordering (Curie temperature T_C for ferromagnetic materials or the Néel temperature T_N for antiferromagnetic materials), and β the average magnetic moment per atom of the alloy expressed in Bohr magnetons.

The function $f(\tau)$ is given as:

$$\begin{aligned} \tau <= 1 \quad &: \quad f(\tau) = 1 - [79\tau^{-1}/140p + (474/497)(1/p-1)(\tau^3/6 + \tau^9/135 + \tau^{15}/600)]/A \\ \tau > 1 \quad &: \quad f(\tau) = -[\tau^{-5}/10 + \tau^{-15}/315 + \tau^{-25}/1500]/A \end{aligned}$$

with $A = 518/1125 + (11692/15975)(1/p-1)$.

These equations were derived by Hillert *et al.* [78Hil] from an expression of the magnetic heat capacity $C_\mathrm{P}^{\mathrm{mag}}$ described by Inden [81Ind].

The value of p depends on the crystal structure. For example, p is equal to 0.28 for fcc and hcp metals and 0.40 for bcc metals [81Ind]. For anti-ferromagnetic alloys the T^* and β are modelled as negative and they are divided by an *anti-ferromagnetic factor* of -1 for bcc and -3 for fcc and hcp before the values are used in equation (2).

For each element, equation (1) is taken from the SGTE unary database. These data have been published previously as the SGTE data for the pure elements by Dinsdale [91Din, 02Din].

The function GHSER_i is also often used to express the thermodynamic functions of metastable structures φ, different from the stable structure of the pure element. The expression ${}^{\circ}G_i^{\varphi}(T) - {}^{\circ}H_i^{\phi}(298.15\ \mathrm{K})$ is equivalent to ${}^{\circ}G_i^{\varphi}(T) - {}^{\circ}G_i^{\phi}(T) + \mathrm{GHSER}_i$. The term ${}^{\circ}G_i^{\varphi}(T) - {}^{\circ}G_i^{\phi}(T)$ is often called the lattice stability of element *i* in phase φ.

Binary compounds

The Gibbs energy of the compound $\mathrm{A_aB_b}$ may be expressed as:

$$G_{\mathrm{A_aB_b}}(T) - \mathrm{a}\ {}^{\circ}H_{\mathrm{A}}^{\phi}(298.15\ \mathrm{K}) - \mathrm{b}\ {}^{\circ}H_{\mathrm{B}}^{\phi}(298.15\ \mathrm{K}) = f(T) \tag{3}$$

where a and b are stoichiometric numbers. The expression for $f(T)$ is identical to that given by equation (1).

Equation (3) can be transformed by applying equation (1) for each component

$$\begin{aligned} f(T) &= G_{\mathrm{A_aB_b}}(T) - \mathrm{a}\ {}^{\circ}G_{\mathrm{A}}^{\phi}(T) - \mathrm{b}\ {}^{\circ}G_{\mathrm{B}}^{\phi}(T) + \mathrm{a\ GHSER_A} + \mathrm{b\ GHSER_B} \\ &= \Delta_{\mathrm{f}}G_{\mathrm{A_aB_b}}(T) + \mathrm{a\ GHSER_A} + \mathrm{b\ GHSER_B} \end{aligned} \tag{4}$$

The term $\Delta_{\mathrm{f}}G_{\mathrm{A_aB_b}}(T)$ is the Gibbs energy of formation of the compound referred to the stable elements at temperature T. It can often be taken as a linear function of T.

Gaseous species

An expression identical to equation (1) may be used to describe the Gibbs energy of the gaseous species with the additional $RT\ln(P/P_0)$ term, where P is the total pressure and P_0 the reference pressure, usually 0.1 MPa. The species in the gas phase are assumed to form an ideal solution. The reference state for each vapour species is taken to be the pure components at 0.1 MPa pressure. The thermodynamic properties of the gas species are normally obtained from vapour pressure measurements coupled to spectroscopic data. Data for gaseous substances are covered in more detail in subvolume (A) for pure substances.

Many species, i.e. molecules, may exist in the gas phase and each has a Gibbs energy of formation. The equilibrium within a gas for a given composition at a given temperature and pressure is calculated by minimising the Gibbs energy varying the fraction of the species. As the Gibbs energy is used as the modelling function in most solution databases it is not possible to calculate the critical point for gas/liquid. The models used for the different liquids are also not compatible with the ideal model for the gas.

Condensed phases

The condensed phases can be divided into three groups.

1: Substitutional solutions

For the substitutional solution ϕ, the molar Gibbs energy is expressed as follows:

$$G_{\mathrm{m}}^{\phi} = G_{\mathrm{m}}^{\phi,\mathrm{srf}} + G_{\mathrm{m}}^{\phi,\mathrm{id}} + G_{\mathrm{m}}^{\phi,\mathrm{E}} \tag{5}$$

with

$$G_{\mathrm{m}}^{\phi,\mathrm{srf}} = \sum_i x_i\ {}^{o}G^{\phi} \tag{6}$$

$$G_{\mathrm{m}}^{\phi,\mathrm{id}} = R\,T \sum_i x_i \ln x_i \tag{7}$$

x_i is the molar fraction of component i with $\sum_i x_i = 1$. The term $G_{\mathrm{m}}^{\phi,\mathrm{srf}}$ is the Gibbs energy of the phase relative to the reference state for the components and $G_{\mathrm{m}}^{\phi,\mathrm{id}}$ is the contribution of ideal mixing entropy.

The Redlich - Kister equation [48Red], a power series expansion, is used to express the excess Gibbs energy, $G_{\rm m}^{\phi,{\rm E}}$, for the interaction between the two elements i and j as follows:

$$G_{\rm m}^{\phi,{\rm E}} \;=\; x_i x_j \sum_{\nu=0} {}^{\nu}L_{ij}^{\phi}\,(x_i - x_j)^{\nu} \tag{8}$$

The model parameter ${}^{\nu}L_{ij}^{\phi}$ can be temperature dependent.

If experimental information for ternary solutions is available then an extra term can be added to equation (8). For a ternary system A–B–C, this term is equal to:

$$x_{\rm A} x_{\rm B} x_{\rm C} L_{\rm ABC} \tag{9}$$

The liquid is in most cases treated as a substitutional solution. For liquids with very strong short range order the associate model [78Som] or the ionic liquid model [85Hil] has sometimes been used.

For magnetic alloys, the composition dependence of T^* and β are expressed by:

$$T^*(x) \;=\; \sum_i x_i \,{}^{\circ}T_i^* + T^{*,{\rm E}} \tag{10}$$

$$\beta(x) \;=\; \sum_i x_i \,{}^{\circ}\beta_i + \beta^{\rm E} \tag{11}$$

where $T^{*,{\rm E}}$ and $\beta^{\rm E}$ are both represented by an expression similar to equation (8).

2: Ordered Phases

The use of the sublattice model, developed by Hillert and Staffansson [70Hil] based on Temkin's model for ionic solutions [45Tem] and extended by Sundman and Ågren [81Sun], allows a variety of solution phases to be treated, for example interstitial solutions, intermediate phases, carbides etc. All of these represent an ordering of the constituents on different sublattices.

As non-stoichiometric phases are formed by several sublattices, they can be schematically described as follows:

$$({\rm A, B, ...})_p({\rm A, B, ...})_q ...$$

where the constituents A, B, ... can be atoms, vacancies, molecules or ions on the different sublattices .... p, q, ... are the number of sites. If $p + q + ... = 1$, then the thermodynamic quantities are referred to one mole of sites. Most often p and q are selected to be the smallest set of integers.

For each sublattice s, the site fraction of the species i, y_i^s, is equal to

$$y_i^s = \frac{n_i^s}{\sum_j n_j^s} = \frac{n_i^s}{n^s} \qquad \text{with} \qquad \sum_i y_i^s = 1 \qquad \text{and} \qquad \sum_s n^s = n \tag{12}$$

where n_i^s is the number of species i in sublattice s, n^s the number of sites in sublattice s, and n the total number of sites. n^s is related to n by $n^s = n \cdot p/(p + q + ...)$. The number of sublattices and the species occupying them, is generally obtained from crystallographical information. The mole fraction of an element is obtained by

$$x_i = \frac{\sum_s n^s y_i^s}{\sum_s n^s (1 - y_{\rm Va}^s)} \tag{13}$$

where $y_{\rm Va}^s$ is the fraction of vacant sites on sublattice s.
This model also describes stoichiometric phases, in which case the sublattices are occupied only by a single species, and substitutional phases which have a single lattice.

The molar Gibbs energy for a phase ϕ expressed by the sublattice model is equal to

$$G_{\rm m}^{\phi} = G_{\rm m}^{\phi,{\rm srf}} + G_{\rm m}^{\phi,{\rm id}} + G_{\rm m}^{\phi,{\rm E}} \tag{14}$$

As an example, a two sublattice phase with two elements A and B in each of the sublattices is considered. Denoting the sublattices with primes at the symbols, the surface of reference for the Gibbs energy is

$$G^{\rm srf} = y_{\rm A}^{'} y_{\rm A}^{''} \, {}^{o}G_{\rm A:A} + y_{\rm A}^{'} y_{\rm B}^{''} \, {}^{o}G_{\rm A:B} + y_{\rm B}^{'} y_{\rm A}^{''} \, {}^{o}G_{\rm B:A} + y_{\rm B}^{'} y_{\rm B}^{''} \, {}^{o}G_{\rm B:B} \tag{15}$$

The terms ${}^{o}G_{\rm A:A}$ and ${}^{o}G_{\rm B:B}$ represent the Gibbs energies of the phase ϕ for the constituent elements A and B. The colon separates the different sublattices. The terms ${}^{o}G_{\rm A:B}$ and ${}^{o}G_{\rm B:A}$ represent the Gibbs energies of the stoichiometric compounds $\rm A_pB_q$ and $\rm B_pA_q$, which may be stable or metastable. ${}^{o}G_{\rm A:A}$, ${}^{o}G_{\rm B:B}$, ${}^{o}G_{\rm A:B}$ and ${}^{o}G_{\rm B:A}$ are numerically given by equations (3) and (1).

The term $G_{\rm m}^{\rm id}$ is related to the molar configurational entropy and is equal to:

$$G_{\rm m}^{\rm id} = R\,T[p(y_{\rm A}^{'} \ln y_{\rm A}^{'} + y_{\rm B}^{'} \ln y_{\rm B}^{'}) + q(y_{\rm A}^{''} \ln y_{\rm A}^{''} + y_{\rm B}^{''} \ln y_{\rm B}^{''})] \tag{16}$$

Finally, the excess Gibbs energy $G_{\rm m}^{\rm E}$ is equal to

$$\begin{aligned} G_{\rm m}^{\rm E} = {} & y_{\rm A}^{'} y_{\rm B}^{'} [y_{\rm A}^{''} L_{\rm A,B:A} + y_{\rm B}^{''} L_{\rm A,B:B}] \\ & + y_{\rm A}^{''} y_{\rm B}^{''} [y_{\rm A}^{'} L_{\rm A:A,B} + y_{\rm B}^{'} L_{\rm B:A,B}] \\ & + y_{\rm A}^{'} y_{\rm B}^{'} y_{\rm A}^{''} y_{\rm B}^{''} L_{\rm A,B:A,B} \end{aligned} \tag{17}$$

The terms $L_{i,j:i}$ and $L_{i:i,j}$ represent the interaction parameters between the atoms on one sublattice for a given occupancy of the other, and can be described by a Redlich - Kister polynomial, as follows:

$$L_{i,j:i} = \sum_{\nu=0} (y_i^{'} - y_j^{'})^{\nu} \, {}^{\nu}L_{i,j:i} \tag{18}$$

The parameters ${}^{\nu}L_{i,j:i}$ can be temperature dependent. The term $L_{i,j:i,j}$ is known as the reciprocal parameter which may be related to the exchange reaction of A and B between the sublattices. It is usually assumed to be composition independent but may depend on temperature.

The above equations can easily be extended to ternary and higher order systems.

3: Phases with order-disorder transformation

Phases with order-disorder transformation, like $A2/B2$ and $A1/L1_2$ can also be described with the sublattice method although this disregards any explicit short range order contributions. A single Gibbs energy function may be used to describe the thermodynamic properties of both the ordered and disordered phases as follows:

$$G_{\rm m} = G_{\rm m}^{\rm dis}(x_i) + \Delta G_{\rm m}^{\rm ord}(y_i^s) \tag{19}$$

where $G_{\rm m}^{\rm dis}(x_i)$ is the molar Gibbs energy of the disordered phase, given by equation (5) and $\Delta G_{\rm m}^{\rm ord}(y_i^s)$ is the ordering energy given by:

$$\Delta G_{\rm m}^{\rm ord} = G_{\rm m}^{\rm subl}(y_i^s) - G_{\rm m}^{\rm subl}(y_i^s = x_i) \tag{20}$$

where $G_{\rm m}^{\rm subl}(y_i^s)$ is given by equation (14). This must be calculated twice, once with the original site fractions y_i^s and once with these site fractions replaced by the mole fractions. If the phase is disordered the site fractions and mole fractions are equal and thus $\Delta G_{\rm m}^{\rm ord}$ equal to zero.

To ensure stability of the disordered phase, the first differential of $G_{\rm m}^{\rm subl}$ with respect to any variation in the site occupancy must be zero at the disordered state. This enforces some relations between the parameters in $G_{\rm m}^{\rm subl}$ as is discussed in [88Ans].

Description of the Tables and Diagrams

The diagrams and tables which are presented for the binary systems provide an overview of the major thermodynamic properties and the mixing behaviour of these systems. Depending on the nature of the respective system, the number and the type of the presented diagrams and tables varies. For all systems, a calculated phase diagram, a short abstract and a table listing the condensed phases are provided. Additional tables and diagrams present data for invariant reactions, integral and partial quantities of the liquid and solid phases, and standard reaction quantities of intermetallic compounds in the system.

The following list gives on overview of the quantities in the tables and diagrams and their designations. The definition of these quantities is provided in the following paragraphs.

Symbol	Unit	Quantity
a_{A}		thermodynamic activity of the component A in a liquid or solid solution
$\Delta_{\mathrm{f}}C_P^{\circ}$	J mol^{-1} K^{-1}	change of the molar heat capacity at constant pressure upon formation of a compound
ΔC_P	J mol^{-1} K^{-1}	change of the molar heat capacity at constant pressure upon formation of a liquid or solid solution
ΔG_{m}	J mol^{-1}	integral Gibbs energy of a liquid or solid solution
$G_{\mathrm{m}}^{\mathrm{E}}$	J mol^{-1}	integral excess Gibbs energy of a liquid or solid solution
ΔG_{A}	J mol^{-1}	partial Gibbs energy of the component A in a liquid or solid solution
$G_{\mathrm{A}}^{\mathrm{E}}$	J mol^{-1}	partial excess Gibbs energy of the component A in a liquid or solid solution
$\Delta_{\mathrm{f}}G^{\circ}$	J mol^{-1}	standard Gibbs energy of formation of a compound
ΔH_{m}	J mol^{-1}	integral enthalpy of a liquid or solid solution
ΔH_{A}	J mol^{-1}	partial enthalpy of the component A in a liquid or solid solution
$\Delta_{\mathrm{f}}H^{\circ}$	J mol^{-1}	standard enthalpy of formation of a compound
$\Delta_{\mathrm{r}}H$	J mol^{-1}	enthalpy of reaction per mole of atoms
p_{i}	Pa	partial pressure of species i
ΔS_{m}	J mol^{-1} K^{-1}	integral entropy of a liquid or solid solution
$S_{\mathrm{m}}^{\mathrm{E}}$	J mol^{-1} K^{-1}	integral excess entropy of a liquid or solid solution
ΔS_{A}	J mol^{-1} K^{-1}	partial entropy of the component A in a liquid or solid solution
$S_{\mathrm{A}}^{\mathrm{E}}$	J mol^{-1} K^{-1}	partial excess entropy of the component A in a liquid or solid solution
$\Delta_{\mathrm{f}}S^{\circ}$	J mol^{-1} K^{-1}	standard entropy of formation of a compound
T	K	thermodynamic temperature
T_{C}	K	Curie temperature
x_{A}		mole fraction of component A in an alloy or compound
γ_{A}		activity coefficient of the component A in a liquid or solid solution

The first diagram shows the phase diagram of the system. The single-phase fields and the compounds are marked with labels which are used in the tables to refer to the respective phases. All boundaries between phases which transform into each other by first-order transformations are drawn with solid lines. Second-order phase transformations and magnetic transformations are denoted by dashed and dotted lines, respectively.

The table “phases, structures and models”, contains crystallographic data and information on the thermodynamic model in the database. The designations of the phases according to Strukturbericht, prototype, Pearson symbol and the space group have been collected from various sources, including the original publication of the assessment and the reference books of Pearson [85Vil], Massalski [90Mas] and Smithells [92Bra]. The SGTE name is used by the accompanying software on the CD-ROM. The last column of this table denotes how the sublattices of the crystals have been mapped into a thermodynamic model. The species which dissolve in a common sublattice are enclosed in parentheses. The indices denote the stoi-

chiometric coefficients of the respective sublattices. If a sublattice is occupied by a single species only, the parentheses have been omitted. Vacancies are denoted by a box (□).

The table of "invariant reactions" provides detailed data for the invariant equilibria and special transition points shown in the phase diagram. For each of these reactions the temperature and the phase compositions are provided. The compositions of the participating phases are listed in the same sequence as given by the symbolic equation. The last column gives the reaction enthalpy on cooling for one mole of atoms according to the respective transformation.

The thermodynamic quantities for the liquid and solid solutions are provided by a set of three tables which are denoted by a suffix a–c after the Roman number. The first of these tables lists the integral quantities as well as the change of the molar heat capacity. The other two tables give the partial quantities for the respective two components.

The integral and partial quantities can often be obtained easily from experiments. Partial molar quantities are used to describe the thermodynamic behaviour of the individual components. In a binary system, the partial molar Gibbs energy G_{A} of component A can be calculated from the molar Gibbs energy, G_{m}, at constant temperature and pressure by the well-known relation:

$$G_{\mathrm{A}} = G_{\mathrm{m}} + (1 - x_{\mathrm{A}})(\partial G_{\mathrm{m}}/\partial x_{\mathrm{A}})_{P,T} \tag{21}$$

G_{A} is also known as the chemical potential of component A and denoted by the symbol μ_{A}. Similar relations hold for the partial molar enthalpy, H_{A}, and the partial molar entropy, S_{A}.

Partial quantities provide the difference between the values of thermodynamic functions of a component in a solution and the corresponding values for the pure components. Thus, the partial Gibbs energy ΔG_{A} of component A is calculated from G_{A} in the solution and G°_{A} in the pure substance by:

$$\Delta G_{\mathrm{A}} = G_{\mathrm{A}} - G^{\circ}_{\mathrm{A}} \tag{22}$$

Usually, the values of the pure components are given for their most stable modification at the respective temperature and pressure. But in order to avoid ambiguities the reference states for each component are given at the tables. The quantities ΔH_{A} and ΔS_{A} are defined accordingly.

The thermodynamic activity a_{A} of a component A is closely related to the partial Gibbs energy by:

$$a_{\mathrm{A}} = \exp(\Delta G_{\mathrm{A}}/RT) \tag{23}$$

Therefore, the activity is 1 for pure components in the chosen reference state.

The integral Gibbs energy, ΔG_{m} is equal to the difference between the Gibbs energy of one mole of a solution G_{m} and the sum of the molar Gibbs energies of the pure components G°_{i} at the same temperature and pressure. For a binary system the integral Gibbs energy is:

$$\Delta G_{\mathrm{m}} = G_{\mathrm{m}} - x_{\mathrm{A}} G^{\circ}_{\mathrm{A}} - x_{\mathrm{B}} G^{\circ}_{\mathrm{B}} \tag{24}$$

If the reference state of the components is the same phase as the mixture, ΔG_{m} is also called the Gibbs energy of mixing. If the reference state of at least one component is different from the phase of the mixture then ΔG_{m} contains the difference in Gibbs energies for the pure components between two phases. In these cases ΔG_{m} is called the Gibbs energy of formation of the mixture. The quantities ΔH_{m} and ΔS_{m} are defined accordingly.

The excess quantities describe the deviation of the mixture from the ideal mixing behaviour. The molar excess Gibbs energy, $G^{\mathrm{E}}_{\mathrm{m}}$, is given by the difference of the integral Gibbs energy and the Gibbs energy of mixing for an ideal mixture:

$$G^{\mathrm{E}}_{\mathrm{m}} = \Delta G_{\mathrm{m}} - G^{\mathrm{id}}_{\mathrm{m}} \tag{25}$$

In case of a a simple substitutional solution, $G_{\mathrm{m}}^{\mathrm{id}}$ is given by equation (7) and for solid solutions with several sublattices an expression similar to equation (16) applies.

The partial excess quantities can be derived from the integral excess functions by relations similar to those between partial and integral quantities. Thus, analogous to equation (21), the partial excess Gibbs energy of component A is given by:

$$G_{\mathrm{A}}^{\mathrm{E}} = G_{\mathrm{m}}^{\mathrm{E}} + (1 - x_{\mathrm{A}})(\partial G_{\mathrm{m}}^{E}/\partial x_{\mathrm{A}})_{P,T} \tag{26}$$

Since the heat of mixing is zero for an ideal mixture, the excess enthalpy is identical to the heat of mixing and the partial excess enthalpy of a component is equal to its partial enthalpy. Therefore, the partial excess entropy can be calculated from the partial excess Gibbs energy by a temperature derivative or by the difference from the partial enthalpy:

$$S_{\mathrm{A}}^{\mathrm{E}} = -(\partial G_{\mathrm{A}}^{\mathrm{E}}/\partial T)_{P,x_{\mathrm{A}}} = (\Delta H_{\mathrm{A}} - G_{\mathrm{A}}^{\mathrm{E}})/T \tag{27}$$

The activity coefficient is related to the partial excess Gibbs energy by an expression analogous to equation (23):

$$\gamma_{\mathrm{A}} = \exp(G_{\mathrm{A}}^{\mathrm{E}}/RT) \tag{28}$$

For the case of simple substitutional solutions the activity of a component A is related to its mole fraction by: $a_A = \gamma_A x_A$.

The preceding equations describe the thermodynamic behaviour of a single phase. In an unconstrained equilibrium between two phases each component has the same chemical potential and the same activity in each phase and the integral quantities are linear functions of the composition in a two-phase region. In the diagrams, the functions are drawn with dashed lines in these regions.

Special considerations apply to stoichiometric compounds. Here, the partial quantities cannot be defined by the expression given in equation (21) because the composition cannot be varied. Instead, the chemical potentials are defined by the equilibrium with the next adjacent stable phase.

The table of “standard reaction quantities” provides the Gibbs energy, the enthalpy, and the entropy of formation for the given compounds from the pure elements in their most stable state at 298.15 K and 0.1 MPa. Phosphorus deviates from this rule since here the white modification is conventionally chosen as a reference state instead of the more stable red form. All values in this table are given for the reaction of a total amount of 1 mole of atoms.

Description of the Software

The software provided with the volumes can calculate the printed phase diagrams but it also has some additional capabilities.

Phase Names

The phase names are the same as used in the volumes. If the phase has a miscibility gap or could appear as both ordered and disordered in the same system, a ”COMPOSITION SET” number is appended to the name after a hash sign. For example LIQUID and LIQUID#2 may appear as phase names if there is a miscibility gap in the liquid phase. Normally the composition set 1 is not identified explicitly. As both phases are thermodynamically identical the assignment of a specific composition set number is arbitrary. For ordering in the Au-Cu system for example there are four different composition sets for the FCC phase.

Diagram Selection

The two basic windows for SGTEbin are shown in Fig. 3. In the text area of the base window references for data and other key textual information may appear. For the selection of a system press any two of the elements highlighted in bold print. The four buttons at the bottom of the window will become available. Four basic types of diagrams can be generated by use of specific buttons. These are,

- the phase diagram,
- the Gibbs energy curves for all phases as a function of composition at a specific temperature
- the activity curves of the two elements as a function of composition at a specific temperature
- a plot of the phase fractions as a function of the temperature for a given composition

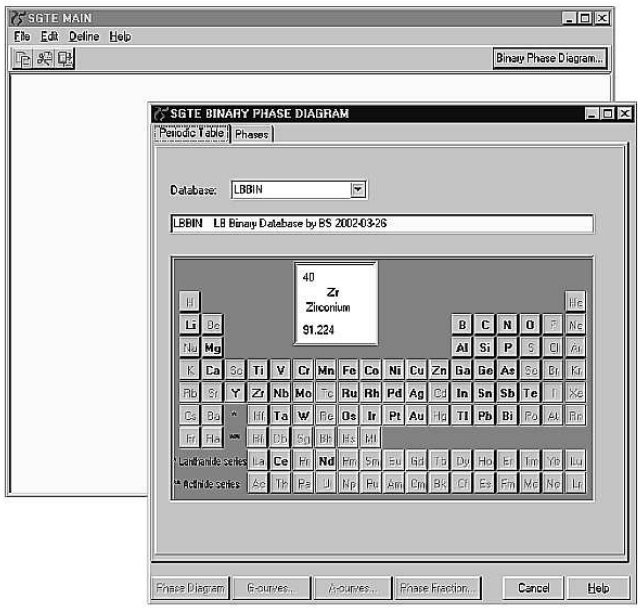

Fig. 3. Base window and periodic chart window.

The basic diagrams are obtained by just selecting two elements and the specific button. From these four calculations an infinite number of modified diagrams can be generated. Some of these will be discussed below.
In addition to selecting the two elements one can also select the set of phases. The folder tagged ”PHASE” gives the default selection of stable phases for the selected system. By changing this selection various metastable diagrams can be calculated.

Phase Diagram

This button will generate a standard temperature - composition phase diagram with the axes in mole fractions and degrees Celsius, see the example in Fig. 4a and 4b. Magnifications and phase labels can be obtained using specific buttons in the graphical window. The REDEFINE button provides a menu, which will allow a change of the axes as shown in Fig. 5. Fig. 6 is equivalent to Fig. 4 but now plotted with activity and temperature in Celsius as axes variables.

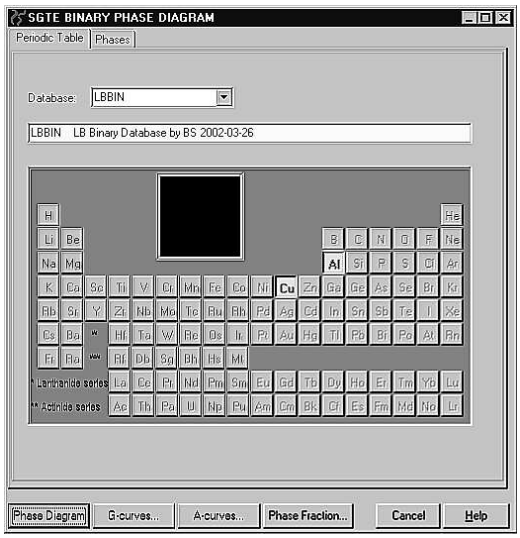

Fig. 4a. The periodic chart window shows the selected elements in red. Note that the buttons in the lower area are activated.

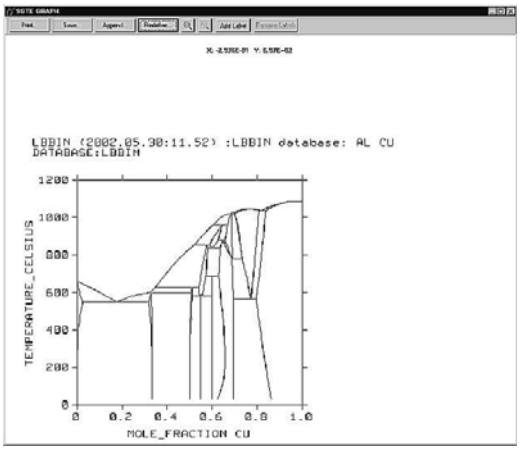

Fig. 4b. A binary phase diagram, here Al-Cu.

There are a number of different possible choices for the axis variable, some will be more sensible than others for a particular phase diagram. You may find it instructive to try a few on your own.

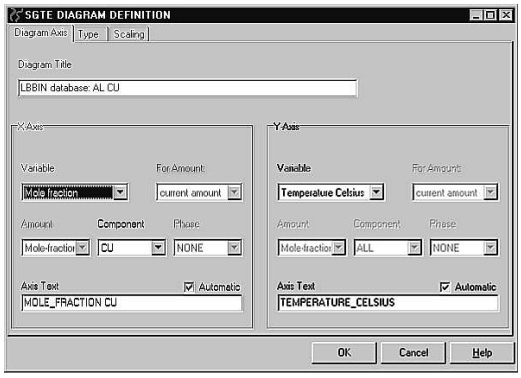

Fig. 5. The REDEFINE window for Al-Cu.

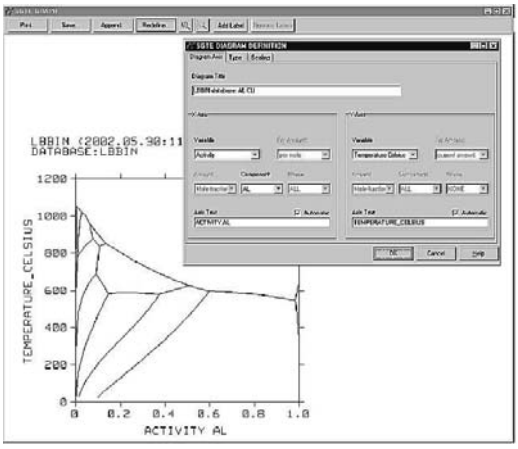

Fig. 6. The calculated Al-Cu system using the activity of Al and the Celsius temperature as axis variables.

G-Curves

In this diagram the Gibbs energies for each phase will be plotted vs composition at a given temperature. This diagram is related to the phase diagram in that the stable combination of phases is given by the lowest Gibbs energy at each composition. An example is given in Fig. 7. The number listed to the right of the diagram identifies each curve. Some phases have limited ranges of existence and stoichiometric phases appear with a small + sign. It is possible to change the axis to plot any integral quantity such as the enthalpy or entropy of the phases. In most cases the default for the reference phase for each element is the stable phase at 298.15 K.

A-Curves

In this diagram the activities of the two elements are plotted vs composition at a given temperature as shown in Fig. 8. The horizontal lines represent two-phase equilibria. It may be useful to change the activity axis to a logarithmic scale in the REDEFINE window or to plot the chemical potential instead. In most cases the default for the reference phase for each element is the stable phase at 298.15 K.

Note the difference between A-CURVES and G-CURVES. In the latter all phases are calculated for their range of composition. In the A-CURVES diagram the phases are included only where they are stable.

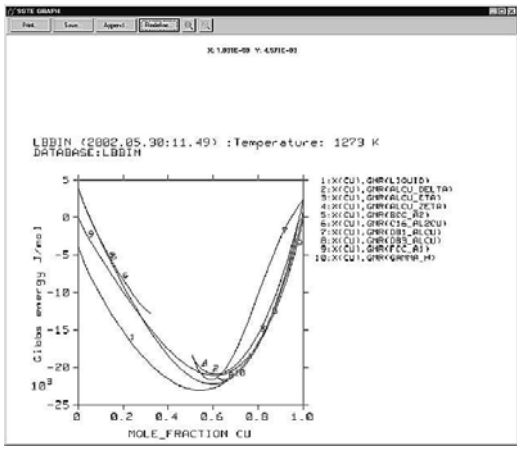

Fig. 7. The diagram calculated by pressing the G curves button. The Gibbs energy curves are shown for all phases of the Al-Cu system at 1273 K.

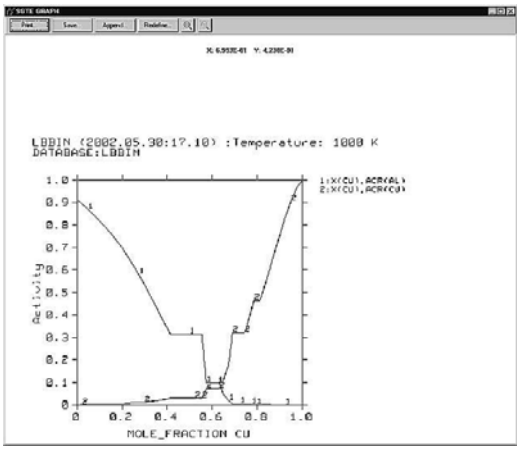

Fig. 8. The diagram calculated by pressing the A curves button. The component activities in the system Al-Cu are shown at 1000 K.

Phase Fraction

This diagram gives the amount of the stable phases as a function of temperature for a given composition as shown in Fig. 9. The amount is given as mass fraction of phase. If one is interested to know how the amount of the phases varies with composition for a given temperature one can use the A-CURVES button and then change the axis with REDEFINE.

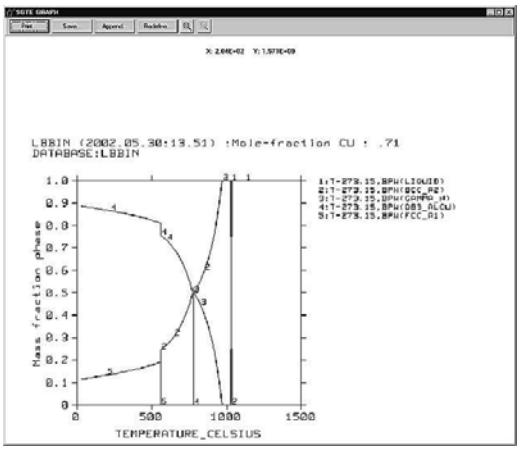

Fig. 9. The diagram calculated by pressing the phase fraction button. The curves show the amount of phase as function of the temperature at a given composition; the mole-fraction of copper is set to 0.71.

Features and Errors

Unfortunately all software has errors. If you find a problem with the software please provide details by sending an email to info@thermocalc.se. Please provide the minimum number of actions needed to reproduce the error. If you would like to suggest an additional feature send an email to the same address. One known problem may occur in the calculation of metastable phase diagrams where there may be a miscibility gap.

References

[45Tem] M. Temkin: Acta Phys. Chim. **20** (1945) 411–420.
[48Red] O. Redlich, A. Kister: Ind. Eng. Chem. **40** (1948) 345–348.
[70Hil] M. Hillert, L.-I. Staffanson: Acta Chem. Scand. **24** (1970) 3618–3626.
[78Hil] M. Hillert, M. Jarl: Calphad **2** (1978) 227–238.
[78Som] F. Sommer: Calphad **2** (1978) 319–324.
[81Ind] G. Inden: Physica **103B** (1981) 82–100.
[81Sun] B. Sundman, J. Ågren: J. Phys. Chem. Solids **42** (1981) 297–301.
[85Hil] M. Hillert, B. Jansson, B. Sundman, Ågren: Metall. Trans. A **16A** (1985) 261–266.
[85Vil] P. Villars, L.D. Calvert: "Pearson's Handbook of Crystallographic Data for Intermetallic Phases", Vol. 1–3, ASM, Metals Park, Ohio, USA, 1985.
[88Ans] I. Ansara, P. Willemin, B. Sundman: Acta metall. **36** (1988) 977–982.
[90Mas] T.B. Massalski, H. Okamoto, P.R. Subramanian, L. Kacprzak: "Binary Alloy Phase Diagrams", 2nd ed., ASM International, Materials Park, Ohio, USA, 1990.
[91Din] A.T. Dinsdale: Calphad **15** (1991) 317–425.
[92Bra] E.A. Brandes, G.B. Brook (eds.): "Smithells Metals Reference Book", 7th ed., Butterworth-Heinemann Ltd., Oxford, 1992.
[97Ans] I. Ansara, N. Dupin, H.L. Lukas, B. Sundman: J. Alloys Compd. **247** (1997) 20–30.
[98Sau] N. Saunders, A.P. Miodownik: "CALPHAD Calculation of Phase Diagrams", Elsevier Science Ltd., Oxford, 1998.
[02Din] A.T. Dinsdale: to be published (2002).

LANDOLT-BÖRNSTEIN

GROUP IV: Physical Chemistry

VOLUME 19: Thermodynamic Properties of Inorganic Materials

SUBVOLUME B: Binary Systems

PART 5: Binary Systems Supplement 1

- In systems
  - In-La
  - In-Pd
- Ir systems
  - Ir-C
  - Ir-Cu
  - Ir-Ni
  - Ir-Pt
  - Ir-Rh
  - Ir-Ru
  - Ir-Zr
- La systems
  - La-In
  - La-Mg
- Li systems
  - Li-Ca
  - Li-Gd
  - Li-N
  - Li-Na
  - Li-Sn
- Mg systems
  - Mg-Dy
  - Mg-Ga
  - Mg-Gd
  - Mg-Ho
  - Mg-La
  - Mg-Tm
  - Mg-Yb
- Mn systems
  - Mn-Gd
  - Mn-Sc
- Mo systems
  - Mo-Ag
  - Mo-Gd
  - Mo-Hf
  - Mo-V
  - Mo-Zr
- N systems
  - N-Li
  - N-Si
- Na systems
  - Na-Li
- Nb systems
  - Nb-Ag
  - Nb-Hf
  - Nb-Ta
- Ni systems
  - Ni-Au
  - Ni-Ce
  - Ni-Hf
  - Ni-Ir
  - Ni-Pb
  - Ni-Ru
  - Ni-Zn
- O systems
  - O-Ag
  - O-Co
- Os systems
  - Os-C
  - Os-Si
- Pb systems
  - Pb-Au
  - Pb-Ni
- Pd systems
  - Pd-Bi
  - Pd-C
  - Pd-Co
  - Pd-Eu
  - Pd-In
  - Pd-Rh
  - Pd-Sm
  - Pd-Tb
- Pt systems
  - Pt-C
  - Pt-Ir
- Rh systems
  - Rh-C
  - Rh-Ir
  - Rh-Pd
- Ru systems
  - Ru-Al
  - Ru-Ba
  - Ru-C
  - Ru-Ca
  - Ru-Cr
  - Ru-Fe
  - Ru-Ir
  - Ru-Ni
  - Ru-Si
  - Ru-Zr
- Sb systems
  - Sb-Fe
- Sc systems
  - Sc-Al
  - Sc-Mn
- Si systems
  - Si-Ga
  - Si-N
  - Si-Os
  - Si-Ru
- Sm systems
  - Sm-Pd
- Sn systems
  - Sn-Al
  - Sn-Eu
  - Sn-Hg
  - Sn-Li
  - Sn-V
- Sr systems
  - Sr-Al
- Ta systems
  - Ta-Nb
- Tb systems
  - Tb-Pd
- Te systems
  - Te-Ag
  - Te-Hg
- Ti systems
  - Ti-Au
  - Ti-Ga
- Tm systems
  - Tm-Mg
- V systems
  - V-Ag
  - V-Mo
  - V-Sn
  - V-W
- W systems
  - W-Ag
  - W-Hf
  - W-V
  - W-Zr
- Y systems
  - Y-Cd
  - Y-Co
- Yb systems
  - Yb-Mg
- Zn systems
  - Zn-C
  - Zn-Co
  - Zn-Hg
  - Zn-Ni
- Zr systems
  - Zr-Au
  - Zr-B
  - Zr-Gd
  - Zr-Ir
  - Zr-Mo
  - Zr-Ru
  - Zr-W

Ag – Pb (Silver – Lead)

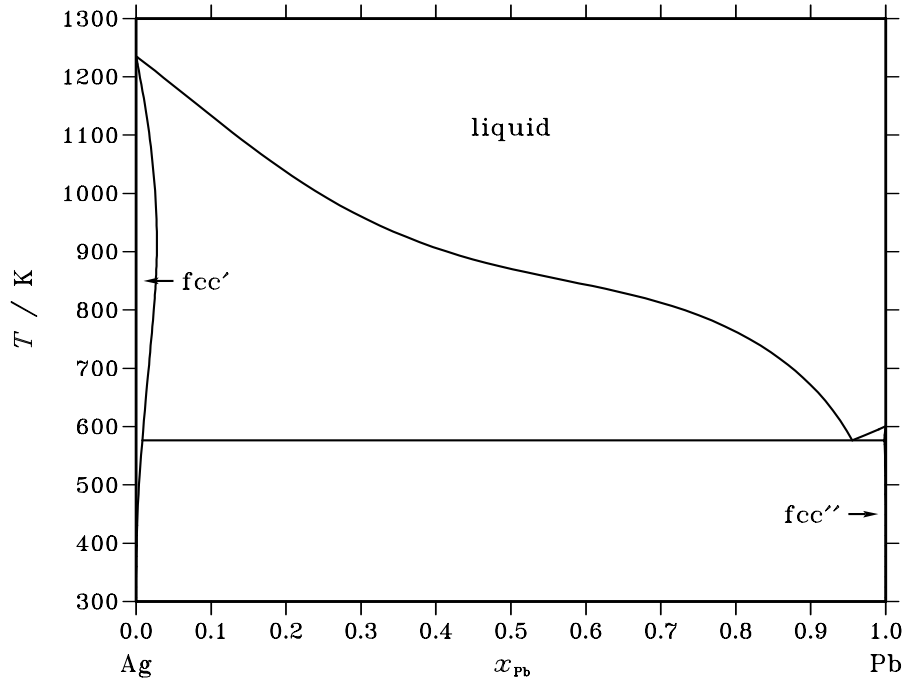

Fig. 1. Calculated phase diagram for the system Ag-Pb.

The silver-lead system is part of the commonly used solder system Pb-Sn-Ag-Bi-Sb-Zn. Therefore, the Ag-Pb system has been studied experimentally many times. A detailed review of experimental data is presented in [80Ell]. The thermodynamic parameters for the Ag-Pb system have been assessed several times [76Zim, 81Ash, 86Hay, 87Kar, 94Lee, 98Roe, 00Luk]. The assessment of [00Luk] has been accepted here. It is based on the same experimental data as [76Zim] and additionally includes a very precise determination of the liquidus for Pb-rich compositions [79Esd].
The system is characterised by a continuous solution of the elements in the liquid phase and a wide miscibility gap in the solid state. The solubility of Pb in fcc-Ag has been determined by thermoelectric power measurements, micrographically and by lattice parameter data. The solubility of Ag in solid Pb is derived from diffusion measurements, thermo-resistometric investigations, electrical resistivity and lattice parameter measurements. In liquid Ag-Pb alloys, the enthalpy of mixing has been measured calorimetrically and the activities of Pb and Ag have been derived from EMF and vapour pressure measurements. All phases are modelled by the substitutional solution model. The calculated thermodynamic quantities and the phase diagram are in good agreement with the experimental data.

Table I. Phases, structures and models.

Phase	Struktur-bericht	Prototype	Pearson symbol	Space group	SGTE name	Model
liquid					LIQUID	$(Ag,Pb)_1$
fcc	$A1$	Cu	$cF4$	$Fm\overline{3}m$	FCC_A1	$(Ag,Pb)_1$

Table II. Invariant reactions.

Reaction	Type	T / K	Compositions / x_{Pb}			$\Delta_{\mathrm{r}}H$ / (J/mol)
liquid $\rightleftharpoons$ fcc′ + fcc″	eutectic	576.4	0.955	0.008	0.998	−5434

Table IIIa. Integral quantities for the liquid phase at 1300 K.

x_{Pb}	ΔG_{m} [J/mol]	ΔH_{m} [J/mol]	ΔS_{m} [J/(mol·K)]	$G^{\mathrm{E}}_{\mathrm{m}}$ [J/mol]	$S^{\mathrm{E}}_{\mathrm{m}}$ [J/(mol·K)]	ΔC_p [J/(mol·K)]
0.000	0	0	0.000	0	0.000	0.000
0.100	−3295	1149	3.419	219	0.716	0.698
0.200	−4834	2127	5.354	575	1.194	1.242
0.300	−5653	2901	6.580	950	1.501	1.630
0.400	−6021	3440	7.278	1253	1.682	1.863
0.500	−6069	3713	7.525	1423	1.761	1.940
0.600	−5851	3689	7.338	1424	1.742	1.863
0.700	−5355	3337	6.686	1248	1.607	1.630
0.800	−4493	2625	5.476	916	1.315	1.242
0.900	−3039	1523	3.510	475	0.807	0.698
1.000	0	0	0.000	0	0.000	0.000

Reference states: Ag(liquid), Pb(liquid)

Table IIIb. Partial quantities for Ag in the liquid phase at 1300 K.

x_{Ag}	ΔG_{Ag} [J/mol]	ΔH_{Ag} [J/mol]	ΔS_{Ag} [J/(mol·K)]	$G^{\mathrm{E}}_{\mathrm{Ag}}$ [J/mol]	$S^{\mathrm{E}}_{\mathrm{Ag}}$ [J/(mol·K)]	a_{Ag}	γ_{Ag}
1.000	0	0	0.000	0	0.000	1.000	1.000
0.900	−1229	81	1.008	−90	0.132	0.893	0.992
0.800	−2603	365	2.283	−191	0.428	0.786	0.983
0.700	−3962	916	3.752	−106	0.786	0.693	0.990
0.600	−5247	1794	5.417	274	1.170	0.615	1.026
0.500	−6513	3064	7.367	979	1.604	0.547	1.095
0.400	−7949	4787	9.796	1955	2.178	0.479	1.198
0.300	−9948	7024	13.055	3066	3.045	0.398	1.328
0.200	−13305	9838	17.802	4091	4.421	0.292	1.460
0.100	−20160	13290	25.730	4729	6.585	0.155	1.549
0.000	$-\infty$	17441	∞	4594	9.883	0.000	1.530

Reference state: Ag(liquid)

Table IIIc. Partial quantities for Pb in the liquid phase at 1300 K.

x_{Pb}	ΔG_{Pb} [J/mol]	ΔH_{Pb} [J/mol]	ΔS_{Pb} [J/(mol·K)]	$G^{\mathrm{E}}_{\mathrm{Pb}}$ [J/mol]	$S^{\mathrm{E}}_{\mathrm{Pb}}$ [J/(mol·K)]	a_{Pb}	γ_{Pb}
0.000	$-\infty$	12251	∞	1043	8.621	0.000	1.101
0.100	−21885	10767	25.117	3003	5.972	0.132	1.320
0.200	−13760	9173	17.641	3637	4.259	0.280	1.400
0.300	−9600	7533	13.179	3414	3.168	0.411	1.371
0.400	−7182	5908	10.069	2722	2.450	0.515	1.286
0.500	−5625	4362	7.682	1867	1.919	0.594	1.189
0.600	−4452	2957	5.699	1069	1.452	0.662	1.104
0.700	−3386	1756	3.956	469	0.990	0.731	1.044
0.800	−2290	822	2.394	122	0.539	0.809	1.011
0.900	−1137	216	1.041	2	0.165	0.900	1.000
1.000	0	0	0.000	0	0.000	1.000	1.000

Reference state: Pb(liquid)

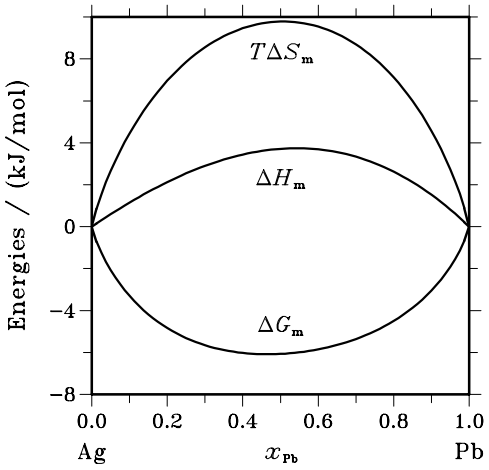

Fig. 2. Integral quantities of the liquid phase at T=1300 K.

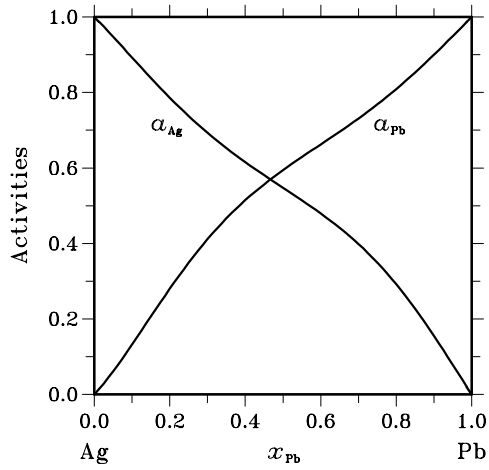

Fig. 3. Activities in the liquid phase at T=1300 K.

References

[76Zim] B. Zimmermann: Ph.D. Thesis, Universität Stuttgart, Stuttgart, 1976.
[79Esd] J.D. Esdaile, N.G. Siviour: Met. Trans. **10A** (1979) 382–384.
[80Ell] R.P. Elliot, F.A. Shunk: Bull. Alloy Phase Diagrams **1** (1980) 56–59.
[81Ash] S. Ashtakala, A.D. Pelton, C.W. Bale: Bull. Alloy Phase Diagrams **2** (1981) 81–83.
[86Hay] F.H. Hayes, H.L. Lukas, G. Effenberg, G. Petzow: Z. Metallkd. **77** (1986) 749–754.
[87Kar] I. Karakaya, W.T. Thompson: Bull. Alloy Phase Diagrams **8** (1987) 326–334.
[94Lee] B.-Z. Lee, C.-S. Oh, D.N. Lee: J. Alloys Comp. **215** (1994) 293–301.
[98Roe] F. Roemermann, R. Blachnik: J. Alloys Comp. **280** (1998) 147–157.
[00Luk] H.L. Lukas: unpublished optimization, 2000.

Ag – Pd (Silver – Palladium)

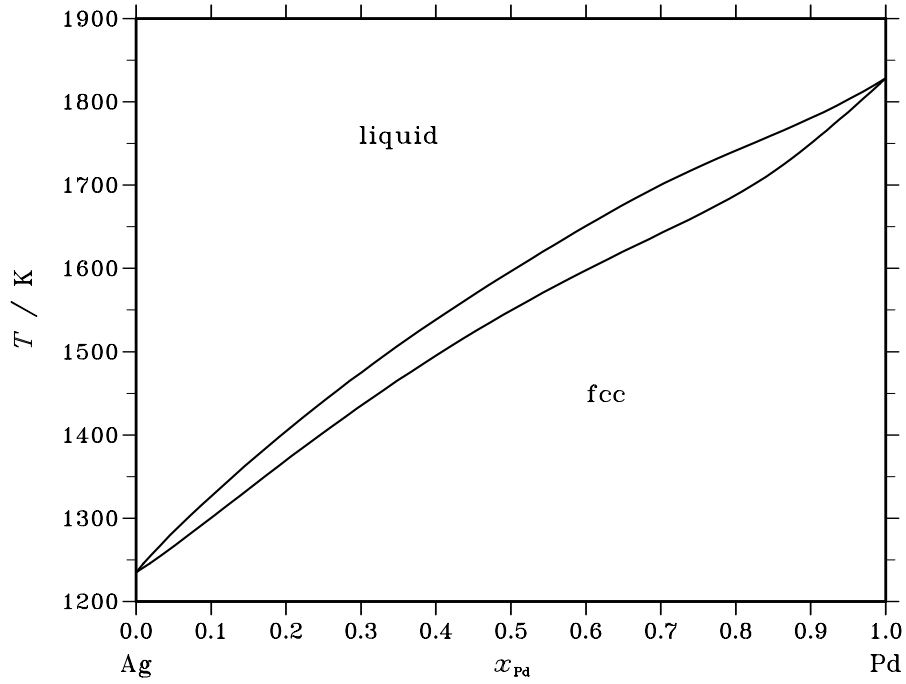

Fig. 1. Calculated phase diagram for the system Ag-Pd.

Alloys of Ag and Pd form a complete range of solid and liquid solutions. The selected thermodynamic data for the system are based on the phase diagram presented by Massalski together with the results obtained by Karakaya and Thompson [87Kar]. A simple substitutional solution model has been used to represent the thermodynamic properties of the liquid and fcc phases. The data are valid for all compositions and temperatures, but particularly in the range 1000 – 2000 K. The present assessment [98Spe] is preferred over that of [99Gho] because the latter presents mixing enthalpies of relatively high magnitude for the liquid and solid phases which is rather surprising for a system with the given complete miscibility ranges.

Table I. Phases, structures and models.

Phase	Struktur-bericht	Prototype	Pearson symbol	Space group	SGTE name	Model
liquid					LIQUID	$(Ag,Pd)_1$
fcc	$A1$	Cu	$cF4$	$Fm\overline{3}m$	FCC_A1	$(Ag,Pd)_1$

Table IIa. Integral quantities for the liquid phase at 1850 K.

x_{Pd}	ΔG_{m} [J/mol]	ΔH_{m} [J/mol]	ΔS_{m} [J/(mol·K)]	$G_{\mathrm{m}}^{\mathrm{E}}$ [J/mol]	$S_{\mathrm{m}}^{\mathrm{E}}$ [J/(mol·K)]	ΔC_p [J/(mol·K)]
0.000	0	0	0.000	0	0.000	0.000
0.100	−6744	−1744	2.703	−1744	0.000	0.000
0.200	−10241	−2544	4.161	−2544	0.000	0.000
0.300	−12016	−2620	5.079	−2620	0.000	0.000
0.400	−12536	−2184	5.596	−2184	0.000	0.000
0.500	−12106	−1444	5.763	−1444	0.000	0.000
0.600	−10952	−600	5.596	−600	0.000	0.000
0.700	−9244	152	5.079	152	0.000	0.000
0.800	−7073	624	4.161	624	0.000	0.000
0.900	−4368	632	2.703	632	0.000	0.000
1.000	0	0	0.000	0	0.000	0.000

Reference states: Ag(liquid), Pd(liquid)

Table IIb. Partial quantities for Ag in the liquid phase at 1850 K.

x_{Ag}	ΔG_{Ag} [J/mol]	ΔH_{Ag} [J/mol]	ΔS_{Ag} [J/(mol·K)]	$G_{\mathrm{Ag}}^{\mathrm{E}}$ [J/mol]	$S_{\mathrm{Ag}}^{\mathrm{E}}$ [J/(mol·K)]	a_{Ag}	γ_{Ag}
1.000	0	0	0.000	0	0.000	1.000	1.000
0.900	−2129	−509	0.876	−509	0.000	0.871	0.967
0.800	−5172	−1740	1.855	−1740	0.000	0.714	0.893
0.700	−8751	−3265	2.966	−3265	0.000	0.566	0.809
0.600	−12529	−4672	4.247	−4672	0.000	0.443	0.738
0.500	−16231	−5569	5.763	−5569	0.000	0.348	0.696
0.400	−19674	−5580	7.619	−5580	0.000	0.278	0.696
0.300	−22868	−4349	10.010	−4349	0.000	0.226	0.754
0.200	−26292	−1536	13.382	−1536	0.000	0.181	0.905
0.100	−32239	3179	19.145	3179	0.000	0.123	1.230
0.000	$-\infty$	10100	∞	10100	0.000	0.000	1.928

Reference state: Ag(liquid)

Table IIc. Partial quantities for Pd in the liquid phase at 1850 K.

x_{Pd}	ΔG_{Pd} [J/mol]	ΔH_{Pd} [J/mol]	ΔS_{Pd} [J/(mol·K)]	$G_{\mathrm{Pd}}^{\mathrm{E}}$ [J/mol]	$S_{\mathrm{Pd}}^{\mathrm{E}}$ [J/(mol·K)]	a_{Pd}	γ_{Pd}
0.000	$-\infty$	−22900	∞	−22900	0.000	0.000	0.226
0.100	−48277	−12859	19.145	−12859	0.000	0.043	0.433
0.200	−30516	−5760	13.382	−5760	0.000	0.138	0.688
0.300	−19634	−1115	10.010	−1115	0.000	0.279	0.930
0.400	−12546	1548	7.619	1548	0.000	0.442	1.106
0.500	−7981	2681	5.763	2681	0.000	0.595	1.190
0.600	−5137	2720	4.247	2720	0.000	0.716	1.193
0.700	−3405	2081	2.966	2081	0.000	0.801	1.145
0.800	−2268	1164	1.855	1164	0.000	0.863	1.079
0.900	−1271	349	0.876	349	0.000	0.921	1.023
1.000	0	0	0.000	0	0.000	1.000	1.000

Reference state: Pd(liquid)

Ag – B (Silver – Boron)

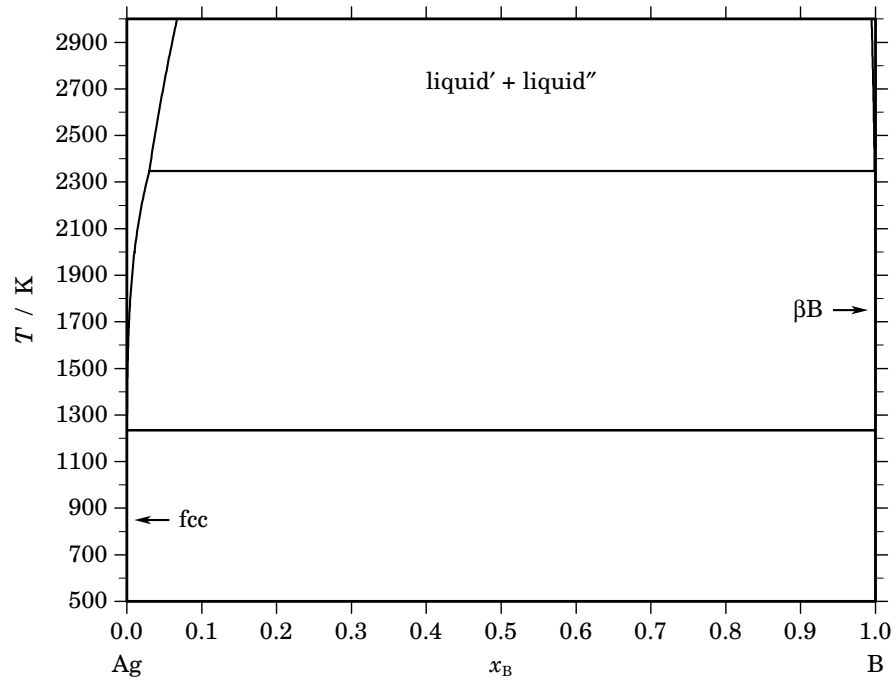

Fig. 1. Calculated phase diagram for the system Ag-B.

No phase diagram data are available for the Ag-B system, except for the invariant equilibrium at 1235 K reported by Wald and Stormont [1970Wal]. Ag and B are immiscible in both the liquid and solid state [1965Wal]. This is consistent with the reported insolubility of B in liquid Ag even at 1873 K [1915Gie]. However, reliable information on the extent of minor solubilities is not available. The compound AgB_2 was obtained by direct synthesis at an unspecified temperature and identified as having a hexagonal structure [1961Obr]. However, X-ray results of alloys with 66.6 at.% B [1965Wal] annealed for two months at 1173 K did not confirm the existence of AgB_2 [1990Kar]. The thermodynamic assessment of the Ag-B system was carried out by Korb [2004Kor]. The calculated phase diagram is in good agreement with available experimental information.

Table I. Phases, structures and models.

Phase	Struktur-bericht	Prototype	Pearson symbol	Space group	SGTE name	Model
liquid					LIQUID	$(Ag,B)_1$
fcc	$A1$	Cu	$cF4$	$Fm\bar{3}m$	FCC_A1	$Ag_1(B,\Box)_1$
βB	$\cdots$	βB	$hR105$	$R\bar{3}m$	BETA_RHOMBO_B	$B_{93}B_{12}$

Table II. Invariant reactions.

Reaction	Type	T / K	Compositions / x_B			$\Delta_r H$ / (J/mol)
liquid″ $\rightleftharpoons$ liquid′ + βB	monotectic	2346.9	0.999	0.030	1.000	−50292
liquid + βB $\rightleftharpoons$ fcc	degenerate	1234.9	0.000	1.000	0.000	−11297

References

[1915Gie] H. Giebelhausen: Z. Anorg. Chem. **91** (1915) 261–262.
[1961Obr] W. Obrowski: Naturwissenschaften **48** (1961) 428.
[1965Wal] F. Wald, R.W. Stormont: J. Less-Common Met. **9** (1965) 423–433.
[1970Wal] F. Wald: Electron. Technol. **3** (1970) 103–108.
[1990Kar] I. Karakaya, W.T. Thompson: Bull. Alloy Phase Diagrams **11** (1990) 547.
[2004Kor] J. Korb, unpublished assessment, GTT-Technologies, 2004.

Ag – Ba (Silver – Barium)

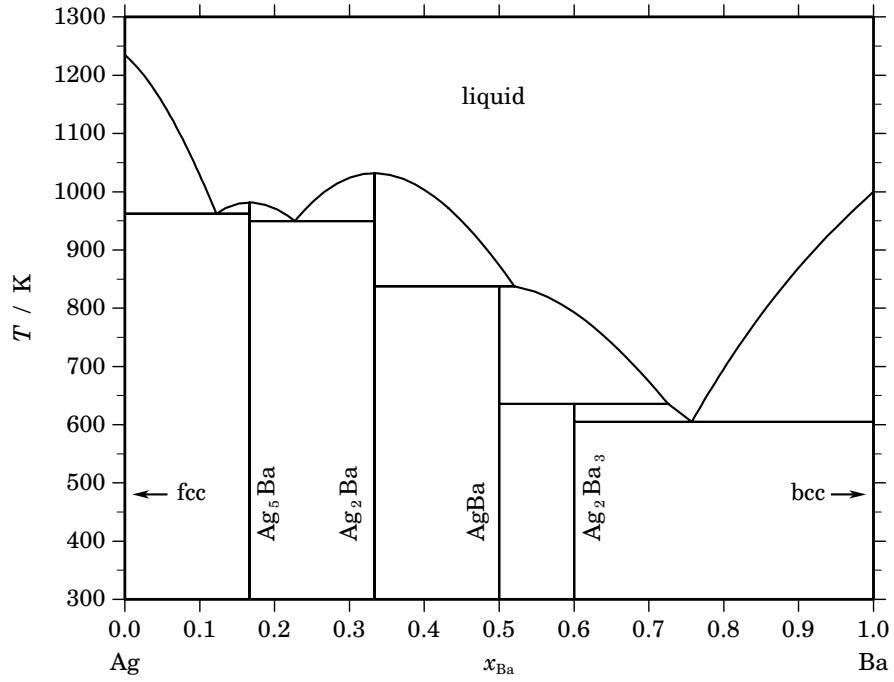

Fig. 1. Calculated phase diagram for the system Ag-Ba.

The Ag-Ba binary system contains two components interesting in the nuclear field, silver being part of AIC control rods (Ag-In-Cd). The phase diagram reported in the compilation of Okamoto [1992Oka] is mainly based on the experimental work of Bruzzone *et al.* [1987Bru] using DTA, X-ray and metallography. The older work of Weibke [1930Wei] using DTA has been discarded. Four intermetallic phases have been identified: Ag_5Ba, with a wide non-stoichiometry range, and three stoichiometric compounds, Ag_2Ba, AgBa, and Ag_2Ba_3. The first two melt congruently at 988 K and 1043 K, the two others decompose peritectically at 833 K and 633 K. There are two eutectic reactions located at 973 K on the silver side and at 513 K on the barium side. There is no reported mutual solubility of both elements in the solid state, and a complete miscibility in the liquid state. The enthalpy of mixing of liquid alloys of silver with barium and rare earth metals (La, Ce, Sm, Eu, Gd, Dy and Yb) have been measured by Ivanov and Witusiewicz [1992Iva] using isoperibolic calorimetry. No experimental data are available for thermodynamic properties of the intermetallic solid phases. This system was assessed by Chevalier and Fischer [1995Che]. The excess Gibbs energy of the liquid and the Gibbs energy of the intermetallic compounds which are all treated as stoichiometric were optimised from selected data for the phase diagram [1987Bru] and the enthalpy of mixing in the melt [1992Iva]. A sub-regular substitution model was used for the liquid. The heat capacity versus temperature and the entropy at 298.15 K of the compounds were estimated from the pure elements by using the Neumann-Kopp rule. The enthalpy of formation was optimised in consistency with other data. The calculations are in very satisfactory agreement with the selected experimental data.

Table I. Phases, structures and models.

Phase	Struktur-bericht	Prototype	Pearson symbol	Space group	SGTE name	Model
liquid					LIQUID	$(Ag,Ba)_1$
fcc	$A1$	Cu	$cF4$	$Fm\bar{3}m$	FCC_A1	Ag_1
Ag_5Ba	$D2_d$	$CaCu_5$	$hP6$	$P6/mmm$	AG5BA	Ag_5Ba_1
Ag_2Ba	$\cdots$	$CeCu_2$	$oI12$	$Imma$	AG2BA	Ag_2Ba_1
AgBa	$B27$	FeB	$oP8$	$Pnma$	AGBA	Ag_1Ba_1
Ag_2Ba_3	$\cdots$	Er_3Ni_2	$hR45$	$R\bar{3}$	AG2BA3	Ag_2Ba_3
bcc	$A2$	W	$cI2$	$Im\bar{3}m$	BCC_A2	Ba_1

Table II. Invariant reactions.

Reaction	Type	T / K	Compositions / x_{Ba}			$\Delta_r H$ / (J/mol)
liquid $\rightleftharpoons$ Ag_2Ba	congruent	1031.9	0.333	0.333		−14037
liquid $\rightleftharpoons$ Ag_5Ba	congruent	981.7	0.167	0.167		−12181
liquid $\rightleftharpoons$ fcc + Ag_5Ba	eutectic	962.0	0.122	0.000	0.167	−11382
liquid $\rightleftharpoons$ Ag_5Ba + Ag_2Ba	eutectic	949.7	0.227	0.167	0.333	−12377
Ag_2Ba + liquid $\rightleftharpoons$ AgBa	peritectic	837.6	0.333	0.520	0.500	−10493
AgBa + liquid $\rightleftharpoons$ Ag_2Ba_3	peritectic	635.8	0.500	0.726	0.600	−3753
liquid $\rightleftharpoons$ Ag_2Ba_3 + bcc	eutectic	604.8	0.757	0.600	1.000	−7906

Table IIIa. Integral quantities for the liquid phase at 1273 K.

x_{Ba}	ΔG_m [J/mol]	ΔH_m [J/mol]	ΔS_m [J/(mol·K)]	G_m^E [J/mol]	S_m^E [J/(mol·K)]	ΔC_P [J/(mol·K)]
0.000	0	0	0.000	0	0.000	0.000
0.100	−9744	−6304	2.703	−6304	0.000	0.000
0.200	−16034	−10738	4.161	−10738	0.000	0.000
0.300	−19944	−13478	5.079	−13478	0.000	0.000
0.400	−21824	−14701	5.596	−14701	0.000	0.000
0.500	−21918	−14581	5.763	−14581	0.000	0.000
0.600	−20418	−13295	5.596	−13295	0.000	0.000
0.700	−17484	−11018	5.079	−11018	0.000	0.000
0.800	−13223	−7926	4.161	−7926	0.000	0.000
0.900	−7636	−4195	2.703	−4195	0.000	0.000
1.000	0	0	0.000	0	0.000	0.000

Reference states: Ag(liquid), Ba(liquid)

Table IIIb. Partial quantities for Ag in the liquid phase at 1273 K.

x_{Ag}	ΔG_{Ag} [J/mol]	ΔH_{Ag} [J/mol]	ΔS_{Ag} [J/(mol·K)]	G^E_{Ag} [J/mol]	S^E_{Ag} [J/(mol·K)]	a_{Ag}	γ_{Ag}
1.000	0	0	0.000	0	0.000	1.000	1.000
0.900	−2079	−964	0.876	−964	0.000	0.822	0.913
0.800	−5983	−3622	1.855	−3622	0.000	0.568	0.710
0.700	−11397	−7621	2.966	−7621	0.000	0.341	0.487
0.600	−18019	−12612	4.247	−12612	0.000	0.182	0.304
0.500	−25579	−18242	5.763	−18242	0.000	0.089	0.178
0.400	−33858	−24160	7.619	−24160	0.000	0.041	0.102
0.300	−42757	−30014	10.010	−30014	0.000	0.018	0.059
0.200	−52488	−35453	13.382	−35453	0.000	0.007	0.035
0.100	−64497	−40126	19.145	−40126	0.000	0.002	0.023
0.000	−∞	−43680	∞	−43680	0.000	0.000	0.016

Reference state: Ag(liquid)

Table IIIc. Partial quantities for Ba in the liquid phase at 1273 K.

x_{Ba}	ΔG_{Ba} [J/mol]	ΔH_{Ba} [J/mol]	ΔS_{Ba} [J/(mol·K)]	G^E_{Ba} [J/mol]	S^E_{Ba} [J/(mol·K)]	a_{Ba}	γ_{Ba}
0.000	−∞	−72968	∞	−72968	0.000	0.000	0.001
0.100	−78731	−54359	19.145	−54359	0.000	0.001	0.006
0.200	−56237	−39202	13.382	−39202	0.000	0.005	0.025
0.300	−39887	−27144	10.010	−27144	0.000	0.023	0.077
0.400	−27532	−17834	7.619	−17834	0.000	0.074	0.185
0.500	−18257	−10920	5.763	−10920	0.000	0.178	0.356
0.600	−11458	−6052	4.247	−6052	0.000	0.339	0.565
0.700	−6652	−2877	2.966	−2877	0.000	0.533	0.762
0.800	−3406	−1044	1.855	−1044	0.000	0.725	0.906
0.900	−1318	−202	0.876	−202	0.000	0.883	0.981
1.000	0	0	0.000	0	0.000	1.000	1.000

Reference state: Ba(liquid)

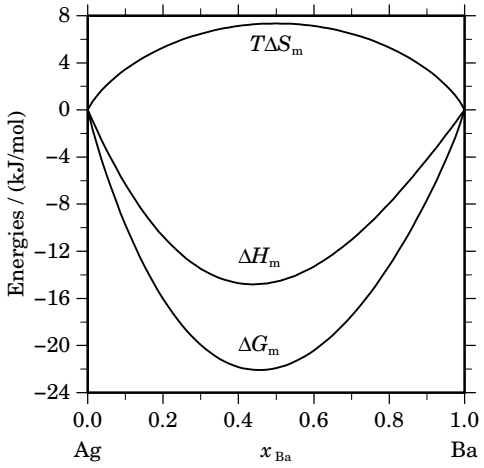

Fig. 2. Integral quantities of the liquid phase at T=1273 K.

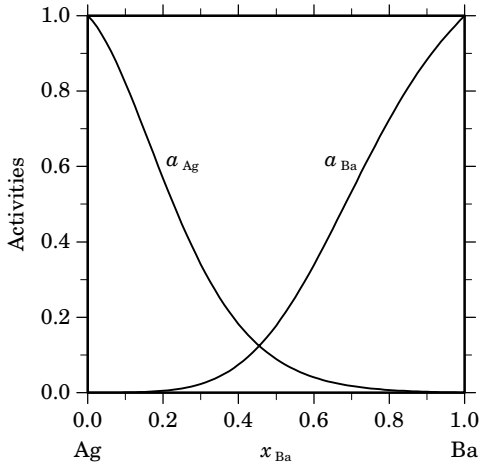

Fig. 3. Activities in the liquid phase at T=1273 K.

Table IV. Standard reaction quantities at 298.15 K for the compounds per mole of atoms.

Compound	x_{Ba}	$\Delta_{\mathrm{f}}G^{\circ}$ / (J/mol)	$\Delta_{\mathrm{f}}H^{\circ}$ / (J/mol)	$\Delta_{\mathrm{f}}S^{\circ}$ / (J/(mol·K))	$\Delta_{\mathrm{f}}C_P^{\circ}$ / (J/(mol·K))
Ag_5Ba_1	0.167	−11206	−11205	0.001	0.000
Ag_2Ba_1	0.333	−18356	−18356	0.001	0.000
Ag_1Ba_1	0.500	−17045	−17045	0.001	0.000
Ag_2Ba_3	0.600	−13868	−13868	0.001	0.000

References

[1930Wei] F. Weibke: Z. Anorg. Allg. Chem. **193** (1930) 297–310.
[1987Bru] G. Bruzzone, M. Ferretti, F. Merlo: J. Less-Common Met. **128** (1987) 259–264.
[1992Iva] M.I. Ivanov, V.T. Witusiewicz: J. Alloys Comp. **186** (1992) 255–266.
[1992Oka] H. Okamoto: J. Phase Equilibria **13** (1992) 434–435.
[1995Che] P.-Y. Chevalier, E. Fischer, unpublished work, 1995.

Ag – Be (Silver – Beryllium)

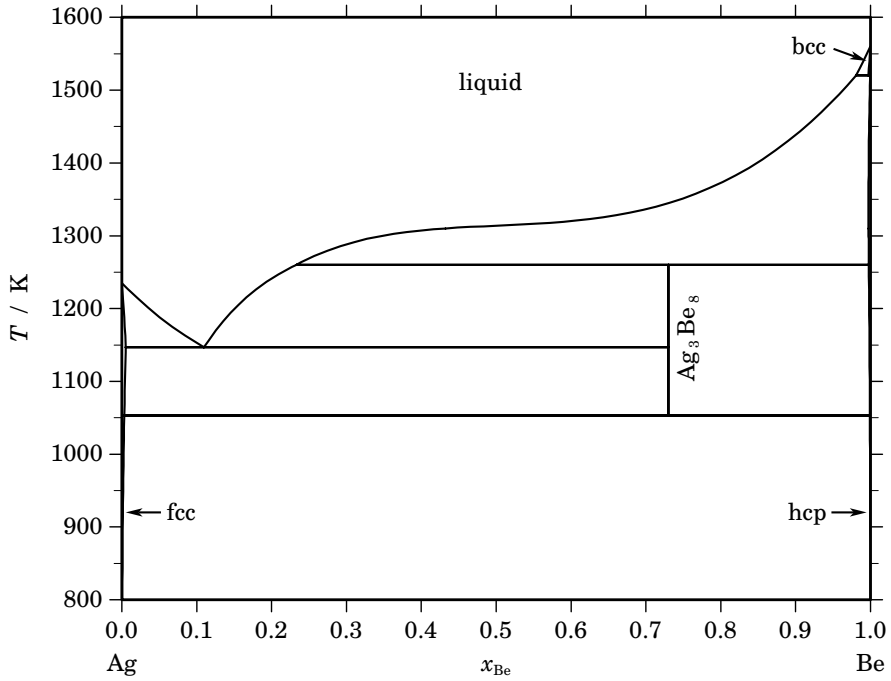

Fig. 1. Calculated phase diagram for the system Ag-Be.

The equilibrium phases of the Ag-Be system are the liquid, the Ag-based fcc solid solution, the Be-based bcc and the hcp solid solution phases, as well as the high-temperature intermetallic compound Ag_3Be_8 which exists only within a limited temperature range between 1033 K and 1283 K [1973Gol, 1979Ald]. The compound is a Laves phase of the Cu_2Mg type but it has been represented by the formula Ag_3Be_8 since it exists only in a very narrow range at the off-stoichiometric composition of about 73 at.% Be. The Ag-Be system was critically assessed by Korb [2004Kor]. The calculated Ag-Be phase diagram compares well with the data compilation in [1987Oka].

Table I. Phases, structures and models.

Phase	Struktur-bericht	Prototype	Pearson symbol	Space group	SGTE name	Model
liquid					LIQUID	$(Ag,Be)_1$
fcc	$A1$	Cu	$cF4$	$Fm\bar{3}m$	FCC_A1	$(Ag,Be)_1$
Ag_3Be_8	$C15$	Cu_2Mg	$cF24$	$Fd\bar{3}m$	AG3BE8	Ag_3Be_8
bcc	$A2$	W	$cI2$	$Im\bar{3}m$	BCC_A2	$(Ag,Be)_1$
hcp	$A3$	Mg	$hP2$	$P6_3/mmc$	HCP_A3	$(Ag,Be)_1$

Table II. Invariant reactions.

Reaction	Type	T / K	Compositions / x_{Be}			$\Delta_r H$ / (J/mol)
bcc $\rightleftharpoons$ liquid + hcp	metatectic	1520.5	0.997	0.981	0.999	−5040
liquid + hcp $\rightleftharpoons$ Ag_3B_8	peritectic	1260.1	0.233	0.998	0.730	−3200
liquid $\rightleftharpoons$ fcc + Ag_3B_8	eutectic	1146.7	0.110	0.005	0.730	−13223
Ag_3B_8 $\rightleftharpoons$ fcc + hcp	eutectoid	1053.2	0.730	0.003	0.999	−2484

Table IIIa. Integral quantities for the liquid phase at 1600 K.

x_{Be}	ΔG_{m} [J/mol]	ΔH_{m} [J/mol]	ΔS_{m} [J/(mol·K)]	$G_{\mathrm{m}}^{\mathrm{E}}$ [J/mol]	$S_{\mathrm{m}}^{\mathrm{E}}$ [J/(mol·K)]	ΔC_P [J/(mol·K)]
0.000	0	0	0.000	0	0.000	0.000
0.100	−2444	1988	2.770	1880	0.067	0.000
0.200	−3311	3522	4.270	3346	0.110	0.000
0.300	−3729	4608	5.211	4397	0.132	0.000
0.400	−3922	5249	5.732	5031	0.136	0.000
0.500	−3974	5450	5.890	5247	0.127	0.000
0.600	−3910	5215	5.703	5043	0.107	0.000
0.700	−3709	4548	5.161	4418	0.082	0.000
0.800	−3287	3454	4.213	3370	0.053	0.000
0.900	−2427	1936	2.727	1898	0.024	0.000
1.000	0	0	0.000	0	0.000	0.000

Reference states: Ag(liquid), Be(liquid)

Table IIIb. Partial quantities for Ag in the liquid phase at 1600 K.

x_{Ag}	ΔG_{Ag} [J/mol]	ΔH_{Ag} [J/mol]	ΔS_{Ag} [J/(mol·K)]	$G_{\mathrm{Ag}}^{\mathrm{E}}$ [J/mol]	$S_{\mathrm{Ag}}^{\mathrm{E}}$ [J/(mol·K)]	a_{Ag}	γ_{Ag}
1.000	0	0	0.000	0	0.000	1.000	1.000
0.900	−1195	227	0.889	207	0.013	0.914	1.016
0.800	−2140	903	1.902	829	0.046	0.851	1.064
0.700	−2876	2019	3.059	1869	0.094	0.806	1.151
0.600	−3465	3568	4.395	3331	0.148	0.771	1.285
0.500	−4004	5539	5.964	5217	0.201	0.740	1.480
0.400	−4660	7925	7.865	7529	0.247	0.704	1.761
0.300	−5744	10717	10.288	10272	0.278	0.649	2.164
0.200	−7963	13907	13.668	13448	0.287	0.550	2.748
0.100	−13572	17486	19.411	17059	0.266	0.361	3.605
0.000	$-\infty$	21445	∞	21110	0.210	0.000	4.888

Reference state: Ag(liquid)

Table IIIc. Partial quantities for Be in the liquid phase at 1600 K.

x_{Be}	ΔG_{Be} [J/mol]	ΔH_{Be} [J/mol]	ΔS_{Be} [J/(mol·K)]	$G_{\mathrm{Be}}^{\mathrm{E}}$ [J/mol]	$S_{\mathrm{Be}}^{\mathrm{E}}$ [J/(mol·K)]	a_{Be}	γ_{Be}
0.000	$-\infty$	22155	∞	20867	0.805	0.000	4.800
0.100	−13690	17831	19.701	16941	0.556	0.357	3.573
0.200	−7994	13997	13.745	13417	0.363	0.548	2.742
0.300	−5721	10647	10.230	10296	0.219	0.650	2.168
0.400	−4608	7771	7.737	7582	0.118	0.707	1.768
0.500	−3944	5361	5.816	5277	0.052	0.743	1.487
0.600	−3410	3409	4.262	3385	0.015	0.774	1.290
0.700	−2836	1905	2.963	1909	−0.003	0.808	1.154
0.800	−2118	841	1.849	850	−0.006	0.853	1.066
0.900	−1189	209	0.873	213	−0.003	0.915	1.016
1.000	0	0	0.000	0	0.000	1.000	1.000

Reference state: Be(liquid)

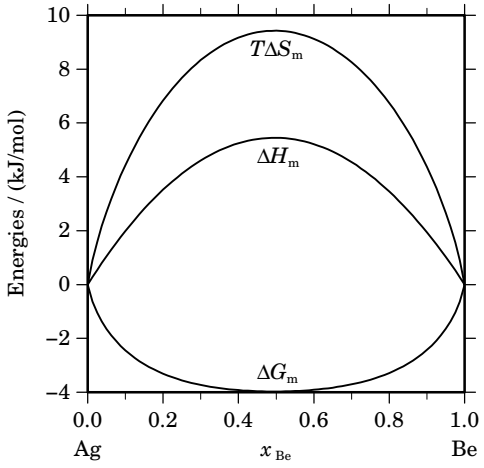

Fig. 2. Integral quantities of the liquid phase at T=1600 K.

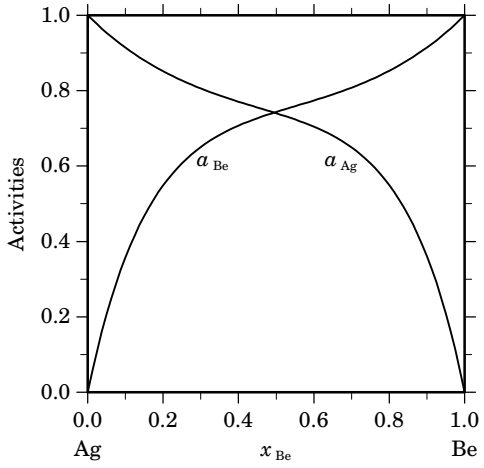

Fig. 3. Activities in the liquid phase at T=1600 K.

Table IV. Standard reaction quantities at 298.15 K for the compounds per mole of atoms.

Compound	x_{Be}	$\Delta_f G^\circ$ / (J/mol)	$\Delta_f H^\circ$ / (J/mol)	$\Delta_f S^\circ$ / (J/(mol·K))	$\Delta_f C_P^\circ$ / (J/(mol·K))
Ag_3Be_8	0.730	1838	2569	2.452	0.000

References

[1973Gol] O. von Goldbeck in: Beryllium: Physico-Chemical Properties of Its Compounds and Alloys, O. Kubaschewski, ed., Atomic Energy Review Special Issue No. 4, International Atomic Energy Agency, Vienna, 1973, pp.45–46.

[1979Ald] F. Aldinger, G. Petzow in: "Beryllium Science and Technology", vol. 1, D. Webster, G.J. London, eds., Plenum Press, New York, 1979, 235–305.

[1987Oka] H. Okamoto, L.E. Tanner in: "Phase Diagrams of Binary Beryllium Alloys", H. Okamoto, L.E. Tanner, eds., ASM, Metals Park, 1987, 4–8.

[2004Kor] J. Korb, unpublished assessment, GTT-Technologies, 2004.

Ag – C (Silver – Carbon)

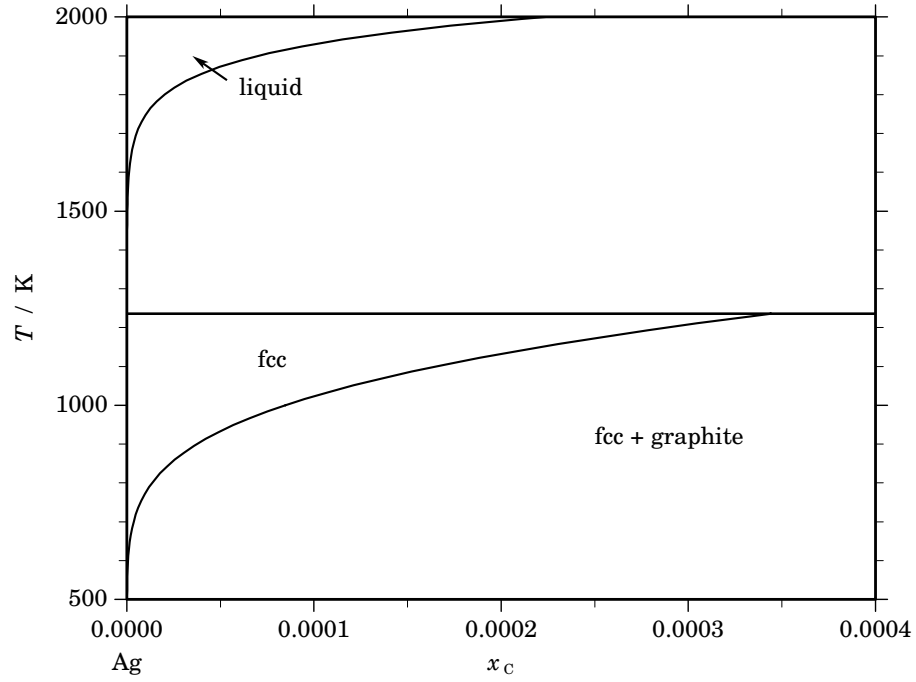

Fig. 1. Calculated phase diagram for the system Ag-C.

The Ag-C phase diagram has been studied by various experimental techniques [1919Ruf, 1949Ves, 1959Sne, 1969McL]. The Ag-C system displays the liquid, fcc and graphite phases. This system exhibits immiscibility to a very high degree [1988Kar]. The solubility of Ag in graphite is extremely low, but not known precisely [1988Kar]. The solid solubility of graphite in fcc-Ag has been studied by a vapour transport technique [1969McL] in the range from 1058 to 1230 K. The solubility of carbon in solid silver at its melting point has been found to be 0.036 at.% C. The solubility of carbon in liquid silver is much lower and has been reported in [1919Ruf]. Some compounds of Ag and C have been reported, such as Ag_4C and AgC [1959Sne] and Ag_2C_2 [1949Ves, 1959Sne]. Their existence has not been confirmed by other investigations. The data for the Ag-C system were critically assessed by Korb [2004Kor]. The calculated phase diagram is in good agreement with the data compilation in [1988Kar].

Table I. Phases, structures and models.

Phase	Struktur-bericht	Prototype	Pearson symbol	Space group	SGTE name	Model
liquid					LIQUID	$(Ag,C)_1$
fcc	$A1$	Cu	$cF4$	$Fm\bar{3}m$	FCC_A1	$Ag_1(C,\Box)_1$
graphite	$A9$	C(graphite)	$hP4$	$P6_3/mmc$	GRAPHITE	C_1

Table II. Invariant reactions.

Reaction	Type	T / K	Compositions / x_C			$\Delta_r H$ / (J/mol)
liquid + graphite $\rightleftharpoons$ fcc	peritectic	1235.5	0.000	1.000	0.000	−11273

References

[1919Ruf] O. Ruff, B. Bergdahl: Z. Anorg. Allg. Chem. **106** (1919) 76–94.
[1949Ves] R. Vestin, E. Ralf: Acta Chem. Scand. **3** (1949) 101–124.
[1959Sne] M.C. Sneed, J.L. Maynard, R.C. Brasted: "Comprehensive Inorganic Chemistry", Vol. II, D, Van Nostrand Co., Inc., New York (1959).
[1969McL] R.B. McLellan: Scr. Metall. **3** (1969) 389–391.
[1988Kar] I. Karakaya, W.T. Thompson: Bull. Alloy Phase Diagrams **9** (1988) 226–227.
[2004Kor] J. Korb: unpublished assessment, GTT-Technologies, 2004.

Ag – Ca (Silver – Calcium)

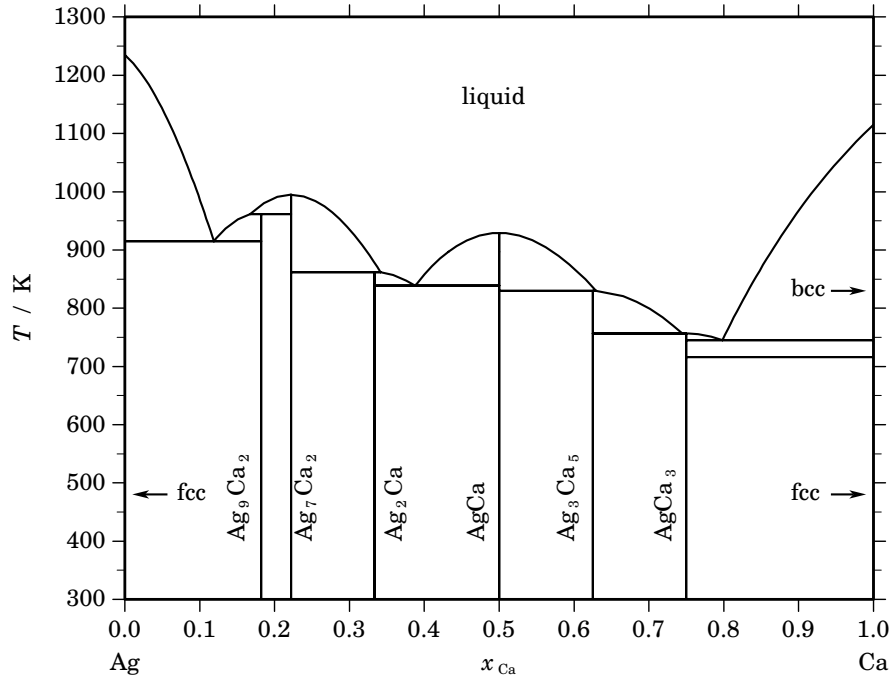

Fig. 1. Calculated phase diagram for the system Ag-Ca.

The Ag-Ca binary system contains two components interesting the nuclear field, silver being part of AIC control rods (Ag-In-Cd) and calcium being a major component of the concrete basemat in its oxide form (CaO). The phase diagram reported in the compilation of Moffatt [1981Mof] and reported by Baren [1988Bar] is based on investigations of Alexander *et al.* [1969Ale] using DTA, X-ray and metallography, and Pascal *et al.* [1970Pas] using DTA. Baar's results from thermal analysis [1911Baa] were reported by Hansen and Anderko [1958Han]. Six intermetallic stoichiometric compounds were clearly identified, Ag_9Ca_2, Ag_7Ca_2, Ag_2Ca, AgCa, Ag_3Ca_5, and $AgCa_3$. In addition, Calvert and Rand [1964Cal] identified Ag_8Ca_3 by X-ray analysis, but it was not confirmed by thermal analysis. Ag_7Ca_2 and AgCa melt congruently at 1004 K and 938 K, respectively, while the four others decompose peritectically. There is no reported mutual solubility of both elements in the solid state, and a complete miscibility in the liquid state. The thermodynamic properties of liquid alloys were electrochemically determined by Delcet and Egan [1978Del] and by Fischbach [1985Fis] using the Knudsen effusion technique. The enthalpy of formation of the compounds was measured potentiometrically [1981Not]. No experimental data are available for the thermodynamic properties of the other compounds. This system was assessed by Chevalier and Fischer [1996Che]. The excess Gibbs energy of the liquid and the Gibbs energy of the intermetallic compounds considered as stoichiometric ones were optimised from the selected experimental information. A sub-regular substitution model was used for the liquid. The enthalpy of formation was optimised in consistency with other data. The agreement with the experimental phase diagram information [1969Ale, 1970Pas] is quite satisfactory. The calculated activity of calcium at 1073 K is in satisfactory agreement with the experiments.

Table I. Phases, structures and models.

Phase	Struktur-bericht	Prototype	Pearson symbol	Space group	SGTE name	Model
liquid					LIQUID	$(Ag,Ca)_1$
fcc	$A1$	Cu	$cF4$	$Fm\bar{3}m$	FCC_A1	$(Ag,Ca)_1$
Ag_9Ca_2	···	···	···	···	AG9CA2	Ag_9Ca_2
Ag_7Ca_2	···	···	$hP18$	$P6_322$	AG7CA2	Ag_7Ca_2
Ag_2Ca	···	···	$oI12$	$Imma$	AG2CA	Ag_2Ca_1
AgCa	B_f	CrB	$oC8$	$Cmcm$	AGCA	Ag_1Ca_1
Ag_3Ca_5	$D8_1$	Cr_5B_3	$tI32$	$I4/mcm$	AG3CA5	Ag_3Ca_5
$AgCa_3$	···	···	···	···	AGCA3	$AgCa_3$
bcc	$A2$	W	$cI2$	$Im\bar{3}m$	BCC_A2	Ca_1

Table II. Invariant reactions.

Reaction	Type	T / K	Compositions / x_{Ca}			$\Delta_r H$ / (J/mol)
liquid $\rightleftharpoons$ Ag_7Ca_2	congruent	994.8	0.222	0.222		−13435
liquid + Ag_7Ca_2 $\rightleftharpoons$ Ag_9Ca_2	peritectic	961.4	0.167	0.222	0.182	−9076
liquid $\rightleftharpoons$ AgCa	congruent	929.4	0.500	0.500		−14074
liquid $\rightleftharpoons$ fcc + Ag_9Ca_2	eutectic	915.0	0.119	0.000	0.182	−11050
Ag_7Ca_2 + liquid $\rightleftharpoons$ Ag_2Ca	peritectic	861.6	0.222	0.341	0.333	−11746
liquid $\rightleftharpoons$ Ag_2Ca + AgCa	eutectic	838.5	0.388	0.333	0.500	−12503
AgCa + liquid $\rightleftharpoons$ Ag_3Ca_5	peritectic	829.6	0.500	0.630	0.625	−12107
liquid $\rightleftharpoons$ $AgCa_3$	congruent	756.7	0.750	0.750		−11010
liquid $\rightleftharpoons$ Ag_3Ca_5 + $AgCa_3$	eutectic	756.6	0.745	0.625	0.750	−11039
liquid $\rightleftharpoons$ $AgCa_3$ + bcc	eutectic	745.4	0.798	0.750	1.000	−10351
bcc $\rightleftharpoons$ $AgCa_3$ + fcc	degenerate	716.0	1.000	0.750	1.000	−929

Table IIIa. Integral quantities for the liquid phase at 1273 K.

x_{Ca}	ΔG_m [J/mol]	ΔH_m [J/mol]	ΔS_m [J/(mol·K)]	G_m^E [J/mol]	S_m^E [J/(mol·K)]	ΔC_P [J/(mol·K)]
0.000	0	0	0.000	0	0.000	0.000
0.100	−12625	−9184	2.703	−9184	0.000	0.000
0.200	−20995	−15698	4.161	−15698	0.000	0.000
0.300	−26244	−19779	5.079	−19779	0.000	0.000
0.400	−28785	−21661	5.596	−21661	0.000	0.000
0.500	−28918	−21581	5.763	−21581	0.000	0.000
0.600	−26899	−19775	5.596	−19775	0.000	0.000
0.700	−22944	−16478	5.079	−16478	0.000	0.000
0.800	−17222	−11926	4.161	−11926	0.000	0.000
0.900	−9795	−6355	2.703	−6355	0.000	0.000
1.000	0	0	0.000	0	0.000	0.000

Reference states: Ag(liquid), Ca(liquid)

Table IIIb. Partial quantities for Ag in the liquid phase at 1273 K.

x_{Ag}	ΔG_{Ag} [J/mol]	ΔH_{Ag} [J/mol]	ΔS_{Ag} [J/(mol·K)]	G^E_{Ag} [J/mol]	S^E_{Ag} [J/(mol·K)]	a_{Ag}	γ_{Ag}
1.000	0	0	0.000	0	0.000	1.000	1.000
0.900	−2489	−1374	0.876	−1374	0.000	0.790	0.878
0.800	−7544	−5182	1.855	−5182	0.000	0.490	0.613
0.700	−14727	−10952	2.966	−10952	0.000	0.249	0.355
0.600	−23620	−18213	4.247	−18213	0.000	0.107	0.179
0.500	−33830	−26493	5.763	−26493	0.000	0.041	0.082
0.400	−45020	−35321	7.619	−35321	0.000	0.014	0.036
0.300	−56968	−44225	10.010	−44225	0.000	0.005	0.015
0.200	−69769	−52734	13.382	−52734	0.000	0.001	0.007
0.100	−84747	−60375	19.145	−60375	0.000	0.000	0.003
0.000	−∞	−66678	∞	−66678	0.000	0.000	0.002

Reference state: Ag(liquid)

Table IIIc. Partial quantities for Ca in the liquid phase at 1273 K.

x_{Ca}	ΔG_{Ca} [J/mol]	ΔH_{Ca} [J/mol]	ΔS_{Ca} [J/(mol·K)]	G^E_{Ca} [J/mol]	S^E_{Ca} [J/(mol·K)]	a_{Ca}	γ_{Ca}
0.000	−∞	−105973	∞	−105973	0.000	0.000	0.000
0.100	−103844	−79473	19.145	−79473	0.000	0.000	0.001
0.200	−74798	−57763	13.382	−57763	0.000	0.001	0.004
0.300	−53118	−40374	10.010	−40374	0.000	0.007	0.022
0.400	−36532	−26833	7.619	−26833	0.000	0.032	0.079
0.500	−24006	−16670	5.763	−16670	0.000	0.104	0.207
0.600	−14818	−9411	4.247	−9411	0.000	0.247	0.411
0.700	−8362	−4586	2.966	−4586	0.000	0.454	0.648
0.800	−4086	−1724	1.855	−1724	0.000	0.680	0.850
0.900	−1468	−352	0.876	−352	0.000	0.871	0.967
1.000	0	0	0.000	0	0.000	1.000	1.000

Reference state: Ca(liquid)

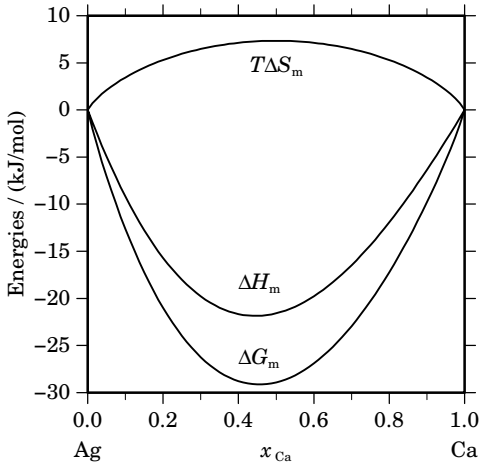

Fig. 2. Integral quantities of the liquid phase at T=1273 K.

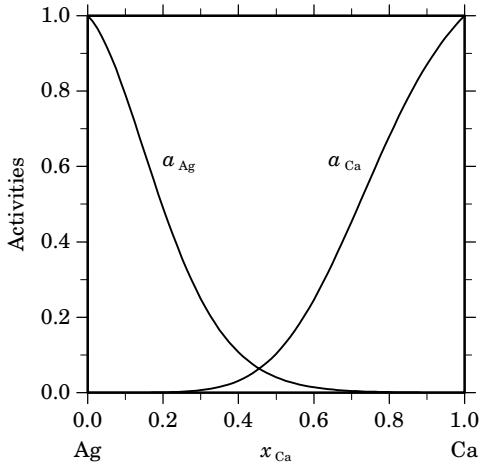

Fig. 3. Activities in the liquid phase at T=1273 K.

Table IV. Standard reaction quantities at 298.15 K for the compounds per mole of atoms.

Compound	x_{Ca}	$\Delta_{\mathrm{f}}G^{\circ}$ / (J/mol)	$\Delta_{\mathrm{f}}H^{\circ}$ / (J/mol)	$\Delta_{\mathrm{f}}S^{\circ}$ / (J/(mol·K))	$\Delta_{\mathrm{f}}C_P^{\circ}$ / (J/(mol·K))
Ag_9Ca_2	0.182	−16462	−16583	−0.407	0.175
Ag_7Ca_2	0.222	−19522	−19671	−0.498	0.214
Ag_2Ca_1	0.333	−22563	−22786	−0.748	0.321
Ag_1Ca_1	0.500	−25291	−25626	−1.122	0.481
Ag_3Ca_5	0.625	−21322	−21740	−1.403	0.601
Ag_1Ca_3	0.750	−15106	−15608	−1.684	0.722

References

[1911Baa] N. Baar: Z. Anorg. Allg. Chem. **70** (1911) 383–392.

[1958Han] M. Hansen, K. Anderko, "Constitution of Binary Alloys", McGraw-Hill, New-York, 1958.

[1964Cal] L.D. Calvert, R.P. Rand: Acta Cryst. **17** (1964) 1175–1176.

[1969Ale] W.A. Alexander, L.D.Calvert, A.Desaulniers, H.S.Dunsmore, D.F.Sargent: Can. J. Chem. **47** (1969) 611–614.

[1970Pas] B. Pascal, M. Caillet, M. Allibert: C.R. Acad. Sci. Paris, Ser. C **270** (1970) 520–522.

[1978Del] J. Delcet, J.J. Egan: J. Less-Common Met. **59** (1978) 229–236.

[1981Mof] W.G. Moffatt, "The Handbook of Binary Phase Diagrams", General Electric Corp. (1981).

[1981Not] M. Notin, J. Hertz: J. Less-Common Met. **80** (1981) 1–8.

[1985Fis] H. Fischbach: J. Less-Common Met. **108** (1985) 151–162.

[1988Bar] M.R. Baren: Bull. Alloy Phase Diagrams **9** (1988) 228–231.

[1996Che] P.-Y. Chevalier, E. Fischer, unpublished assessment, 1996.

Ag – Cd (Silver – Cadmium)

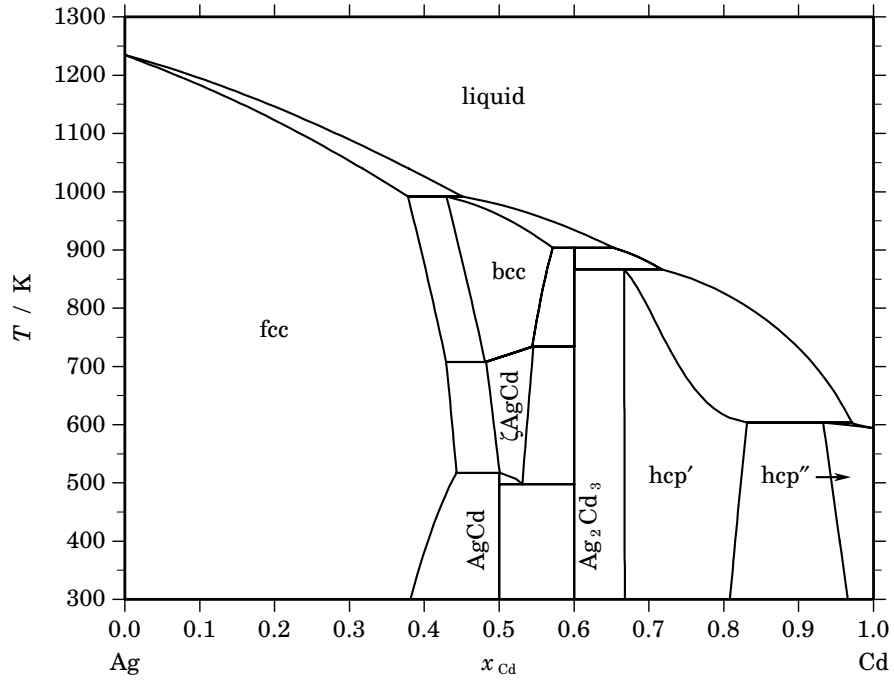

Fig. 1. Calculated phase diagram for the system Ag-Cd.

The Ag-Cd binary system contains two components interesting in the nuclear field, silver and cadmium being part of AIC control rods (Ag-In-Cd). The phase diagram has been reported in several compilations of binary systems [1958Han, 1965Ell, 1969Shu]. It is mainly based on the investigation of phase equilibria by [1905Ros, 1910Bru, 1911Pet, 1937Hum, 1939Owe] with additional results of [1896Gau, 1928Ast, 1928Nat, 1931Dur, 1935Dur, 1957Ray, 1959Pya, 1960Qua, 1962Mas]. The Ag-Cd system is a typical representative for the formation of intermetallic electron phases which are characterised by certain ratios of valence electrons to atoms. Among them are the β-, γ- and ϵ-brasses which are here denoted as the bcc, Ag_2Cd_3 and hcp$'$ phases, respectively. The latter hexagonal phase and the terminal Cd-rich solid solution (hcp$''$) have been modelled as a single hexagonal phase with a miscibility gap. A third hexagonal solid solution, ζAgCd, has been described as a separate phase. The intermetallic compounds AgCd and Ag_2Cd_3 have been approximated with stoichiometric descriptions. Ag_2Cd_3 has the γ-brass structure at higher temperature and a related superstructure at lower temperature but it has been described as a single phase only. The thermodynamic properties of liquid and solid alloys have been compiled from the literature in [1973Des] based on the measured activities of cadmium [1933Öla, 1942Sch, 1949Bir, 1956Her, 1956Sca, 1963Fil, 1969Con, 1970Mas, 1984Hou] and on calorimetric investigations [1956Kle, 1958And, 1958Orr, 1958Hul, 1969Wal]. This system has been assessed by Chevalier [2004Che]. A simple substitution model has been used for all solution phases (liquid, fcc, bcc, ζAgCd, and hcp) the excess interaction parameters being described by a Redlich-Kister polynomial of maximal second order. The heat capacity of the compounds was estimated from the pure solid components by using the Neumann-Kopp rule. The enthalpy and entropy of formation were optimised in consistency with other data. The agreement with the experimental information is quite satisfactory, as well for phase diagram [1905Ros, 1910Bru, 1911Pet, 1958Han, 1937Hum, 1939Owe] as thermodynamic data of solid and liquid phases (partial Gibbs energy and enthalpy of formation).

Table I. Phases, structures and models.

Phase	Struktur-bericht	Prototype	Pearson symbol	Space group	SGTE name	Model
liquid					LIQUID	$(Ag,Cd)_1$
fcc	$A1$	Cu	$cF4$	$Fm\bar{3}m$	FCC_A1	$(Ag,Cd)_1$
bcc	$A2$	W	$cI2$	$Im\bar{3}m$	BCC_A2	$(Ag,Cd)_1$
ζAgCd	$A3$	Mg	$hP2$	$P6_3/mmc$	AGCD_ZETA	$(Ag,Cd)_1$
AgCd	$B2$	CsCl	$cP2$	$Pm3m$	AGCD_B2	Ag_1Cd_1
Ag_2Cd_3	$D8_2$	Cu_5Zn_8	$cI52$	$I\bar{4}3m$	AG2CD3	Ag_2Cd_3
hcp	$A3$	Mg	$hP2$	$P6_3/mmc$	HCP_A3	$(Ag,Cd)_1$

Table II. Invariant reactions.

Reaction	Type	T / K	Compositions / x_{Cd}			$\Delta_{\mathrm{r}}H$ / (J/mol)
fcc + liquid $\rightleftharpoons$ bcc	peritectic	991.8	0.378	0.450	0.430	−4390
bcc + liquid $\rightleftharpoons$ Ag_2Cd_3	peritectic	903.4	0.572	0.653	0.600	−2763
Ag_2Cd_3 + liquid $\rightleftharpoons$ hcp′	peritectic	866.6	0.600	0.717	0.667	−4172
bcc + Ag_2Cd_3 $\rightleftharpoons$ ζAgCd	peritectoid	734.4	0.544	0.600	0.546	−193
bcc $\rightleftharpoons$ fcc + ζAgCd	eutectoid	707.6	0.481	0.429	0.483	−206
hcp′ + liquid $\rightleftharpoons$ hcp″	peritectic	603.3	0.831	0.971	0.933	−4437
fcc + ζAgCd $\rightleftharpoons$ AgCd	peritectoid	516.9	0.443	0.501	0.500	−1030
ζAgCd $\rightleftharpoons$ AgCd + Ag_2Cd_3	eutectoid	497.8	0.531	0.500	0.600	−738

Table IIIa. Integral quantities for the liquid phase at 1273 K.

x_{Cd}	ΔG_{m} [J/mol]	ΔH_{m} [J/mol]	ΔS_{m} [J/(mol·K)]	$G_{\mathrm{m}}^{\mathrm{E}}$ [J/mol]	$S_{\mathrm{m}}^{\mathrm{E}}$ [J/(mol·K)]	ΔC_P [J/(mol·K)]
0.000	0	0	0.000	0	0.000	0.000
0.100	−5117	−3523	1.252	−1676	−1.451	0.000
0.200	−8006	−5993	1.582	−2710	−2.579	0.000
0.300	−9667	−7510	1.694	−3201	−3.385	0.000
0.400	−10376	−8177	1.727	−3252	−3.868	0.000
0.500	−10301	−8095	1.734	−2965	−4.030	0.000
0.600	−9564	−7365	1.727	−2440	−3.868	0.000
0.700	−8246	−6089	1.694	−1780	−3.385	0.000
0.800	−6382	−4369	1.582	−1085	−2.579	0.000
0.900	−3899	−2305	1.252	−458	−1.451	0.000
1.000	0	0	0.000	0	0.000	0.000

Reference states: Ag(liquid), Cd(liquid)

Table IIIb. Partial quantities for Ag in the liquid phase at 1273 K.

x_{Ag}	ΔG_{Ag} [J/mol]	ΔH_{Ag} [J/mol]	ΔS_{Ag} [J/(mol·K)]	G^E_{Ag} [J/mol]	S^E_{Ag} [J/(mol·K)]	a_{Ag}	γ_{Ag}
1.000	0	0	0.000	0	0.000	1.000	1.000
0.900	−1454	−544	0.715	−339	−0.161	0.872	0.969
0.800	−3581	−2040	1.211	−1219	−0.645	0.713	0.891
0.700	−6213	−4284	1.515	−2438	−1.451	0.556	0.794
0.600	−9199	−7075	1.668	−3792	−2.579	0.419	0.699
0.500	−12416	−10210	1.734	−5080	−4.030	0.309	0.619
0.400	−15795	−13484	1.816	−6097	−5.803	0.225	0.562
0.300	−19384	−16695	2.112	−6640	−7.898	0.160	0.534
0.200	−23542	−19640	3.066	−6507	−10.316	0.108	0.541
0.100	−29867	−22116	6.089	−5495	−13.056	0.060	0.595
0.000	−∞	−23920	∞	−3401	−16.119	0.000	0.725

Reference state: Ag(liquid)

Table IIIc. Partial quantities for Cd in the liquid phase at 1273 K.

x_{Cd}	ΔG_{Cd} [J/mol]	ΔH_{Cd} [J/mol]	ΔS_{Cd} [J/(mol·K)]	G^E_{Cd} [J/mol]	S^E_{Cd} [J/(mol·K)]	a_{Cd}	γ_{Cd}
0.000	−∞	−40838	∞	−20319	−16.119	0.000	0.147
0.100	−38089	−30338	6.089	−13718	−13.056	0.027	0.274
0.200	−25708	−21805	3.066	−8673	−10.316	0.088	0.441
0.300	−17726	−15037	2.112	−4982	−7.898	0.187	0.625
0.400	−12141	−9829	1.816	−2442	−5.803	0.318	0.794
0.500	−8187	−5980	1.734	−850	−4.030	0.461	0.923
0.600	−5409	−3286	1.668	−3	−2.579	0.600	1.000
0.700	−3472	−1544	1.515	303	−1.451	0.720	1.029
0.800	−2092	−551	1.211	270	−0.645	0.821	1.026
0.900	−1014	−104	0.715	101	−0.161	0.909	1.010
1.000	0	0	0.000	0	0.000	1.000	1.000

Reference state: Cd(liquid)

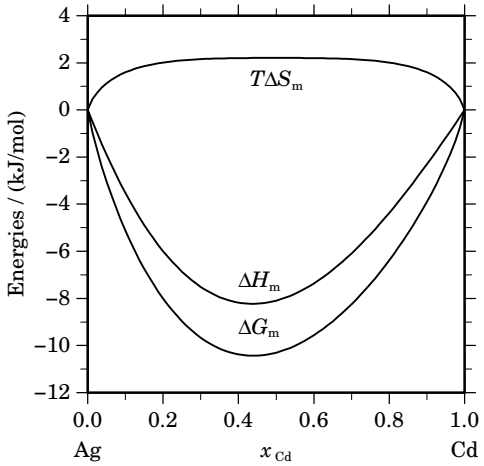

Fig. 2. Integral quantities of the liquid phase at T=1273 K.

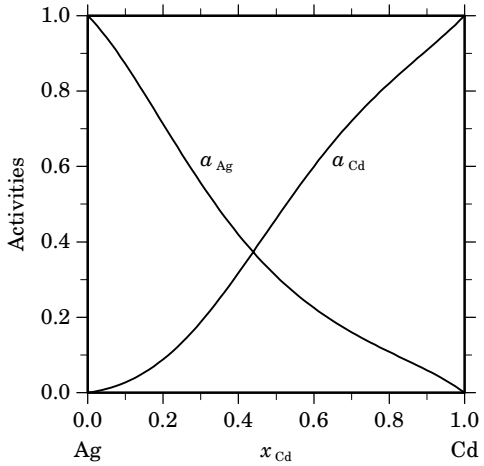

Fig. 3. Activities in the liquid phase at T=1273 K.

Table IVa. Integral quantities for the stable phases at 573 K.

Phase	x_{Cd}	ΔG_{m} [J/mol]	ΔH_{m} [J/mol]	ΔS_{m} [J/(mol·K)]	$G_{\mathrm{m}}^{\mathrm{E}}$ [J/mol]	$S_{\mathrm{m}}^{\mathrm{E}}$ [J/(mol·K)]	ΔC_P [J/(mol·K)]
fcc	0.000	0	0	0.000	0	0.000	0.000
	0.100	−4031	−2890	1.992	−2483	−0.710	0.038
	0.200	−6550	−4878	2.918	−4166	−1.243	0.076
	0.300	−8050	−6055	3.482	−5139	−1.597	0.114
	0.400	−8700	−6510	3.823	−5494	−1.773	0.152
	0.439	−8750	−6511	3.908	−5483	−1.794	0.167
ζAgCd	0.496	−8744	−6291	4.282	−5442	−1.481	0.000
	0.500	−8743	−6292	4.278	−5441	−1.486	0.000
	0.536	−8676	−6252	4.230	−5385	−1.513	0.000
Ag_2Cd_3	0.600	−8461	−6277	3.811			0.000
hcp′	0.667	−7885	−5944	3.387	−4854	−1.902	0.000
	0.700	−7499	−5686	3.164	−4589	−1.915	0.000
	0.800	−5396	−4004	2.429	−3012	−1.732	0.000
	0.829	−4665	−3403	2.203	−2483	−1.607	0.000
hcp″	0.936	−1878	−1197	1.188	−746	−0.787	0.000
	1.000	0	0	0.000	0	0.000	0.000

Reference states: Ag(fcc), Cd(hcp)

Table IVb. Partial quantities for Ag in the stable phases at 573 K.

Phase	x_{Ag}	ΔG_{Ag} [J/mol]	ΔH_{Ag} [J/mol]	ΔS_{Ag} [J/(mol·K)]	$G_{\mathrm{Ag}}^{\mathrm{E}}$ [J/mol]	$S_{\mathrm{Ag}}^{\mathrm{E}}$ [J/(mol·K)]	a_{Ag}	γ_{Ag}
fcc	1.000	0	0	0.000	0	0.000	1.000	1.000
	0.900	−917	−466	0.787	−415	−0.089	0.825	0.917
	0.800	−2602	−1743	1.499	−1539	−0.356	0.579	0.724
	0.700	−4892	−3652	2.164	−3193	−0.802	0.358	0.512
	0.600	−7631	−6013	2.822	−5197	−1.425	0.202	0.336
	0.561	−8792	−7021	3.090	−6037	−1.717	0.158	0.282
ζAgCd	0.504	−8792	−6062	4.764	−5532	−0.925	0.158	0.313
	0.500	−8974	−6222	4.803	−5672	−0.961	0.152	0.304
	0.464	−10460	−7526	5.120	−6807	−1.256	0.111	0.240
Ag_2Cd_3	0.400	−10460	−6044	7.707			0.111	
	0.400	−13595	−9247	7.588			0.058	
hcp′	0.333	−13595	−9103	7.840	−8351	−1.311	0.058	0.173
	0.300	−17868	−13264	8.035	−12132	−1.975	0.024	0.078
	0.200	−25480	−20527	8.645	−17813	−4.737	0.005	0.024
	0.171	−26143	−21035	8.914	−17741	−5.749	0.004	0.024
hcp″	0.064	−26143	−19093	12.303	−13038	−10.568	0.004	0.065
	0.000	$-\infty$	−18991	∞	−10818	−14.262	0.000	0.103

Reference state: Ag(fcc)

Table IVc. Partial quantities for Cd in the stable phases at 573 K.

Phase	x_{Cd}	ΔG_{Cd} [J/mol]	ΔH_{Cd} [J/mol]	ΔS_{Cd} [J/(mol·K)]	G^E_{Cd} [J/mol]	S^E_{Cd} [J/(mol·K)]	a_{Cd}	γ_{Cd}
fcc	0.000	$-\infty$	−33703	∞	−29121	−7.995	0.000	0.002
	0.100	−32064	−24705	12.842	−21094	−6.303	0.001	0.012
	0.200	−22341	−17418	8.593	−14674	−4.789	0.009	0.046
	0.300	−15418	−11661	6.557	−9682	−3.453	0.039	0.131
	0.400	−10304	−7254	5.323	−5939	−2.295	0.115	0.288
	0.439	−8696	−5859	4.952	−4775	−1.891	0.161	0.367
ζAgCd	0.496	−8696	−6524	3.791	−5351	−2.047	0.161	0.325
	0.500	−8512	−6362	3.753	−5210	−2.011	0.168	0.335
	0.536	−7128	−5147	3.458	−4153	−1.735	0.224	0.418
Ag_2Cd_3	0.600	−7128	−6433	1.213			0.224	
	0.600	−5038	−4297	1.292			0.347	
hcp′	0.667	−5038	−4369	1.167	−3111	−2.196	0.347	0.520
	0.700	−3055	−2438	1.076	−1356	−1.889	0.527	0.752
	0.800	−375	126	0.875	688	−0.980	0.924	1.155
	0.829	−222	244	0.814	674	−0.750	0.954	1.152
hcp″	0.936	−222	24	0.429	93	−0.120	0.954	1.020
	1.000	0	0	0.000	0	0.000	1.000	1.000

Reference state: Cd(hcp)

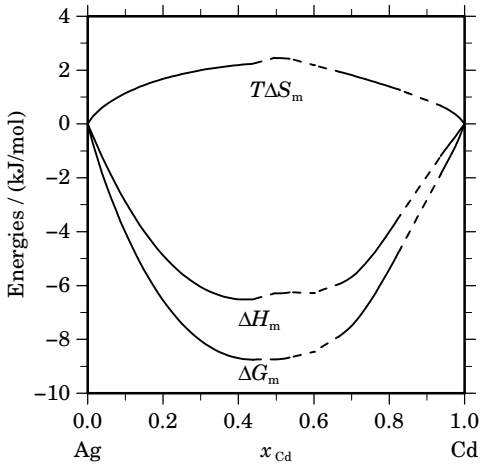

Fig. 4. Integral quantities of the stable phases at T=573 K.

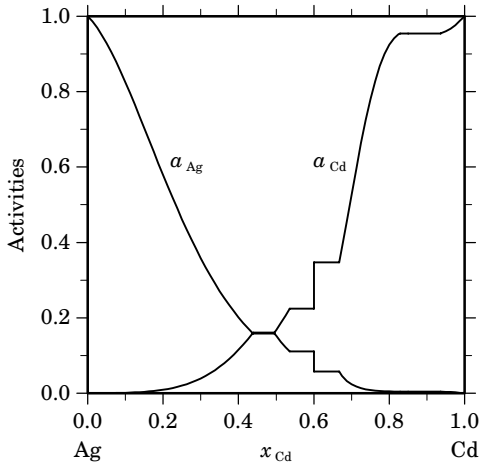

Fig. 5. Activities in the stable phases at T=573 K.

Table V. Standard reaction quantities at 298.15 K for the compounds per mole of atoms.

Compound	x_{Cd}	$\Delta_f G^\circ$ / (J/mol)	$\Delta_f H^\circ$ / (J/mol)	$\Delta_f S^\circ$ / (J/(mol·K))	$\Delta_f C^\circ_P$ / (J/(mol·K))
Ag_1Cd_1	0.500	−8005	−7325	2.279	0.000
Ag_2Cd_3	0.600	−7413	−6277	3.811	0.000

References

[1896Gau] H. Gautier: Bull. Soc. Encour. Ind. Natl. **1** (1896) 1315.
[1905Ros] T.K. Rose: Proc. Roy. Soc. (London), **74** (1905) 218–230.
[1910Bru] G. Bruni, E. Quercigh: Z. Anorg. Chem. **68** (1910) 198–206.
[1911Pet] G.J. Petrenko, A.S. Fedorow: Z. Anorg. Chem. **70** (1911) 157–168.
[1928Ast] V.H. Astrand, A. Westgren: Z. Anorg. Chem. **175** (1928) 90–96.
[1928Nat] G. Natta, M. Freri: Atti Reale Acad. Lincei Rend. **7** (1928) 406–410.
[1931Dur] P.J. Durrant: J. Inst. Met. **45** (1931) 99–118.
[1933Öla] A. Ölander: Z. Phys. Chem. A **163A** (1933) 107–121.
[1935Dur] P.J. Durrant: J. Inst. Met. **56** (1935) 155–164.
[1937Hum] W. Hume-Rothery, P.W. Reynolds: Proc. Roy. Soc. (London) A **160A** (1937) 282–303.
[1939Owe] E.A. Owen, J. Rogers, J.C. Guthrie: J. Inst. Met. **65** (1939) 457–472.
[1942Sch] A. Schneider, H. Schmid: Z. Elektrochem. **48** (1942) 627–639.
[1949Bir] C.E. Birchenall, C.H. Cheng: J. Met. **185** (1949) 428–434.
[1956Her] P. Herasymenko: Acta Metall. **4** (1956) 1–6.
[1956Kle] O.J. Kleppa: J. Phys. Chem. **60** (1956) 848–852.
[1956Sca] G. Scatchard, R.H. Boyd: J. Am. Chem. Soc. **78** (1956) 3889–3893.
[1957Ray] H.W. Rayson, W.A. Alexander: Can. J. Chem. **35** (1957) 1571–1575.
[1958Han] M. Hansen, K. Anderko: "Constitution of Binary Alloys", McGraw-Hill, New-York, 1958.
[1958And] P.D. Anderson: J. Am. Chem. Soc. **80** (1958) 3171–3175.
[1958Orr] R.L. Orr, A. Goldberg, R. Hultgren: J. Phys. Chem. **62** (1958) 325–327.
[1958Hul] R. Hultgren, K.N. Rao: Trans. Ind. Inst. Met. **11** (1958) 55–58.
[1959Pya] V.N. Pyatnitskii, A.T. Grigor'ev, E.M. Sokolovskaya, E.V. Lysova: Russ. J. Inorg. Chem. **4** (1959) 925–926.
[1960Qua] A. Quader: Ind. J. Phys. Proc. Ind. Ass. Cult. Sci. (1960) 506–515.
[1962Mas] T.B. Massalski, H.W. King: Acta Metall. **10** (1962) 1171–1181.
[1963Fil] J.D. Filby, J.N. Pratt: Acta Metall. **11** (1963) 427–434.
[1965Ell] R.P. Elliott: "Constitution of Binary Alloys", 1st Suppl., McGraw-Hill, New-York, 1965.
[1969Con] D.R. Conant, H.S. Swofford: J. Chem. Eng. Data **14** (1969) 369–372.
[1969Shu] F.A. Shunk, "Constitution of Binary Alloys", 2nd Suppl., McGraw-Hill, 1969.
[1969Wal] J. Waldman, A.K. Jena, M. Bever: Trans. Metall. Soc. AIME **245** (1969) 1039–1043.
[1970Mas] D.B. Masson, J.L. Sheu: Metall. Trans. **1** (1970) 3005–3009.
[1973Des] P.D. Desai in: "Selected Values of the Thermodynamic Properties of Binary Alloys", R. Hultgren, P.D. Desai, D.T. Hawkins, M. Gleiser, K.K. Kelley (Eds.), ASM, Metals Park, Oh, 1973, pp.36–43.
[1984Hou] B.L. Houseman, D.R. Conant: High Temp. Sci. **17** (1984) 251–265.
[2004Che] P.-Y. Chevalier, unpublished work, 2004.

Ag – Ce (Silver – Cerium)

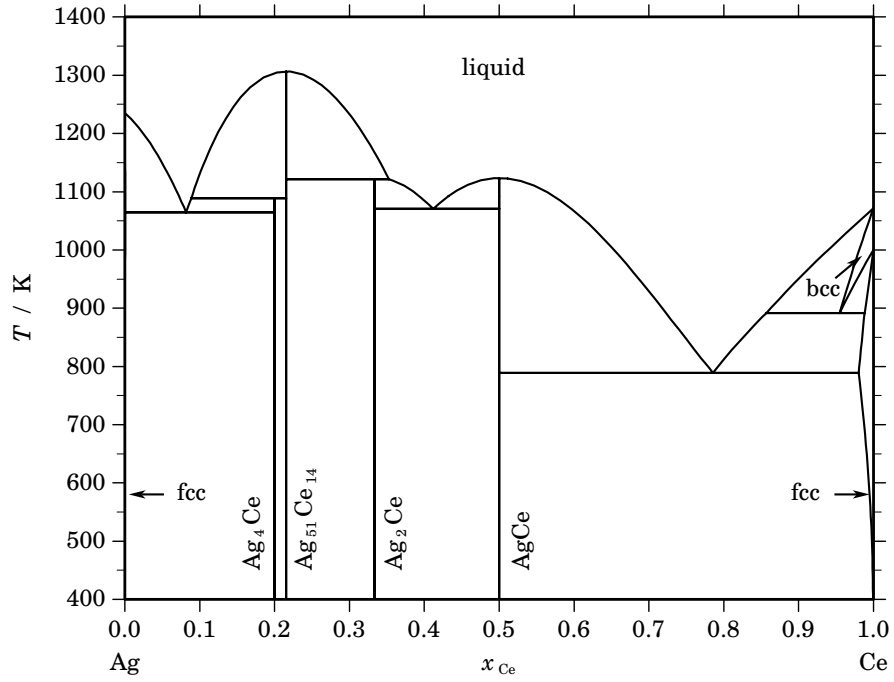

Fig. 1. Calculated phase diagram for the system Ag-Ce.

Ag-rare earth binary alloys are potential electronic materials and amorphous materials. They attract the interest of theoretical research and industrial purposes.

The phase diagram of the the Ag-Ce system has been studied in several investigations [1943Rol, 1970McM, 1975Del, 1980Heu, 1983Sta, 1984Sta] with some disagreement on the number of the intermetallic phases, their stoichiometry and the data of the invariant reactions. A review on the the literature of the Ag-Ce system has been given in [1985Gsc] and the existence of four stable intermetallic compounds has been accepted: Ag_4Ce, $Ag_{51}Ce_{14}$, Ag_2Ce and AgCe. [1980Heu] reported the maximum solubility of Ce in Ag and the solubility of Ag in Ce has been reported by [1975Del, 1983Sta]. [1987Iva] measured the thermodynamic activity of liquid phase at 1090°C by means of the Knudsen effusion method and found a large deviation from ideal behaviour. [1992Iva] determined the heats of mixing of liquid alloys of the Ag-Ce system by means of isoperibolic calorimetry. [1993Fit] measured the standard enthalpies of formation of AgCe, $Ag_{51}Ce_{14}$ and the enthalpies of mixing of the liquid, which agreed well with that of [1992Iva]. The measured standard enthalpy of formation of AgCe is abnormally less negative compared to that of equi-atomic compounds in other Ag-rare earth systems.

The thermodynamic assessment of the Ag-Ce system is from [2002Yin]. The terminal solid solutions fcc, bcc, hcp and the liquid phase were described by a substitutional solution model using the Redlich-Kister equation. The intermetallic compounds AgCe, Ag_2Ce, $Ag_{51}Ce_{14}$, and Ag_4Ce are treated as stoichiometric phases. Due to a lack of data the high and low temperature modifications of Ag_2Ce and AgCe have not been distinguished.

The calculated phase diagram is in excellent agreement with that reported by [1975Del, 1983Sta, 1984Sta]. The assessed enthalpy of formation of $Ag_{51}Ce_{14}$ agree very well with experimental results, the assessed value for AgCe is more negative. The agreement of optimised results with the experimental activities at 1090°C and with the experimental enthalpies of mixing is good.

Table I. Phases, structures and models.

Phase	Struktur-bericht	Prototype	Pearson symbol	Space group	SGTE name	Model
liquid					LIQUID	$(Ag,Ce)_1$
fcc	$A1$	Cu	$cF4$	$Fm\bar{3}m$	FCC_A1	$(Ag,Ce)_1$
Ag_4Ce	⋯	⋯	⋯	⋯	AG4CE	Ag_4Ce_1
$Ag_{51}Ce_{14}$	⋯	$Ag_{51}Gd_{14}$	$hP65$	$P6/m$	AG51CE14	$Ag_{51}Ce_{14}$
αAg_2Ce	⋯	Cu_2Ce	$oI12$	$Imma$	AG2CE	Ag_2Ce_1
βAg_2Ce	⋯	⋯	⋯	⋯	AG2CE	Ag_2Ce_1
γAg_2Ce	⋯	⋯	⋯	⋯	AG2CE	Ag_2Ce_1
αAgCe	$B2$	CsCl	$cP2$	$Pm\bar{3}m$	AGCE	Ag_1Ce_1
βAgCe	⋯	⋯	⋯	⋯	AGCE	Ag_1Ce_1
bcc	$A2$	W	$cI2$	$Im\bar{3}m$	BCC_A2	$(Ag,Ce)_1$

Table II. Invariant reactions.

Reaction	Type	T / K	Compositions / x_{Ce}			$\Delta_r H$ / (J/mol)
liquid ⇌ $Ag_{51}Ce_{14}$	congruent	1306.7	0.215	0.215		−14455
liquid ⇌ AgCe	congruent	1123.3	0.500	0.500		−14644
$Ag_{51}Ce_{14}$ + liquid ⇌ Ag_2Ce	peritectic	1121.3	0.215	0.353	0.333	−10513
liquid + $Ag_{51}Ce_{14}$ ⇌ Ag_4Ce	peritectic	1089.0	0.089	0.215	0.200	−1524
liquid ⇌ Ag_2Ce + AgCe	eutectic	1070.4	0.412	0.333	0.500	−12794
liquid ⇌ fcc + Ag_4Ce	eutectic	1064.5	0.082	0.000	0.200	−10720
bcc ⇌ liquid + fcc	metatectic	891.8	0.955	0.857	0.988	−795
liquid ⇌ AgCe + fcc	eutectic	789.0	0.786	0.500	0.980	−9716

Table IIIa. Integral quantities for the liquid phase at 1323 K.

x_{Ce}	ΔG_m [J/mol]	ΔH_m [J/mol]	ΔS_m [J/(mol·K)]	G_m^E [J/mol]	S_m^E [J/(mol·K)]	ΔC_P [J/(mol·K)]
0.000	0	0	0.000	0	0.000	0.000
0.100	−10380	−8832	1.170	−6804	−1.532	0.000
0.200	−17064	−14566	1.888	−11560	−2.272	0.000
0.300	−21187	−17628	2.690	−14467	−2.389	0.000
0.400	−23131	−18444	3.543	−15728	−2.053	0.000
0.500	−23169	−17439	4.331	−15544	−1.432	0.000
0.600	−21520	−15039	4.899	−14117	−0.697	0.000
0.700	−18367	−11670	5.062	−11647	−0.017	0.000
0.800	−13842	−7756	4.600	−8337	0.439	0.000
0.900	−7963	−3724	3.204	−4388	0.501	0.000
1.000	0	0	0.000	0	0.000	0.000

Reference states: Ag(liquid), Ce(liquid)

Table IIIb. Partial quantities for Ag in the liquid phase at 1323 K.

x_{Ag}	ΔG_{Ag} [J/mol]	ΔH_{Ag} [J/mol]	ΔS_{Ag} [J/(mol·K)]	G^E_{Ag} [J/mol]	S^E_{Ag} [J/(mol·K)]	a_{Ag}	γ_{Ag}
1.000	0	0	0.000	0	0.000	1.000	1.000
0.900	−2217	−1620	0.452	−1058	−0.424	0.817	0.908
0.800	−6419	−5912	0.383	−3964	−1.472	0.558	0.697
0.700	−12239	−12024	0.162	−8315	−2.804	0.329	0.470
0.600	−19327	−19106	0.167	−13708	−4.080	0.173	0.288
0.500	−27365	−26307	0.800	−19741	−4.963	0.083	0.166
0.400	−36089	−32774	2.506	−26009	−5.113	0.038	0.094
0.300	−45356	−37657	5.819	−32112	−4.191	0.016	0.054
0.200	−55349	−40104	11.523	−37645	−1.859	0.007	0.033
0.100	−67535	−39265	21.368	−42207	2.223	0.002	0.022
0.000	−∞	−34288	∞	−45393	8.394	0.000	0.016

Reference state: Ag(liquid)

Table IIIc. Partial quantities for Ce in the liquid phase at 1323 K.

x_{Ce}	ΔG_{Ce} [J/mol]	ΔH_{Ce} [J/mol]	ΔS_{Ce} [J/(mol·K)]	G^E_{Ce} [J/mol]	S^E_{Ce} [J/(mol·K)]	a_{Ce}	γ_{Ce}
0.000	−∞	−105226	∞	−78962	−19.852	0.000	0.001
0.100	−83850	−73741	7.641	−58521	−11.504	0.000	0.005
0.200	−59646	−49185	7.907	−41942	−5.474	0.004	0.022
0.300	−42066	−30705	8.587	−28822	−1.423	0.022	0.073
0.400	−28838	−17451	8.607	−18759	0.988	0.073	0.182
0.500	−18973	−8572	7.862	−11348	2.099	0.178	0.356
0.600	−11808	−3216	6.494	−6189	2.247	0.342	0.570
0.700	−6800	−532	4.738	−2877	1.772	0.539	0.770
0.800	−3465	331	2.869	−1010	1.014	0.730	0.912
0.900	−1344	225	1.186	−185	0.310	0.885	0.983
1.000	0	0	0.000	0	0.000	1.000	1.000

Reference state: Ce(liquid)

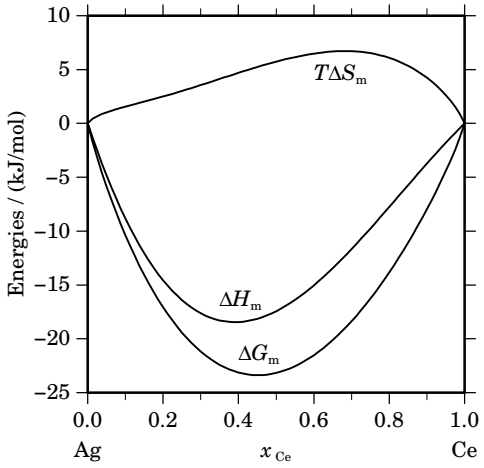

Fig. 2. Integral quantities of the liquid phase at T=1323 K.

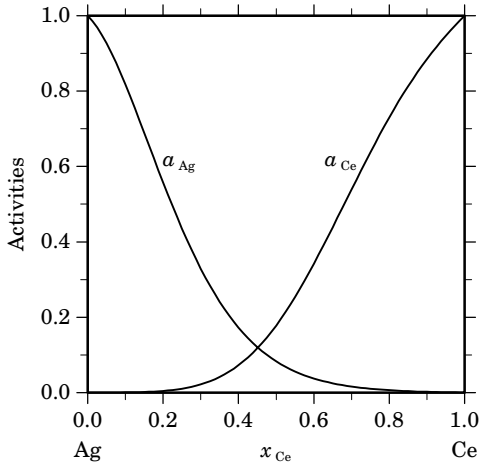

Fig. 3. Activities in the liquid phase at T=1323 K.

Table IV. Standard reaction quantities at 298.15 K for the compounds per mole of atoms.

Compound	x_{Ce}	$\Delta_{\mathrm{f}}G^{\circ}$ / (J/mol)	$\Delta_{\mathrm{f}}H^{\circ}$ / (J/mol)	$\Delta_{\mathrm{f}}S^{\circ}$ / (J/(mol·K))	$\Delta_{\mathrm{f}}C_P^{\circ}$ / (J/(mol·K))
Ag_4Ce_1	0.200	−17765	−17863	−0.329	0.000
$Ag_{51}Ce_{14}$	0.215	−18949	−18998	−0.166	0.000
Ag_2Ce_1	0.333	−20412	−20194	0.734	0.000
Ag_1Ce_1	0.500	−22272	−22331	−0.197	0.000

References

[1943Rol] L. Rolla, A. Jandelli, G. Canneri, R. Vogel: Z. Metallkd. **35** (1943) 29–42.

[1970McM] O.D. McMaster, K.A. Gschneidner Jr., R.F. Venteicher: Acta Cryst. B **26B** (1970) 1224–1229.

[1975Del] S. Delfino, R. Ferro, R. Cappeli, A. Borsese: J. Less-Common Met. **41** (1975) 59–64.

[1980Heu] T. Heumann, A. Preval: J. Less-Common Met. **76** (1980) 263–270.

[1983Sta] I. Stapf, H. Jehn: J. Less-Common Met. **92** (1983) 167–175.

[1984Sta] I. Stapf, H. Jehn: J. Less-Common Met. **98** (1983) 173–183.

[1985Gsc] K.A. Gschneidner Jr., F.W. Calderwood: Bull. Alloy Phase Diagrams **6** (1985) 439–443.

[1987Iva] M.I. Ivanov, G.M. Lukashenko: J. Less-Common Met. **133** (1987) 181–192.

[1992Iva] M.I. Ivanov, V.T. Witusiewicz: J. Alloys Comp. **186** (1992) 255–266.

[1993Fit] K. Fitzner, O.J. Kleppa: Metall. Mater. Trans. A **24A** (1993) 1827–1834.

[2002Yin] F. Yin, M. Huang, X. Su, P. Zhang, Z. Li, Y. Shi: J. Alloys Comp. **334** (2002) 154–158.

Ag – Cr (Silver – Chromium)

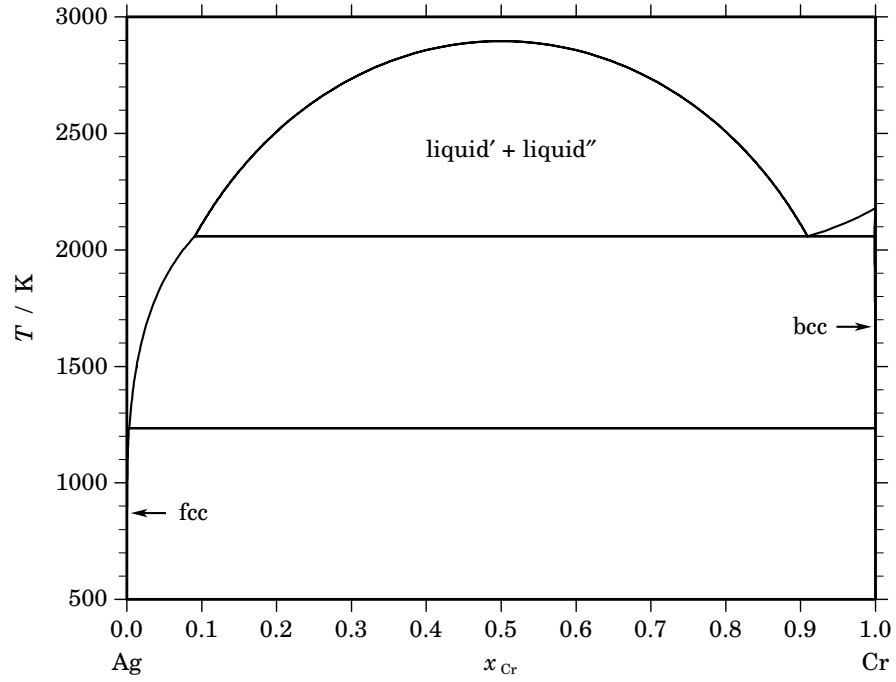

Fig. 1. Calculated phase diagram for the system Ag-Cr.

The Ag-Cr system shows a wide range of immiscibility in the liquid phase. A monotectic reaction according to Allen [1967All] occurs at about 1723 K, where the Ag-rich liquid contains about 3 at.% Cr [1990Ven]. The assessed equilibrium Ag-Cr phase diagram is based on the studies of Hindrichs [1908Hin], Grigorev *et al.* [1954Gri], and Allen [1967All]. The boundaries of the liquid miscibility gap above the monotectic temperature have not been established. The absence of intermediate phases was confirmed by the thin-film studies of Simic and Marinkovic [1978Sim]. The solubility of Cr in liquid Ag was measured by Allen [1967All]. Neumann *et al.* [1981Neu] determined the solubility of Cr in solid Ag in the temperature range 973 K to 1233 K. Formation of a metastable solid solution of Cr in Ag beyond the equilibrium concentration was observed by Ning [1983Nin], who quenched liquid Ag-rich alloys at cooling rates of 105 to 106 K/s. The observed metastable solid solubility limit corresponds to the solubility of Cr in liquid Ag at the monotectic temperature. The thermodynamic assessment of the Ag-Cr system was carried out by Korb [2004Kor]. The melting point of pure Cr at 2136 K reported in [1990Ven] does not correspond with the value of 2180 K given by SGTE [1991Din]. The calculated monotectic temperature using the SGTE data is about 2058 K. The experimental data are well represented by the calculated phase equilibria.

Table I. Phases, structures and models.

Phase	Struktur-bericht	Prototype	Pearson symbol	Space group	SGTE name	Model
liquid					LIQUID	$(Ag,Cr)_1$
fcc	$A1$	Cu	$cF4$	$Fm\overline{3}m$	FCC_A1	$(Ag,Cr)_1$
bcc	$A2$	W	$cI2$	$Im\overline{3}m$	BCC_A2	$(Ag,Cr)_1$

Table II. Invariant reactions.

Reaction	Type	T / K	Compositions / x_{Cr}			$\Delta_{\mathrm{r}}H$ / (J/mol)
liquid $\rightleftharpoons$ liquid′ + liquid″	critical	2896.9	0.500	0.500	0.500	0
liquid″ $\rightleftharpoons$ liquid′ + bcc	monotectic	2058.4	0.091	0.909	0.998	−23354
liquid′ $\rightleftharpoons$ fcc + bcc	eutectic	1234.0	0.003	0.003	1.000	−11353

References

[1908Hin] G. Hindrichs: Z. Anorg. Chem. **59** (1908) 414–449.

[1954Gri] A.T. Grigorev, E.M. Sokolovskaya, M.I. Kruglova: Vestn. Mosk. Univ., Fiz.-Mat. Estest. Nauk **9** (1954) 77–81.

[1967All] B.C. Allen: Trans. Metall. Soc. AIME **239** (1967) 1026–1029.

[1978Sim] V. Simic, Z. Marinkovic: Nauchno Tekh. Pregl. **28** (1978) 3–12.

[1981Neu] G. Neumann, M. Pfundstein, P. Reimers: Phys. Stat. Solidi A **64A** (1981) 225–232.

[1983Nin] Y. Ning: Chin Shu Hsueh Pao **19** (1983) A316-A353.

[1991Din] A.T. Dinsdale: Calphad **15** (1991) 317–425.

[1990Ven] M. Venkatraman, J.P. Neumann: Bull. Alloy Phase Diagrams **11** (1990) 263–265.

[2004Kor] J. Korb, unpublished assessment, GTT-Technologies, 2004.

Ag – Cu (Silver – Copper)

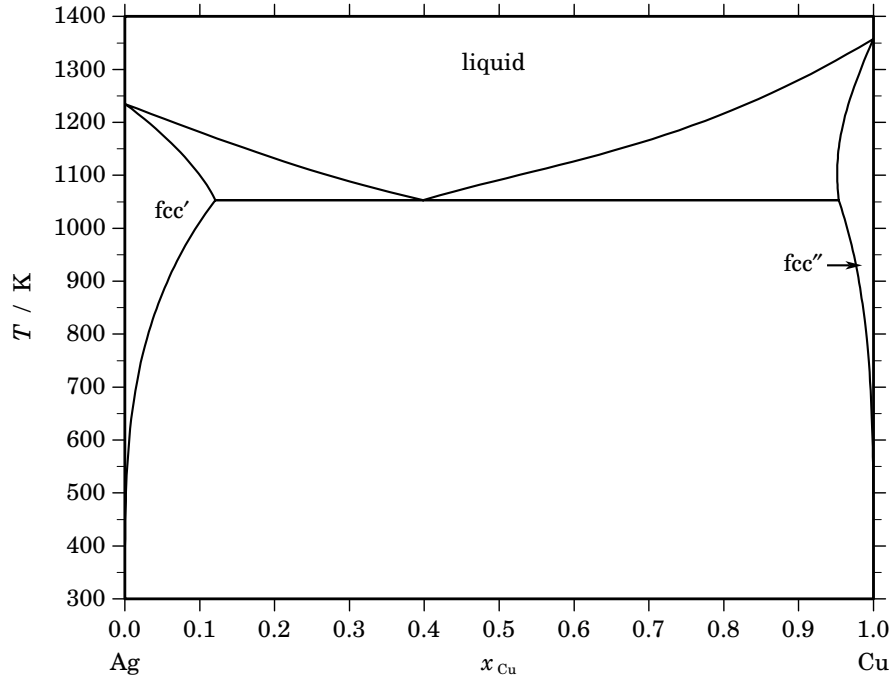

Fig. 1. Calculated phase diagram for the system Ag-Cu.

The combination of silver and copper is encountered in gold alloys for dental applications, jewelry and coinage. Copper-Silver alloys with high contents of phosphorus are used for brazing. The thermodynamics of the binary Ag-Cu system has been re-assessed recently in [2004Wit] in the course of the optimisation of the ternary Ag-Al-Cu system. The phase diagram of the Ag-Cu binary is a simple eutectic with appreciable solid solubilities of the metallic elements. The evaluation takes into account literature data for the phase boundaries in the phase diagram from many experimental investigations. For the description of the liquid phase, several experimental studies of the mixing enthalpy have been taken into account. The evaluated dataset of [2004Wit] is preferred over that of [2002Kus] because more recent calorimetric data for the mixing properties of the liquid [1999Fit] have been included.

Table I. Phases, structures and models.

Phase	Struktur-bericht	Prototype	Pearson symbol	Space group	SGTE name	Model
liquid					LIQUID	$(Ag,Cu)_1$
fcc	$A1$	Cu	$cF4$	$Fm\overline{3}m$	FCC_A1	$(Ag,Cu)_1$

Table II. Invariant reactions.

Reaction	Type	T / K	Compositions / x_{Cu}			$\Delta_r H$ / (J/mol)
liquid $\rightleftharpoons$ fcc′ + fcc″	eutectic	1053.4	0.398	0.121	0.953	−12438

Table IIIa. Integral quantities for the liquid phase at 1373 K.

x_{Cu}	ΔG_{m} [J/mol]	ΔH_{m} [J/mol]	ΔS_{m} [J/(mol·K)]	$G_{\mathrm{m}}^{\mathrm{E}}$ [J/mol]	$S_{\mathrm{m}}^{\mathrm{E}}$ [J/(mol·K)]	ΔC_P [J/(mol·K)]
0.000	0	0	0.000	0	0.000	0.000
0.100	−2632	1234	2.816	1079	0.113	0.000
0.200	−3779	2224	4.373	1933	0.212	0.000
0.300	−4415	2959	5.371	2558	0.292	0.000
0.400	−4735	3426	5.944	2948	0.349	0.000
0.500	−4817	3616	6.142	3095	0.379	0.000
0.600	−4688	3516	5.975	2995	0.379	0.000
0.700	−4332	3116	5.424	2642	0.345	0.000
0.800	−3684	2404	4.434	2029	0.273	0.000
0.900	−2561	1369	2.862	1150	0.159	0.000
1.000	0	0	0.000	0	0.000	0.000

Reference states: Ag(liquid), Cu(liquid)

Table IIIb. Partial quantities for Ag in the liquid phase at 1373 K.

x_{Ag}	ΔG_{Ag} [J/mol]	ΔH_{Ag} [J/mol]	ΔS_{Ag} [J/(mol·K)]	$G_{\mathrm{Ag}}^{\mathrm{E}}$ [J/mol]	$S_{\mathrm{Ag}}^{\mathrm{E}}$ [J/(mol·K)]	a_{Ag}	γ_{Ag}
1.000	0	0	0.000	0	0.000	1.000	1.000
0.900	−1092	120	0.883	111	0.007	0.909	1.010
0.800	−2096	496	1.888	452	0.033	0.832	1.040
0.700	−3038	1150	3.050	1034	0.085	0.766	1.095
0.600	−3962	2105	4.418	1870	0.171	0.707	1.178
0.500	−4941	3382	6.062	2971	0.299	0.649	1.297
0.400	−6110	5005	8.095	4350	0.477	0.586	1.464
0.300	−7726	6995	10.722	6018	0.712	0.508	1.694
0.200	−10385	9376	14.393	7988	1.011	0.403	2.013
0.100	−16016	12169	20.528	10270	1.383	0.246	2.459
0.000	$-\infty$	15397	∞	12878	1.835	0.000	3.090

Reference state: Ag(liquid)

Table IIIc. Partial quantities for Cu in the liquid phase at 1373 K.

x_{Cu}	ΔG_{Cu} [J/mol]	ΔH_{Cu} [J/mol]	ΔS_{Cu} [J/(mol·K)]	$G_{\mathrm{Cu}}^{\mathrm{E}}$ [J/mol]	$S_{\mathrm{Cu}}^{\mathrm{E}}$ [J/(mol·K)]	a_{Cu}	γ_{Cu}
0.000	$-\infty$	13529	∞	11886	1.197	0.000	2.832
0.100	−16498	11261	20.218	9788	1.073	0.236	2.357
0.200	−10512	9137	14.311	7861	0.929	0.398	1.991
0.300	−7629	7178	10.785	6116	0.774	0.513	1.709
0.400	−5896	5408	8.233	4564	0.615	0.597	1.492
0.500	−4693	3849	6.222	3219	0.459	0.663	1.326
0.600	−3739	2523	4.561	2092	0.314	0.721	1.201
0.700	−2877	1453	3.154	1195	0.188	0.777	1.110
0.800	−2008	661	1.944	539	0.089	0.839	1.048
0.900	−1066	169	0.899	137	0.023	0.911	1.012
1.000	0	0	0.000	0	0.000	1.000	1.000

Reference state: Cu(liquid)

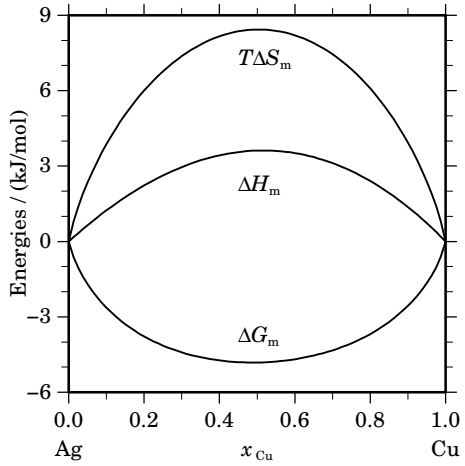

Fig. 2. Integral quantities of the liquid phase at T=1373 K.

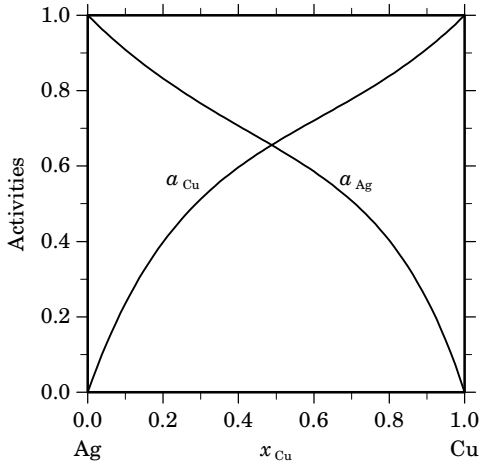

Fig. 3. Activities in the liquid phase at T=1373 K.

References

[1999Fit] K. Fitzner, Q. Guo, J. Wang, O.J. Kleppa: J. Alloys Comp. **291** (1999) 190–200.
[2002Kus] A. Kusoffsky: Acta Mater. **50** (2002) 5139–5145.
[2004Wit] V.T. Witusiewicz, U. Hecht, S.G. Fries, S. Rex: J. Alloys Comp. **385** (2004) 133–143.

Ag – Fe (Silver – Iron)

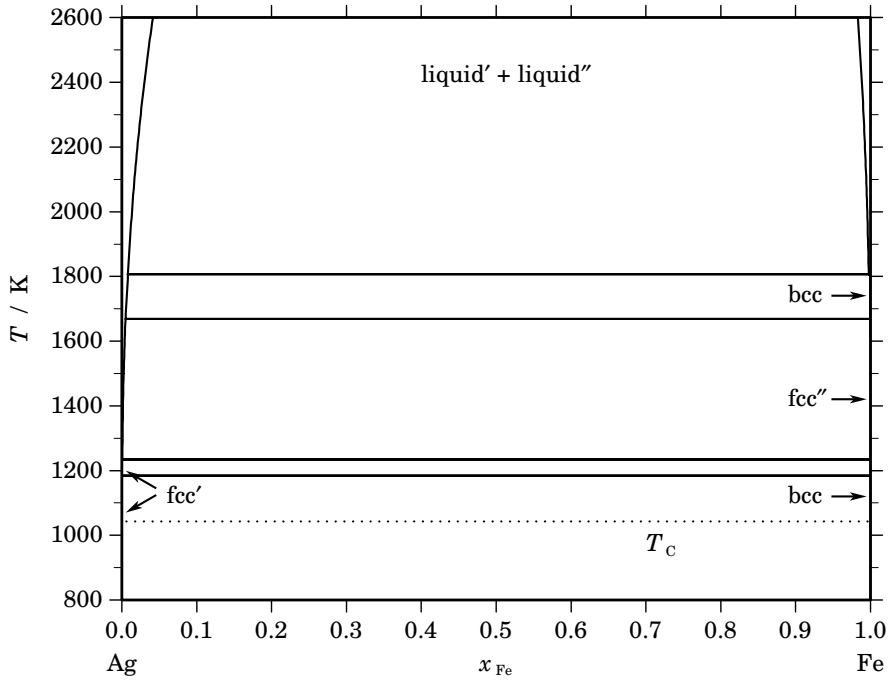

Fig. 1. Calculated phase diagram for the system Ag-Fe.

The Ag-Fe system has been reviewed in [1984Swa] and a critical thermodynamic assessment has been done by Korb [2004Kor]. The equilibrium phases of the Ag-Fe system are the liquid, the bcc solid solution based on low-temperature α-Fe as well as high-temperature δ-Fe, and the fcc phase with a large miscibility gap between the Ag- and γ-Fe-based terminal solutions. The mutual solubility of Ag and Fe is indeed very low in both the solid and the liquid state. According to [1973Wri] the solubility of Ag in solid γ-Fe reaches a maximum of approximately 0.022 at.% at 1671 K. Data on the Fe-rich side for the solubility of Ag in the fcc phase were taken from [1973Wri]. On the Ag-rich side, the data of [1969Ber] were used for the solubility of Fe between 923 and 1185 K. The assessed phase diagram is based on the results of [1930Tam, 1955Chi, 1958Gib].

Table I. Phases, structures and models.

Phase	Struktur-bericht	Prototype	Pearson symbol	Space group	SGTE name	Model
liquid					LIQUID	$(Ag,Fe)_1$
fcc	$A1$	Cu	$cF4$	$Fm\overline{3}m$	FCC_A1	$(Ag,Fe)_1$
bcc	$A2$	W	$cI2$	$Im\overline{3}m$	BCC_A2	$(Ag,Fe)_1$

Table II. Invariant reactions.

Reaction	Type	T / K	Compositions / x_{Fe}			$\Delta_r H$ / (J/mol)
liquid″ $\rightleftharpoons$ liquid′ + bcc	monotectic	1807.3	0.998	0.008	1.000	−13929
liquid′ + bcc $\rightleftharpoons$ fcc″	peritectic	1668.9	0.005	1.000	1.000	−825
liquid′ $\rightleftharpoons$ fcc′ + fcc″	eutectic	1234.6	0.001	0.000	1.000	−11330
fcc″ $\rightleftharpoons$ fcc′ + bcc	eutectoid	1184.7	1.000	0.000	1.000	−1014

References

[1930Tam] G. Tamman, W. Oelsen: Z. Anorg. Chem. **186** (1930) 277–279.
[1955Chi] J. Chipman, T.P. Floridis: Acta Metall. **3** (1955) 456–459.
[1958Gib] W.S. Gibson, W. Hume-Rothery: J. Iron Steel Inst. **189** (1958) 243–250.
[1969Ber] J. Bernardini, A. Combe-Brun, J. Cabane: C.R. Hebd. Séances Acad. Sci. **269** (1969) 287–289.
[1973Wri] H.A. Wriedt, W.B. Morrison, W.E. Cole: Metall. Trans. **4** (1973) 1453–1456.
[1984Swa] L.J. Swartzendruber: Bull. Alloy Phase Diagrams **5** (1984) 560–564.
[2004Kor] J. Korb, unpublished assessment, GTT-Technologies, 2004.

Ag – Mo (Silver – Molybdenum)

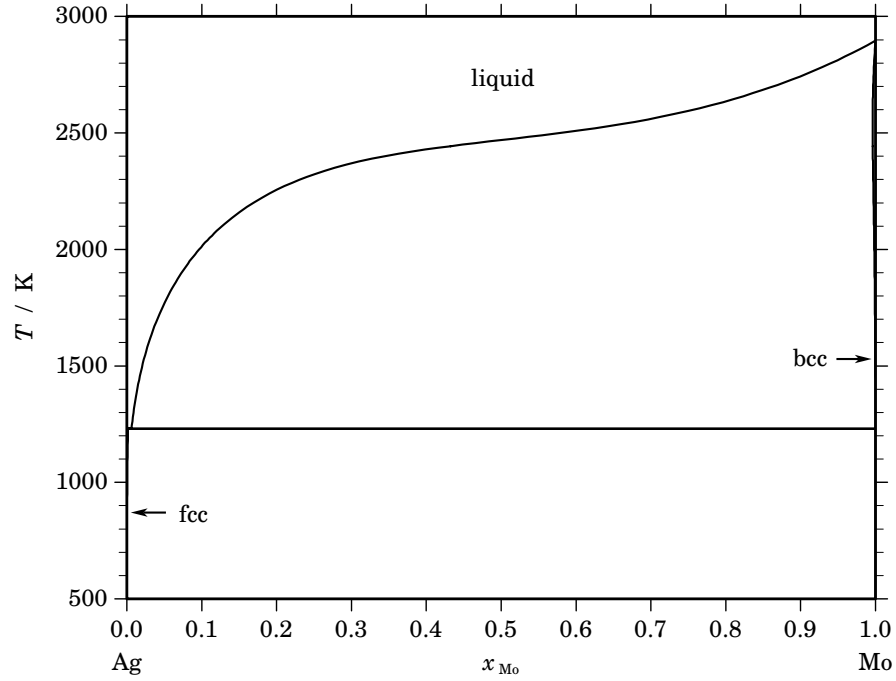

Fig. 1. Calculated phase diagram for the system Ag-Mo.

The experimental information on the Ag-Mo system is limited [1990Bar]. The Ag-Mo system is characterised by the liquid, the fcc phase based on Ag and the bcc phase based on Mo with very small solubility for Ag. The experimental studies [1924Dre, 1948Lin] indicate the insolubility of Mo in solid silver as determined by X-ray investigations and microscopy. According to Dreibholz [1924Dre] liquid Ag can dissolve at least 5.6 at.% Mo at about 1873 K. Linel [1948Lin] observed that several percent of Mo are soluble in liquid Ag at 1673 K. An assessment for the Ag-Mo system has been provided by Korb [2004Kor]. The invariant at 1231 K reported by Baren in [1990Bar] can be reproduced well by the calculations.

Table I. Phases, structures and models.

Phase	Struktur-bericht	Prototype	Pearson symbol	Space group	SGTE name	Model
liquid					LIQUID	$(Ag,Mo)_1$
fcc	$A1$	Cu	$cF4$	$Fm\bar{3}m$	FCC_A1	$(Ag,Mo)_1$
bcc	$A2$	W	$cI2$	$Im\bar{3}m$	BCC_A2	$(Ag,Mo)_1$

Table II. Invariant reactions.

Reaction	Type	T / K	Compositions / x_{Mo}			$\Delta_{\mathrm{r}}H$ / (J/mol)
liquid $\rightleftharpoons$ fcc + bcc	eutectic	1230.0	0.006	0.002	1.000	−11513

Table IIIa. Integral quantities for the liquid phase at 2900 K.

x_{Mo}	ΔG_{m} [J/mol]	ΔH_{m} [J/mol]	ΔS_{m} [J/(mol·K)]	$G_{\mathrm{m}}^{\mathrm{E}}$ [J/mol]	$S_{\mathrm{m}}^{\mathrm{E}}$ [J/(mol·K)]	ΔC_P [J/(mol·K)]
0.000	0	0	0.000	0	0.000	0.000
0.100	−4484	1954	2.220	3355	−0.483	0.000
0.200	−6128	3444	3.300	5938	−0.860	0.000
0.300	−6969	4481	3.948	7760	−1.131	0.000
0.400	−7397	5076	4.301	8831	−1.295	0.000
0.500	−7555	5241	4.412	9159	−1.351	0.000
0.600	−7474	4986	4.296	8754	−1.299	0.000
0.700	−7103	4323	3.940	7626	−1.139	0.000
0.800	−6281	3264	3.291	5785	−0.869	0.000
0.900	−4599	1819	2.213	3240	−0.490	0.000
1.000	0	0	0.000	0	0.000	0.000

Reference states: Ag(liquid), Mo(liquid)

Table IIIb. Partial quantities for Ag in the liquid phase at 2900 K.

x_{Ag}	ΔG_{Ag} [J/mol]	ΔH_{Ag} [J/mol]	ΔS_{Ag} [J/(mol·K)]	$G_{\mathrm{Ag}}^{\mathrm{E}}$ [J/mol]	$S_{\mathrm{Ag}}^{\mathrm{E}}$ [J/(mol·K)]	a_{Ag}	γ_{Ag}
1.000	0	0	0.000	0	0.000	1.000	1.000
0.900	−2153	234	0.823	387	−0.053	0.915	1.016
0.800	−3845	921	1.643	1536	−0.212	0.853	1.066
0.700	−5174	2038	2.487	3426	−0.479	0.807	1.153
0.600	−6277	3564	3.393	6040	−0.854	0.771	1.285
0.500	−7355	5474	4.424	9358	−1.339	0.737	1.474
0.400	−8733	7748	5.683	13361	−1.935	0.696	1.740
0.300	−11001	10363	7.367	18029	−2.643	0.634	2.112
0.200	−15463	13296	9.917	23344	−3.465	0.527	2.633
0.100	−26234	16525	14.745	29286	−4.400	0.337	3.369
0.000	$-\infty$	20027	∞	35836	−5.451	0.000	4.420

Reference state: Ag(liquid)

Table IIIc. Partial quantities for Mo in the liquid phase at 2900 K.

x_{Mo}	ΔG_{Mo} [J/mol]	ΔH_{Mo} [J/mol]	ΔS_{Mo} [J/(mol·K)]	$G_{\mathrm{Mo}}^{\mathrm{E}}$ [J/mol]	$S_{\mathrm{Mo}}^{\mathrm{E}}$ [J/(mol·K)]	a_{Mo}	γ_{Mo}
0.000	$-\infty$	21898	∞	37433	−5.357	0.000	4.723
0.100	−25458	17434	14.790	30062	−4.354	0.348	3.479
0.200	−15259	13536	9.929	23548	−3.453	0.531	2.655
0.300	−11158	10180	7.358	17873	−2.653	0.630	2.099
0.400	−9078	7344	5.663	13016	−1.956	0.686	1.716
0.500	−7754	5007	4.400	8959	−1.363	0.725	1.450
0.600	−6634	3144	3.372	5683	−0.875	0.759	1.266
0.700	−5432	1735	2.472	3168	−0.494	0.798	1.140
0.800	−3985	756	1.635	1395	−0.220	0.848	1.060
0.900	−2195	185	0.821	346	−0.055	0.913	1.014
1.000	0	0	0.000	0	0.000	1.000	1.000

Reference state: Mo(liquid)

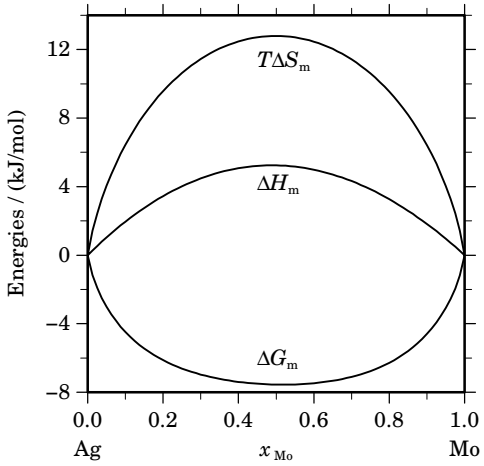

Fig. 2. Integral quantities of the liquid phase at T=2900 K.

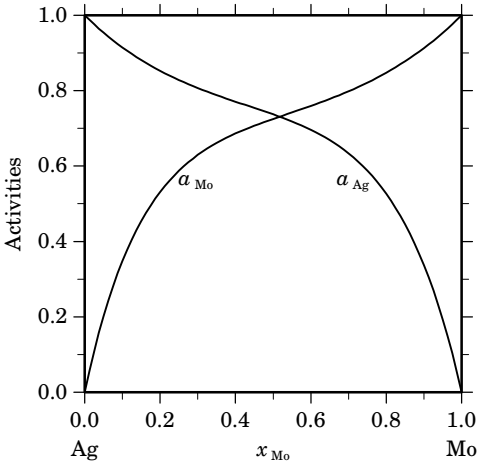

Fig. 3. Activities in the liquid phase at T=2900 K.

References

[1924Dre] L. Dreibholz: Z. Phys. Chem. **108** (1924) 1–50.
[1948Lin] F.V. Linel: Trans. Metall. Soc. AIME **175** (1948) 878–905.
[1990Bar] M.R. Baren: Bull. Alloy Phase Diagrams **11** (1990) 548–549.
[2004Kor] J. Korb, unpublished assessment, GTT-Technologies, 2004.

Ag – Nb (Silver – Niobium)

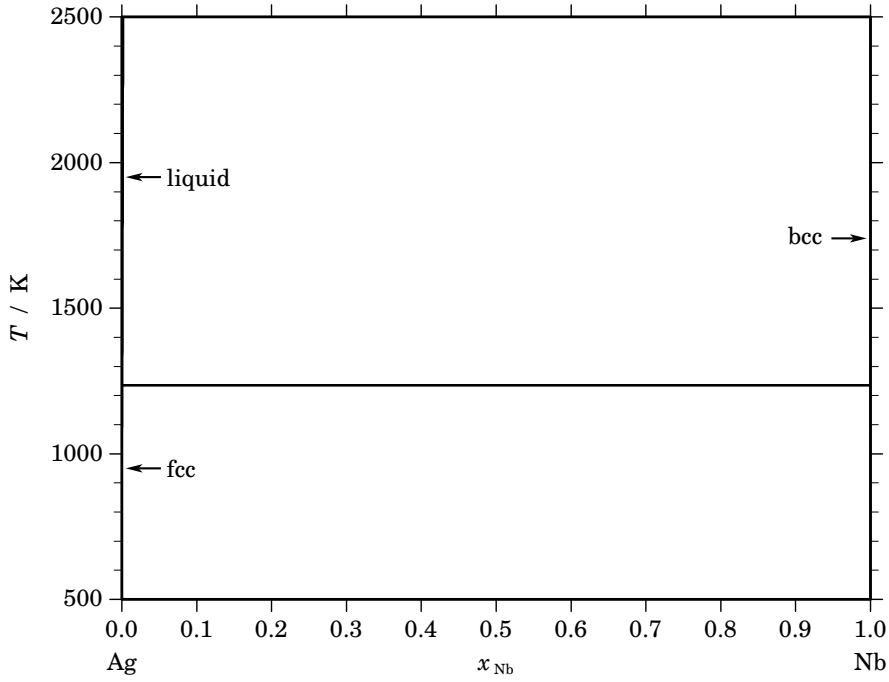

Fig. 1. Calculated phase diagram for the system Ag-Nb.

A review on the scarce information about the Ag-Nb system has been given by [1989Bar]. Results of X-ray diffraction, electrical conductivity, and metallographic studies [1963Kie] showed that the solubility of Nb in liquid Ag is extremely small. No intermediate compounds have been reported for the Ag-Nb system, which apparently is similar to the Ag-W, Ag-Mo, and Ag-V systems. Based on the information of the systems mentioned above the thermodynamic descriptions for all the stable phases (liquid, fcc, bcc) in the Ag-Nb system have been estimated by Korb [2004Kor].

Table I. Phases, structures and models.

Phase	Struktur-bericht	Prototype	Pearson symbol	Space group	SGTE name	Model
liquid					LIQUID	$(Ag,Nb)_1$
fcc	$A1$	Cu	$cF4$	$Fm\overline{3}m$	FCC_A1	$(Ag,Nb)_1$
bcc	$A2$	W	$cI2$	$Im\overline{3}m$	BCC_A2	$(Ag,Nb)_1$

Table II. Invariant reactions.

Reaction	Type	T / K	Compositions / x_{Nb}			$\Delta_{\mathrm{r}}H$ / (J/mol)
liquid + bcc $\rightleftharpoons$ fcc	peritectic	1235.2	0.001	1.000	0.001	−11256

References

[1963Kie] R. Kieffer, H. Nowotny: Metallwiss. Tech. (Berlin) **17** (1963) 669–677.
[1989Bar] M.R. Baren: Bull. Alloy Phase Diagrams **10** (1989) 640.
[2004Kor] J. Korb, unpublished assessment, GTT-Technologies, 2004.

Ag – O (Silver – Oxygen)

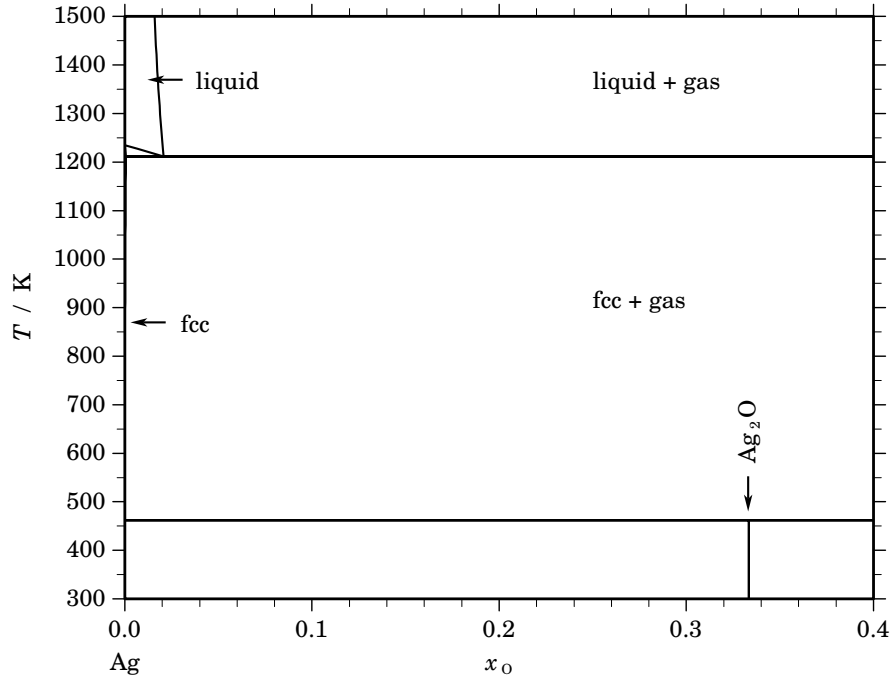

Fig. 1. Calculated phase diagram for the system Ag-O.

The silver-oxygen system has been reviewed and a thermodynamic assessment has been given by [1997Ass]. The stable phases in the system are the liquid, solid silver (fcc) with limited solubility for oxygen and at higher oxygen activities Ag_2O. The optimisation of the dataset is based on the evaluation of a large amount of experimental data from the literature. It includes the solubility and the activities of oxygen in the liquid phase, the solubility of oxygen in solid silver, the oxygen activities in the 2-phase equilibria of the condensed phases, and data for the heat capacity of Ag_2O as well as formation energies for this oxide. In a recent update [2003Hal] the description of the oxygen solubility in solid silver has been switched to an interstitial model.

Table I. Phases, structures and models.

Phase	Struktur-bericht	Prototype	Pearson symbol	Space group	SGTE name	Model
liquid					IONIC_LIQUID	$Ag_p^{1+}(O^{2-},\Box)_q$
fcc	$A1$	Cu	$cF4$	$Fm\bar{3}m$	FCC_A1	$Ag_1(O,\Box)_1$
Ag_2O	$C3$	Cu_2O	$cP6$	$Pn\bar{3}m$	CU2O	Ag_2O_1

Table II. Invariant reactions.

Reaction	Type	T / K	Compositions / x_O			$\Delta_r H$ / (J/mol)
liquid $\rightleftharpoons$ fcc + gas	gas-eutectic	1211.4	0.021	0.001	1.000	−10696
fcc + gas $\rightleftharpoons$ Ag_2O	gas-peritectoid	462.1	0.000	1.000	0.333	−9952

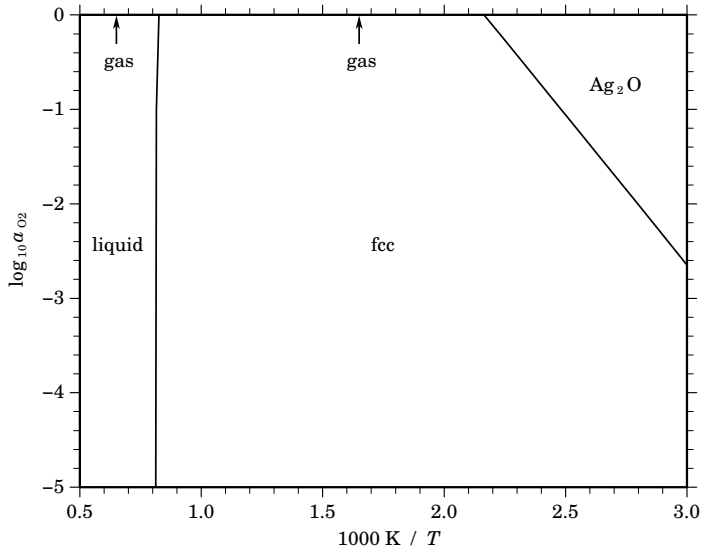

Fig. 2. Calculated temperature-activity phase diagram. Reference state: $\frac{1}{2}O_2$(gas, 0.1 MPa).

Table III. Standard reaction quantities at 298.15 K for the compounds per mole of atoms.

Compound	x_O	$\Delta_f G^\circ$ / (J/mol)	$\Delta_f H^\circ$ / (J/mol)	$\Delta_f S^\circ$ / (J/(mol·K))	$\Delta_f C_P^\circ$ / (J/(mol·K))
Ag_2O	0.333	−3599	−10228	−22.233	0.279

References

[1997Ass] J. Assal, B. Hallstedt, L. Gauckler: J. Am. Ceram. Soc. **80** (1997) 3054–3060; J. Am. Ceram. Soc. **81** (1998) 450–451.

[2003Hal] B. Hallstedt, L.J. Gauckler: Calphad **27** (2003) 177–191.

Ag – Te (Silver – Tellurium)

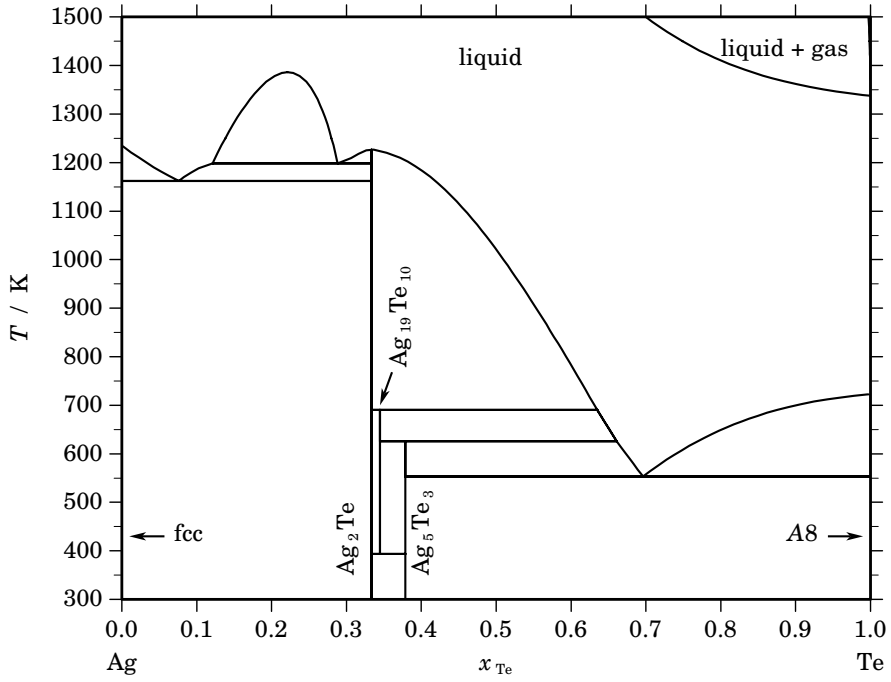

Fig. 1. Calculated phase diagram for the system Ag-Te.

The data for the Ag-Te system were critically assessed by Korb [2004Kor]. The condensed phases of the Ag-Te system are the liquid, with a miscibility gap and the solid phases fcc and hcp and three compounds, Ag_2Te, $Ag_{1.9}Te$, and Ag_5Te_3 [1991Kar]. The experimental investigations of the near-stoichiometric compounds Ag_2Te and Ag_5Te_3 were reported by [1964Hon]. With the exception of the miscibility gap, the phase boundaries for the liquid field were established from cooling curves [1910Pel, 1916Chi]. The presence of a miscibility gap was established by [1940Kra, 1966Kra]. The mutual solid solubilities of the elements in each other are negligible [1939Koe]. The calculated phase diagram agrees well with available experimental data. All three intermetallic compounds are known to have polymorphic modifications but they are not modelled in the assessment.

Table I. Phases, structures and models.

Phase	Struktur-bericht	Prototype	Pearson symbol	Space group	SGTE name	Model
liquid					LIQUID	$(Ag,Te)_1$
fcc	$A1$	Cu	$cF4$	$Fm\bar{3}m$	FCC_A1	$(Ag,Te)_1$
αAg_2Te	···	αAg_2Te	$mP12$	$P21/c$	AG2TE	Ag_2Te_1
βAg_2Te	···	···	$cF12$	···	AG2TE	Ag_2Te_1
γAg_2Te	···	···	$cI*$	···	AG2TE	Ag_2Te_1
$\alpha Ag_{19}Te_{10}$	···	···	···	···	AG19TE10	$Ag_{19}Te_{10}$
$\beta Ag_{19}Te_{10}$	···	···	···	···	AG19TE10	$Ag_{19}Te_{10}$
αAg_5Te_3	···	···	$hP55$	$P6/mmm$	AG5TE3	$Ag_{41}Te_{25}$
βAg_5Te_3	···	···	···	···	AG5TE3	$Ag_{41}Te_{25}$
$A8$	$A8$	γSe	$hP3$	$P3_121$	HEXAGONAL_A8	Te_1

Table II. Invariant reactions.

Reaction	Type	T / K	Compositions / x_{Te}			$\Delta_{\mathrm{r}}H$ / (J/mol)
liquid $\rightleftharpoons$ liquid′ + liquid″	critical	1386.1	0.221	0.221	0.221	0
liquid″ $\rightleftharpoons$ Ag_2Te	congruent	1226.7	0.333	0.333		−18105
liquid″ $\rightleftharpoons$ liquid′ + Ag_2Te	monotectic	1198.8	0.288	0.121	0.333	−14876
liquid′ $\rightleftharpoons$ fcc + Ag_2Te	eutectic	1162.1	0.076	0.000	0.333	−14022
Ag_2Te + liquid″ $\rightleftharpoons$ $Ag_{19}Te_{10}$	peritectic	690.3	0.333	0.635	0.345	−938
$Ag_{19}Te_{10}$ + liquid″ $\rightleftharpoons$ Ag_5Te_3	peritectic	626.0	0.345	0.661	0.379	−1728
liquid″ $\rightleftharpoons$ Ag_5Te_3 + $A8$	eutectic	553.1	0.696	0.379	1.000	−11555
$Ag_{19}Te_{10}$ $\rightleftharpoons$ Ag_2Te + Ag_5Te_3	eutectoid	393.9	0.345	0.333	0.379	−1899

Table IIIa. Integral quantities for the liquid phase at 1281 K.

x_{Te}	ΔG_{m} [J/mol]	ΔH_{m} [J/mol]	ΔS_{m} [J/(mol·K)]	$G^{\mathrm{E}}_{\mathrm{m}}$ [J/mol]	$S^{\mathrm{E}}_{\mathrm{m}}$ [J/(mol·K)]	ΔC_P [J/(mol·K)]
0.000	0	0	0.000	0	0.000	0.000
0.100	−7490	−446	5.499	−4028	2.796	0.000
0.200	−13829	−1950	9.274	−8500	5.113	0.000
0.300	−20108	−5544	11.370	−13602	6.291	0.026
0.400	−23244	−8352	11.625	−16076	6.029	0.029
0.500	−23374	−9254	11.023	−15991	5.259	0.002
0.600	−21475	−9042	9.705	−14307	4.110	0.000
0.700	−17976	−7816	7.931	−11469	2.852	0.000
0.800	−13192	−5784	5.782	−7862	1.622	0.000
0.900	−7290	−3132	3.246	−3827	0.543	0.000
1.000	0	0	0.000	0	0.000	0.000

Reference states: Ag(liquid), Te(liquid)

Table IIIb. Partial quantities for Ag in the liquid phase at 1281 K.

x_{Ag}	ΔG_{Ag} [J/mol]	ΔH_{Ag} [J/mol]	ΔS_{Ag} [J/(mol·K)]	$G^{\mathrm{E}}_{\mathrm{Ag}}$ [J/mol]	$S^{\mathrm{E}}_{\mathrm{Ag}}$ [J/(mol·K)]	a_{Ag}	γ_{Ag}
1.000	0	0	0.000	0	0.000	1.000	1.000
0.900	−949	419	1.068	173	0.192	0.915	1.016
0.800	−1273	2661	3.071	1103	1.216	0.887	1.109
0.700	−2479	9885	9.652	1320	6.686	0.792	1.132
0.600	−18047	−2821	11.886	−12606	7.638	0.184	0.306
0.500	−28182	−7479	16.162	−20799	10.398	0.071	0.142
0.400	−38051	−13561	19.118	−28292	11.499	0.028	0.070
0.300	−47257	−19459	21.701	−34434	11.690	0.012	0.039
0.200	−56038	−24735	24.437	−38896	11.055	0.005	0.026
0.100	−65420	−29343	28.163	−40896	9.018	0.002	0.022
0.000	$-\infty$	−33340	∞	26577	−46.774	0.000	12.125

Reference state: Ag(liquid)

Table IIIc. Partial quantities for Te in the liquid phase at 1281 K.

x_{Te}	ΔG_{Te} [J/mol]	ΔH_{Te} [J/mol]	ΔS_{Te} [J/(mol·K)]	$G^{\mathrm{E}}_{\mathrm{Te}}$ [J/mol]	$S^{\mathrm{E}}_{\mathrm{Te}}$ [J/(mol·K)]	a_{Te}	γ_{Te}
0.000	$-\infty$	−994	∞	−38904	29.594	0.000	0.026
0.100	−66362	−8231	45.379	−41837	26.234	0.002	0.020
0.200	−64053	−20390	34.085	−46911	20.703	0.002	0.012
0.300	−61242	−41543	15.377	−48418	5.367	0.003	0.011
0.400	−31039	−16649	11.234	−21280	3.615	0.054	0.136
0.500	−18566	−11029	5.884	−11183	0.120	0.175	0.350
0.600	−10424	−6030	3.430	−4983	−0.817	0.376	0.626
0.700	−5426	−2826	2.030	−1627	−0.936	0.601	0.858
0.800	−2480	−1047	1.119	−103	−0.737	0.792	0.990
0.900	−831	−220	0.477	291	−0.399	0.925	1.028
1.000	0	0	0.000	0	0.000	1.000	1.000

Reference state: Te(liquid)

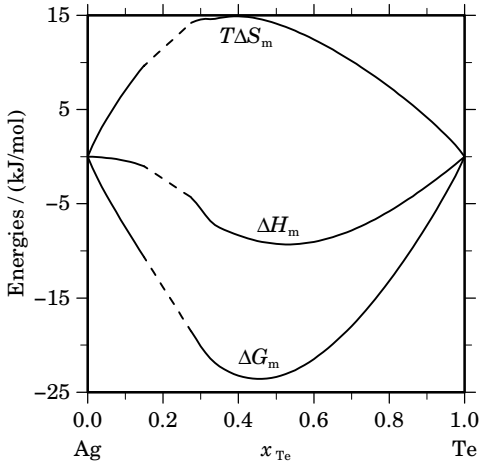

Fig. 2. Integral quantities of the liquid phase at T=1281 K.

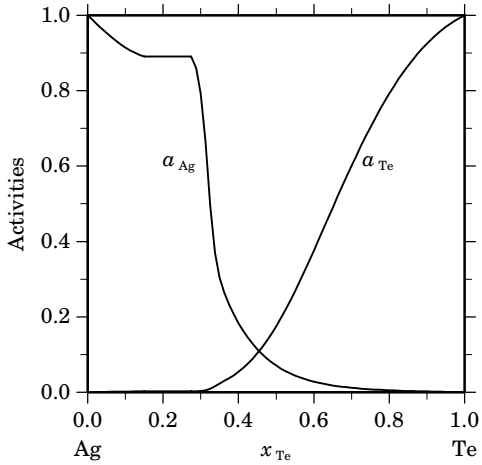

Fig. 3. Activities in the liquid phase at T=1281 K.

Table IV. Standard reaction quantities at 298.15 K for the compounds per mole of atoms.

Compound	x_{Te}	$\Delta_{\mathrm{f}}G^{\circ}$ / (J/mol)	$\Delta_{\mathrm{f}}H^{\circ}$ / (J/mol)	$\Delta_{\mathrm{f}}S^{\circ}$ / (J/(mol·K))	$\Delta_{\mathrm{f}}C^{\circ}_{P}$ / (J/(mol·K))
Ag_2Te_1	0.333	−14104	−12117	6.662	2.830
$Ag_{19}Te_{10}$	0.345	−13542	−9839	12.418	0.000
Ag_5Te_3	0.379	−13942	−12236	5.721	3.630

References

[1910Pel] G. Pellini, E. Quercigh: Atti. Accad. Naz. Lincei **19** (1910) 415–421.
[1916Chi] M. Chikashige, I. Saito: Mem. Coll. Sci. Kyoto Univ. **1** (1916) 361–368.
[1939Koe] V. Koern: Naturwissenschaften **27** (1939) 432.
[1940Kra] F.C. Kracek, C.J. Ksanda: Trans. Am. Geophys. Union (1940) 363.
[1964Hon] R.N. Honea: Am. Mineralogist **49** (1964) 325–338.
[1966Kra] F.C. Kracek, C.J. Ksanda, L.J. Cabri: Am. Mineralogist **51** (1966) 14–28.
[1991Kar] I. Karakaya, W.T. Thompson: J. Phase Equilibria **12** (1991) 56–63.
[2004Kor] J. Korb, unpublished assessment, GTT-Technologies, 2004.

Ag – V (Silver – Vanadium)

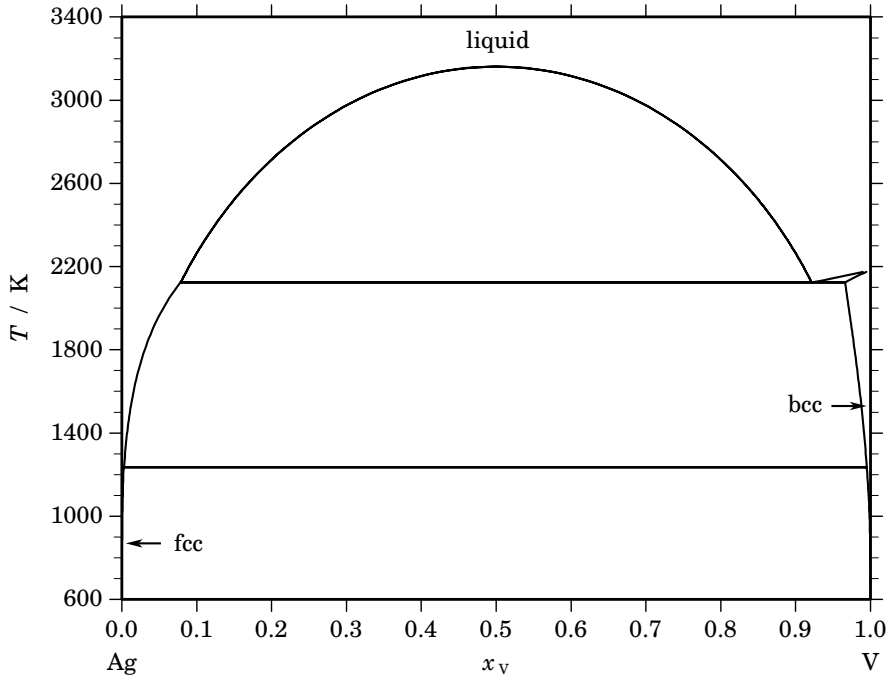

Fig. 1. Calculated phase diagram for the system Ag-V.

Ag-V is a simple system involving one eutectic and one monotectic invariant reaction. The system exhibits the liquid as well as two solid solutions, based on fcc-Ag and bcc-V, respectively. Experimental studies [1915Gie, 1954Ros] reported the existence of a miscibility gap in the liquid phase. With increasing temperature the solubility of Ag in bcc-V increases reaching a composition near 3.2 at.% Ag at the monotectic temperature 2124 K [1989Smi]. The solubility of V in fcc-Ag is negligible.
The Ag-V system has been critically assessed by Korb [2004Kor]. The calculated phase diagram is in good agreement with the experimental thermodynamic data. The small solubility of Ag in solid vanadium is reproduced well by the calculations.

Table I. Phases, structures and models.

Phase	Struktur-bericht	Prototype	Pearson symbol	Space group	SGTE name	Model
liquid					LIQUID	$(Ag,V)_1$
fcc	$A1$	Cu	$cF4$	$Fm\bar{3}m$	FCC_A1	$(Ag,V)_1$
bcc	$A2$	W	$cI2$	$Im\bar{3}m$	BCC_A2	$(Ag,V)_1$

Table II. Invariant reactions.

Reaction	Type	T / K	Compositions / x_V			$\Delta_r H$ / (J/mol)
liquid $\rightleftharpoons$ liquid′ + liquid″	critical	3161.6	0.500	0.500	0.500	0
liquid″ $\rightleftharpoons$ liquid′ + bcc	monotectic	2124.3	0.079	0.921	0.966	−21632
liquid′ $\rightleftharpoons$ fcc + bcc	eutectic	1234.4	0.002	0.003	0.995	−11335

Table IIIa. Integral quantities for the liquid phase at 3200 K.

x_{V}	ΔG_{m} [J/mol]	ΔH_{m} [J/mol]	ΔS_{m} [J/(mol·K)]	$G_{\mathrm{m}}^{\mathrm{E}}$ [J/mol]	$S_{\mathrm{m}}^{\mathrm{E}}$ [J/(mol·K)]	ΔC_P [J/(mol·K)]
0.000	0	0	0.000	0	0.000	0.000
0.100	−3914	4456	2.616	4735	−0.087	0.000
0.200	−4896	7922	4.006	8418	−0.155	0.000
0.300	−5205	10398	4.876	11048	−0.203	0.000
0.400	−5280	11883	5.363	12627	−0.232	0.000
0.500	−5289	12378	5.521	13153	−0.242	0.000
0.600	−5280	11883	5.363	12627	−0.232	0.000
0.700	−5205	10398	4.876	11048	−0.203	0.000
0.800	−4896	7922	4.006	8418	−0.155	0.000
0.900	−3914	4456	2.616	4735	−0.087	0.000
1.000	0	0	0.000	0	0.000	0.000

Reference states: Ag(liquid), V(liquid)

Table IIIb. Partial quantities for Ag in the liquid phase at 3200 K.

x_{Ag}	ΔG_{Ag} [J/mol]	ΔH_{Ag} [J/mol]	ΔS_{Ag} [J/(mol·K)]	$G_{\mathrm{Ag}}^{\mathrm{E}}$ [J/mol]	$S_{\mathrm{Ag}}^{\mathrm{E}}$ [J/(mol·K)]	a_{Ag}	γ_{Ag}
1.000	0	0	0.000	0	0.000	1.000	1.000
0.900	−2277	495	0.866	526	−0.010	0.918	1.020
0.800	−3833	1980	1.817	2104	−0.039	0.866	1.082
0.700	−4755	4456	2.878	4735	−0.087	0.836	1.195
0.600	−5173	7922	4.092	8418	−0.155	0.823	1.372
0.500	−5289	12378	5.521	13153	−0.242	0.820	1.639
0.400	−5439	17824	7.270	18940	−0.349	0.815	2.038
0.300	−6254	24261	9.536	25780	−0.475	0.791	2.635
0.200	−9150	31688	12.762	33671	−0.620	0.709	3.545
0.100	−18648	40105	18.360	42615	−0.785	0.496	4.961
0.000	$-\infty$	49512	∞	52611	−0.969	0.000	7.224

Reference state: Ag(liquid)

Table IIIc. Partial quantities for V in the liquid phase at 3200 K.

x_{V}	ΔG_{V} [J/mol]	ΔH_{V} [J/mol]	ΔS_{V} [J/(mol·K)]	$G_{\mathrm{V}}^{\mathrm{E}}$ [J/mol]	$S_{\mathrm{V}}^{\mathrm{E}}$ [J/(mol·K)]	a_{V}	γ_{V}
0.000	$-\infty$	49512	∞	52611	−0.969	0.000	7.224
0.100	−18648	40105	18.360	42615	−0.785	0.496	4.961
0.200	−9150	31688	12.762	33671	−0.620	0.709	3.545
0.300	−6254	24261	9.536	25780	−0.475	0.791	2.635
0.400	−5439	17824	7.270	18940	−0.349	0.815	2.038
0.500	−5289	12378	5.521	13153	−0.242	0.820	1.639
0.600	−5173	7922	4.092	8418	−0.155	0.823	1.372
0.700	−4755	4456	2.878	4735	−0.087	0.836	1.195
0.800	−3833	1980	1.817	2104	−0.039	0.866	1.082
0.900	−2277	495	0.866	526	−0.010	0.918	1.020
1.000	0	0	0.000	0	0.000	1.000	1.000

Reference state: V(liquid)

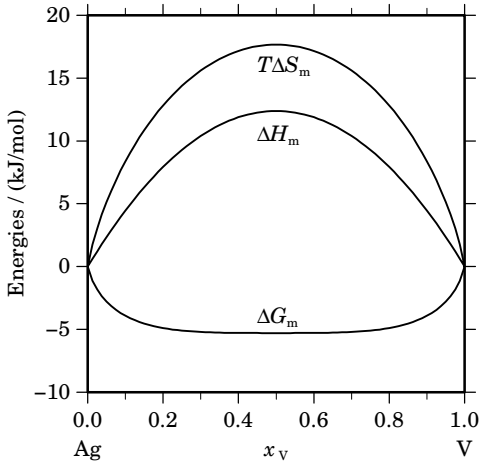

Fig. 2. Integral quantities of the liquid phase at T=3200 K.

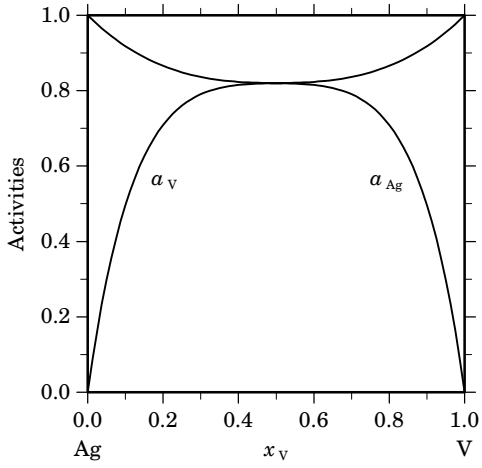

Fig. 3. Activities in the liquid phase at T=3200 K.

References

[1915Gie] H. Giebelhausen: Z. Anorg. Chem. **91** (1915) 251–263.
[1954Ros] W. Rostoker, A. Yamamoto: Trans. Am. Soc. Met. **46** (1954) 1136–1167.
[1989Smi] J.F. Smith in: Phase Diagrams of Binary Vanadium Alloys, J.F. Smith (ed.), ASM, Metals Park, 1989, 4–6.
[2004Kor] J. Korb, unpublished assessment, GTT-Technologies, 2004.

Ag – W (Silver – Tungsten)

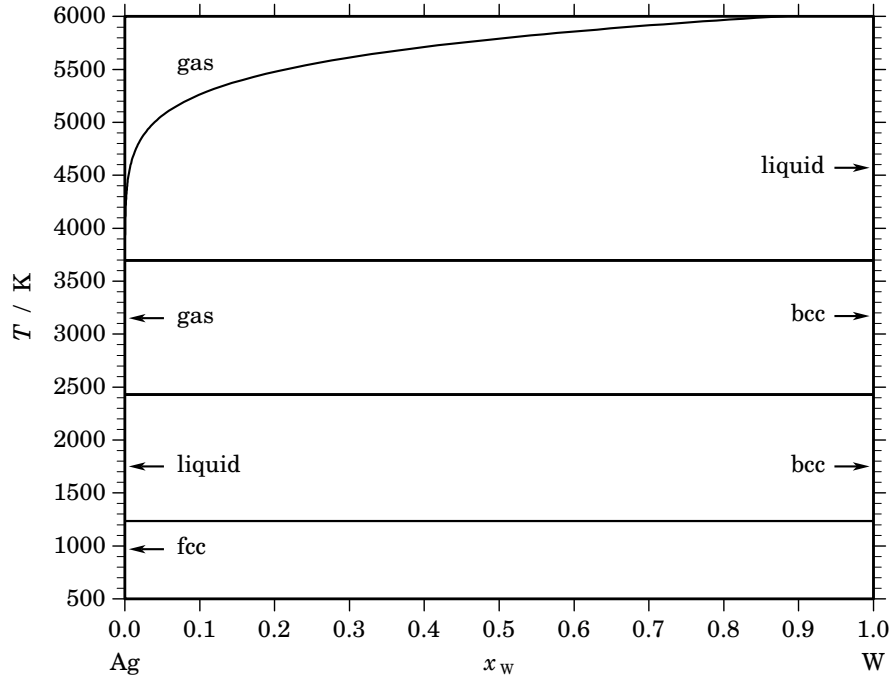

Fig. 1. Calculated phase diagram for the system Ag-W.

A review on the very limited information of the Ag-W system has been given in [1991Nag] and a thermodynamic dataset has been assessed by Korb [2004Kor]. Only three condensed phases are stable: the liquid, Ag-based fcc and the W-based bcc phases. According to experimental investigations [1860Ber, 1929Sch] the Ag-W system exhibits nearly complete immiscibility in both the liquid and the solid states.

Table I. Phases, structures and models.

Phase	Struktur-bericht	Prototype	Pearson symbol	Space group	SGTE name	Model
liquid					LIQUID	$(Ag,W)_1$
fcc	$A1$	Cu	$cF4$	$Fm\bar{3}m$	FCC_A1	$(Ag,W)_1$
bcc	$A2$	W	$cI2$	$Im\bar{3}m$	BCC_A2	$(Ag,W)_1$

Table II. Invariant reactions.

Reaction	Type	T / K	Compositions / x_W			$\Delta_r H$ / (J/mol)
liquid $\rightleftharpoons$ gas + bcc	degenerate	3694.8	1.000	0.000	1.000	−52306
gas + bcc $\rightleftharpoons$ liquid	degenerate	2430.0	0.000	1.000	0.000	−245459
liquid + bcc $\rightleftharpoons$ fcc	degenerate	1235.1	0.000	1.000	0.000	−11297

References

[1860Ber] F.A. Bernoulli: Pogg. Ann. **111** (1860) 587–588.
[1929Sch] M.V. Schwarz: "Metall- u. Legierungskunde" Ferd. Enke Verlag, Stuttgart (1929) 73.
[1991Nag] S.V. Nagender Naidu, P. Rama Rao in: Phase Diagrams of Binary Tungsten Alloys, S.V. Nagender Naidu, P. Rama Rao (eds.), The Indian Institute of Metals, Calcutta, 1991, 5–6.
[2004Kor] J. Korb, unpublished assessment, GTT-Technologies, 2004.

Al – Be (Aluminium – Beryllium)

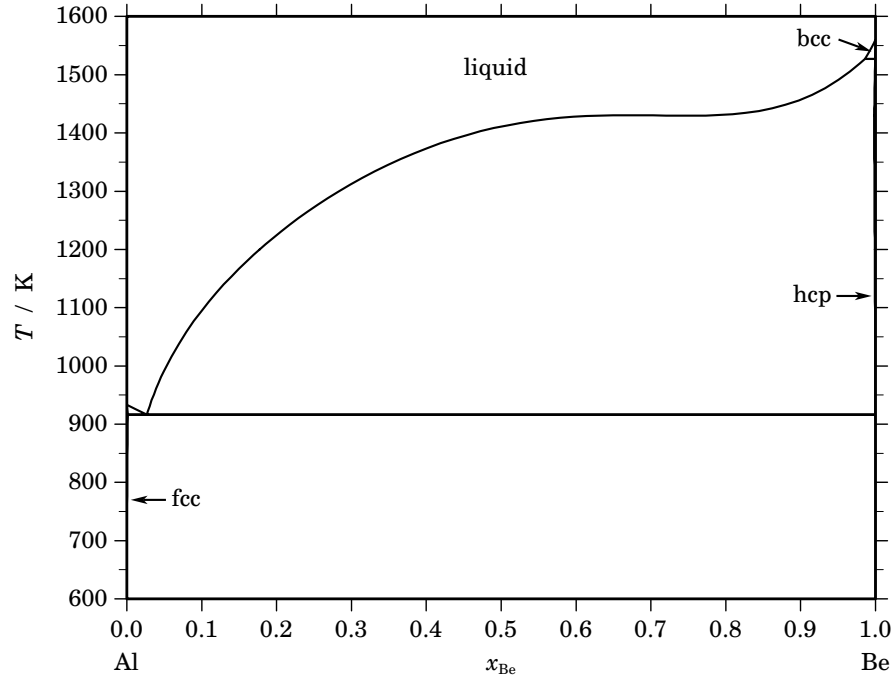

Fig. 1. Calculated phase diagram for the system Al-Be.

The Al–Be system has been reviewed in [1987Mur, 2004Pan] and a thermodynamic assessment has been given in [2004Pan]. The phase diagram shows a simple eutectic with the melting minimum close to the Al-side and with only small mutual solid solubility of the elements. The thermodynamic optimisation is based on experimental data from the literature as well as on new experiments reported in [2004Pan]. Data for the liquidus and for the solubility of beryllium in aluminium from several investigations are taken into account. In addition, activity data for the elements in the liquid have been included in the assessment.

Table I. Phases, structures and models.

Phase	Struktur-bericht	Prototype	Pearson symbol	Space group	SGTE name	Model
liquid					LIQUID	$(Al,Be)_1$
fcc	$A1$	Cu	$cF4$	$Fm\bar{3}m$	FCC_A1	$(Al,Be)_1$
bcc	$A2$	W	$cI2$	$Im\bar{3}m$	BCC_A2	$(Al,Be)_1$
hcp	$A3$	Mg	$hP2$	$P6_3/mmc$	HCP_A3	$(Al,Be)_1$

Table II. Invariant reactions.

Reaction	Type	T / K	Compositions / x_{Be}			$\Delta_r H$ / (J/mol)
liquid + bcc $\rightleftharpoons$ hcp	peritectic	1527.0	0.986	1.000	1.000	−6848
liquid $\rightleftharpoons$ fcc + hcp	eutectic	916.5	0.027	0.001	1.000	−12033

Table IIIa. Integral quantities for the liquid phase at 1600 K.

x_{Be}	ΔG_{m} [J/mol]	ΔH_{m} [J/mol]	ΔS_{m} [J/(mol·K)]	$G_{\mathrm{m}}^{\mathrm{E}}$ [J/mol]	$S_{\mathrm{m}}^{\mathrm{E}}$ [J/(mol·K)]	ΔC_P [J/(mol·K)]
0.000	0	0	0.000	0	0.000	0.000
0.100	−3942	4415	5.223	383	2.520	0.000
0.200	−5661	8164	8.641	996	4.480	0.000
0.300	−6405	11129	10.959	1721	5.880	0.000
0.400	−6513	13192	12.316	2440	6.720	0.000
0.500	−6186	14235	12.763	3035	7.000	0.000
0.600	−5567	14138	12.316	3386	6.720	0.000
0.700	−4749	12785	10.959	3377	5.880	0.000
0.800	−3769	10056	8.641	2888	4.480	0.000
0.900	−2523	5834	5.223	1802	2.520	0.000
1.000	0	0	0.000	0	0.000	0.000

Reference states: Al(liquid), Be(liquid)

Table IIIb. Partial quantities for Al in the liquid phase at 1600 K.

x_{Al}	ΔG_{Al} [J/mol]	ΔH_{Al} [J/mol]	ΔS_{Al} [J/(mol·K)]	$G_{\mathrm{Al}}^{\mathrm{E}}$ [J/mol]	$S_{\mathrm{Al}}^{\mathrm{E}}$ [J/(mol·K)]	a_{Al}	γ_{Al}
1.000	0	0	0.000	0	0.000	1.000	1.000
0.900	−1537	313	1.156	−135	0.280	0.891	0.990
0.800	−3350	1410	2.975	−382	1.120	0.777	0.972
0.700	−5249	3528	5.486	−504	2.520	0.674	0.963
0.600	−7061	6903	8.727	−266	4.480	0.588	0.980
0.500	−8650	11771	12.763	571	7.000	0.522	1.044
0.400	−9948	18369	17.698	2241	10.080	0.473	1.183
0.300	−11035	26934	23.730	4982	13.720	0.436	1.454
0.200	−12380	37703	31.302	9031	17.920	0.394	1.972
0.100	−16009	50911	41.825	14623	22.680	0.300	3.002
0.000	$-\infty$	66795	∞	21995	28.000	0.000	5.225

Reference state: Al(liquid)

Table IIIc. Partial quantities for Be in the liquid phase at 1600 K.

x_{Be}	ΔG_{Be} [J/mol]	ΔH_{Be} [J/mol]	ΔS_{Be} [J/(mol·K)]	$G_{\mathrm{Be}}^{\mathrm{E}}$ [J/mol]	$S_{\mathrm{Be}}^{\mathrm{E}}$ [J/(mol·K)]	a_{Be}	γ_{Be}
0.000	$-\infty$	47083	∞	2283	28.000	0.000	1.187
0.100	−25589	41331	41.825	5043	22.680	0.146	1.461
0.200	−14903	35179	31.302	6507	17.920	0.326	1.631
0.300	−9103	28866	23.730	6914	13.720	0.504	1.682
0.400	−5691	22627	17.698	6499	10.080	0.652	1.630
0.500	−3722	16699	12.763	5499	7.000	0.756	1.512
0.600	−2646	11318	8.727	4150	4.480	0.820	1.366
0.700	−2056	6721	5.486	2689	2.520	0.857	1.224
0.800	−1616	3145	2.975	1353	1.120	0.886	1.107
0.900	−1024	826	1.156	378	0.280	0.926	1.029
1.000	0	0	0.000	0	0.000	1.000	1.000

Reference state: Be(liquid)

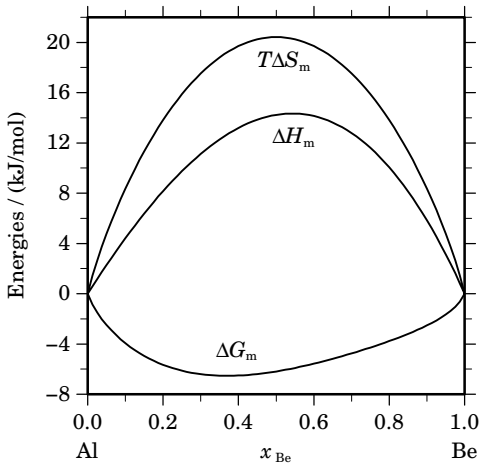

Fig. 2. Integral quantities of the liquid phase at T=1600 K.

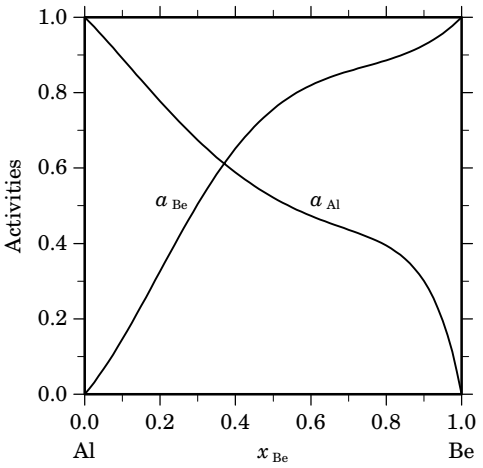

Fig. 3. Activities in the liquid phase at T=1600 K.

References

[1987Mur] J.L. Murray, D.J. Kahan in: "Phase Diagrams of Binary Beryllium Alloys", H. Okamoto, L.E. Tanner, Eds., ASM Int., Metals Park, OH, 1987, pp. 9–14.

[2004Pan] Z. Pan, Y. Du, B.Y. Huang, Y. Liu, R.C. Wang: Calphad **28** (2004) 371–378.

Al – Dy (Aluminium – Dysprosium)

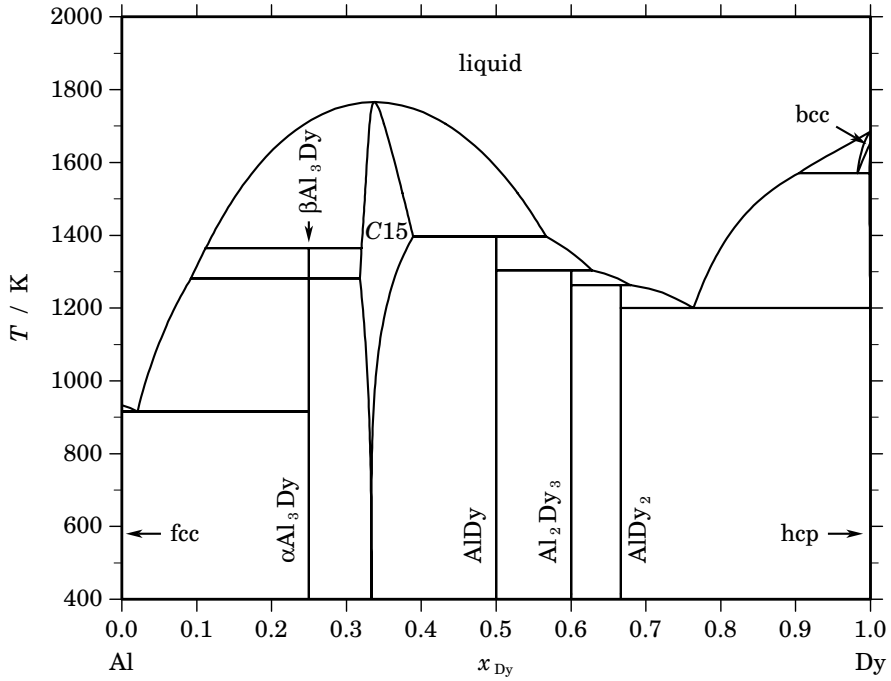

Fig. 1. Calculated phase diagram for the system Al-Dy.

The rare earth elements have attracted some attention as additives to light metal alloys in the aerospace and automotive industry due to the improvement of mechanical properties of Al- and Mg-alloys at high temperatures. Cacciamani *et al.* [2003Cac] prepared a thermodynamic optimisation of the complete Al-Dy system, which is based on a review of the Al-rich part [1988Gsc] and an experimental investigation of the phase equilibria in the range from 0 to 67 at.% Al [2000Sac]. Except for the standard enthalpy of formation of the Al_2Dy phase [1985Col] no other thermodynamic data for the intermetallic compounds have been available. Despite this lack of data, the assessment [2003Cac] can be considered as quite reasonable since other similar systems (Al-Gd, Al-Ho) have been evaluated simultaneously and data have been estimated taking advantage of the close relations between the involved rare earth elements. The dataset should not be used at too high temperatures because an artificial inverse miscibility gap opens in the liquid above 3500 K.

Table I. Phases, structures and models.

Phase	Struktur-bericht	Prototype	Pearson symbol	Space group	SGTE name	Model
liquid					LIQUID	$(Al,Dy)_1$
fcc	$A1$	Cu	$cF4$	$Fm\bar{3}m$	FCC_A1	Al_1
αAl_3Dy	$D0_{24}$	Ni_3Ti	$hP16$	$P6_3/mmc$	AL3DY	Al_3Dy_1
βAl_3Dy	···	Al_3Ho	$hR20$	$R\bar{3}m$	AL3LN	Al_3Dy_1
$C15$	$C15$	Cu_2Mg	$cF24$	$Fd\bar{3}m$	C15_LAVES	$(Al,Dy)_2(Al,Dy)_1$
AlDy	···	AlEr	$oP16$	$Pmma$	ALLN	Al_1Dy_1
Al_2Dy_3	···	Al_2Zr_3	$tP20$	$P4_2/mnm$	AL2LN3	Al_2Dy_3
$AlDy_2$	$C23$	Co_2Si	$oP12$	$Pnma$	ALLN2	Al_1Dy_2
bcc	$A2$	W	$cI2$	$Im\bar{3}m$	BCC_A2	$(Al,Dy)_1$
hcp	$A3$	Mg	$hP2$	$P6_3/mmc$	HCP_A3	$(Al,Dy)_1$

Table II. Invariant reactions.

Reaction	Type	T / K	Compositions / x_{Dy}			$\Delta_{\mathrm{r}}H$ / (J/mol)
liquid $\rightleftharpoons C15$	congruent	1765.9	0.337	0.337		−28321
bcc $\rightleftharpoons$ liquid + hcp	metatectic	1571.1	0.983	0.904	0.999	−2316
$C15$ + liquid $\rightleftharpoons$ AlDy	peritectic	1396.2	0.389	0.567	0.500	−14359
liquid + $C15 \rightleftharpoons \beta Al_3Dy$	peritectic	1364.8	0.112	0.320	0.250	−1293
AlDy + liquid $\rightleftharpoons Al_2Dy_3$	peritectic	1303.9	0.500	0.628	0.600	−14224
$\beta Al_3Dy \rightleftharpoons \alpha Al_3Dy$	polymorphic	1281.2	0.250	0.250		−5000
Al_2Dy_3 + liquid $\rightleftharpoons AlDy_2$	peritectic	1262.9	0.600	0.680	0.667	−13697
liquid $\rightleftharpoons AlDy_2$ + hcp	eutectic	1200.0	0.763	0.667	1.000	−13069
liquid $\rightleftharpoons$ fcc + αAl_3Dy	eutectic	916.1	0.021	0.000	0.250	−10950

Table IIIa. Integral quantities for the liquid phase at 1800 K.

x_{Dy}	ΔG_{m} [J/mol]	ΔH_{m} [J/mol]	ΔS_{m} [J/(mol·K)]	$G_{\mathrm{m}}^{\mathrm{E}}$ [J/mol]	$S_{\mathrm{m}}^{\mathrm{E}}$ [J/(mol·K)]	ΔC_P [J/(mol·K)]
0.000	0	0	0.000	0	0.000	0.000
0.100	−10561	−15104	−2.523	−5696	−5.226	0.000
0.200	−17753	−26988	−5.131	−10264	−9.291	0.000
0.300	−22522	−35330	−7.116	−13380	−12.195	0.000
0.400	−24950	−39964	−8.341	−14877	−13.937	0.000
0.500	−25117	−40875	−8.754	−14744	−14.517	0.000
0.600	−23193	−38207	−8.341	−13121	−13.937	0.000
0.700	−19448	−32256	−7.116	−10305	−12.195	0.000
0.800	−14239	−23474	−5.131	−6750	−9.291	0.000
0.900	−7926	−12468	−2.523	−3061	−5.226	0.000
1.000	0	0	0.000	0	0.000	0.000

Reference states: Al(liquid), Dy(liquid)

Table IIIb. Partial quantities for Al in the liquid phase at 1800 K.

x_{Al}	ΔG_{Al} [J/mol]	ΔH_{Al} [J/mol]	ΔS_{Al} [J/(mol·K)]	$G_{\mathrm{Al}}^{\mathrm{E}}$ [J/mol]	$S_{\mathrm{Al}}^{\mathrm{E}}$ [J/(mol·K)]	a_{Al}	γ_{Al}
1.000	0	0	0.000	0	0.000	1.000	1.000
0.900	−2075	−1543	0.295	−498	−0.581	0.871	0.967
0.800	−5838	−6679	−0.467	−2498	−2.323	0.677	0.846
0.700	−11752	−15821	−2.261	−6414	−5.226	0.456	0.651
0.600	−19838	−28917	−5.044	−12193	−9.291	0.266	0.443
0.500	−29692	−45450	−8.754	−19319	−14.517	0.138	0.275
0.400	−40523	−64439	−13.287	−26809	−20.905	0.067	0.167
0.300	−51239	−84438	−18.444	−33220	−28.454	0.033	0.109
0.200	−60727	−103536	−23.783	−36640	−37.165	0.017	0.086
0.100	−69155	−119360	−27.892	−34694	−47.037	0.010	0.098
0.000	$-\infty$	−129070	∞	−24544	−58.070	0.000	0.194

Reference state: Al(liquid)

Table IIIc. Partial quantities for Dy in the liquid phase at 1800 K.

x_{Dy}	ΔG_{Dy} [J/mol]	ΔH_{Dy} [J/mol]	ΔS_{Dy} [J/(mol·K)]	$G^{\mathrm{E}}_{\mathrm{Dy}}$ [J/mol]	$S^{\mathrm{E}}_{\mathrm{Dy}}$ [J/(mol·K)]	a_{Dy}	γ_{Dy}
0.000	$-\infty$	−165670	∞	−61144	−58.070	0.000	0.017
0.100	−86943	−137148	−27.892	−52482	−47.037	0.003	0.030
0.200	−65412	−108221	−23.783	−41325	−37.165	0.013	0.063
0.300	−47652	−80851	−18.444	−29633	−28.454	0.041	0.138
0.400	−32617	−56533	−13.287	−18904	−20.905	0.113	0.283
0.500	−20542	−36300	−8.754	−10169	−14.517	0.253	0.507
0.600	−11640	−20719	−5.044	−3995	−9.291	0.459	0.766
0.700	−5823	−9892	−2.261	−485	−5.226	0.678	0.968
0.800	−2617	−3459	−0.467	722	−2.323	0.840	1.049
0.900	−1123	−591	0.295	454	−0.581	0.928	1.031
1.000	0	0	0.000	0	0.000	1.000	1.000

Reference state: Dy(liquid)

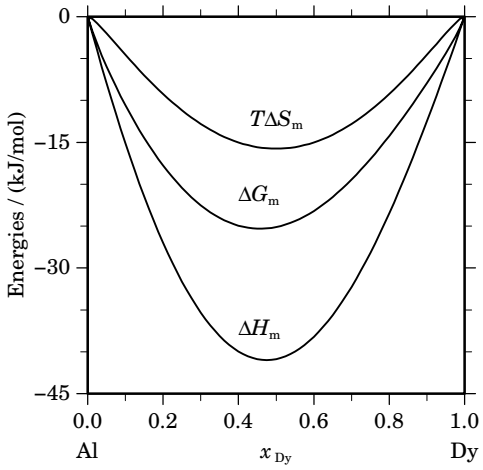

Fig. 2. Integral quantities of the liquid phase at T=1800 K.

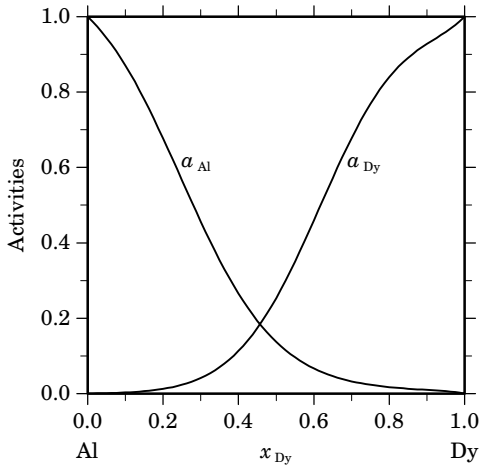

Fig. 3. Activities in the liquid phase at T=1800 K.

Table IV. Standard reaction quantities at 298.15 K for the compounds per mole of atoms.

Compound	x_{Dy}	$\Delta_{\mathrm{f}}G^{\circ}$ / (J/mol)	$\Delta_{\mathrm{f}}H^{\circ}$ / (J/mol)	$\Delta_{\mathrm{f}}S^{\circ}$ / (J/(mol·K))	$\Delta_{\mathrm{f}}C^{\circ}_{P}$ / (J/(mol·K))
αAl_3Dy_1	0.250	−39408	−42486	−10.324	−0.192
βAl_3Dy_1	0.250	−35571	−37486	−6.422	−0.192
$C15$	0.333	−49997	−53981	−13.362	−0.256
AlDy	0.500	−45439	−49471	−13.523	−0.385
Al_2Dy_3	0.600	−40130	−43966	−12.864	−0.462
Al_1Dy_2	0.667	−35022	−38462	−11.538	−0.513

References

[1985Col] C. Colinet, A. Pasturel, K.H.J. Buschow: J. Chem. Thermodyn. **17** (1985) 1133–1139.
[1988Gsc] K.A. Gschneidner, F.W. Calderwood: Bull. Alloy Phase Diagrams **9** (1988) 673–675.
[2000Sac] A. Saccone, A.M. Cardinale, S. Delfino, R. Ferro: Z. Metallkd. **91** (2000) 17–23.
[2003Cac] G. Cacciamani, S. de Negri, A. Saccone, R. Ferro: Intermetallics **11** (2003) 1135–1151.

Al – Gd (Aluminium – Gadolinium)

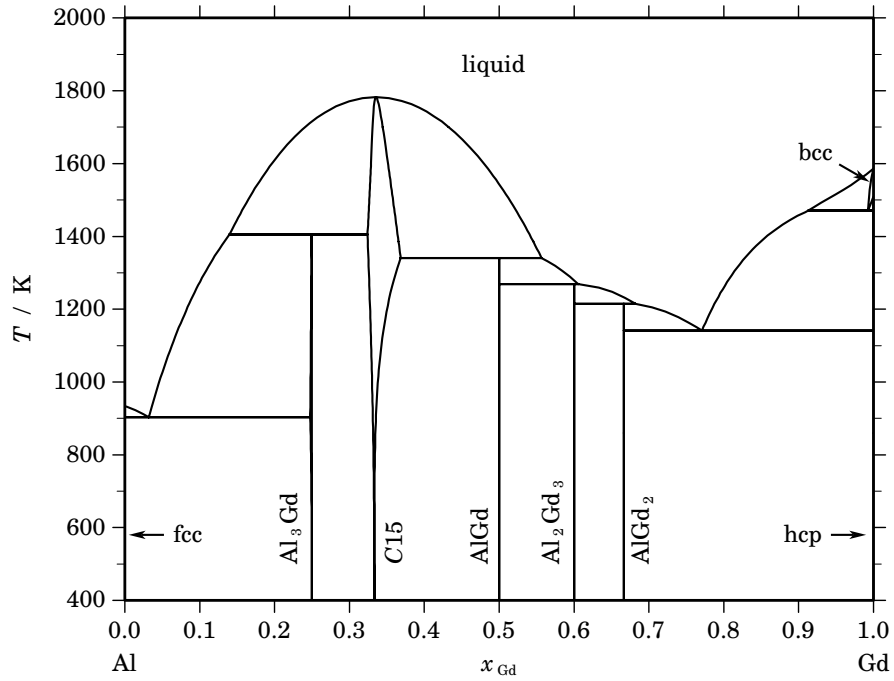

Fig. 1. Calculated phase diagram for the system Al-Gd.

The rare earth elements have attracted some attention as additives to light metal alloys in the aerospace and automotive industry due to the improvement of mechanical properties of Al- and Mg-alloys at high temperatures. For the Al-Gd system two thermodynamic optimisations have been reported in the literature [2001Grö, 2003Cac], however, no parameters have been given in [2001Grö]. The optimisation of Cacciamani *et al.* [2003Cac] is based on an experimental revision of the phase equilibria in the concentration range from 0 to 67 at.% Al [2000Sac] and for the Al-rich part on the review [1988Gsc]. In addition, the assessment takes into account the standard enthalpies of formation for the five intermetallic compounds from the literature [1987Som, 1988Col]. The dataset should not be used at too high temperatures because an artificial inverse miscibility gap opens in the liquid above 3900 K.

Table I. Phases, structures and models.

Phase	Struktur-bericht	Prototype	Pearson symbol	Space group	SGTE name	Model
liquid					LIQUID	$(Al,Gd)_1$
fcc	$A1$	Cu	$cF4$	$Fm\bar{3}m$	FCC_A1	$(Al,Gd)_1$
Al_3Gd	$D0_{19}$	Ni_3Sn	$hP8$	$P6_3/mmc$	AL3LN	$Al_3(Al,Gd)_1$
$C15$	$C15$	Cu_2Mg	$cF24$	$Fd\bar{3}m$	C15_LAVES	$(Al,Gd)_2(Al,Gd)_1$
AlGd	⋯	AlEr	$oP16$	$Pmma$	ALLN	Al_1Gd_1
Al_2Gd_3	⋯	Al_2Zr_3	$tP20$	$P4_2/mnm$	AL2LN3	Al_2Gd_3
$AlGd_2$	$C23$	Co_2Si	$oP12$	$Pnma$	ALLN2	Al_1Gd_2
bcc	$A2$	W	$cI2$	$Im\bar{3}m$	BCC_A2	$(Al,Gd)_1$
hcp	$A3$	Mg	$hP2$	$P6_3/mmc$	HCP_A3	$(Al,Gd)_1$

Table II. Invariant reactions.

Reaction	Type	T / K	Compositions / x_{Gd}			$\Delta_{\mathrm{r}}H$ / (J/mol)
liquid $\rightleftharpoons$ $C15$	congruent	1782.9	0.335	0.335		−25768
bcc $\rightleftharpoons$ liquid + hcp	metatectic	1471.0	0.993	0.913	1.000	−2797
liquid + $C15$ $\rightleftharpoons$ Al_3Gd	peritectic	1405.0	0.140	0.324	0.249	−6300
$C15$ + liquid $\rightleftharpoons$ AlGd	peritectic	1341.0	0.368	0.557	0.500	−14046
AlGd + liquid $\rightleftharpoons$ Al_2Gd_3	peritectic	1268.6	0.500	0.606	0.600	−16460
Al_2Gd_3 + liquid $\rightleftharpoons$ $AlGd_2$	peritectic	1214.3	0.600	0.682	0.667	−12817
liquid $\rightleftharpoons$ $AlGd_2$ + hcp	eutectic	1141.0	0.771	0.667	1.000	−12777
liquid $\rightleftharpoons$ fcc + Al_3Gd	eutectic	903.0	0.032	0.000	0.248	−10769

Table IIIa. Integral quantities for the liquid phase at 1800 K.

x_{Gd}	ΔG_{m} [J/mol]	ΔH_{m} [J/mol]	ΔS_{m} [J/(mol·K)]	$G^{\mathrm{E}}_{\mathrm{m}}$ [J/mol]	$S^{\mathrm{E}}_{\mathrm{m}}$ [J/(mol·K)]	ΔC_P [J/(mol·K)]
0.000	0	0	0.000	0	0.000	0.000
0.100	−12014	−15631	−2.009	−7149	−4.712	0.000
0.200	−20267	−27857	−4.217	−12777	−8.378	0.000
0.300	−25691	−36341	−5.917	−16549	−10.996	0.000
0.400	−28377	−40924	−6.971	−18305	−12.566	0.000
0.500	−28437	−41625	−7.327	−18063	−13.090	0.000
0.600	−26093	−38640	−6.971	−16021	−12.566	0.000
0.700	−21695	−32344	−5.917	−12552	−10.996	0.000
0.800	−15699	−23289	−4.217	−8210	−8.378	0.000
0.900	−8588	−12205	−2.009	−3723	−4.712	0.000
1.000	0	0	0.000	0	0.000	0.000

Reference states: Al(liquid), Gd(liquid)

Table IIIb. Partial quantities for Al in the liquid phase at 1800 K.

x_{Al}	ΔG_{Al} [J/mol]	ΔH_{Al} [J/mol]	ΔS_{Al} [J/(mol·K)]	$G^{\mathrm{E}}_{\mathrm{Al}}$ [J/mol]	$S^{\mathrm{E}}_{\mathrm{Al}}$ [J/(mol·K)]	a_{Al}	γ_{Al}
1.000	0	0	0.000	0	0.000	1.000	1.000
0.900	−2266	−1632	0.352	−689	−0.524	0.859	0.955
0.800	−6634	−7065	−0.239	−3295	−2.094	0.642	0.802
0.700	−13561	−16706	−1.747	−8223	−4.712	0.404	0.577
0.600	−22994	−30428	−4.130	−15348	−8.378	0.215	0.359
0.500	−34384	−47573	−7.327	−24011	−13.090	0.101	0.201
0.400	−46730	−66946	−11.231	−33016	−18.850	0.044	0.110
0.300	−58658	−86820	−15.646	−40639	−25.656	0.020	0.066
0.200	−68706	−104937	−20.129	−44619	−33.510	0.010	0.051
0.100	−76623	−118503	−23.267	−42162	−42.412	0.006	0.060
0.000	$-\infty$	−124190	∞	−29942	−52.360	0.000	0.135

Reference state: Al(liquid)

Table IIIc. Partial quantities for Gd in the liquid phase at 1800 K.

x_{Gd}	ΔG_{Gd} [J/mol]	ΔH_{Gd} [J/mol]	ΔS_{Gd} [J/(mol·K)]	$G^{\mathrm{E}}_{\mathrm{Gd}}$ [J/mol]	$S^{\mathrm{E}}_{\mathrm{Gd}}$ [J/(mol·K)]	a_{Gd}	γ_{Gd}
0.000	$-\infty$	−171770	∞	−77522	−52.360	0.000	0.006
0.100	−99746	−141627	−23.267	−65286	−42.412	0.001	0.013
0.200	−74796	−111027	−20.129	−50709	−33.510	0.007	0.034
0.300	−53995	−82158	−15.646	−35976	−25.656	0.027	0.090
0.400	−36452	−56668	−11.231	−22739	−18.850	0.088	0.219
0.500	−22489	−35678	−7.327	−12116	−13.090	0.223	0.445
0.600	−12336	−19770	−4.130	−4691	−8.378	0.439	0.731
0.700	−5853	−8998	−1.747	−515	−4.712	0.676	0.966
0.800	−2447	−2877	−0.239	892	−2.094	0.849	1.061
0.900	−1029	−395	0.352	548	−0.524	0.934	1.037
1.000	0	0	0.000	0	0.000	1.000	1.000

Reference state: Gd(liquid)

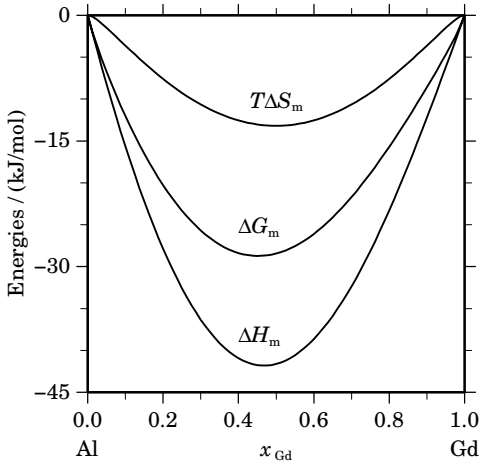

Fig. 2. Integral quantities of the liquid phase at T=1800 K.

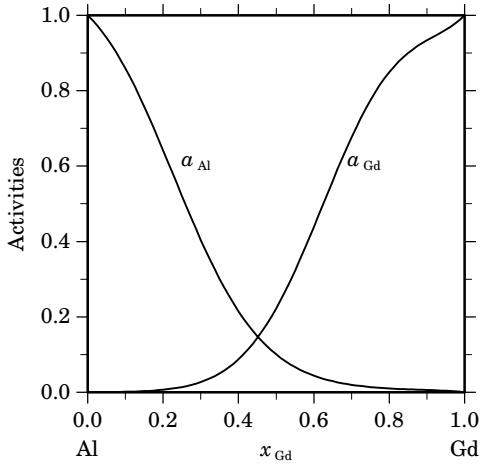

Fig. 3. Activities in the liquid phase at T=1800 K.

Table IV. Standard reaction quantities at 298.15 K for the compounds per mole of atoms.

Compound	x_{Gd}	$\Delta_{\mathrm{f}}G^{\circ}$ / (J/mol)	$\Delta_{\mathrm{f}}H^{\circ}$ / (J/mol)	$\Delta_{\mathrm{f}}S^{\circ}$ / (J/(mol·K))	$\Delta_{\mathrm{f}}C^{\circ}_{P}$ / (J/(mol·K))
Al_3Gd	0.250	−39008	−41063	−6.892	−3.243
$C15$	0.333	−50043	−53084	−10.200	−4.326
AlGd	0.500	−45501	−48626	−10.480	−6.489
Al_2Gd_3	0.600	−40583	−43551	−9.953	−7.786
Al_1Gd_2	0.667	−35386	−38001	−8.773	−8.652

References

[1987Som] F. Sommer, M. Keita: J. Less-Common Met. **136** (1987) 95–99.
[1988Col] C. Colinet, A. Pasturel: Physica B **150B** (1988) 397–403.
[1988Gsc] K.A. Gschneidner Jr., F.W. Calderwood: Bull. Alloy Phase Diagrams **9** (1988) 680–683.
[2000Sac] A. Saccone, A.M. Cardinale, S. Delfino, R. Ferro: Z. Metallkd. **91** (2000) 17–23.
[2001Grö] J. Gröbner, D. Kevorkov, R. Schmid-Fetzer: Z. Metallkd. **92** (2001) 22–27.
[2003Cac] G. Cacciamani, S. de Negri, A. Saccone, R. Ferro: Intermetallics **11** (2003) 1135–1151.

Al – Ho (Aluminium – Holmium)

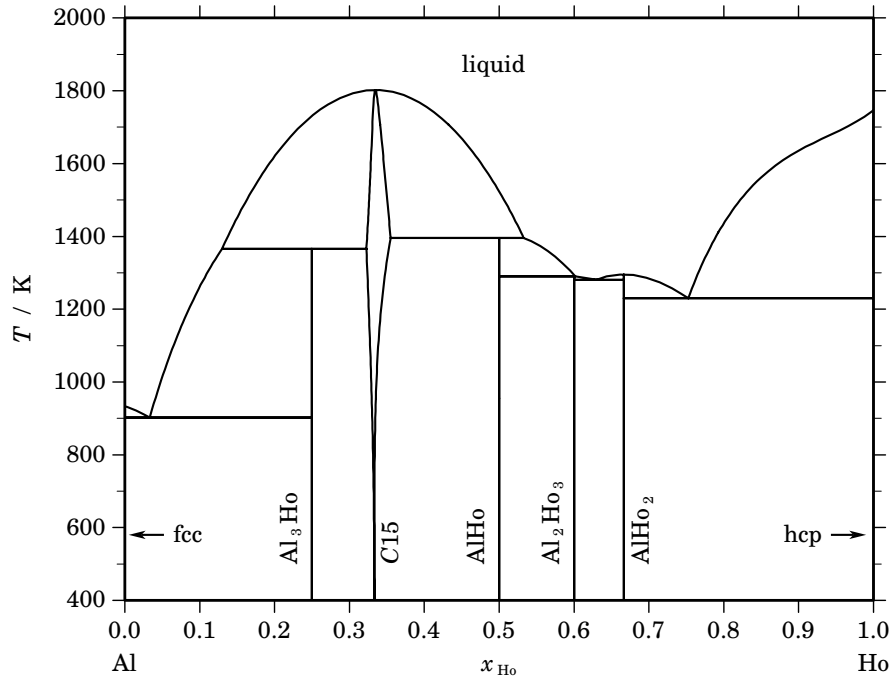

Fig. 1. Calculated phase diagram for the system Al-Ho.

The rare earth elements have attracted some attention as additives to light metal alloys in the aerospace and automotive industry due to the improvement of mechanical properties of Al- and Mg-alloys at high temperatures. Cacciamani *et al.* [2003Cac] prepared a thermodynamic optimisation of the Al-Ho system, which is based on an experimental investigation of the phase equilibria involving the liquid [1966Mey] and one datum for the standard enthalpy of formation of the Al_2Ho phase [1985Col]. Although no other thermodynamic data for the system are available, the assessment [2003Cac] can be still considered as reasonable since other similar systems (Al-Dy, Al-Gd) have been evaluated simultaneously and data have been estimated taking advantage of the close relations between the involved rare earth elements.

Table I. Phases, structures and models.

Phase	Struktur-bericht	Prototype	Pearson symbol	Space group	SGTE name	Model
liquid					LIQUID	$(Al,Ho)_1$
fcc	$A1$	Cu	$cF4$	$Fm\bar{3}m$	FCC_A1	Al_1
Al_3Ho	$\cdots$	Al_3Ho	$hR20$	$R\bar{3}m$	AL3LN	Al_3Ho_1
$C15$	$C15$	Cu_2Mg	$cF24$	$Fd\bar{3}m$	C15_LAVES	$(Al,Ho)_2(Al,Ho)_1$
AlHo	$\cdots$	AlEr	$oP16$	$Pmma$	ALLN	Al_1Ho_1
Al_2Ho_3	$\cdots$	Al_2Zr_3	$tP20$	$P4_2/mnm$	AL2LN3	Al_2Ho_3
$AlHo_2$	$C23$	Co_2Si	$oP12$	$Pnma$	ALLN2	Al_1Ho_2
hcp	$A3$	Mg	$hP2$	$P6_3/mmc$	HCP_A3	$(Al,Ho)_1$

Table II. Invariant reactions.

Reaction	Type	T / K	Compositions / x_{Ho}			$\Delta_{\mathrm{r}}H$ / (J/mol)
liquid $\rightleftharpoons C15$	congruent	1802.3	0.334	0.334		−25506
$C15$ + liquid $\rightleftharpoons$ AlHo	peritectic	1396.1	0.355	0.533	0.500	−14730
liquid + $C15$ $\rightleftharpoons$ Al_3Ho	peritectic	1365.6	0.130	0.323	0.250	−5566
liquid $\rightleftharpoons$ $AlHo_2$	congruent	1295.3	0.667	0.667		−15956
AlHo + liquid $\rightleftharpoons$ Al_2Ho_3	peritectic	1290.6	0.500	0.602	0.600	−15536
liquid $\rightleftharpoons$ Al_2Ho_3 + $AlHo_2$	eutectic	1280.8	0.630	0.600	0.667	−15675
liquid $\rightleftharpoons$ $AlHo_2$ + hcp	eutectic	1229.8	0.752	0.667	1.000	−13831
liquid $\rightleftharpoons$ fcc + Al_3Ho	eutectic	902.2	0.033	0.000	0.250	−10736

Table IIIa. Integral quantities for the liquid phase at 1800 K.

x_{Ho}	ΔG_{m} [J/mol]	ΔH_{m} [J/mol]	ΔS_{m} [J/(mol·K)]	$G^{\mathrm{E}}_{\mathrm{m}}$ [J/mol]	$S^{\mathrm{E}}_{\mathrm{m}}$ [J/(mol·K)]	ΔC_P [J/(mol·K)]
0.000	0	0	0.000	0	0.000	0.000
0.100	−12708	−16944	−2.353	−7843	−5.056	0.000
0.200	−21753	−30444	−4.828	−14264	−8.989	0.000
0.300	−27915	−40009	−6.719	−18773	−11.798	0.000
0.400	−31163	−45361	−7.887	−21091	−13.483	0.000
0.500	−31523	−46430	−8.282	−21149	−14.045	0.000
0.600	−29164	−43362	−7.887	−19092	−13.483	0.000
0.700	−24418	−36511	−6.719	−15275	−11.798	0.000
0.800	−17756	−26446	−4.828	−10267	−8.989	0.000
0.900	−9710	−13946	−2.353	−4845	−5.056	0.000
1.000	0	0	0.000	0	0.000	0.000

Reference states: Al(liquid), Ho(liquid)

Table IIIb. Partial quantities for Al in the liquid phase at 1800 K.

x_{Al}	ΔG_{Al} [J/mol]	ΔH_{Al} [J/mol]	ΔS_{Al} [J/(mol·K)]	$G^{\mathrm{E}}_{\mathrm{Al}}$ [J/mol]	$S^{\mathrm{E}}_{\mathrm{Al}}$ [J/(mol·K)]	a_{Al}	γ_{Al}
1.000	0	0	0.000	0	0.000	1.000	1.000
0.900	−2188	−1622	0.314	−611	−0.562	0.864	0.960
0.800	−6545	−7250	−0.392	−3205	−2.247	0.646	0.807
0.700	−13784	−17548	−2.091	−8446	−5.056	0.398	0.569
0.600	−24010	−32544	−4.742	−16365	−8.989	0.201	0.335
0.500	−36728	−51635	−8.282	−26354	−14.045	0.086	0.172
0.400	−50888	−73579	−12.606	−37174	−20.225	0.033	0.083
0.300	−64969	−96501	−17.518	−46950	−27.528	0.013	0.043
0.200	−77257	−117889	−22.573	−53170	−35.955	0.006	0.029
0.100	−87150	−134599	−26.361	−52689	−45.506	0.003	0.030
0.000	$-\infty$	−142850	∞	−41726	−56.180	0.000	0.062

Reference state: Al(liquid)

Table IIIc. Partial quantities for Ho in the liquid phase at 1800 K.

x_{Ho}	ΔG_{Ho} [J/mol]	ΔH_{Ho} [J/mol]	ΔS_{Ho} [J/(mol·K)]	$G^{\mathrm{E}}_{\mathrm{Ho}}$ [J/mol]	$S^{\mathrm{E}}_{\mathrm{Ho}}$ [J/(mol·K)]	a_{Ho}	γ_{Ho}
0.000	$-\infty$	−184490	∞	−83366	−56.180	0.000	0.004
0.100	−107387	−154836	−26.361	−72926	−45.506	0.001	0.008
0.200	−82587	−123219	−22.573	−58500	−35.955	0.004	0.020
0.300	−60888	−92420	−17.518	−42869	−27.528	0.017	0.057
0.400	−41893	−64585	−12.606	−28180	−20.225	0.061	0.152
0.500	−26318	−41225	−8.282	−15944	−14.045	0.172	0.345
0.600	−14682	−23217	−4.742	−7037	−8.989	0.375	0.625
0.700	−7039	−10802	−2.091	−1701	−5.056	0.625	0.893
0.800	−2880	−3586	−0.392	459	−2.247	0.825	1.031
0.900	−1105	−540	0.314	472	−0.562	0.929	1.032
1.000	0	0	0.000	0	0.000	1.000	1.000

Reference state: Ho(liquid)

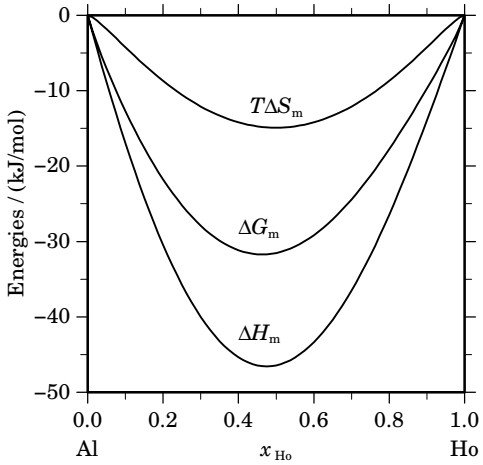

Fig. 2. Integral quantities of the liquid phase at T=1800 K.

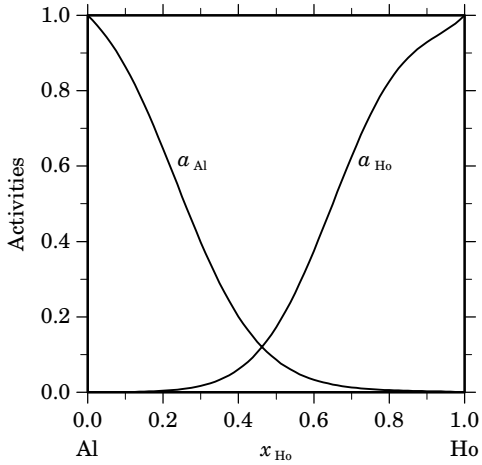

Fig. 3. Activities in the liquid phase at T=1800 K.

Table IV. Standard reaction quantities at 298.15 K for the compounds per mole of atoms.

Compound	x_{Ho}	$\Delta_{\mathrm{f}}G^{\circ}$ / (J/mol)	$\Delta_{\mathrm{f}}H^{\circ}$ / (J/mol)	$\Delta_{\mathrm{f}}S^{\circ}$ / (J/(mol·K))	$\Delta_{\mathrm{f}}C^{\circ}_{P}$ / (J/(mol·K))
Al_3Ho	0.250	−40754	−43000	−7.532	0.000
$C15$	0.333	−52687	−56000	−11.113	0.000
AlHo	0.500	−47389	−50500	−10.435	0.000
Al_2Ho_3	0.600	−41638	−44500	−9.600	0.000
Al_1Ho_2	0.667	−37302	−40000	−9.050	0.000

References

[1966Mey] A. Meyer: J. Less-Common Met. **10** (1966) 121–129.
[1985Col] C. Colinet, A. Pasturel, K.H.J. Buschow: J. Chem. Thermodyn. **17** (1985) 1133–1139.
[2003Cac] G. Cacciamani, S. de Negri, A. Saccone, R. Ferro: Intermetallics **11** (2003) 1135–1151.

Al – Ru (Aluminium – Ruthenium)

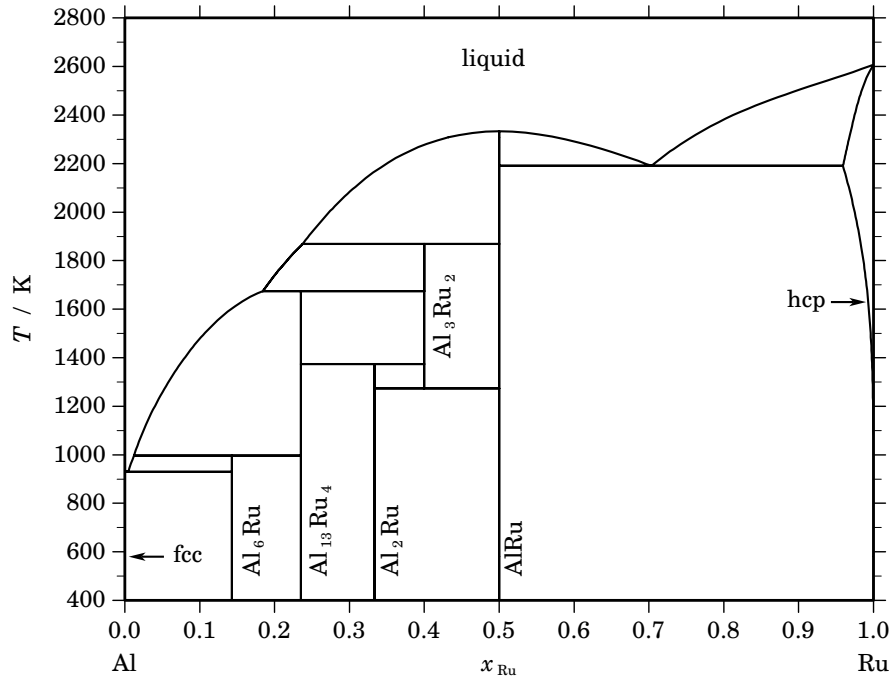

Fig. 1. Calculated phase diagram for the system Al-Ru.

The Al-Ru system contains two components interesting for the nuclear field, aluminium being a major component of the concrete basemat in its oxide form (Al_2O_3) and Ru being one selected component representative of a family of non volatile fission products. The system has been thermodynamically optimised by Chevalier and Fischer [1996Che] and Prins *et al.* [2003Pri] but the latter work is not recommended due to the modelling of the imprecise non-stoichiometry range of $Al_{13}Ru$, Al_2Ru, Al_3Ru_2 and AlRu leading to different temperatures of decomposition of these compounds. The phase diagram reported in the compilation of Moffatt [1981Mof] is based on the phase diagram of Obrowski [1963Obr] which has been obtained from microscopy, X-ray, and DTA experiments, and the investigation of Al-rich alloys by Anlage *et al.* [1988Anl] using scanning electron microscopy, X-ray, and thermal analysis. Five intermetallic compounds were identified, Al_6Ru, $Al_{13}Ru_4$, Al_2Ru, Al_3Ru_2 and AlRu. The three last show a non-negligible stoichiometry range. AlRu melts congruently at about 2323 K. The standard molar enthalpy of formation of AlRu has been determined calorimetrically by Jung and Kleppa [1992Jun]. The excess Gibbs energy of the liquid and hcp solution phases and the Gibbs energy of the intermetallics which have been described as stoichiometric compounds were optimised from the selected experimental information. A sub-regular substitution model was used for the liquid and a regular solution for the hcp phase. The enthalpy of formation was optimised in consistency with other data. The agreement with the experimental information [1963Obr, 1988Anl, 1992Jun] is quite satisfactory. However, a revised phase diagram for Al-rich alloys has been published in [2003Mi] which presents different equilibria at higher temperatures and an additional high-temperature compound, Al_5Ru_2.

Table I. Phases, structures and models.

Phase	Struktur-bericht	Prototype	Pearson symbol	Space group	SGTE name	Model
liquid					LIQUID	$(Al,Ru)_1$
fcc	$A1$	Cu	$cF4$	$Fm\overline{3}m$	FCC_A1	$(Al,Ru)_1$
Al_6Ru	$D2_h$	Al_6Mn	$oC28$	$Cmcm$	AL6RU	Al_6Ru_1
$Al_{13}Ru_4$	$\cdots$	$Al_{13}Fe_4$	$mC102$	$C2/m$	AL13RU4	$Al_{13}Ru_4$
Al_2Ru	$C54$	$TiSi_2$	$oF24$	$Fddd$	AL2RU	Al_2Ru_1
Al_3Ru_2	$\cdots$	Al_3Os_2	$tI10$	$I4/mmm$	AL3RU2	Al_3Ru_2
AlRu	$B2$	CsCl	$cP2$	$Pm\overline{3}m$	ALRU	Al_1Ru_1
hcp	$A3$	Mg	$hP2$	$P6_3/mmc$	HCP_A3	$(Al,Ru)_1$

Table II. Invariant reactions.

Reaction	Type	T / K	Compositions / x_{Ru}			$\Delta_r H$ / (J/mol)
liquid $\rightleftharpoons$ AlRu	congruent	2332.7	0.500	0.500		−63621
liquid $\rightleftharpoons$ AlRu + hcp	eutectic	2191.0	0.703	0.500	0.959	−48684
liquid + AlRu $\rightleftharpoons$ Al_3Ru_2	peritectic	1868.3	0.237	0.500	0.400	−11339
liquid + Al_3Ru_2 $\rightleftharpoons$ $Al_{13}Ru_4$	peritectic	1674.6	0.184	0.400	0.235	−23684
$Al_{13}Ru_4$ + Al_3Ru_2 $\rightleftharpoons$ Al_2Ru	peritectoid	1373.4	0.235	0.400	0.333	−2645
Al_3Ru_2 $\rightleftharpoons$ Al_2Ru + AlRu	eutectoid	1273.1	0.400	0.333	0.500	−3175
liquid + $Al_{13}Ru_4$ $\rightleftharpoons$ Al_6Ru	peritectic	996.0	0.012	0.235	0.143	−7091
liquid $\rightleftharpoons$ fcc + Al_6Ru	eutectic	929.8	0.005	0.000	0.143	−11078

Table IIIa. Integral quantities for the liquid phase at 2700 K.

x_{Ru}	ΔG_m [J/mol]	ΔH_m [J/mol]	ΔS_m [J/(mol·K)]	G_m^E [J/mol]	S_m^E [J/(mol·K)]	ΔC_P [J/(mol·K)]
0.000	0	0	0.000	0	0.000	0.000
0.100	−19011	−11713	2.703	−11713	0.000	0.000
0.200	−30522	−19288	4.161	−19288	0.000	0.000
0.300	−37015	−23302	5.079	−23302	0.000	0.000
0.400	−39437	−24329	5.596	−24329	0.000	0.000
0.500	−38505	−22945	5.763	−22945	0.000	0.000
0.600	−34834	−19725	5.596	−19725	0.000	0.000
0.700	−28959	−15245	5.079	−15245	0.000	0.000
0.800	−21315	−10081	4.161	−10081	0.000	0.000
0.900	−12105	−4807	2.703	−4807	0.000	0.000
1.000	0	0	0.000	0	0.000	0.000

Reference states: Al(liquid), Ru(liquid)

Table IIIb. Partial quantities for Al in the liquid phase at 2700 K.

x_{Al}	ΔG_{Al} [J/mol]	ΔH_{Al} [J/mol]	ΔS_{Al} [J/(mol·K)]	$G^{\mathrm{E}}_{\mathrm{Al}}$ [J/mol]	$S^{\mathrm{E}}_{\mathrm{Al}}$ [J/(mol·K)]	a_{Al}	γ_{Al}
1.000	0	0	0.000	0	0.000	1.000	1.000
0.900	−4530	−2165	0.876	−2165	0.000	0.817	0.908
0.800	−12901	−7891	1.855	−7891	0.000	0.563	0.704
0.700	−24036	−16029	2.966	−16029	0.000	0.343	0.490
0.600	−36894	−25427	4.247	−25427	0.000	0.193	0.322
0.500	−50494	−34933	5.763	−34933	0.000	0.105	0.211
0.400	−63969	−43399	7.619	−43399	0.000	0.058	0.145
0.300	−76699	−49671	10.010	−49671	0.000	0.033	0.109
0.200	−88730	−52600	13.382	−52600	0.000	0.019	0.096
0.100	−102725	−51034	19.145	−51034	0.000	0.010	0.103
0.000	−∞	−43823	∞	−43823	0.000	0.000	0.142

Reference state: Al(liquid)

Table IIIc. Partial quantities for Ru in the liquid phase at 2700 K.

x_{Ru}	ΔG_{Ru} [J/mol]	ΔH_{Ru} [J/mol]	ΔS_{Ru} [J/(mol·K)]	$G^{\mathrm{E}}_{\mathrm{Ru}}$ [J/mol]	$S^{\mathrm{E}}_{\mathrm{Ru}}$ [J/(mol·K)]	a_{Ru}	γ_{Ru}
0.000	−∞	−139734	∞	−139734	0.000	0.000	0.002
0.100	−149338	−97647	19.145	−97647	0.000	0.001	0.013
0.200	−101007	−64876	13.382	−64876	0.000	0.011	0.056
0.300	−67300	−40272	10.010	−40272	0.000	0.050	0.166
0.400	−43252	−22682	7.619	−22682	0.000	0.146	0.364
0.500	−26516	−10956	5.763	−10956	0.000	0.307	0.614
0.600	−15410	−3943	4.247	−3943	0.000	0.503	0.839
0.700	−8498	−491	2.966	−491	0.000	0.685	0.978
0.800	−4460	549	1.855	549	0.000	0.820	1.025
0.900	−2036	329	0.876	329	0.000	0.913	1.015
1.000	0	0	0.000	0	0.000	1.000	1.000

Reference state: Ru(liquid)

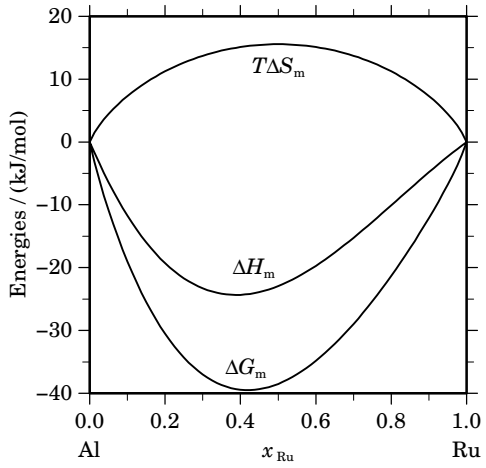

Fig. 2. Integral quantities of the liquid phase at T=2700 K.

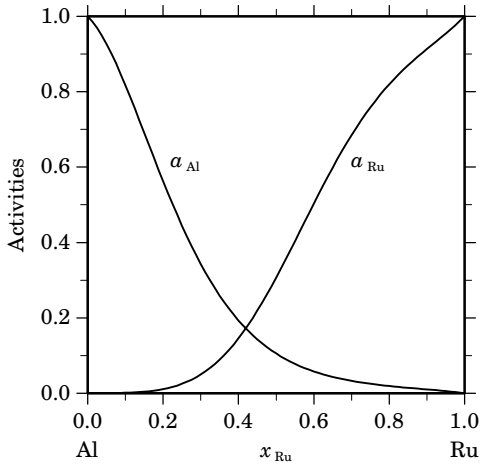

Fig. 3. Activities in the liquid phase at T=2700 K.

Table IV. Standard reaction quantities at 298.15 K for the compounds per mole of atoms.

Compound	x_{Ru}	$\Delta_{\mathrm{f}}G^{\circ}$ / (J/mol)	$\Delta_{\mathrm{f}}H^{\circ}$ / (J/mol)	$\Delta_{\mathrm{f}}S^{\circ}$ / (J/(mol·K))	$\Delta_{\mathrm{f}}C_P^{\circ}$ / (J/(mol·K))
Al_6Ru_1	0.143	−26312	−28000	−5.660	0.000
$Al_{13}Ru_4$	0.235	−40494	−42300	−6.056	0.000
Al_2Ru_1	0.333	−48062	−51000	−9.854	4.971
Al_3Ru_2	0.400	−50011	−52245	−7.494	4.474
Al_1Ru_1	0.500	−59012	−62050	−10.188	3.728

References

[1963Obr] W. Obrowski: Metallwiss. Tech. (Berlin) **17** (1963) 108–112.
[1981Mof] W.G. Moffatt, "The Handbook of Binary Phase Diagrams", General Electric Corp. (1981).
[1988Anl] S.M. Anlage, P. Nash, R. Ramachandran, R.B. Schwarz: J. Less-Common Met. **136** (1988) 237–247.
[1992Jun] W.G. Jung, O.J. Kleppa: Metall. Trans. B **23B** (1992) 53–56.
[1996Che] P.-Y. Chevalier, E. Fischer, unpublished work, 1996.
[2003Mi] S. Mi, S. Balanetskyy, B. Grushko: Intermetallics **11** (2003) 643–649.
[2003Pri] S.N. Prins, L.A. Cornish, W.E. Stumpf, B. Sundman: Calphad **27** (2003) 79–80.

Al – Sc (Aluminium – Scandium)

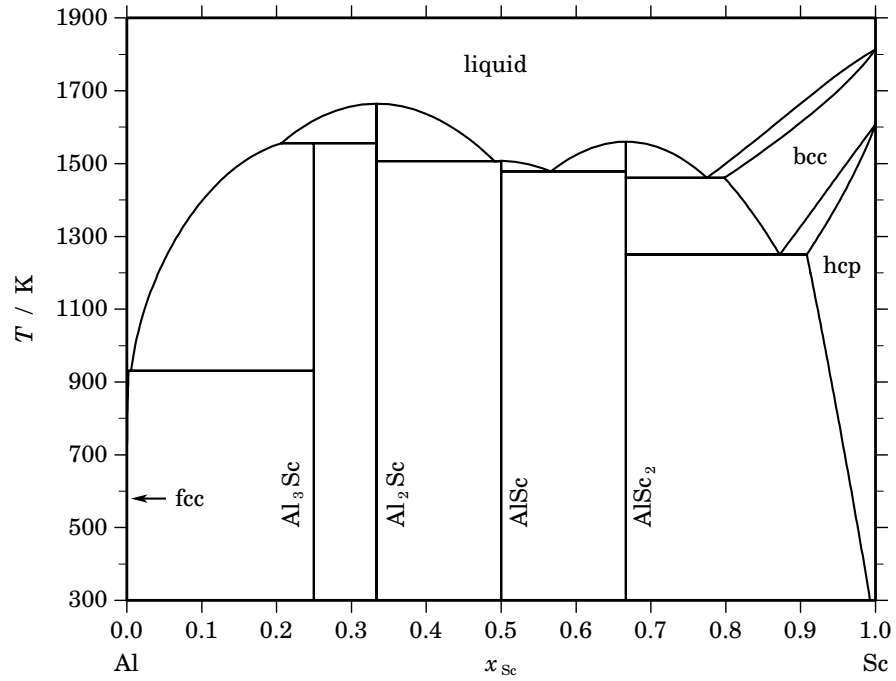

Fig. 1. Calculated phase diagram for the system Al-Sc.

Additions of Sc to Al- and Mg-alloys are of potential interest for the aerospace and automotive industry because the mechanical properties of the alloys can be improved at higher temperatures. Thermodynamic assessments and reviews of the literature of the Al-Sc system have been reported in [1998Mur, 1999Cac]. The assessment of [1999Cac] is selected here, because it includes a set of additional experimental data which are reported in that paper. The optimisation takes into account data for the phase equilibria from several literature sources as well as new DTA investigations [1999Cac]. According to these results, the solubility of Al in bcc-Sc and hcp-Sc is much higher than in previous reports. Furthermore, the assessment takes account of investigations of mixing enthalpies in the liquid [1986Lit] and heats of formation for the intermetallic compounds from the literature as well as from new experiments [1999Cac].

Table I. Phases, structures and models.

Phase	Struktur-bericht	Prototype	Pearson symbol	Space group	SGTE name	Model
liquid					LIQUID	$(Al,Sc)_1$
fcc	$A1$	Cu	$cF4$	$Fm\bar{3}m$	FCC_A1	$(Al,Sc)_1$
Al_3Sc	$L1_2$	$AuCu_3$	$cP4$	$Pm\bar{3}m$	AL3SC	Al_3Sc_1
Al_2Sc	$C15$	Cu_2Mg	$cF24$	$Fd\bar{3}m$	AL2SC	Al_2Sc_1
AlSc	$B2$	CsCl	$cP2$	$Pm\bar{3}m$	ALSC	Al_1Sc_1
$AlSc_2$	$B8_2$	Ni_2In	$hP6$	$P6_3/mmc$	ALSC2	Al_1Sc_2
bcc	$A2$	W	$cI2$	$Im\bar{3}m$	BCC_A2	$(Al,Sc)_1$
hcp	$A3$	Mg	$hP2$	$P6_3/mmc$	HCP_A3	$(Al,Sc)_1$

Table II. Invariant reactions.

Reaction	Type	T / K	Compositions / x_{Sc}			$\Delta_{\mathrm{r}}H$ / (J/mol)
liquid $\rightleftharpoons$ Al_2Sc	congruent	1664.8	0.333	0.333		−33033
liquid $\rightleftharpoons$ $AlSc_2$	congruent	1560.3	0.667	0.667		−24360
liquid + Al_2Sc $\rightleftharpoons$ Al_3Sc	peritectic	1556.1	0.207	0.333	0.250	−19839
liquid $\rightleftharpoons$ AlSc	congruent	1507.3	0.500	0.500		−28477
liquid $\rightleftharpoons$ Al_2Sc + AlSc	eutectic	1506.8	0.491	0.333	0.500	−28528
liquid $\rightleftharpoons$ AlSc + $AlSc_2$	eutectic	1478.3	0.566	0.500	0.667	−25832
liquid $\rightleftharpoons$ $AlSc_2$ + bcc	eutectic	1460.8	0.775	0.667	0.798	−9058
bcc $\rightleftharpoons$ $AlSc_2$ + hcp	eutectoid	1250.3	0.872	0.667	0.908	−5731
liquid $\rightleftharpoons$ fcc + Al_3Sc	eutectic	930.9	0.006	0.002	0.250	−10819

Table IIIa. Integral quantities for the liquid phase at 1873 K.

x_{Sc}	ΔG_{m} [J/mol]	ΔH_{m} [J/mol]	ΔS_{m} [J/(mol·K)]	$G_{\mathrm{m}}^{\mathrm{E}}$ [J/mol]	$S_{\mathrm{m}}^{\mathrm{E}}$ [J/(mol·K)]	ΔC_P [J/(mol·K)]
0.000	0	0	0.000	0	0.000	0.000
0.100	−13456	−11364	1.117	−8393	−1.586	0.000
0.200	−22715	−20203	1.341	−14922	−2.820	0.000
0.300	−29098	−26517	1.378	−19585	−3.701	0.000
0.400	−32863	−30305	1.366	−22383	−4.230	0.000
0.500	−34110	−31568	1.357	−23315	−4.406	0.000
0.600	−32863	−30305	1.366	−22383	−4.230	0.000
0.700	−29098	−26517	1.378	−19585	−3.701	0.000
0.800	−22715	−20203	1.341	−14922	−2.820	0.000
0.900	−13456	−11364	1.117	−8393	−1.586	0.000
1.000	0	0	0.000	0	0.000	0.000

Reference states: Al(liquid), Sc(liquid)

Table IIIb. Partial quantities for Al in the liquid phase at 1873 K.

x_{Al}	ΔG_{Al} [J/mol]	ΔH_{Al} [J/mol]	ΔS_{Al} [J/(mol·K)]	$G_{\mathrm{Al}}^{\mathrm{E}}$ [J/mol]	$S_{\mathrm{Al}}^{\mathrm{E}}$ [J/(mol·K)]	a_{Al}	γ_{Al}
1.000	0	0	0.000	0	0.000	1.000	1.000
0.900	−2573	−1263	0.700	−933	−0.176	0.848	0.942
0.800	−7205	−5051	1.150	−3730	−0.705	0.630	0.787
0.700	−13948	−11364	1.379	−8393	−1.586	0.408	0.583
0.600	−22877	−20203	1.427	−14922	−2.820	0.230	0.384
0.500	−34110	−31568	1.357	−23315	−4.406	0.112	0.224
0.400	−47843	−45457	1.274	−33574	−6.345	0.046	0.116
0.300	−64447	−61873	1.375	−45698	−8.636	0.016	0.053
0.200	−84751	−80813	2.102	−59687	−11.279	0.004	0.022
0.100	−111399	−102279	4.869	−75541	−14.276	0.001	0.008
0.000	$-\infty$	−126270	∞	−93260	−17.624	0.000	0.003

Reference state: Al(liquid)

Table IIIc. Partial quantities for Sc in the liquid phase at 1873 K.

x_{Sc}	ΔG_{Sc} [J/mol]	ΔH_{Sc} [J/mol]	ΔS_{Sc} [J/(mol·K)]	G^E_{Sc} [J/mol]	S^E_{Sc} [J/(mol·K)]	a_{Sc}	γ_{Sc}
0.000	$-\infty$	−126270	∞	−93261	−17.624	0.000	0.003
0.100	−111399	−102279	4.869	−75541	−14.276	0.001	0.008
0.200	−84751	−80813	2.102	−59687	−11.279	0.004	0.022
0.300	−64447	−61873	1.375	−45698	−8.636	0.016	0.053
0.400	−47843	−45457	1.274	−33574	−6.345	0.046	0.116
0.500	−34110	−31568	1.357	−23315	−4.406	0.112	0.224
0.600	−22877	−20203	1.427	−14922	−2.820	0.230	0.384
0.700	−13948	−11364	1.379	−8393	−1.586	0.408	0.583
0.800	−7205	−5051	1.150	−3730	−0.705	0.630	0.787
0.900	−2573	−1263	0.700	−933	−0.176	0.848	0.942
1.000	0	0	0.000	0	0.000	1.000	1.000

Reference state: Sc(liquid)

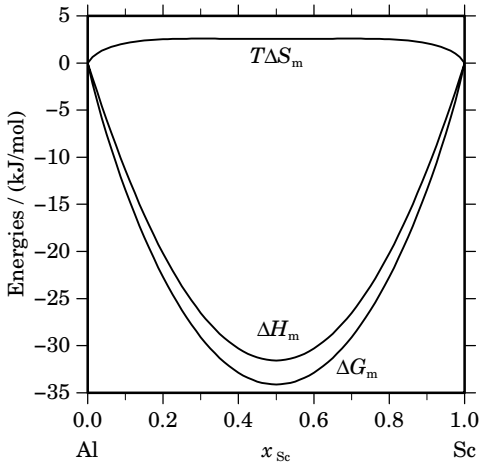

Fig. 2. Integral quantities of the liquid phase at T=1873 K.

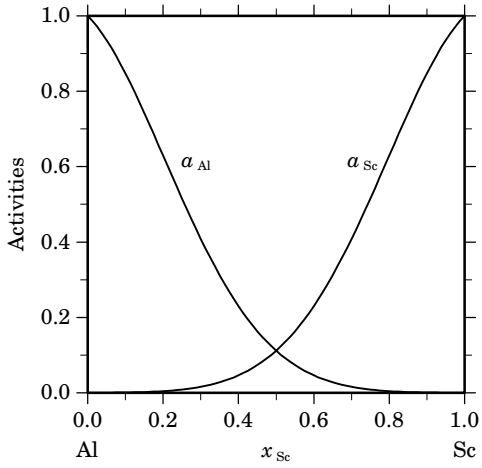

Fig. 3. Activities in the liquid phase at T=1873 K.

Table IV. Standard reaction quantities at 298.15 K for the compounds per mole of atoms.

Compound	x_{Sc}	$\Delta_f G^\circ$ / (J/mol)	$\Delta_f H^\circ$ / (J/mol)	$\Delta_f S^\circ$ / (J/(mol·K))	$\Delta_f C^\circ_P$ / (J/(mol·K))
Al_3Sc_1	0.250	−39855	−42000	−7.193	0.000
Al_2Sc_1	0.333	−45764	−48000	−7.500	0.000
Al_1Sc_1	0.500	−43932	−46000	−6.937	0.000
Al_1Sc_2	0.667	−35887	−37000	−3.733	0.000

References

[1986Lit] V.V. Litovskii, M.G. Valishev, Yu.O. Esin, P.V. Geld, M.S. Petrushevskii: Russ. J. Phys. Chem. **60** (1986) 1385–1386.

[1998Mur] J.L. Murray: J. Phase Equilibria **19** (1998) 380–384.

[1999Cac] G. Cacciamani, P. Riani, G. Borzone, N. Parodi, A. Saccone, R. Ferro, A. Pisch, R. Schmid-Fetzer: Intermetallics **7** (1999) 101–108.

Al – Sn (Aluminium – Tin)

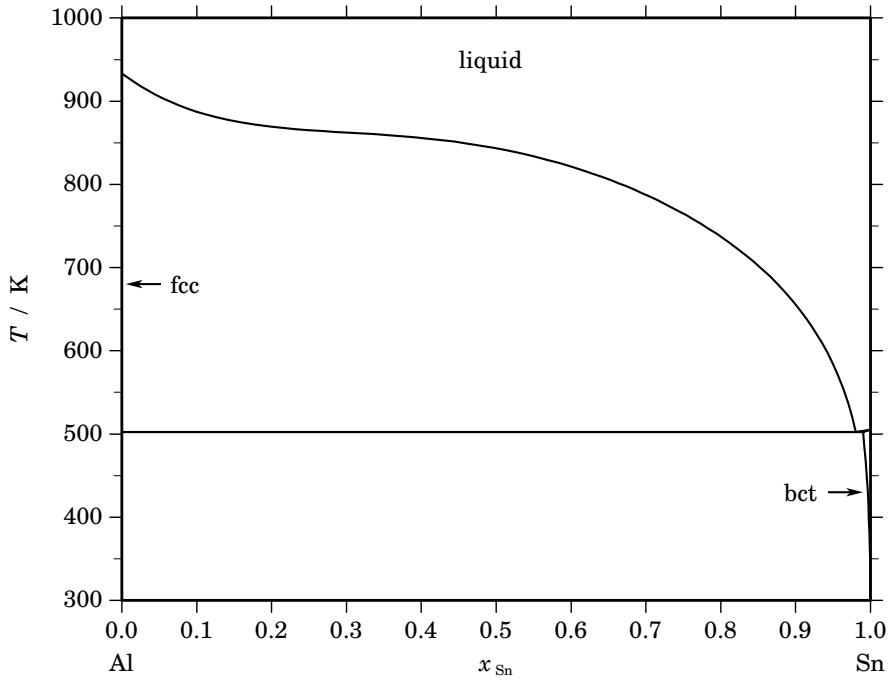

Fig. 1. Calculated phase diagram for the system Al-Sn.

The Al-Sn is a simple eutectic system with the eutectic point close to the tin side. The mutual solubility in the solid metals is quite low. An optimised dataset for the Al-Sn system has been reported by [1998Fri] which has been corrected recently [2003Luk]. A review of the system has been given in [1983McA]. Since then no additional experimental investigations on the thermodynamics of Al-Sn have been reported. The liquidus has been measured across the whole composition range in several investigations using various techniques [1906Gwy, 1949Sul, 1964Bon]. The mixing enthalpy in the liquid has been determined at different temperatures [1930Kaw, 1958Oel, 1963Wit] and measurements of the activities of Al in the liquid are reported in [1964Bon, 1966Tik, 1968Bat, 1969Lee]. The solubility of Sn in fcc-Al has been determined by [1976Dor].

Table I. Phases, structures and models.

Phase	Struktur-bericht	Prototype	Pearson symbol	Space group	SGTE name	Model
liquid					LIQUID	$(Al,Sn)_1$
fcc	$A1$	Cu	$cF4$	$Fm\bar{3}m$	FCC_A1	$(Al,Sn)_1$
bct	$A5$	βSn	$tI4$	$I4_1/amd$	BCT_A5	$(Al,Sn)_1$

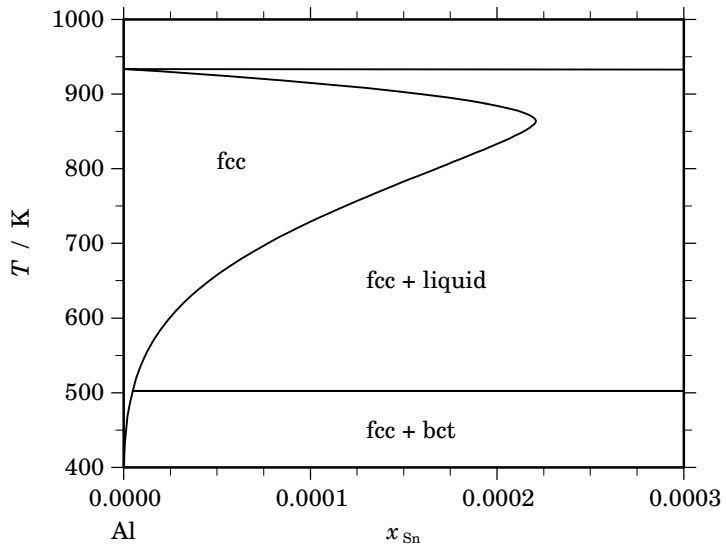

Fig. 2. Partial phase diagram for the system Al-Sn.

Table II. Invariant reactions.

Reaction	Type	T / K	Compositions / x_{Sn}			$\Delta_{\mathrm{r}}H$ / (J/mol)
liquid $\rightleftharpoons$ fcc + bct	eutectic	502.4	0.980	0.000	0.990	−7139

Table IIIa. Integral quantities for the liquid phase at 973 K.

x_{Sn}	ΔG_{m} [J/mol]	ΔH_{m} [J/mol]	ΔS_{m} [J/(mol·K)]	$G_{\mathrm{m}}^{\mathrm{E}}$ [J/mol]	$S_{\mathrm{m}}^{\mathrm{E}}$ [J/(mol·K)]	ΔC_P [J/(mol·K)]
0.000	0	0	0.000	0	0.000	0.000
0.100	−1312	1867	3.267	1318	0.564	0.000
0.200	−1855	3109	5.101	2194	0.941	0.000
0.300	−2239	3834	6.241	2703	1.162	0.000
0.400	−2534	4133	6.852	2911	1.257	0.000
0.500	−2737	4082	7.009	2870	1.246	0.000
0.600	−2821	3739	6.742	2624	1.146	0.000
0.700	−2742	3143	6.048	2200	0.969	0.000
0.800	−2429	2320	4.880	1619	0.720	0.000
0.900	−1742	1275	3.102	887	0.399	0.000
1.000	0	0	0.000	0	0.000	0.000

Reference states: Al(liquid), Sn(liquid)

Table IIIb. Partial quantities for Al in the liquid phase at 973 K.

x_{Al}	ΔG_{Al} [J/mol]	ΔH_{Al} [J/mol]	ΔS_{Al} [J/(mol·K)]	G^E_{Al} [J/mol]	S^E_{Al} [J/(mol·K)]	a_{Al}	γ_{Al}
1.000	0	0	0.000	0	0.000	1.000	1.000
0.900	−617	332	0.976	235	0.100	0.927	1.029
0.800	−973	1176	2.208	833	0.353	0.887	1.108
0.700	−1229	2339	3.667	1657	0.701	0.859	1.227
0.600	−1525	3681	5.350	2608	1.103	0.828	1.380
0.500	−1989	5110	7.297	3618	1.534	0.782	1.564
0.400	−2755	6589	9.603	4658	1.985	0.711	1.778
0.300	−4010	8128	12.475	5730	2.465	0.609	2.030
0.200	−6148	9789	16.379	6872	2.998	0.468	2.338
0.100	−10469	11686	22.770	8159	3.625	0.274	2.741
0.000	−∞	13983	∞	9697	4.406	0.000	3.315

Reference state: Al(liquid)

Table IIIc. Partial quantities for Sn in the liquid phase at 973 K.

x_{Sn}	ΔG_{Sn} [J/mol]	ΔH_{Sn} [J/mol]	ΔS_{Sn} [J/(mol·K)]	G^E_{Sn} [J/mol]	S^E_{Sn} [J/(mol·K)]	a_{Sn}	γ_{Sn}
0.000	−∞	22207	∞	15680	6.708	0.000	6.946
0.100	−7561	15683	23.889	11067	4.745	0.393	3.927
0.200	−5382	10842	16.674	7638	3.292	0.514	2.571
0.300	−4597	7322	12.249	5143	2.239	0.567	1.888
0.400	−4047	4813	9.106	3365	1.487	0.606	1.516
0.500	−3485	3054	6.721	2122	0.958	0.650	1.300
0.600	−2865	1839	4.834	1267	0.587	0.702	1.170
0.700	−2198	1007	3.294	688	0.328	0.762	1.089
0.800	−1499	452	2.006	306	0.150	0.831	1.039
0.900	−773	119	0.916	80	0.040	0.909	1.010
1.000	0	0	0.000	0	0.000	1.000	1.000

Reference state: Sn(liquid)

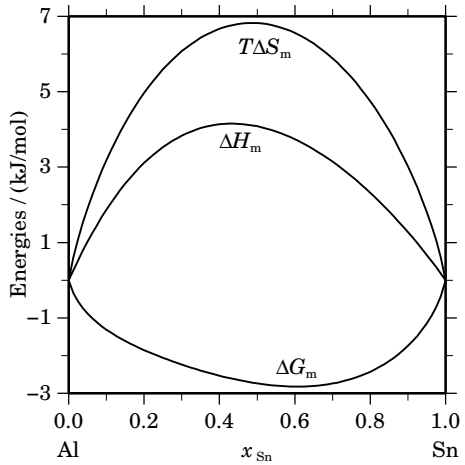

Fig. 3. Integral quantities of the liquid phase at T=973 K.

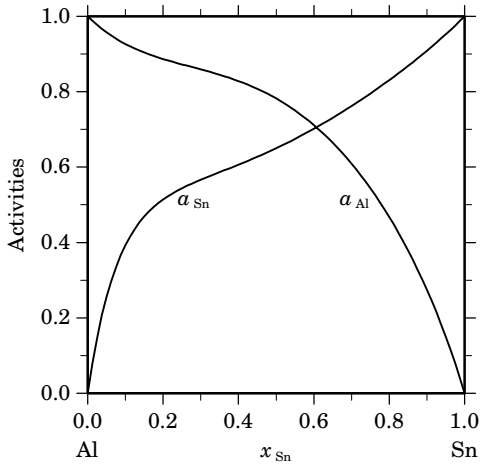

Fig. 4. Activities in the liquid phase at T=973 K.

References

[1906Gwy] A.C.G. Gwyer: Z. Anorg. Allg. Chem. **49** (1906) 311–316.
[1930Kaw] M. Kawakami: Sci. Rep. Res. Inst. Tohoku Univ. **19** (1930) 521–549.
[1949Sul] A.H. Sully, H.K. Hardy, T.J. Heal: J. Inst. Met. **76** (1949) 269–294.
[1958Oel] W. Oelsen, P. Zuhlke, O. Oelsen: Arch. Eisenhüttenwes. **29** (1958) 799–805.
[1963Wit] F.E. Wittig, G. Keil: Z. Metallkd. **54** (1963) 576–590.
[1964Bon] E. Bonnier, F. Durand, G. Massart: C. R. Acad. Sci. Paris **259** (1964) 380–383; G. Massart, F. Durand, E. Bonnier: Bull. Soc. Chim. Fr. **1** (1965) 87–90.
[1966Tik] A.A. Tikhomorov, I.T. Svyvalim, D.A. Esim, B.M. Lepinskikh: Izv. V.U.Z. Tsvetn. Metall. **4** (1966) 22-27.
[1968Bat] G.I. Batalin, E.A. Beloborodova, L.A. Kyachko: Ukr. Khim. Zh. **34** (1968) 663–669.
[1969Lee] Y.K. Lee, A. Yazawa: J. Jpn. Inst. Met. **33** (1969) 323–328.
[1976Dor] R.C. Dorward: Metall. Trans. A **7A** (1976) 308–310.
[1983McA] A.J. McAlister, D.J. Kahan: Bull. Alloy Phase Diagrams **4** (1983) 410–414.
[1998Fri] S.G. Fries, H.L. Lukas in: I. Ansara, A.T. Dinsdale, M.H. Rand (eds.): COST 507, "Thermochemical database for light metal alloys", Vol. 2, EUR 18499, 1998, 81–82.
[2003Luk] H.L. Lukas, unpublished work, 2003.

Al – Sr (Aluminium – Strontium)

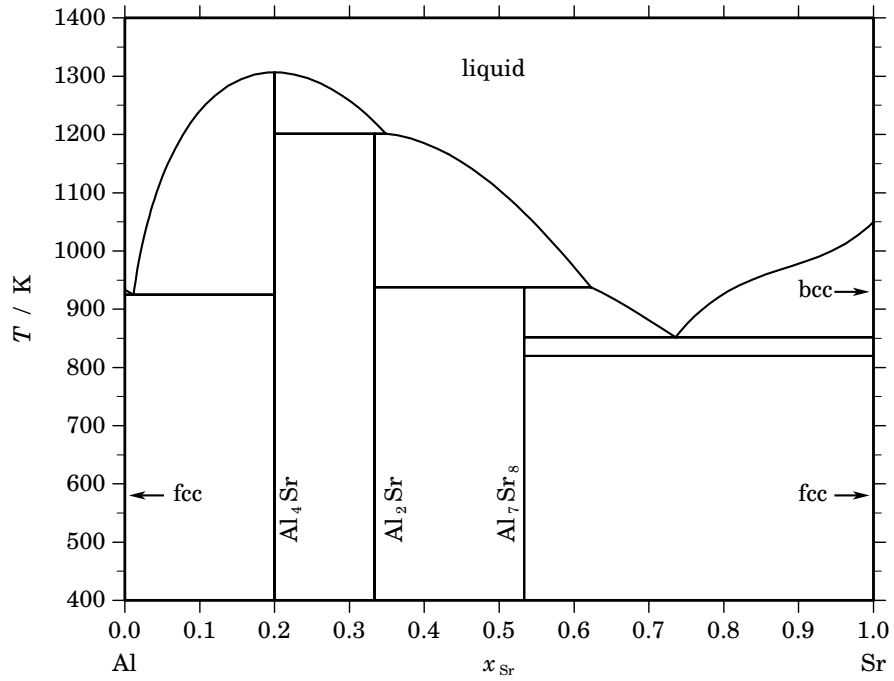

Fig. 1. Calculated phase diagram for the system Al-Sr.

Small amounts of strontium are added to Al-Si alloys in order to improve their eutectic microstructure. For this purpose, aluminium-strontium master alloys are used with Sr-concentrations up to 90%. Reviews and thermodynamical assessments for the Al-Sr system have been prepared by [1989Gsc, 2003Wan] the latter dataset being selected here. The optimisation is based on investigations of the phase diagram from the literature which are well reproduced within the scatter of data between the various literature sources. The thermodynamics of the liquid has been evaluated throughout the whole composition range using data for the mixing enthalpy and the activity of Sr at several temperatures. In lack of experimental data for the thermodynamics of the three intermetallic compounds, results for the enthalpy of formation from first-principle calculations have been used in the optimisation. The dataset should not be used at too high temperatures because an artificial inverse miscibility gap opens in the liquid above 3100 K.

Table I. Phases, structures and models.

Phase	Struktur-bericht	Prototype	Pearson symbol	Space group	SGTE name	Model
liquid					LIQUID	$(Al,Sr)_1$
fcc	$A1$	Cu	$cF4$	$Fm\bar{3}m$	FCC_A1	$(Al,Sr)_1$
Al_4Sr	$D1_3$	Al_4Ba	$tI10$	$I4/mmm$	D13_AL4SR	Al_4Sr_1
Al_2Sr	···	$CeCu_2$	$oI12$	$Imma$	AL2SR	Al_2Sr_1
Al_7Sr_8	···	Al_7Sr_8	$cP60$	$P2_13$	AL7SR8	Al_7Sr_8
bcc	$A2$	W	$cI2$	$Im\bar{3}m$	BCC_A2	$(Al,Sr)_1$

Table II. Invariant reactions.

Reaction	Type	T / K	Compositions / x_{Sr}			$\Delta_{\mathrm{r}}H$ / (J/mol)
liquid $\rightleftharpoons$ Al_4Sr	congruent	1306.7	0.200	0.200		−20921
Al_4Sr + liquid $\rightleftharpoons$ Al_2Sr	peritectic	1201.3	0.200	0.349	0.333	−19401
Al_2Sr + liquid $\rightleftharpoons$ Al_7Sr_8	peritectic	937.6	0.333	0.623	0.533	−7067
liquid $\rightleftharpoons$ fcc + Al_4Sr	eutectic	924.7	0.012	0.000	0.200	−10987
liquid $\rightleftharpoons$ Al_7Sr_8 + bcc	eutectic	851.9	0.736	0.533	1.000	−8737
bcc $\rightleftharpoons$ Al_7Sr_8 + fcc	eutectoid	820.0	1.000	0.533	1.000	−837

Table IIIa. Integral quantities for the liquid phase at 1400 K.

x_{Sr}	ΔG_{m} [J/mol]	ΔH_{m} [J/mol]	ΔS_{m} [J/(mol·K)]	$G^{\mathrm{E}}_{\mathrm{m}}$ [J/mol]	$S^{\mathrm{E}}_{\mathrm{m}}$ [J/(mol·K)]	ΔC_P [J/(mol·K)]
0.000	0	0	0.000	0	0.000	0.000
0.100	−6688	−9102	−1.724	−2904	−4.427	0.000
0.200	−10614	−15292	−3.341	−4789	−7.502	0.000
0.300	−12857	−18767	−4.221	−5747	−9.300	0.000
0.400	−13732	−19805	−4.338	−5897	−9.934	0.000
0.500	−13457	−18758	−3.787	−5388	−9.550	0.000
0.600	−12227	−16056	−2.735	−4393	−8.331	0.000
0.700	−10224	−12206	−1.416	−3114	−6.495	0.000
0.800	−7604	−7793	−0.135	−1779	−4.296	0.000
0.900	−4431	−3478	0.680	−647	−2.022	0.000
1.000	0	0	0.000	0	0.000	0.000

Reference states: Al(liquid), Sr(liquid)

Table IIIb. Partial quantities for Al in the liquid phase at 1400 K.

x_{Al}	ΔG_{Al} [J/mol]	ΔH_{Al} [J/mol]	ΔS_{Al} [J/(mol·K)]	$G^{\mathrm{E}}_{\mathrm{Al}}$ [J/mol]	$S^{\mathrm{E}}_{\mathrm{Al}}$ [J/(mol·K)]	a_{Al}	γ_{Al}
1.000	0	0	0.000	0	0.000	1.000	1.000
0.900	−1749	−1483	0.190	−523	−0.686	0.860	0.956
0.800	−4579	−5705	−0.805	−1981	−2.660	0.675	0.843
0.700	−8302	−12154	−2.752	−4150	−5.717	0.490	0.700
0.600	−12668	−20085	−5.298	−6722	−9.545	0.337	0.561
0.500	−17375	−28521	−7.962	−9306	−13.725	0.225	0.450
0.400	−22098	−36257	−10.114	−11432	−17.732	0.150	0.375
0.300	−26558	−41852	−10.924	−12544	−20.935	0.102	0.340
0.200	−30741	−43639	−9.213	−12006	−22.595	0.071	0.356
0.100	−35904	−39714	−2.722	−9101	−21.867	0.046	0.458
0.000	$-\infty$	−27947	∞	−3027	−17.800	0.000	0.771

Reference state: Al(liquid)

Table IIIc. Partial quantities for Sr in the liquid phase at 1400 K.

x_{Sr}	ΔG_{Sr} [J/mol]	ΔH_{Sr} [J/mol]	ΔS_{Sr} [J/(mol·K)]	$G^{\mathrm{E}}_{\mathrm{Sr}}$ [J/mol]	$S^{\mathrm{E}}_{\mathrm{Sr}}$ [J/(mol·K)]	a_{Sr}	γ_{Sr}
0.000	$-\infty$	−106053	∞	−34373	−51.200	0.000	0.052
0.100	−51138	−77674	−18.954	−24335	−38.099	0.012	0.124
0.200	−34753	−53636	−13.488	−16019	−26.870	0.051	0.253
0.300	−23486	−34198	−7.651	−9472	−17.662	0.133	0.443
0.400	−15327	−19386	−2.899	−4661	−10.518	0.268	0.670
0.500	−9538	−8995	0.388	−1470	−5.375	0.441	0.881
0.600	−5646	−2589	2.184	300	−2.063	0.616	1.026
0.700	−3224	499	2.659	928	−0.306	0.758	1.083
0.800	−1820	1168	2.134	777	0.279	0.855	1.069
0.900	−934	548	1.058	292	0.182	0.923	1.025
1.000	0	0	0.000	0	0.000	1.000	1.000

Reference state: Sr(liquid)

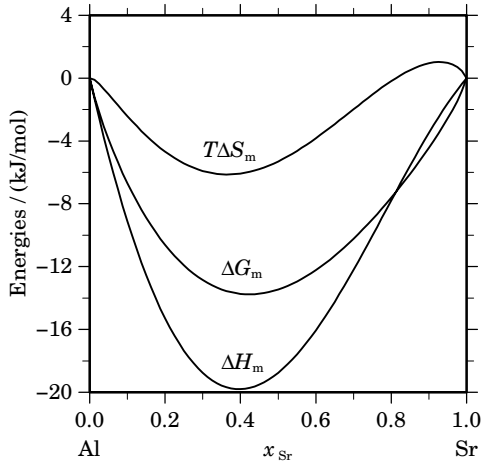

Fig. 2. Integral quantities of the liquid phase at T=1400 K.

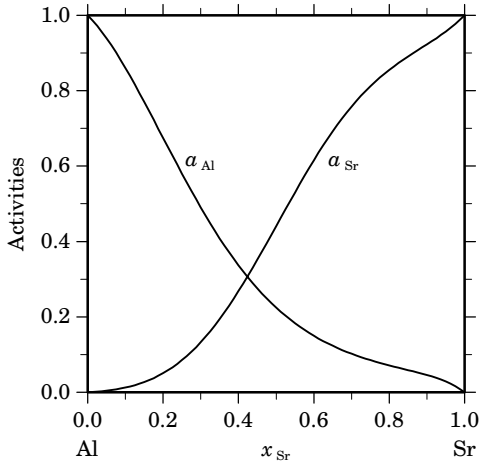

Fig. 3. Activities in the liquid phase at T=1400 K.

Table IV. Standard reaction quantities at 298.15 K for the compounds per mole of atoms.

Compound	x_{Sr}	$\Delta_{\mathrm{f}}G^{\circ}$ / (J/mol)	$\Delta_{\mathrm{f}}H^{\circ}$ / (J/mol)	$\Delta_{\mathrm{f}}S^{\circ}$ / (J/(mol·K))	$\Delta_{\mathrm{f}}C^{\circ}_{P}$ / (J/(mol·K))
Al_4Sr_1	0.200	−23484	−26069	−8.670	0.000
Al_2Sr_1	0.333	−27361	−30903	−11.880	0.000
Al_7Sr_8	0.533	−19291	−21385	−7.020	0.000

References

[1989Gsc] K.A. Gschneidner Jr., F.W. Calderwood: Bull. Alloy Phase Diagrams **10** (1989) 34–36.
[2003Wan] C. Wang, Z. Jin, Y. Du: J. Alloys Comp. **358** (2003) 288–293.

Au – B (Gold – Boron)

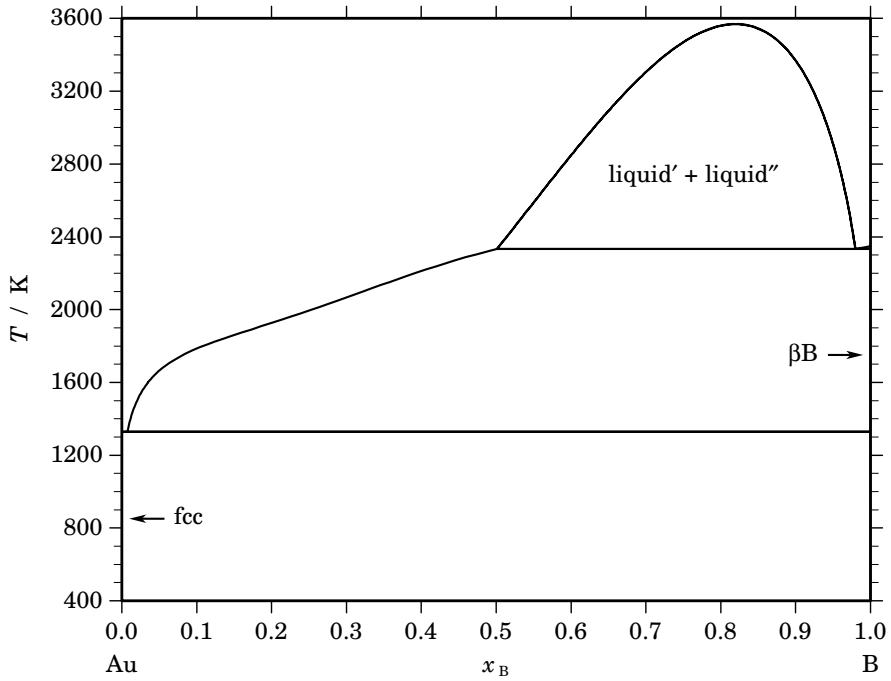

Fig. 1. Calculated phase diagram for the system Au-B.

The Au-B binary system was assessed by Chevalier [1998Che]. The phase diagram reported in the compilation of Moffatt [1981Mof] is based on the investigations of Wald and Stormont [1965Wal] using X-ray analysis, optical metallography, and thermal analysis. The compound AuB_2 previously reported by Elliott [1965Ell] could not be confirmed. An eutectic reaction deported on the gold side, was determined at 1329 K and less than 5 at.% B. A liquid miscibility gap is believed to exist at compositions of more than 50 at.% B, with a monotectic reaction at about 15 K below the melting point of boron, which has been given at 2498 K [1981Mof]. However, in the optimisation [1998Che] the recommended melting temperature for boron of 2348 K [91Din] has been used and consequently the calculated monotectic temperature is located 15 K lower at 2333 K. No mutual solubility of both elements is known in the solid state and no thermodynamic properties are available for that system.

Table I. Phases, structures and models.

Phase	Struktur-bericht	Prototype	Pearson symbol	Space group	SGTE name	Model
liquid					LIQUID	$(Au,B)_1$
fcc	$A1$	Cu	$cF4$	$Fm\bar{3}m$	FCC_A1	$Au_1(B,\Box)_1$
βB	$\cdots$	βB	$hR105$	$R\bar{3}m$	BETA_RHOMBO_B	$B_{93}B_{12}$

Table II. Invariant reactions.

Reaction	Type	T / K	Compositions / x_B			$\Delta_r H$ / (J/mol)
liquid $\rightleftharpoons$ liquid′ + liquid″	critical	3560.0	0.819	0.819	0.819	0
liquid″ $\rightleftharpoons$ liquid′ + βB	monotectic	2333.0	0.501	0.980	1.000	−49219
liquid′ $\rightleftharpoons$ fcc + βB	eutectic	1328.8	0.000	0.008	1.000	−13079

Table IIIa. Integral quantities for the liquid phase at 2000 K.

x_{B}	ΔG_{m} [J/mol]	ΔH_{m} [J/mol]	ΔS_{m} [J/(mol·K)]	$G^{\mathrm{E}}_{\mathrm{m}}$ [J/mol]	$S^{\mathrm{E}}_{\mathrm{m}}$ [J/(mol·K)]	ΔC_P [J/(mol·K)]
0.000	0	0	0.000	0	0.000	0.000
0.100	−1953	7689	4.821	3453	2.118	0.149
0.200	−2312	14483	8.397	6009	4.237	0.297
0.253	−2239	17903	10.071	7172	5.366	0.376

Reference states: Au(liquid), B(βB)

Table IIIb. Partial quantities for Au in the liquid phase at 2000 K.

x_{Au}	ΔG_{Au} [J/mol]	ΔH_{Au} [J/mol]	ΔS_{Au} [J/(mol·K)]	$G^{\mathrm{E}}_{\mathrm{Au}}$ [J/mol]	$S^{\mathrm{E}}_{\mathrm{Au}}$ [J/(mol·K)]	a_{Au}	γ_{Au}
1.000	0	0	0.000	0	0.000	1.000	1.000
0.900	−1212	541	0.876	541	0.000	0.930	1.033
0.800	−2256	1455	1.855	1455	0.000	0.873	1.091
0.747	−2999	1858	2.429	1858	0.000	0.835	1.118

Reference state: Au(liquid)

Table IIIc. Partial quantities for B in the liquid phase at 2000 K.

x_{B}	ΔG_{B} [J/mol]	ΔH_{B} [J/mol]	ΔS_{B} [J/(mol·K)]	$G^{\mathrm{E}}_{\mathrm{B}}$ [J/mol]	$S^{\mathrm{E}}_{\mathrm{B}}$ [J/(mol·K)]	a_{B}	γ_{B}
0.000	$-\infty$	83388	∞	41022	21.183	0.000	11.786
0.100	−8628	72028	40.328	29662	21.183	0.595	5.952
0.200	−2535	66595	34.565	24228	21.183	0.859	4.293
0.253	0	65201	32.600	22834	21.183	1.000	3.948

Reference state: B(βB)

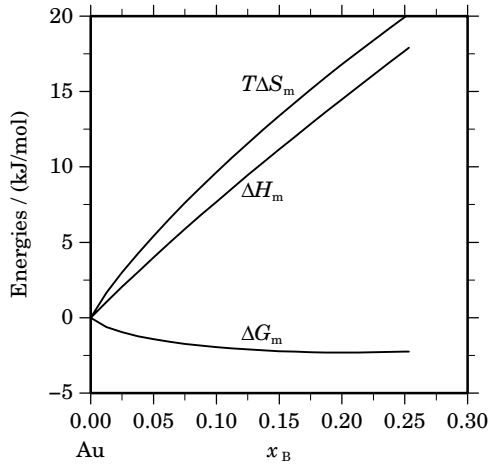

Fig. 2. Integral quantities of the liquid phase at T=2000 K.

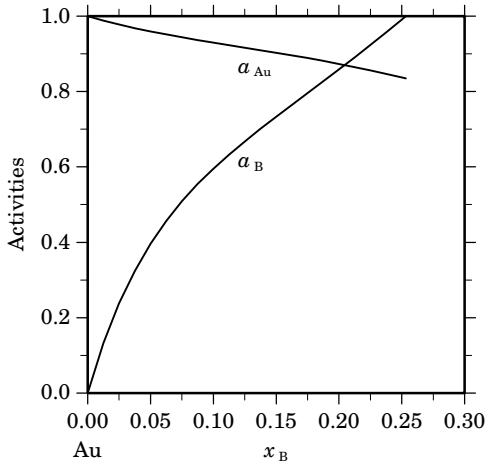

Fig. 3. Activities in the liquid phase at T=2000 K.

References

[1965Ell] R.P. Elliott, “Constitution of Binary Alloys”, 1st Suppl., McGraw-Hill, New-York, 1965.
[1965Wal] F. Wald, R. W. Stormont: J. Less-Common Met. **9** (1965) 423–433.
[1981Mof] W.G. Moffatt, “The Handbook of Binary Phase Diagrams”, General Electric Corp. (1981).
[1991Din] A.T. Dinsdale: Calphad **15** (1991) 317–425.
[1998Che] P.-Y. Chevalier, unpublished work, 1998.

Au – Co (Gold – Cobalt)

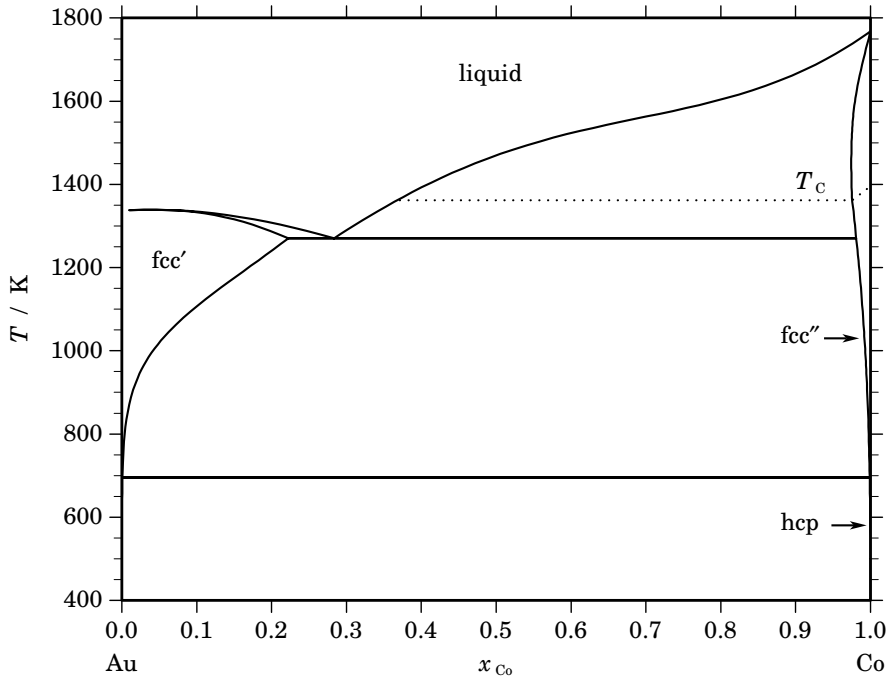

Fig. 1. Calculated phase diagram for the system Au-Co.

The equilibrium phases of the Au-Co system are: the liquid, the fcc solid solution which is separated by a large miscibility gap into a gold-rich phase dissolving up to 22 at.% Co and a Co-rich phase with an Au-solubility of less than 2 at.%, and the hcp-Co based phase containing less than 0.05 at.% Au. The thermodynamic descriptions for the Au-Co system has been obtained by Korb [2004Kor]. The assessed phase boundaries are based mainly on the experimental data of [1950Rau] and [1984Tas]. The liquidus boundary in equilibrium with Co-rich alloys is based on the results of [1984Tas]. The calculated phase diagram is in good agreement with the critical review of [1987Oka].

Table I. Phases, structures and models.

Phase	Struktur-bericht	Prototype	Pearson symbol	Space group	SGTE name	Model
liquid					LIQUID	$(Au,Co)_1$
fcc	$A1$	Cu	$cF4$	$Fm\bar{3}m$	FCC_A1	$(Au,Co)_1$
hcp	$A3$	Mg	$hP2$	$P6_3/mmc$	HCP_A3	$(Au,Co)_1$

Table II. Invariant reactions.

Reaction	Type	T / K	Compositions / x_{Co}			$\Delta_r H$ / (J/mol)
liquid $\rightleftharpoons$ fcc′ + fcc″	eutectic	1270.7	0.284	0.222	0.981	−7702
fcc′ + fcc″ $\rightleftharpoons$ hcp	peritectoid	695.4	0.001	0.999	0.999	−422

Table IIIa. Integral quantities for the liquid phase at 1800 K.

x_{Co}	ΔG_{m} [J/mol]	ΔH_{m} [J/mol]	ΔS_{m} [J/(mol·K)]	$G_{\mathrm{m}}^{\mathrm{E}}$ [J/mol]	$S_{\mathrm{m}}^{\mathrm{E}}$ [J/(mol·K)]	ΔC_P [J/(mol·K)]
0.000	0	0	0.000	0	0.000	0.000
0.100	−4152	1527	3.155	714	0.452	0.000
0.200	−5963	2754	4.843	1526	0.682	0.000
0.300	−6802	3667	5.816	2340	0.737	0.000
0.400	−7013	4250	6.257	3060	0.661	0.000
0.500	−6785	4490	6.264	3589	0.500	0.000
0.600	−6242	4370	5.895	3831	0.299	0.000
0.700	−5453	3876	5.183	3689	0.104	0.000
0.800	−4421	2993	4.119	3068	−0.042	0.000
0.900	−2995	1706	2.612	1870	−0.091	0.000
1.000	0	0	0.000	0	0.000	0.000

Reference states: Au(liquid), Co(liquid)

Table IIIb. Partial quantities for Au in the liquid phase at 1800 K.

x_{Au}	ΔG_{Au} [J/mol]	ΔH_{Au} [J/mol]	ΔS_{Au} [J/(mol·K)]	$G_{\mathrm{Au}}^{\mathrm{E}}$ [J/mol]	$S_{\mathrm{Au}}^{\mathrm{E}}$ [J/(mol·K)]	a_{Au}	γ_{Au}
1.000	0	0	0.000	0	0.000	1.000	1.000
0.900	−1642	147	0.994	−65	0.118	0.896	0.996
0.800	−3472	609	2.267	−132	0.412	0.793	0.991
0.700	−5347	1415	3.757	−9	0.791	0.700	0.999
0.600	−7147	2595	5.412	498	1.165	0.620	1.034
0.500	−8793	4178	7.206	1581	1.443	0.556	1.111
0.400	−10280	6196	9.154	3433	1.535	0.503	1.258
0.300	−11772	8677	11.361	6247	1.350	0.455	1.518
0.200	−13872	11652	14.180	10215	0.799	0.396	1.979
0.100	−18931	15151	18.934	15530	−0.211	0.282	2.823
0.000	$-\infty$	19202	∞	22385	−1.768	0.000	4.463

Reference state: Au(liquid)

Table IIIc. Partial quantities for Co in the liquid phase at 1800 K.

x_{Co}	ΔG_{Co} [J/mol]	ΔH_{Co} [J/mol]	ΔS_{Co} [J/(mol·K)]	$G_{\mathrm{Co}}^{\mathrm{E}}$ [J/mol]	$S_{\mathrm{Co}}^{\mathrm{E}}$ [J/(mol·K)]	a_{Co}	γ_{Co}
0.000	$-\infty$	16714	∞	6324	5.772	0.000	1.526
0.100	−26736	13941	22.599	7724	3.454	0.168	1.676
0.200	−15928	11334	15.146	8159	1.764	0.345	1.725
0.300	−10198	8921	10.622	7821	0.611	0.506	1.686
0.400	−6811	6734	7.525	6902	−0.094	0.634	1.586
0.500	−4777	4801	5.321	5596	−0.442	0.727	1.453
0.600	−3550	3152	3.723	4096	−0.524	0.789	1.315
0.700	−2745	1818	2.535	2593	−0.431	0.832	1.189
0.800	−2059	828	1.604	1281	−0.252	0.871	1.089
0.900	−1225	212	0.798	352	−0.078	0.921	1.024
1.000	0	0	0.000	0	0.000	1.000	1.000

Reference state: Co(liquid)

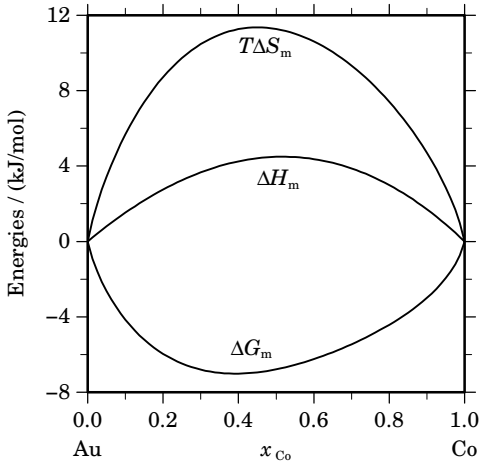

Fig. 2. Integral quantities of the liquid phase at T=1800 K.

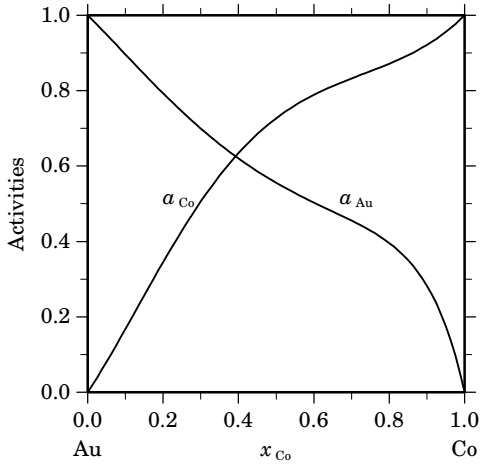

Fig. 3. Activities in the liquid phase at T=1800 K.

Table IVa. Integral quantities for the stable phases at 1270 K.

Phase	x_{Co}	ΔG_m [J/mol]	ΔH_m [J/mol]	ΔS_m [J/(mol·K)]	G_m^E [J/mol]	S_m^E [J/(mol·K)]	ΔC_P [J/(mol·K)]
fcc′	0.000	0	0	0.000	0	0.000	0.000
	0.100	−1838	6193	6.323	1595	3.620	−1.404
	0.200	−2067	10445	9.852	3217	5.692	−2.806
	0.222	−2027	11142	10.369	3562	5.968	−3.113
fcc″	0.981	−225	925	0.905	782	0.113	1.395
	1.000	0	0	0.000	0	0.000	0.000

Reference states: Au(fcc), Co(fcc)

Table IVb. Partial quantities for Au in the stable phases at 1270 K.

Phase	x_{Au}	ΔG_{Au} [J/mol]	ΔH_{Au} [J/mol]	ΔS_{Au} [J/(mol·K)]	G_{Au}^E [J/mol]	S_{Au}^E [J/(mol·K)]	a_{Au}	γ_{Au}
fcc′	1.000	0	0	0.000	0	0.000	1.000	1.000
	0.900	−1149	1012	1.701	−37	0.825	0.897	0.997
	0.800	−2319	3714	4.751	37	2.895	0.803	1.003
	0.778	−2554	4482	5.540	95	3.455	0.785	1.009
fcc″	0.019	−2554	48730	40.382	39130	7.559	0.785	40.679
	0.000	$-\infty$	47080	∞	41882	4.093	0.000	52.791

Reference state: Au(fcc)

Table IVc. Partial quantities for Co in the stable phases at 1270 K.

Phase	x_{Co}	ΔG_{Co} [J/mol]	ΔH_{Co} [J/mol]	ΔS_{Co} [J/(mol·K)]	$G^{\mathrm{E}}_{\mathrm{Co}}$ [J/mol]	$S^{\mathrm{E}}_{\mathrm{Co}}$ [J/(mol·K)]	a_{Co}	γ_{Co}
fcc′	0.000	$-\infty$	72457	∞	15352	44.965	0.000	4.280
	0.100	−8039	52821	47.922	16275	28.777	0.467	4.670
	0.200	−1059	37370	30.259	15935	16.878	0.905	4.523
	0.222	−179	34495	27.303	15719	14.784	0.983	4.431
fcc″	0.981	−179	−16	0.128	27	−0.034	0.983	1.003
	1.000	0	0	0.000	0	0.000	1.000	1.000

Reference state: Co(fcc)

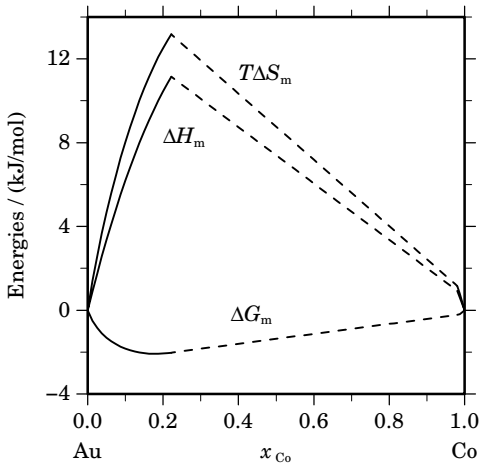

Fig. 4. Integral quantities of the stable phases at T=1270 K.

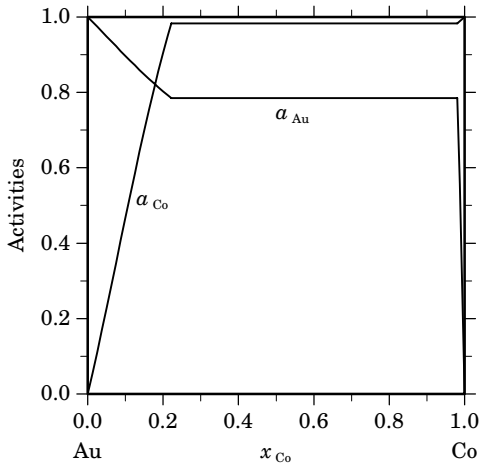

Fig. 5. Activities in the stable phases at T=1270 K.

References

[1950Rau] E. Raub, P. Walter: Z. Metallkd. **41** (1950) 234–238.
[1963Kle] W. Klement, Jr.: Trans. Metall. AIME **227** (1963) 965–970.
[1966Fuj] S. Fujime: Jpn. J. Appl. Phys. **5** (1966) 739–740.
[1983Liu] B.X. Liu, M.A. Nicolet: Thin Solid Films **101** (1983) 201–206.
[1984Tas] P. Taskinen: Scand. J. Metall. **13** (1984) 39–45.
[1987Oka] H. Okamoto, T.B. Massalski, M. Hasebe, T. Nishizawa in: Phase Diagrams of Binary Gold Alloys, H. Okamoto, T.B. Massalski (eds.), ASM, Metals Park, Ohio, 1987, 63–68.
[2004Kor] J. Korb, unpublished assessment, GTT-Technologies, 2004.

Au – Hf (Gold – Hafnium)

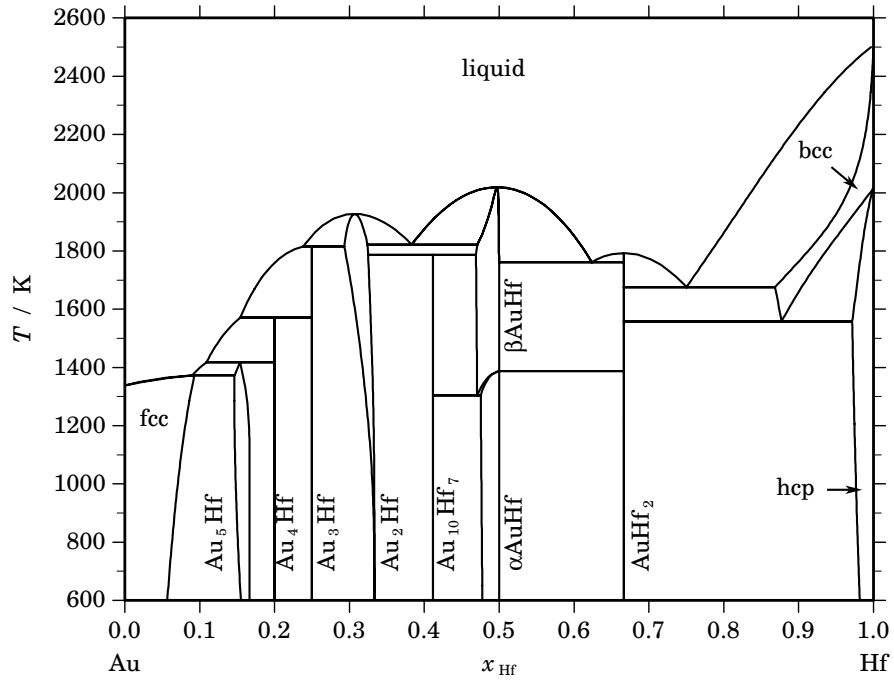

Fig. 1. Calculated phase diagram for the system Au-Hf.

The Au-Hf system has been reviewed in [1984Oka, 2000Oka, 2003Du] and a thermodynamic dataset has been optimised in [2003Du]. The assessment is based mainly on investigations of the phase diagram by [2000Lom] using differential thermal analysis, x-ray diffraction, and electron microprobe analysis. Seven intermetallic compounds have been identified in agreement with previous studies of the phase diagram by [1962Sto]. The enthalpies of formation of the compounds Au_3Hf, Au_2Hf, AuHf and $AuHf_2$ have been determined by [1992Fit]. The terminal solid solutions bcc, hcp, fcc and the liquid phase were described by substitutional solution models using Redlich-Kister polynomials. The three intermetallic compounds Au_5Hf, Au_2Hf, αAuHf and βAuHf with certain homogeneity ranges were treated by two-sublattice models with Au and Hf in one sublattice and the other filled with Au only. The four other compounds Au_4Hf, Au_3Hf, $Au_{10}Hf_7$, $AuHf_2$ were considered as stoichiometric. Satisfactory agreement is obtained between the calculated and experimental data.

Table I. Phases, structures and models.

Phase	Struktur-bericht	Prototype	Pearson symbol	Space group	SGTE name	Model
liquid					LIQUID	$(Au,Hf)_1$
fcc	$A1$	Cu	$cF4$	$Fm\overline{3}m$	FCC_A1	$(Au,Hf)_1$
Au_5Hf	$D1_a$	$MoNi_4$	$tI10$	$I4/m$	AU5HF	$Au_5(Au,Hf)_1$
Au_4Hf	$\cdots$	Au_4Zr	$oP20$	$Pnma$	AU4HF	Au_4Hf_1
Au_3Hf	$D0_a$	βCu_3Ti	$oP8$	$Pmmn$	AU3HF	Au_3Hf_1
Au_2Hf	$C11_b$	$MoSi_2$	$tI6$	$I4/mmm$	AU2HF	$Au_2(Au,Hf)_1$
$Au_{10}Hf_7$	$\cdots$	$Ni_{10}Zr_7$	$oC68$	$C2ca$	AU10HF7	$Au_{10}Hf_7$
αAuHf	$B11$	γCuTi	$tP4$	$P4/nmm$	AUHF_ALPHA	$Au_1(Au,Hf)_1$
βAuHf	$\cdots$	$\cdots$	$\cdots$	$\cdots$	AUHF_BETA	$Au_1(Au,Hf)_1$
$AuHf_2$	$C11_b$	$MoSi_2$	$tI6$	$I4/mmm$	AUHF2	Au_1Hf_2
bcc	$A2$	W	$cI2$	$Im\overline{3}m$	BCC_A2	$(Au,Hf)_1$
hcp	$A3$	Mg	$hP2$	$P6_3/mmc$	HCP_A3	$(Au,Hf)_1$

Table II. Invariant reactions.

Reaction	Type	T / K	Compositions / x_{Hf}			$\Delta_r H$ / (J/mol)
liquid $\rightleftharpoons$ βAuHf	congruent	2019.4	0.497	0.497		−19153
liquid $\rightleftharpoons$ Au_2Hf	congruent	1927.4	0.307	0.307		−13252
liquid $\rightleftharpoons$ Au_2Hf + βAuHf	eutectic	1821.8	0.383	0.324	0.471	−14870
liquid + Au_2Hf $\rightleftharpoons$ Au_3Hf	peritectic	1815.4	0.238	0.293	0.250	−13909
liquid $\rightleftharpoons$ $AuHf_2$	congruent	1793.0	0.667	0.667		−15652
Au_2Hf + βAuHf $\rightleftharpoons$ $Au_{10}Hf_7$	peritectoid	1786.0	0.325	0.469	0.412	−3431
liquid $\rightleftharpoons$ βAuHf + $AuHf_2$	eutectic	1761.3	0.624	0.500	0.667	−15378
liquid $\rightleftharpoons$ $AuHf_2$ + bcc	eutectic	1675.8	0.750	0.667	0.868	−14897
liquid + Au_3Hf $\rightleftharpoons$ Au_4Hf	peritectic	1570.9	0.154	0.250	0.200	−11984
bcc $\rightleftharpoons$ $AuHf_2$ + hcp	eutectoid	1558.3	0.877	0.667	0.971	−5377
liquid + Au_4Hf $\rightleftharpoons$ Au_5Hf	peritectic	1418.1	0.109	0.200	0.154	−11632
βAuHf + $AuHf_2$ $\rightleftharpoons$ αAuHf	peritectoid	1386.9	0.500	0.667	0.500	−1117
liquid + Au_5Hf $\rightleftharpoons$ fcc	peritectic	1373.1	0.090	0.146	0.093	−12475
βAuHf $\rightleftharpoons$ $Au_{10}Hf_7$ + αAuHf	eutectoid	1304.0	0.471	0.412	0.475	−651

Table IIIa. Integral quantities for the liquid phase at 2573 K.

x_{Hf}	ΔG_{m} [J/mol]	ΔH_{m} [J/mol]	ΔS_{m} [J/(mol·K)]	$G_{\mathrm{m}}^{\mathrm{E}}$ [J/mol]	$S_{\mathrm{m}}^{\mathrm{E}}$ [J/(mol·K)]	ΔC_P [J/(mol·K)]
0.000	0	0	0.000	0	0.000	0.000
0.100	−13352	−28636	−5.940	−6397	−8.643	0.000
0.200	−22532	−48065	−9.923	−11826	−14.084	0.000
0.300	−29186	−59351	−11.724	−16118	−16.803	0.000
0.400	−33498	−63563	−11.685	−19101	−17.281	0.000
0.500	−35434	−61767	−10.234	−20605	−15.998	0.000
0.600	−34859	−55030	−7.839	−20461	−13.435	0.000
0.700	−31568	−44418	−4.994	−18499	−10.073	0.000
0.800	−25254	−30998	−2.232	−14548	−6.393	0.000
0.900	−15393	−15836	−0.172	−8439	−2.875	0.000
1.000	0	0	0.000	0	0.000	0.000

Reference states: Au(liquid), Hf(liquid)

Table IIIb. Partial quantities for Au in the liquid phase at 2573 K.

x_{Au}	ΔG_{Au} [J/mol]	ΔH_{Au} [J/mol]	ΔS_{Au} [J/(mol·K)]	$G_{\mathrm{Au}}^{\mathrm{E}}$ [J/mol]	$S_{\mathrm{Au}}^{\mathrm{E}}$ [J/(mol·K)]	a_{Au}	γ_{Au}
1.000	0	0	0.000	0	0.000	1.000	1.000
0.900	−2710	−4782	−0.805	−456	−1.681	0.881	0.979
0.800	−6823	−17705	−4.229	−2049	−6.085	0.727	0.909
0.700	−12752	−36636	−9.283	−5121	−12.248	0.551	0.787
0.600	−20940	−59442	−14.964	−10012	−19.211	0.376	0.626
0.500	−31890	−83990	−20.249	−17061	−26.012	0.225	0.450
0.400	−46212	−108145	−24.070	−26609	−31.689	0.115	0.288
0.300	−64754	−129775	−25.271	−38997	−35.281	0.048	0.162
0.200	−88995	−146746	−22.445	−54564	−35.827	0.016	0.078
0.100	−122910	−156925	−13.220	−73650	−32.365	0.003	0.032
0.000	$-\infty$	−158179	∞	−96597	−23.934	0.000	0.011

Reference state: Au(liquid)

Table IIIc. Partial quantities for Hf in the liquid phase at 2573 K.

x_{Hf}	ΔG_{Hf} [J/mol]	ΔH_{Hf} [J/mol]	ΔS_{Hf} [J/(mol·K)]	$G_{\mathrm{Hf}}^{\mathrm{E}}$ [J/mol]	$S_{\mathrm{Hf}}^{\mathrm{E}}$ [J/(mol·K)]	a_{Hf}	γ_{Hf}
0.000	$-\infty$	−335959	∞	−68244	−104.048	0.000	0.041
0.100	−109131	−243326	−52.155	−59871	−71.300	0.006	0.061
0.200	−85366	−169502	−32.700	−50935	−46.082	0.018	0.092
0.300	−67532	−112353	−17.420	−41775	−27.430	0.043	0.142
0.400	−52336	−69745	−6.766	−32734	−14.384	0.087	0.217
0.500	−38978	−39545	−0.220	−24149	−5.984	0.162	0.323
0.600	−27291	−19620	2.981	−16363	−1.266	0.279	0.465
0.700	−17345	−7836	3.696	−9714	0.730	0.445	0.635
0.800	−9318	−2060	2.821	−4544	0.965	0.647	0.809
0.900	−3447	−160	1.278	−1193	0.402	0.851	0.946
1.000	0	0	0.000	0	0.000	1.000	1.000

Reference state: Hf(liquid)

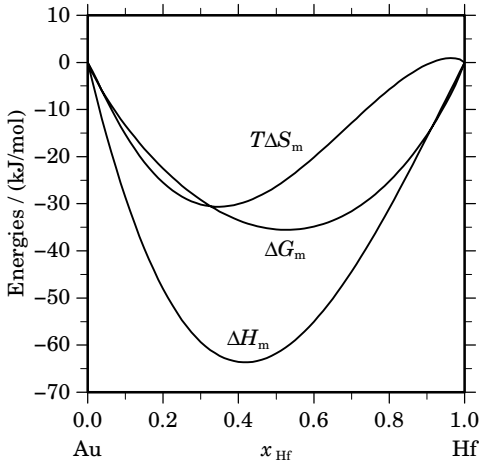

Fig. 2. Integral quantities of the liquid phase at T=2573 K.

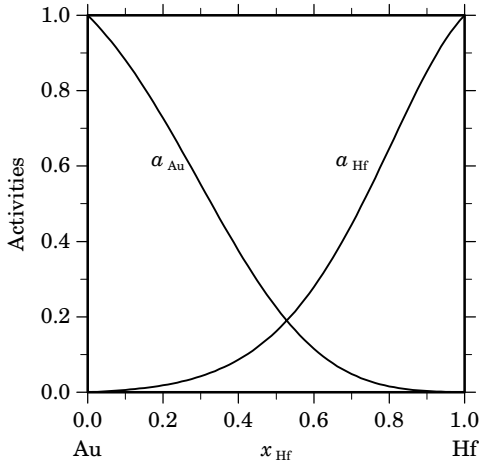

Fig. 3. Activities in the liquid phase at T=2573 K.

Table IV. Standard reaction quantities at 298.15 K for the compounds per mole of atoms.

Compound	x_{Hf}	$\Delta_f G^\circ$ / (J/mol)	$\Delta_f H^\circ$ / (J/mol)	$\Delta_f S^\circ$ / (J/(mol·K))	$\Delta_f C_P^\circ$ / (J/(mol·K))
Au_5Hf	0.167	−44927	−49061	−13.867	0.000
Au_4Hf_1	0.200	−47656	−51155	−11.738	0.000
Au_3Hf_1	0.250	−51314	−54301	−10.020	0.000
Au_2Hf	0.333	−56382	−59453	−10.299	0.000
$Au_{10}Hf_7$	0.412	−60171	−63666	−11.719	0.000
αAuHf	0.500	−58264	−61203	−9.858	0.000
βAuHf	0.500	−57386	−60085	−9.052	0.000
Au_1Hf_2	0.667	−39665	−40794	−3.784	0.000

References

[1962Sto] E. Stolz, K. Schubert: Z. Metallkd. **53** (1962) 433–444.
[1984Oka] H. Okamoto, T.B. Massalski: Bull. Alloy Phase Diagrams **5** (1984) 379–380.
[1992Fit] K. Fitzner, O.J. Kleppa: Metall. Trans. A **23A** (1992) 997–1003.
[2000Lom] M. Lomello-Tafin, P. Galez, P. Feschotte, J.L. Jorda: J. Alloys Comp. **296** (2000) 103–111.
[2000Oka] H. Okamoto: J. Phase Equilibria **21** (2000) 410.
[2003Du] Z. Du, L. Yang: J. Alloys Comp. **353** (2003) 213–216.

Au – Ni (Gold – Nickel)

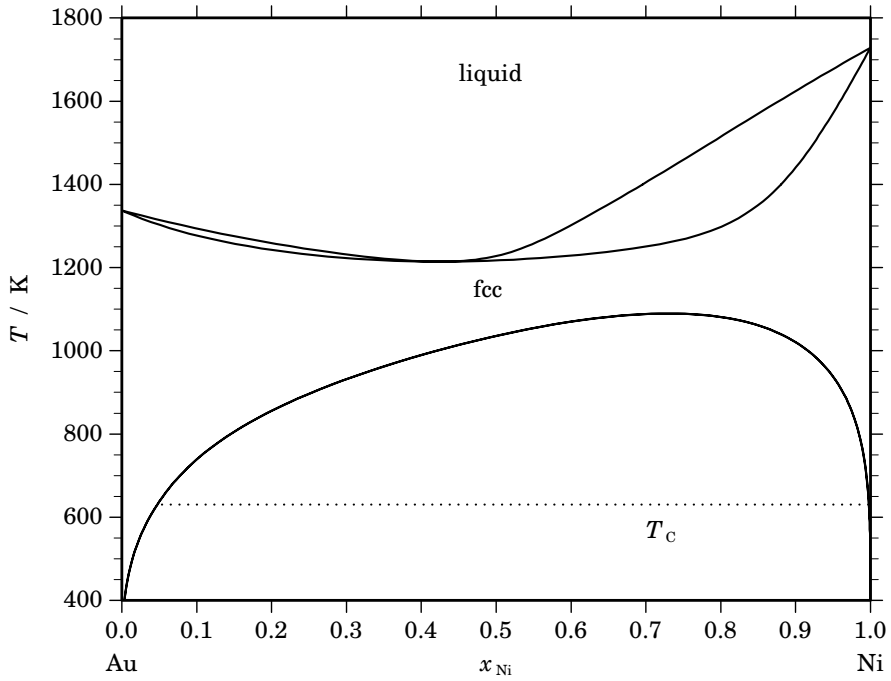

Fig. 1. Calculated phase diagram for the system Au-Ni.

Nickel is a common addition for improving the strength of gold alloys and these materials are frequently encountered in jewellery. A thorough review on the thermodynamics of the gold-nickel system has been given in [1991Oka] and a thermodynamic optimisation has been reported in [2005Wan]. The phase diagram consists of only two phases, the liquid and the the fcc solid solution phase which hosts a broad miscibility gap. The optimisation is based on many experimental investigations of Au-Ni alloys from the literature including phase equilibrium studies, calorimetric and EMF investigations of liquid and solid alloys, and experiments using Knudsen techniques.

Table I. Phases, structures and models.

Phase	Struktur-bericht	Prototype	Pearson symbol	Space group	SGTE name	Model
liquid					LIQUID	$(Au,Ni)_1$
fcc	$A1$	Cu	$cF4$	$Fm\bar{3}m$	FCC_A1	$(Au,Ni)_1$

Table II. Invariant reactions.

Reaction	Type	T / K	Compositions / x_{Ni}			$\Delta_r H$ / (J/mol)
liquid $\rightleftharpoons$ fcc	congruent	1214.3	0.424	0.424		−9990
fcc $\rightleftharpoons$ fcc′ + fcc″	critical	1089.2	0.713	0.713	0.713	0

Table IIIa. Integral quantities for the liquid phase at 1820 K.

x_{Ni}	ΔG_{m} [J/mol]	ΔH_{m} [J/mol]	ΔS_{m} [J/(mol·K)]	$G_{\mathrm{m}}^{\mathrm{E}}$ [J/mol]	$S_{\mathrm{m}}^{\mathrm{E}}$ [J/(mol·K)]	ΔC_P [J/(mol·K)]
0.000	0	0	0.000	0	0.000	0.000
0.100	−4837	971	3.192	82	0.489	0.000
0.200	−7478	1675	5.029	94	0.869	0.000
0.300	−9188	2131	6.219	56	1.140	0.000
0.400	−10198	2357	6.899	−14	1.303	0.000
0.500	−10584	2375	7.120	−95	1.357	0.000
0.600	−10353	2203	6.899	−169	1.303	0.000
0.700	−9459	1859	6.219	−216	1.140	0.000
0.800	−7788	1365	5.029	−216	0.869	0.000
0.900	−5070	739	3.192	−150	0.489	0.000
1.000	0	0	0.000	0	0.000	0.000

Reference states: Au(liquid), Ni(liquid)

Table IIIb. Partial quantities for Au in the liquid phase at 1820 K.

x_{Au}	ΔG_{Au} [J/mol]	ΔH_{Au} [J/mol]	ΔS_{Au} [J/(mol·K)]	$G_{\mathrm{Au}}^{\mathrm{E}}$ [J/mol]	$S_{\mathrm{Au}}^{\mathrm{E}}$ [J/(mol·K)]	a_{Au}	γ_{Au}
1.000	0	0	0.000	0	0.000	1.000	1.000
0.900	−1556	137	0.930	38	0.054	0.902	1.003
0.800	−3250	522	2.072	127	0.217	0.807	1.008
0.700	−5170	1116	3.454	227	0.489	0.711	1.015
0.600	−7429	1882	5.116	301	0.869	0.612	1.020
0.500	−10181	2779	7.120	308	1.357	0.510	1.021
0.400	−13654	3769	9.573	212	1.954	0.406	1.014
0.300	−18247	4813	12.671	−28	2.660	0.299	0.998
0.200	−24805	5873	16.856	−450	3.475	0.194	0.971
0.100	−35937	6911	23.542	−1093	4.397	0.093	0.930
0.000	$-\infty$	7886	∞	−1995	5.429	0.000	0.876

Reference state: Au(liquid)

Table IIIc. Partial quantities for Ni in the liquid phase at 1820 K.

x_{Ni}	ΔG_{Ni} [J/mol]	ΔH_{Ni} [J/mol]	ΔS_{Ni} [J/(mol·K)]	$G_{\mathrm{Ni}}^{\mathrm{E}}$ [J/mol]	$S_{\mathrm{Ni}}^{\mathrm{E}}$ [J/(mol·K)]	a_{Ni}	γ_{Ni}
0.000	$-\infty$	11114	∞	1233	5.429	0.000	1.085
0.100	−34368	8479	23.542	476	4.397	0.103	1.032
0.200	−24392	6287	16.856	−37	3.475	0.200	0.998
0.300	−18564	4497	12.671	−345	2.660	0.293	0.977
0.400	−14351	3071	9.573	−486	1.954	0.387	0.968
0.500	−10988	1972	7.120	−499	1.357	0.484	0.968
0.600	−8152	1158	5.116	−422	0.869	0.583	0.972
0.700	−5693	594	3.454	−296	0.489	0.686	0.981
0.800	−3534	238	2.072	−157	0.217	0.792	0.990
0.900	−1640	53	0.930	−46	0.054	0.897	0.997
1.000	0	0	0.000	0	0.000	1.000	1.000

Reference state: Ni(liquid)

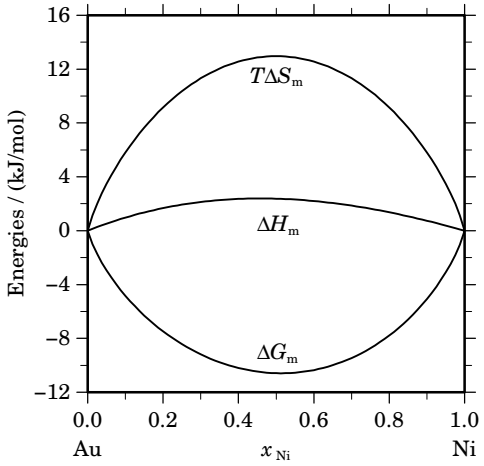

Fig. 2. Integral quantities of the liquid phase at T=1820 K.

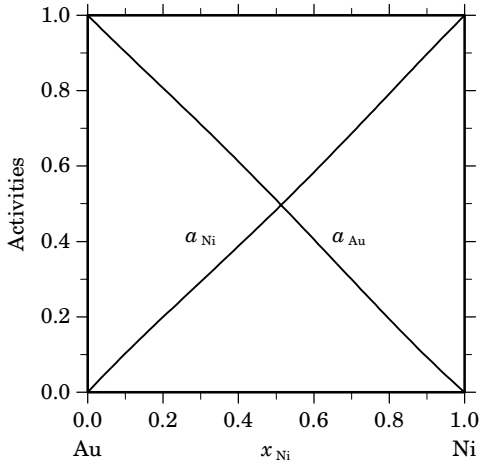

Fig. 3. Activities in the liquid phase at T=1820 K.

Table IVa. Integral quantities for the stable phases at 1150 K.

Phase	x_{Ni}	ΔG_m [J/mol]	ΔH_m [J/mol]	ΔS_m [J/(mol·K)]	G_m^E [J/mol]	S_m^E [J/(mol·K)]	ΔC_P [J/(mol·K)]
fcc	0.000	0	0	0.000	0	0.000	0.000
	0.100	−1825	1944	3.277	1283	0.575	−0.015
	0.200	−2492	3694	5.380	2292	1.219	−0.030
	0.300	−2775	5204	6.939	3066	1.860	−0.045
	0.400	−2818	6403	8.018	3617	2.422	−0.060
	0.500	−2691	7196	8.597	3937	2.833	−0.075
	0.600	−2445	7462	8.615	3990	3.019	−0.089
	0.700	−2122	7059	7.984	3719	2.905	−0.100
	0.800	−1745	5817	6.576	3039	2.415	−0.103
	0.900	−1264	3539	4.177	1844	1.474	−0.081
	1.000	0	0	0.000	0	0.000	0.000

Reference states: Au(fcc), Ni(fcc)

Table IVb. Partial quantities for Au in the stable phases at 1150 K.

Phase	x_{Au}	ΔG_{Au} [J/mol]	ΔH_{Au} [J/mol]	ΔS_{Au} [J/(mol·K)]	G_{Au}^E [J/mol]	S_{Au}^E [J/(mol·K)]	a_{Au}	γ_{Au}
fcc	1.000	0	0	0.000	0	0.000	1.000	1.000
	0.900	−862	91	0.829	145	−0.047	0.914	1.015
	0.800	−1615	414	1.765	519	−0.091	0.845	1.056
	0.700	−2331	1100	2.983	1079	0.018	0.784	1.119
	0.600	−3024	2349	4.673	1860	0.425	0.729	1.215
	0.500	−3662	4438	7.044	2966	1.280	0.682	1.364
	0.400	−4187	7715	10.350	4574	2.731	0.645	1.613
	0.300	−4576	12605	14.940	6936	4.929	0.620	2.066
	0.200	−5011	19616	21.415	10378	8.033	0.592	2.961
	0.100	−6715	29351	31.361	15302	12.216	0.495	4.955
	0.000	$-\infty$	42539	∞	22194	17.692	0.000	10.187

Reference state: Au(fcc)

Table IVc. Partial quantities for Ni in the stable phases at 1150 K.

Phase	x_{Ni}	ΔG_{Ni} [J/mol]	ΔH_{Ni} [J/mol]	ΔS_{Ni} [J/(mol·K)]	$G^{\mathrm{E}}_{\mathrm{Ni}}$ [J/mol]	$S^{\mathrm{E}}_{\mathrm{Ni}}$ [J/(mol·K)]	a_{Ni}	γ_{Ni}
fcc	0.000	$-\infty$	20313	∞	14391	5.150	0.000	4.504
	0.100	−10493	18621	25.316	11524	6.171	0.334	3.337
	0.200	−6001	16814	19.839	9388	6.458	0.534	2.669
	0.300	−3811	14782	16.168	7701	6.157	0.671	2.238
	0.400	−2508	12484	13.036	6253	5.418	0.769	1.923
	0.500	−1719	9953	10.150	4908	4.387	0.835	1.671
	0.600	−1283	7293	7.458	3601	3.211	0.874	1.457
	0.700	−1071	4682	5.002	2340	2.037	0.894	1.277
	0.800	−929	2367	2.866	1205	1.011	0.907	1.134
	0.900	−659	671	1.156	349	0.280	0.933	1.037
	1.000	0	0	0.000	0	0.000	1.000	1.000

Reference state: Ni(fcc)

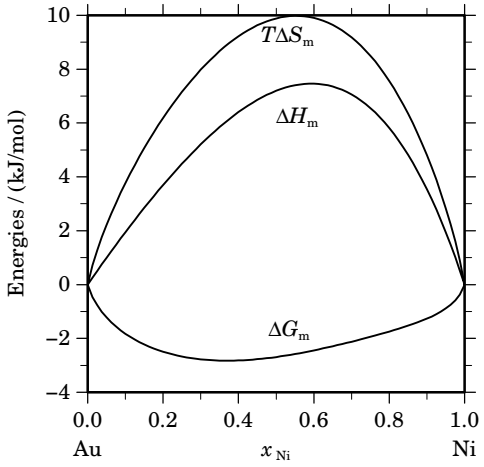

Fig. 4. Integral quantities of the stable phases at T=1150 K.

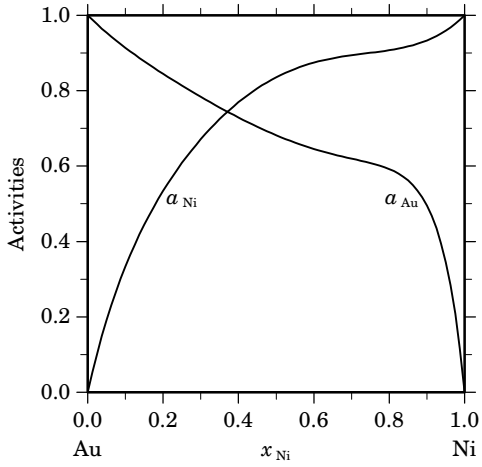

Fig. 5. Activities in the stable phases at T=1150 K.

References

[1991Oka] H. Okamoto, T.B. Massalski in: Phase Diagrams of Binary Nickel Alloys, P. Nash, Ed., ASM Intl., Materials Park, 1991, pp. 16–30.

[2005Wan] J. Wang, X.-G. Lu, B. Sundman, X. Su: Calphad **29** (2005) 263–268.

Au – Pb (Gold – Lead)

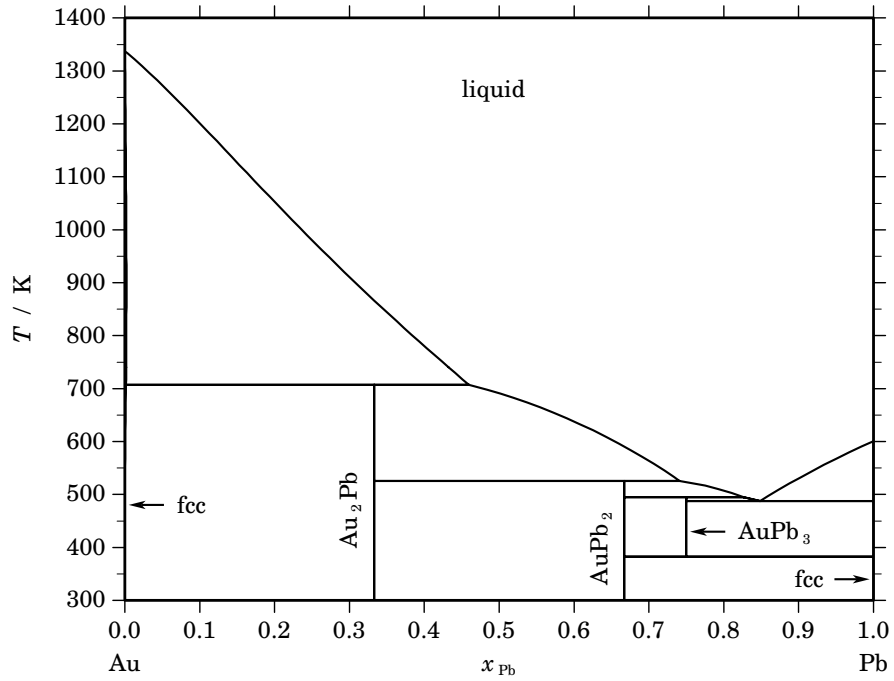

Fig. 1. Calculated phase diagram for the system Au-Pb.

The knowledge of the Au-Pb system is required for an understanding of the interactions between Sn-Pb solder and gold-plated contacts of electronic components. An old thermodynamic assessment of this system has been presented in the first volume of this series [2002SGTE]. Since then several additional investigations of Au-Pb have been published which have been incorporated in a recent optimisation [2004Wan]. The assessment takes into account several experimental investigations on the phase diagram from the literature, measurements of the enthalpy of mixing in the liquid at different temperatures and determination of the Pb activities in the liquid from several sources. In addition the assessment takes account of the experimental standard enthalpies of formation of the compounds. The mixing properties of the melt seem to be very temperature dependent and there are pronounced discrepancies between the various experimental datasets in the literature.

Table I. Phases, structures and models.

Phase	Struktur-bericht	Prototype	Pearson symbol	Space group	SGTE name	Model
liquid					LIQUID	$(Au,Pb)_1$
fcc	$A1$	Cu	$cF4$	$Fm\bar{3}m$	FCC_A1	$(Au,Pb)_1$
Au_2Pb	$C15$	Cu_2Mg	$cF24$	$Fd\bar{3}m$	AU2PB	Au_2Pb_1
$AuPb_2$	$C16$	Al_2Cu	$tI12$	$I4/mcm$	AUPB2	Au_1Pb_2
$AuPb_3$	$\cdots$	αV_3S	$tI32$	$I\bar{4}2m$	AUPB3	Au_1Pb_3

Table II. Invariant reactions.

Reaction	Type	T / K	Compositions / x_{Pb}			$\Delta_{\mathrm{r}}H$ / (J/mol)
fcc + liquid $\rightleftharpoons$ Au_2Pb	peritectic	707.1	0.002	0.459	0.333	−8256
Au_2Pb + liquid $\rightleftharpoons$ $AuPb_2$	peritectic	525.7	0.333	0.741	0.667	−6003
$AuPb_2$ + liquid $\rightleftharpoons$ $AuPb_3$	peritectic	495.2	0.667	0.827	0.750	−2800
liquid $\rightleftharpoons$ $AuPb_3$ + fcc	eutectic	487.8	0.848	0.750	1.000	−5443
$AuPb_3$ $\rightleftharpoons$ $AuPb_2$ + fcc	eutectoid	382.4	0.750	0.667	1.000	−202

Table IIIa. Integral quantities for the liquid phase at 1373 K.

x_{Pb}	ΔG_{m} [J/mol]	ΔH_{m} [J/mol]	ΔS_{m} [J/(mol·K)]	$G^{\mathrm{E}}_{\mathrm{m}}$ [J/mol]	$S^{\mathrm{E}}_{\mathrm{m}}$ [J/(mol·K)]	ΔC_P [J/(mol·K)]
0.000	0	0	0.000	0	0.000	0.000
0.100	−5425	394	4.238	−1713	1.535	1.299
0.200	−8608	615	6.717	−2895	2.557	2.310
0.300	−10576	695	8.209	−3602	3.130	3.031
0.400	−11574	666	8.915	−3891	3.319	3.464
0.500	−11730	560	8.951	−3817	3.188	3.609
0.600	−11121	410	8.398	−3438	2.802	3.464
0.700	−9784	246	7.305	−2810	2.226	3.031
0.800	−7703	102	5.685	−1990	1.524	2.310
0.900	−4746	9	3.463	−1035	0.760	1.299
1.000	0	0	0.000	0	0.000	0.000

Reference states: Au(liquid), Pb(liquid)

Table IIIb. Partial quantities for Au in the liquid phase at 1373 K.

x_{Au}	ΔG_{Au} [J/mol]	ΔH_{Au} [J/mol]	ΔS_{Au} [J/(mol·K)]	$G^{\mathrm{E}}_{\mathrm{Au}}$ [J/mol]	$S^{\mathrm{E}}_{\mathrm{Au}}$ [J/(mol·K)]	a_{Au}	γ_{Au}
1.000	0	0	0.000	0	0.000	1.000	1.000
0.900	−1478	92	1.143	−275	0.267	0.879	0.976
0.800	−3573	325	2.839	−1025	0.983	0.731	0.914
0.700	−6209	635	4.985	−2138	2.019	0.580	0.829
0.600	−9330	957	7.493	−3499	3.245	0.442	0.736
0.500	−12908	1229	10.296	−4995	4.533	0.323	0.646
0.400	−16975	1384	13.371	−6514	5.753	0.226	0.565
0.300	−21688	1360	16.787	−7943	6.776	0.150	0.499
0.200	−27541	1092	20.855	−9168	7.473	0.090	0.448
0.100	−36363	516	26.860	−10077	7.715	0.041	0.414
0.000	$-\infty$	−432	∞	−10555	7.373	0.000	0.397

Reference state: Au(liquid)

Table IIIc. Partial quantities for Pb in the liquid phase at 1373 K.

x_{Pb}	ΔG_{Pb} [J/mol]	ΔH_{Pb} [J/mol]	ΔS_{Pb} [J/(mol·K)]	$G^{\mathrm{E}}_{\mathrm{Pb}}$ [J/mol]	$S^{\mathrm{E}}_{\mathrm{Pb}}$ [J/(mol·K)]	a_{Pb}	γ_{Pb}
0.000	$-\infty$	4915	∞	−19981	18.132	0.000	0.174
0.100	−40943	3115	32.089	−14657	12.944	0.028	0.277
0.200	−28748	1777	22.232	−10375	8.850	0.081	0.403
0.300	−20764	836	15.732	−7020	5.722	0.162	0.541
0.400	−14939	230	11.048	−4479	3.429	0.270	0.675
0.500	−10552	−108	7.607	−2639	1.843	0.397	0.794
0.600	−7219	−240	5.083	−1387	0.835	0.531	0.886
0.700	−4682	−231	3.242	−611	0.276	0.664	0.948
0.800	−2743	−146	1.892	−196	0.037	0.786	0.983
0.900	−1233	−47	0.864	−30	−0.012	0.898	0.997
1.000	0	0	0.000	0	0.000	1.000	1.000

Reference state: Pb(liquid)

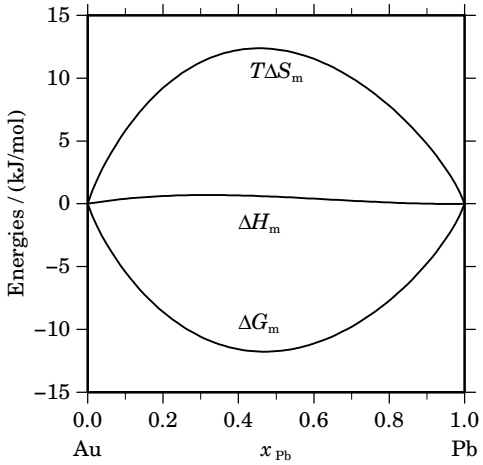

Fig. 2. Integral quantities of the liquid phase at T=1373 K.

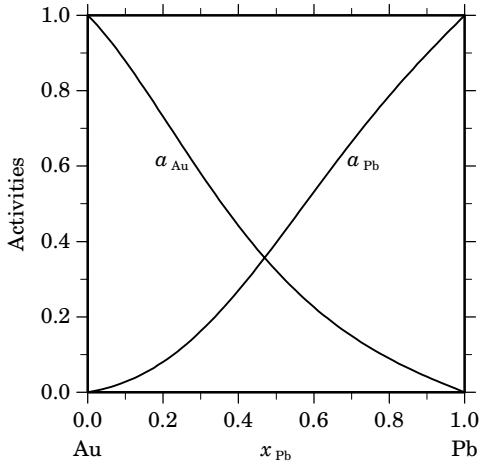

Fig. 3. Activities in the liquid phase at T=1373 K.

Table IV. Standard reaction quantities at 298.15 K for the compounds per mole of atoms.

Compound	x_{Pb}	$\Delta_{\mathrm{f}}G^{\circ}$ / (J/mol)	$\Delta_{\mathrm{f}}H^{\circ}$ / (J/mol)	$\Delta_{\mathrm{f}}S^{\circ}$ / (J/(mol·K))	$\Delta_{\mathrm{f}}C^{\circ}_{P}$ / (J/(mol·K))
Au_2Pb_1	0.333	−2861	−3010	−0.500	0.000
Au_1Pb_2	0.667	−2368	−2800	−1.450	0.000
Au_1Pb_3	0.750	−1733	−1900	−0.560	0.000

References

[2002SGTE] SGTE in: Landolt-Börnstein, New Series, IV/19 B1, Springer-Verlag, Berlin Heidelberg, 2002, pp. 280–282.

[2004Wan] J. Wang, H.S. Liu, Z.P. Jin: Calphad **28** (2004) 91–95.

Au – Ti (Gold – Titanium)

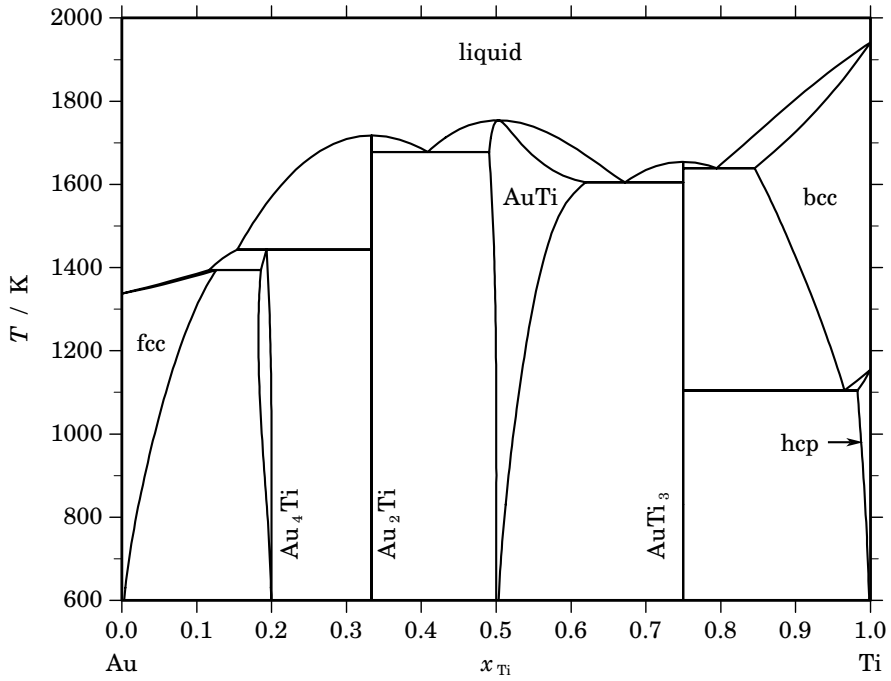

Fig. 1. Calculated phase diagram for the system Au-Ti.

Alloys of gold and titanium as well as gold platings on titanium are encountered in jewelry and also in dental applications. A thorough review of the literature on the thermodynamics of the Au-Ti system has been given in [1987Mur] and a thermodynamic optimised dataset has been reported by [2001Luo]. The optimisation takes into account 5 experimental datasets for the phase diagram from the literature, a calorimetric investigation of the mixing enthalpy in Au-rich melts and reported standard enthalpies of formation for three of the intermetallic compounds, $AuTi_3$, AuTi, and Au_2Ti which have been obtained from direct synthesis calorimetry. The low-temperature modifications of the AuTi compound have not been included in the optimisation due to a lack of data.

References

[1987Mur] J.L. Murray in: Phase Diagrams of Binary Titanium Alloys, J.L. Murray, Ed., ASM Intl., Metals Park, OH, 1987, pp. 27–32.

[2001Luo] W. Luo, Z. Jin, H. Liu, T. Wang: Calphad **25** (2001) 19–26.

Table I. Phases, structures and models.

Phase	Strukturbericht	Prototype	Pearson symbol	Space group	SGTE name	Model
liquid					LIQUID	$(Au,Ti)_1$
fcc	$A1$	Cu	$cF4$	$Fm\bar{3}m$	FCC_A1	$(Au,Ti)_1$
Au_4Ti	$D1_a$	$MoNi_4$	$tI10$	$I4/m$	AU4TI	$Au_4(Au,Ti)_1$
Au_2Ti	$C11_b$	$MoSi_2$	$tI6$	$I4/mmm$	AU2TI	Au_2Ti_1
αAuTi	$B11$	CuTi	$tP4$	$P4/nmm$	AUTI	$(Au,Ti)_1(Ti,\Box)_1$
βAuTi	$B19$	AuCd	$oP4$	$Pmma$	AUTI	$(Au,Ti)_1(Ti,\Box)_1$
γAuTi	$B2$	CsCl	$cP2$	$Pm\bar{3}m$	AUTI	$(Au,Ti)_1(Ti,\Box)_1$
$AuTi_3$	$A15$	Cr_3Si	$cP8$	$Pm3n$	AUTI3	Au_1Ti_3
bcc	$A2$	W	$cI2$	$Im\bar{3}m$	BCC_A2	$(Au,Ti)_1$
hcp	$A3$	Mg	$hP2$	$P6_3/mmc$	HCP_A3	$(Au,Ti)_1$

Table II. Invariant reactions.

Reaction	Type	T / K	Compositions / x_{Ti}			$\Delta_r H$ / (J/mol)
liquid $\rightleftharpoons$ AuTi	congruent	1754.6	0.503	0.503		−28799
liquid $\rightleftharpoons$ Au_2Ti	congruent	1717.9	0.333	0.333		−43289
liquid $\rightleftharpoons$ Au_2Ti + AuTi	eutectic	1678.0	0.409	0.333	0.490	−35388
liquid $\rightleftharpoons$ $AuTi_3$	congruent	1654.4	0.750	0.750		−23842
liquid $\rightleftharpoons$ $AuTi_3$ + bcc	eutectic	1639.3	0.794	0.750	0.845	−18241
liquid $\rightleftharpoons$ AuTi + $AuTi_3$	eutectic	1604.9	0.672	0.619	0.750	−21471
liquid + Au_2Ti $\rightleftharpoons$ Au_4Ti	peritectic	1443.7	0.154	0.333	0.193	−21679
liquid + Au_4Ti $\rightleftharpoons$ fcc	peritectic	1394.1	0.116	0.186	0.126	−8854
bcc $\rightleftharpoons$ $AuTi_3$ + hcp	eutectoid	1104.9	0.965	0.750	0.982	−5129

Table IIIa. Integral quantities for the liquid phase at 2000 K.

x_{Ti}	ΔG_m [J/mol]	ΔH_m [J/mol]	ΔS_m [J/(mol·K)]	G_m^E [J/mol]	S_m^E [J/(mol·K)]	ΔC_P [J/(mol·K)]
0.000	0	0	0.000	0	0.000	0.000
0.100	−19206	−12370	3.418	−13800	0.715	0.000
0.200	−31822	−20984	5.419	−23501	1.258	0.000
0.300	−39648	−26222	6.713	−29490	1.634	0.000
0.400	−43347	−28459	7.444	−32155	1.848	0.000
0.500	−43409	−28074	7.668	−31883	1.904	0.000
0.600	−40251	−25442	7.404	−29059	1.809	0.000
0.700	−34231	−20942	6.644	−24073	1.565	0.000
0.800	−25630	−14950	5.340	−17309	1.179	0.000
0.900	−14562	−7844	3.359	−9156	0.656	0.000
1.000	0	0	0.000	0	0.000	0.000

Reference states: Au(liquid), Ti(liquid)

Table IIIb. Partial quantities for Au in the liquid phase at 2000 K.

x_{Au}	ΔG_{Au} [J/mol]	ΔH_{Au} [J/mol]	ΔS_{Au} [J/(mol·K)]	$G^{\mathrm{E}}_{\mathrm{Au}}$ [J/mol]	$S^{\mathrm{E}}_{\mathrm{Au}}$ [J/(mol·K)]	a_{Au}	γ_{Au}
1.000	0	0	0.000	0	0.000	1.000	1.000
0.900	−3866	−1940	0.963	−2114	0.087	0.793	0.881
0.800	−11650	−7258	2.196	−7939	0.341	0.496	0.620
0.700	−22633	−15198	3.718	−16702	0.752	0.256	0.366
0.600	−36123	−25007	5.558	−27629	1.311	0.114	0.190
0.500	−51471	−35931	7.770	−39945	2.007	0.045	0.091
0.400	−68114	−47215	10.449	−52877	2.831	0.017	0.042
0.300	−85671	−58105	13.783	−65650	3.773	0.006	0.019
0.200	−104255	−67846	18.205	−77492	4.823	0.002	0.009
0.100	−125916	−75684	25.116	−87627	5.971	0.001	0.005
0.000	−∞	−80866	∞	−95281	7.208	0.000	0.003

Reference state: Au(liquid)

Table IIIc. Partial quantities for Ti in the liquid phase at 2000 K.

x_{Ti}	ΔG_{Ti} [J/mol]	ΔH_{Ti} [J/mol]	ΔS_{Ti} [J/(mol·K)]	$G^{\mathrm{E}}_{\mathrm{Ti}}$ [J/mol]	$S^{\mathrm{E}}_{\mathrm{Ti}}$ [J/(mol·K)]	a_{Ti}	γ_{Ti}
0.000	−∞	−143724	∞	−159779	8.028	0.000	0.000
0.100	−157262	−106234	25.514	−118973	6.370	0.000	0.001
0.200	−112511	−75892	18.309	−85747	4.928	0.001	0.006
0.300	−79350	−51944	13.703	−59330	3.693	0.008	0.028
0.400	−54182	−33637	10.272	−38945	2.654	0.038	0.096
0.500	−35347	−20216	7.565	−23820	1.802	0.119	0.239
0.600	−21676	−10927	5.374	−13181	1.127	0.272	0.453
0.700	−12185	−5015	3.585	−6253	0.619	0.481	0.687
0.800	−5974	−1726	2.124	−2263	0.269	0.698	0.873
0.900	−2189	−306	0.942	−437	0.066	0.877	0.974
1.000	0	0	0.000	0	0.000	1.000	1.000

Reference state: Ti(liquid)

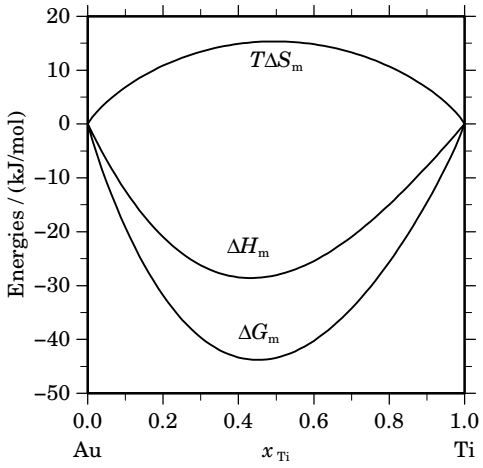

Fig. 2. Integral quantities of the liquid phase at T=2000 K.

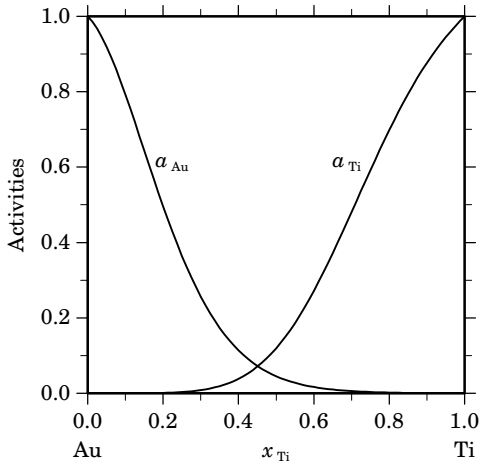

Fig. 3. Activities in the liquid phase at T=2000 K.

Table IVa. Integral quantities for the stable phases at 1300 K.

Phase	x_{Ti}	ΔG_{m} [J/mol]	ΔH_{m} [J/mol]	ΔS_{m} [J/(mol·K)]	$G_{\mathrm{m}}^{\mathrm{E}}$ [J/mol]	$S_{\mathrm{m}}^{\mathrm{E}}$ [J/(mol·K)]	ΔC_P [J/(mol·K)]
fcc	0.000	0	0	0.000	0	0.000	0.000
	0.098	−16627	−12738	2.992	−13162	0.326	0.555
Au_4Ti	0.183	−28381	−36195	−6.011	−23239	−9.966	1.036
	0.197	−30204	−39797	−7.379	−24840	−11.505	1.117
Au_2Ti	0.333	−45454	−59020	−10.435			1.889
AuTi	0.499	−43625	−46728	−2.387	−36133	−8.150	3.677
	0.500	−43609	−46730	−2.401	−36117	−8.164	3.820
	0.549	−41077	−42600	−1.171	−33636	−6.895	3.931
$AuTi_3$	0.750	−28254	−31825	−2.746			4.250
bcc	0.928	−8823	−5846	2.290	−6027	0.139	0.000
	1.000	0	0	0.000	0	0.000	0.000

Reference states: Au(fcc), Ti(bcc)

Table IVb. Partial quantities for Au in the stable phases at 1300 K.

Phase	x_{Au}	ΔG_{Au} [J/mol]	ΔH_{Au} [J/mol]	ΔS_{Au} [J/(mol·K)]	$G_{\mathrm{Au}}^{\mathrm{E}}$ [J/mol]	$S_{\mathrm{Au}}^{\mathrm{E}}$ [J/(mol·K)]	a_{Au}	γ_{Au}
fcc	1.000	0	0	0.000	0	0.000	1.000	1.000
	0.902	−3051	−1910	0.878	−1936	0.020	0.754	0.836
Au_4Ti	0.817	−3051	10000	10.039	−869	8.360	0.754	0.923
	0.803	−8140	10000	13.954	−5767	12.128	0.471	0.587
Au_2Ti	0.667	−8140	−11983	−2.957			0.471	
	0.667	−49135	−83749	−26.627			0.011	
AuTi	0.501	−49135	−31745	13.377	−41665	7.631	0.011	0.021
	0.500	−53273	−58340	−3.897	−45781	−9.660	0.007	0.014
	0.451	−75984	−92162	−12.445	−67389	−19.056	0.001	0.002
$AuTi_3$	0.250	−75984	−71932	3.117			0.001	
	0.250	−110118	−141273	−23.965			0.000	
bcc	0.072	−110118	−81613	21.927	−81676	0.049	0.000	0.001
	0.000	$-\infty$	−80242	∞	−85583	4.108	0.000	0.000

Reference state: Au(fcc)

Table IVc. Partial quantities for Ti in the stable phases at 1300 K.

Phase	x_{Ti}	ΔG_{Ti} [J/mol]	ΔH_{Ti} [J/mol]	ΔS_{Ti} [J/(mol·K)]	$G^{\mathrm{E}}_{\mathrm{Ti}}$ [J/mol]	$S^{\mathrm{E}}_{\mathrm{Ti}}$ [J/(mol·K)]	a_{Ti}	γ_{Ti}
fcc	0.000	$-\infty$	−150030	∞	−154550	3.477	0.000	0.000
	0.098	−141592	−112406	22.450	−116485	3.137	0.000	0.000
Au_4Ti	0.183	−141592	−242664	−77.748	−123225	−91.876	0.000	0.000
	0.197	−120094	−242664	−94.284	−102540	−107.788	0.000	0.000
Au_2Ti	0.333	−120094	−153107	−25.394			0.000	
	0.333	−38092	−9553	21.953			0.029	
AuTi	0.499	−38092	−61773	−18.216	−30577	−23.997	0.029	0.059
	0.500	−33945	−35121	−0.905	−26452	−6.668	0.043	0.087
	0.549	−12344	−1803	8.109	−5853	3.115	0.319	0.582
$AuTi_3$	0.750	−12344	−18456	−4.701			0.319	
	0.750	−966	4658	4.327			0.914	
bcc	0.928	−966	31	0.767			0.914	0.985
	1.000	0	0	0.000	0	0.000	1.000	1.000

Reference state: Ti(bcc)

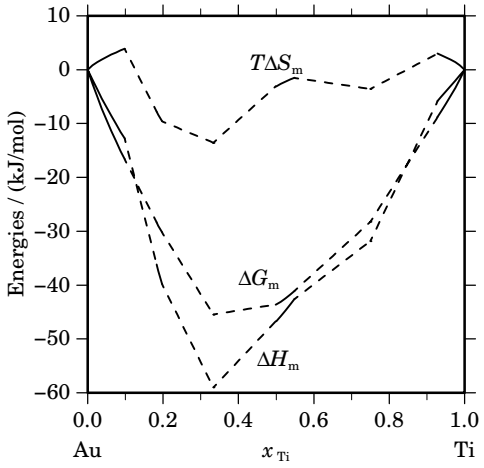

Fig. 4. Integral quantities of the stable phases at T=1300 K.

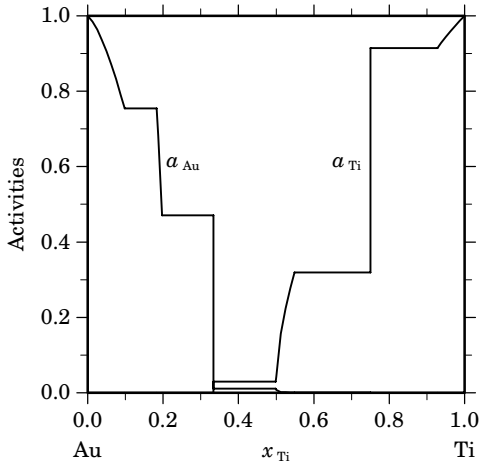

Fig. 5. Activities in the stable phases at T=1300 K.

Table V. Standard reaction quantities at 298.15 K for the compounds per mole of atoms.

Compound	x_{Ti}	$\Delta_{\mathrm{f}}G^{\circ}$ / (J/mol)	$\Delta_{\mathrm{f}}H^{\circ}$ / (J/mol)	$\Delta_{\mathrm{f}}S^{\circ}$ / (J/(mol·K))	$\Delta_{\mathrm{f}}C^{\circ}_{P}$ / (J/(mol·K))
Au_4Ti	0.200	−37730	−39855	−7.125	0.000
Au_2Ti_1	0.333	−55074	−57889	−9.443	0.000
AuTi	0.500	−44914	−45242	−1.098	0.013
Au_1Ti_3	0.750	−29128	−29281	−0.514	0.000

Au – Zr (Gold – Zirconium)

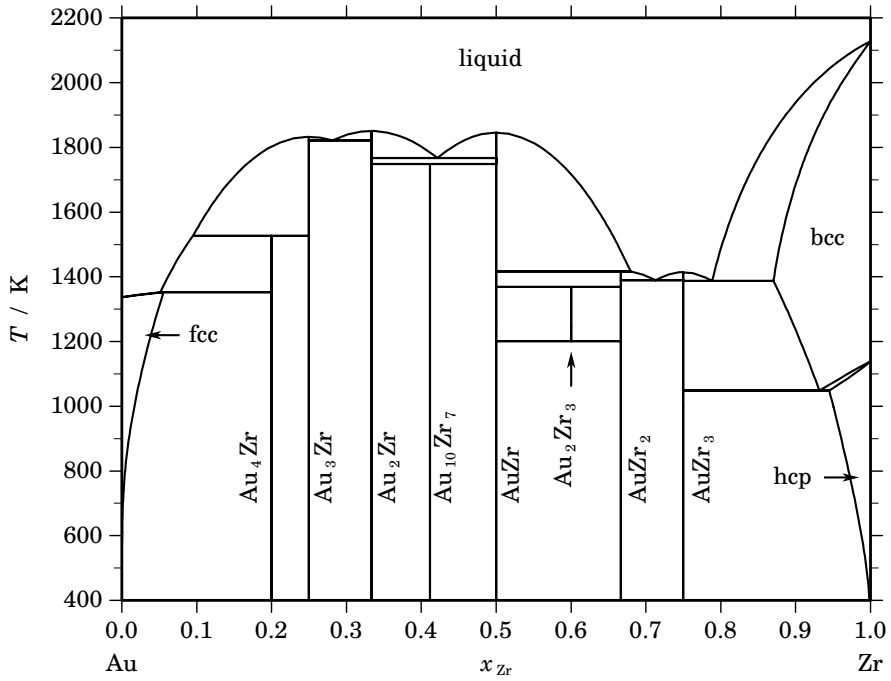

Fig. 1. Calculated phase diagram for the system Au-Zr.

The alloy systems or intermetallic compounds composed of Zr and Au have attracted much attention for the theoretical study of the solid state and for many industrial purposes such as the use of amorphous Au-Zr alloys as catalysts for CO hydrogenation and oxidation. The Au-rich side of the Au-Zr phase diagram was studied by [1948Rau]. [1997Lom] reexamined this system by means of differential thermal analysis, x-ray diffraction and electron probe microanalysis, and established the phase diagram in its present form. He suggested that the compounds $AuZr_3$, AuZr, Au_2Zr and Au_3Zr melt congruently. $AuZr_2$ and Au_4Zr form peritectically. Au_2Zr_3 and $Au_{10}Zr_7$ are formed by peritectoid reactions. The maximum solid solubility of Au in βZr is 16 at.% Au. The αZr has a narrow homogeneity range. The maximum solid solubility of Zr in Au is about 8 at.% Zr. This value agrees with that of [1948Rau]. A literature review was presented by [1999Oka]. According to [1999Oka], Au_4Zr_5 does not exist. The experimental standard enthalpies of formation of the congruently melting compounds $AuZr_2$, Au_4Zr_5, Au_2Zr, Au_3Zr were determined by [1992Fit], those of the compounds $AuZr_3$, $AuZr_2$, Au_4Zr_5, AuZr, $Au_{10}Zr_7$, Au_2Zr, Au_3Zr, Au_4Zr were determined by [1998Lom]. The enthalpies of mixing of solid Zr in liquid Au and the enthalpies of mixing for the liquid alloys were also measured by [1998Lom] and [1992Fit], respectively. The thermodynamic evaluation of the Au-Zr system was made by [2000Su]. The terminal solid solutions bcc, hcp, fcc and the liquid phase were described by a substitutional solution model using the Redlich-Kister equation. The intermetallic compounds $AuZr_3$, $AuZr_2$, Au_2Zr_3, AuZr, $Au_{10}Zr_7$, Au_2Zr, Au_3Zr, Au_4Zr are modelled as stoichiometric phases. The calculated phase diagram is in good agreement with the experiments reported by [1998Lom]. All invariant equilibria in the system are reproduced well. The assessed terminal solubilities of Zr in Au, and of Au in Zr do not agree well with the experimental data, but the review of [1999Oka] showed a thermodynamic improbability. The assessed enthalpies of formation agree well with experimental data. The calculated partial and integral molar enthalpies of mixing of solid Zr in liquid is good below 11 at.% Zr; above this composition, the measurements of the enthalpies of mixing are not accurate due to the occurrence of solid Au_4Zr at the experimental temperature. More experimental work on the liquid/βZr and βZr/αZr boundaries may be necessary to improve the description.

Table I. Phases, structures and models.

Phase	Struktur-bericht	Prototype	Pearson symbol	Space group	SGTE name	Model
liquid					LIQUID	$(Au,Zr)_1$
fcc	$A1$	Cu	$cF4$	$Fm\overline{3}m$	FCC_A1	$(Au,Zr)_1$
Au_4Zr	$\cdots$	$AuZr_4$	$oP20$	$Pnma$	AU4ZR	Au_4Zr_1
Au_3Zr	$D0_a$	βCu_3Ti	$oP8$	$Pmmn$	AU3ZR	Au_3Zr_1
Au_2Zr	$C11_b$	$MoSi_2$	$tI6$	$I4/mmm$	AU2ZR	Au_2Zr_1
$Au_{10}Zr_7$	$\cdots$	$\cdots$	$tI34$	$\cdots$	AU10ZR7	$Au_{10}Zr_7$
AuZr	$\cdots$	$\cdots$	$\cdots$	$\cdots$	AUZR	Au_1Zr_1
Au_2Zr_3	$\cdots$	$\cdots$	$\cdots$	$\cdots$	AU2ZR3	Au_2Zr_3
$AuZr_2$	$C11_b$	$MoSi_2$	$tI6$	$I4/mmm$	AUZR2	Au_1Zr_2
$AuZr_3$	$A15$	Cr_3Si	$cP8$	$Pm3n$	AUZR3	Au_1Zr_3
bcc	$A2$	W	$cI2$	$Im\overline{3}m$	BCC_A2	$(Au,Zr)_1$
hcp	$A3$	Mg	$hP2$	$P6_3/mmc$	HCP_A3	$(Au,Zr)_1$

Table II. Invariant reactions.

Reaction	Type	T / K	Compositions / x_{Zr}			$\Delta_r H$ / (J/mol)
liquid $\rightleftharpoons$ Au_2Zr	congruent	1850.8	0.333	0.333		−30587
liquid $\rightleftharpoons$ AuZr	congruent	1845.5	0.500	0.500		−25408
liquid $\rightleftharpoons$ Au_3Zr	congruent	1833.0	0.250	0.250		−29297
liquid $\rightleftharpoons$ Au_3Zr + Au_2Zr	eutectic	1821.4	0.282	0.250	0.333	−29490
liquid $\rightleftharpoons$ Au_2Zr + AuZr	eutectic	1767.1	0.422	0.333	0.500	−26518
Au_2Zr + AuZr $\rightleftharpoons$ $Au_{10}Zr_7$	peritectoid	1749.0	0.333	0.500	0.412	−2
liquid + Au_3Zr $\rightleftharpoons$ Au_4Zr	peritectic	1527.1	0.095	0.250	0.200	−5907
AuZr + liquid $\rightleftharpoons$ $AuZr_2$	peritectic	1416.3	0.500	0.680	0.667	−18469
liquid $\rightleftharpoons$ $AuZr_3$	congruent	1414.5	0.750	0.750		−14774
liquid $\rightleftharpoons$ $AuZr_2$ + $AuZr_3$	eutectic	1389.8	0.713	0.667	0.750	−16664
liquid $\rightleftharpoons$ $AuZr_3$ + bcc	eutectic	1387.1	0.788	0.750	0.870	−11324
AuZr + $AuZr_2$ $\rightleftharpoons$ Au_2Zr_3	peritectoid	1368.8	0.500	0.667	0.600	−6
liquid + Au_4Zr $\rightleftharpoons$ fcc	peritectic	1352.3	0.052	0.200	0.056	−10372
Au_2Zr_3 $\rightleftharpoons$ AuZr + $AuZr_2$	eutectoid	1200.8	0.600	0.500	0.667	−5
bcc $\rightleftharpoons$ $AuZr_3$ + hcp	eutectoid	1049.0	0.932	0.750	0.945	−4531

Table IIIa. Integral quantities for the liquid phase at 2200 K.

x_{Zr}	ΔG_{m} [J/mol]	ΔH_{m} [J/mol]	ΔS_{m} [J/(mol·K)]	$G_{\mathrm{m}}^{\mathrm{E}}$ [J/mol]	$S_{\mathrm{m}}^{\mathrm{E}}$ [J/(mol·K)]	ΔC_P [J/(mol·K)]
0.000	0	0	0.000	0	0.000	0.000
0.100	−18209	−16976	0.561	−12263	−2.142	0.000
0.200	−30826	−30591	0.107	−21673	−4.054	0.000
0.300	−39452	−40691	−0.564	−28278	−5.643	0.000
0.400	−44436	−47122	−1.221	−32125	−6.817	0.000
0.500	−45943	−49729	−1.721	−33264	−7.484	0.000
0.600	−44052	−48358	−1.957	−31741	−7.553	0.000
0.700	−38780	−42854	−1.852	−27606	−6.931	0.000
0.800	−30058	−33062	−1.365	−20905	−5.526	0.000
0.900	−17633	−18829	−0.544	−11687	−3.246	0.000
1.000	0	0	0.000	0	0.000	0.000

Reference states: Au(liquid), Zr(liquid)

Table IIIb. Partial quantities for Au in the liquid phase at 2200 K.

x_{Au}	ΔG_{Au} [J/mol]	ΔH_{Au} [J/mol]	ΔS_{Au} [J/(mol·K)]	$G_{\mathrm{Au}}^{\mathrm{E}}$ [J/mol]	$S_{\mathrm{Au}}^{\mathrm{E}}$ [J/(mol·K)]	a_{Au}	γ_{Au}
1.000	0	0	0.000	0	0.000	1.000	1.000
0.900	−3362	−1655	0.776	−1435	−0.100	0.832	0.925
0.800	−9756	−6824	1.333	−5674	−0.523	0.587	0.733
0.700	−19147	−15818	1.514	−12623	−1.452	0.351	0.502
0.600	−31529	−28944	1.175	−22185	−3.072	0.178	0.297
0.500	−46943	−46512	0.196	−34264	−5.567	0.077	0.154
0.400	−65525	−68830	−1.502	−48764	−9.121	0.028	0.070
0.300	−87612	−96208	−3.907	−65589	−13.917	0.008	0.028
0.200	−114083	−128954	−6.759	−84643	−20.141	0.002	0.010
0.100	−147949	−167377	−8.831	−105831	−27.976	0.000	0.003
0.000	$-\infty$	−211786	∞	−129055	−37.605	0.000	0.001

Reference state: Au(liquid)

Table IIIc. Partial quantities for Zr in the liquid phase at 2200 K.

x_{Zr}	ΔG_{Zr} [J/mol]	ΔH_{Zr} [J/mol]	ΔS_{Zr} [J/(mol·K)]	$G_{\mathrm{Zr}}^{\mathrm{E}}$ [J/mol]	$S_{\mathrm{Zr}}^{\mathrm{E}}$ [J/(mol·K)]	a_{Zr}	γ_{Zr}
0.000	$-\infty$	−186046	∞	−137056	−22.268	0.000	0.001
0.100	−151838	−154867	−1.377	−109719	−20.522	0.000	0.002
0.200	−115107	−125659	−4.796	−85668	−18.178	0.002	0.009
0.300	−86828	−98730	−5.410	−64805	−15.420	0.009	0.029
0.400	−63797	−74390	−4.815	−47036	−12.434	0.031	0.076
0.500	−44943	−52947	−3.638	−32264	−9.401	0.086	0.171
0.600	−29737	−34709	−2.260	−20393	−6.508	0.197	0.328
0.700	−17851	−19987	−0.971	−11327	−3.937	0.377	0.538
0.800	−9052	−9089	−0.017	−4970	−1.872	0.610	0.762
0.900	−3154	−2324	0.377	−1227	−0.499	0.842	0.935
1.000	0	0	0.000	0	0.000	1.000	1.000

Reference state: Zr(liquid)

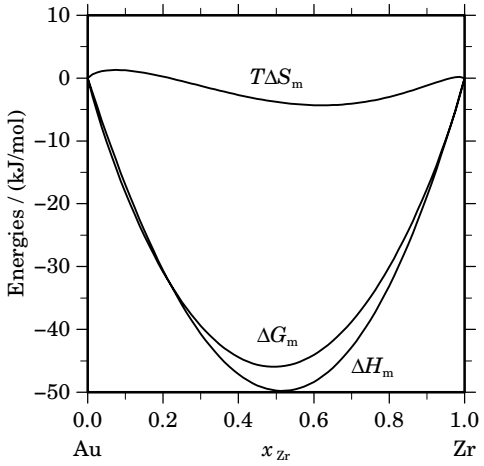

Fig. 2. Integral quantities of the liquid phase at T=2200 K.

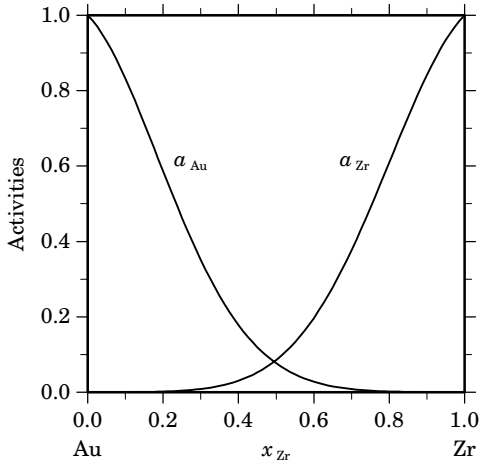

Fig. 3. Activities in the liquid phase at T=2200 K.

Table IV. Standard reaction quantities at 298.15 K for the compounds per mole of atoms.

Compound	x_{Zr}	$\Delta_f G^\circ$ / (J/mol)	$\Delta_f H^\circ$ / (J/mol)	$\Delta_f S^\circ$ / (J/(mol·K))	$\Delta_f C_P^\circ$ / (J/(mol·K))
Au_4Zr_1	0.200	−40169	−41759	−5.335	0.000
Au_3Zr_1	0.250	−49395	−51453	−6.903	0.000
Au_2Zr_1	0.333	−57045	−59445	−8.050	0.000
$Au_{10}Zr_7$	0.412	−57473	−59624	−7.217	0.000
Au_1Zr_1	0.500	−57951	−59823	−6.278	0.000
Au_2Zr_3	0.600	−51184	−53114	−6.472	−0.063
Au_1Zr_2	0.667	−46730	−48743	−6.754	0.000
Au_1Zr_3	0.750	−35657	−36536	−2.950	0.000

References

[1948Rau] E. Raub, M. Engel: Z. Metallkd. **39** (1948) 172–177.
[1992Fit] K. Fitzner, O.J. Kleppa: Metall. Trans. A **23A** (1992) 997–1003.
[1997Lom] M. Lomello-Tafin, P. Galez, J.C. Gachon, P. Feschotte, J.L. Jorda: J. Alloys Comp. **257** (1997) 215–223.
[1998Lom] M. Lomello-Tafin, P. Galez, P. Feschotte, J.J. Kuntz, J.L. Jorda, J.C. Gachon: J. Alloys Comp. **267** (1998) 142–148.
[1999Oka] H. Okamoto: J. Phase Equilibria **20** (1999) 349.
[2000Su] X. Su, F. Yin, Z. Li, Y. Shi: Z. Metallkd. **91** (2000) 744–747.

B – Zr (Boron – Zirconium)

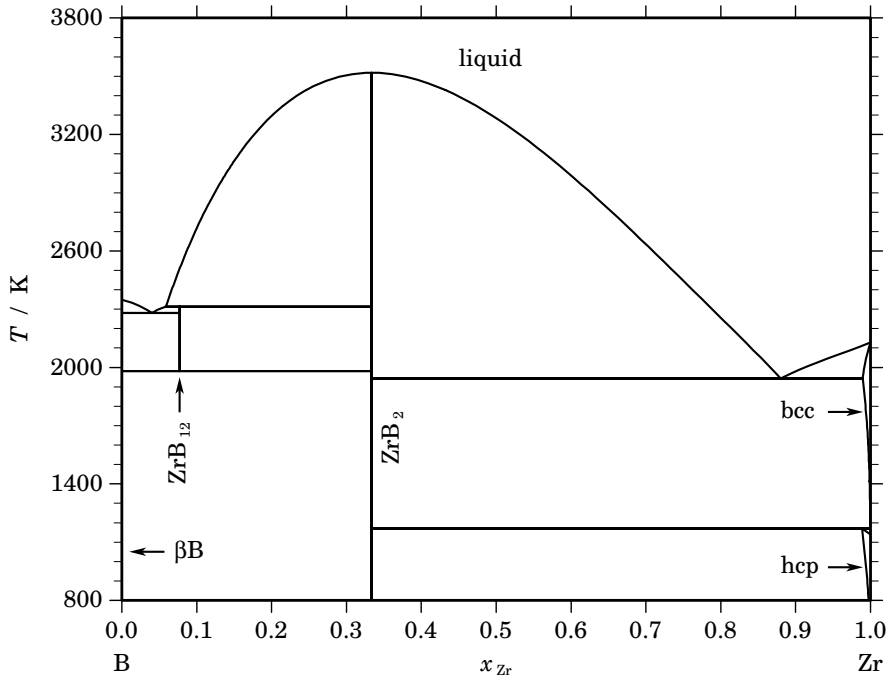

Fig. 1. Calculated phase diagram for the system B-Zr.

A review and a thermodynamic assessment for the system B-Zr has been published in [1988Rog] which has been revised later [1998Dus]. The data for the phase diagram are based mostly on the results from [1966Rud] and from [1970Por]. The liquidus data show a very high scatter due to the aggressive attack of the B-melt on the crucible materials. Thermodynamic properties have been determined only for ZrB_2. The experimental data for this compound have been reviewed by [1976Alc] and recommended values have been given which are used in the assessment [1998Dus].

Table I. Phases, structures and models.

Phase	Struktur-bericht	Prototype	Pearson symbol	Space group	SGTE name	Model
liquid					LIQUID	$(B,Zr)_1$
βB	$\cdots$	βB	$hR105$	$R\bar{3}m$	BETA_RHOMBO_B	$B_{93}B_{12}$
ZrB_{12}	$D2_f$	UB_{12}	$cF52$	$Fm\bar{3}m$	ZRB12	Zr_1B_{12}
ZrB_2	$C32$	AlB_2	$hP3$	$P6/mmm$	ZRB2	Zr_1B_2
bcc	$A2$	W	$cI2$	$Im\bar{3}m$	BCC_A2	$Zr_1(B,\Box)_3$
hcp	$A3$	Mg	$hP2$	$P6_3/mmc$	HCP_A3	$Zr_2(B,\Box)_1$

Table II. Invariant reactions.

Reaction	Type	T / K	Compositions / x_{Zr}			$\Delta_{\mathrm{r}}H$ / (J/mol)
liquid $\rightleftharpoons$ ZrB_2	congruent	3518.0	0.333	0.333		−99035
liquid + ZrB_2 $\rightleftharpoons$ ZrB_{12}	peritectic	2312.9	0.059	0.333	0.077	−39109
liquid $\rightleftharpoons$ βB + ZrB_{12}	eutectic	2280.1	0.040	0.000	0.077	−45880
ZrB_{12} $\rightleftharpoons$ βB + ZrB_2	eutectoid	1980.7	0.077	0.000	0.333	−8121
liquid $\rightleftharpoons$ ZrB_2 + bcc	eutectic	1942.9	0.880	0.333	0.989	−22987
ZrB_2 + bcc $\rightleftharpoons$ hcp	peritectoid	1169.7	0.333	1.000	0.989	−3541

Table IIIa. Integral quantities for the liquid phase at 3600 K.

x_{Zr}	ΔG_{m} [J/mol]	ΔH_{m} [J/mol]	ΔS_{m} [J/(mol·K)]	$G_{\mathrm{m}}^{\mathrm{E}}$ [J/mol]	$S_{\mathrm{m}}^{\mathrm{E}}$ [J/(mol·K)]	ΔC_P [J/(mol·K)]
0.000	0	0	0.000	0	0.000	0.000
0.100	−28519	−28323	0.054	−18789	−2.649	0.000
0.200	−45818	−47791	−0.548	−30840	−4.708	0.000
0.300	−55400	−59363	−1.101	−37115	−6.180	0.000
0.400	−58719	−64000	−1.467	−38574	−7.063	0.000
0.500	−56926	−62664	−1.594	−36179	−7.357	0.000
0.600	−51033	−56314	−1.467	−30889	−7.063	0.000
0.700	−41950	−45913	−1.101	−23665	−6.180	0.000
0.800	−30447	−32419	−0.548	−15469	−4.708	0.000
0.900	−16990	−16795	0.054	−7260	−2.649	0.000
1.000	0	0	0.000	0	0.000	0.000

Reference states: B(liquid), Zr(liquid)

Table IIIb. Partial quantities for B in the liquid phase at 3600 K.

x_{B}	ΔG_{B} [J/mol]	ΔH_{B} [J/mol]	ΔS_{B} [J/(mol·K)]	$G_{\mathrm{B}}^{\mathrm{E}}$ [J/mol]	$S_{\mathrm{B}}^{\mathrm{E}}$ [J/(mol·K)]	a_{B}	γ_{B}
1.000	0	0	0.000	0	0.000	1.000	1.000
0.900	−6682	−4588	0.582	−3529	−0.294	0.800	0.889
0.800	−19513	−17072	0.678	−12834	−1.177	0.521	0.651
0.700	−36670	−35529	0.317	−25994	−2.649	0.294	0.420
0.600	−56378	−58038	−0.461	−41088	−4.708	0.152	0.253
0.500	−76941	−82679	−1.594	−56194	−7.357	0.076	0.153
0.400	−96817	−107529	−2.976	−69390	−10.594	0.039	0.098
0.300	−114793	−130667	−4.409	−78756	−14.420	0.022	0.072
0.200	−130543	−150172	−5.452	−82369	−18.834	0.013	0.064
0.100	−147231	−164121	−4.692	−78309	−23.837	0.007	0.073
0.000	$-\infty$	−170595	∞	−64654	−29.428	0.000	0.115

Reference state: B(liquid)

Table IIIc. Partial quantities for Zr in the liquid phase at 3600 K.

x_{Zr}	ΔG_{Zr} [J/mol]	ΔH_{Zr} [J/mol]	ΔS_{Zr} [J/(mol·K)]	$G^{\mathrm{E}}_{\mathrm{Zr}}$ [J/mol]	$S^{\mathrm{E}}_{\mathrm{Zr}}$ [J/(mol·K)]	a_{Zr}	γ_{Zr}
0.000	$-\infty$	−330715	∞	−224774	−29.428	0.000	0.001
0.100	−225049	−241940	−4.692	−156128	−23.837	0.001	0.005
0.200	−151039	−170667	−5.452	−102865	−18.834	0.006	0.032
0.300	−99102	−114975	−4.409	−63064	−14.420	0.036	0.122
0.400	−62231	−72943	−2.976	−34804	−10.594	0.125	0.313
0.500	−36911	−42649	−1.594	−16164	−7.357	0.291	0.583
0.600	−20511	−22171	−0.461	−5221	−4.708	0.504	0.840
0.700	−10731	−9589	0.317	−55	−2.649	0.699	0.998
0.800	−5422	−2981	0.678	1257	−1.177	0.834	1.043
0.900	−2519	−425	0.582	634	−0.294	0.919	1.021
1.000	0	0	0.000	0	0.000	1.000	1.000

Reference state: Zr(liquid)

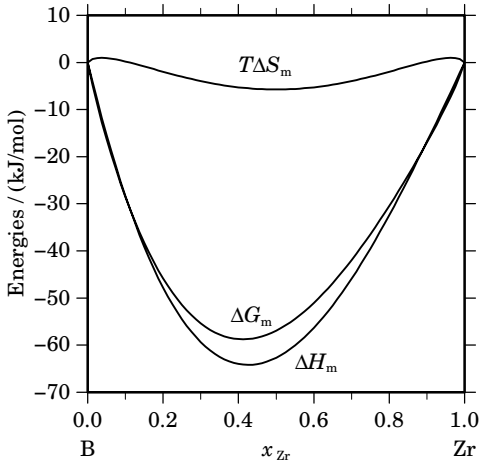

Fig. 2. Integral quantities of the liquid phase at T=3600 K.

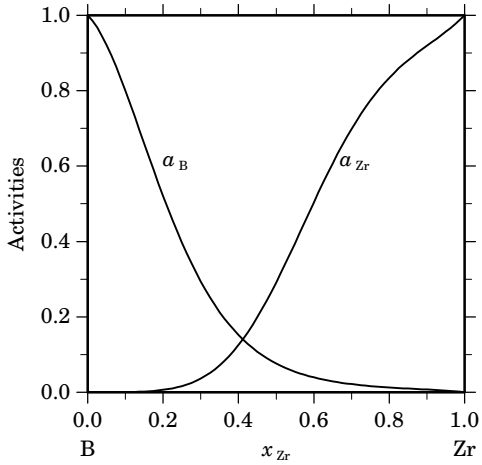

Fig. 3. Activities in the liquid phase at T=3600 K.

Table IV. Standard reaction quantities at 298.15 K for the compounds per mole of atoms.

Compound	x_{Zr}	$\Delta_{\mathrm{f}}G^{\circ}$ / (J/mol)	$\Delta_{\mathrm{f}}H^{\circ}$ / (J/mol)	$\Delta_{\mathrm{f}}S^{\circ}$ / (J/(mol·K))	$\Delta_{\mathrm{f}}C^{\circ}_{P}$ / (J/(mol·K))
Zr_1B_{12}	0.077	−18871	−18306	1.897	0.000
Zr_1B_2	0.333	−107409	−108899	−5.000	0.142

References

[1966Rud] E. Rudy, St. Windisch: Techn. Rept. AFML-TR-65-2, pt. I, vol. VIII, Wright Patterson AFB, Ohio, 1966, 1–33.

[1970Por] K.P. Portnoi, V.M. Romashov, L.I. Vyroshina: Poroshkov. Metall. **91** (1970) 68–71.

[1976Alc] C.B. Alcock, K.T. Jacob, S. Zador in: "Zirconium: physoco-chemical properties of its compounds and alloys", Atomic Energy Review, Spec. Issue No. 6, O. Kubaschewski, Ed., IAEA, Vienna, 1976, pp. 7–65.

[1988Rog] P. Rogl, P.E. Potter: Calphad **12** (1988) 191–204.

[1993Oka] H. Okamoto: J. Phase Equilibria **14** (1993) 261–262.

[1998Dus] H. Duschanek, P. Rogl in: "Phase Diagrams of Ternary Metal-Boron-Carbon Systems", P. Rogl, ASM, Materials Park, 1998, pp. 445–485.

Ba – Ru (Barium – Ruthenium)

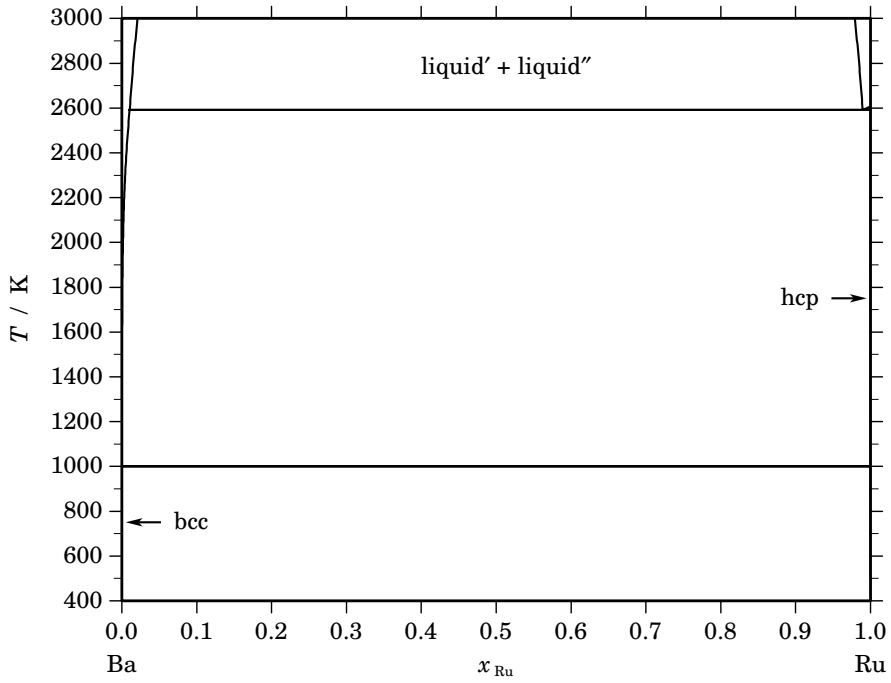

Fig. 1. Calculated phase diagram for the system Ba-Ru.

The Ba-Ru binary system contains two components of interest in the nuclear field, selected as representative of families of non volatile fission products. The classical compilations of binary phase diagrams, give no information at all on this system. Consequently, it has been supposed that there is a negligible mutual solubility of the elements barium and ruthenium in the solid state, and a wide miscibility gap in the liquid state, the mutual solubility increasing at high temperature. Thus, the assessed diagram is only qualitative, and solubilities may only be estimated. No thermodynamic properties are available for that system. The system was assessed by Chevalier and Fischer [1995Che]. The excess Gibbs energy of the liquid was estimated to be highly positive, to produce a small mutual solubility of pure components at low temperature and a large miscibility gap at high temperature. Similarly, highly positive interaction parameters in the bcc and hcp phases allow to produce a negligible mutual solubility of the components. No experimental data are available for comparison with the calculated phase diagram.

Table I. Phases, structures and models.

Phase	Struktur-bericht	Prototype	Pearson symbol	Space group	SGTE name	Model
liquid					LIQUID	$(Ba,Ru)_1$
bcc	$A2$	W	$cI2$	$Im\overline{3}m$	BCC_A2	$(Ba,Ru)_1$
hcp	$A3$	Mg	$hP2$	$P6_3/mmc$	HCP_A3	$(Ba,Ru)_1$

Table II. Invariant reactions.

Reaction	Type	T / K	Compositions / x_{Ru}			$\Delta_{\mathrm{r}}H$ / (J/mol)
liquid″ $\rightleftharpoons$ liquid′ + hcp	eutectic	2592.3	0.989	0.011	1.000	−39195
liquid′ $\rightleftharpoons$ bcc + hcp	eutectic	1000.0	0.000	0.000	1.000	−7120

References

[1995Che] P.-Y. Chevalier, E. Fischer, unpublished work, 1995.

Bi – Pd (Bismuth – Palladium)

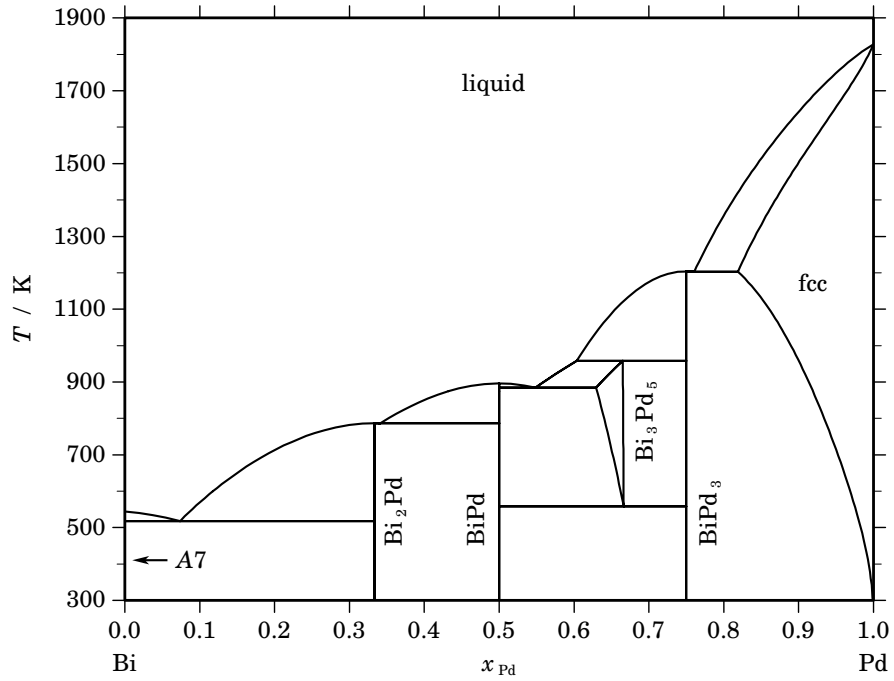

Fig. 1. Calculated phase diagram for the system Bi-Pd.

This system was assessed by Vřešťál *et al.* [2006Vre], from the available experimental information, and ab-initio calculations of the total energies of BiPd and Bi_2Pd. Bismuth is an important component both as a solvent of uranium in nuclear metallurgy, and also in lead-free solder materials, the substrates of which often containing palladium. The phase diagram is based on the experimental work of Zhuravlev and Zhdanov[1953], Zhuravlev [1957Zhu], Brasier and Hume-Rothery [1959Bra], using cooling curve analysis, Schweitzer and Weeks [1961Sch] who analysed the liquidus after equilibrating annealing. The experimental Bi-Pd phase diagram was assessed by Okamoto [1994Oka]. It presents three solution phases, the liquid with a complete miscibility range, the palladium rich terminal solid solution (fcc), and the intermediate solution phase Bi_3Pd_5 (62-71 at.%Pd). The following intermediate compounds have been identified with a very narrow non-stoichiometry range and two allotropic forms, αBi_2Pd, βBi_2Pd (1.5 at.%, 653 K), αBiPd, βBiPd (1 at.%, 483 K), $\alpha BiPd_3$, $\beta BiPd_3$ (1073 K). The structures of the intermetallic phases were experimentally studied by Schubert *et al.* [1953Sch], Zhuravlev and Zhdanov [1953Zhu], Kheiker *et al.* [1953Khe], Levin *et al.* [1953Lev], Zhdanov [1954Zhd], Zhuravlev [1958Zhu] and Bhatt and Schubert [1979Bat]. Two other compounds, Bi_2Pd_5 and $Bi_{12}Pd_{31}$, were put in evidence by Sarah and Schubert [1979Sar], the second one in a very limited temperature range (823 K - 878 K). However, in diffusion couple experiments using BiPd and pure Pd [2001Obe] only the formation of $BiPd_3$ and Bi_3Pd_5 has been observed but neither Bi_2Pd_5 nor $Bi_{12}Pd_{31}$ have been detected. Therefore, only three stoichiometric compounds, Bi_2Pd, BiPd and $BiPd_3$ without structural transformation were modelled by the assessor [2006Vre]. There is no reported solubility of palladium in rhombohedral bismuth. In addition, the solubility of bismuth in palladium at lower temperature has been determined [2001Obe] and the integral enthalpy of mixing of liquid Bi-Pd alloys has been measured by high temperature solution calorimetry in the range of 0-50 at.% Pd at 1028 K.

Table I. Phases, structures and models.

Phase	Struktur-bericht	Prototype	Pearson symbol	Space group	SGTE name	Model
liquid					LIQUID	$(Bi,Pd)_1$
$A7$	$A7$	αAs	$hR2$	$R\bar{3}m$	RHOMBOHEDRAL_A7	$(Bi,Pd)_1$
αBi_2Pd	⋯	⋯	$mC12$	$C2/m$	A_BI2PD	Bi_2Pd_1
βBi_2Pd	$C11_b$	$MoSi_2$	$tI6$	$I4/mmm$	B_BI2PD	Bi_2Pd_1
$\alpha BiPd$	⋯	⋯	$mP32$	$P2_1$	A_BIPD	Bi_1Pd_1
$\beta BiPd$	⋯	⋯	$oC32$	$Cmc2_1$	B_BIPD	Bi_1Pd_1
Bi_3Pd_5	⋯	⋯	$hP16$	⋯	BI3PD5	$(Bi,Pd)_1$
Bi_2Pd_5	⋯	⋯	$mC28$	$C2/m$	⋯	⋯
$Bi_{12}Pd_{31}$	⋯	⋯	$hR44$	$R3$	⋯	⋯
$\alpha BiPd_3$	⋯	⋯	$oP16$	$Pmma$	A_BIPD3	Bi_1Pd_3
$\beta BiPd_3$	⋯	⋯	⋯	⋯	B_BIPD3	Bi_1Pd_3
fcc	$A1$	Cu	$cF4$	$Fm\bar{3}m$	FCC_A1	$(Bi,Pd)_1$

Table II. Invariant reactions.

Reaction	Type	T / K	Compositions / x_{Pd}			$\Delta_r H$ / (J/mol)
liquid $\rightleftharpoons$ $BiPd_3$	congruent	1204.6	0.750	0.750		−13032
liquid $\rightleftharpoons$ $BiPd_3$ + fcc	eutectic	1203.1	0.761	0.750	0.819	−11662
liquid + $BiPd_3$ $\rightleftharpoons$ Bi_3Pd_5	peritectic	958.1	0.604	0.750	0.665	−6996
liquid $\rightleftharpoons$ BiPd	congruent	895.9	0.500	0.500		−18429
liquid $\rightleftharpoons$ BiPd + Bi_3Pd_5	eutectic	884.1	0.548	0.500	0.629	−15299
liquid $\rightleftharpoons$ Bi_2Pd	congruent	787.0	0.333	0.333		−14229
liquid $\rightleftharpoons$ Bi_2Pd + BiPd	eutectic	786.7	0.342	0.333	0.500	−14308
Bi_3Pd_5 $\rightleftharpoons$ BiPd + $BiPd_3$	eutectoid	558.5	0.666	0.500	0.750	−1146
liquid $\rightleftharpoons$ A7 + Bi_2Pd	eutectic	518.1	0.074	0.000	0.333	−10706

Table IIIa. Integral quantities for the liquid phase at 1828 K.

x_{Pd}	ΔG_m [J/mol]	ΔH_m [J/mol]	ΔS_m [J/(mol·K)]	G_m^E [J/mol]	S_m^E [J/(mol·K)]	ΔC_P [J/(mol·K)]
0.000	0	0	0.000	0	0.000	0.000
0.100	−9182	−8190	0.543	−4242	−2.160	0.000
0.200	−15786	−15200	0.321	−8180	−3.840	0.000
0.300	−20861	−20790	0.039	−11577	−5.040	0.000
0.400	−24420	−24720	−0.164	−14191	−5.760	0.000
0.500	−26317	−26750	−0.237	−15782	−6.000	0.000
0.600	−26340	−26640	−0.164	−16111	−5.760	0.000
0.700	−24221	−24150	0.039	−14937	−5.040	0.000
0.800	−19626	−19040	0.321	−12021	−3.840	0.000
0.900	−12062	−11070	0.543	−7122	−2.160	0.000
1.000	0	0	0.000	0	0.000	0.000

Reference states: Bi(liquid), Pd(liquid)

Table IIIb. Partial quantities for Bi in the liquid phase at 1828 K.

x_{Bi}	ΔG_{Bi} [J/mol]	ΔH_{Bi} [J/mol]	ΔS_{Bi} [J/(mol·K)]	$G^{\mathrm{E}}_{\mathrm{Bi}}$ [J/mol]	$S^{\mathrm{E}}_{\mathrm{Bi}}$ [J/(mol·K)]	a_{Bi}	γ_{Bi}
1.000	0	0	0.000	0	0.000	1.000	1.000
0.900	−1713	−550	0.636	−111	−0.240	0.893	0.993
0.800	−4157	−2520	0.895	−765	−0.960	0.761	0.951
0.700	−7863	−6390	0.806	−2442	−2.160	0.596	0.852
0.600	−13385	−12640	0.407	−5620	−3.840	0.415	0.691
0.500	−21317	−21750	−0.237	−10782	−6.000	0.246	0.492
0.400	−32333	−34200	−1.021	−18406	−8.640	0.119	0.298
0.300	−47272	−50470	−1.750	−28973	−11.760	0.045	0.149
0.200	−67424	−71040	−1.978	−42962	−15.360	0.012	0.059
0.100	−95851	−96390	−0.295	−60854	−19.440	0.002	0.018
0.000	$-\infty$	−127000	∞	−83128	−24.000	0.000	0.004

Reference state: Bi(liquid)

Table IIIc. Partial quantities for Pd in the liquid phase at 1828 K.

x_{Pd}	ΔG_{Pd} [J/mol]	ΔH_{Pd} [J/mol]	ΔS_{Pd} [J/(mol·K)]	$G^{\mathrm{E}}_{\mathrm{Pd}}$ [J/mol]	$S^{\mathrm{E}}_{\mathrm{Pd}}$ [J/(mol·K)]	a_{Pd}	γ_{Pd}
0.000	$-\infty$	−87000	∞	−43128	−24.000	0.000	0.059
0.100	−76411	−76950	−0.295	−41414	−19.440	0.007	0.066
0.200	−62304	−65920	−1.978	−37842	−15.360	0.017	0.083
0.300	−51192	−54390	−1.750	−32893	−11.760	0.034	0.115
0.400	−40973	−42840	−1.021	−27046	−8.640	0.067	0.169
0.500	−31317	−31750	−0.237	−20782	−6.000	0.127	0.255
0.600	−22345	−21600	0.407	−14581	−3.840	0.230	0.383
0.700	−14343	−12870	0.806	−8922	−2.160	0.389	0.556
0.800	−7677	−6040	0.895	−4285	−0.960	0.603	0.754
0.900	−2753	−1590	0.636	−1151	−0.240	0.834	0.927
1.000	0	0	0.000	0	0.000	1.000	1.000

Reference state: Pd(liquid)

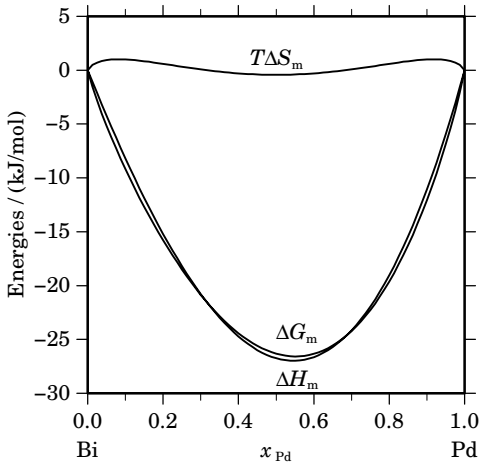

Fig. 2. Integral quantities of the liquid phase at T=1828 K.

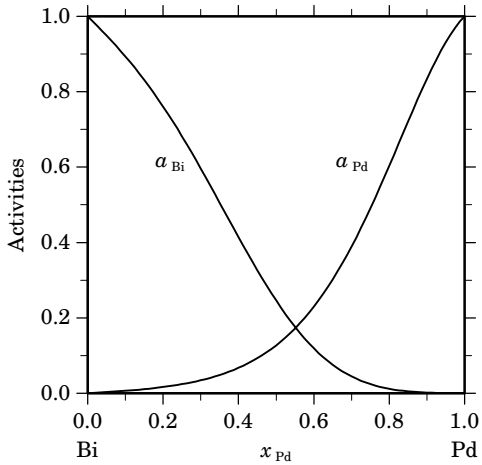

Fig. 3. Activities in the liquid phase at T=1828 K.

Table IVa. Integral quantities for the stable phases at 1028 K.

Phase	x_{Pd}	ΔG_{m} [J/mol]	ΔH_{m} [J/mol]	ΔS_{m} [J/(mol·K)]	$G_{\mathrm{m}}^{\mathrm{E}}$ [J/mol]	$S_{\mathrm{m}}^{\mathrm{E}}$ [J/(mol·K)]	ΔC_P [J/(mol·K)]
liquid	0.000	0	0	0.000	0	0.000	0.000
	0.100	−8134	−6964	1.139	−5356	−1.564	0.405
	0.200	−14302	−12747	1.513	−10025	−2.648	0.809
	0.300	−18989	−17111	1.827	−13768	−3.252	1.214
	0.400	−22097	−19814	2.220	−16344	−3.375	1.619
	0.500	−23438	−20618	2.744	−17514	−3.019	2.024
	0.600	−22789	−19281	3.413	−17037	−2.183	2.428
	0.626	−22253	−18539	3.613	−16605	−1.881	2.535
$BiPd_3$	0.750	−19375	−25134	−5.603			0.000
fcc	0.882	−10260	−8275	1.931	−7162	−1.083	0.000
	0.900	−8995	−7164	1.782	−6217	−0.921	0.000
	1.000	0	0	0.000	0	0.000	0.000

Reference states: Bi(liquid), Pd(fcc)

Table IVb. Partial quantities for Bi in the stable phases at 1028 K.

Phase	x_{Bi}	ΔG_{Bi} [J/mol]	ΔH_{Bi} [J/mol]	ΔS_{Bi} [J/(mol·K)]	$G_{\mathrm{Bi}}^{\mathrm{E}}$ [J/mol]	$S_{\mathrm{Bi}}^{\mathrm{E}}$ [J/(mol·K)]	a_{Bi}	γ_{Bi}
liquid	1.000	0	0	0.000	0	0.000	1.000	1.000
	0.900	−1204	−550	0.636	−303	−0.240	0.869	0.965
	0.800	−3440	−2520	0.895	−1533	−0.960	0.669	0.836
	0.700	−7218	−6390	0.806	−4170	−2.160	0.430	0.614
	0.600	−13059	−12640	0.407	−8692	−3.840	0.217	0.362
	0.500	−21507	−21750	−0.237	−15582	−6.000	0.081	0.162
	0.400	−33150	−34200	−1.021	−25318	−8.640	0.021	0.052
	0.374	−36850	−38115	−1.231	−28432	−9.419	0.013	0.036
$BiPd_3$	0.250	−36850	14909	50.349			0.013	
	0.250	−71081	−120776	−48.342			0.000	
fcc	0.118	−71081	−62143	8.695	−52799	−9.089	0.000	0.002
	0.100	−74921	−64616	10.025	−55241	−9.120	0.000	0.002
	0.000	$-\infty$	−79436	∞	−69865	−9.310	0.000	0.000

Reference state: Bi(liquid)

Table IVc. Partial quantities for Pd in the stable phases at 1028 K.

Phase	x_{Pd}	ΔG_{Pd} [J/mol]	ΔH_{Pd} [J/mol]	ΔS_{Pd} [J/(mol·K)]	$G^{\mathrm{E}}_{\mathrm{Pd}}$ [J/mol]	$S^{\mathrm{E}}_{\mathrm{Pd}}$ [J/(mol·K)]	a_{Pd}	γ_{Pd}
liquid	0.000	$-\infty$	−74735	∞	−56192	−18.038	0.000	0.001
	0.100	−70510	−64685	5.666	−50829	−13.478	0.000	0.003
	0.200	−57750	−53655	3.983	−43994	−9.398	0.001	0.006
	0.300	−46455	−42125	4.212	−36164	−5.798	0.004	0.015
	0.400	−35654	−30575	4.940	−27822	−2.678	0.015	0.039
	0.500	−25370	−19485	5.725	−19446	−0.038	0.051	0.103
	0.600	−15882	−9335	6.369	−11516	2.122	0.156	0.260
	0.626	−13550	−6866	6.501	−9552	2.613	0.205	0.327
$BiPd_3$	0.750	−13550	−38482	−24.253			0.205	
	0.750	−2139	6747	8.644			0.779	
fcc	0.882	−2139	−1082	1.028	−1068	−0.014	0.779	0.883
	0.900	−1670	−780	0.866	−770	−0.010	0.822	0.914
	1.000	0	0	0.000	0	0.000	1.000	1.000

Reference state: Pd(fcc)

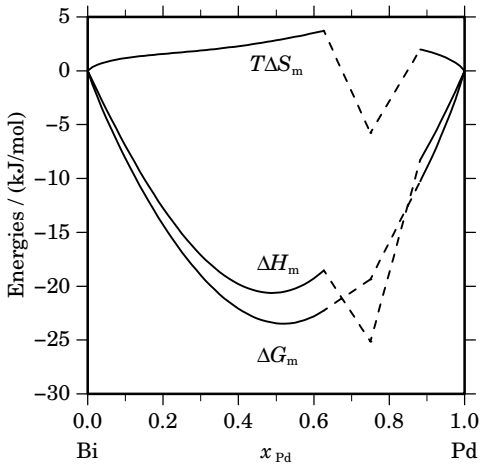

Fig. 4. Integral quantities of the stable phases at T=1028 K.

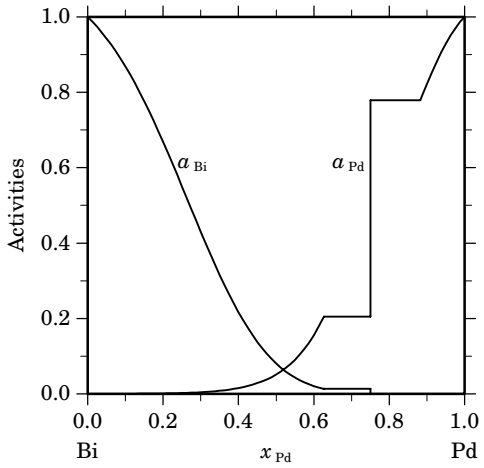

Fig. 5. Activities in the stable phases at T=1028 K.

Table V. Standard reaction quantities at 298.15 K for the compounds per mole of atoms.

Compound	x_{Pd}	$\Delta_{\mathrm{f}}G^{\circ}$ / (J/mol)	$\Delta_{\mathrm{f}}H^{\circ}$ / (J/mol)	$\Delta_{\mathrm{f}}S^{\circ}$ / (J/(mol·K))	$\Delta_{\mathrm{f}}C^{\circ}_{P}$ / (J/(mol·K))
Bi_2Pd_1	0.333	−24355	−25100	−2.500	0.000
Bi_1Pd_1	0.500	−31319	−33600	−7.650	0.000
Bi_1Pd_3	0.750	−22181	−22300	−0.400	0.000

References

[1953Khe] D.M. Kheiker, G.S. Zhdanov, N.N. Zhuravlev: Zh. Eksp. Teoret. Fiz. **25** (1953) 621–627.
[1953Lev] L.S. Levin, G.S. Zhdanov, N.N. Zhuravlev: Zh. Eksp. Teoret. Fiz. **25** (1953) 751–754.
[1953Sch] K. Schubert, K. Anderko, M. Kluge, H. Beeskov, M. Ilschner, E. Dorre, P. Esslinger: Naturwiss. **40** (1953) 269.
[1953Zhu] N.N. Zhuravlev, G.S. Zhdanov: Zh. Eksp. Teoret. Fiz. **25** (1953) 485–490.
[1954Zhd] G.S. Zhdanov: Tr. Inst. Kristallogr. Akad. Nauk SSSR **10** (1954) 99–116.
[1957Zhu] N.N. Zhuravlev: Zh. Eksp. Teoret. Fiz. **32** (1957) 1305–1312; transl.: Sov. Phys. JETP **5** (1957) 1064–1072.
[1958Zhu] N.N. Zhuravlev: Kristallogr. **3** (1958) 503–504; transl.: Sov. Phys. Crystallogr. **3** (1958) 506.
[1959Bra] J. Brasier, W. Hume-Rothery: J. Less-Common Met. **1** (1959) 157–164.
[1961Sch] D.G. Schweitzer, J.R. Weeks: Trans. Q. ASM **54** (1961) 185-200.
[1979Bat] Y.C. Bhatt, K. Schubert: J. Less-Common Met. **64** (1979) P17–P24.
[1979Sar] N. Sarah, K. Schubert: J. Less-Common Met. **63** (1979) 75–82.
[1994Oka] H. Okamoto: J. Phase Equilibria **15** (1994) 191–194.
[2001Obe] P. Oberndorff: Ph.D. Thesis, TU Eindhoven, 2001.
[2006Vre] J. Vřešťál, J. Pinkas, A. Watson, A. Scott, J. Houserová, A. Kroupa: Calphad **30** (2006) 14–17.

C – Ir (Carbon – Iridium)

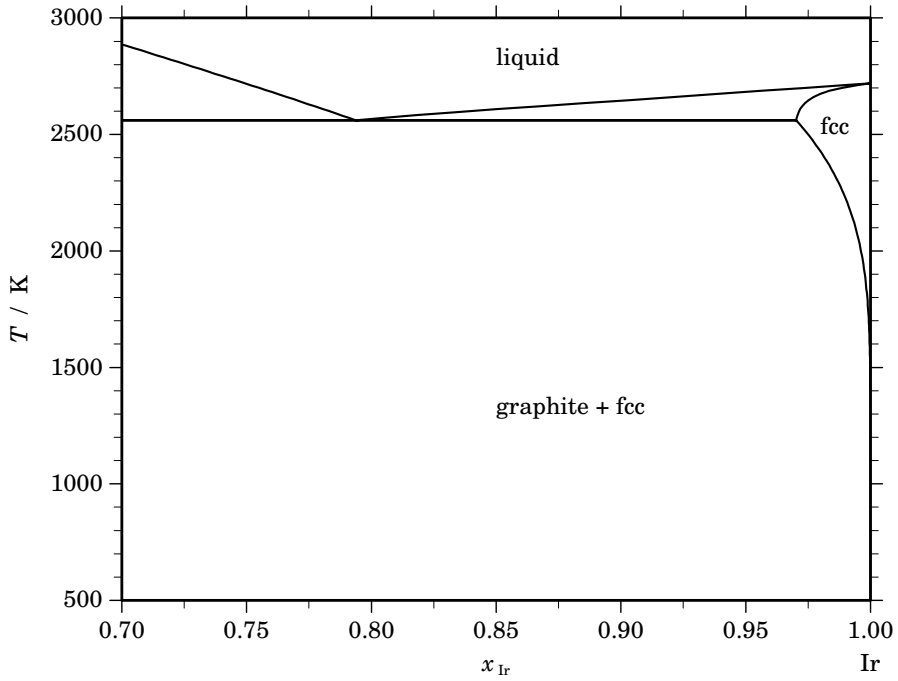

Fig. 1. Calculated phase diagram for the system C-Ir.

The C-Ir phase diagram displays the liquid phase, the fcc phase based on Ir with quite small solubility of C and the graphite phase. Burylev [1967Bur, 1969Bur] estimated the solubility of C in liquid Ir assuming systematic changes with atomic number in the interaction between the elements. Vol and Kagan [1976Vol] constructed the Ir-C phase diagram based on the above information [1990Mas]. The C-Ir system has been critically assessed by Korb [2004Kor]. The eutectic was experimentally determined by Nadler and Kempter [1960Nad], and later confirmed by the experimental investigations carried out by Dinsdale [2004Din]. The calculated eutectic temperature agrees well the experimental value [2004Din].

Table I. Phases, structures and models.

Phase	Struktur-bericht	Prototype	Pearson symbol	Space group	SGTE name	Model
liquid					LIQUID	$(C,Ir)_1$
graphite	$A9$	C(graphite)	$hP4$	$P6_3/mmc$	GRAPHITE	C_1
fcc	$A1$	Cu	$cF4$	$Fm\overline{3}m$	FCC_A1	$Ir_1(C,\square)_1$

Table II. Invariant reactions.

Reaction	Type	T / K	Compositions / x_{Ir}			$\Delta_r H$ / (J/mol)
liquid $\rightleftharpoons$ graphite + fcc	eutectic	2561.1	0.794	0.000	0.970	−34244

Table IIIa. Integral quantities for the liquid phase at 2800 K.

x_{Ir}	ΔG_{m} [J/mol]	ΔH_{m} [J/mol]	ΔS_{m} [J/(mol·K)]	$G_{\mathrm{m}}^{\mathrm{E}}$ [J/mol]	$S_{\mathrm{m}}^{\mathrm{E}}$ [J/(mol·K)]	ΔC_P [J/(mol·K)]
0.726	−3135	10139	4.740	10539	−0.143	0.000
0.800	−3257	6890	3.624	8393	−0.537	0.000
0.900	−2764	3270	2.155	4804	−0.548	0.000
1.000	0	0	0.000	0	0.000	0.000

Reference states: C(graphite), Ir(liquid)

Table IIIb. Partial quantities for C in the liquid phase at 2800 K.

x_{C}	ΔG_{C} [J/mol]	ΔH_{C} [J/mol]	ΔS_{C} [J/(mol·K)]	$G_{\mathrm{C}}^{\mathrm{E}}$ [J/mol]	$S_{\mathrm{C}}^{\mathrm{E}}$ [J/(mol·K)]	a_{C}	γ_{C}
0.274	0	45194	16.141	30127	5.381	1.000	3.648
0.200	−4008	38780	15.281	33461	1.900	0.842	4.209
0.100	−11724	33413	16.120	41882	−3.025	0.604	6.044
0.000	$-\infty$	32865	∞	55649	−8.137	0.000	10.917

Reference state: C(graphite)

Table IIIc. Partial quantities for Ir in the liquid phase at 2800 K.

x_{Ir}	ΔG_{Ir} [J/mol]	ΔH_{Ir} [J/mol]	ΔS_{Ir} [J/(mol·K)]	$G_{\mathrm{Ir}}^{\mathrm{E}}$ [J/mol]	$S_{\mathrm{Ir}}^{\mathrm{E}}$ [J/(mol·K)]	a_{Ir}	γ_{Ir}
0.726	−4318	−3101	0.435	3141	−2.229	0.831	1.144
0.800	−3070	−1083	0.710	2125	−1.146	0.876	1.096
0.900	−1769	−79	0.603	684	−0.273	0.927	1.030
1.000	0	0	0.000	0	0.000	1.000	1.000

Reference state: Ir(liquid)

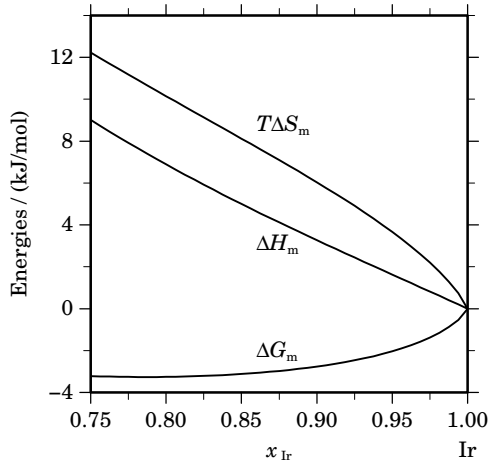

Fig. 2. Integral quantities of the liquid phase at T=2800 K.

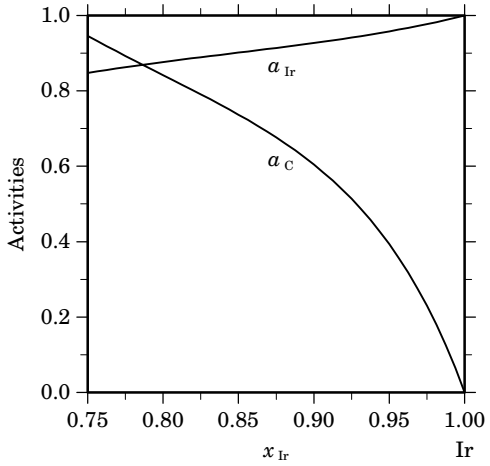

Fig. 3. Activities in the liquid phase at T=2800 K.

References

[1960Nad] M.R. Nadler, C.P. Kempter: J. Phys. Chem. **64** (1960) 1468-1471.
[1967Bur] B.P. Burylev: Izv. V.U.Z. Chern. Metall. **10** (1967) 20-22.
[1969Bur] B.P. Burylev: Izv. V.U.Z. Tsvetn. Metall. **12** (1969) 112–116.
[1976Vol] A.E. Vol, I.K. Kagan in: "Handbook of Binary Metallic Systems", Nauka Publishers, Moscow (1976); TR: National Bureau of Standards, pp. 788–789 (1985).
[1990Mas] T.B. Massalski (Ed.): "Binary Alloy Phase Diagrams", 2nd Ed., ASM Int., Materials Park, OH, 1990.
[2004Din] A.T. Dinsdale, NPL, Teddington, U.K., private communication, 2004.
[2004Kor] J. Korb, unpublished assessment, GTT-Technologies, 2004.

C – Os (Carbon – Osmium)

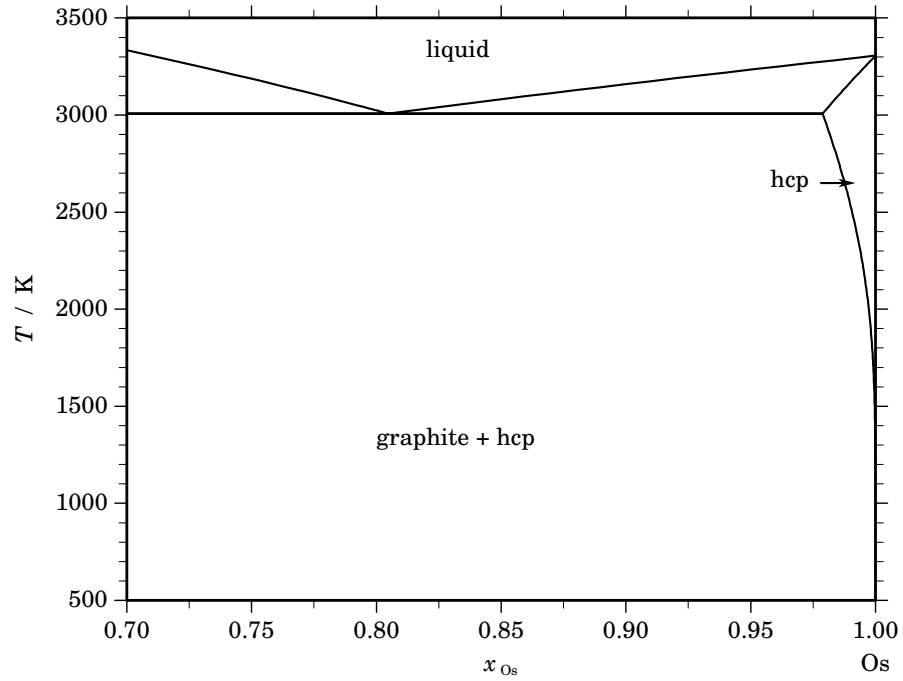

Fig. 1. Calculated phase diagram for the system C-Os.

The C-Os phase diagram is eutectic and includes the liquid phase, the hcp phase based on Os and graphite [1990Mas]. Experimental data on the C-Os system are limited and as the basis for the optimisation the phase diagram data given in [1976Mof] are used. OsC does not exist, according to [1964Rau]. The thermodynamic assessment of the C-Os system was carried out by Korb and Jantzen [2004Kor]. The experimentally determined invariant equilibria [1960Nad] agree satisfactorily with the calculations.

Table I. Phases, structures and models.

Phase	Struktur-bericht	Prototype	Pearson symbol	Space group	SGTE name	Model
liquid					LIQUID	$(C,Os)_1$
graphite	$A9$	C(graphite)	$hP4$	$P6_3/mmc$	GRAPHITE	C_1
hcp	$A3$	Mg	$hP2$	$P6_3/mmc$	HCP_A3	$Os_2(C,\square)_1$

Table II. Invariant reactions.

Reaction	Type	T / K	Compositions / x_{Os}			$\Delta_r H$ / (J/mol)
liquid $\rightleftharpoons$ graphite + hcp	eutectic	3007.5	0.805	0.000	0.979	−63629

Table IIIa. Integral quantities for the liquid phase at 3350 K.

x_{Os}	ΔG_{m} [J/mol]	ΔH_{m} [J/mol]	ΔS_{m} [J/(mol·K)]	$G^{\mathrm{E}}_{\mathrm{m}}$ [J/mol]	$S^{\mathrm{E}}_{\mathrm{m}}$ [J/(mol·K)]	ΔC_P [J/(mol·K)]
0.694	−7299	35054	12.643	9844	7.525	0.000
0.700	−7355	34413	12.468	9660	7.389	0.000
0.800	−7574	22866	9.087	6364	4.926	0.000
0.900	−5911	11395	5.166	3144	2.463	0.000
1.000	0	0	0.000	0	0.000	0.000

Reference states: C(graphite), Os(liquid)

Table IIIb. Partial quantities for C in the liquid phase at 3350 K.

x_{C}	ΔG_{C} [J/mol]	ΔH_{C} [J/mol]	ΔS_{C} [J/(mol·K)]	$G^{\mathrm{E}}_{\mathrm{C}}$ [J/mol]	$S^{\mathrm{E}}_{\mathrm{C}}$ [J/(mol·K)]	a_{C}	γ_{C}
0.306	0	115537	34.489	33026	24.630	1.000	3.273
0.300	−538	115507	34.640	32997	24.630	0.981	3.270
0.200	−12402	114937	38.012	32427	24.630	0.641	3.203
0.100	−32354	114291	43.775	31781	24.630	0.313	3.130
0.000	$-\infty$	113569	∞	31059	24.630	0.000	3.050

Reference state: C(graphite)

Table IIIc. Partial quantities for Os in the liquid phase at 3350 K.

x_{Os}	ΔG_{Os} [J/mol]	ΔH_{Os} [J/mol]	ΔS_{Os} [J/(mol·K)]	$G^{\mathrm{E}}_{\mathrm{Os}}$ [J/mol]	$S^{\mathrm{E}}_{\mathrm{Os}}$ [J/(mol·K)]	a_{Os}	γ_{Os}
0.694	−10510	−355	3.032	−355	0.000	0.686	0.987
0.700	−10277	−342	2.966	−342	0.000	0.691	0.988
0.800	−6367	−152	1.855	−152	0.000	0.796	0.995
0.900	−2973	−38	0.876	−38	0.000	0.899	0.999
1.000	0	0	0.000	0	0.000	1.000	1.000

Reference state: Os(liquid)

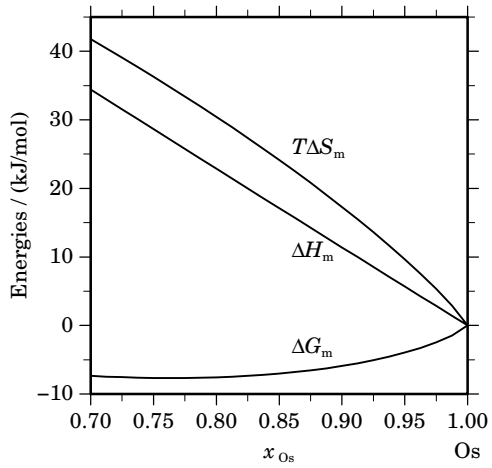

Fig. 2. Integral quantities of the liquid phase at T=3350 K.

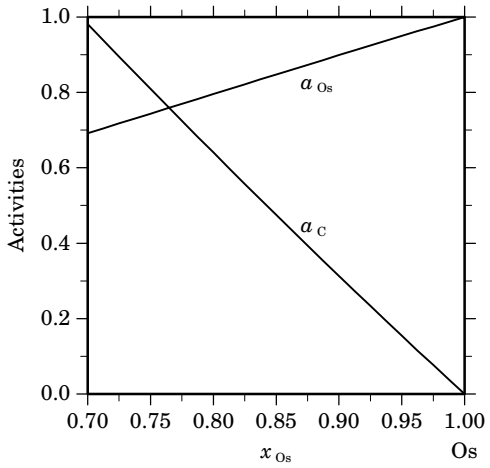

Fig. 3. Activities in the liquid phase at T=3350 K.

References

[1960Nad] M.R. Nadler, C.P. Kempter: J. Phys. Chem. **64** (1960) 1468–1471.
[1964Rau] E. Raub, G. Falkenberg: Z. Metallkd. **55** (1964) 186–189.
[1976Mof] W.G. Moffatt, (ed.): "Handbook of Binary Phase Diagrams", General Electric Co., Schenectady, NY (1976).
[90Mas] T.B. Massalski (ed.), Binary Alloy Phase Diagrams, ASM International (1990).
[2004Kor] J. Korb, T. Jantzen, unpublished assessment, GTT-Technologies, 2004.

C – Pd (Carbon – Palladium)

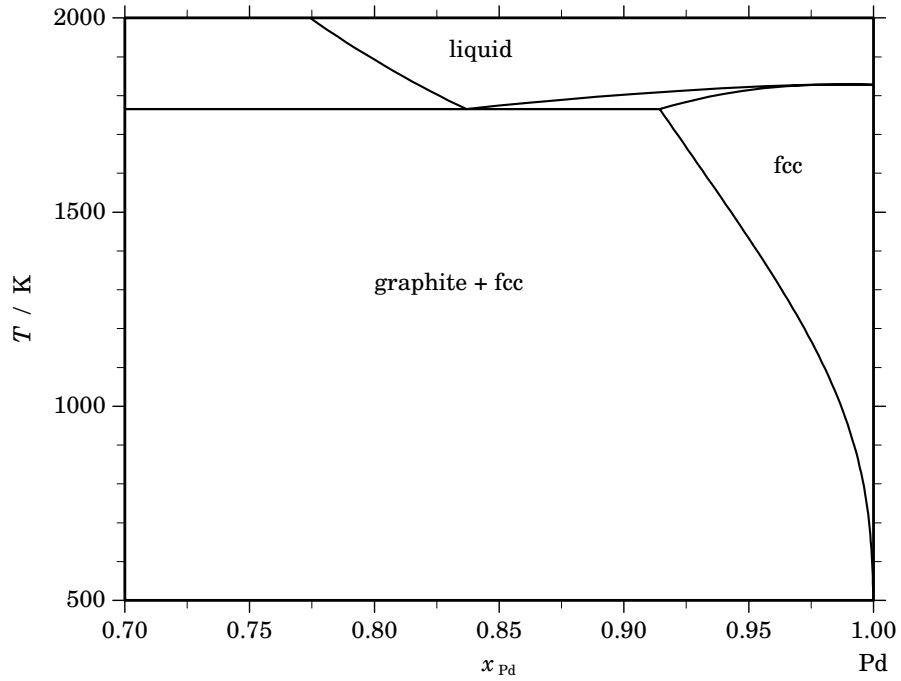

Fig. 1. Calculated phase diagram for the system C-Pd.

The C-Pd phase diagram is eutectic and includes the liquid phase, the fcc phase based on Pd and graphite [1990Mas]. Experimental data on the C-Pd system are limited and as the basis for the optimisation the phase diagram data given by [1996Mas, 2004Din] are used. The solid solubility of C in Pd was determined by Siller and Oates [1968Sil] in the temperature range 1173 to 1473 K. The eutectic reaction was studied by different authors using various methods. Nadler and Kempter [1960Nad] reported the eutectic temperature at about 1777 K, Bhatt and Venkataramani [1987Bha] at about 1783 K. Later investigations carried out by Dinsdale [2004Din] pointed out the temperature 1765 K, which has been used for the data assessment. The thermodynamic assessment of the C-Pd system was carried out by Korb [2004Kor]. The most recent experimental [2004Din] and the calculated invariant equilibria agree well.

Table I. Phases, structures and models.

Phase	Struktur-bericht	Prototype	Pearson symbol	Space group	SGTE name	Model
liquid					LIQUID	$(C,Pd)_1$
graphite	$A9$	C(graphite)	$hP4$	$P6_3/mmc$	GRAPHITE	C_1
fcc	$A1$	Cu	$cF4$	$Fm\bar{3}m$	FCC_A1	$Pd_1(C,\Box)_1$

Table II. Invariant reactions.

Reaction	Type	T / K	Compositions / x_{Pd}			$\Delta_r H$ / (J/mol)
liquid $\rightleftharpoons$ fcc	congruent	1828.8	0.989	0.989		−16895
liquid $\rightleftharpoons$ graphite + fcc	eutectic	1765.2	0.837	0.000	0.914	−19546

Table IIIa. Integral quantities for the liquid phase at 1900 K.

x_{Pd}	ΔG_{m} [J/mol]	ΔH_{m} [J/mol]	ΔS_{m} [J/(mol·K)]	$G_{\mathrm{m}}^{\mathrm{E}}$ [J/mol]	$S_{\mathrm{m}}^{\mathrm{E}}$ [J/(mol·K)]	ΔC_P [J/(mol·K)]
0.798	−2452	10441	6.786	5494	2.604	0.000
0.800	−2458	10367	6.750	5447	2.589	0.000
0.900	−2205	5990	4.313	2930	1.611	0.000
1.000	0	0	0.000	0	0.000	0.000

Reference states: C(graphite), Pd(liquid)

Table IIIb. Partial quantities for C in the liquid phase at 1900 K.

x_{C}	ΔG_{C} [J/mol]	ΔH_{C} [J/mol]	ΔS_{C} [J/(mol·K)]	$G_{\mathrm{C}}^{\mathrm{E}}$ [J/mol]	$S_{\mathrm{C}}^{\mathrm{E}}$ [J/(mol·K)]	a_{C}	γ_{C}
0.202	0	41741	21.969	25276	8.666	1.000	4.953
0.200	−163	41820	22.096	25263	8.714	0.990	4.949
0.100	−9681	51016	31.946	26694	12.801	0.542	5.418
0.000	$-\infty$	71579	∞	33028	20.290	0.000	8.090

Reference state: C(graphite)

Table IIIc. Partial quantities for Pd in the liquid phase at 1900 K.

x_{Pd}	ΔG_{Pd} [J/mol]	ΔH_{Pd} [J/mol]	ΔS_{Pd} [J/(mol·K)]	$G_{\mathrm{Pd}}^{\mathrm{E}}$ [J/mol]	$S_{\mathrm{Pd}}^{\mathrm{E}}$ [J/(mol·K)]	a_{Pd}	γ_{Pd}
0.798	−3073	2523	2.945	490	1.070	0.823	1.031
0.800	−3032	2504	2.913	493	1.058	0.825	1.032
0.900	−1375	987	1.243	290	0.367	0.917	1.018
1.000	0	0	0.000	0	0.000	1.000	1.000

Reference state: Pd(liquid)

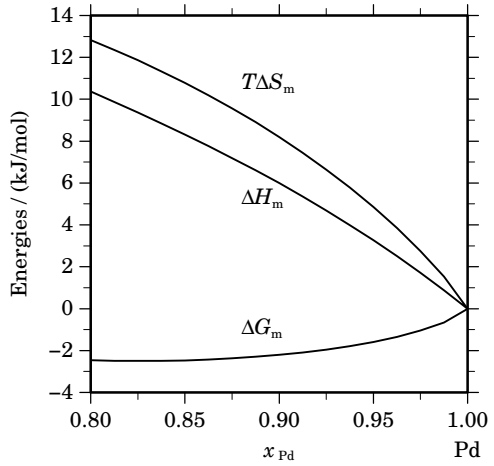

Fig. 2. Integral quantities of the liquid phase at T=1900 K.

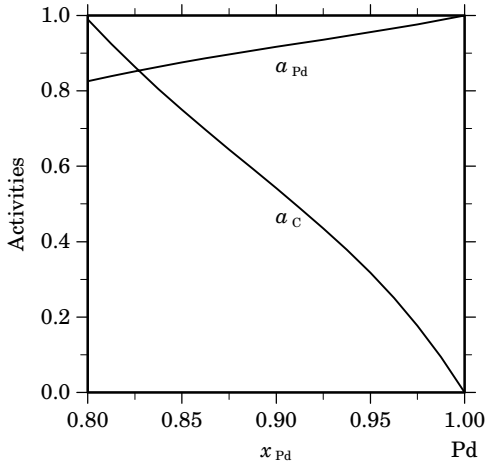

Fig. 3. Activities in the liquid phase at T=1900 K.

References

[1960Nad] M.R. Nadler, C.P. Kempter: J. Phys. Chem. **64** (1960) 1468–1471.
[1968Sil] R.H. Siller, W.A. Oates, R.B. McLellan: J. Less-Common Met. **16** (1968) 71–73.
[1987Bha] Y.J. Bhatt, R. Venkataramani, S.P. Garg: J. Less-Common Met. **132** (1987) L21–L24.
[1990Mas] T.B. Massalski (Ed.): "Binary Alloy Phase Diagrams", 2nd Ed., ASM Int., Materials Park, OH, 1990.
[2004Din] A.T. Dinsdale, NPL, Teddington, U.K., private communication, 2004.
[2004Kor] J. Korb, unpublished assessment, GTT-Technologies, 2004.

C – Pt (Carbon – Platinum)

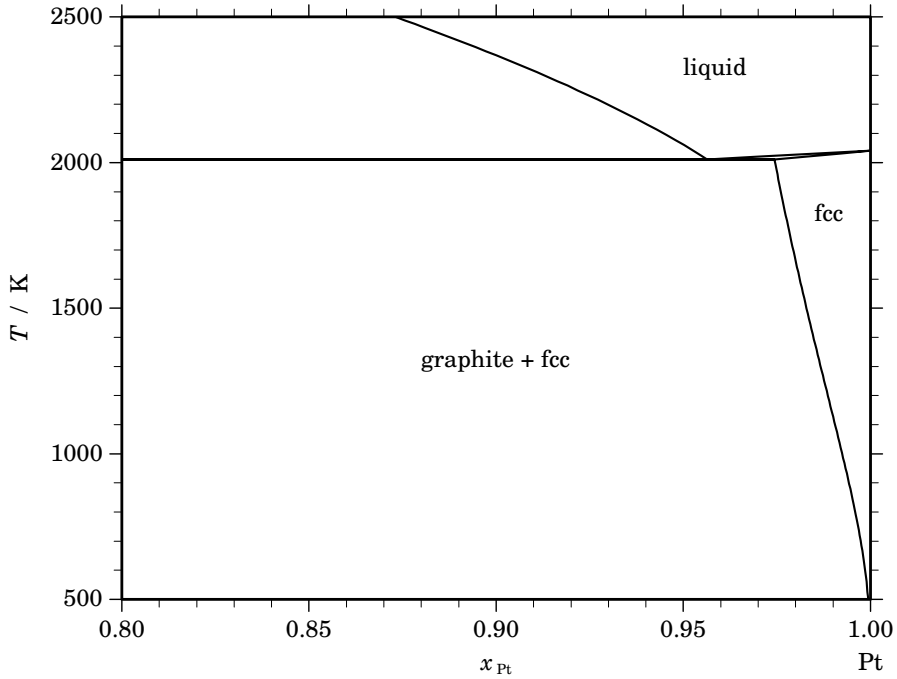

Fig. 1. Calculated phase diagram for the system C-Pt.

The C-Pt phase diagram has been studied by [1960Har, 1966Rhe, 1968Shi] using various experimental techniques. The system consists of the liquid, the fcc phase with very small solubility of C in Pt and the graphite phase with practically no solubility for Pt. No compounds were found to form at 65 kbar and 2973 K [1960Har]. The solid solubility of C in Pt was determined by [1968Sil] in the range from 1149 to 1518 K. According to [1996Mas] the solubility of C in Pt is less than 3 at.% C. This behaviour can be reproduced well by the calculations. Earlier investigations of the eutectic reaction at about 1978 K in the C-Pt system were carried out by Rhee [1966Rhe]. Later measurements done by Bhatt and Venkataramani [1987Bha], Park and Yamada [1999Par], and Dinsdale [2004Din] do not confirm previous experimental work. These investigations are however in good accord with each other and report the eutectic reaction between 2010 and 2011 K. The thermodynamic assessment of the C-Pt system was carried out by Korb and Jantzen [2004Kor]. The calculated eutectic temperature agrees very well with the experimental values [1987Bha, 2000Par, 2004Din].

Table I. Phases, structures and models.

Phase	Struktur-bericht	Prototype	Pearson symbol	Space group	SGTE name	Model
liquid					LIQUID	$(C,Pt)_1$
graphite	$A9$	C(graphite)	$hP4$	$P6_3/mmc$	GRAPHITE	C_1
fcc	$A1$	Cu	$cF4$	$Fm\overline{3}m$	FCC_A1	$Pt_1(C,\Box)_1$

Table II. Invariant reactions.

Reaction	Type	T / K	Compositions / x_{Pt}			$\Delta_r H$ / (J/mol)
liquid $\rightleftharpoons$ graphite + fcc	eutectic	2011.0	0.956	0.000	0.974	−25116

Table IIIa. Integral quantities for the liquid phase at 2100 K.

x_{Pt}	ΔG_{m} [J/mol]	ΔH_{m} [J/mol]	ΔS_{m} [J/(mol·K)]	$G^{\mathrm{E}}_{\mathrm{m}}$ [J/mol]	$S^{\mathrm{E}}_{\mathrm{m}}$ [J/(mol·K)]	ΔC_P [J/(mol·K)]
0.945	−986	5603	3.138	2745	1.361	0.000
0.950	−987	5066	2.882	2480	1.232	0.000
0.975	−812	2522	1.588	1229	0.616	0.000
1.000	0	0	0.000	0	0.000	0.000

Reference states: C(graphite), Pt(liquid)

Table IIIb. Partial quantities for C in the liquid phase at 2100 K.

x_{C}	ΔG_{C} [J/mol]	ΔH_{C} [J/mol]	ΔS_{C} [J/(mol·K)]	$G^{\mathrm{E}}_{\mathrm{C}}$ [J/mol]	$S^{\mathrm{E}}_{\mathrm{C}}$ [J/(mol·K)]	a_{C}	γ_{C}
0.055	0	102285	48.707	50562	24.630	1.000	18.098
0.050	−1913	102117	49.538	50394	24.630	0.896	17.924
0.025	−14829	101303	55.301	49580	24.630	0.428	17.109
0.000	$-\infty$	100469	∞	48746	24.630	0.000	16.310

Reference state: C(graphite)

Table IIIc. Partial quantities for Pt in the liquid phase at 2100 K.

x_{Pt}	ΔG_{Pt} [J/mol]	ΔH_{Pt} [J/mol]	ΔS_{Pt} [J/(mol·K)]	$G^{\mathrm{E}}_{\mathrm{Pt}}$ [J/mol]	$S^{\mathrm{E}}_{\mathrm{Pt}}$ [J/(mol·K)]	a_{Pt}	γ_{Pt}
0.945	−1044	−52	0.473	−52	0.000	0.942	0.997
0.950	−938	−42	0.426	−42	0.000	0.948	0.998
0.975	−453	−11	0.211	−11	0.000	0.974	0.999
1.000	0	0	0.000	0	0.000	1.000	1.000

Reference state: Pt(liquid)

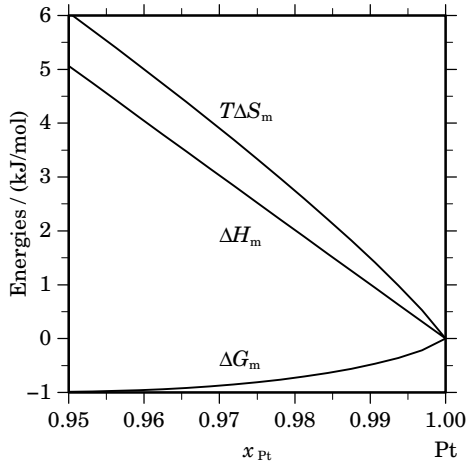

Fig. 2. Integral quantities of the liquid phase at T=2100 K.

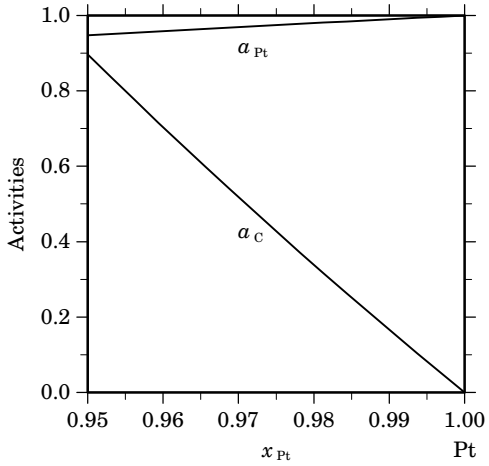

Fig. 3. Activities in the liquid phase at T=2100 K.

References

[1960Har] J.S. Harvey *et al.*: Tech. Rep. WADC-TR-59-655, 1960.

[1966Rhe] S.K. Rhee, Diss. Abstr. B **27** (1966) 1963; see also Platinum Met. Rev. **11** (1967) 112.

[1968Sil] R.H. Siller, W.A. Oates, R.B. McLellan: J. Less-Common Met. **16** (1968) 71–73.

[1987Bha] Y.J. Bhatt, R. Venkataramani, S.P. Garg: J. Less-Common Met. **132** (1987) L21–L24.

[1990Mas] T.B. Massalski (Ed.): "Binary Alloy Phase Diagrams", 2nd Ed., ASM Int., Materials Park, OH, 1990.

[2000Par] S.N. Park, Y. Yamada: SAE Mulli **40** (2000) 322–328.

[2004Din] A.T. Dinsdale, NPL, Teddington, U.K., private communication, 2004.

[2004Kor] J. Korb, T. Jantzen, unpublished assessment, GTT-Technologies, 2004.

C – Rh (Carbon – Rhodium)

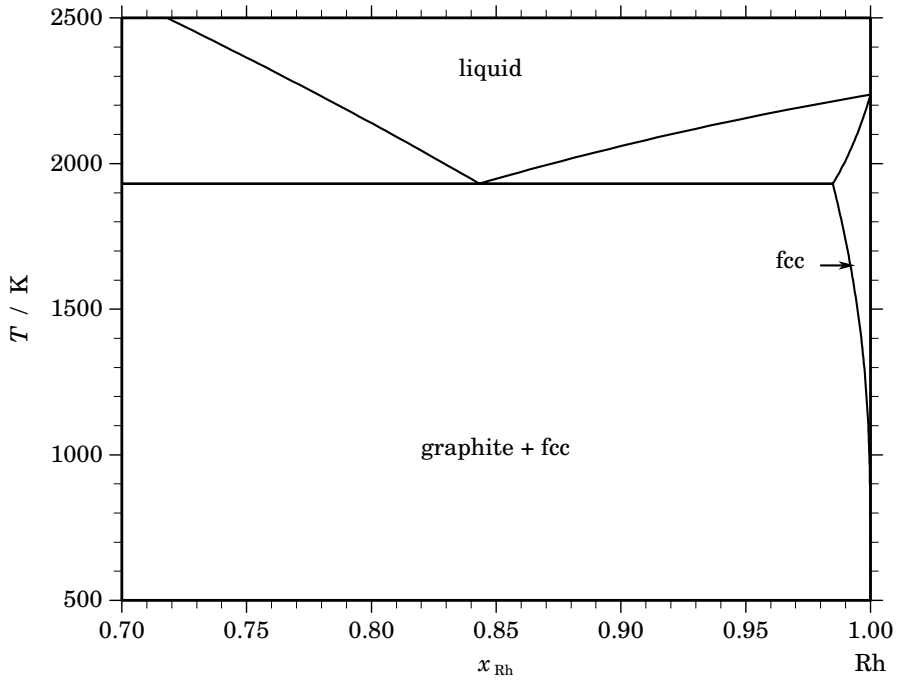

Fig. 1. Calculated phase diagram for the system C-Rh.

The C-Rh phase diagram is eutectic and includes the liquid phase, the fcc phase based on Rh and graphite [1990Mas]. Experimental data on the C-Rh system are limited and as the basis for the optimisation the phase diagram data given in [1990Mas] and the experimental data about the eutectic temperature [2004Din] are used. The solubility ranges for C in fcc-Rh were investigated by Barabash and Koval [1986Bar] in the temperature range from 1073 to 1523 K. The invariant equilibrium experimental data have been determined by Nadler and Kempter [1960Nad] who reported the eutectic temperature 1967±17 K, by Bhatt and Venkataramani (1947 K) [1987Bha] and by Dinsdale (1930 K) [2004Din]. The experimental investigations are in reasonable agreement, except for the eutectic temperature. The most recent measurement [2004Din] was used in the data assessment. The C-Rh system has been critically assessed by Korb and Jantzen [2004Kor]. The calculated and experimental [1967Gie, 2004Din] phase diagram are in good agreement.

Table I. Phases, structures and models.

Phase	Struktur-bericht	Prototype	Pearson symbol	Space group	SGTE name	Model
liquid					LIQUID	$(C,Rh)_1$
graphite	$A9$	C(graphite)	$hP4$	$P6_3/mmc$	GRAPHITE	C_1
fcc	$A1$	Cu	$cF4$	$Fm\bar{3}m$	FCC_A1	$Rh_1(C,\Box)_1$

Table II. Invariant reactions.

Reaction	Type	T / K	Compositions / x_{Rh}			$\Delta_r H$ / (J/mol)
liquid $\rightleftharpoons$ graphite + fcc	eutectic	1931.0	0.843	0.000	0.985	−30031

Table IIIa. Integral quantities for the liquid phase at 2250 K.

x_{Rh}	ΔG_{m} [J/mol]	ΔH_{m} [J/mol]	ΔS_{m} [J/(mol·K)]	$G^{\mathrm{E}}_{\mathrm{m}}$ [J/mol]	$S^{\mathrm{E}}_{\mathrm{m}}$ [J/(mol·K)]	ΔC_P [J/(mol·K)]
0.776	−5313	14560	8.832	4643	4.408	0.000
0.800	−5420	12660	8.035	3941	3.875	0.000
0.900	−4507	5652	4.515	1575	1.812	0.000
1.000	0	0	0.000	0	0.000	0.000

Reference states: C(graphite), Rh(liquid)

Table IIIb. Partial quantities for C in the liquid phase at 2250 K.

x_{C}	ΔG_{C} [J/mol]	ΔH_{C} [J/mol]	ΔS_{C} [J/(mol·K)]	$G^{\mathrm{E}}_{\mathrm{C}}$ [J/mol]	$S^{\mathrm{E}}_{\mathrm{C}}$ [J/(mol·K)]	a_{C}	γ_{C}
0.224	0	76727	34.101	27971	21.669	1.000	4.460
0.200	−3836	74143	34.657	26273	21.276	0.815	4.073
0.100	−23898	62622	38.453	19178	19.308	0.279	2.788
0.000	$-\infty$	49732	∞	12087	16.731	0.000	1.908

Reference state: C(graphite)

Table IIIc. Partial quantities for Rh in the liquid phase at 2250 K.

x_{Rh}	ΔG_{Rh} [J/mol]	ΔH_{Rh} [J/mol]	ΔS_{Rh} [J/(mol·K)]	$G^{\mathrm{E}}_{\mathrm{Rh}}$ [J/mol]	$S^{\mathrm{E}}_{\mathrm{Rh}}$ [J/(mol·K)]	a_{Rh}	γ_{Rh}
0.776	−6848	−3407	1.530	−2099	−0.581	0.693	0.894
0.800	−5816	−2711	1.380	−1642	−0.475	0.733	0.916
0.900	−2352	−678	0.744	−381	−0.132	0.882	0.980
1.000	0	0	0.000	0	0.000	1.000	1.000

Reference state: Rh(liquid)

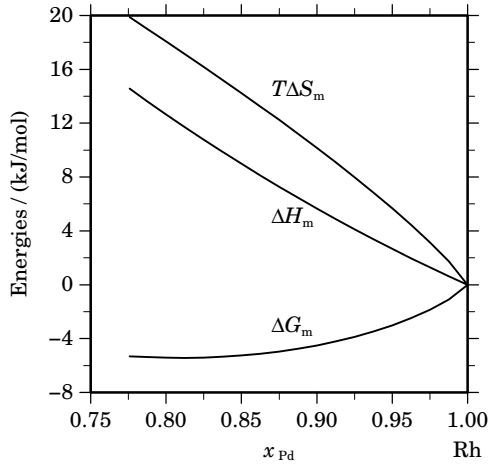

Fig. 2. Integral quantities of the liquid phase at T=2250 K.

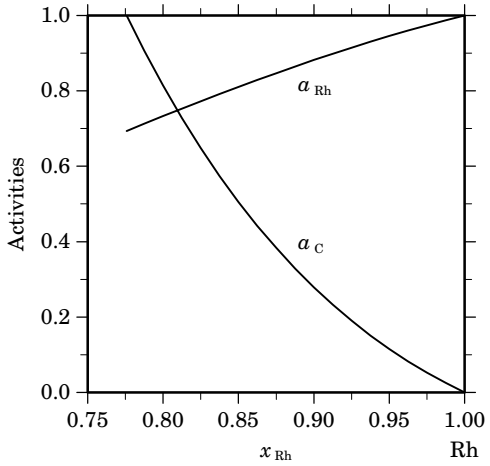

Fig. 3. Activities in the liquid phase at T=2250 K.

References

[1960Nad] M.R. Nadler, C.P. Kempter: J. Phys. Chem. **64** (1960) 1468–1471.
[1967Gie] B.C. Giessen, P.N. Dangel, N.J. Grant: J. Less-Common Met. **13** (1967) 62–70.
[1986Bar] O.M. Barabash, Yu.N. Koval: "Crystal Structure of Metals and Alloys", Naukova Dumka, Kiev, (1986) 209.
[1987Bha] Y.J. Bhatt, R. Venkataramani, S.P. Garg: J. Less-Common Met. **132** (1987) L21–L24.
[1990Mas] T.B. Massalski (Ed.): "Binary Alloy Phase Diagrams", 2nd Ed., ASM Int., Materials Park, OH, 1990.
[2004Din] A.T. Dinsdale, NPL, Teddington, U.K., private communication, 2004.
[2004Kor] J. Korb, T. Jantzen, unpublished assessment, GTT-Technologies, 2004.

C – Ru (Carbon – Ruthenium)

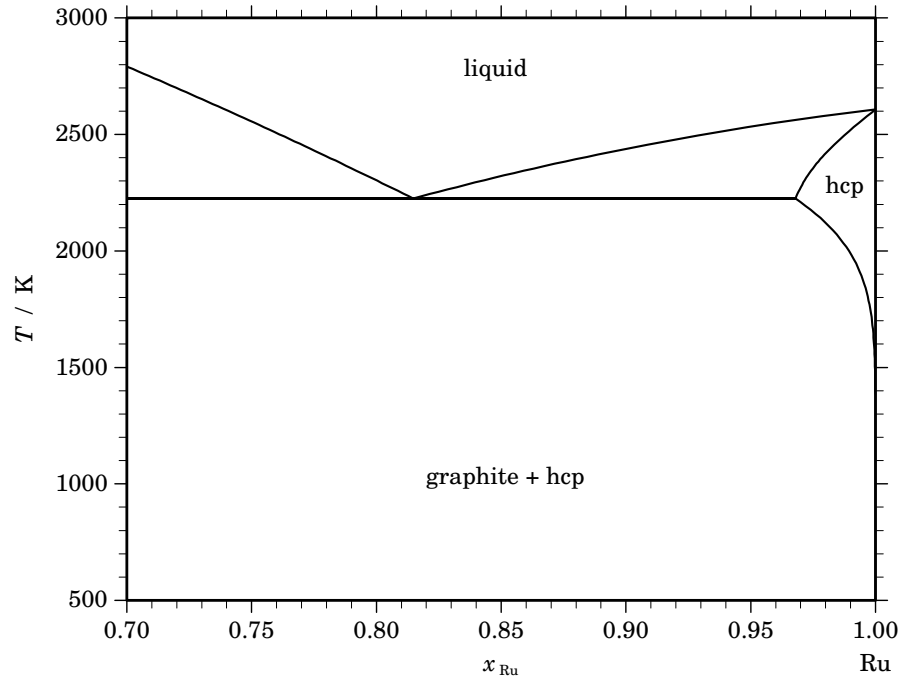

Fig. 1. Calculated phase diagram for the system C-Ru.

The C-Ru phase diagram is eutectic and includes the liquid phase, the hcp phase based on Ru and graphite [1990Mas]. The solubility range of C in hcp-Ru was investigated by Barabash and Koval [1986Bar] in the temperature range from 1073 to 1523 K. Experimental data on the C-Ru system are limited. The assessment is based on the phase diagram data given in [1990Mas] which have been measured by Fromm and Gebhardt [1978Fro]. The experimental data for the eutectic temperature are consistent and do not contradict each other. According to Fromm and Gebhardt [1978Fro] the invariant reaction occurs at 2213 K, Bhatt and Venkatarami [1987Bha] reported the temperature 2231 K, while Park and Yamada [2000Par] as well as Dinsdale [2004Din] found the eutectic temperature to be 2225 K. The latter value was used in the data assessment. The C-Ru system has been critically assessed by Korb and Jantzen [2004Kor]. The calculated and experimentally determined phase diagram agree well.

Table I. Phases, structures and models.

Phase	Struktur-bericht	Prototype	Pearson symbol	Space group	SGTE name	Model
liquid					LIQUID	$(Ru,C)_1$
graphite	$A9$	C(graphite)	$hP4$	$P6_3/mmc$	GRAPHITE	C_1
hcp	$A3$	Mg	$hP2$	$P6_3/mmc$	HCP_A3	$Ru_2(C,\Box)_1$

Table II. Invariant reactions.

Reaction	Type	T / K	Compositions / x_{Ru}			$\Delta_r H$ / (J/mol)
liquid $\rightleftharpoons$ graphite + hcp	eutectic	2225.1	0.815	0.000	0.968	−38728

Table IIIa. Integral quantities for the liquid phase at 2700 K.

x_{Ru}	ΔG_{m} [J/mol]	ΔH_{m} [J/mol]	ΔS_{m} [J/(mol·K)]	$G_{\mathrm{m}}^{\mathrm{E}}$ [J/mol]	$S_{\mathrm{m}}^{\mathrm{E}}$ [J/(mol·K)]	ΔC_P [J/(mol·K)]
0.720	−8999	22946	11.831	4316	6.900	0.000
0.800	−9227	15307	9.087	2007	4.926	0.000
0.900	−7005	6943	5.166	293	2.463	0.000
1.000	0	0	0.000	0	0.000	0.000

Reference states: C(graphite), Ru(liquid)

Table IIIb. Partial quantities for C in the liquid phase at 2700 K.

x_{C}	ΔG_{C} [J/mol]	ΔH_{C} [J/mol]	ΔS_{C} [J/(mol·K)]	$G_{\mathrm{C}}^{\mathrm{E}}$ [J/mol]	$S_{\mathrm{C}}^{\mathrm{E}}$ [J/(mol·K)]	a_{C}	γ_{C}
0.280	0	95067	35.210	28566	24.630	1.000	3.570
0.200	−15087	87545	38.012	21044	24.630	0.511	2.553
0.100	−42169	76024	43.775	9523	24.630	0.153	1.528
0.000	$-\infty$	61882	∞	−4619	24.630	0.000	0.814

Reference state: C(graphite)

Table IIIc. Partial quantities for Ru in the liquid phase at 2700 K.

x_{Ru}	ΔG_{Ru} [J/mol]	ΔH_{Ru} [J/mol]	ΔS_{Ru} [J/(mol·K)]	$G_{\mathrm{Ru}}^{\mathrm{E}}$ [J/mol]	$S_{\mathrm{Ru}}^{\mathrm{E}}$ [J/(mol·K)]	a_{Ru}	γ_{Ru}
0.720	−12501	−5121	2.733	−5121	0.000	0.573	0.796
0.800	−7762	−2753	1.855	−2753	0.000	0.708	0.885
0.900	−3098	−733	0.876	−733	0.000	0.871	0.968
1.000	0	0	0.000	0	0.000	1.000	1.000

Reference state: Ru(liquid)

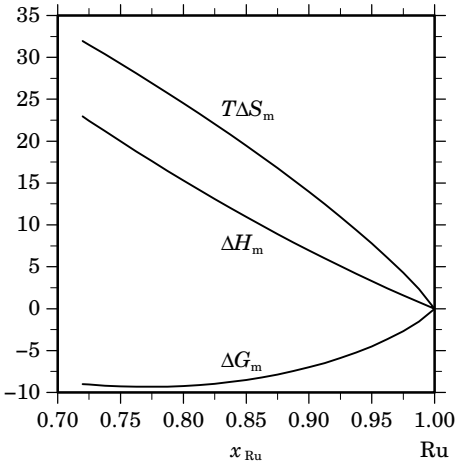

Fig. 2. Integral quantities of the liquid phase at T=2700 K.

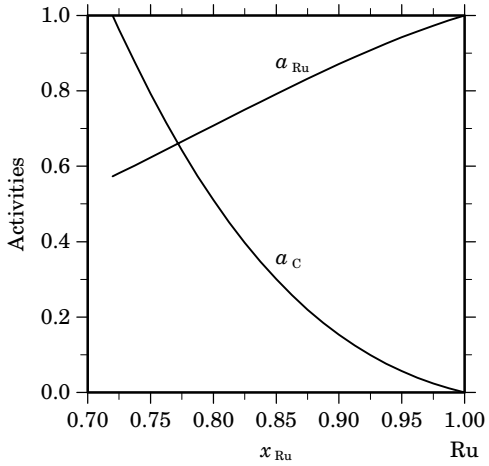

Fig. 3. Activities in the liquid phase at T=2700 K.

References

[1978Fro] E. Fromm, T.E. Gebhardt: "Gasses and Carbon in Metals", Metallurgiya, Moscow, 1978.

[1986Bar] O.M. Barabash, Yu.N. Koval: "Crystal Structure of Metals and Alloys", Naukova Dumka, Kiev, (1986) 209–210.

[1987Bha] Y.J. Bhatt, R. Venkataramani, S.P. Garg: J. Less-Common Met. **132** (1987) L21–L24.

[1990Mas] T.B. Massalski (Ed.): "Binary Alloy Phase Diagrams", 2nd Ed., ASM Int., Materials Park, OH, 1990.

[2000Par] S.N. Park, Y. Yamada: SAE Mulli **40** (2000) 322–328.

[2004Din] A.T. Dinsdale, NPL, Teddington, U.K., private communication, 2004.

[2004Kor] J. Korb, T. Jantzen, unpublished assessment, GTT-Technologies, 2004.

C – Zn (Carbon – Zinc)

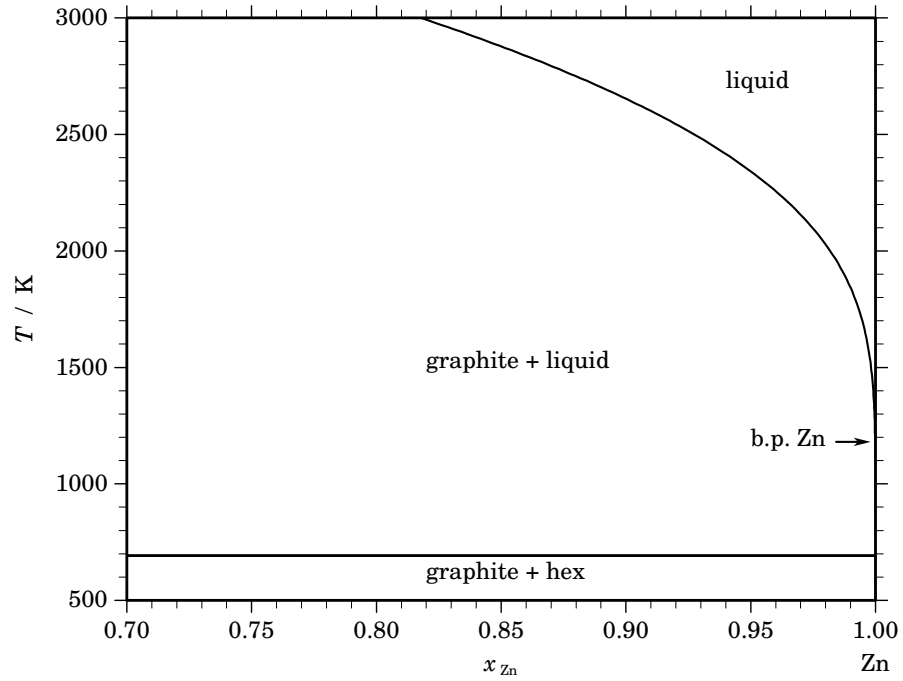

Fig. 1. Calculated phase diagram for the system C-Zn.

Only minor information is available on the carbon-zinc system. The solubility of C in liquid Zn at the boiling point of Zn is only small but no reliable value has been measured [1919Ruf]. The solubility of C in solid Zn is unknown. In an assessment of the ternary system C-Co-Zn, Hämäläinen and Isomäki [2005Häm] evaluated the interaction between carbon and zinc in the melt which allows the calculation of the binary C-Zn phase diagram. This result compares well with the phase diagram given by [2000Tur] which has been calculated with different preconditions. The boiling point of Zn is indicated in the phase diagram although the gas phase has been suppressed in the calculation.

Table I. Phases, structures and models.

Phase	Struktur-bericht	Prototype	Pearson symbol	Space group	SGTE name	Model
liquid					LIQUID	$(C,Zn)_1$
graphite	$A9$	C(graphite)	$hP4$	$P6_3/mmc$	GRAPHITE	C_1
hex	$A3$	Mg	$hP2$	$P6_3/mmc$	HCP_ZN	Zn_1

Table II. Invariant reactions.

Reaction	Type	T / K	Compositions / x_{Zn}			$\Delta_r H$ / (J/mol)
liquid $\rightleftharpoons$ graphite + hex	eutectic	692.7	1.000	0.000	1.000	−7322

References

[1919Ruf] O. Ruff, B. Bergdahl: Z. Anorg. Chem. **106** (1919) 91–94.
[2000Tur] V.Z. Turkevich: J. Superhard Mater. **22** (2000) 11–15.
[2005Häm] M. Hämäläinen, I. Isomäki: J. Alloys Comp. **392** (2005) 220–224.

Ca – Li (Calcium – Lithium)

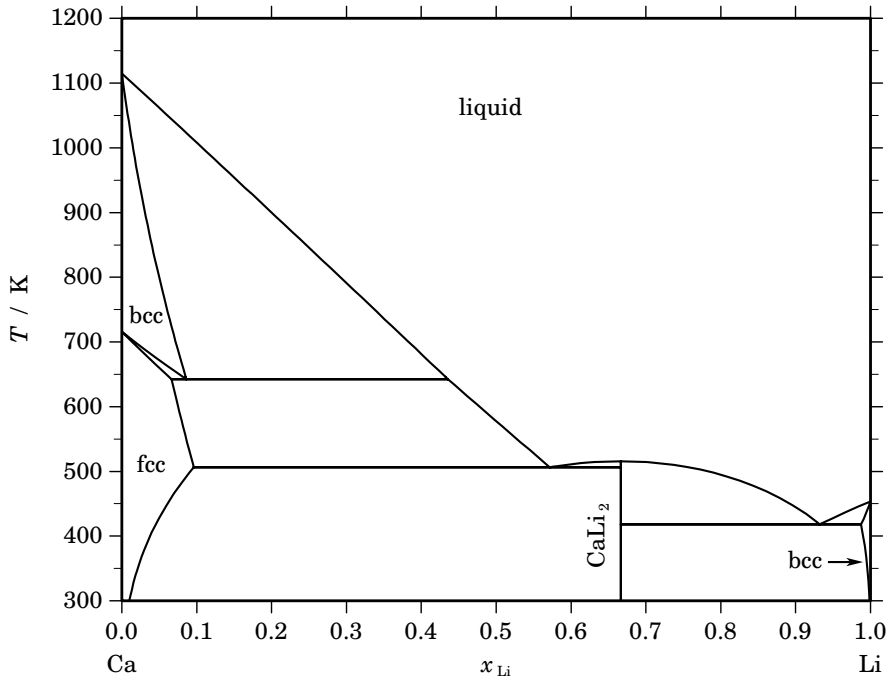

Fig. 1. Calculated phase diagram for the system Ca-Li.

Calcium and lithium are both important alloying elements for magnesium. Calcium acts as a grain refiner and it improves the creep resistance while Li decreases the density of the alloys. The literature on the Ca-Li system has been reviewed in [1987Bal, 2002Grö] and a thermodynamic assessment has been given in [2002Grö]. The phase diagram has been thoroughly investigated by [1966Car]. The enthalpy of formation of $CaLi_2$ has been measured by drop solution calorimetry [2002Grö]. Based on these data, the critical recommendations for the phase diagram and the invariants given in [1987Bal] and using the SGTE element data the thermodynamic description for Ca-Li has been optimised.

Table I. Phases, structures and models.

Phase	Struktur-bericht	Prototype	Pearson symbol	Space group	SGTE name	Model
liquid					LIQUID	$(Ca,Li)_1$
fcc	$A1$	Cu	$cF4$	$Fm\bar{3}m$	FCC_A1	$(Ca,Li)_1$
$CaLi_2$	$C14$	$MgZn_2$	$hP12$	$P6_3/mmc$	CALI2	Ca_1Li_2
bcc	$A2$	W	$cI2$	$Im\bar{3}m$	BCC_A2	$(Ca,Li)_1$
hcp	$A3$	Mg	$hP2$	$P6_3/mmc$	HCP_A3	$(Ca,Li)_1$

Table II. Invariant reactions.

Reaction	Type	T / K	Compositions / x_{Li}			$\Delta_r H$ / (J/mol)
bcc $\rightleftharpoons$ fcc + liquid	metatectic	642.5	0.086	0.066	0.435	−708
liquid $\rightleftharpoons$ $CaLi_2$	congruent	515.5	0.667	0.667		−8244
liquid $\rightleftharpoons$ fcc + $CaLi_2$	eutectic	506.5	0.572	0.096	0.667	−8117
liquid $\rightleftharpoons$ $CaLi_2$ + bcc	eutectic	418.1	0.932	0.667	0.987	−3723

Table IIIa. Integral quantities for the liquid phase at 1200 K.

x_{Li}	ΔG_{m} [J/mol]	ΔH_{m} [J/mol]	ΔS_{m} [J/(mol·K)]	$G^{\mathrm{E}}_{\mathrm{m}}$ [J/mol]	$S^{\mathrm{E}}_{\mathrm{m}}$ [J/(mol·K)]	ΔC_P [J/(mol·K)]
0.000	0	0	0.000	0	0.000	0.000
0.100	−4098	−508	2.991	−854	0.289	0.000
0.200	−6511	−903	4.674	−1518	0.513	0.000
0.300	−8088	−1185	5.752	−1993	0.673	0.000
0.400	−8992	−1354	6.365	−2277	0.770	0.000
0.500	−9288	−1410	6.565	−2372	0.802	0.000
0.600	−8992	−1354	6.365	−2277	0.770	0.000
0.700	−8088	−1185	5.752	−1993	0.673	0.000
0.800	−6511	−903	4.674	−1518	0.513	0.000
0.900	−4098	−508	2.991	−854	0.289	0.000
1.000	0	0	0.000	0	0.000	0.000

Reference states: Ca(liquid), Li(liquid)

Table IIIb. Partial quantities for Ca in the liquid phase at 1200 K.

x_{Ca}	ΔG_{Ca} [J/mol]	ΔH_{Ca} [J/mol]	ΔS_{Ca} [J/(mol·K)]	$G^{\mathrm{E}}_{\mathrm{Ca}}$ [J/mol]	$S^{\mathrm{E}}_{\mathrm{Ca}}$ [J/(mol·K)]	a_{Ca}	γ_{Ca}
1.000	0	0	0.000	0	0.000	1.000	1.000
0.900	−1146	−56	0.908	−95	0.032	0.891	0.991
0.800	−2606	−226	1.984	−380	0.128	0.770	0.963
0.700	−4413	−508	3.254	−854	0.289	0.643	0.918
0.600	−6615	−903	4.760	−1518	0.513	0.515	0.859
0.500	−9288	−1410	6.565	−2372	0.802	0.394	0.788
0.400	−12558	−2031	8.773	−3416	1.154	0.284	0.710
0.300	−16662	−2764	11.582	−4650	1.571	0.188	0.627
0.200	−22131	−3610	15.434	−6073	2.052	0.109	0.544
0.100	−30660	−4569	21.742	−7686	2.597	0.046	0.463
0.000	$-\infty$	−5641	∞	−9489	3.207	0.000	0.386

Reference state: Ca(liquid)

Table IIIc. Partial quantities for Li in the liquid phase at 1200 K.

x_{Li}	ΔG_{Li} [J/mol]	ΔH_{Li} [J/mol]	ΔS_{Li} [J/(mol·K)]	$G^{\mathrm{E}}_{\mathrm{Li}}$ [J/mol]	$S^{\mathrm{E}}_{\mathrm{Li}}$ [J/(mol·K)]	a_{Li}	γ_{Li}
0.000	$-\infty$	−5641	∞	−9489	3.207	0.000	0.386
0.100	−30660	−4569	21.742	−7686	2.597	0.046	0.463
0.200	−22131	−3610	15.434	−6073	2.052	0.109	0.544
0.300	−16662	−2764	11.582	−4650	1.571	0.188	0.627
0.400	−12558	−2031	8.773	−3416	1.154	0.284	0.710
0.500	−9288	−1410	6.565	−2372	0.802	0.394	0.788
0.600	−6615	−903	4.760	−1518	0.513	0.515	0.859
0.700	−4413	−508	3.254	−854	0.289	0.643	0.918
0.800	−2606	−226	1.984	−380	0.128	0.770	0.963
0.900	−1146	−56	0.908	−95	0.032	0.891	0.991
1.000	0	0	0.000	0	0.000	1.000	1.000

Reference state: Li(liquid)

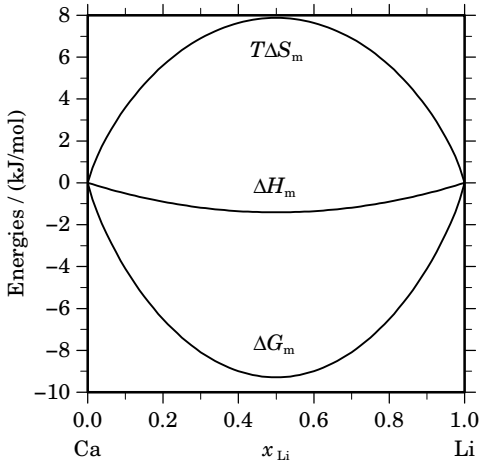

Fig. 2. Integral quantities of the liquid phase at T=1200 K.

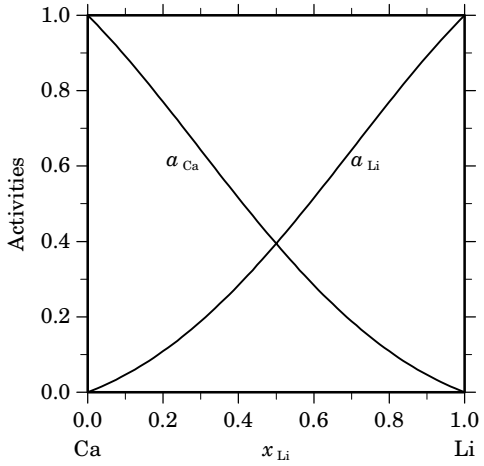

Fig. 3. Activities in the liquid phase at T=1200 K.

Table IV. Standard reaction quantities at 298.15 K for the compounds per mole of atoms.

Compound	x_{Li}	$\Delta_f G^\circ$ / (J/mol)	$\Delta_f H^\circ$ / (J/mol)	$\Delta_f S^\circ$ / (J/(mol·K))	$\Delta_f C_P^\circ$ / (J/(mol·K))
Ca_1Li_2	0.667	−3258	−3894	−2.132	0.000

References

[1966Car] D.G. Carfagno, Ph.D. Thesis, Syracuse Univ., Syracuse, NY, 1966.
[1987Bal] C.W. Bale, A.D. Pelton: Bull. Alloy Phase Diagrams **8** (1987) 125–127.
[2002Grö] J. Gröbner, R. Schmid-Fetzer, A. Pisch, C. Colinet, V.V. Pavlyuk, G.S. Dmytriv, D.G. Kevorkov, O.I. Bodak: Thermochim. Acta **389** (2002) 85–94.

Ca – Ru (Calcium – Ruthenium)

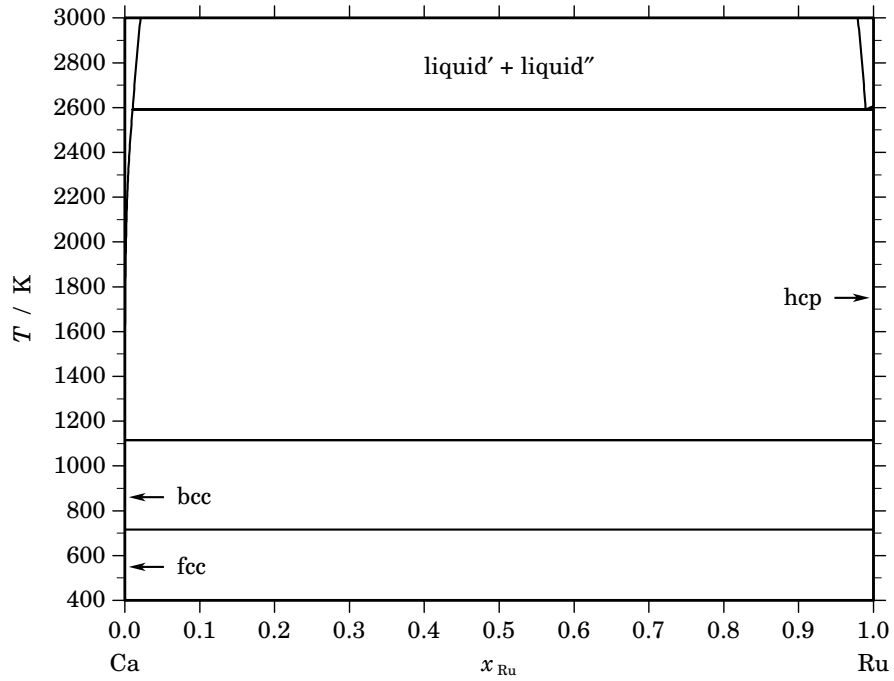

Fig. 1. Calculated phase diagram for the system Ca-Ru.

The Ca-Ru binary system contains two components of interest in the nuclear field, calcium being a major component of the concrete basemat in its oxide form (CaO) and Ru selected as representative of a family of non-volatile fission products.
The classical compilations of binary phase diagrams, give no information at all on this system. Consequently, it has been supposed that there is a negligible mutual solid solubility of calcium and ruthenium in each other, and a wide miscibility gap in the liquid state, the mutual solubility increasing at high temperature. Thus, the assessed diagram is only qualitative and the solid and liquid solubilities are entirely estimated. No thermodynamic property is available for that system. The system was assessed by Chevalier and Fischer [1996Che].
The excess Gibbs energy of the liquid was estimated to be highly positive, to produce a small solubility of components at low temperature and a large miscibility gap at high temperature. Similarly, highly positive interaction parameters in the bcc, fcc and hcp phases allow to produce a negligible mutual solubility. No comparison of the calculated phase diagram with experimental data is possible.

Table I. Phases, structures and models.

Phase	Struktur-bericht	Prototype	Pearson symbol	Space group	SGTE name	Model
liquid					LIQUID	$(Ca,Ru)_1$
fcc	$A1$	Cu	$cF4$	$Fm\overline{3}m$	FCC_A1	Ca_1
bcc	$A2$	W	$cI2$	$Im\overline{3}m$	BCC_A2	Ca_1
hcp	$A3$	Mg	$hP2$	$P6_3/mmc$	HCP_A3	Ru_1

Table II. Invariant reactions.

Reaction	Type	T / K	Compositions / x_{Ru}			$\Delta_{\mathrm{r}}H$ / (J/mol)
liquid $\rightleftharpoons$ liquid + hcp	eutectic	2592.3	0.989	0.011	1.000	−39195
liquid $\rightleftharpoons$ bcc + hcp	eutectic	1115.0	0.000	0.000	1.000	−8540
bcc + hcp $\rightleftharpoons$ fcc	peritectoid	716.0	0.000	1.000	0.000	−929

References

[1996Che] P.-Y. Chevalier, E. Fischer, unpublished work, 1996.

Cd – Y (Cadmium – Yttrium)

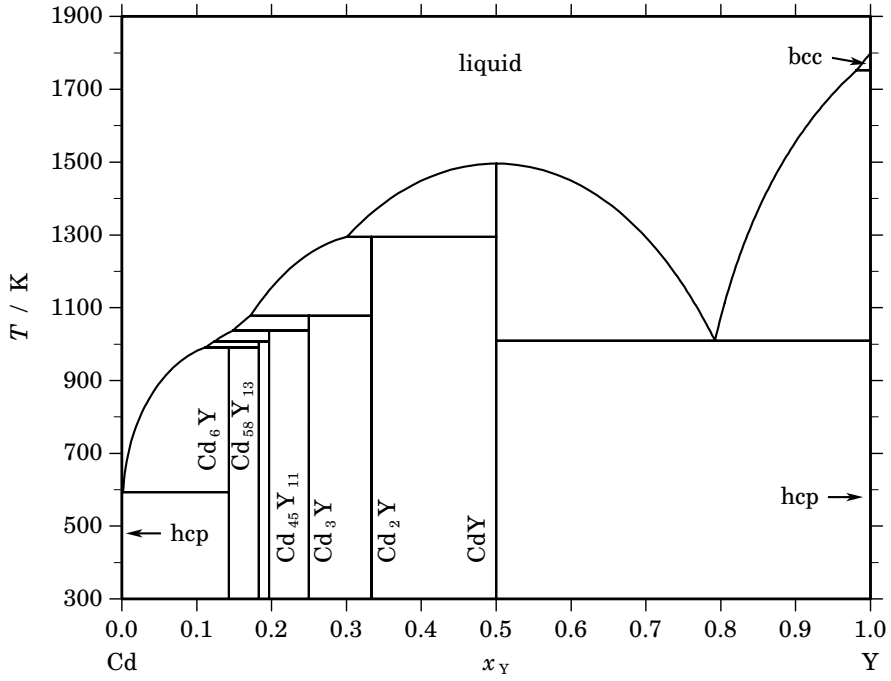

Fig. 1. Calculated phase diagram for the system Cd-Y.

The design of pyrometallurgically reprocessing for recycling nuclear reactor fuels needs thermodynamic information on multicomponent systems of actinides and rare earths solute with cadmium.
The experimental data for the Cd-Y system are relatively limited. There are no information on the mutual solubility of cadmium and yttrium in the solid state. Only the partial phase diagram covering the range 63 to 100 at.% Cd was reported by [1969Ryb]. Phase boundaries were determined by differential thermal analysis, metallography and x-ray diffraction methods. The Cd-richest compound is Cd_6Y which decomposes peritectically. [1988Gsc] reviewed this system. [1995Sak] determined the activity of yttrium using electromotive force measurements. The thermodynamic assessment of the Cd-Y system is from [2001Kur]. The liquid phase was described by a substitutional solution model using the Redlich-Kister equation. The intermetallic compounds Cd_6Y, $Cd_{58}Y_{13}$, $Cd_{45}Y_{11}$, Cd_3Y, Cd_2Y and CdY are treated as stoichiometric compounds. The calculated phase diagram presents slight differences with experimental data. These differences may be due to a lack of experimental solubility data. The activities are well reproduced.

Table I. Phases, structures and models.

Phase	Struktur-bericht	Prototype	Pearson symbol	Space group	SGTE name	Model
liquid					LIQUID	$(Cd,Y)_1$
hcp	$A3$	Mg	$hP2$	$P6_3/mmc$	HCP_A3	$(Cd,Y)_1$
Cd_6Y	$\cdots$	Cd_6Y	$cI168$	$Im\bar{3}$	CD6Y	Cd_6Y_1
$Cd_{58}Y_{13}$	$\cdots$	$Pu_{13}Zn_{58}$	$hp142$	$P6_3/mmc$	CD58Y13	$Cd_{58}Y_{13}$
$Cd_{45}Y_{11}$	$\cdots$	$Cd_{45}Sm_{11}$	$cF448$	$F\bar{4}3m$	CD45Y11	$Cd_{45}Y_{11}$
Cd_3Y	$\cdots$	Cd_3Er	$oC16$	$Cmcm$	CD3Y	Cd_3Y_1
Cd_2Y	$C6$	CdI_2	$hP3$	$P\bar{3}m1$	CD2Y	Cd_2Y_1
CdY	$B2$	CsCl	$cP2$	$Pm\bar{3}m$	CDY	Cd_1Y_1
bcc	$A2$	W	$cI2$	$Im\bar{3}m$	BCC_A2	Y_1

Table II. Invariant reactions.

Reaction	Type	T / K	Compositions / x_{Y}			$\Delta_{\mathrm{r}}H$ / (J/mol)
liquid + bcc $\rightleftharpoons$ hcp	peritectic	1752.0	0.981	1.000	1.000	−4995
liquid $\rightleftharpoons$ CdY	congruent	1496.0	0.500	0.500		−29146
liquid + CdY $\rightleftharpoons$ Cd_2Y	peritectic	1294.9	0.301	0.500	0.333	−12898
liquid + Cd_2Y $\rightleftharpoons$ Cd_3Y	peritectic	1078.2	0.172	0.333	0.250	−6733
liquid + Cd_3Y $\rightleftharpoons$ $Cd_{45}Y_{11}$	peritectic	1036.9	0.148	0.250	0.196	−6945
liquid $\rightleftharpoons$ CdY + hcp	eutectic	1009.5	0.792	0.500	1.000	−9786
liquid + $Cd_{45}Y_{11}$ $\rightleftharpoons$ $Cd_{58}Y_{13}$	peritectic	1007.6	0.124	0.196	0.183	−2237
liquid + $Cd_{58}Y_{13}$ $\rightleftharpoons$ Cd_6Y	peritectic	990.7	0.112	0.183	0.143	−6087
liquid $\rightleftharpoons$ hcp + Cd_6Y	eutectic	593.4	0.002	0.000	0.143	−6219

Table IIIa. Integral quantities for the liquid phase at 1800 K.

x_{Y}	ΔG_{m} [J/mol]	ΔH_{m} [J/mol]	ΔS_{m} [J/(mol·K)]	$G_{\mathrm{m}}^{\mathrm{E}}$ [J/mol]	$S_{\mathrm{m}}^{\mathrm{E}}$ [J/(mol·K)]	ΔC_P [J/(mol·K)]
0.000	0	0	0.000	0	0.000	0.000
0.100	−9464	−11889	−1.347	−4599	−4.050	0.000
0.200	−15665	−21136	−3.039	−8176	−7.200	0.000
0.300	−19873	−27741	−4.371	−10731	−9.450	0.000
0.400	−22336	−31704	−5.204	−12264	−10.800	0.000
0.500	−23149	−33025	−5.487	−12775	−11.250	0.000
0.600	−22336	−31704	−5.204	−12264	−10.800	0.000
0.700	−19873	−27741	−4.371	−10731	−9.450	0.000
0.800	−15665	−21136	−3.039	−8176	−7.200	0.000
0.900	−9464	−11889	−1.347	−4599	−4.050	0.000
1.000	0	0	0.000	0	0.000	0.000

Reference states: Cd(liquid), Y(liquid)

Table IIIb. Partial quantities for Cd in the liquid phase at 1800 K.

x_{Cd}	ΔG_{Cd} [J/mol]	ΔH_{Cd} [J/mol]	ΔS_{Cd} [J/(mol·K)]	$G_{\mathrm{Cd}}^{\mathrm{E}}$ [J/mol]	$S_{\mathrm{Cd}}^{\mathrm{E}}$ [J/(mol·K)]	a_{Cd}	γ_{Cd}
1.000	0	0	0.000	0	0.000	1.000	1.000
0.900	−2088	−1321	0.426	−511	−0.450	0.870	0.966
0.800	−5384	−5284	0.055	−2044	−1.800	0.698	0.872
0.700	−9937	−11889	−1.084	−4599	−4.050	0.515	0.735
0.600	−15821	−21136	−2.953	−8176	−7.200	0.347	0.579
0.500	−23149	−33025	−5.487	−12775	−11.250	0.213	0.426
0.400	−32109	−47556	−8.581	−18396	−16.200	0.117	0.293
0.300	−43058	−64729	−12.040	−25039	−22.050	0.056	0.188
0.200	−56791	−84544	−15.418	−32704	−28.800	0.022	0.112
0.100	−75852	−107001	−17.305	−41391	−36.450	0.006	0.063
0.000	$-\infty$	−132100	∞	−51100	−45.000	0.000	0.033

Reference state: Cd(liquid)

Table IIIc. Partial quantities for Y in the liquid phase at 1800 K.

x_Y	ΔG_Y [J/mol]	ΔH_Y [J/mol]	ΔS_Y [J/(mol·K)]	G_Y^E [J/mol]	S_Y^E [J/(mol·K)]	a_Y	γ_Y
0.000	$-\infty$	−132100	∞	−51100	−45.000	0.000	0.033
0.100	−75852	−107001	−17.305	−41391	−36.450	0.006	0.063
0.200	−56791	−84544	−15.418	−32704	−28.800	0.022	0.112
0.300	−43058	−64729	−12.040	−25039	−22.050	0.056	0.188
0.400	−32109	−47556	−8.581	−18396	−16.200	0.117	0.293
0.500	−23149	−33025	−5.487	−12775	−11.250	0.213	0.426
0.600	−15821	−21136	−2.953	−8176	−7.200	0.347	0.579
0.700	−9937	−11889	−1.084	−4599	−4.050	0.515	0.735
0.800	−5384	−5284	0.055	−2044	−1.800	0.698	0.872
0.900	−2088	−1321	0.426	−511	−0.450	0.870	0.966
1.000	0	0	0.000	0	0.000	1.000	1.000

Reference state: Y(liquid)

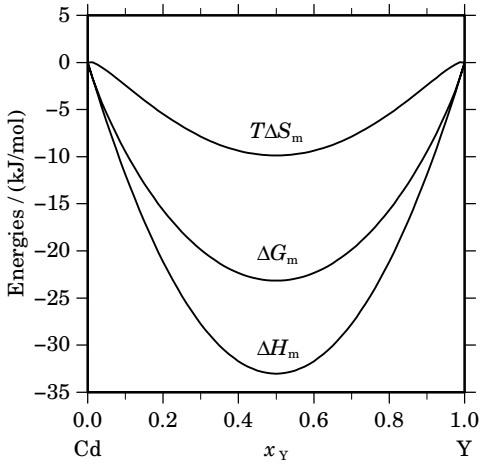

Fig. 2. Integral quantities of the liquid phase at T=1800 K.

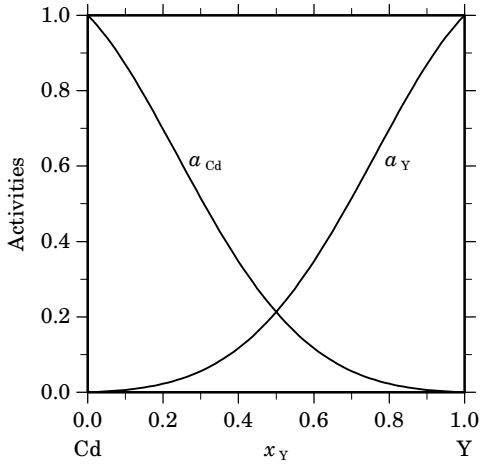

Fig. 3. Activities in the liquid phase at T=1800 K.

Table IV. Standard reaction quantities at 298.15 K for the compounds per mole of atoms.

Compound	x_Y	$\Delta_f G^\circ$ / (J/mol)	$\Delta_f H^\circ$ / (J/mol)	$\Delta_f S^\circ$ / (J/(mol·K))	$\Delta_f C_P^\circ$ / (J/(mol·K))
Cd_6Y_1	0.143	−19674	−20876	−4.031	0.000
$Cd_{58}Y_{13}$	0.183	−23837	−25529	−5.673	0.000
$Cd_{45}Y_{11}$	0.196	−25033	−26825	−6.011	0.000
Cd_3Y_1	0.250	−29083	−31104	−6.777	0.000
Cd_2Y_1	0.333	−35289	−37814	−8.469	0.000
Cd_1Y_1	0.500	−47210	−51936	−15.852	0.000

References

[1969Ryb] E. Ryba, P.K. Kejriwal, R. Elmendorf: J. Less-Common Met. **18** (1969) 419–422.
[1988Gsc] K.A. Gschneidner Jr., F.W. Calderwood: Bull. Alloy Phase Diagrams **9** (1988) 139–140.
[1995Sak] Y. Sakamura, T. Inoue, T.S. Storvick, L.F. Grantham: Proc. Int. Conf. Evaluation of Emerging Nuclear Fuel Cycle Systems, Global 95, Versailles, France, Sept. 11-14, vol. 2, 1185–1192 (1995).
[2001Kur] M. Kurata, Y. Sakamura: J. Phase Equilibria **22** (2001) 232–240.

Ce – Ni (Cerium – Nickel)

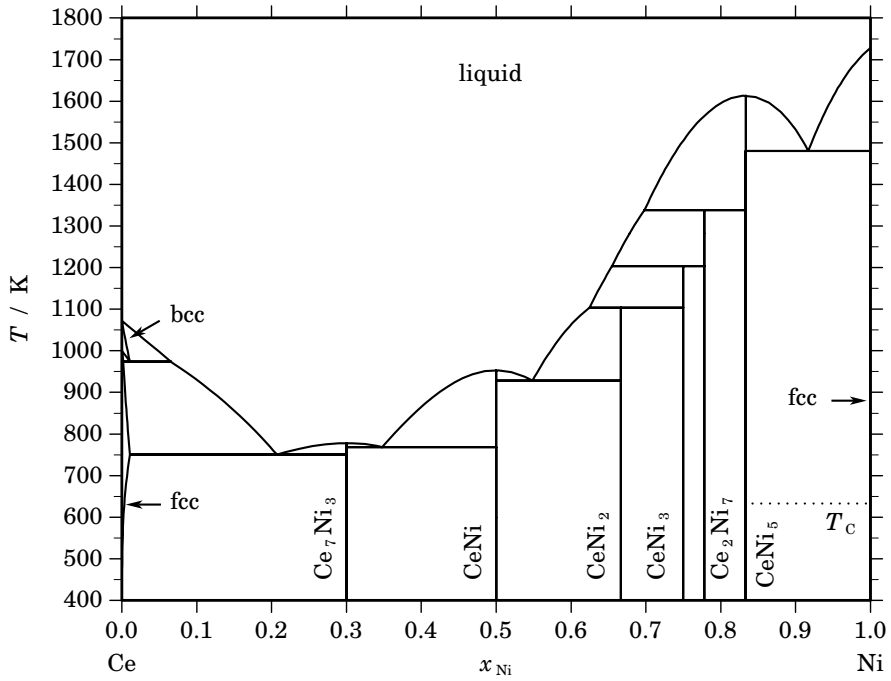

Fig. 1. Calculated phase diagram for the system Ce-Ni.

The interest in the Ce-Ni system is related to its potential use in hydrogen storage materials or in permanent magnets. A review on the thermodynamic literature of the Ce-Ni system has been given by Nash and Tung [1991Nas] and a thermodynamic optimisation has been prepared by Du *et al.* [2004Du]. The optimisation is based mainly on experimental information on the phase diagram [1947Vog, 1964Dus, 1965Per, 1967Geb]. No thermodynamic data are available for the melt. Calorimetric data for the standard enthalpy of formation for intermetallic compounds have been reported only for $CeNi_5$ [1983Col, 1998Guo] and for CeNi [1998Guo].

Table I. Phases, structures and models.

Phase	Strukturbericht	Prototype	Pearson symbol	Space group	SGTE name	Model
liquid					LIQUID	$(Ce,Ni)_1$
fcc	$A1$	Cu	$cF4$	$Fm\bar{3}m$	FCC_A1	$(Ce,Ni)_1$
bcc	$A2$	W	$cI2$	$Im\bar{3}m$	BCC_A2	$(Ce,Ni)_1$
Ce_7Ni_3	$D10_2$	Fe_3Th_7	$hP20$	$P6_3mc$	CE7NI3	Ce_7Ni_3
CeNi	$B33$	CrB	$oC8$	$Cmcm$	CENI	Ce_1Ni_1
$CeNi_2$	$C15$	Cu_2Mg	$cF24$	$Fd\bar{3}m$	CENI2	Ce_1Ni_2
$CeNi_3$	···	$CeNi_3$	$hP*$	$P6_3/mmc$	CENI3	Ce_1Ni_3
Ce_2Ni_7	···	$CeNi_3$	$hP*$	$P6_3/mmc$	CE2NI7	Ce_2Ni_7
$CeNi_5$	$D2_d$	$CaCu_5$	$hP6$	$P6/mmm$	CENI5	Ce_1Ni_5

Table II. Invariant reactions.

Reaction	Type	T / K	Compositions / x_{Ni}			$\Delta_{\mathrm{r}}H$ / (J/mol)
liquid $\rightleftharpoons$ $CeNi_5$	congruent	1613.2	0.833	0.833		−21520
liquid $\rightleftharpoons$ $CeNi_5$ + fcc	eutectic	1480.4	0.917	0.833	1.000	−17066
liquid + $CeNi_5$ $\rightleftharpoons$ Ce_2Ni_7	peritectic	1337.9	0.698	0.833	0.778	−5737
liquid + Ce_2Ni_7 $\rightleftharpoons$ $CeNi_3$	peritectic	1203.3	0.655	0.778	0.750	−2925
liquid + $CeNi_3$ $\rightleftharpoons$ $CeNi_2$	peritectic	1103.3	0.625	0.750	0.667	−7964
bcc $\rightleftharpoons$ fcc + liquid	metatectic	974.1	0.011	0.002	0.065	−1778
liquid $\rightleftharpoons$ CeNi	congruent	953.3	0.500	0.500		−13001
liquid $\rightleftharpoons$ CeNi + $CeNi_2$	eutectic	928.2	0.548	0.500	0.667	−11999
liquid $\rightleftharpoons$ Ce_7Ni_3	congruent	778.2	0.300	0.300		−16211
liquid $\rightleftharpoons$ Ce_7Ni_3 + CeNi	eutectic	768.2	0.348	0.300	0.500	−14826
liquid $\rightleftharpoons$ fcc + Ce_7Ni_3	eutectic	750.2	0.207	0.011	0.300	−13593

Table IIIa. Integral quantities for the liquid phase at 1800 K.

x_{Ni}	ΔG_{m} [J/mol]	ΔH_{m} [J/mol]	ΔS_{m} [J/(mol·K)]	$G_{\mathrm{m}}^{\mathrm{E}}$ [J/mol]	$S_{\mathrm{m}}^{\mathrm{E}}$ [J/(mol·K)]	ΔC_P [J/(mol·K)]
0.000	0	0	0.000	0	0.000	0.000
0.100	−14339	−6471	4.371	−9474	1.668	0.000
0.200	−25006	−13551	6.364	−17517	2.203	0.000
0.300	−33018	−20473	6.969	−23876	1.890	0.000
0.400	−38371	−26469	6.612	−28298	1.016	0.000
0.500	−40905	−30772	5.630	−30532	−0.133	0.000
0.600	−40394	−32612	4.324	−30322	−1.272	0.000
0.700	−36559	−31223	2.965	−27417	−2.114	0.000
0.800	−29053	−25837	1.787	−21564	−2.374	0.000
0.900	−17374	−15685	0.939	−12509	−1.764	0.000
1.000	0	0	0.000	0	0.000	0.000

Reference states: Ce(liquid), Ni(liquid)

Table IIIb. Partial quantities for Ce in the liquid phase at 1800 K.

x_{Ce}	ΔG_{Ce} [J/mol]	ΔH_{Ce} [J/mol]	ΔS_{Ce} [J/(mol·K)]	$G_{\mathrm{Ce}}^{\mathrm{E}}$ [J/mol]	$S_{\mathrm{Ce}}^{\mathrm{E}}$ [J/(mol·K)]	a_{Ce}	γ_{Ce}
1.000	0	0	0.000	0	0.000	1.000	1.000
0.900	−2250	433	1.490	−673	0.614	0.860	0.956
0.800	−6370	707	3.932	−3030	2.076	0.653	0.817
0.700	−12915	−712	6.779	−7577	3.814	0.422	0.603
0.600	−22464	−5361	9.501	−14819	5.254	0.223	0.372
0.500	−35636	−14775	11.589	−25262	5.826	0.092	0.185
0.400	−53126	−30490	12.575	−39412	4.957	0.029	0.072
0.300	−75795	−54042	12.085	−57776	2.075	0.006	0.021
0.200	−104946	−86966	9.989	−80859	−3.393	0.001	0.005
0.100	−143627	−130797	7.128	−109166	−12.017	0.000	0.001
0.000	$-\infty$	−187072	∞	−143205	−24.371	0.000	0.000

Reference state: Ce(liquid)

Table IIIc. Partial quantities for Ni in the liquid phase at 1800 K.

x_{Ni}	ΔG_{Ni} [J/mol]	ΔH_{Ni} [J/mol]	ΔS_{Ni} [J/(mol·K)]	$G^{\mathrm{E}}_{\mathrm{Ni}}$ [J/mol]	$S^{\mathrm{E}}_{\mathrm{Ni}}$ [J/(mol·K)]	a_{Ni}	γ_{Ni}
0.000	$-\infty$	−59100	∞	−101047	23.304	0.000	0.001
0.100	−123138	−68603	30.298	−88678	11.153	0.000	0.003
0.200	−99550	−70585	16.091	−75463	2.710	0.001	0.006
0.300	−79926	−66583	7.413	−61907	−2.598	0.005	0.016
0.400	−62232	−58132	2.278	−48518	−5.341	0.016	0.039
0.500	−46175	−46768	−0.330	−35801	−6.093	0.046	0.091
0.600	−31907	−34027	−1.178	−24262	−5.425	0.119	0.198
0.700	−19744	−21444	−0.944	−14406	−3.910	0.267	0.382
0.800	−10080	−10554	−0.264	−6740	−2.119	0.510	0.637
0.900	−3346	−2895	0.251	−1769	−0.625	0.800	0.888
1.000	0	0	0.000	0	0.000	1.000	1.000

Reference state: Ni(liquid)

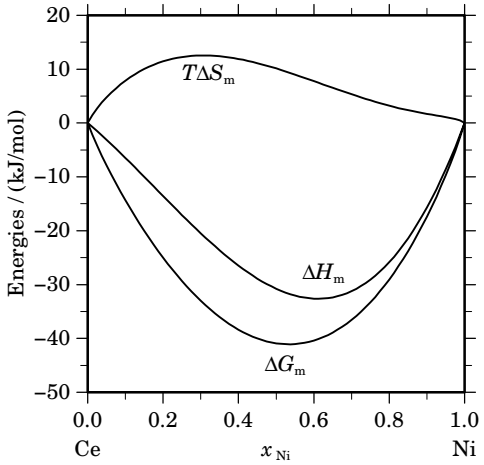

Fig. 2. Integral quantities of the liquid phase at T=1800 K.

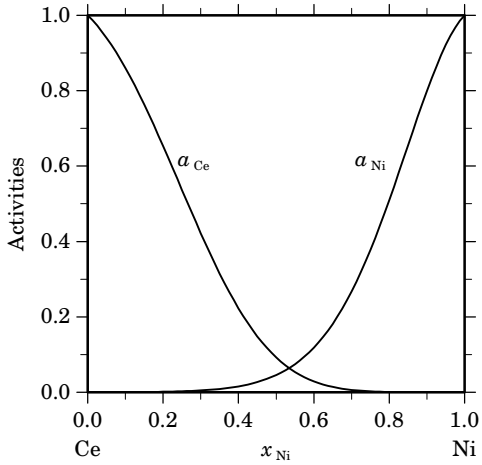

Fig. 3. Activities in the liquid phase at T=1800 K.

Table IV. Standard reaction quantities at 298.15 K for the compounds per mole of atoms.

Compound	x_{Ni}	$\Delta_{\mathrm{f}}G^{\circ}$ / (J/mol)	$\Delta_{\mathrm{f}}H^{\circ}$ / (J/mol)	$\Delta_{\mathrm{f}}S^{\circ}$ / (J/(mol·K))	$\Delta_{\mathrm{f}}C^{\circ}_{P}$ / (J/(mol·K))
Ce_7Ni_3	0.300	−24116	−25508	−4.667	−0.229
Ce_1Ni_1	0.500	−31122	−30422	2.345	−0.382
Ce_1Ni_2	0.667	−30676	−29654	3.427	−0.510
Ce_1Ni_3	0.750	−29610	−28955	2.198	−0.573
Ce_2Ni_7	0.778	−29044	−28532	1.717	−0.595
Ce_1Ni_5	0.833	−27602	−27521	0.274	−0.637

References

[1947Vog] R. Vogel: Z. Metallkd. **38** (1947) 97–103.
[1964Dui] U.K. Duisemaliev: Zh. Neorg. Khim. **9** (1964) 755–756.
[1965Per] R.H. Perkins, L.A. Geoffrion, J.C. Biery: Trans. AIME **233** (1965) 1703–1710.
[1967Geb] J.M. Gebhart III, D.E. Etter, P.A. Tucker in: Proceedings of the 6th Conference on Rare Earth Research, May 1967, pp. 417–457.
[1983Col] C. Colinet, A. Pasturel: Phys. Stat. Solidi A **80A** (1983) 75–79.
[1991Nas] P. Nash, C. Tung in: "Phase Diagrams of Binary Nickel Alloys", P. Nash, Ed., ASM Intl., Metals Park, OH, 1991, pp. 62–67.
[1998Guo] Q. Guo, O.J. Kleppa: J. Alloys Comp. **270** (1998) 212–217.
[2004Du] Z. Du, L. Yang, G. Ling: J. Alloys Comp. **375** (2004) 186–190.

Co – Gd (Cobalt – Gadolinium)

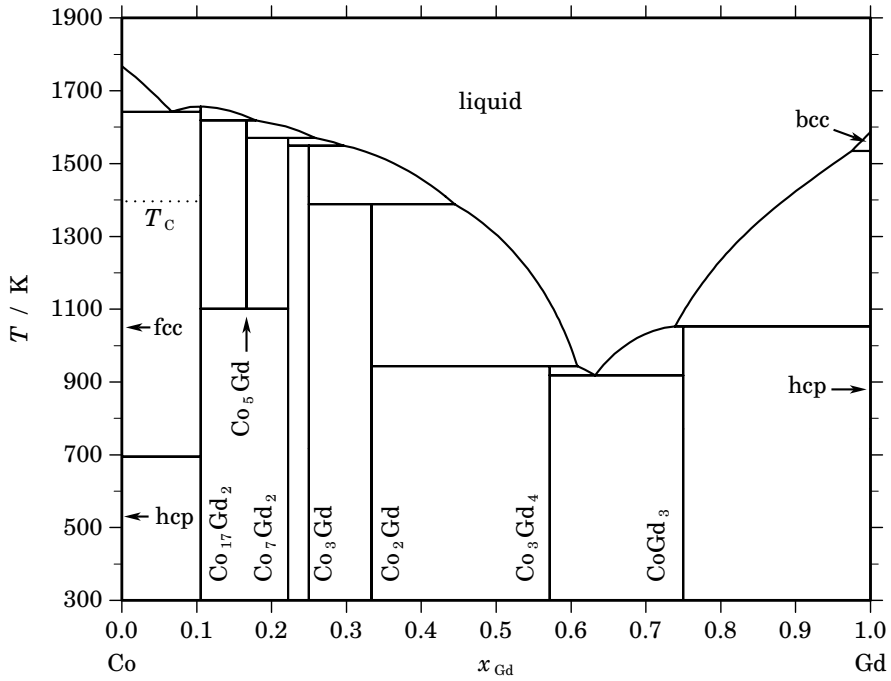

Fig. 1. Calculated phase diagram for the system Co-Gd.

Intermetallic compounds formed between rare earth and transition metals, especially 3d elements are of particular interest regarding their magnetic properties and their reversible absorption of hydrogen gas at room temperature and nearly atmospheric pressure. The phase diagram of the Co-Gd system was measured by [1961Nov, 1969Bus, 1992Ge]. [1992Oka] reviewed this system. The results of [1961Nov] are quite different from those of the studies of [1969Bus, 1992Ge] and are discarded. The last two investigations gave the same kind of relationships, i.e. two eutectic reactions, congruent melting of $Co_{17}Gd_2$ and incongruent melting of all other compounds. Co_5Gd is unstable at low temperatures. Both Co_5Gd and $Co_{17}Gd_2$ were reported to have a certain homogeneity region at high temperatures. $Co_{17}Gd_2$ and Co_7Gd_2 are dimorphic, but their transformation temperatures are unknown. The heat of mixing in the liquid phase at 1823 K was measured by [1989Nik] for the entire composition range. The enthalpies of formation of the compounds were measured by various authors [1976Deo, 1986Sch, 1987Col1] with the most complete set being that by [1987Col1, 1987Col2]. The heat capacities of Co_5Gd and Co_2Gd were measured by [1974Kel, 1989Leg] in the temperature ranges 5-300 K and 300-473 K, respectively. [1987Bar] measured the heat capacity at the composition 63.2 at.% Gd in the temperature range 800-980 K. Magnetic measurements of the compounds are reported by [1966Lem1, 1966Lem2, 1972Bur]. The thermodynamic assessment of the Co-Gd system is from [1995Liu]. The fcc, hcp, bcc, and the liquid phases were described by a substitutional solution model using the Redlich-Kister equation. A magnetic contribution is added for the fcc, hcp and bcc phases, and no solubility range is assumed for these phases. The seven intermetallic compounds $Co_{17}Gd_2$, Co_5Gd, Co_7Gd_2, Co_3Gd, Co_2Gd, Co_3Gd_4, and $CoGd_3$ are all treated as stoichiometric compounds because of limited information. Good agreement is obtained between the calculation and the experimental results.

Table I. Phases, structures and models.

Phase	Struktur-bericht	Prototype	Pearson symbol	Space group	SGTE name	Model
liquid					LIQUID	$(Co,Gd)_1$
fcc	$A1$	Cu	$cF4$	$Fm\bar{3}m$	FCC_A1	$(Co,Gd)_1$
hcp	$A3$	Mg	$hP2$	$P6_3/mmc$	HCP_A3	$(Co,Gd)_1$
$Co_{17}Gd_2$	$\cdots$	Th_2Zn_{17}	$hR19$	$R\bar{3}m$	CO17GD2	$Co_{17}Gd_2$
Co_5Gd	$D2_d$	$CaCu_5$	$hP6$	$P6/mmm$	CO5GD	Co_5Gd_1
Co_7Gd_2	$\cdots$	Co_7Er_2	$hR18$	$R\bar{3}m$	CO7GD2	Co_7Gd_2
Co_3Gd	$\cdots$	Be_3Nb	$hR12$	$R\bar{3}m$	CO3GD	Co_3Gd_1
Co_2Gd	$C15$	Cu_2Mg	$cF24$	$Fd\bar{3}m$	CO2GD	Co_2Gd_1
Co_3Gd_4	$\cdots$	Co_3Ho_4	$hP22$	$P6_3/m$	CO3GD4	Co_3Gd_4
$CoGd_3$	$D0_{11}$	Fe_3C	$oP16$	$Pnma$	COGD3	Co_1Gd_3
bcc	$A2$	W	$cI2$	$Im\bar{3}m$	BCC_A2	$(Co,Gd)_1$

Table II. Invariant reactions.

Reaction	Type	T / K	Compositions / x_{Gd}			$\Delta_r H$ / (J/mol)
liquid $\rightleftharpoons$ $Co_{17}Gd_2$	congruent	1657.0	0.105	0.105		−21931
liquid $\rightleftharpoons$ fcc + $Co_{17}Gd_2$	eutectic	1641.6	0.067	0.000	0.105	−19536
$Co_{17}Gd_2$ + liquid $\rightleftharpoons$ Co_5Gd	peritectic	1618.6	0.105	0.179	0.167	−17447
Co_5Gd + liquid $\rightleftharpoons$ Co_7Gd_2	peritectic	1570.2	0.167	0.258	0.222	−14393
Co_7Gd_2 + liquid $\rightleftharpoons$ Co_3Gd	peritectic	1549.5	0.222	0.297	0.250	−8145
liquid + bcc $\rightleftharpoons$ hcp	peritectic	1534.9	0.975	1.000	1.000	−3677
Co_3Gd + liquid $\rightleftharpoons$ Co_2Gd	peritectic	1388.2	0.250	0.445	0.333	−5201
Co_5Gd $\rightleftharpoons$ $Co_{17}Gd_2$ + Co_7Gd_2	eutectoid	1100.8	0.167	0.105	0.222	−790
liquid + hcp $\rightleftharpoons$ $CoGd_3$	peritectic	1053.0	0.739	1.000	0.750	−6517
Co_2Gd + liquid $\rightleftharpoons$ Co_3Gd_4	peritectic	943.1	0.333	0.608	0.571	−4822
liquid $\rightleftharpoons$ Co_3Gd_4 + $CoGd_3$	eutectic	917.9	0.632	0.571	0.750	−5018
fcc + $Co_{17}Gd_2$ $\rightleftharpoons$ hcp	peritectoid	695.0	0.000	0.105	0.000	−428

Table IIIa. Integral quantities for the liquid phase at 1823 K.

x_{Gd}	ΔG_m [J/mol]	ΔH_m [J/mol]	ΔS_m [J/(mol·K)]	G_m^E [J/mol]	S_m^E [J/(mol·K)]	ΔC_P [J/(mol·K)]
0.000	0	0	0.000	0	0.000	0.000
0.100	−6889	−7349	−0.253	−1961	−2.956	3.085
0.200	−10761	−12756	−1.094	−3176	−5.255	5.484
0.300	−13021	−16335	−1.818	−3762	−6.897	7.197
0.400	−14036	−18203	−2.286	−3834	−7.882	8.226
0.500	−14016	−18477	−2.447	−3510	−8.210	8.568
0.600	−13105	−17273	−2.286	−2904	−7.882	8.226
0.700	−11393	−14707	−1.818	−2134	−6.897	7.197
0.800	−8901	−10895	−1.094	−1316	−5.255	5.484
0.900	−5493	−5954	−0.253	−566	−2.956	3.085
1.000	0	0	0.000	0	0.000	0.000

Reference states: Co(liquid), Gd(liquid)

Table IIIb. Partial quantities for Co in the liquid phase at 1823 K.

x_{Co}	ΔG_{Co} [J/mol]	ΔH_{Co} [J/mol]	ΔS_{Co} [J/(mol·K)]	G^{E}_{Co} [J/mol]	S^{E}_{Co} [J/(mol·K)]	a_{Co}	γ_{Co}
1.000	0	0	0.000	0	0.000	1.000	1.000
0.900	−1989	−991	0.548	−392	−0.328	0.877	0.974
0.800	−4796	−3809	0.542	−1414	−1.314	0.729	0.911
0.700	−8239	−8221	0.010	−2833	−2.956	0.581	0.830
0.600	−12159	−13996	−1.007	−4417	−5.255	0.448	0.747
0.500	−16438	−20899	−2.447	−5932	−8.210	0.338	0.676
0.400	−21035	−28700	−4.204	−7147	−11.823	0.250	0.624
0.300	−26078	−37165	−6.082	−7829	−16.092	0.179	0.597
0.200	−32140	−46061	−7.637	−7745	−21.018	0.120	0.600
0.100	−41564	−55157	−7.456	−6663	−26.601	0.064	0.644
0.000	−∞	−64219	∞	−4350	−32.841	0.000	0.751

Reference state: Co(liquid)

Table IIIc. Partial quantities for Gd in the liquid phase at 1823 K.

x_{Gd}	ΔG_{Gd} [J/mol]	ΔH_{Gd} [J/mol]	ΔS_{Gd} [J/(mol·K)]	G^{E}_{Gd} [J/mol]	S^{E}_{Gd} [J/(mol·K)]	a_{Gd}	γ_{Gd}
0.000	−∞	−83597	∞	−23728	−32.841	0.000	0.209
0.100	−50982	−64575	−7.456	−16080	−26.601	0.035	0.346
0.200	−34620	−48542	−7.637	−10225	−21.018	0.102	0.509
0.300	−24179	−35266	−6.082	−5930	−16.092	0.203	0.676
0.400	−16850	−24514	−4.204	−2961	−11.823	0.329	0.823
0.500	−11594	−16055	−2.447	−1087	−8.210	0.465	0.931
0.600	−7819	−9655	−1.007	−76	−5.255	0.597	0.995
0.700	−5100	−5082	0.010	306	−2.956	0.714	1.020
0.800	−3091	−2104	0.542	291	−1.314	0.816	1.019
0.900	−1485	−487	0.548	112	−0.328	0.907	1.007
1.000	0	0	0.000	0	0.000	1.000	1.000

Reference state: Gd(liquid)

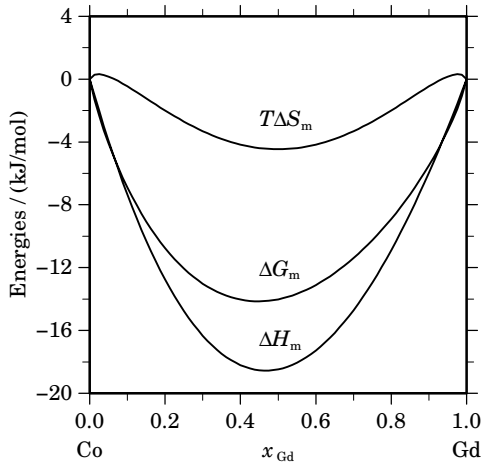

Fig. 2. Integral quantities of the liquid phase at T=1823 K.

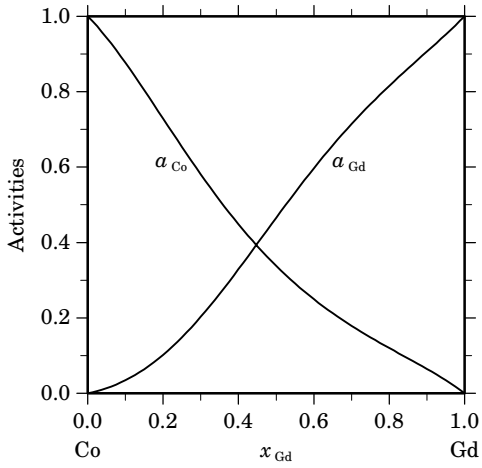

Fig. 3. Activities in the liquid phase at T=1823 K.

Table IV. Standard reaction quantities at 298.15 K for the compounds per mole of atoms.

Compound	x_{Gd}	$\Delta_{\mathrm{f}}G^{\circ}$ / (J/mol)	$\Delta_{\mathrm{f}}H^{\circ}$ / (J/mol)	$\Delta_{\mathrm{f}}S^{\circ}$ / (J/(mol·K))	$\Delta_{\mathrm{f}}C_P^{\circ}$ / (J/(mol·K))
$Co_{17}Gd_2$	0.105	−7717	−7229	1.637	−0.130
Co_5Gd_1	0.167	−11347	−11449	−0.345	1.594
Co_7Gd_2	0.222	−15390	−15925	−1.793	−0.113
Co_3Gd_1	0.250	−16463	−17141	−2.274	−0.109
Co_2Gd_1	0.333	−15798	−16270	−1.584	−0.097
Co_3Gd_4	0.571	−12787	−13930	−3.833	1.546
Co_1Gd_3	0.750	−8984	−9906	−3.094	1.572

References

[1961Nov] V.F. Novy, R.C. Vickery, E.V. Kleber: Trans. Metall. Soc. AIME **221** (1961) 588–590.
[1966Lem1] R. Lemaire: Cobalt **32** (1966) 132–140.
[1966Lem2] R. Lemaire: Cobalt **33** (1966) 201–211.
[1969Bus] K.H.J. Buschow, A.S. van der Goot: J. Less-Common Met. **17** (1969) 249–255.
[1972Bur] E. Burzo: Phys. Rev. B **6B** (1972) 2882–2887.
[1974Kel] D.A. Keller, S.G. Sankar, R.S. Craig, W.E. Wallace: Am. Inst. Phys. Conf. Proc. **18** (1974) 1207–1211.
[1976Deo] S.S. Deodhar, P.J. Ficalora: High Temp. Sci. **8** (1976) 185–193.
[1986Sch] J. Schott, F. Sommer: J. Less-Common Met. **119** (1986) 307–317.
[1987Bar] M. Barrico, C. Antonions and L. Battezzati: Scr. Metall. **21** (1987) 849–852.
[1987Col1] C. Colinet, A. Pasturel, K.H.J. Buschow: Metall. Trans. A **18A** (1987) 903–907.
[1987Col2] C. Colinet, A. Pasturel: Calphad **11** (1987) 323–324.
[1989Nik] I.V. Nikolaenko, M.A. Turchanin: Rasplavy **5** (1989) 77–79.
[1989Leg] S.B.K. Leghari: J. Nat. Sci. Math. **29** (1989) 69–85.
[1992Ge] W.Q. Ge, C.H. Wu, Y.C. Chuang: Z. Metallkd. **83** (1992) 300–303.
[1992Oka] H. Okamoto: J. Phase Equilibria **13** (1992) 673–674.
[1995Liu] Z.-K. Liu, W. Zhang, B. Sundman: J. Alloys Comp. **226** (1995) 33–45.

Co – Ge (Cobalt – Germanium)

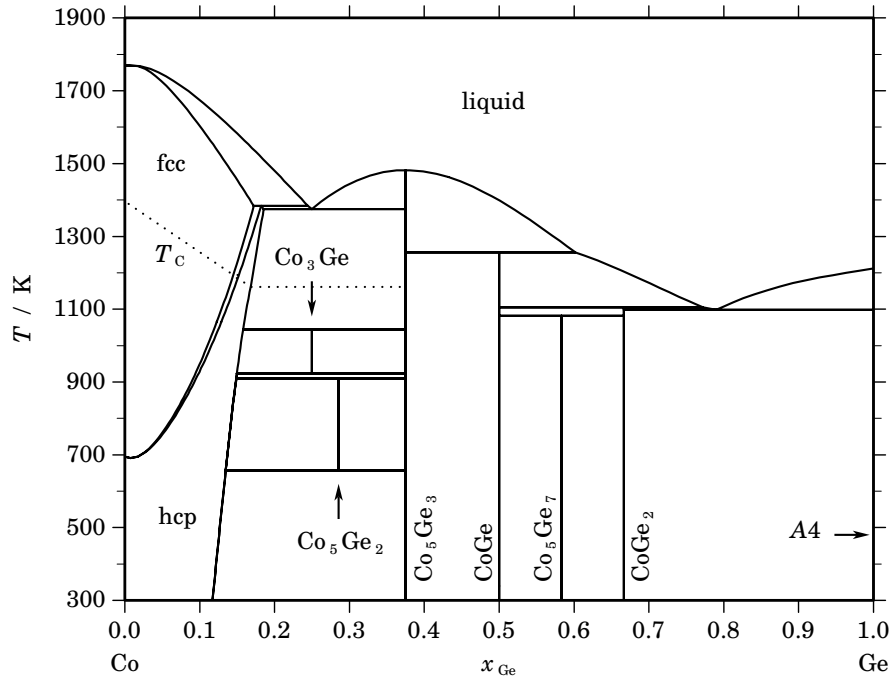

Fig. 1. Calculated phase diagram for the system Co-Ge.

The equilibrium phases are the liquid, the Co-rich fcc solid solution, the Co-rich hcp solid solution, the Ge-rich solid solution, with negligible solid solubility of Co and 6 near-stoichiometric compounds Co_3Ge, Co_5Ge_2, Co_5Ge_3, CoGe, Co_5Ge_7 and $CoGe_2$. Two compounds, CoGe and $CoGe_2$, decompose peritectically at 1258 and 1105 K, respectively. CoGe has a narrow homogeneity range of about 2.5 at.% with a stoichiometric composition at the peritectic temperature. The compound Co_5Ge_7 is stable up to the peritectoid temperature of 1079 K. Co_3Ge is formed below about 1043 K, the hexagonal phase Co_5Ge_2 is stable between 655 and 909 K. The phase Co_5Ge_3 which exhibits a fairly wide homogeneity range of almost 10 at.% melts congruently at 1483 K. The thermodynamic assessment of the Co-Ge system carried out by Korb [2004Kor] is based on [1949Pfi, 1980Day, 1990Eno], with review of the data of [1952Kös, 1973Aga, 1976Bal]. All compounds have been treated as stoichiometric, including Co_5Ge_3 and CoGe. Taking into account this simplification the calculated and the published [1991Ish] phase diagram agree well.

Table I. Phases, structures and models.

Phase	Struktur-bericht	Prototype	Pearson symbol	Space group	SGTE name	Model
liquid					LIQUID	$(Co,Ge)_1$
fcc	$A1$	Cu	$cF4$	$Fm\bar{3}m$	FCC_A1	$(Co,Ge)_1$
hcp	$A3$	Mg	$hP2$	$P6_3/mmc$	HCP_A3	$(Co,Ge)_1$
Co_3Ge	$A15$ (?)	Cr_3Si (?)	$cP8$ (?)	$Pm\bar{3}n$ (?)	CO3GE	Co_3Ge_1
Co_5Ge_2	···	···	$hP*$	···	CO5GE2	Co_5Ge_2
αCo_5Ge_3	···	···	$oP*$	$Pbnm$?	CO5GE3	Co_5Ge_3
βCo_5Ge_3	$B8_2$	$InNi_2$	$hP6$	$P6_3/mmc$	CO5GE3	Co_5Ge_3
CoGe	···	···	$mC16$	$C2/m$	COGE	Co_1Ge_1
Co_5Ge_7	···	···	$tI24$	$I4mm$	CO5GE7	Co_5Ge_7
$CoGe_2$	···	···	$oC24$	$Aba2$	COGE2	Co_1Ge_2
$A4$	$A4$	C(diamond)	$cF8$	$Fd\bar{3}m$	DIAMOND_A4	Ge_1

Table II. Invariant reactions.

Reaction	Type	T / K	Compositions / x_{Ge}			$\Delta_r H$ / (J/mol)
liquid $\rightleftharpoons$ Co_5Ge_3	congruent	1481.9	0.375	0.375		−64617
fcc + liquid $\rightleftharpoons$ hcp	peritectic	1383.8	0.172	0.245	0.182	−6168
liquid $\rightleftharpoons$ hcp + Co_5Ge_3	eutectic	1374.7	0.250	0.186	0.375	−42156
Co_5Ge_3 + liquid $\rightleftharpoons$ CoGe	peritectic	1256.3	0.375	0.602	0.500	−32569
CoGe + liquid $\rightleftharpoons$ $CoGe_2$	peritectic	1105.1	0.500	0.772	0.667	−32166
liquid $\rightleftharpoons$ $CoGe_2$ + $A4$	eutectic	1098.1	0.790	0.667	1.000	−49871
CoGe + $CoGe_2$ $\rightleftharpoons$ Co_5Ge_7	peritectoid	1081.8	0.500	0.667	0.583	−1493
hcp + Co_5Ge_3 $\rightleftharpoons$ Co_3Ge	peritectoid	1044.0	0.158	0.375	0.250	−588
Co_3Ge $\rightleftharpoons$ hcp + Co_5Ge_3	eutectoid	922.8	0.250	0.150	0.375	−463
hcp + Co_5Ge_3 $\rightleftharpoons$ Co_5Ge_2	peritectoid	908.6	0.149	0.375	0.286	−613
fcc $\rightleftharpoons$ hcp	congruent	695.3	0.000	0.000		−428
Co_5Ge_2 $\rightleftharpoons$ hcp + Co_5Ge_3	eutectoid	655.8	0.286	0.135	0.375	−403

Table IIIa. Integral quantities for the liquid phase at 1823 K.

x_{Ge}	ΔG_m [J/mol]	ΔH_m [J/mol]	ΔS_m [J/(mol·K)]	G_m^E [J/mol]	S_m^E [J/(mol·K)]	ΔC_P [J/(mol·K)]
0.000	0	0	0.000	0	0.000	0.000
0.100	−30063	−11514	10.175	−25135	7.472	0.000
0.200	−50222	−18422	17.444	−42637	13.283	0.000
0.300	−62532	−21491	22.513	−53273	17.434	0.000
0.400	−68012	−21489	25.520	−57811	19.924	0.000
0.500	−67526	−19185	26.518	−57020	20.754	0.000
0.600	−61868	−15345	25.520	−51667	19.924	0.000
0.700	−51780	−10739	22.513	−42521	17.434	0.000
0.800	−37934	−6134	17.444	−30349	13.283	0.000
0.900	−20847	−2298	10.175	−15919	7.472	0.000
1.000	0	0	0.000	0	0.000	0.000

Reference states: Co(liquid), Ge(liquid)

Table IIIb. Partial quantities for Co in the liquid phase at 1823 K.

x_{Co}	ΔG_{Co} [J/mol]	ΔH_{Co} [J/mol]	ΔS_{Co} [J/(mol·K)]	G^{E}_{Co} [J/mol]	S^{E}_{Co} [J/(mol·K)]	a_{Co}	γ_{Co}
1.000	0	0	0.000	0	0.000	1.000	1.000
0.900	−5542	−2431	1.706	−3945	0.830	0.694	0.771
0.800	−18138	−8702	5.176	−14755	3.321	0.302	0.378
0.700	−36301	−17274	10.437	−30895	7.472	0.091	0.130
0.600	−58572	−26614	17.530	−50829	13.283	0.021	0.035
0.500	−83526	−35185	26.518	−73020	20.754	0.004	0.008
0.400	−109821	−41450	37.505	−95933	29.886	0.001	0.002
0.300	−136280	−43874	50.689	−118031	40.679	0.000	0.000
0.200	−162174	−40920	66.513	−137779	53.132	0.000	0.000
0.100	−188542	−31054	86.389	−153641	67.245	0.000	0.000
0.000	−∞	−12738	∞	−164080	83.018	0.000	0.000

Reference state: Co(liquid)

Table IIIc. Partial quantities for Ge in the liquid phase at 1823 K.

x_{Ge}	ΔG_{Ge} [J/mol]	ΔH_{Ge} [J/mol]	ΔS_{Ge} [J/(mol·K)]	G^{E}_{Ge} [J/mol]	S^{E}_{Ge} [J/(mol·K)]	a_{Ge}	γ_{Ge}
0.000	−∞	−140738	∞	−292080	83.018	0.000	0.000
0.100	−250750	−93262	86.389	−215849	67.245	0.000	0.000
0.200	−178558	−57304	66.513	−154163	53.132	0.000	0.000
0.300	−123736	−31330	50.689	−105487	40.679	0.000	0.001
0.400	−82173	−13802	37.505	−68285	29.886	0.004	0.011
0.500	−51526	−3185	26.518	−41020	20.754	0.033	0.067
0.600	−29900	2058	17.530	−22157	13.283	0.139	0.232
0.700	−15565	3462	10.437	−10159	7.472	0.358	0.512
0.800	−6873	2562	5.176	−3491	3.321	0.635	0.794
0.900	−2214	897	1.706	−617	0.830	0.864	0.960
1.000	0	0	0.000	0	0.000	1.000	1.000

Reference state: Ge(liquid)

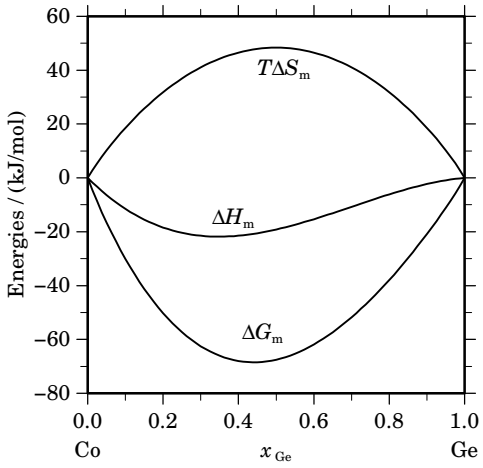

Fig. 2. Integral quantities of the liquid phase at T=1823 K.

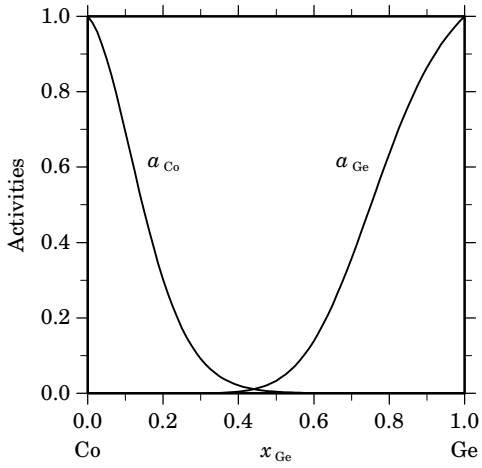

Fig. 3. Activities in the liquid phase at T=1823 K.

Table IV. Standard reaction quantities at 298.15 K for the compounds per mole of atoms.

Compound	x_{Ge}	$\Delta_{\mathrm{f}}G^{\circ}$ / (J/mol)	$\Delta_{\mathrm{f}}H^{\circ}$ / (J/mol)	$\Delta_{\mathrm{f}}S^{\circ}$ / (J/(mol·K))	$\Delta_{\mathrm{f}}C_P^{\circ}$ / (J/(mol·K))
Co_3Ge_1	0.250	−41387	−39698	5.668	−0.109
Co_5Ge_2	0.286	−47219	−46188	3.458	−0.104
Co_5Ge_3	0.375	−60000	−60000	0.001	−0.287
Co_1Ge_1	0.500	−51800	−51800	0.001	−0.228
Co_5Ge_7	0.583	−44163	−44167	−0.015	−0.060
Co_1Ge_2	0.667	−36403	−37120	−2.405	−0.149

References

[1949Pfi] H. Pfisterer, K. Schubert: Z. Metallkd. **40** (1949) 378–383.
[1952Kös] W. Köster, E. Horn: Z. Metallkd. **43** (1952) 333–33.
[1973Aga] T.P. Agalakova, V.L. Zagryzhskii, P.V. Geld: Izv. Akad. Nauk SSSR, Neorg. Mater. **9** (1973) 1180–1185; TR: Inorg. Mater. **9** (1973) 1048–1051.
[1976Bal] J.B. Ballance, H. Stadelmaier: Z. Metallkd. **67** (1976) 729–731.
[1980Day] A. Dayer, P. Feschotte: J. Less-Common Met. **72** (1980) 51–70.
[1990Eno] H. Enoki, K. Ishida, T. Nishizawa: J. Less-Common Met. **160** (1990) 153–160.
[1991Ish] K. Ishida, T. Nishizawa: J. Phase Equilibria **12** (1991) 77–83.
[2004Kor] J. Korb, unpublished assessment, GTT-Technologies, 2004.

Co – O (Cobalt – Oxygen)

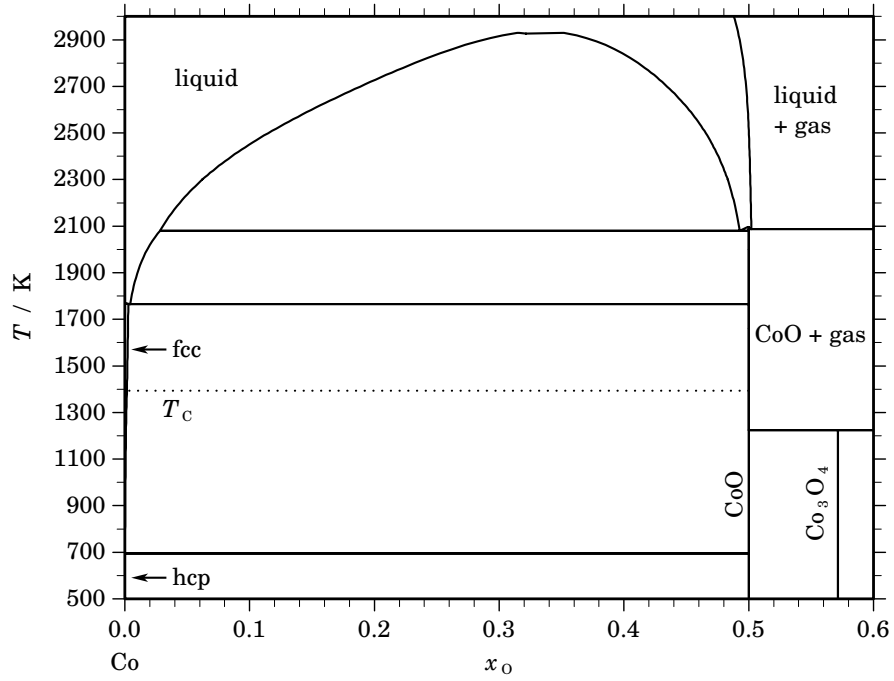

Fig. 1. Calculated phase diagram for the system Co-O.

A thorough review on the cobalt-oxygen system and a thermodynamic assessment has been given by [2003Che]. The stable phases in the system are the liquid, metallic cobalt (hcp and fcc) with limited solubility for oxygen and two oxides, CoO and Co_3O_4, which are described as stoichiometric compounds. The optimisation of the dataset is based on the evaluation of a large amount of experimental data from the literature. It includes the solubility and the activities of oxygen in the liquid phase, the solubility of oxygen in Co metal, the oxygen activities in the 2-phase equilibria of the condensed phases, data for the heat capacity and the heat content of both oxides as well as the enthalpies of formation and the entropy of these oxides at 298.15 K.

Table I. Phases, structures and models.

Phase	Strukturbericht	Prototype	Pearson symbol	Space group	SGTE name	Model
liquid					IONIC_L	$(Co^{2+},Co^{3+})_p(O^{2-},\square)_q$
fcc	$A1$	Cu	$cF4$	$Fm\overline{3}m$	FCC_A1	$Co_1(O,\square)_1$
hcp	$A3$	Mg	$hP2$	$P6_3/mmc$	HCP_A3	$Co_2(O,\square)_1$
CoO	$B1$	NaCl	$cF8$	$Fm\overline{3}m$	CO1O1	Co_1O_1
Co_3O_4	$H1_1$	$MgAl_2O_4$	$cF56$	$Fd\overline{3}m$	CO3O4	$(Co^{2+},Co^{3+})_1(Co^{2+},Co^{3+})_2O_4$

Table II. Invariant reactions.

Reaction	Type	T / K	Compositions / x_O			$\Delta_r H$ / (J/mol)
liquid ⇌ liquid′ + liquid″	critical	2935.5	0.334	0.334	0.334	0
liquid″ ⇌ CoO	congruent	2096.6	0.500	0.500		−21226
liquid″ ⇌ CoO + gas	gas-eutectic	2087.3	0.502	0.500	1.000	−20259
liquid″ ⇌ liquid′ + CoO	monotectic	2079.9	0.493	0.028	0.500	−22325
liquid′ ⇌ fcc + CoO	eutectic	1765.6	0.004	0.003	0.500	−16693
CoO + gas ⇌ Co_3O_4	gas-peritectoid	1223.7	0.500	1.000	0.571	−23383
fcc ⇌ hcp + CoO	degenerate	694.9	0.000	0.000	0.500	−429

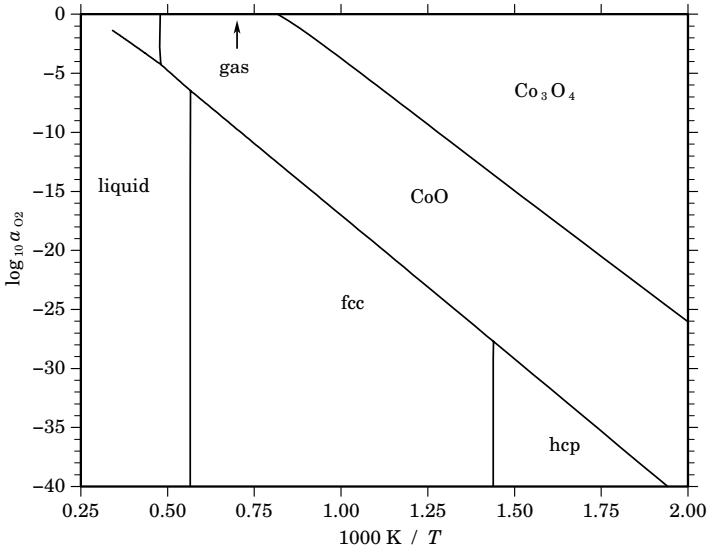

Fig. 2. Calculated temperature-activity phase diagram. Reference state: $\frac{1}{2}O_2$(gas, 0.1 MPa).

Table III. Standard reaction quantities at 298.15 K for the compounds per mole of atoms.

Compound	x_O	$\Delta_f G^\circ$ / (J/mol)	$\Delta_f H^\circ$ / (J/mol)	$\Delta_f S^\circ$ / (J/(mol·K))	$\Delta_f C_P^\circ$ / (J/(mol·K))
Co_1O_1	0.500	−106765	−118430	−39.123	7.567
Co_3O_4	0.571	−114126	−130769	−55.822	−1.712

References

[2003Che] M. Chen, B. Hallstedt, L.J. Gauckler: J. Phase Equilibria **24** (2003) 212–227.

Co – Pd (Cobalt – Palladium)

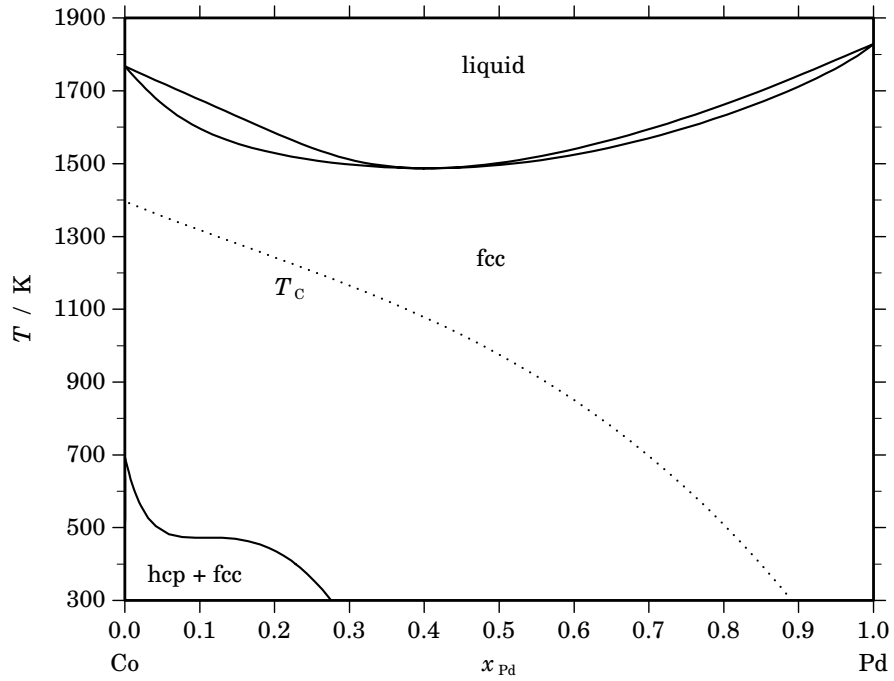

Fig. 1. Calculated phase diagram for the system Co-Pd.

The Co-Pd phase diagram is quite simple, consisting only of the melt, a broad fcc solution phase and at lower temperature the Co-based hcp phase. The present thermochemical optimisation of the Co-Pd system has been done by [2004Fra]. The phase diagram of the Co-Pd system and the T_C curve of fcc alloys have been determined essentially by Grube and Kästner [1936Gru]. The mixing enthalpy in the melt has been measured calorimetrically at 1873 K [1977Vat] and the excess properties of mixing have been determined by Knudsen mass spectrometry for the melt [1994Tom] as well as for solid solutions [1995Wan]. The activity of Co in fcc solid solutions has been measured in gas equilibration experiments [1965Sch] and by EMF methods [1965Sch, 1970Bid]. The experimental results of Vatolin and Kozlov [1977Vat] are in conflict with the results of Tomiska *et al.* [1994Tom]. [1977Vat] obtained slightly positive mixing enthalpies in the liquid whereas [1994Tom] found considerable negative mixing enthalpies. However, the same group investigated also the solid solutions [1995Wan] and both of their datasets are in accord with the phase diagram. Therefore, the results of [1977Vat] have been excluded from the present assessment. Another assessment for Co-Pd has been reported in [1999Gho] but the results of [1977Vat] have been adopted and the dataset predicts the presence of a miscibility gap in the fcc phase below 846 K at 17 at.% Pd which is not supported by experiments.

References

[1936Gru] G. Grube, H. Kästner: Z. Elektrochem. **42** (1936) 156–160.
[1965Sch] K. Schwerdtfeger, A. Muan: Acta Metall. **13** (1965) 509–515.
[1970Bid] L.R. Bidwell, F.E. Rizzo, J.V. Smith: Acta Metall. **18** (1970) 1013–1019.
[1977Vat] N.A. Vatolin, Yu.S. Kozlov: Russ. Metall., No. 1, (1977) 67–71.
[1994Tom] J. Tomiska, M.S. Belegratis, H. Wang: Ber. Bunsenges. Phys. Chem. **98** (1994) 1091–1095.
[1995Wan] H. Wang, M.S. Belegratis, J. Theiner, J. Tomiska: J. Alloys Comp. **220** (1995) 32–38.
[1999Gho] G. Ghosh, C. Kantner, G.B. Olsen: J. Phase Equilibria **20** (1999) 295–308.
[2004Fra] P. Franke, unpublished work, 2004.

Table I. Phases, structures and models.

Phase	Struktur-bericht	Prototype	Pearson symbol	Space group	SGTE name	Model
liquid					LIQUID	$(Co,Pd)_1$
fcc	$A1$	Cu	$cF4$	$Fm\bar{3}m$	FCC_A1	$(Co,Pd)_1$
hcp	$A3$	Mg	$hP2$	$P6_3/mmc$	HCP_A3	$(Co,Pd)_1$

Table II. Invariant reactions.

Reaction	Type	T / K	Compositions / x_{Pd}		$\Delta_{\mathrm{r}}H$ / (J/mol)
liquid $\rightleftharpoons$ fcc	congruent	1487.2	0.405	0.405	−13821

Table IIIa. Integral quantities for the liquid phase at 1850 K.

x_{Pd}	ΔG_{m} [J/mol]	ΔH_{m} [J/mol]	ΔS_{m} [J/(mol·K)]	$G_{\mathrm{m}}^{\mathrm{E}}$ [J/mol]	$S_{\mathrm{m}}^{\mathrm{E}}$ [J/(mol·K)]	ΔC_P [J/(mol·K)]
0.000	0	0	0.000	0	0.000	0.000
0.100	−6109	−3427	1.450	−1109	−1.253	0.000
0.200	−10037	−6430	1.949	−2339	−2.211	0.000
0.300	−12949	−8883	2.198	−3553	−2.881	0.000
0.400	−14965	−10660	2.327	−4613	−3.269	0.000
0.500	−16041	−11633	2.383	−5380	−3.380	0.000
0.600	−16068	−11675	2.375	−5716	−3.221	0.000
0.700	−14881	−10659	2.282	−5484	−2.797	0.000
0.800	−12244	−8460	2.045	−4546	−2.115	0.000
0.900	−7765	−4949	1.522	−2764	−1.181	0.000
1.000	0	0	0.000	0	0.000	0.000

Reference states: Co(liquid), Pd(liquid)

Table IIIb. Partial quantities for Co in the liquid phase at 1850 K.

x_{Co}	ΔG_{Co} [J/mol]	ΔH_{Co} [J/mol]	ΔS_{Co} [J/(mol·K)]	$G_{\mathrm{Co}}^{\mathrm{E}}$ [J/mol]	$S_{\mathrm{Co}}^{\mathrm{E}}$ [J/(mol·K)]	a_{Co}	γ_{Co}
1.000	0	0	0.000	0	0.000	1.000	1.000
0.900	−1537	−190	0.728	84	−0.148	0.905	1.005
0.800	−3282	−931	1.271	151	−0.585	0.808	1.010
0.700	−5561	−2475	1.668	−74	−1.298	0.697	0.995
0.600	−8725	−5077	1.972	−868	−2.275	0.567	0.945
0.500	−13168	−8990	2.258	−2506	−3.505	0.425	0.850
0.400	−19358	−14468	2.643	−5264	−4.975	0.284	0.710
0.300	−27937	−21764	3.337	−9417	−6.674	0.163	0.542
0.200	−39999	−31132	4.793	−15243	−8.589	0.074	0.371
0.100	−58434	−42826	8.437	−23016	−10.708	0.022	0.224
0.000	$-\infty$	−57100	∞	−33013	−13.020	0.000	0.117

Reference state: Co(liquid)

Table IIIc. Partial quantities for Pd in the liquid phase at 1850 K.

x_{Pd}	ΔG_{Pd} [J/mol]	ΔH_{Pd} [J/mol]	ΔS_{Pd} [J/(mol·K)]	$G^{\mathrm{E}}_{\mathrm{Pd}}$ [J/mol]	$S^{\mathrm{E}}_{\mathrm{Pd}}$ [J/(mol·K)]	a_{Pd}	γ_{Pd}
0.000	$-\infty$	−35960	∞	−10023	−14.020	0.000	0.521
0.100	−47261	−32552	7.951	−11843	−11.194	0.046	0.463
0.200	−37056	−28426	4.665	−12300	−8.717	0.090	0.449
0.300	−30190	−23836	3.435	−11670	−6.576	0.140	0.468
0.400	−24324	−19034	2.859	−10229	−4.759	0.206	0.514
0.500	−18915	−14275	2.508	−8253	−3.255	0.292	0.585
0.600	−13875	−9812	2.196	−6018	−2.051	0.406	0.676
0.700	−9285	−5900	1.830	−3799	−1.136	0.547	0.781
0.800	−5305	−2791	1.359	−1872	−0.497	0.708	0.885
0.900	−2135	−740	0.754	−514	−0.122	0.870	0.967
1.000	0	0	0.000	0	0.000	1.000	1.000

Reference state: Pd(liquid)

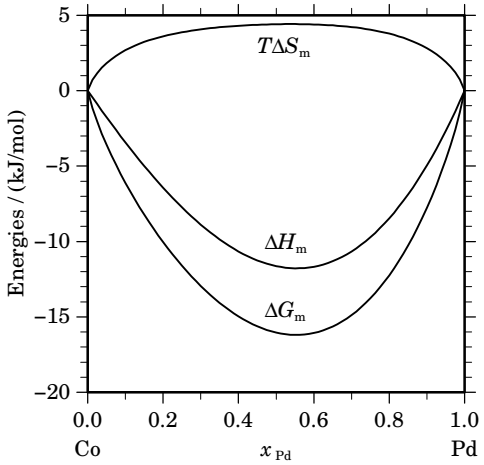

Fig. 2. Integral quantities of the liquid phase at T=1850 K.

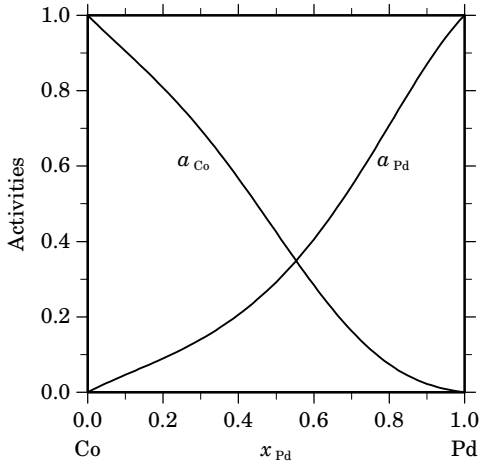

Fig. 3. Activities in the liquid phase at T=1850 K.

Table IVa. Integral quantities for the stable phases at 1473 K.

Phase	x_{Pd}	ΔG_{m} [J/mol]	ΔH_{m} [J/mol]	ΔS_{m} [J/(mol·K)]	$G^{\mathrm{E}}_{\mathrm{m}}$ [J/mol]	$S^{\mathrm{E}}_{\mathrm{m}}$ [J/(mol·K)]	ΔC_P [J/(mol·K)]
fcc	0.000	0	0	0.000	0	0.000	0.000
	0.100	−4321	−1872	1.662	−339	−1.041	−1.600
	0.200	−7231	−4160	2.085	−1102	−2.076	−2.216
	0.300	−9574	−6488	2.095	−2093	−2.984	−2.422
	0.400	−11364	−8544	1.915	−3122	−3.681	−2.425
	0.500	−12497	−10049	1.662	−4008	−4.101	−2.296
	0.600	−12814	−10738	1.409	−4572	−4.186	−2.043
	0.700	−12116	−10353	1.197	−4634	−3.882	−1.657
	0.800	−10144	−8623	1.032	−4016	−3.128	−1.155
	0.900	−6513	−5267	0.846	−2532	−1.857	−0.585
	1.000	0	0	0.000	0	0.000	0.000

Reference states: Co(fcc), Pd(fcc)

Table IVb. Partial quantities for Co in the stable phases at 1473 K.

Phase	x_{Co}	ΔG_{Co} [J/mol]	ΔH_{Co} [J/mol]	ΔS_{Co} [J/(mol·K)]	G^{E}_{Co} [J/mol]	S^{E}_{Co} [J/(mol·K)]	a_{Co}	γ_{Co}
fcc	1.000	0	0	0.000	0	0.000	1.000	1.000
	0.900	−1044	278	0.898	246	0.022	0.918	1.020
	0.800	−2018	567	1.755	715	−0.101	0.848	1.060
	0.700	−3339	235	2.427	1029	−0.539	0.761	1.088
	0.600	−5427	−1243	2.841	829	−1.407	0.642	1.070
	0.500	−8724	−4348	2.971	−235	−2.792	0.491	0.981
	0.400	−13735	−9563	2.832	−2513	−4.786	0.326	0.814
	0.300	−21113	−17431	2.500	−6368	−7.511	0.178	0.595
	0.200	−31891	−28584	2.245	−12180	−11.137	0.074	0.370
	0.100	−48529	−43656	3.308	−20329	−15.837	0.019	0.190
	0.000	−∞	−63128	∞	−31164	−21.700	0.000	0.079

Reference state: Co(fcc)

Table IVc. Partial quantities for Pd in the stable phases at 1473 K.

Phase	x_{Pd}	ΔG_{Pd} [J/mol]	ΔH_{Pd} [J/mol]	ΔS_{Pd} [J/(mol·K)]	G^{E}_{Pd} [J/mol]	S^{E}_{Pd} [J/(mol·K)]	a_{Pd}	γ_{Pd}
fcc	0.000	−∞	−15101	∞	−575	−9.862	0.000	0.954
	0.100	−33806	−21225	8.541	−5605	−10.604	0.063	0.633
	0.200	−28083	−23066	3.405	−8371	−9.976	0.101	0.505
	0.300	−24121	−22174	1.322	−9376	−8.688	0.140	0.465
	0.400	−20270	−19496	0.526	−9048	−7.093	0.191	0.478
	0.500	−16270	−15749	0.354	−7781	−5.409	0.265	0.530
	0.600	−12200	−11521	0.461	−5944	−3.786	0.369	0.615
	0.700	−8260	−7319	0.639	−3891	−2.327	0.509	0.728
	0.800	−4707	−3633	0.729	−1974	−1.126	0.681	0.851
	0.900	−1845	−1001	0.573	−554	−0.303	0.860	0.956
	1.000	0	0	0.000	0	0.000	1.000	1.000

Reference state: Pd(fcc)

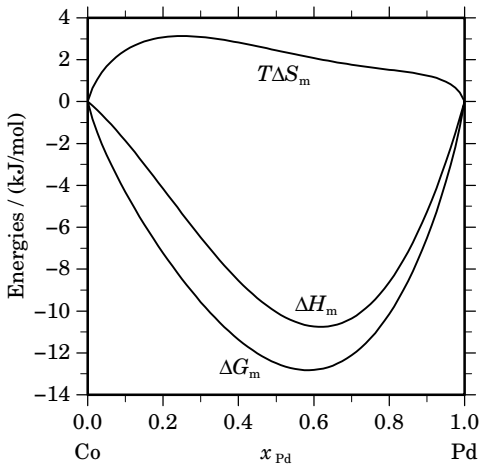

Fig. 4. Integral quantities of the stable phases at T=1473 K.

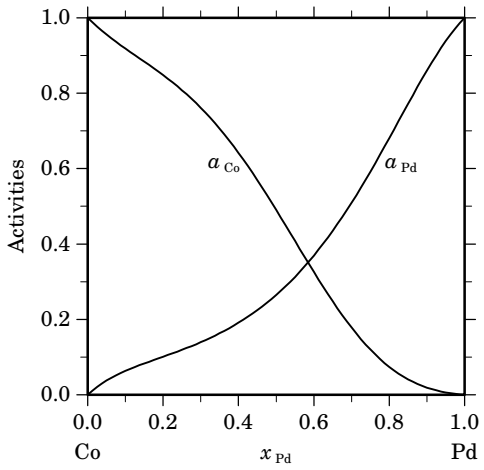

Fig. 5. Activities in the stable phases at T=1473 K.

Co – Y (Cobalt – Yttrium)

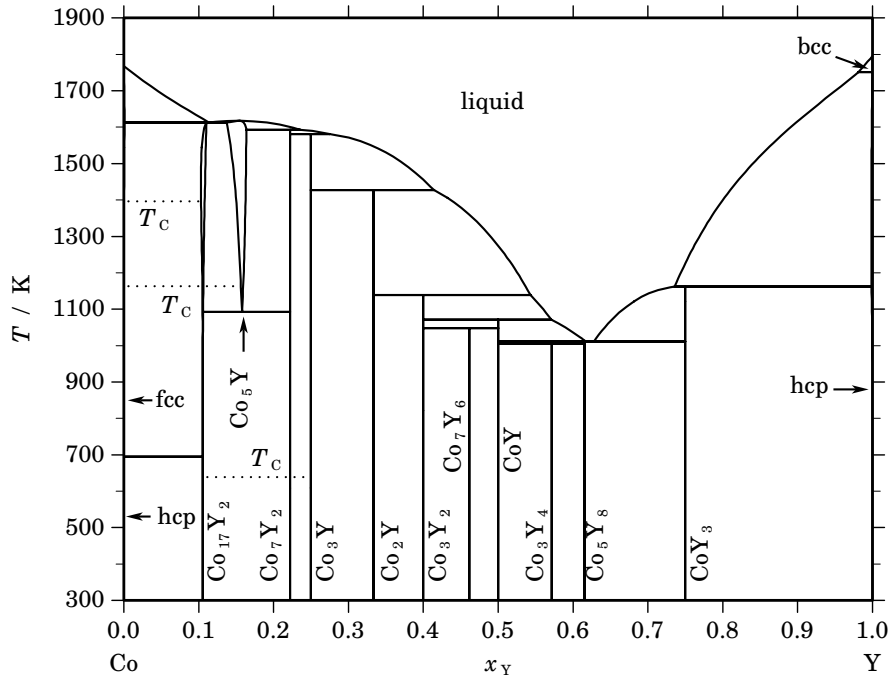

Fig. 1. Calculated phase diagram for the system Co-Y.

The Co-Y system is of interest for permanent magnets ($Co_{17}Y_2$) and for its potential use as hydrogen storage materials. A survey on the literature of the Co-Y system and a thermodynamic assessment has been been given by [2004Du]. The optimisation is based on experimental data on the phase diagram which are taken mainly from [1974Kha, 1991Wu] and on thermochemical data for the intermetallic compounds [1985Sub, 1987Col, 1987Mey]. For the liquid, no data have been available. A polymorphic transformation between $\alpha Co_{17}Y_2$ and $\beta Co_{17}Y_2$ at about 1573 K has been omitted in the assessment. At higher temperature the compounds $Co_{17}Y_2$ and Co_5Y deviate from their stoichiometric compositions due to an excess of Y in $Co_{17}Y_2$ and excess Co in Co_5Y. Since their crystal structures are closely related, [2004Du] have described both compounds as a single phase with a miscibility gap. However, since both structures are different, the phases are still denoted as different compounds in the present diagrams and tables. The dataset should not be used at too high temperatures because an artificial inverse miscibility gap opens in the liquid above 3800 K.

Table I. Phases, structures and models.

Phase	Strukturbericht	Prototype	Pearson symbol	Space group	SGTE name	Model
liquid					LIQUID	$(Co,Y)_1$
fcc	$A1$	Cu	$cF4$	$Fm\bar{3}m$	FCC_A1	$(Co,Y)_1$
hcp	$A3$	Mg	$hP2$	$P6_3/mmc$	HCP_A3	$(Co,Y)_1$
$\alpha Co_{17}Y_2$	$\cdots$	Th_2Zn_{17}	$hR19$	$R\bar{3}m$	CO17RE2	$Co_{15}(Co_2,Y)_2(Co_2,Y)_1$
$\beta Co_{17}Y_2$	$\cdots$	$Ni_{17}Th_2$	$hP38$	$P6_3/mmc$	CO17RE2	$Co_{15}(Co_2,Y)_2(Co_2,Y)_1$
Co_5Y	$D2_{\mathrm{d}}$	$CaCu_5$	$hP6$	$P6/mmm$	CO17RE2	$Co_{15}(Co_2,Y)_2(Co_2,Y)_1$
Co_7Y_2	$\cdots$	Co_7Er_2	$hR18$	$R\bar{3}m$	CO7Y2	Co_7Y_2
Co_3Y	$\cdots$	Be_3Nb	$hR12$	$R\bar{3}m$	CO3Y	Co_3Y_1
Co_2Y	$C15$	Cu_2Mg	$cF24$	$Fd\bar{3}m$	CO2Y	Co_2Y_1
Co_3Y_2	$\cdots$	$\cdots$	$cP*$	$\cdots$	CO3Y2	Co_3Y_2
Co_7Y_6	$\cdots$	$\cdots$	$\cdots$	$\cdots$	CO7Y6	Co_7Y_6
CoY	$B33$	CrB	$oC8$	$Cmcm$	COY	Co_1Y_1
Co_3Y_4	$\cdots$	Co_3Ho_4	$hP22$	$P6_3/m$	CO3Y4	Co_3Y_4
Co_5Y_8	$\cdots$	$\cdots$	$mP52$	$P2_1/c$	CO5Y8	Co_5Y_8
CoY_3	$D0_{11}$	Fe_3C	$oP16$	$Pnma$	COY3	Co_1Y_3
bcc	$A2$	W	$cI2$	$Im\bar{3}m$	BCC_A2	$(Co,Y)_1$

Table II. Invariant reactions.

Reaction	Type	T / K	Compositions / x_{Y}			$\Delta_{\mathrm{r}}H$ / (J/mol)
liquid + bcc $\rightleftharpoons$ hcp	peritectic	1751.2	0.981	1.000	1.000	−4896
liquid $\rightleftharpoons$ Co_5Y	congruent	1617.5	0.155	0.155		−33578
fcc + liquid $\rightleftharpoons$ $Co_{17}Y_2$	peritectic	1613.3	0.001	0.114	0.110	−31923
liquid $\rightleftharpoons$ $Co_{17}Y_2$ + Co_5Y	eutectic	1613.3	0.114	0.110	0.137	−32696
Co_5Y + liquid $\rightleftharpoons$ Co_7Y_2	peritectic	1593.0	0.164	0.236	0.222	−28455
Co_7Y_2 + liquid $\rightleftharpoons$ Co_3Y	peritectic	1580.8	0.222	0.275	0.250	−18188
Co_3Y + liquid $\rightleftharpoons$ Co_2Y	peritectic	1427.0	0.250	0.414	0.333	−16225
liquid + hcp $\rightleftharpoons$ CoY_3	peritectic	1161.9	0.736	0.999	0.750	−16777
Co_2Y + liquid $\rightleftharpoons$ Co_3Y_2	peritectic	1139.0	0.333	0.543	0.400	−10918
Co_5Y $\rightleftharpoons$ $Co_{17}Y_2$ + Co_7Y_2	eutectoid	1092.0	0.158	0.106	0.222	−1372
Co_3Y_2 + liquid $\rightleftharpoons$ CoY	peritectic	1071.0	0.400	0.571	0.500	−16986
Co_3Y_2 + CoY $\rightleftharpoons$ Co_7Y_6	peritectoid	1048.0	0.400	0.500	0.462	−2465
CoY + liquid $\rightleftharpoons$ Co_5Y_8	peritectic	1012.6	0.500	0.616	0.615	−20645
liquid $\rightleftharpoons$ Co_5Y_8 + CoY_3	eutectic	1011.3	0.628	0.615	0.750	−20133
CoY + Co_5Y_8 $\rightleftharpoons$ Co_3Y_4	peritectoid	1005.0	0.500	0.615	0.571	−595
fcc + $Co_{17}Y_2$ $\rightleftharpoons$ hcp	peritectoid	695.0	0.000	0.105	0.000	−428

Table IIIa. Integral quantities for the liquid phase at 1800 K.

x_{Y}	ΔG_{m} [J/mol]	ΔH_{m} [J/mol]	ΔS_{m} [J/(mol·K)]	$G_{\mathrm{m}}^{\mathrm{E}}$ [J/mol]	$S_{\mathrm{m}}^{\mathrm{E}}$ [J/(mol·K)]	ΔC_P [J/(mol·K)]
0.000	0	0	0.000	0	0.000	0.000
0.100	−11761	1932	7.607	−6896	4.905	0.000
0.200	−20390	−4115	9.042	−12901	4.881	0.000
0.300	−26679	−12995	7.602	−17537	2.523	0.000
0.400	−30533	−20885	5.360	−20461	−0.236	0.000
0.500	−31841	−25284	3.643	−21467	−2.120	0.000
0.600	−30556	−25014	3.079	−20484	−2.517	0.000
0.700	−26719	−20221	3.610	−17577	−1.469	0.000
0.800	−20436	−12373	4.479	−12947	0.319	0.000
0.900	−11796	−4261	4.186	−6930	1.483	0.000
1.000	0	0	0.000	0	0.000	0.000

Reference states: Co(liquid), Y(liquid)

Table IIIb. Partial quantities for Co in the liquid phase at 1800 K.

x_{Co}	ΔG_{Co} [J/mol]	ΔH_{Co} [J/mol]	ΔS_{Co} [J/(mol·K)]	$G_{\mathrm{Co}}^{\mathrm{E}}$ [J/mol]	$S_{\mathrm{Co}}^{\mathrm{E}}$ [J/(mol·K)]	a_{Co}	γ_{Co}
1.000	0	0	0.000	0	0.000	1.000	1.000
0.900	−1931	4958	3.827	−354	2.951	0.879	0.977
0.800	−5463	12308	9.872	−2123	8.017	0.694	0.868
0.700	−11398	13741	13.966	−6060	11.000	0.467	0.667
0.600	−20153	4918	13.929	−12508	9.682	0.260	0.434
0.500	−31781	−14531	9.583	−21407	3.820	0.120	0.239
0.400	−46000	−41009	2.773	−32287	−4.845	0.046	0.116
0.300	−62289	−66949	−2.589	−44270	−12.599	0.016	0.052
0.200	−80159	−80815	−0.364	−56072	−13.746	0.005	0.024
0.100	−100462	−67104	18.532	−66001	−0.612	0.001	0.012
0.000	$-\infty$	−6341	∞	−71957	36.453	0.000	0.008

Reference state: Co(liquid)

Table IIIc. Partial quantities for Y in the liquid phase at 1800 K.

x_{Y}	ΔG_{Y} [J/mol]	ΔH_{Y} [J/mol]	ΔS_{Y} [J/(mol·K)]	$G_{\mathrm{Y}}^{\mathrm{E}}$ [J/mol]	$S_{\mathrm{Y}}^{\mathrm{E}}$ [J/(mol·K)]	a_{Y}	γ_{Y}
0.000	$-\infty$	79683	∞	−71480	83.979	0.000	0.008
0.100	−100230	−25296	41.630	−65769	22.485	0.001	0.012
0.200	−80098	−69804	5.719	−56011	−7.663	0.005	0.024
0.300	−62336	−75379	−7.246	−44317	−17.257	0.016	0.052
0.400	−46103	−59590	−7.493	−32390	−15.111	0.046	0.115
0.500	−31900	−36037	−2.298	−21527	−8.061	0.119	0.237
0.600	−20260	−14351	3.283	−12615	−0.964	0.258	0.430
0.700	−11475	−195	6.267	−6137	3.301	0.465	0.664
0.800	−5505	4737	5.690	−2165	3.835	0.692	0.865
0.900	−1944	2721	2.592	−367	1.716	0.878	0.976
1.000	0	0	0.000	0	0.000	1.000	1.000

Reference state: Y(liquid)

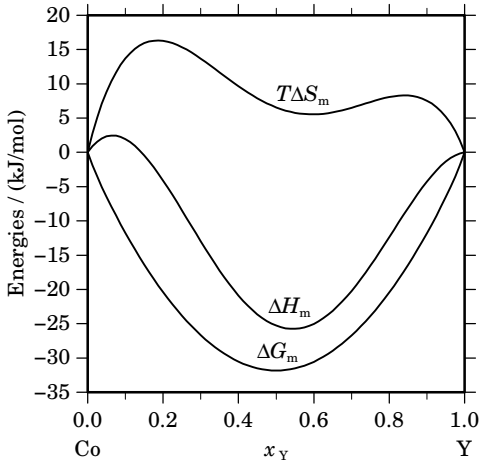

Fig. 2. Integral quantities of the liquid phase at T=1800 K.

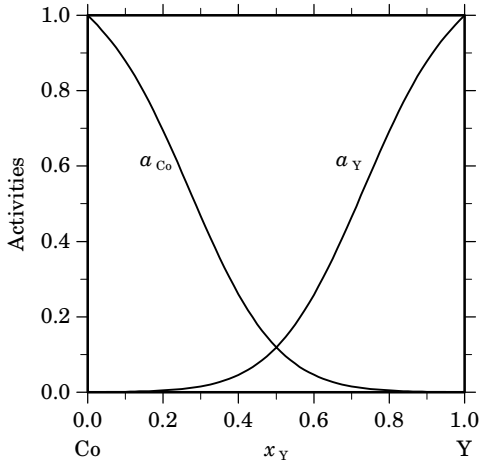

Fig. 3. Activities in the liquid phase at T=1800 K.

Table IV. Standard reaction quantities at 298.15 K for the compounds per mole of atoms.

Compound	x_Y	$\Delta_f G^\circ$ / (J/mol)	$\Delta_f H^\circ$ / (J/mol)	$\Delta_f S^\circ$ / (J/(mol·K))	$\Delta_f C_P^\circ$ / (J/(mol·K))
$Co_{17}Y_2$	0.105	−10488	−10226	−0.878	−0.078
Co_7Y_2	0.222	−19841	−19935	−0.314	0.307
Co_3Y_1	0.250	−21765	−21643	0.407	5.028
Co_2Y_1	0.333	−27238	−27815	−1.935	−0.097
Co_3Y_2	0.400	−30600	−32522	−6.446	−0.087
Co_7Y_6	0.462	−33450	−36853	−11.412	−0.078
Co_1Y_1	0.500	−32365	−35553	−10.693	−0.072
Co_3Y_4	0.571	−29319	−32133	−9.437	−0.062
Co_5Y_8	0.615	−26768	−29066	−7.708	−0.056
Co_1Y_3	0.750	−18245	−18892	−2.171	−0.036

References

[1974Kha] Y. Khan: Z. Metallkd. **65** (1974) 489–495.
[1985Sub] P.R. Subramanian, J.F. Smith: Metall. Trans. A **16A** (1985) 1195–1201.
[1987Col] C. Colinet, A. Pasturel: Calphad **11** (1987) 323–334.
[1987Mey] F. Meyer-Liautaud, S. Derkaoui, C.H. Allibert, R. Castanet: J. Less-Common Met. **127** (1987) 231–242.
[1991Wu] C.H. Wu, Y.C. Chuang, X.P. Su: Z. Metallkd. **82** (1991) 73–79.
[2004Du] Z. Du, D. Lü: J. Alloys Comp. **373** (2004) 171–178.

Co – Zn (Cobalt – Zinc)

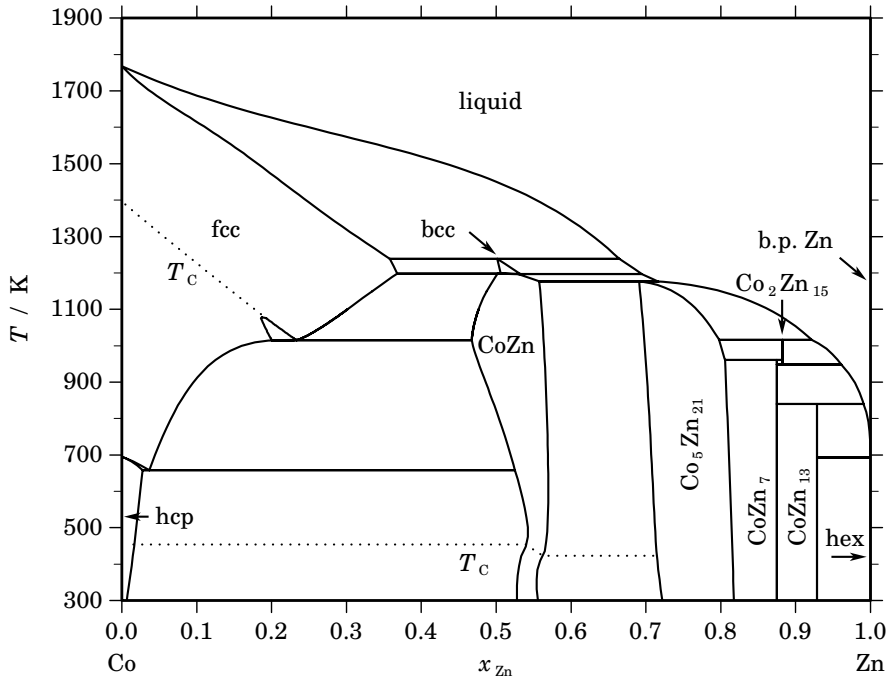

Fig. 1. Calculated phase diagram for the system Co-Zn.

The Co-Zn system has been reviewed and a thermodynamic dataset has been optimised in [2004Vas]. The Co-Zn system has been studied thoroughly by Schramm using metallographic and thermal analyses, x-ray diffraction and magnetic methods [1938Sch1, 1938Sch2, 1938Sch3, 1938Sch4, 1941Sch]. Later, various parts of the phase diagram have been re-investigated [1955Kös, 1955Lih, 1976Bud1, 1995Tak]. Thermodynamic properties of Co-Zn solutions have been reported for solid alloys [1976Bud2, 1977Bud, 1981Ali, 1982Cöm] as well as more limited data for the melt [1982Cöm]. The assessed dataset which is shown here [2004Vas] provides a good representation of the experimental data. The dataset should not be used at too high temperatures because an artificial inverse miscibility gap opens in the liquid above 2600 K. Another assessment for Co-Zn has been reported by [2004Iso] but here the phase diagram has been modelled with less detail.

Table I. Phases, structures and models.

Phase	Struktur-bericht	Prototype	Pearson symbol	Space group	SGTE name	Model
liquid					LIQUID	$(Co,Zn)_1$
fcc	$A1$	Cu	$cF4$	$Fm\bar{3}m$	FCC_A1	$(Co,Zn)_1$
hcp	$A3$	Mg	$hP2$	$P6_3/mmc$	HCP_A3	$(Co,Zn)_1$
bcc	$A2$	W	$cI2$	$Im\bar{3}m$	COZN_A2	$(Co,Zn)_1$
CoZn	$A13$	βMn	$cP20$	$P4_132$	COZN_A13	$(Co,Zn)_1$
Co_5Zn_{21}	$D8_3$	Al_4Cu_9	$cP52$	$P4\bar{3}m$	CO5ZN21	$(Co,Zn)_1$
$CoZn_7$	···	···	$c*^*$	···	COZN7	Co_1Zn_7
Co_2Zn_{15}	···	···	···	···	CO2ZN15	Co_2Zn_{15}
$CoZn_{13}$	···	···	$mC28$	$C2/m$	COZN13	Co_1Zn_{13}
hex	$A3$	Mg	$hP2$	$P6_3/mmc$	HCP_ZN	Zn_1

Table II. Invariant reactions.

Reaction	Type	T / K	Compositions / x_{Zn}			$\Delta_{\mathrm{r}}H$ / (J/mol)
fcc + liquid ⇌ bcc	peritectic	1239.0	0.358	0.664	0.501	−3900
fcc + bcc ⇌ CoZn	peritectoid	1198.0	0.368	0.506	0.502	−6720
bcc ⇌ CoZn + liquid	metatectic	1197.0	0.532	0.529	0.694	−6865
CoZn + liquid ⇌ Co_5Zn_{21}	peritectic	1176.8	0.558	0.716	0.691	−14659
fcc ⇌ fcc′ + fcc″	critical	1089.0	0.184	0.184	0.184	0
Co_5Zn_{21} + liquid ⇌ Co_2Zn_{15}	peritectic	1016.4	0.798	0.921	0.882	−5328
fcc″ ⇌ fcc′ + CoZn	monotectoid	1014.7	0.234	0.200	0.467	−1182
Co_5Zn_{21} + Co_2Zn_{15} ⇌ $CoZn_7$	peritectoid	961.1	0.806	0.882	0.875	−3846
Co_2Zn_{15} ⇌ $CoZn_7$ + liquid	eutectic	948.1	0.882	0.875	0.961	−3068
$CoZn_7$ + liquid ⇌ $CoZn_{13}$	peritectic	840.2	0.875	0.991	0.929	−3437
liquid ⇌ $CoZn_{13}$ + hex	eutectic	692.6	1.000	0.929	1.000	−7327
fcc′ ⇌ hcp + CoZn	eutectoid	658.0	0.037	0.028	0.525	−685

Table IIIa. Integral quantities for the liquid phase at 1800 K.

x_{Zn}	ΔG_{m} [J/mol]	ΔH_{m} [J/mol]	ΔS_{m} [J/(mol·K)]	$G^{\mathrm{E}}_{\mathrm{m}}$ [J/mol]	$S^{\mathrm{E}}_{\mathrm{m}}$ [J/(mol·K)]	ΔC_P [J/(mol·K)]
0.000	0	0	0.000	0	0.000	0.000
0.100	−4283	2375	3.699	582	0.996	0.000
0.200	−6397	2566	4.979	1093	0.819	0.000
0.300	−7633	1194	4.904	1509	−0.175	0.000
0.400	−8261	−1120	3.967	1811	−1.628	0.000
0.500	−8397	−3754	2.579	1977	−3.184	0.000
0.600	−8089	−6088	1.111	1984	−4.484	0.000
0.700	−7331	−7501	−0.094	1811	−5.174	0.000
0.800	−6052	−7371	−0.733	1437	−4.894	0.000
0.900	−4024	−5078	−0.585	841	−3.288	0.000
1.000	0	0	0.000	0	0.000	0.000

Reference states: Co(liquid), Zn(liquid)

Table IIIb. Partial quantities for Co in the liquid phase at 1800 K.

x_{Co}	ΔG_{Co} [J/mol]	ΔH_{Co} [J/mol]	ΔS_{Co} [J/(mol·K)]	$G^{\mathrm{E}}_{\mathrm{Co}}$ [J/mol]	$S^{\mathrm{E}}_{\mathrm{Co}}$ [J/(mol·K)]	a_{Co}	γ_{Co}
1.000	0	0	0.000	0	0.000	1.000	1.000
0.900	−1544	1196	1.522	32	0.646	0.902	1.002
0.800	−3181	3954	3.964	158	2.109	0.809	1.011
0.700	−4917	7033	6.639	421	3.674	0.720	1.029
0.600	−6782	9191	8.874	863	4.627	0.636	1.059
0.500	−8846	9185	10.017	1528	4.254	0.554	1.107
0.400	−11255	5774	9.460	2458	1.842	0.471	1.179
0.300	−14321	−2286	6.686	3698	−3.324	0.384	1.280
0.200	−18797	−16236	1.423	5290	−11.959	0.285	1.424
0.100	−27184	−37318	−5.630	7277	−24.775	0.163	1.626
0.000	−∞	−66775	∞	9702	−42.487	0.000	1.912

Reference state: Co(liquid)

Table IIIc. Partial quantities for Zn in the liquid phase at 1800 K.

x_{Zn}	ΔG_{Zn} [J/mol]	ΔH_{Zn} [J/mol]	ΔS_{Zn} [J/(mol·K)]	$G^{\mathrm{E}}_{\mathrm{Zn}}$ [J/mol]	$S^{\mathrm{E}}_{\mathrm{Zn}}$ [J/(mol·K)]	a_{Zn}	γ_{Zn}
0.000	$-\infty$	36741	∞	6110	17.017	0.000	1.504
0.100	−28930	12991	23.289	5531	4.144	0.145	1.447
0.200	−19257	−2986	9.040	4830	−4.342	0.276	1.381
0.300	−13969	−12431	0.855	4050	−9.156	0.393	1.311
0.400	−10479	−16586	−3.393	3234	−11.011	0.496	1.241
0.500	−7948	−16694	−4.859	2425	−10.622	0.588	1.176
0.600	−5978	−13997	−4.455	1667	−8.702	0.671	1.118
0.700	−4336	−9736	−3.000	1002	−5.966	0.748	1.069
0.800	−2865	−5155	−1.272	474	−3.128	0.826	1.032
0.900	−1451	−1496	−0.025	126	−0.901	0.908	1.008
1.000	0	0	0.000	0	0.000	1.000	1.000

Reference state: Zn(liquid)

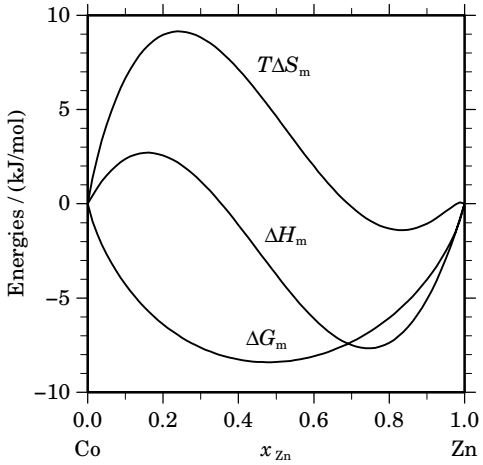

Fig. 2. Integral quantities of the liquid phase at T=1800 K.

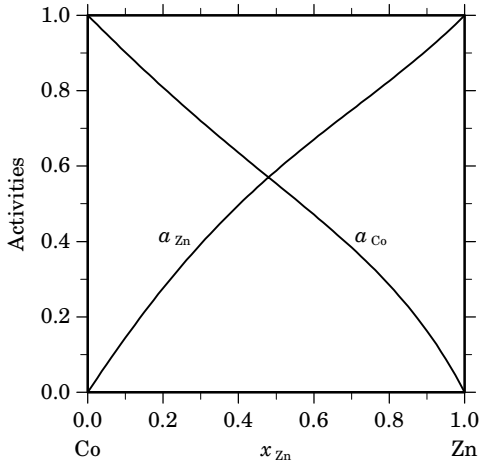

Fig. 3. Activities in the liquid phase at T=1800 K.

Table IV. Standard reaction quantities at 298.15 K for the compounds per mole of atoms.

Compound	x_{Zn}	$\Delta_{\mathrm{f}}G^{\circ}$ / (J/mol)	$\Delta_{\mathrm{f}}H^{\circ}$ / (J/mol)	$\Delta_{\mathrm{f}}S^{\circ}$ / (J/(mol·K))	$\Delta_{\mathrm{f}}C^{\circ}_{P}$ / (J/(mol·K))
Co_1Zn_7	0.875	−9901	−10986	−3.638	−0.018
Co_2Zn_{15}	0.882	−6739	−6491	0.830	−0.017
Co_1Zn_{13}	0.929	−5795	−6101	−1.029	−0.010

References

[1938Sch] J. Schramm: Z. Metallkd. **30** (1938) 10–14.
[1938Sch2] J. Schramm: Z. Metallkd. **30** (1938) 122–130.
[1938Sch3] J. Schramm: Z. Metallkd. **30** (1938) 131–135.
[1938Sch4] J. Schramm: Z. Metallkd. **30** (1938) 327–334.
[1941Sch] J. Schramm: Z. Metallkd. **33** (1941) 46–48.
[1955Kös] W. Köster, H. Schmid: Z. Metallkd. **46** (1955) 468–469.
[1955Lih] F. Lihl, E. Weisberg: Z. Metallkd. **46** (1955) 579–581.
[1976Bud1] S. Budurov, G.P. Vassilev: Z. Metallkd. **67** (1976) 170–172.
[1976Bud2] S. Budurov, G.P. Vassilev, L. Mandadjieva: Z. Metallkd. **67** (1976) 307–310.
[1977Bud] S. Budurov, G.P. Vassilev: Z. Metallkd. **68** (1977) 795–798.
[1981Ali] S. Ali, V. Geiderich: Zh. Fiz. Khim. **67** (1981) 1248–51.
[1982Cöm] H. Cömert, J.N. Pratt: Thermochim. Acta **59** (1982) 267–285.
[1995Tak] T. Takayama, S. Shinohara, K. Ishida, T. Nishizawa: J. Phase Equilibria **16** (1995) 390–395.
[2004Iso] I. Isomäki, M. Hämäläinen: J. Alloys Comp. **375** (2004) 191–195.
[2004Vas] G.P. Vassilev, M. Jiang: J. Phase Equil. Diff. **25** (2004) 259–268.

Cr – Ru (Chromium – Ruthenium)

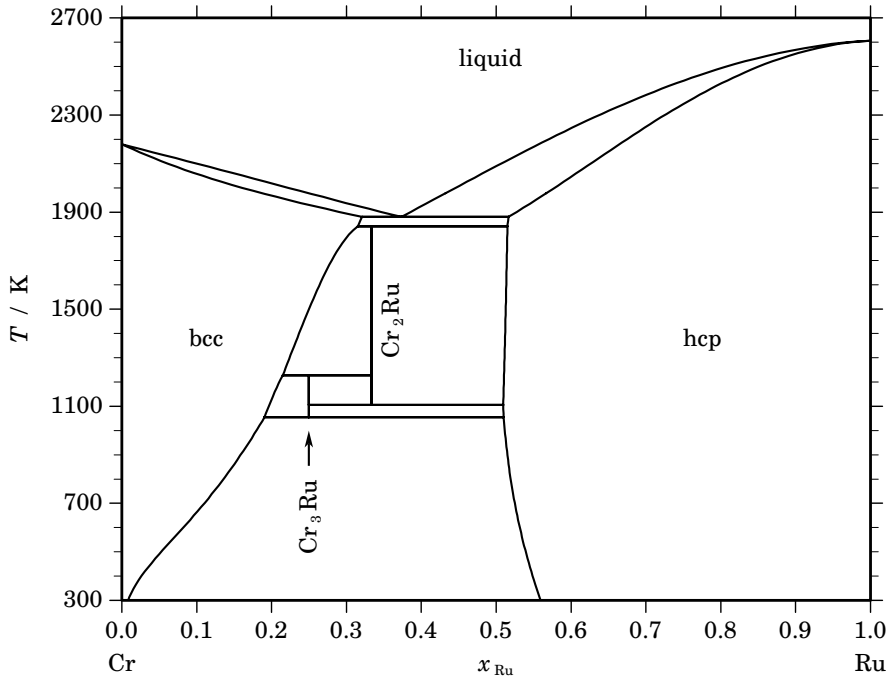

Fig. 1. Calculated phase diagram for the system Cr-Ru.

The Cr-Ru binary system contains two components interesting for the nuclear field, chromium being a major component of stainless steel structures of the vessel, and ruthenium being selected as representative of a family of non-volatile fission products. Experimental information on the phase diagram has been reported in several compilations of binary systems [1958Han, 1965Ell, 1969Shu, 1981Mof] and in the review of Venkatraman and Neumann [1987Ven]. Raub and Mahler [1955Rau] and Greenfield and Beck [1956Gre] firstly put in evidence the existence of the bcc and hcp terminal solid solutions, and intermetallic phases, Cr_4Ru, Cr_3Ru and Cr_2Ru (σ). The diagram constructed by Savitskii *et al.* [1961Sav] by classical methods is in poor agreement with the selected one. Shurin and Dmitrieva [1964Shu] determined liquidus and solidus data. Cr_4Ru was not confirmed. The high temperature data are in agreement with [1961Sav] and [1964Shu], the low temperature transitions of Cr_3Ru were determined by Wopersnow and Raub [1979Wop]. The solubility of Ru in bcc was determined by Waterstrat [1981Wat] at 1373 K and 1073 K. No thermodynamic properties are available for that system.

The system was assessed by Chevalier and Fischer [1998Che]. The excess Gibbs energy of the liquid, bcc, hcp and the Gibbs energy of the intermetallic compounds, Cr_3Ru and σ which are considered as stoichiometric was optimised from the selected phase diagram experimental information. A sub-regular substitution model was used for solution phases. The heat capacity of the compounds was estimated from the pure solid components by using the Neumann-Kopp rule. The enthalpy and entropy of formation was optimised in consistency with other data. The agreement with the experimental information [1961Sav, 1964Shu, 1979Wop, 1981Wat, 1987Ven] is satisfactory.

Table I. Phases, structures and models.

Phase	Struktur-bericht	Prototype	Pearson symbol	Space group	SGTE name	Model
liquid					LIQUID	$(Cr,Ru)_1$
bcc	$A2$	W	$cI2$	$Im\overline{3}m$	BCC_A2	$(Cr,Ru)_1$
Cr_3Ru	$A15$	Cr_3Si	$cP8$	$Pm\overline{3}n$	CR3RU	Cr_3Ru
Cr_2Ru	$D8_b$	σCrFe	$tP30$	$P4_2/mnm$	CR2RU	Cr_2Ru
hcp	$A3$	Mg	$hP2$	$P6_3/mmc$	HCP_A3	$(Cr,Ru)_1$

Table II. Invariant reactions.

Reaction	Type	T / K	Compositions / x_{Ru}			$\Delta_r H$ / (J/mol)
liquid $\rightleftharpoons$ bcc + hcp	eutectic	1880.5	0.373	0.321	0.516	−19351
bcc + hcp $\rightleftharpoons$ Cr_2Ru	peritectoid	1841.2	0.315	0.515	0.333	−1241
bcc + Cr_2Ru $\rightleftharpoons$ Cr_3Ru	peritectoid	1227.8	0.215	0.333	0.250	−163
Cr_2Ru $\rightleftharpoons$ Cr_3Ru + hcp	eutectoid	1106.1	0.333	0.250	0.509	−499
Cr_3Ru $\rightleftharpoons$ bcc + hcp	eutectoid	1054.9	0.250	0.191	0.510	−321

Table IIIa. Integral quantities for the liquid phase at 2700 K.

x_{Ru}	ΔG_m [J/mol]	ΔH_m [J/mol]	ΔS_m [J/(mol·K)]	G_m^E [J/mol]	S_m^E [J/(mol·K)]	ΔC_P [J/(mol·K)]
0.000	0	0	0.000	0	0.000	0.000
0.100	−10400	−3102	2.703	−3102	0.000	0.000
0.200	−17311	−6077	4.161	−6077	0.000	0.000
0.300	−22427	−8714	5.079	−8714	0.000	0.000
0.400	−25911	−10802	5.596	−10802	0.000	0.000
0.500	−27692	−12131	5.763	−12131	0.000	0.000
0.600	−27598	−12489	5.596	−12489	0.000	0.000
0.700	−25379	−11666	5.079	−11666	0.000	0.000
0.800	−20684	−9451	4.161	−9451	0.000	0.000
0.900	−12930	−5632	2.703	−5632	0.000	0.000
1.000	0	0	0.000	0	0.000	0.000

Reference states: Cr(liquid), Ru(liquid)

Table IIIb. Partial quantities for Cr in the liquid phase at 2700 K.

x_{Cr}	ΔG_{Cr} [J/mol]	ΔH_{Cr} [J/mol]	ΔS_{Cr} [J/(mol·K)]	G^E_{Cr} [J/mol]	S^E_{Cr} [J/(mol·K)]	a_{Cr}	γ_{Cr}
1.000	0	0	0.000	0	0.000	1.000	1.000
0.900	−2394	−28	0.876	−28	0.000	0.899	0.999
0.800	−5404	−395	1.855	−395	0.000	0.786	0.983
0.700	−9528	−1521	2.966	−1521	0.000	0.654	0.935
0.600	−15296	−3828	4.247	−3828	0.000	0.506	0.843
0.500	−23299	−7738	5.763	−7738	0.000	0.354	0.708
0.400	−34243	−13673	7.619	−13673	0.000	0.218	0.544
0.300	−49083	−22055	10.010	−22055	0.000	0.112	0.374
0.200	−69435	−33304	13.382	−33304	0.000	0.045	0.227
0.100	−99535	−47844	19.145	−47844	0.000	0.012	0.119
0.000	−∞	−66094	∞	−66094	0.000	0.000	0.053

Reference state: Cr(liquid)

Table IIIc. Partial quantities for Ru in the liquid phase at 2700 K.

x_{Ru}	ΔG_{Ru} [J/mol]	ΔH_{Ru} [J/mol]	ΔS_{Ru} [J/(mol·K)]	G^E_{Ru} [J/mol]	S^E_{Ru} [J/(mol·K)]	a_{Ru}	γ_{Ru}
0.000	−∞	−30953	∞	−30953	0.000	0.000	0.252
0.100	−82456	−30765	19.145	−30765	0.000	0.025	0.254
0.200	−64937	−28806	13.382	−28806	0.000	0.055	0.277
0.300	−52527	−25499	10.010	−25499	0.000	0.096	0.321
0.400	−41834	−21264	7.619	−21264	0.000	0.155	0.388
0.500	−32084	−16524	5.763	−16524	0.000	0.240	0.479
0.600	−23167	−11700	4.247	−11700	0.000	0.356	0.594
0.700	−15221	−7214	2.966	−7214	0.000	0.508	0.725
0.800	−8497	−3487	1.855	−3487	0.000	0.685	0.856
0.900	−3307	−942	0.876	−942	0.000	0.863	0.959
1.000	0	0	0.000	0	0.000	1.000	1.000

Reference state: Ru(liquid)

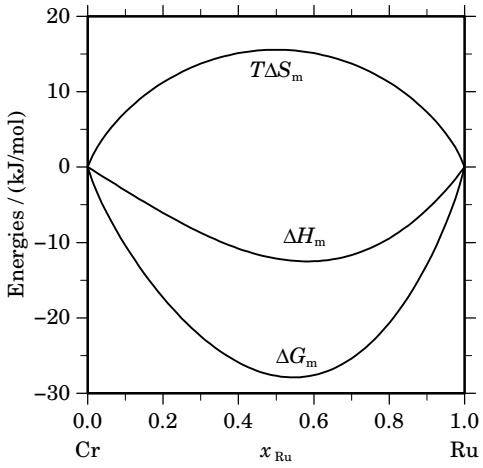

Fig. 2. Integral quantities of the liquid phase at T=2700 K.

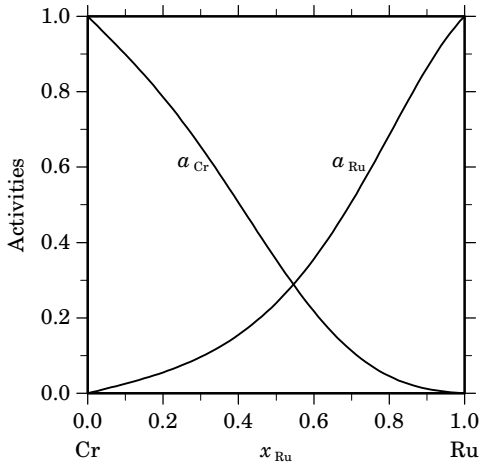

Fig. 3. Activities in the liquid phase at T=2700 K.

Table IVa. Integral quantities for the stable phases at 1600 K.

Phase	x_{Ru}	ΔG_{m} [J/mol]	ΔH_{m} [J/mol]	ΔS_{m} [J/(mol·K)]	$G_{\mathrm{m}}^{\mathrm{E}}$ [J/mol]	$S_{\mathrm{m}}^{\mathrm{E}}$ [J/(mol·K)]	ΔC_P [J/(mol·K)]
bcc	0.000	0	0	0.000	0	0.000	0.000
	0.100	−5552	−420	3.208	−1228	0.505	0.000
	0.200	−9103	−831	5.171	−2447	1.010	0.000
	0.264	−10803	−992	6.132	−3125	1.333	0.000
Cr_2Ru	0.333	−12415	−2806	6.006			0.000
hcp	0.513	−16189	−6973	5.760	−6973	0.000	0.000
	0.600	−17466	−8513	5.596	−8513	0.000	0.000
	0.700	−17328	−9202	5.079	−9202	0.000	0.000
	0.800	−14961	−8304	4.161	−8304	0.000	0.000
	0.900	−9707	−5383	2.703	−5383	0.000	0.000
	1.000	0	0	0.000	0	0.000	0.000

Reference states: Cr(bcc), Ru(hcp)

Table IVb. Partial quantities for Cr in the stable phases at 1600 K.

Phase	x_{Cr}	ΔG_{Cr} [J/mol]	ΔH_{Cr} [J/mol]	ΔS_{Cr} [J/(mol·K)]	$G_{\mathrm{Cr}}^{\mathrm{E}}$ [J/mol]	$S_{\mathrm{Cr}}^{\mathrm{E}}$ [J/(mol·K)]	a_{Cr}	γ_{Cr}
bcc	1.000	0	0	0.000	0	0.000	1.000	1.000
	0.900	−1371	31	0.876	31	0.000	0.902	1.002
	0.800	−3126	−158	1.855	−158	0.000	0.791	0.988
	0.736	−4666	−588	2.549	−588	0.000	0.704	0.957
Cr_2Ru	0.667	−4666	5917	6.614			0.704	
	0.667	−5431	4905	6.460			0.665	
hcp	0.487	−5431	4153	5.990	4153	0.000	0.665	1.366
	0.400	−12684	−495	7.619	−495	0.000	0.385	0.964
	0.300	−25438	−9421	10.011	−9421	0.000	0.148	0.493
	0.200	−44407	−22996	13.382	−22996	0.000	0.036	0.178
	0.100	−72727	−42096	19.145	−42096	0.000	0.004	0.042
	0.000	$-\infty$	−67593	∞	−67593	0.000	0.000	0.006

Reference state: Cr(bcc)

Table IVc. Partial quantities for Ru in the stable phases at 1600 K.

Phase	x_{Ru}	ΔG_{Ru} [J/mol]	ΔH_{Ru} [J/mol]	ΔS_{Ru} [J/(mol·K)]	$G^{\mathrm{E}}_{\mathrm{Ru}}$ [J/mol]	$S^{\mathrm{E}}_{\mathrm{Ru}}$ [J/(mol·K)]	a_{Ru}	γ_{Ru}
bcc	0.000	$-\infty$	−3535	∞	−11615	5.050	0.000	0.418
	0.100	−43185	−4473	24.195	−12553	5.050	0.039	0.389
	0.200	−33013	−3522	18.432	−11602	5.050	0.084	0.418
	0.264	−27914	−2116	16.123	−10196	5.050	0.123	0.465
Cr_2Ru	0.333	−27914	−20252	4.788			0.123	
	0.333	−26384	−18229	5.097			0.138	
hcp	0.513	−26384	−17516	5.542	−17516	0.000	0.138	0.268
	0.600	−20654	−13858	4.247	−13858	0.000	0.212	0.353
	0.700	−13853	−9108	2.966	−9108	0.000	0.353	0.504
	0.800	−7600	−4631	1.855	−4631	0.000	0.565	0.706
	0.900	−2705	−1304	0.876	−1304	0.000	0.816	0.907
	1.000	0	0	0.000	0	0.000	1.000	1.000

Reference state: Ru(hcp)

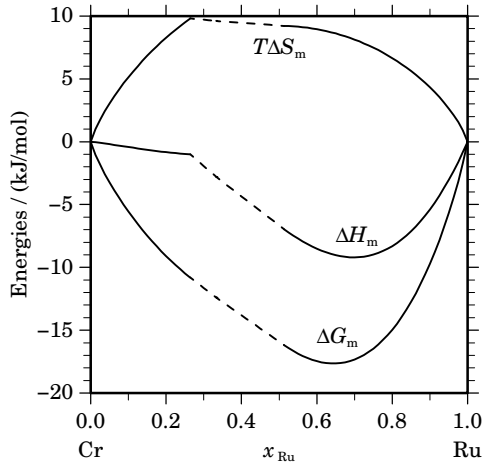

Fig. 4. Integral quantities of the stable phases at T=1600 K.

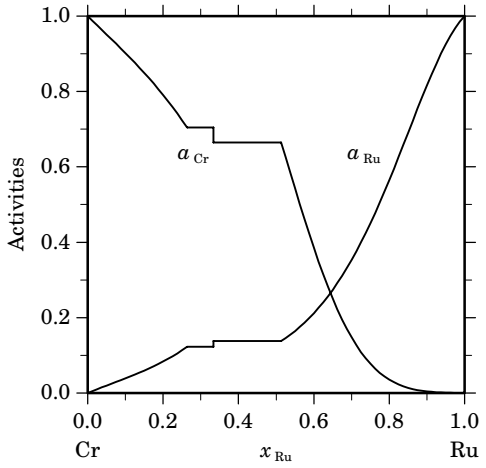

Fig. 5. Activities in the stable phases at T=1600 K.

Table V. Standard reaction quantities at 298.15 K for the compounds per mole of atoms.

Compound	x_{Ru}	$\Delta_{\mathrm{f}}G^{\circ}$ / (J/mol)	$\Delta_{\mathrm{f}}H^{\circ}$ / (J/mol)	$\Delta_{\mathrm{f}}S^{\circ}$ / (J/(mol·K))	$\Delta_{\mathrm{f}}C^{\circ}_{P}$ / (J/(mol·K))
Cr_3R_1	0.250	−3237	−1604	5.476	−0.110
Cr_2Ru	0.333	−4596	−2800	6.024	−0.098

References

[1955Rau] E. Raub, W. Mahler: Z. Metallkde. **46** (1955) 210–215.
[1956Gre] P. Greenfield, P.A. Beck: Trans. AIME **206** (1956) 265–276.
[1958Han] M. Hansen, K. Anderko, "Constitution of Binary Alloys", McGraw-Hill, New-York, 1958.
[1961Sav] E.M. Savitskii, V.F. Terekhova, N.A. Birun: Russ. J. Inorg. Chem. **6** (1961) 1002–1003.
[1964Shu] A.K. Shurin, G.P. Dmitrieva: Sbornik Nauchn. Rab. Inst. Metallofiz. Akad. Nauk Ukr. SSR, **18** (1964) 170–174.
[1965Ell] R.P. Elliott, "Constitution of Binary Alloys", 1st Suppl., McGraw-Hill, New-York, 1965.
[1969Shu] F.A. Shunk, "Constitution of Binary Alloys", 2nd Suppl., McGraw-Hill, New-York, 1969.
[1979Wop] W. Wopersnow, J. Raub: Metallwiss. Tech. **33** (1979) 1261–1265.
[1981Mof] W.G. Moffatt, "The Handbook of Binary Phase Diagrams", General Electric Corp. (1981).
[1981Wat] R.M. Waterstrat: J. Less-Common Met. **80** (1981) 31–36.
[1987Ven] M.Venkatraman, J.P. Neumann: Bull. Alloy Phase Diagrams **8** (1987) 109–112.
[1998Che] P.-Y. Chevalier, E. Fischer, unpublished work, 1998.

Cu – Ir (Copper – Iridium)

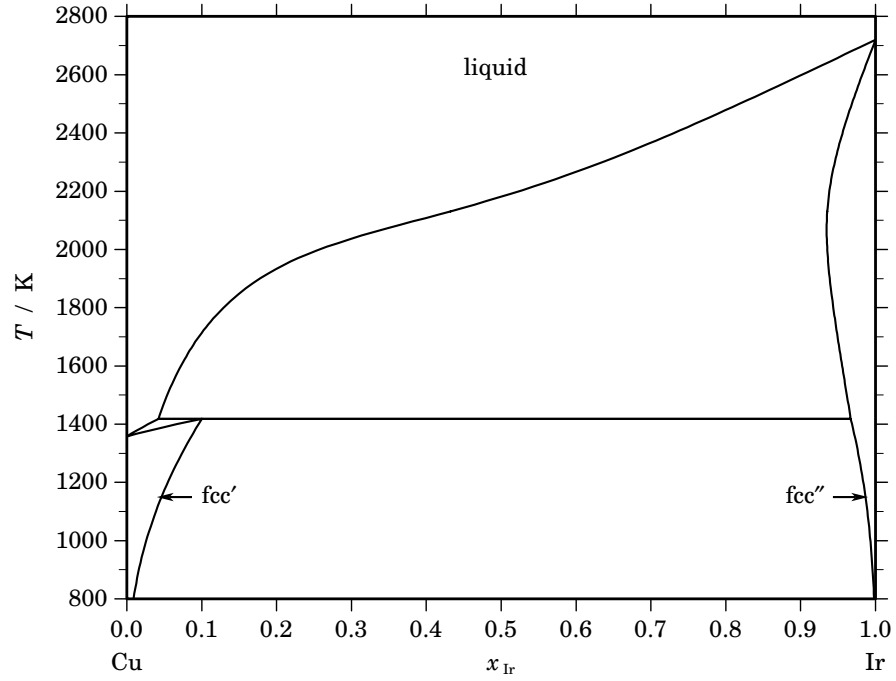

Fig. 1. Calculated phase diagram for the system Cu-Ir.

The thermodynamic description of the Cu-Ir system is based on the only reported phase diagram study below 1473 K [1969Rau]. The higher temperature part of the diagram (above 1473 K) was estimated from calculations based on thermodynamic modelling of the experimental phase diagram data. The equilibrium phases of the Cu-Ir system are the liquid, miscible in all proportions and stable down to the melting point of Cu, the fcc solid solution based on Cu, which has a maximum solubility of about 8 at.% Ir at the peritectic temperature and the fcc solid solution based on Ir, which has a maximum solubility of 6.3 at.% Cu at 2123 K [1987Cha]. According to [1969Rau] the peritectic temperature is 1411±5 K, and the corresponding compositions of the liquid, fcc', and fcc" phases are 4, 8, 97 at.% Ir, respectively. This behaviour can be reproduced well by the calculations. The calculated Cu-Ir phase diagram indicates a good agreement with published experimental data [1987Cha].

Table I. Phases, structures and models.

Phase	Struktur-bericht	Prototype	Pearson symbol	Space group	SGTE name	Model
liquid					LIQUID	$(Cu,Ir)_1$
fcc	$A1$	Cu	$cF4$	$Fm\bar{3}m$	FCC_A1	$(Cu,Ir)_1$

Table II. Invariant reactions.

Reaction	Type	T / K	Compositions / x_{Ir}			$\Delta_r H$ / (J/mol)
liquid + fcc″ $\rightleftharpoons$ fcc′	peritectic	1418.6	0.042	0.967	0.100	−10622

Table IIIa. Integral quantities for the liquid phase at 2800 K.

x_{Ir}	ΔG_{m} [J/mol]	ΔH_{m} [J/mol]	ΔS_{m} [J/(mol·K)]	$G_{\mathrm{m}}^{\mathrm{E}}$ [J/mol]	$S_{\mathrm{m}}^{\mathrm{E}}$ [J/(mol·K)]	ΔC_P [J/(mol·K)]
0.000	0	0	0.000	0	0.000	0.000
0.100	−4682	1492	2.205	2886	−0.498	0.000
0.200	−6724	2448	3.276	4926	−0.885	0.000
0.300	−8025	2943	3.917	6196	−1.162	0.000
0.400	−8895	3056	4.268	6774	−1.328	0.000
0.500	−9401	2863	4.380	6735	−1.383	0.000
0.600	−9510	2441	4.268	6159	−1.328	0.000
0.700	−9102	1867	3.917	5120	−1.162	0.000
0.800	−7954	1218	3.276	3696	−0.885	0.000
0.900	−5605	570	2.205	1964	−0.498	0.000
1.000	0	0	0.000	0	0.000	0.000

Reference states: Cu(liquid), Ir(liquid)

Table IIIb. Partial quantities for Cu in the liquid phase at 2800 K.

x_{Cu}	ΔG_{Cu} [J/mol]	ΔH_{Cu} [J/mol]	ΔS_{Cu} [J/(mol·K)]	$G_{\mathrm{Cu}}^{\mathrm{E}}$ [J/mol]	$S_{\mathrm{Cu}}^{\mathrm{E}}$ [J/(mol·K)]	a_{Cu}	γ_{Cu}
1.000	0	0	0.000	0	0.000	1.000	1.000
0.900	−2017	281	0.821	436	−0.055	0.917	1.019
0.800	−3554	1022	1.634	1641	−0.221	0.858	1.073
0.700	−4841	2069	2.468	3463	−0.498	0.812	1.160
0.600	−6147	3268	3.362	5746	−0.885	0.768	1.280
0.500	−7800	4465	4.380	8337	−1.383	0.715	1.431
0.400	−10249	5507	5.627	11083	−1.991	0.644	1.610
0.300	−14200	6240	7.300	13829	−2.710	0.543	1.811
0.200	−21046	6510	9.842	16423	−3.540	0.405	2.025
0.100	−34896	6164	14.664	18709	−4.480	0.223	2.234
0.000	$-\infty$	5047	∞	20536	−5.531	0.000	2.416

Reference state: Cu(liquid)

Table IIIc. Partial quantities for Ir in the liquid phase at 2800 K.

x_{Ir}	ΔG_{Ir} [J/mol]	ΔH_{Ir} [J/mol]	ΔS_{Ir} [J/(mol·K)]	$G_{\mathrm{Ir}}^{\mathrm{E}}$ [J/mol]	$S_{\mathrm{Ir}}^{\mathrm{E}}$ [J/(mol·K)]	a_{Ir}	γ_{Ir}
0.000	$-\infty$	17860	∞	33348	−5.531	0.000	4.189
0.100	−28669	12391	14.664	24936	−4.480	0.292	2.919
0.200	−19406	8150	9.842	18063	−3.540	0.434	2.172
0.300	−15456	4984	7.300	12574	−2.710	0.515	1.716
0.400	−13017	2740	5.627	8315	−1.991	0.572	1.429
0.500	−11003	1262	4.380	5134	−1.383	0.623	1.247
0.600	−9017	398	3.362	2876	−0.885	0.679	1.131
0.700	−6917	−7	2.468	1387	−0.498	0.743	1.061
0.800	−4681	−106	1.634	514	−0.221	0.818	1.022
0.900	−2350	−52	0.821	103	−0.055	0.904	1.004
1.000	0	0	0.000	0	0.000	1.000	1.000

Reference state: Ir(liquid)

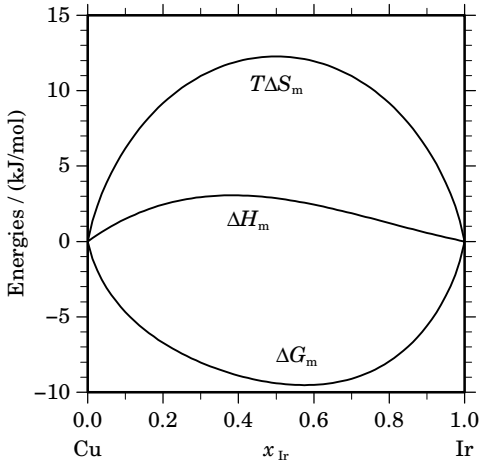

Fig. 2. Integral quantities of the liquid phase at T=2800 K.

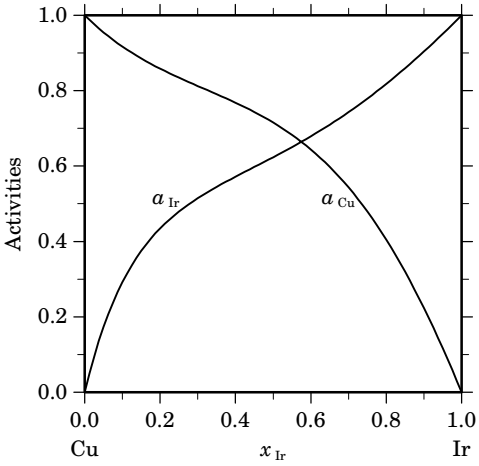

Fig. 3. Activities in the liquid phase at T=2800 K.

References

[1969Rau] E. Raub, E. Röschel: Z. Metallkd. **60** (1969) 142–144.
[1987Cha] D.J. Chakrabarti, D.E. Laughlin: Bull. Alloy Phase Diagrams **8** (1987) 132–136.
[2004Kor] J. Korb, unpublished assessment, GTT-Technologies, 2004.

Dy – Mg (Dysprosium – Magnesium)

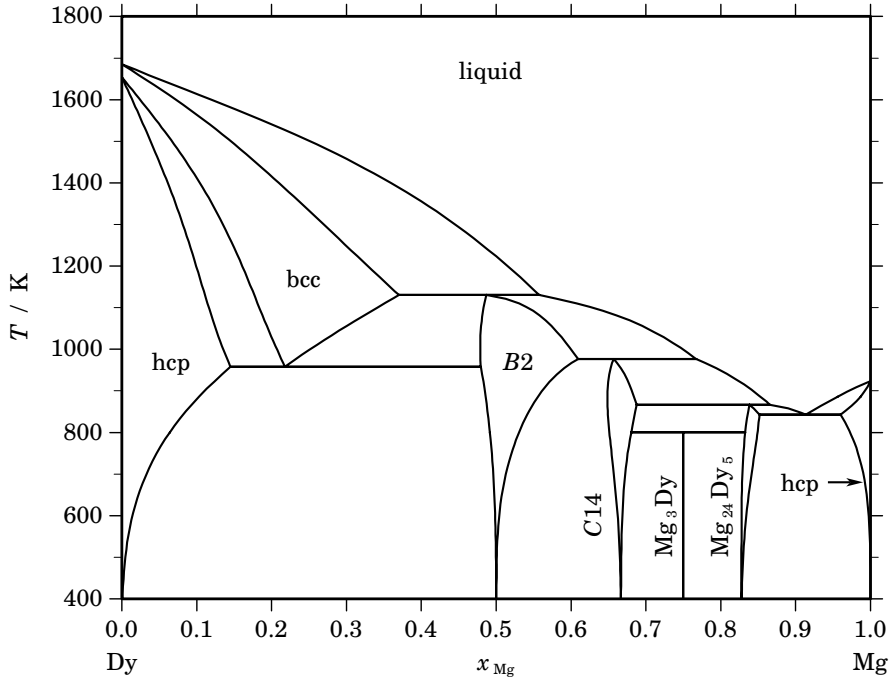

Fig. 1. Calculated phase diagram for the system Dy-Mg.

The rare earth elements have attracted some attention as additives to light metal alloys in the aerospace and automotive industry due to the improvement of mechanical properties of Al- and Mg-alloys at high temperatures. Cacciamani *et al.* [2003Cac] prepared a thermodynamic optimisation of the complete Dy-Mg system, which is primarily based on an experimental investigation of the phase equilibria at elevated temperatures throughout the whole composition range [1991Sac]. The solid solubilities have been measured by [1965Jos] for Mg in hcp-Dy and by [1978Rok] for Dy in magnesium. Since no thermodynamic data have been available for the Dy-Mg system the assessors estimated the values based on other systems of Mg with rare-earth metals which have been evaluated in the same publication.

Table I. Phases, structures and models.

Phase	Struktur-bericht	Prototype	Pearson symbol	Space group	SGTE name	Model
liquid					LIQUID	$(Dy,Mg)_1$
hcp	$A3$	Mg	$hP2$	$P6_3/mmc$	HCP_A3	$(Dy,Mg)_1$
bcc	$A2$	W	$cI2$	$Im\bar{3}m$	BCC_A2	$(Dy,Mg)_1$
$B2$	$B2$	CsCl	$cP2$	$Pm3m$	BCC_B2	$(Dy,Mg)_1(Dy,Mg)_1$
$C14$	$C14$	$MgZn_2$	$hP12$	$P6_3/mmc$	LAVES_C14	$(Dy,Mg)_2(Dy,Mg)_1$
Mg_3Dy	$D0_3$	BiF_3	$cF16$	$Fm\bar{3}m$	MG3LN	Mg_3Dy_1
$Mg_{24}Dy_5$	$A12$	αMn	$cI58$	$I\bar{4}3m$	MG24DY5	$Mg_{24}(Dy,Mg)_5$

Table II. Invariant reactions.

Reaction	Type	T / K	Compositions / x_{Mg}			$\Delta_{\mathrm{r}}H$ / (J/mol)
bcc + liquid $\rightleftharpoons B2$	peritectic	1130.3	0.370	0.558	0.487	−10978
$B2$ + liquid $\rightleftharpoons C14$	peritectic	976.6	0.609	0.767	0.657	−7979
bcc $\rightleftharpoons$ hcp + $B2$	eutectoid	958.3	0.218	0.145	0.479	−3053
$C14$ + liquid $\rightleftharpoons$ $Mg_{24}Dy_5$	peritectic	866.8	0.688	0.866	0.838	−12106
liquid $\rightleftharpoons$ $Mg_{24}Dy_5$ + hcp	eutectic	843.0	0.914	0.852	0.960	−9819
$C14$ + $Mg_{24}Dy_5$ $\rightleftharpoons$ Mg_3Dy	peritectoid	800.7	0.681	0.833	0.750	−597

Table IIIa. Integral quantities for the liquid phase at 1800 K.

x_{Mg}	ΔG_{m} [J/mol]	ΔH_{m} [J/mol]	ΔS_{m} [J/(mol·K)]	$G_{\mathrm{m}}^{\mathrm{E}}$ [J/mol]	$S_{\mathrm{m}}^{\mathrm{E}}$ [J/(mol·K)]	ΔC_P [J/(mol·K)]
0.000	0	0	0.000	0	0.000	0.000
0.100	−5405	244	3.138	−540	0.435	0.000
0.200	−8648	−330	4.621	−1158	0.460	0.000
0.300	−10924	−1436	5.271	−1782	0.192	0.000
0.400	−12407	−2786	5.345	−2334	−0.251	0.000
0.500	−13116	−4095	5.012	−2742	−0.752	0.000
0.600	−13003	−5076	4.404	−2931	−1.192	0.000
0.700	−11968	−5444	3.624	−2826	−1.455	0.000
0.800	−9841	−4911	2.739	−2352	−1.422	0.000
0.900	−6300	−3192	1.727	−1435	−0.976	0.000
1.000	0	0	0.000	0	0.000	0.000

Reference states: Dy(liquid), Mg(liquid)

Table IIIb. Partial quantities for Dy in the liquid phase at 1800 K.

x_{Dy}	ΔG_{Dy} [J/mol]	ΔH_{Dy} [J/mol]	ΔS_{Dy} [J/(mol·K)]	$G_{\mathrm{Dy}}^{\mathrm{E}}$ [J/mol]	$S_{\mathrm{Dy}}^{\mathrm{E}}$ [J/(mol·K)]	a_{Dy}	γ_{Dy}
1.000	0	0	0.000	0	0.000	1.000	1.000
0.900	−1525	457	1.101	52	0.225	0.903	1.003
0.800	−3231	1444	2.598	108	0.742	0.806	1.007
0.700	−5319	2391	4.283	20	1.318	0.701	1.001
0.600	−8008	2724	5.962	−363	1.715	0.586	0.976
0.500	−11562	1870	7.462	−1189	1.699	0.462	0.924
0.400	−16320	−743	8.654	−2607	1.035	0.336	0.840
0.300	−22785	−5688	9.498	−4766	−0.512	0.218	0.727
0.200	−31903	−13537	10.203	−7816	−3.179	0.119	0.593
0.100	−46366	−24864	11.946	−11905	−7.199	0.045	0.451
0.000	$-\infty$	−40240	∞	−17184	−12.809	0.000	0.317

Reference state: Dy(liquid)

Table IIIc. Partial quantities for Mg in the liquid phase at 1800 K.

x_{Mg}	ΔG_{Mg} [J/mol]	ΔH_{Mg} [J/mol]	ΔS_{Mg} [J/(mol·K)]	$G^{\mathrm{E}}_{\mathrm{Mg}}$ [J/mol]	$S^{\mathrm{E}}_{\mathrm{Mg}}$ [J/(mol·K)]	a_{Mg}	γ_{Mg}
0.000	$-\infty$	7480	∞	−4755	6.797	0.000	0.728
0.100	−40326	−1672	21.474	−5865	2.329	0.068	0.676
0.200	−30312	−7429	12.713	−6225	−0.669	0.132	0.660
0.300	−24003	−10365	7.577	−5984	−2.434	0.201	0.670
0.400	−19005	−11051	4.419	−5291	−3.200	0.281	0.702
0.500	−14670	−10060	2.561	−4296	−3.202	0.375	0.750
0.600	−10792	−7965	1.570	−3147	−2.677	0.486	0.810
0.700	−7332	−5340	1.107	−1994	−1.859	0.613	0.875
0.800	−4325	−2755	0.872	−986	−0.983	0.749	0.936
0.900	−1848	−784	0.591	−271	−0.285	0.884	0.982
1.000	0	0	0.000	0	0.000	1.000	1.000

Reference state: Mg(liquid)

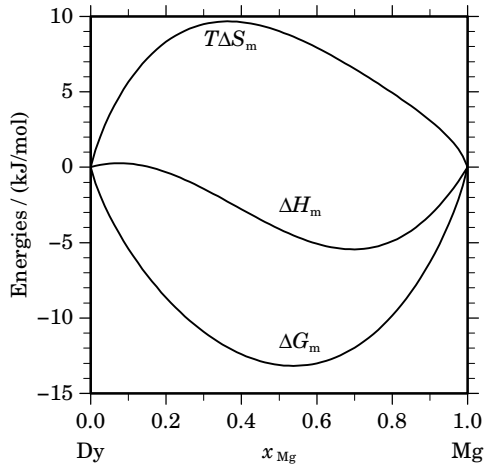

Fig. 2. Integral quantities of the liquid phase at T=1800 K.

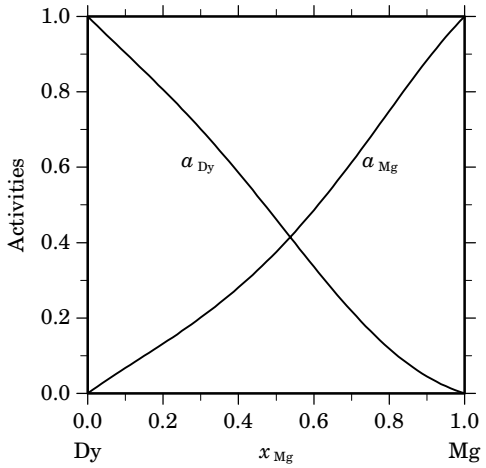

Fig. 3. Activities in the liquid phase at T=1800 K.

Table IV. Standard reaction quantities at 298.15 K for the compounds per mole of atoms.

Compound	x_{Mg}	$\Delta_{\mathrm{f}}G^{\circ}$ / (J/mol)	$\Delta_{\mathrm{f}}H^{\circ}$ / (J/mol)	$\Delta_{\mathrm{f}}S^{\circ}$ / (J/(mol·K))	$\Delta_{\mathrm{f}}C^{\circ}_{P}$ / (J/(mol·K))
$B2$	0.500	−12298	−13952	−5.550	−0.383
$C14$	0.667	−12142	−13981	−6.167	−0.241
Mg_3Dy	0.750	−10504	−12386	−6.312	−0.192
$Mg_{24}Dy_5$	0.828	−8790	−10680	−6.339	−0.133

References

[1965Jos] R.R. Joseph, K.A. Gschneidner jr.: Trans. Metall. Soc. AIME **233** (1965) 2063–2069.
[1978Rok] L.L. Rokhlin in: "Probl. Metalloved. Tsvetn. Splavov", N.M. Zhavoronkov (Ed.), Izd. Nauka, Moscow, 1978, pp. 59–70.
[1991Sac] A. Saccone, S. Delfino, D. Macció, R. Ferro: Z. Metallkd. **82** (1991) 568–573.
[2003Cac] G. Cacciamani, S. de Negri, A. Saccone, R. Ferro: Intermetallics **11** (2003) 1135–1151.

Eu – Pd (Europium – Palladium)

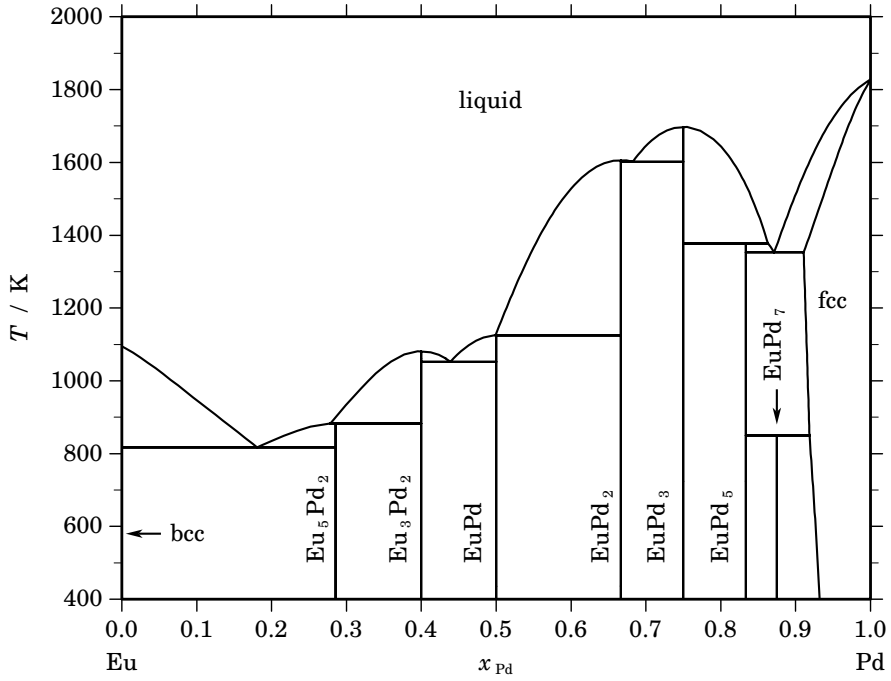

Fig. 1. Calculated phase diagram for the system Eu-Pd.

Intermetallic compounds of palladium with rare earth metals are of interest due to their potential use in hydrogen diffusion membranes for purification and isotope enrichment. A review of the Eu-Pd system and a thermodynamic assessment has been given by [2001Du]. The optimisation is based on data on the the phase diagram which have been reported in [1974Ian] for equilibria with the liquid across the whole composition range and in addition results for equilibria involving the compound $EuPd_7$ which have been reported by [1990Tak]. No thermodynamic data have been available for the melt or the intermetallic compounds. Due to the close chemical relationships among the rare earth metals, [2001Du] have considered in the optimisation of the intermetallic compounds the corresponding enthalpies of formation in the systems Gd-Pd and Pd-Sm which have been available in the literature. The dataset should not be used at too high temperatures because an artificial inverse miscibility gap opens in the liquid above 3550 K.

Table I. Phases, structures and models.

Phase	Struktur-bericht	Prototype	Pearson symbol	Space group	SGTE name	Model
liquid					LIQUID	$(Eu,Pd)_1$
bcc	$A2$	W	$cI2$	$Im\bar{3}m$	BCC_A2	$(Eu,Pd)_1$
Eu_5Pd_2	$\cdots$	Mn_5C_2	$mC28$	$C2/c$	EU5PD2	Eu_5Pd_2
Eu_3Pd_2	$\cdots$	Er_3Ni_2	$hR15$	$R\bar{3}$	EU3PD2	Eu_3Pd_2
EuPd	$B33$	CrB	$oC8$	$Cmcm$	EUPD	Eu_1Pd_1
$EuPd_2$	$C15$	$MgCu_2$	$cF24$	$Fd\bar{3}m$	EUPD2	Eu_1Pd_2
$EuPd_3$	$L1_2$	$AuCu_3$	$cP4$	$Pm\bar{3}m$	EUPD3	Eu_1Pd_3
$EuPd_5$	$\cdots$	$\cdots$	$o*72$	$\cdots$	EUPD5	Eu_1Pd_5
$EuPd_7$	$\cdots$	$\cdots$	$c**$	$\cdots$	EUPD7	Eu_1Pd_7
fcc	$A1$	Cu	$cF4$	$Fm\bar{3}m$	FCC_A1	$(Eu,Pd)_1$

Table II. Invariant reactions.

Reaction	Type	T / K	Compositions / x_{Pd}			$\Delta_{\mathrm{r}}H$ / (J/mol)
liquid $\rightleftharpoons$ $EuPd_3$	congruent	1697.8	0.750	0.750		−33450
liquid $\rightleftharpoons$ $EuPd_2$	congruent	1606.7	0.667	0.667		−36671
liquid $\rightleftharpoons$ $EuPd_2$ + $EuPd_3$	eutectic	1602.1	0.683	0.667	0.750	−35350
$EuPd_3$ + liquid $\rightleftharpoons$ $EuPd_5$	peritectic	1377.4	0.750	0.863	0.833	−10688
liquid $\rightleftharpoons$ $EuPd_5$ + fcc	eutectic	1353.1	0.871	0.833	0.911	−12830
liquid + $EuPd_2$ $\rightleftharpoons$ EuPd	peritectic	1125.2	0.499	0.667	0.500	−18832
liquid $\rightleftharpoons$ Eu_3Pd_2	congruent	1081.6	0.400	0.400		−17263
liquid $\rightleftharpoons$ Eu_3Pd_2 + EuPd	eutectic	1052.4	0.439	0.400	0.500	−17403
liquid + Eu_3Pd_2 $\rightleftharpoons$ Eu_5Pd_2	peritectic	882.9	0.278	0.400	0.286	−17452
$EuPd_5$ + fcc $\rightleftharpoons$ $EuPd_7$	peritectoid	850.1	0.833	0.918	0.875	−1004
liquid $\rightleftharpoons$ bcc + Eu_5Pd_2	eutectic	817.4	0.181	0.000	0.286	−19097

Table IIIa. Integral quantities for the liquid phase at 1900 K.

x_{Pd}	ΔG_{m} [J/mol]	ΔH_{m} [J/mol]	ΔS_{m} [J/(mol·K)]	$G^{\mathrm{E}}_{\mathrm{m}}$ [J/mol]	$S^{\mathrm{E}}_{\mathrm{m}}$ [J/(mol·K)]	ΔC_P [J/(mol·K)]
0.000	0	0	0.000	0	0.000	0.000
0.100	−40633	−7879	17.239	−35497	14.536	0.000
0.200	−70223	−21784	25.494	−62318	21.334	0.000
0.300	−90408	−38799	27.163	−80758	22.084	0.000
0.400	−101744	−56007	24.072	−91112	18.477	0.000
0.500	−104627	−70492	17.966	−93677	12.203	0.000
0.600	−99380	−79337	10.548	−88748	4.953	0.000
0.700	−86270	−79627	3.496	−76620	−1.583	0.000
0.800	−65494	−68445	−1.554	−57589	−5.714	0.000
0.900	−37086	−42875	−3.047	−31950	−5.750	0.000
1.000	0	0	0.000	0	0.000	0.000

Reference states: Eu(liquid), Pd(liquid)

Table IIIb. Partial quantities for Eu in the liquid phase at 1900 K.

x_{Eu}	ΔG_{Eu} [J/mol]	ΔH_{Eu} [J/mol]	ΔS_{Eu} [J/(mol·K)]	$G^{\mathrm{E}}_{\mathrm{Eu}}$ [J/mol]	$S^{\mathrm{E}}_{\mathrm{Eu}}$ [J/(mol·K)]	a_{Eu}	γ_{Eu}
1.000	0	0	0.000	0	0.000	1.000	1.000
0.900	−6052	3499	5.027	−4388	4.151	0.682	0.757
0.800	−20681	10108	16.205	−17156	14.349	0.270	0.338
0.700	−43349	13994	30.180	−37714	27.215	0.064	0.092
0.600	−73541	9324	43.613	−65471	39.366	0.010	0.016
0.500	−110785	−9735	53.184	−99835	47.421	0.001	0.002
0.400	−154691	−49014	55.619	−140215	48.001	0.000	0.000
0.300	−205041	−114347	47.734	−186021	37.723	0.000	0.000
0.200	−262085	−211566	26.589	−236660	13.207	0.000	0.000
0.100	−327917	−346505	−9.783	−291542	−28.928	0.000	0.000
0.000	$-\infty$	−524995	∞	−350075	−92.063	0.000	0.000

Reference state: Eu(liquid)

Table IIIc. Partial quantities for Pd in the liquid phase at 1900 K.

x_{Pd}	ΔG_{Pd} [J/mol]	ΔH_{Pd} [J/mol]	ΔS_{Pd} [J/(mol·K)]	$G^{\mathrm{E}}_{\mathrm{Pd}}$ [J/mol]	$S^{\mathrm{E}}_{\mathrm{Pd}}$ [J/(mol·K)]	a_{Pd}	γ_{Pd}
0.000	$-\infty$	−38939	∞	−399340	189.685	0.000	0.000
0.100	−351860	−110282	127.147	−315485	108.002	0.000	0.000
0.200	−268391	−149351	62.653	−242966	49.271	0.000	0.000
0.300	−200213	−161981	20.122	−181193	10.112	0.000	0.000
0.400	−144049	−154002	−5.238	−129574	−12.857	0.000	0.000
0.500	−98469	−131249	−17.253	−87519	−23.016	0.002	0.004
0.600	−62505	−99553	−19.499	−54436	−23.746	0.019	0.032
0.700	−35368	−64748	−15.463	−29733	−18.429	0.107	0.152
0.800	−16346	−32665	−8.589	−12821	−10.444	0.355	0.444
0.900	−4771	−9138	−2.299	−3107	−3.175	0.739	0.821
1.000	0	0	0.000	0	0.000	1.000	1.000

Reference state: Pd(liquid)

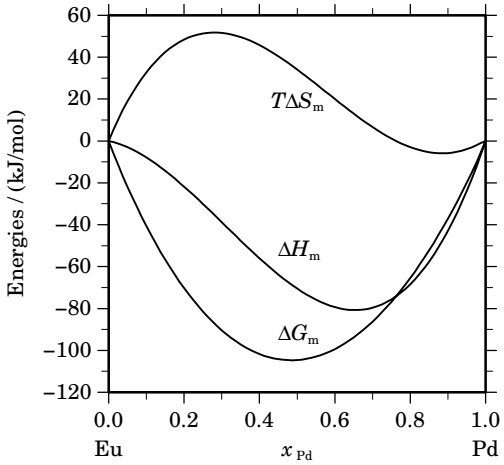

Fig. 2. Integral quantities of the liquid phase at T=1900 K.

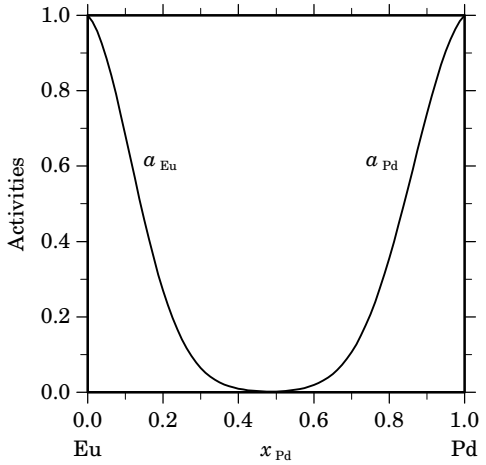

Fig. 3. Activities in the liquid phase at T=1900 K.

Table IV. Standard reaction quantities at 298.15 K for the compounds per mole of atoms.

Compound	x_{Pd}	$\Delta_{\mathrm{f}}G^{\circ}$ / (J/mol)	$\Delta_{\mathrm{f}}H^{\circ}$ / (J/mol)	$\Delta_{\mathrm{f}}S^{\circ}$ / (J/(mol·K))	$\Delta_{\mathrm{f}}C^{\circ}_{P}$ / (J/(mol·K))
Eu_5Pd_2	0.286	−48926	−44766	13.953	0.000
Eu_3Pd_2	0.400	−67389	−62722	15.652	0.000
Eu_1Pd_1	0.500	−81068	−78545	8.461	0.000
Eu_1Pd_2	0.667	−101882	−104636	−9.236	0.000
Eu_1Pd_3	0.750	−92103	−95334	−10.836	0.000
Eu_1Pd_5	0.833	−63717	−65892	−7.294	0.000
Eu_1Pd_7	0.875	−49326	−51176	−6.207	0.000

References

[1974Ian] A. Iandelli, A. Palenzona: J. Less-Common Met. **39** (1974) 1–7.
[1990Tak] K. Takao, K.L. Zhao, Y. Sakamoto: J. Mater. Sci. **25** (1990) 1255–1260.
[2001Du] Z. Du, Y. He: J. Alloys Comp. **327** (2001) 127–131.

Eu – Sn (Europium – Tin)

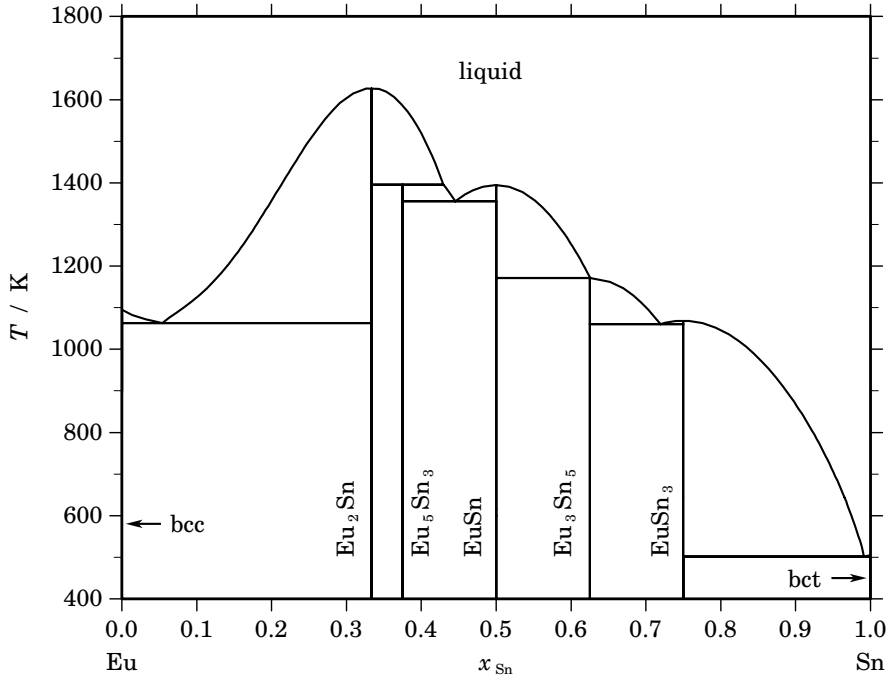

Fig. 1. Calculated phase diagram for the system Eu-Sn.

A review on the Eu-Sn system and a thermodynamic assessment has been given by [2004Liu]. The optimisation is based mostly on data for the phase diagram which have been reported in [1998Pal] throughout the whole composition range. Some additional thermodynamic data have been available from the literature. Bacha *et al.* [1973Bac] have obtained by EMF experiments the enthalpy of formation of $EuSn_3$ as well as the partial enthalpy of Eu in Sn-melts at low concentrations of Eu. Using also EMF techniques Kober *et al.* [1987Kob] have reported activities of Eu in Sn-melts at low Eu contents.

Table I. Phases, structures and models.

Phase	Struktur-bericht	Prototype	Pearson symbol	Space group	SGTE name	Model
liquid					LIQUID	$(Eu,Sn)_1$
bcc	$A2$	W	$cI2$	$Im\bar{3}m$	BCC_A2	Eu_1
Eu_2Sn	$C23$	Co_2Si	$oP12$	$Pnma$	EU2SN	Eu_2Sn_1
Eu_5Sn_3	$D8_m$	W_5Si_3	$tI32$	$I4/mcm$	EU5SN3	Eu_5Sn_3
EuSn	$B33$	CrB	$oC8$	$Cmcm$	EUSN	Eu_1Sn_1
Eu_3Sn_5	$\cdots$	Pu_3Pd_5	$oC32$	$Cmcm$	EU3SN5	Eu_3Sn_5
$EuSn_3$	$L1_2$	$AuCu_3$	$cP4$	$Pm\bar{3}m$	EUSN3	Eu_1Sn_3
bct	$A5$	βSn	$tI4$	$I4_1/amd$	BCT_A5	Sn_1

Table II. Invariant reactions.

Reaction	Type	T / K	Compositions / x_{Sn}			$\Delta_{\mathrm{r}}H$ / (J/mol)
liquid ⇌ Eu_2Sn	congruent	1628.2	0.333	0.333		−11150
Eu_2Sn + liquid ⇌ Eu_5Sn_3	peritectic	1396.0	0.333	0.430	0.375	−6967
liquid ⇌ EuSn	congruent	1394.7	0.500	0.500		−21211
liquid ⇌ Eu_5Sn_3 + EuSn	eutectic	1356.1	0.445	0.375	0.500	−17190
EuSn + liquid ⇌ Eu_3Sn_5	peritectic	1171.0	0.500	0.626	0.625	−21415
liquid ⇌ bcc + Eu_2Sn	eutectic	1063.0	0.054	0.001	0.333	−9740
liquid ⇌ $EuSn_3$	congruent	1068.7	0.750	0.750		−27396
liquid ⇌ Eu_3Sn_5 + $EuSn_3$	eutectic	1060.3	0.719	0.625	0.750	−25335
liquid ⇌ $EuSn_3$ + bct	eutectic	501.6	0.992	0.750	1.000	−7253

Table IIIa. Integral quantities for the liquid phase at 1800 K.

x_{Sn}	ΔG_{m} [J/mol]	ΔH_{m} [J/mol]	ΔS_{m} [J/(mol·K)]	$G_{\mathrm{m}}^{\mathrm{E}}$ [J/mol]	$S_{\mathrm{m}}^{\mathrm{E}}$ [J/(mol·K)]	ΔC_P [J/(mol·K)]
0.000	0	0	0.000	0	0.000	0.000
0.100	−13921	−10202	2.066	−9056	−0.637	0.000
0.200	−26170	−20665	3.059	−18681	−1.102	0.000
0.300	−36515	−30097	3.566	−27373	−1.513	0.000
0.400	−44007	−37403	3.669	−33934	−1.927	0.000
0.500	−47848	−41685	3.424	−37475	−2.339	0.000
0.600	−47479	−42240	2.911	−37407	−2.685	0.000
0.700	−42592	−38562	2.239	−33449	−2.840	0.000
0.800	−33115	−30339	1.542	−25626	−2.619	0.000
0.900	−19130	−17458	0.929	−14265	−1.774	0.000
1.000	0	0	0.000	0	0.000	0.000

Reference states: Eu(liquid), Sn(liquid)

Table IIIb. Partial quantities for Eu in the liquid phase at 1800 K.

x_{Eu}	ΔG_{Eu} [J/mol]	ΔH_{Eu} [J/mol]	ΔS_{Eu} [J/(mol·K)]	$G_{\mathrm{Eu}}^{\mathrm{E}}$ [J/mol]	$S_{\mathrm{Eu}}^{\mathrm{E}}$ [J/(mol·K)]	a_{Eu}	γ_{Eu}
1.000	0	0	0.000	0	0.000	1.000	1.000
0.900	−1017	362	0.766	560	−0.110	0.934	1.038
0.800	−3254	−373	1.601	85	−0.254	0.805	1.006
0.700	−9308	−4491	2.677	−3970	−0.289	0.537	0.767
0.600	−20883	−13692	3.995	−13238	−0.252	0.248	0.413
0.500	−38806	−29088	5.399	−28432	−0.365	0.075	0.150
0.400	−63067	−51202	6.592	−49354	−1.027	0.015	0.037
0.300	−92907	−79968	7.189	−74888	−2.822	0.002	0.007
0.200	−127092	−114732	6.867	−103005	−6.515	0.000	0.001
0.100	−165221	−154253	6.093	−130760	−13.052	0.000	0.000
0.000	$-\infty$	−196701	∞	−154292	−23.561	0.000	0.000

Reference state: Eu(liquid)

Table IIIc. Partial quantities for Sn in the liquid phase at 1800 K.

x_{Sn}	ΔG_{Sn} [J/mol]	ΔH_{Sn} [J/mol]	ΔS_{Sn} [J/(mol·K)]	$G^{\mathrm{E}}_{\mathrm{Sn}}$ [J/mol]	$S^{\mathrm{E}}_{\mathrm{Sn}}$ [J/(mol·K)]	a_{Sn}	γ_{Sn}
0.000	$-\infty$	−95926	∞	−81950	−7.764	0.000	0.004
0.100	−130063	−105277	13.770	−95602	−5.375	0.000	0.002
0.200	−117833	−101833	8.889	−93746	−4.493	0.000	0.002
0.300	−99997	−89844	5.641	−81978	−4.370	0.001	0.004
0.400	−78693	−72969	3.180	−64980	−4.439	0.005	0.013
0.500	−56891	−54282	1.449	−46517	−4.314	0.022	0.045
0.600	−37087	−36266	0.456	−29442	−3.791	0.084	0.140
0.700	−21028	−20816	0.117	−15690	−2.848	0.245	0.351
0.800	−9620	−9241	0.211	−6281	−1.644	0.526	0.657
0.900	−2898	−2258	0.355	−1321	−0.521	0.824	0.916
1.000	0	0	0.000	0	0.000	1.000	1.000

Reference state: Sn(liquid)

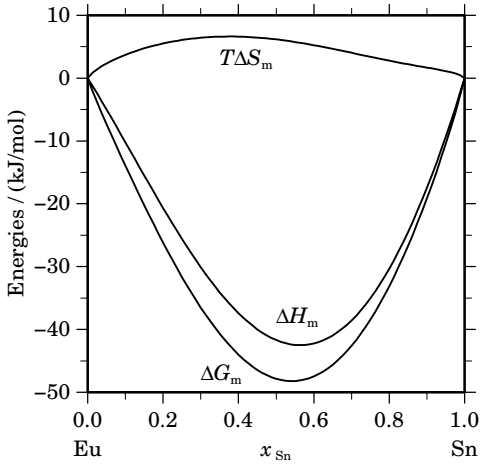

Fig. 2. Integral quantities of the liquid phase at T=1800 K.

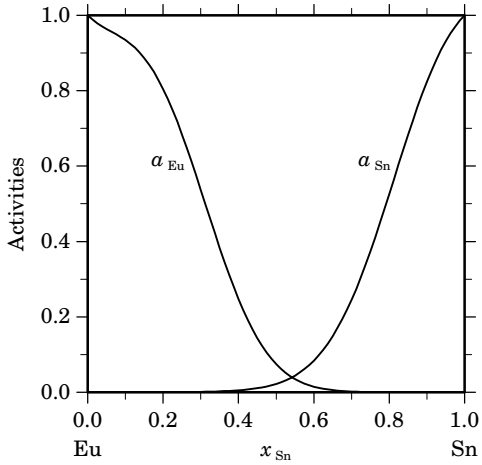

Fig. 3. Activities in the liquid phase at T=1800 K.

Table IV. Standard reaction quantities at 298.15 K for the compounds per mole of atoms.

Compound	x_{Sn}	$\Delta_{\mathrm{f}}G^{\circ}$ / (J/mol)	$\Delta_{\mathrm{f}}H^{\circ}$ / (J/mol)	$\Delta_{\mathrm{f}}S^{\circ}$ / (J/(mol·K))	$\Delta_{\mathrm{f}}C^{\circ}_{P}$ / (J/(mol·K))
Eu_2Sn_1	0.333	−38759	−37010	5.867	0.000
Eu_5Sn_3	0.375	−42913	−41643	4.260	0.000
Eu_1Sn_1	0.500	−55167	−55544	−1.265	0.000
Eu_3Sn_5	0.625	−54359	−55526	−3.912	0.000
Eu_1Sn_3	0.750	−51517	−54877	−11.271	0.000

References

[1973Bac] A. Bacha, C. Chatillon-Colinet, A. Percheron, J.-C. Mathieu, J.-C. Achard: C. R. Acad. Sci., Ser. C **276** (1973) 995–998.

[1987Kob] V.I. Kober, I.F. Nichkov, S.P. Raspopin, S.S. Zvontsov: Izv. V.U.Z. Tsvetn. Metall., No. 2 (1987) 120–121.

[1998Pal] A. Palenzona, P. Manfrinetti, M.L. Fornasini: J. Alloys Comp. **280** (1998) 211–214.

[2004Liu] L. Liu, C. Li, F. Wang, Z. Du, W. Zhang: J. Alloys Comp. **379** (2004) 148–153.

Fe – Ru (Iron – Ruthenium)

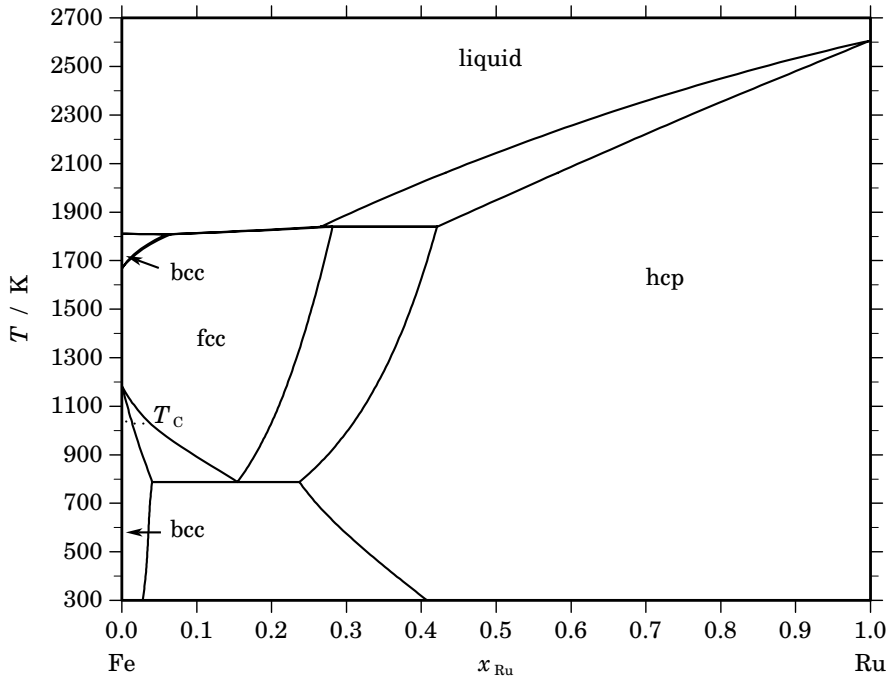

Fig. 1. Calculated phase diagram for the system Fe-Ru.

The Fe-Ru binary system contains two components interesting for the nuclear field, iron being a major component of stainless steel structures of the vessel, and ruthenium being selected as representative of a family of non-volatile fission products. Experimental information on the phase diagram has been reported in several compilations of binary systems [1958Han, 1965Ell, 1969Shu]. The components are completely miscible in the liquid state. The maximal solubility of ruthenium reaches 5 at.% at 1809 K and 4.8 at.% at 773 K in iron-rich bcc terminal solid solutions, and varies from 9.3 at.% at 773 K to 29.5 at.% at 1863 K in the iron-rich fcc terminal solid solution. The solubility of iron in ruthenium-rich hcp terminal solid solutions varies from 76.5 at.% at 773 K to 64.5 at.% at 1863 K. The transition temperatures fcc/bcc have been studied by Fallot [1938Fal] and Martelly [1938Mar] using X-ray and magnetic analysis. The iron-rich side at high temperature was determined by Gibson and Hume-Rothery [1958Gib] by thermal analysis. Raub and Plate [1960Rau] determined monophasic and diphasic domains between fcc, hcp and bcc in the range from 673 K to 1473 K. The activity of iron in the fcc and hcp domains was determined by Stepakoff and Kaufman [1968Ste] from vapour pressure measurements at 1600 K. The system was assessed by Chevalier and Fischer [2004Che]. The excess Gibbs energy of the liquid, bcc, fcc and hcp solution phases was optimised based on selected experimental information for the phase diagram and thermodynamic properties. A regular substitution model was used for all solution phases. The agreement with the experimental information is satisfactory, but however the vertical shape of the fcc/hcp region [1960Rau] cannot be easily reproduced to be compatible with the peritectic determined by Obrowski [1959Obr]. This point should be re-analysed.

Table I. Phases, structures and models.

Phase	Struktur-bericht	Prototype	Pearson symbol	Space group	SGTE name	Model
liquid					LIQUID	$(Fe,Ru)_1$
fcc	$A1$	Cu	$cF4$	$Fm\bar{3}m$	FCC_A1	$(Fe,Ru)_1$
bcc	$A2$	W	$cI2$	$Im\bar{3}m$	BCC_A2	$(Fe,Ru)_1$
hcp	$A3$	Mg	$hP2$	$P6_3/mmc$	HCP_A3	$(Fe,Ru)_1$

Table II. Invariant reactions.

Reaction	Type	T / K	Compositions / x_{Ru}			$\Delta_{\mathrm{r}}H$ / (J/mol)
liquid + hcp $\rightleftharpoons$ fcc	peritectic	1839.4	0.266	0.421	0.281	−17178
liquid $\rightleftharpoons$ bcc + fcc	eutectic	1808.4	0.061	0.060	0.065	−14565
fcc $\rightleftharpoons$ bcc + hcp	eutectoid	788.2	0.154	0.041	0.237	−3042

Table IIIa. Integral quantities for the liquid phase at 2700 K.

x_{Ru}	ΔG_{m} [J/mol]	ΔH_{m} [J/mol]	ΔS_{m} [J/(mol·K)]	$G^{\mathrm{E}}_{\mathrm{m}}$ [J/mol]	$S^{\mathrm{E}}_{\mathrm{m}}$ [J/(mol·K)]	ΔC_P [J/(mol·K)]
0.000	0	0	0.000	0	0.000	0.000
0.100	−9093	−1795	2.703	−1795	0.000	0.000
0.200	−14426	−3192	4.161	−3192	0.000	0.000
0.300	−17903	−4189	5.079	−4189	0.000	0.000
0.400	−19897	−4788	5.596	−4788	0.000	0.000
0.500	−20548	−4987	5.763	−4987	0.000	0.000
0.600	−19896	−4788	5.596	−4788	0.000	0.000
0.700	−17903	−4189	5.079	−4189	0.000	0.000
0.800	−14426	−3192	4.161	−3192	0.000	0.000
0.900	−9093	−1795	2.703	−1795	0.000	0.000
1.000	0	0	0.000	0	0.000	0.000

Reference states: Fe(liquid), Ru(liquid)

Table IIIb. Partial quantities for Fe in the liquid phase at 2700 K.

x_{Fe}	ΔG_{Fe} [J/mol]	ΔH_{Fe} [J/mol]	ΔS_{Fe} [J/(mol·K)]	$G^{\mathrm{E}}_{\mathrm{Fe}}$ [J/mol]	$S^{\mathrm{E}}_{\mathrm{Fe}}$ [J/(mol·K)]	a_{Fe}	γ_{Fe}
1.000	0	0	0.000	0	0.000	1.000	1.000
0.900	−2565	−199	0.876	−199	0.000	0.892	0.991
0.800	−5807	−798	1.855	−798	0.000	0.772	0.965
0.700	−9803	−1795	2.966	−1795	0.000	0.646	0.923
0.600	−14660	−3192	4.247	−3192	0.000	0.520	0.867
0.500	−20548	−4987	5.763	−4987	0.000	0.400	0.801
0.400	−27752	−7182	7.619	−7182	0.000	0.290	0.726
0.300	−36804	−9775	10.010	−9775	0.000	0.194	0.647
0.200	−48898	−12768	13.382	−12768	0.000	0.113	0.566
0.100	−67850	−16159	19.145	−16159	0.000	0.049	0.487
0.000	$-\infty$	−19950	∞	−19950	0.000	0.000	0.411

Reference state: Fe(liquid)

Table IIIc. Partial quantities for Ru in the liquid phase at 2700 K.

x_{Ru}	ΔG_{Ru} [J/mol]	ΔH_{Ru} [J/mol]	ΔS_{Ru} [J/(mol·K)]	$G^{\mathrm{E}}_{\mathrm{Ru}}$ [J/mol]	$S^{\mathrm{E}}_{\mathrm{Ru}}$ [J/(mol·K)]	a_{Ru}	γ_{Ru}
0.000	$-\infty$	−19950	∞	−19950	0.000	0.000	0.411
0.100	−67850	−16159	19.145	−16159	0.000	0.049	0.487
0.200	−48898	−12768	13.382	−12768	0.000	0.113	0.566
0.300	−36804	−9775	10.010	−9775	0.000	0.194	0.647
0.400	−27752	−7182	7.619	−7182	0.000	0.290	0.726
0.500	−20548	−4987	5.763	−4987	0.000	0.400	0.801
0.600	−14660	−3192	4.247	−3192	0.000	0.520	0.867
0.700	−9803	−1795	2.966	−1795	0.000	0.646	0.923
0.800	−5807	−798	1.855	−798	0.000	0.772	0.965
0.900	−2565	−199	0.876	−199	0.000	0.892	0.991
1.000	0	0	0.000	0	0.000	1.000	1.000

Reference state: Ru(liquid)

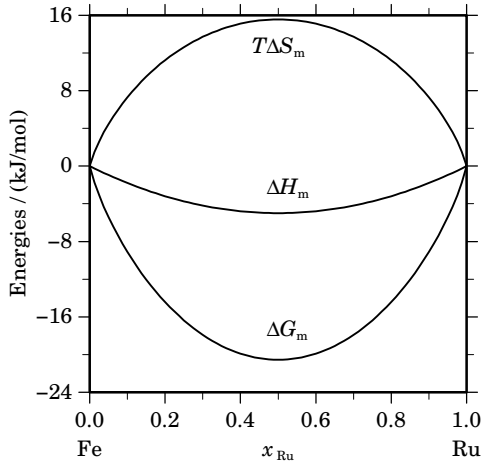

Fig. 2. Integral quantities of the liquid phase at T=2700 K.

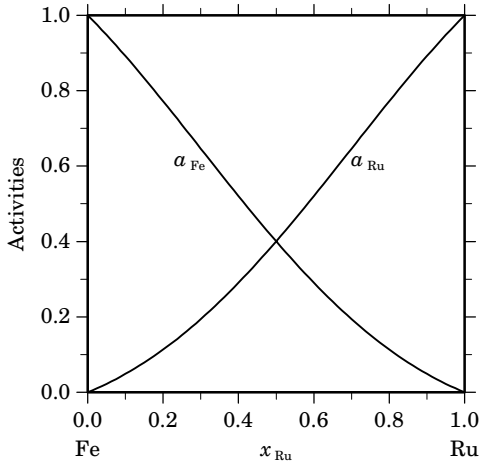

Fig. 3. Activities in the liquid phase at T=2700 K.

Table IVa. Integral quantities for the stable phases at 1600 K.

Phase	x_{Ru}	ΔG_{m} [J/mol]	ΔH_{m} [J/mol]	ΔS_{m} [J/(mol·K)]	$G_{\mathrm{m}}^{\mathrm{E}}$ [J/mol]	$S_{\mathrm{m}}^{\mathrm{E}}$ [J/(mol·K)]	ΔC_P [J/(mol·K)]
fcc	0.000	0	0	0.000	0	0.000	0.000
	0.100	−5240	−1834	2.129	−915	−0.574	0.000
	0.200	−8092	−2983	3.193	−1435	−0.968	0.000
	0.262	−9212	−3352	3.663	−1559	−1.121	0.000
hcp	0.397	−11174	−5881	3.308	−2235	−2.279	0.000
	0.400	−11213	−5886	3.329	−2260	−2.266	0.000
	0.500	−12156	−5850	3.941	−2935	−1.822	0.000
	0.600	−12143	−5437	4.191	−3190	−1.404	0.000
	0.700	−11150	−4645	4.066	−3024	−1.013	0.000
	0.800	−9094	−3475	3.512	−2437	−0.649	0.000
	0.900	−5753	−1927	2.392	−1429	−0.311	0.000
	1.000	0	0	0.000	0	0.000	0.000

Reference states: Fe(fcc), Ru(hcp)

Table IVb. Partial quantities for Fe in the stable phases at 1600 K.

Phase	x_{Fe}	ΔG_{Fe} [J/mol]	ΔH_{Fe} [J/mol]	ΔS_{Fe} [J/(mol·K)]	$G_{\mathrm{Fe}}^{\mathrm{E}}$ [J/mol]	$S_{\mathrm{Fe}}^{\mathrm{E}}$ [J/(mol·K)]	a_{Fe}	γ_{Fe}
fcc	1.000	0	0	0.000	0	0.000	1.000	1.000
	0.900	−1600	−343	0.786	−198	−0.090	0.887	0.985
	0.800	−3760	−1371	1.493	−792	−0.362	0.754	0.942
	0.738	−5406	−2356	1.906	−1361	−0.622	0.666	0.903
hcp	0.603	−5406	−5229	0.111	1330	−4.099	0.666	1.105
	0.600	−5511	−5270	0.151	1284	−4.096	0.661	1.101
	0.500	−9831	−6972	1.787	−610	−3.977	0.478	0.955
	0.400	−15114	−9053	3.788	−2924	−3.830	0.321	0.803
	0.300	−21677	−11512	6.353	−5660	−3.657	0.196	0.653
	0.200	−30227	−14349	9.924	−8816	−3.458	0.103	0.515
	0.100	−43025	−17565	15.913	−12393	−3.232	0.039	0.394
	0.000	$-\infty$	−21158	∞	−16392	−2.979	0.000	0.292

Reference state: Fe(fcc)

Table IVc. Partial quantities for Ru in the stable phases at 1600 K.

Phase	x_{Ru}	ΔG_{Ru} [J/mol]	ΔH_{Ru} [J/mol]	ΔS_{Ru} [J/(mol·K)]	$G^{\mathrm{E}}_{\mathrm{Ru}}$ [J/mol]	$S^{\mathrm{E}}_{\mathrm{Ru}}$ [J/(mol·K)]	a_{Ru}	γ_{Ru}
fcc	0.000	$-\infty$	−21771	∞	−11134	−6.648	0.000	0.433
	0.100	−38005	−15259	14.216	−7373	−4.929	0.057	0.575
	0.200	−25419	−9433	9.991	−4008	−3.391	0.148	0.740
	0.262	−19924	−6156	8.605	−2115	−2.525	0.224	0.853
hcp	0.397	−19924	−6871	8.158	−7644	0.483	0.224	0.563
	0.400	−19765	−6809	8.097	−7575	0.479	0.226	0.566
	0.500	−14482	−4729	6.096	−5261	0.332	0.337	0.673
	0.600	−10162	−3026	4.460	−3367	0.213	0.466	0.776
	0.700	−6639	−1702	3.085	−1894	0.120	0.607	0.867
	0.800	−3810	−757	1.909	−842	0.053	0.751	0.939
	0.900	−1612	−189	0.889	−210	0.013	0.886	0.984
	1.000	0	0	0.000	0	0.000	1.000	1.000

Reference state: Ru(hcp)

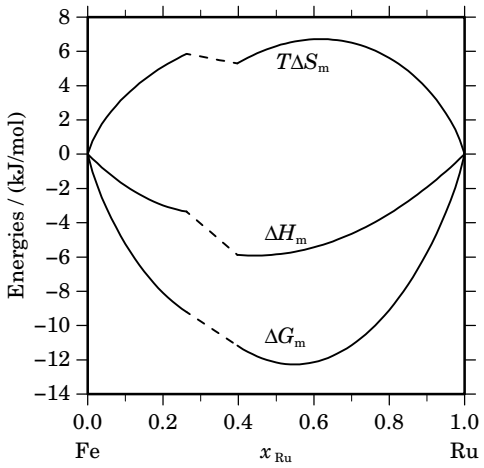

Fig. 4. Integral quantities of the stable phases at T=1600 K.

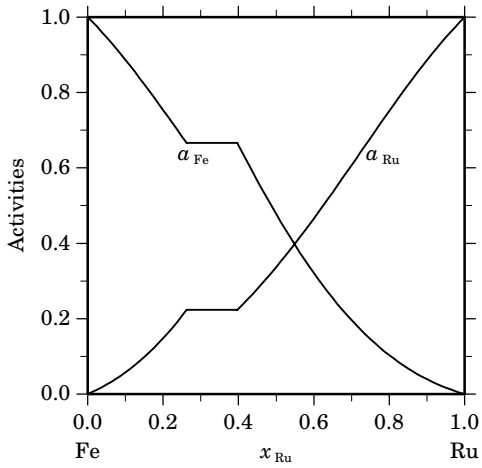

Fig. 5. Activities in the stable phases at T=1600 K.

References

[1938Fal] M. Fallot: Ann. Phys. **10** (1938) 291–332.
[1938Mar] J. Martelly: Ann. Phys. **9** (1938) 318–333.
[1958Gib] W.S. Gibson, F. Hume-Rothery: J. Iron Steel Inst. **189** (1958) 243–250.
[1958Han] M. Hansen, K. Anderko, "Constitution of Binary Alloys", McGraw-Hill, 1958.
[1959Obr] W. Obrowski: Naturwiss. **46** (1959) 624–625.
[1960Rau] E. Raub, W. Plate: Z. Metallkd. **51** (1960) 477–481.
[1965Ell] R.P. Elliott, "Constitution of Binary Alloys", 1st Suppl., McGraw-Hill, New-York, 1965.
[1968Ste] G.L. Stepakoff, L. Kaufman: Acta Metall. **16** (1968) 13–22.
[1969Shu] F.A. Shunk, "Constitution of Binary Alloys", 2nd Suppl., McGraw-Hill, New-York, 1969.
[2004Che] P.-Y. Chevalier, E. Fischer, unpublished work, 2004.

Fe – Sb (Iron – Antimony)

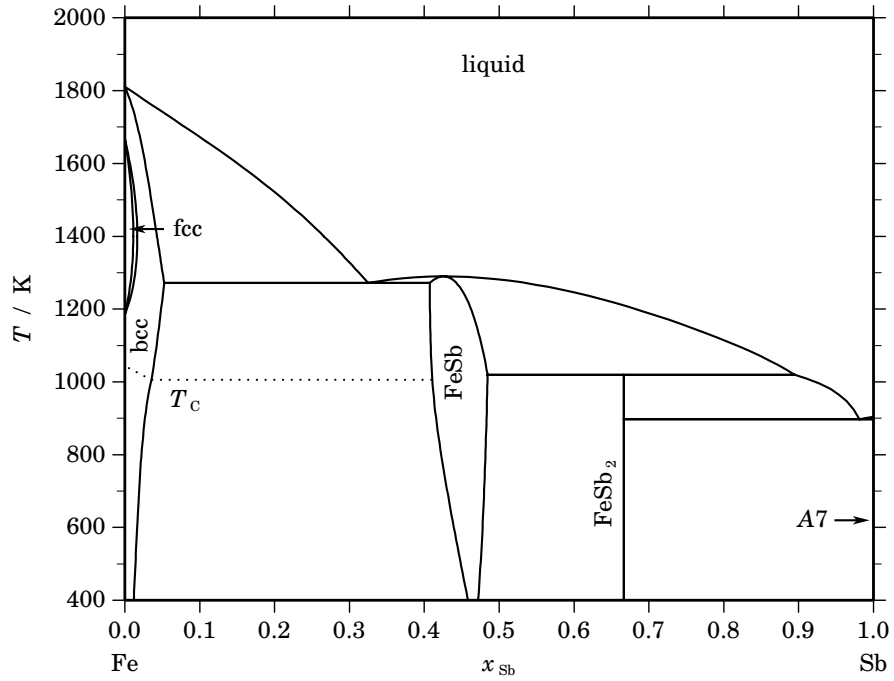

Fig. 1. Calculated phase diagram for the system Fe-Sb.

Iron and antimony are often found as substitutional elements in copper arsenide and sulfide minerals which are used in copper smelting processes. A thermodynamic optimisation of the Fe-Sb system has been reported by [1995Pei]. For the assessment a large number of reports has been evaluated which determine the phase diagram over the complete composition range and temperatures up to the liquidus. In addition, enthalpies of mixing and the activities of both elements have been available for Sb-rich melts as well as in the sub-solidus region across the whole composition range. In the assessment of the phases FeSb and $FeSb_2$ their magnetic properties have not been considered.

Table I. Phases, structures and models.

Phase	Struktur-bericht	Prototype	Pearson symbol	Space group	SGTE name	Model
liquid					LIQUID	$(Fe,Sb)_1$
fcc	$A1$	Cu	$cF4$	$Fm\bar{3}m$	FCC_A1	$(Fe,Sb)_1$
$A2$	$A2$	W	$cI2$	$Im\bar{3}m$	BCC_A2	$(Fe,Sb)_1$
FeSb	$B8_1$	NiAS	$hP4$	$P6_3/mmc$	FESB	$Fe_1(Fe,Sb)_1$
$FeSb_2$	···	···	$oP6$	$Pnn2$	FESB2	Fe_1Sb_2
$A7$	$A7$	αAs	$hR2$	$R\bar{3}m$	RHOMBOHEDRAL_A7	Sb_1

Table II. Invariant reactions.

Reaction	Type	T / K	Compositions / x_{Sb}			$\Delta_r H$ / (J/mol)
liquid $\rightleftharpoons$ $FeSb_2$	congruent	1038.3	0.155	0.155		−10899
liquid $\rightleftharpoons$ bcc + $FeSb_2$	eutectic	1271.5	0.325	0.053	0.407	−14416
$FeSb_2$ + liquid $\rightleftharpoons$ $FeSb_2$	peritectic	1018.9	0.485	0.895	0.667	−13680
liquid $\rightleftharpoons$ $FeSb_2$ + A7	eutectic	897.8	0.981	0.667	1.000	−20180

Table IIIa. Integral quantities for the liquid phase at 1823 K.

x_{Sb}	ΔG_{m} [J/mol]	ΔH_{m} [J/mol]	ΔS_{m} [J/(mol·K)]	$G_{\mathrm{m}}^{\mathrm{E}}$ [J/mol]	$S_{\mathrm{m}}^{\mathrm{E}}$ [J/(mol·K)]	ΔC_P [J/(mol·K)]
0.000	0	0	0.000	0	0.000	0.000
0.100	−3936	−3022	0.501	992	−2.202	0.000
0.200	−5949	−4989	0.526	1636	−3.634	0.000
0.300	−7240	−6007	0.676	2019	−4.403	0.000
0.400	−7995	−6202	0.983	2206	−4.612	0.000
0.500	−8267	−5723	1.396	2239	−4.367	0.000
0.600	−8063	−4741	1.822	2138	−3.773	0.000
0.700	−7359	−3450	2.145	1900	−2.935	0.000
0.800	−6085	−2067	2.204	1499	−1.956	0.000
0.900	−4038	−830	1.760	890	−0.943	0.000
1.000	0	0	0.000	0	0.000	0.000

Reference states: Fe(liquid), Sb(liquid)

Table IIIb. Partial quantities for Fe in the liquid phase at 1823 K.

x_{Fe}	ΔG_{Fe} [J/mol]	ΔH_{Fe} [J/mol]	ΔS_{Fe} [J/(mol·K)]	$G_{\mathrm{Fe}}^{\mathrm{E}}$ [J/mol]	$S_{\mathrm{Fe}}^{\mathrm{E}}$ [J/(mol·K)]	a_{Fe}	γ_{Fe}
1.000	0	0	0.000	0	0.000	1.000	1.000
0.900	−1407	−542	0.474	190	−0.402	0.911	1.013
0.800	−2748	−2042	0.387	634	−1.468	0.834	1.043
0.700	−4216	−4257	−0.023	1190	−2.988	0.757	1.082
0.600	−5956	−6878	−0.506	1787	−4.753	0.675	1.125
0.500	−8090	−9528	−0.789	2417	−6.552	0.586	1.173
0.400	−10746	−11764	−0.559	3142	−8.177	0.492	1.230
0.300	−14157	−13075	0.594	4092	−9.417	0.393	1.310
0.200	−18933	−12881	3.320	5462	−10.062	0.287	1.434
0.100	−27386	−10538	9.242	7515	−9.903	0.164	1.642
0.000	$-\infty$	−5332	∞	10583	−8.730	0.000	2.010

Reference state: Fe(liquid)

Table IIIc. Partial quantities for Sb in the liquid phase at 1823 K.

x_{Sb}	ΔG_{Sb} [J/mol]	ΔH_{Sb} [J/mol]	ΔS_{Sb} [J/(mol·K)]	$G_{\mathrm{Sb}}^{\mathrm{E}}$ [J/mol]	$S_{\mathrm{Sb}}^{\mathrm{E}}$ [J/(mol·K)]	a_{Sb}	γ_{Sb}
0.000	$-\infty$	−35777	∞	12004	−26.210	0.000	2.208
0.100	−26695	−25334	0.747	8206	−18.398	0.172	1.718
0.200	−18751	−16778	1.082	5644	−12.300	0.290	1.451
0.300	−14296	−10091	2.307	3953	−7.704	0.389	1.298
0.400	−11053	−5188	3.217	2835	−4.401	0.482	1.206
0.500	−8445	−1917	3.581	2062	−2.182	0.573	1.146
0.600	−6274	−58	3.410	1468	−0.837	0.661	1.102
0.700	−4446	675	2.809	960	−0.156	0.746	1.065
0.800	−2873	637	1.926	509	0.070	0.827	1.034
0.900	−1444	249	0.929	153	0.053	0.909	1.010
1.000	0	0	0.000	0	0.000	1.000	1.000

Reference state: Sb(liquid)

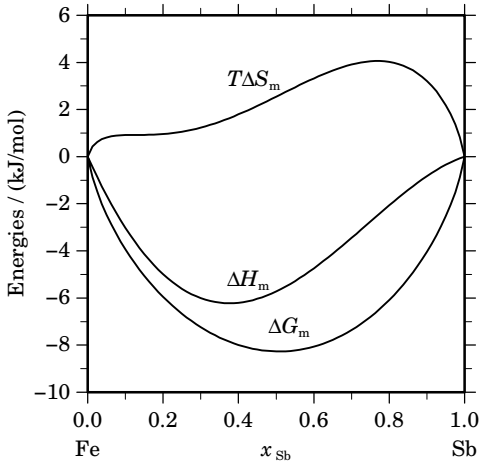

Fig. 2. Integral quantities of the liquid phase at T=1823 K.

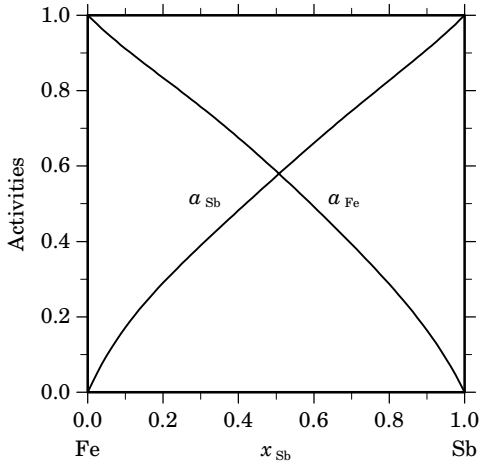

Fig. 3. Activities in the liquid phase at T=1823 K.

Table IV. Standard reaction quantities at 298.15 K for the compounds per mole of atoms.

Compound	x_{Sb}	$\Delta_f G^\circ$ / (J/mol)	$\Delta_f H^\circ$ / (J/mol)	$\Delta_f S^\circ$ / (J/(mol·K))	$\Delta_f C_P^\circ$ / (J/(mol·K))
Fe_1Sb_2	0.667	−7055	−7012	0.145	−0.139

References

[1995Pei] B. Pei, B. Björkman, B. Sundman, B. Jansson: Calphad **19** (1995) 1–15.

Ga – Mg (Gallium – Magnesium)

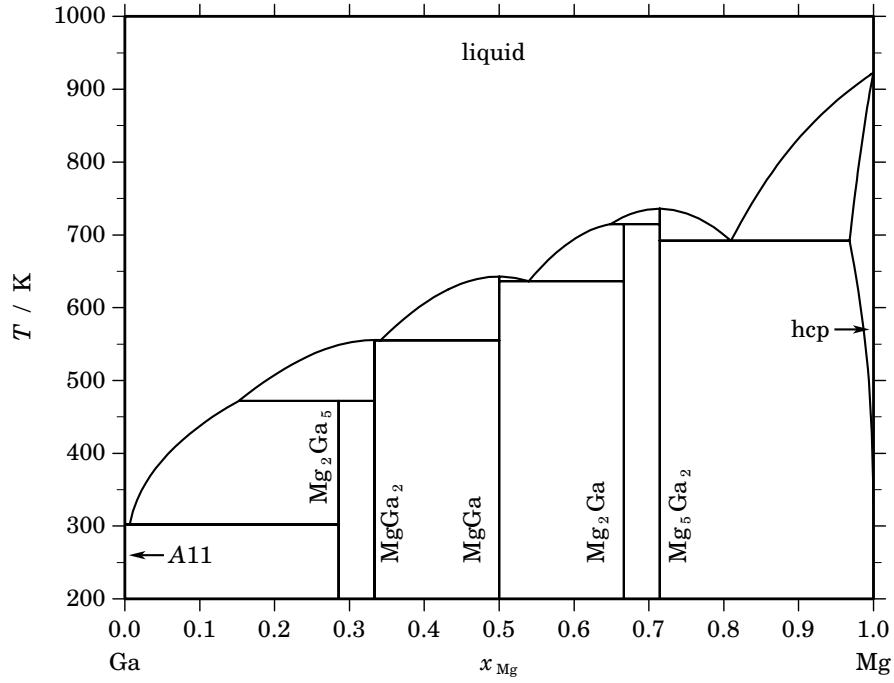

Fig. 1. Calculated phase diagram for the system Ga-Mg.

Magnesium is the major p-type dopant for GaN semiconductors and Ga-Mg melts can be used for this purpose in ion implantation processes. Another interesting applications is the potential use of Ga-based pastes for brazing and soldering Mg-alloys. The Ga-Mg system has been reviewed in [1986Nay] and a new experimental investigation and a thermodynamic optimisation has been reported by [1991Not]. Although this dataset seems to be a good assessment it has not been based on the SGTE description for the element data. Therefore, the system has been re-optimised [2005Fra] using the SGTE element data. For this adjustment the the same selection of experimental data has been used and the same invariant points of the phase diagram as recommended by [1991Not].

Table I. Phases, structures and models.

Phase	Struktur-bericht	Prototype	Pearson symbol	Space group	SGTE name	Model
liquid					LIQUID	$(Ga,Mg)_1$
$A11$	$A11$	αGa	$oC8$	$Cmca$	ORTHORHOMBIC_CMCA	Ga_1
Mg_2Ga_5	$\cdots$	Mg_2Ga_5	$tI28$	$I4/mmm$	MG2GA5	Mg_2Ga_5
$MgGa_2$	$\cdots$	$MgGa_2$	$oP24$	$Pbam$	MGGA2	Mg_1Ga_2
MgGa	$\cdots$	MgGa	$tI32$	$I4_1/a$	MGGA	Mg_1Ga_1
Mg_2Ga	$\cdots$	Mg_2Ga	$hP18$	$P\bar{6}2c$	MG2GA	Mg_2Ga_1
Mg_5Ga_2	$D8_g$	Mg_5Ga_2	$oI28$	$Ibam$	MG5GA2	Mg_5Ga_2
hcp	$A3$	Mg	$hP2$	$P6_3/mmc$	HCP_A3	$(Ga,Mg)_1$

Table II. Invariant reactions.

Reaction	Type	T / K	Compositions / x_{Mg}			$\Delta_{\mathrm{r}}H$ / (J/mol)
liquid $\rightleftharpoons$ Mg_5Ga_2	congruent	736.0	0.714	0.714		−8726
liquid + Mg_5Ga_2 $\rightleftharpoons$ Mg_2Ga	peritectic	714.8	0.649	0.714	0.667	−5944
liquid $\rightleftharpoons$ Mg_5Ga_2 + hcp	eutectic	691.9	0.810	0.714	0.968	−7502
liquid $\rightleftharpoons$ MgGa	congruent	642.8	0.500	0.500		−8683
liquid $\rightleftharpoons$ MgGa + Mg_2Ga	eutectic	636.4	0.540	0.500	0.667	−8284
liquid $\rightleftharpoons$ $MgGa_2$	congruent	555.5	0.333	0.333		−7597
liquid $\rightleftharpoons$ $MgGa_2$ + MgGa	eutectic	555.3	0.342	0.333	0.500	−7593
liquid + $MgGa_2$ $\rightleftharpoons$ Mg_2Ga_5	peritectic	472.1	0.153	0.333	0.286	−2397
liquid $\rightleftharpoons$ $A11$ + Mg_2Ga_5	eutectic	302.0	0.006	0.000	0.286	−5619

Table IIIa. Integral quantities for the liquid phase at 973 K.

x_{Mg}	ΔG_{m} [J/mol]	ΔH_{m} [J/mol]	ΔS_{m} [J/(mol·K)]	$G_{\mathrm{m}}^{\mathrm{E}}$ [J/mol]	$S_{\mathrm{m}}^{\mathrm{E}}$ [J/(mol·K)]	ΔC_P [J/(mol·K)]
0.000	0	0	0.000	0	0.000	0.000
0.100	−5253	−3129	2.183	−2623	−0.520	0.000
0.200	−8875	−6065	2.888	−4827	−1.273	0.000
0.300	−11507	−8595	2.992	−6565	−2.087	0.000
0.400	−13196	−10470	2.802	−7751	−2.794	0.000
0.500	−13898	−11445	2.521	−8290	−3.243	0.000
0.600	−13541	−11326	2.277	−8096	−3.319	0.000
0.700	−12061	−10006	2.112	−7119	−2.967	0.000
0.800	−9415	−7510	1.958	−5367	−2.203	0.000
0.900	−5559	−4037	1.564	−2929	−1.139	0.000
1.000	0	0	0.000	0	0.000	0.000

Reference states: Ga(liquid), Mg(liquid)

Table IIIb. Partial quantities for Ga in the liquid phase at 973 K.

x_{Ga}	ΔG_{Ga} [J/mol]	ΔH_{Ga} [J/mol]	ΔS_{Ga} [J/(mol·K)]	$G_{\mathrm{Ga}}^{\mathrm{E}}$ [J/mol]	$S_{\mathrm{Ga}}^{\mathrm{E}}$ [J/(mol·K)]	a_{Ga}	γ_{Ga}
1.000	0	0	0.000	0	0.000	1.000	1.000
0.900	−1058	−66	1.019	−205	0.143	0.877	0.975
0.800	−2667	−519	2.207	−862	0.352	0.719	0.899
0.700	−5016	−1861	3.243	−2131	0.277	0.538	0.768
0.600	−8369	−4618	3.855	−4236	−0.392	0.355	0.592
0.500	−12974	−9172	3.908	−7367	−1.855	0.201	0.402
0.400	−18996	−15595	3.496	−11583	−4.123	0.096	0.239
0.300	−26464	−23481	3.066	−16724	−6.945	0.038	0.127
0.200	−35333	−31782	3.650	−22313	−9.732	0.013	0.063
0.100	−46089	−38633	7.663	−27461	−11.481	0.003	0.034
0.000	$-\infty$	−41193	∞	−30777	−10.705	0.000	0.022

Reference state: Ga(liquid)

Table IIIc. Partial quantities for Mg in the liquid phase at 973 K.

x_{Mg}	ΔG_{Mg} [J/mol]	ΔH_{Mg} [J/mol]	ΔS_{Mg} [J/(mol·K)]	$G^{\mathrm{E}}_{\mathrm{Mg}}$ [J/mol]	$S^{\mathrm{E}}_{\mathrm{Mg}}$ [J/(mol·K)]	a_{Mg}	γ_{Mg}
0.000	$-\infty$	−31717	∞	−28295	−3.517	0.000	0.030
0.100	−43007	−30697	12.652	−24380	−6.493	0.005	0.049
0.200	−33709	−28249	5.612	−20689	−7.770	0.016	0.078
0.300	−26650	−24308	2.407	−16910	−7.603	0.037	0.124
0.400	−20436	−19247	1.222	−13023	−6.397	0.080	0.200
0.500	−14821	−13719	1.133	−9214	−4.630	0.160	0.320
0.600	−9904	−8480	1.464	−5772	−2.783	0.294	0.490
0.700	−5888	−4231	1.704	−3003	−1.262	0.483	0.690
0.800	−2935	−1442	1.535	−1130	−0.321	0.696	0.870
0.900	−1055	−193	0.886	−203	0.010	0.878	0.975
1.000	0	0	0.000	0	0.000	1.000	1.000

Reference state: Mg(liquid)

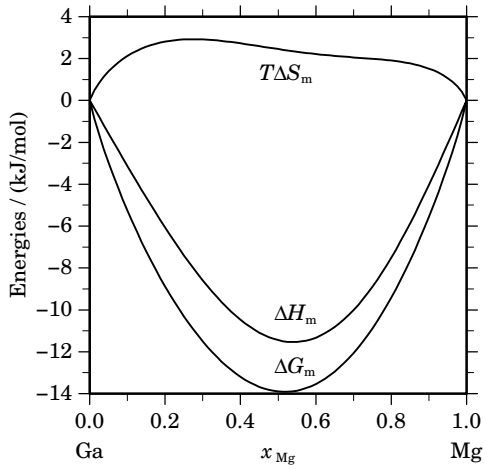

Fig. 2. Integral quantities of the liquid phase at T=973 K.

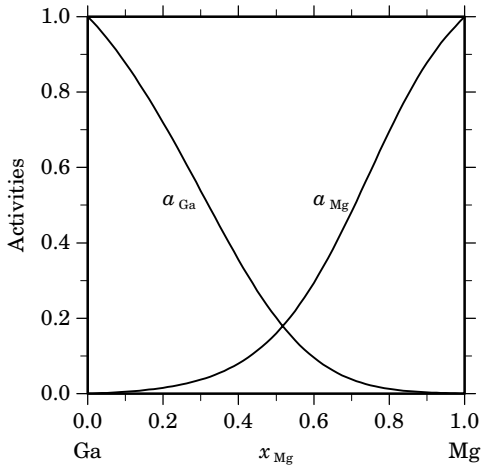

Fig. 3. Activities in the liquid phase at T=973 K.

Table IV. Standard reaction quantities at 298.15 K for the compounds per mole of atoms.

Compound	x_{Mg}	$\Delta_{\mathrm{f}}G^{\circ}$ / (J/mol)	$\Delta_{\mathrm{f}}H^{\circ}$ / (J/mol)	$\Delta_{\mathrm{f}}S^{\circ}$ / (J/(mol·K))	$\Delta_{\mathrm{f}}C^{\circ}_{P}$ / (J/(mol·K))
Mg_2Ga_5	0.286	−10766	−9695	3.594	0.000
Mg_1Ga_2	0.333	−11783	−10388	4.680	0.000
Mg_1Ga_1	0.500	−14015	−13183	2.790	0.000
Mg_2Ga_1	0.667	−12293	−11463	2.785	0.000
Mg_5Ga_2	0.714	−11508	−10927	1.950	0.000

References

[1988Nay] A.A. Nayeb-Hashemi, J.B. Clark in: "Phase Diagrams of Binary Magnesium Alloys", A.A. Nayeb-Hashemi, J.B. Clark, Eds., ASM Intl., Metals Park, OH, 1988, pp. 122–128.

[1991Not] M. Notin, E. Belbacha, J. Charles, J. Hertz: J. Alloys Comp. **176** (1991) 25–38.

[2005Fra] P. Franke: unpublished optimisation, 2005.

Ga – Si (Gallium – Silicon)

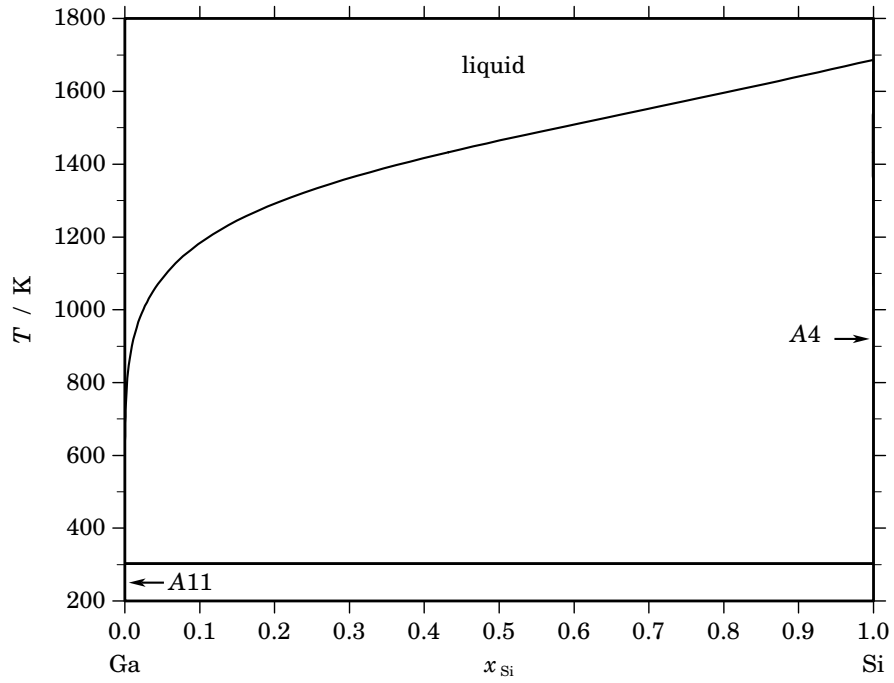

Fig. 1. Calculated phase diagram for the system Ga-Si.

The system Ga-Si is of interest for the semiconductor industry. Ga can be used as a p-type dopant in Si and furthermore, thin films of silicon can be grown from its solution in Ga melts by liquid phase epitaxy. A thorough review on the gallium-silicon system has been given by Olesinski *et al.* [1985Ole]. Since then, it seems that only one major thermodynamic investigation has been published for this system [2004Sud]. The selected dataset has been optimised by [2005Fra]. The phase diagram of Ga-Si is simple eutectic and almost degenerate on the Ga-side. For the optimisation of the liquidus curve, data from 3 experimental investigations have been selected which are in good mutual agreement [1948Kle, 1953Kec, 1977Gir]. For the solid solubility of gallium in crystalline silicon the data of [1960Tru, 1977Gir] have been chosen. In a recent investigation mixing enthalpies for the melt have been reported [2004Sud] across the whole composition range. These data compare well with the partial enthalpy of Si in Ga-rich melts which have been given in [1983Tma].

References

[1948Kle] W. Klemm, L. Klemm, F. Hohmann, H. Volk, E. Orlamünder, H.A. Klein: Z. Anorg. Allg. Chem. **256** (1948) 239–252.
[1953Kec] P.H. Keck, J. Broder: Phys. Rev. Lett. **90** (1953) 521–522.
[1960Tru] F.A. Trumbore: Bell. Sys. Tech. J. **39** (1960) 205–233.
[1977Gir] B. Girault, F. Chevrier, A. Joullie, G. Bougnot: J. Cryst. Growth **37** (1977) 169–177.
[1983Tma] M. Tmar, A. Pasturel, C. Colinet: J. Chem. Thermodyn. **15** (1983) 1037–1040.
[1985Ole] R.W. Olesinski, N. Kanani, G.J. Abbaschian: Bull. Alloy Phase Diagrams **6** (1985) 362–364.
[2004Sud] V.S. Sudavtsova, T.N. Zinevich, N.V. Kotova, E.A. Beloborodova: Zh. Fiz. Khim. **78** (2004) 957–960.
[2005Fra] P. Franke: unpublished optimisation, 2005.

Table I. Phases, structures and models.

Phase	Struktur-bericht	Prototype	Pearson symbol	Space group	SGTE name	Model
liquid					LIQUID	$(Ga,Si)_1$
$A11$	$A11$	αGa	$oC8$	$Cmca$	ORTHORHOMBIC_CMCA	Ga_1
$A4$	$A4$	C(diamond)	$cF8$	$Fd\overline{3}m$	DIAMOND_A4	$(Ga,Si)_1$

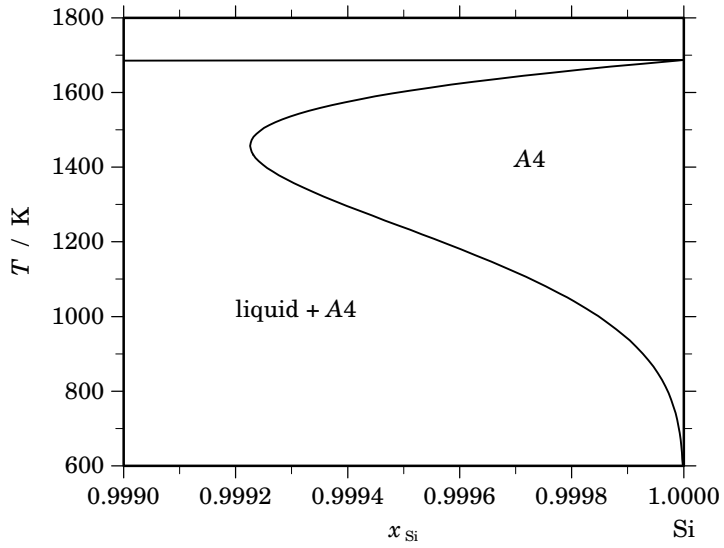

Fig. 2. Partial phase diagram for the system Ga-Si.

Table II. Invariant reactions.

Reaction	Type	T / K	Compositions / x_{Si}			$\Delta_{\mathrm{r}}H$ / (J/mol)
liquid $\rightleftharpoons A11$ + $A4$	eutectic	302.9	0.000	0.000	1.000	-5590

Table IIIa. Integral quantities for the liquid phase at 1750 K.

x_{Si}	ΔG_{m} [J/mol]	ΔH_{m} [J/mol]	ΔS_{m} [J/(mol·K)]	$G_{\mathrm{m}}^{\mathrm{E}}$ [J/mol]	$S_{\mathrm{m}}^{\mathrm{E}}$ [J/(mol·K)]	ΔC_P [J/(mol·K)]
0.000	0	0	0.000	0	0.000	0.000
0.100	−4282	1656	3.393	448	0.690	0.000
0.200	−6485	2944	5.388	796	1.227	0.000
0.300	−7843	3864	6.690	1045	1.611	0.000
0.400	−8598	4416	7.437	1195	1.841	0.000
0.500	−8841	4600	7.681	1244	1.918	0.000
0.600	−8598	4416	7.437	1195	1.841	0.000
0.700	−7843	3864	6.690	1045	1.611	0.000
0.800	−6485	2944	5.388	796	1.227	0.000
0.900	−4282	1656	3.393	448	0.690	0.000
1.000	0	0	0.000	0	0.000	0.000

Reference states: Ga(liquid), Si(liquid)

Table IIIb. Partial quantities for Ga in the liquid phase at 1750 K.

x_{Ga}	ΔG_{Ga} [J/mol]	ΔH_{Ga} [J/mol]	ΔS_{Ga} [J/(mol·K)]	G^E_{Ga} [J/mol]	S^E_{Ga} [J/(mol·K)]	a_{Ga}	γ_{Ga}
1.000	0	0	0.000	0	0.000	1.000	1.000
0.900	−1483	184	0.953	50	0.077	0.903	1.003
0.800	−3048	736	2.162	199	0.307	0.811	1.014
0.700	−4742	1656	3.656	448	0.690	0.722	1.031
0.600	−6636	2944	5.474	796	1.227	0.634	1.056
0.500	−8841	4600	7.681	1244	1.918	0.545	1.089
0.400	−11541	6624	10.380	1792	2.761	0.452	1.131
0.300	−15079	9016	13.769	2439	3.758	0.355	1.182
0.200	−20232	11776	18.291	3186	4.909	0.249	1.245
0.100	−29472	14904	25.358	4032	6.213	0.132	1.319
0.000	−∞	18400	∞	4978	7.670	0.000	1.408

Reference state: Ga(liquid)

Table IIIc. Partial quantities for Si in the liquid phase at 1750 K.

x_{Si}	ΔG_{Si} [J/mol]	ΔH_{Si} [J/mol]	ΔS_{Si} [J/(mol·K)]	G^E_{Si} [J/mol]	S^E_{Si} [J/(mol·K)]	a_{Si}	γ_{Si}
0.000	−∞	18400	∞	4978	7.670	0.000	1.408
0.100	−29472	14904	25.358	4032	6.213	0.132	1.319
0.200	−20232	11776	18.291	3186	4.909	0.249	1.245
0.300	−15079	9016	13.769	2439	3.758	0.355	1.182
0.400	−11541	6624	10.380	1792	2.761	0.452	1.131
0.500	−8841	4600	7.681	1244	1.918	0.545	1.089
0.600	−6636	2944	5.474	796	1.227	0.634	1.056
0.700	−4742	1656	3.656	448	0.690	0.722	1.031
0.800	−3048	736	2.162	199	0.307	0.811	1.014
0.900	−1483	184	0.953	50	0.077	0.903	1.003
1.000	0	0	0.000	0	0.000	1.000	1.000

Reference state: Si(liquid)

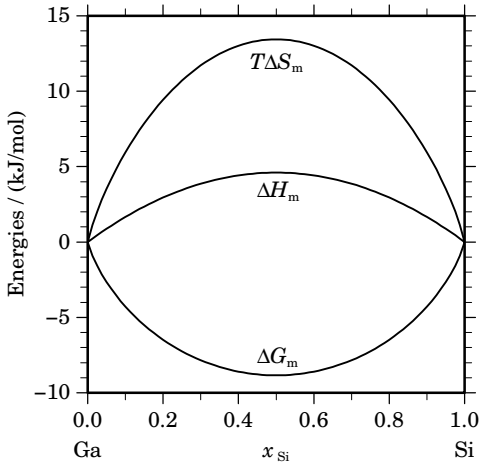

Fig. 3. Integral quantities of the liquid phase at T=1750 K.

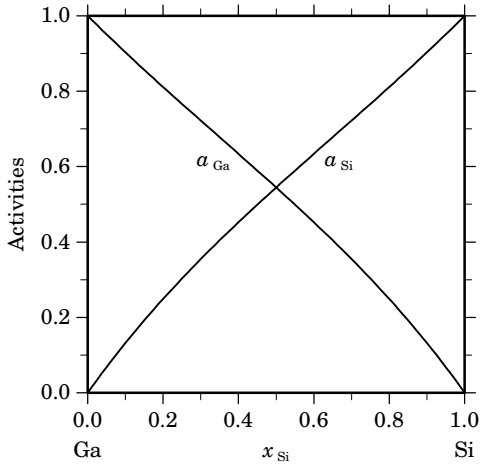

Fig. 4. Activities in the liquid phase at T=1750 K.

Ga – Ti (Gallium – Titanium)

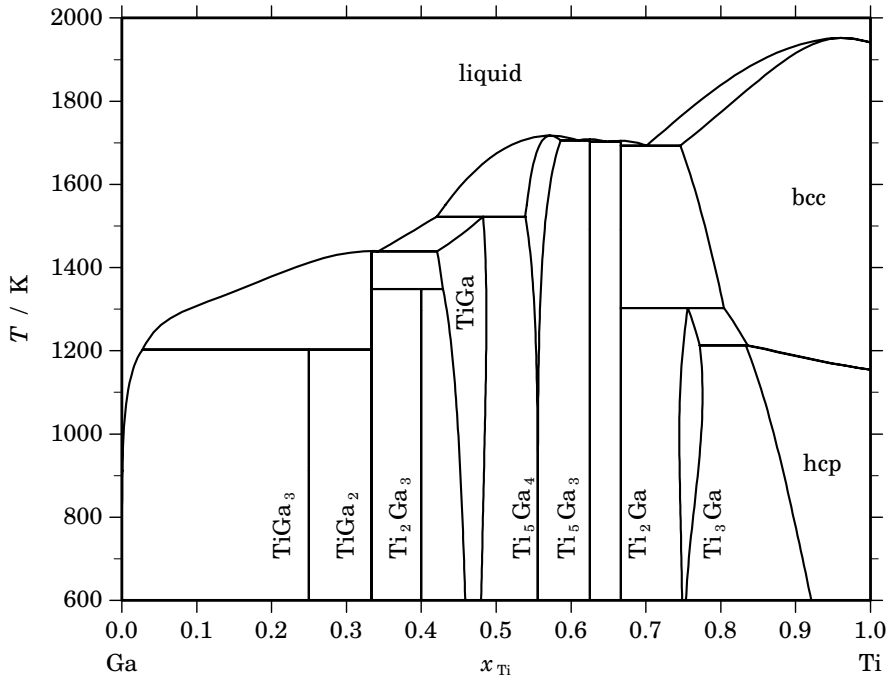

Fig. 1. Calculated phase diagram for the system Ga-Ti.

A review and a thermodynamically optimised dataset for the complete Ga-Ti system has been given by Li *et al.* [2003Li]. In a previous overview by Murray [1985Mur] a phase diagram has been assessed only for the Ti-rich part of the phase diagram because at that time only one experimental investigation [1962Pot] on almost the complete composition range of the phase diagram has been available but various questions remained open in that report. This investigation, a 2nd extended study of the phase diagram from the literature [2001Ant] and other partial evaluations of the phase diagram as well as additional own experiments have been used in [2003Li] to establish a complete phase diagram and an optimised thermodynamic dataset for the Ga-Ti system. The mixing enthalpy in the liquid has been measured by [1974Esi], however the calculated curve from the evaluated dataset shows significant deviations. The partial enthalpies of solution for Ti in Ga-rich melts [1985Nik] are in good agreement with the calculation within the experimental scatter. The experimental chemical potential differences between Ga and Ti in bcc alloys reported by [1973Geg] are in good agreement with the calculation. Except for the standard enthalpy of formation of $GaTi_2$ [1999Mes] no other thermodynamic data for the intermetallic compounds have been available. In order to estimate the respective values of the other compounds Li *et al.* [2003Li] used enthalpies of formation for Ti-Al alloys from the literature as a guide.

Table I. Phases, structures and models.

Phase	Struktur-bericht	Prototype	Pearson symbol	Space group	SGTE name	Model
liquid					LIQUID	$(Ga,Ti)_1$
$A11$	$A11$	αGa	$oC8$	$Cmca$	ORTHORHOMBIC_CMCA	Ga_1
$TiGa_3$	$D0_{22}$	$TiAl_3$	$tI8$	$I4/mmm$	TIGA3	Ti_1Ga_3
$TiGa_2$	$\cdots$	$HfGa_2$	$t*$*	$\cdots$	TIGA2	Ti_1Ga_2
Ti_2Ga_3	$\cdots$	Ti_2Ga_3	$tP10$	$P4/m$	TI2GA3	Ti_2Ga_3
TiGa	$L1_0$	AuCu	$tP4$	$P4/mmm$	TIGA	$(Ga,Ti)_1(Ga,Ti)_1$
Ti_5Ga_4	$\cdots$	Ti_5Ga_4	$hP18$	$P6_3/mcm$	TI5GA4	$(Ga,Ti)_5(Ga,Ti)_4$
Ti_5Ga_3	$D8_{\mathrm{m}}$	W_5Si_3	$tI32$	$I4/mcm$	TI5GA3	Ti_5Ga_3
Ti_2Ga	$B8_2$	Ni_2In	$hP6$	$P6_3/mmc$	TI2GA	Ti_2Ga_1
Ti_3Ga	$D0_{19}$	Ni_3Sn	$hP8$	$P6_3/mmc$	TI3GA	$(Ga,Ti)_3(Ga,Ti)_1$
bcc	$A2$	W	$cI2$	$Im\overline{3}m$	BCC_A2	$(Ga,Ti)_1$
hcp	$A3$	Ti	$hP2$	$P6_3/mmc$	HCP_A3	$(Ga,Ti)_1$

Table II. Invariant reactions.

Reaction	Type	T / K	Compositions / x_{Ti}			$\Delta_{\mathrm{r}}H$ / (J/mol)
liquid $\rightleftharpoons$ bcc	congruent	1952.3	0.962	0.962		−13998
liquid $\rightleftharpoons$ Ti_5Ga_4	congruent	1401.2	0.794	0.794		−5211
liquid $\rightleftharpoons$ Ti_5Ga_3	congruent	1708.6	0.625	0.625		−16906
liquid $\rightleftharpoons$ Ti_5Ga_4 + Ti_5Ga_3	eutectic	1706.1	0.609	0.586	0.625	−15396
liquid $\rightleftharpoons$ Ti_2Ga	congruent	1704.8	0.667	0.667		−17888
liquid $\rightleftharpoons$ Ti_5Ga_3 + Ti_2Ga	eutectic	1702.0	0.650	0.625	0.667	−17414
liquid $\rightleftharpoons$ Ti_2Ga + bcc	eutectic	1693.2	0.701	0.667	0.746	−14630
liquid + Ti_5Ga_4 $\rightleftharpoons$ TiGa	peritectic	1522.2	0.421	0.539	0.482	−9722
liquid $\rightleftharpoons$ $TiGa_2$	congruent	1439.7	0.333	0.333		−22280
liquid $\rightleftharpoons$ $TiGa_2$ + TiGa	eutectic	1439.3	0.343	0.333	0.421	−21733
$TiGa_2$ + TiGa $\rightleftharpoons$ Ti_2Ga_3	peritectoid	1348.0	0.333	0.429	0.400	−408
Ti_2Ga + bcc $\rightleftharpoons$ Ti_3Ga	peritectoid	1303.1	0.667	0.804	0.756	−4499
Ti_3Ga + bcc $\rightleftharpoons$ hcp	peritectoid	1213.2	0.772	0.836	0.833	−1823
liquid + $TiGa_2$ $\rightleftharpoons$ $TiGa_3$	peritectic	1203.1	0.028	0.333	0.250	−7164
liquid $\rightleftharpoons$ $A11$ + $TiGa_3$	eutectic	302.9	0.000	0.000	0.250	−5590

Table IIIa. Integral quantities for the liquid phase at 2000 K.

x_{Ti}	ΔG_{m} [J/mol]	ΔH_{m} [J/mol]	ΔS_{m} [J/(mol·K)]	$G_{\mathrm{m}}^{\mathrm{E}}$ [J/mol]	$S_{\mathrm{m}}^{\mathrm{E}}$ [J/(mol·K)]	ΔC_P [J/(mol·K)]
0.000	0	0	0.000	0	0.000	0.000
0.100	−6656	−7793	−0.569	−1250	−3.271	0.000
0.200	−11774	−15923	−2.074	−3453	−6.235	0.000
0.300	−16000	−23309	−3.655	−5842	−8.734	0.000
0.400	−19017	−29045	−5.014	−7826	−10.610	0.000
0.500	−20513	−32400	−5.944	−8986	−11.707	0.000
0.600	−20272	−32815	−6.271	−9080	−11.867	0.000
0.700	−18195	−29905	−5.855	−8037	−10.934	0.000
0.800	−14283	−23461	−4.589	−5962	−8.750	0.000
0.900	−8538	−13447	−2.455	−3132	−5.157	0.000
1.000	0	0	0.000	0	0.000	0.000

Reference states: Ga(liquid), Ti(liquid)

Table IIIb. Partial quantities for Ga in the liquid phase at 2000 K.

x_{Ga}	ΔG_{Ga} [J/mol]	ΔH_{Ga} [J/mol]	ΔS_{Ga} [J/(mol·K)]	$G_{\mathrm{Ga}}^{\mathrm{E}}$ [J/mol]	$S_{\mathrm{Ga}}^{\mathrm{E}}$ [J/(mol·K)]	a_{Ga}	γ_{Ga}
1.000	0	0	0.000	0	0.000	1.000	1.000
0.900	−1134	363	0.748	618	−0.128	0.934	1.038
0.800	−2346	−76	1.135	1365	−0.721	0.868	1.086
0.700	−4961	−3216	0.873	970	−2.093	0.742	1.060
0.600	−9811	−10433	−0.311	−1316	−4.559	0.554	0.924
0.500	−17246	−22585	−2.669	−5719	−8.433	0.354	0.709
0.400	−27182	−40003	−6.410	−11945	−14.029	0.195	0.488
0.300	−39195	−62498	−11.651	−19175	−21.662	0.095	0.316
0.200	−52833	−89362	−18.264	−26070	−31.646	0.042	0.209
0.100	−69058	−119359	−25.151	−30768	−44.295	0.016	0.157
0.000	$-\infty$	−150737	∞	−30888	−59.925	0.000	0.156

Reference state: Ga(liquid)

Table IIIc. Partial quantities for Ti in the liquid phase at 2000 K.

x_{Ti}	ΔG_{Ti} [J/mol]	ΔH_{Ti} [J/mol]	ΔS_{Ti} [J/(mol·K)]	$G_{\mathrm{Ti}}^{\mathrm{E}}$ [J/mol]	$S_{\mathrm{Ti}}^{\mathrm{E}}$ [J/(mol·K)]	a_{Ti}	γ_{Ti}
0.000	$-\infty$	−72213	∞	−4753	−33.730	0.000	0.751
0.100	−56357	−81197	−12.420	−18067	−31.565	0.034	0.337
0.200	−49488	−79311	−14.911	−22724	−28.293	0.051	0.255
0.300	−41757	−70194	−14.219	−21736	−24.229	0.081	0.271
0.400	−32827	−56964	−12.068	−17590	−19.687	0.139	0.347
0.500	−23780	−42215	−9.218	−12253	−14.981	0.239	0.479
0.600	−15665	−28023	−6.179	−7170	−10.426	0.390	0.650
0.700	−9195	−15936	−3.371	−3264	−6.336	0.575	0.822
0.800	−4645	−6986	−1.170	−935	−3.026	0.756	0.945
0.900	−1813	−1679	0.067	−61	−0.809	0.897	0.996
1.000	0	0	0.000	0	0.000	1.000	1.000

Reference state: Ti(liquid)

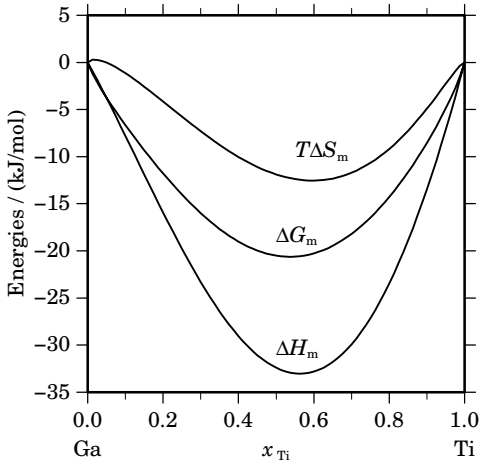

Fig. 2. Integral quantities of the liquid phase at T=2000 K.

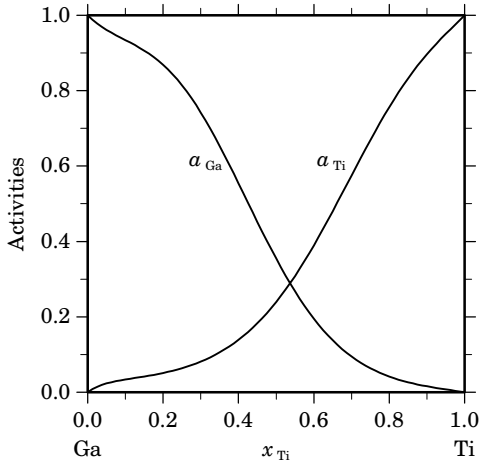

Fig. 3. Activities in the liquid phase at T=2000 K.

Table IV. Standard reaction quantities at 298.15 K for the compounds per mole of atoms.

Compound	x_{Ti}	$\Delta_{\mathrm{f}}G^{\circ}$ / (J/mol)	$\Delta_{\mathrm{f}}H^{\circ}$ / (J/mol)	$\Delta_{\mathrm{f}}S^{\circ}$ / (J/(mol·K))	$\Delta_{\mathrm{f}}C_P^{\circ}$ / (J/(mol·K))
Ti_1Ga_3	0.250	−33809	−35130	−4.429	0.000
Ti_1Ga_2	0.333	−38427	−39867	−4.827	0.000
Ti_2Ga_3	0.400	−38795	−40064	−4.257	0.000
Ti_5Ga_4	0.556	−38491	−39500	−3.384	0.000
Ti_5Ga_3	0.625	−37787	−39125	−4.487	0.000
Ti_2Ga_1	0.667	−37056	−38667	−5.403	0.000
Ti_3Ga	0.750	−32028	−34127	−7.040	0.000

References

[1962Pot] M. Potzschke, K. Schubert: Z. Metallkd. **53** (1962) 474–488.
[1973Geg] H.L. Gegel, M. Hoch in: "Titanium Science and Technology", R.I. Jaffee, H.M. Burte, eds., vol. 2, 1973, pp. 923–933.
[1974Esi] Yu.O. Esin, N.P. Bobrov, M.S. Petrushevskii, P.V. Gel'd: Russ. Metall. 5 (1974) 86–91.
[1985Mur] J.L. Murray: Bull. Alloy Phase Diagrams **6** (1985) 327–330.
[1985Nik] I.V. Nikolaenko, G.I. Batalin, E.A. Beloborodova, Yu.V. Vorobei, V.S. Zhuravlev: Zh. Fiz. Khim. **59** (1985) 728–730.
[1999Mes] S.V. Meschel, O.J. Kleppa: J. Alloys Comp. **290** (1999) 150–156.
[2001Ant] N.V. Antonova, L.A. Tretyachenko: J. Alloys Comp. **317-318** (2001) 398–405.
[2003Li] J.-B. Li, J.-C. Tedenac, M.-C. Record: J. Alloys Comp. **358** (2003) 133–141.

Gd – Li (Gadolinium – Lithium)

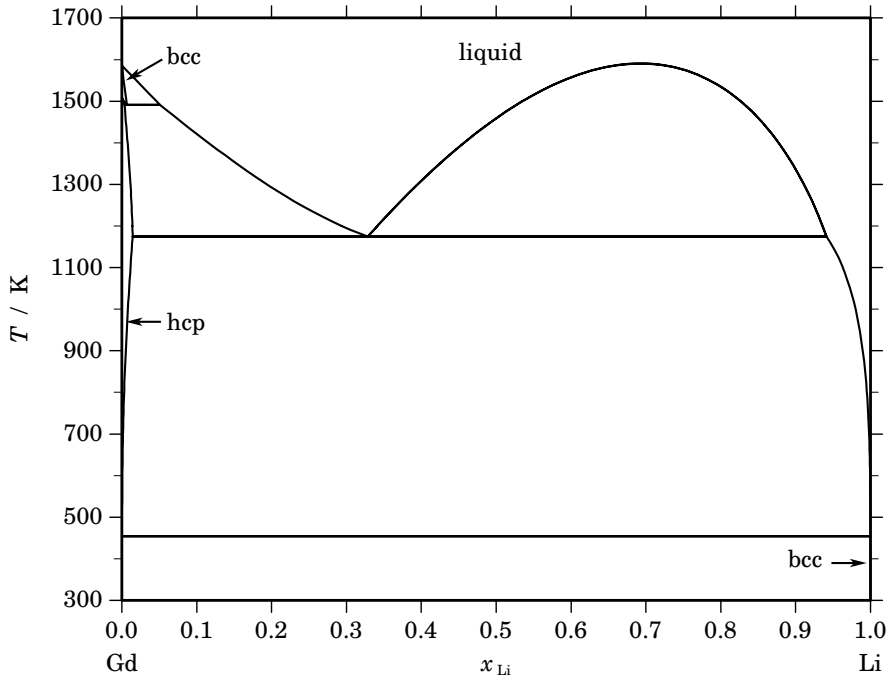

Fig. 1. Calculated phase diagram for the system Gd-Li.

Lithium is a common addition for magnesium alloys in order to decrease their density and to improve the ductility. Rare Earth metals can enable precipitation hardening of magnesium alloys and enhance the castability. Only very few data have been reported about the Gd-Li system. At 473 K no mutual solubility of the elements could be observed [1989Pav]. In DTA experiments [1998Gan] only two invariant temperatures have been detected, a eutectic almost degenerate on the Li-side, and a monotectic at higher temperatures. The existence of the miscibility gap has been verified experimentally [2001Kev] and in the course of an assessment of the ternary system Gd-Li-Mg, the dataset for the binary Gd-Li has been optimised as well [2001Kev].

Table I. Phases, structures and models.

Phase	Struktur-bericht	Prototype	Pearson symbol	Space group	SGTE name	Model
liquid					LIQUID	$(Gd,Li)_1$
bcc	$A2$	W	$cI2$	$Im\bar{3}m$	BCC_A2	$(Gd,Li)_1$
hcp	$A3$	Mg	$hP2$	$P6_3/mmc$	HCP_A3	$(Gd,Li)_1$

Table II. Invariant reactions.

Reaction	Type	T / K	Compositions / x_{Li}			$\Delta_{\mathrm{r}}H$ / (J/mol)
liquid $\rightleftharpoons$ liquid′ + liquid″	critical	1589.4	0.693	0.693	0.693	0
bcc $\rightleftharpoons$ hcp + liquid′	metatectic	1491.4	0.007	0.004	0.051	−2682
liquid′ $\rightleftharpoons$ hcp + liquid″	monotectic	1174.5	0.329	0.014	0.941	−11438
hcp + liquid″ $\rightleftharpoons$ bcc	peritectic	453.7	0.000	1.000	1.000	−2994

Table IIIa. Integral quantities for the liquid phase at 1600 K.

x_{Li}	ΔG_{m} [J/mol]	ΔH_{m} [J/mol]	ΔS_{m} [J/(mol·K)]	$G_{\mathrm{m}}^{\mathrm{E}}$ [J/mol]	$S_{\mathrm{m}}^{\mathrm{E}}$ [J/(mol·K)]	ΔC_P [J/(mol·K)]
0.000	0	0	0.000	0	0.000	0.000
0.100	−3183	1141	2.703	1141	0.000	0.000
0.200	−4327	2330	4.161	2330	0.000	0.000
0.300	−4674	3452	5.079	3452	0.000	0.000
0.400	−4556	4397	5.596	4397	0.000	0.000
0.500	−4171	5050	5.763	5050	0.000	0.000
0.600	−3654	5299	5.596	5299	0.000	0.000
0.700	−3095	5032	5.079	5032	0.000	0.000
0.800	−2523	4134	4.161	4134	0.000	0.000
0.900	−1830	2495	2.703	2495	0.000	0.000
1.000	0	0	0.000	0	0.000	0.000

Reference states: Gd(liquid), Li(liquid)

Table IIIb. Partial quantities for Gd in the liquid phase at 1600 K.

x_{Gd}	ΔG_{Gd} [J/mol]	ΔH_{Gd} [J/mol]	ΔS_{Gd} [J/(mol·K)]	$G_{\mathrm{Gd}}^{\mathrm{E}}$ [J/mol]	$S_{\mathrm{Gd}}^{\mathrm{E}}$ [J/(mol·K)]	a_{Gd}	γ_{Gd}
1.000	0	0	0.000	0	0.000	1.000	1.000
0.900	−1444	−42	0.876	−42	0.000	0.897	0.997
0.800	−2988	−19	1.855	−19	0.000	0.799	0.999
0.700	−4450	295	2.966	295	0.000	0.716	1.022
0.600	−5669	1126	4.247	1126	0.000	0.653	1.088
0.500	−6521	2700	5.763	2700	0.000	0.613	1.225
0.400	−6948	5242	7.619	5242	0.000	0.593	1.483
0.300	−7040	8977	10.010	8977	0.000	0.589	1.964
0.200	−7280	14131	13.382	14131	0.000	0.579	2.893
0.100	−9701	20930	19.145	20930	0.000	0.482	4.823
0.000	$-\infty$	29600	∞	29600	0.000	0.000	9.254

Reference state: Gd(liquid)

Table IIIc. Partial quantities for Li in the liquid phase at 1600 K.

x_{Li}	ΔG_{Li} [J/mol]	ΔH_{Li} [J/mol]	ΔS_{Li} [J/(mol·K)]	$G_{\mathrm{Li}}^{\mathrm{E}}$ [J/mol]	$S_{\mathrm{Li}}^{\mathrm{E}}$ [J/(mol·K)]	a_{Li}	γ_{Li}
0.000	$-\infty$	10800	∞	10800	0.000	0.000	2.252
0.100	−18838	11794	19.145	11794	0.000	0.243	2.427
0.200	−9686	11725	13.382	11725	0.000	0.483	2.414
0.300	−5198	10819	10.010	10819	0.000	0.677	2.255
0.400	−2887	9302	7.619	9302	0.000	0.805	2.012
0.500	−1821	7400	5.763	7400	0.000	0.872	1.744
0.600	−1458	5338	4.247	5338	0.000	0.896	1.494
0.700	−1404	3341	2.966	3341	0.000	0.900	1.285
0.800	−1333	1635	1.855	1635	0.000	0.905	1.131
0.900	−955	446	0.876	446	0.000	0.931	1.034
1.000	0	0	0.000	0	0.000	1.000	1.000

Reference state: Li(liquid)

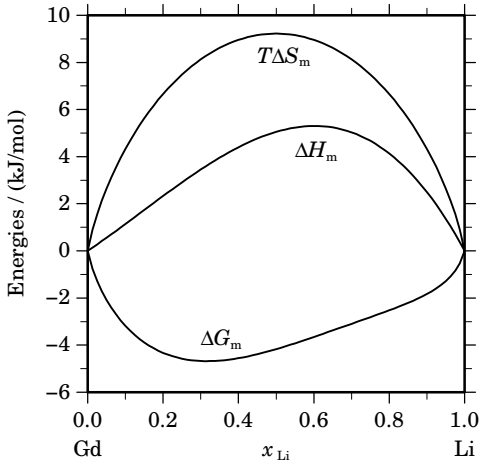

Fig. 2. Integral quantities of the liquid phase at T=1600 K.

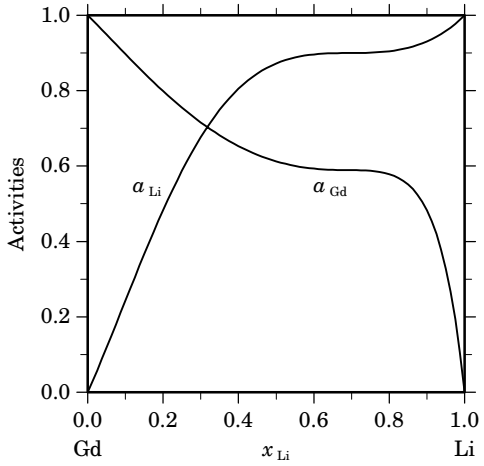

Fig. 3. Activities in the liquid phase at T=1600 K.

References

[1989Pav] V.V. Pavlyuk: Thesis Cand. Chem. Sci., Lviv, 1989.

[1998Gan] I.N. Ganiev, Kh.M. Nazarov, M.D. Badalov: Metally 6 (1998) 109–112.

[2001Kev] D.G. Kevorkov, J. Gröbner, R. Schmid-Fetzer, V.V. Pavlyuk, G.S. Dmytriv, O.I. Bodak: J. Phase Equilibria **22** (2001) 34–42.

Gd – Mg (Gadolinium – Magnesium)

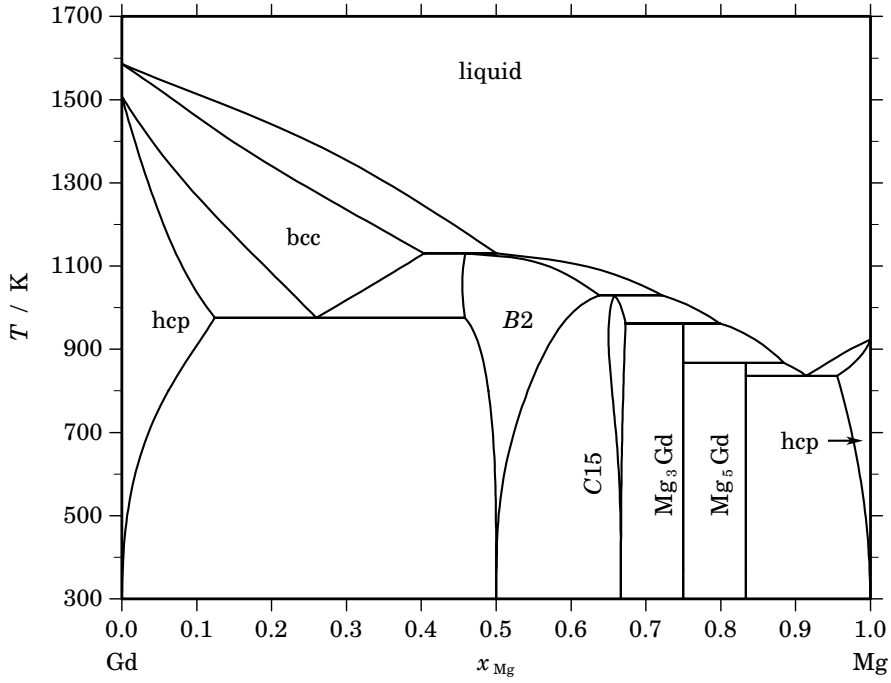

Fig. 1. Calculated phase diagram for the system Gd-Mg.

The rare earth elements have attracted some attention as additives to light metal alloys in the aerospace and automotive industry due to the improvement of mechanical properties of Al- and Mg-alloys at high temperatures. Cacciamani *et al.* [2003Cac] prepared a thermodynamic optimisation of the complete Gd-Mg system, which is mostly based on an experimental investigation of the phase equilibria at elevated temperatures throughout the whole composition range [1986Man]. The solid solubilities have been measured by [1965Jos] for Mg in hcp-Gd and by [1978Rok] for Gd in magnesium. Except for the standard enthalpy of formation of the GdMg phase no other thermodynamic data for the Gd-Mg system have been available. Despite this lack of data, the assessment [2003Cac] can be considered as quite reasonable since other similar systems (Dy-Mg, Ho-Mg) have been evaluated simultaneously and data have been estimated taking advantage of the close relations between the involved rare earth elements.

Table I. Phases, structures and models.

Phase	Struktur-bericht	Prototype	Pearson symbol	Space group	SGTE name	Model
liquid					LIQUID	$(Gd,Mg)_1$
hcp	$A3$	Mg	$hP2$	$P6_3/mmc$	HCP_A3	$(Gd,Mg)_1$
bcc	$A2$	W	$cI2$	$Im\bar{3}m$	BCC_A2	$(Gd,Mg)_1$
$B2$	$B2$	CsCl	$cP2$	$Pm3m$	BCC_B2	$(Gd,Mg)_1(Gd,Mg)_1$
$C15$	$C15$	$MgCu_2$	$cF24$	$Fd\bar{3}m$	LAVES_C15	$(Gd,Mg)_2(Gd,Mg)_1$
Mg_3Gd	$D0_3$	BiF_3	$cF16$	$Fm\bar{3}m$	MG3LN	Mg_3Gd_1
Mg_5Gd	$\cdots$	$GdMg_5$	$cF448$	$F\bar{4}3m$	GDMG5	Mg_5Gd_1

Table II. Invariant reactions.

Reaction	Type	T / K	Compositions / x_{Mg}			$\Delta_{\mathrm{r}}H$ / (J/mol)
bcc + liquid $\rightleftharpoons$ $B2$	peritectic	1130.4	0.404	0.501	0.459	−7962
$B2$ + liquid $\rightleftharpoons$ $C15$	peritectic	1029.5	0.638	0.722	0.658	−7514
bcc $\rightleftharpoons$ hcp + $B2$	eutectoid	976.0	0.260	0.124	0.458	−5479
$C15$ + liquid $\rightleftharpoons$ Mg_3Gd	peritectic	962.2	0.673	0.798	0.750	−8869
Mg_3Gd + liquid $\rightleftharpoons$ Mg_5Gd	peritectic	867.3	0.750	0.884	0.833	−6828
liquid $\rightleftharpoons$ Mg_5Gd + hcp	eutectic	836.1	0.914	0.833	0.955	−9077

Table IIIa. Integral quantities for the liquid phase at 1800 K.

x_{Mg}	ΔG_{m} [J/mol]	ΔH_{m} [J/mol]	ΔS_{m} [J/(mol·K)]	$G_{\mathrm{m}}^{\mathrm{E}}$ [J/mol]	$S_{\mathrm{m}}^{\mathrm{E}}$ [J/(mol·K)]	ΔC_P [J/(mol·K)]
0.000	0	0	0.000	0	0.000	0.000
0.100	−5952	−551	3.001	−1087	0.298	0.000
0.200	−9916	−1734	4.545	−2427	0.385	0.000
0.300	−12977	−3268	5.394	−3834	0.315	0.000
0.400	−15197	−4867	5.739	−5124	0.143	0.000
0.500	−16485	−6250	5.686	−6111	−0.077	0.000
0.600	−16681	−7133	5.305	−6609	−0.291	0.000
0.700	−15574	−7232	4.634	−6432	−0.445	0.000
0.800	−12885	−6266	3.677	−5395	−0.483	0.000
0.900	−8178	−3949	2.350	−3313	−0.353	0.000
1.000	0	0	0.000	0	0.000	0.000

Reference states: Gd(liquid), Mg(liquid)

Table IIIb. Partial quantities for Gd in the liquid phase at 1800 K.

x_{Gd}	ΔG_{Gd} [J/mol]	ΔH_{Gd} [J/mol]	ΔS_{Gd} [J/(mol·K)]	$G_{\mathrm{Gd}}^{\mathrm{E}}$ [J/mol]	$S_{\mathrm{Gd}}^{\mathrm{E}}$ [J/(mol·K)]	a_{Gd}	γ_{Gd}
1.000	0	0	0.000	0	0.000	1.000	1.000
0.900	−1419	364	0.990	158	0.114	0.910	1.011
0.800	−2957	1077	2.241	383	0.385	0.821	1.026
0.700	−5033	1573	3.670	305	0.705	0.714	1.021
0.600	−8093	1286	5.211	−448	0.963	0.582	0.971
0.500	−12619	−350	6.816	−2245	1.053	0.430	0.861
0.400	−19173	−3902	8.484	−5460	0.865	0.278	0.694
0.300	−28481	−9937	10.302	−10462	0.292	0.149	0.497
0.200	−41710	−19021	12.605	−17623	−0.776	0.062	0.308
0.100	−61775	−31720	16.698	−27314	−2.447	0.016	0.161
0.000	$-\infty$	−48600	∞	−39906	−4.830	0.000	0.069

Reference state: Gd(liquid)

Table IIIc. Partial quantities for Mg in the liquid phase at 1800 K.

x_{Mg}	ΔG_{Mg} [J/mol]	ΔH_{Mg} [J/mol]	ΔS_{Mg} [J/(mol·K)]	$G^{\mathrm{E}}_{\mathrm{Mg}}$ [J/mol]	$S^{\mathrm{E}}_{\mathrm{Mg}}$ [J/(mol·K)]	a_{Mg}	γ_{Mg}
0.000	$-\infty$	−1400	∞	−8982	4.212	0.000	0.549
0.100	−46746	−8780	21.092	−12285	1.947	0.044	0.440
0.200	−37752	−12979	13.763	−13665	0.381	0.080	0.401
0.300	−31512	−14563	9.416	−13493	−0.594	0.122	0.406
0.400	−25853	−14098	6.531	−12140	−1.088	0.178	0.444
0.500	−20350	−12150	4.556	−9977	−1.207	0.257	0.513
0.600	−15020	−9286	3.185	−7375	−1.062	0.367	0.611
0.700	−10043	−6073	2.205	−4705	−0.760	0.511	0.730
0.800	−5678	−3077	1.445	−2338	−0.410	0.684	0.855
0.900	−2223	−864	0.755	−646	−0.121	0.862	0.958
1.000	0	0	0.000	0	0.000	1.000	1.000

Reference state: Mg(liquid)

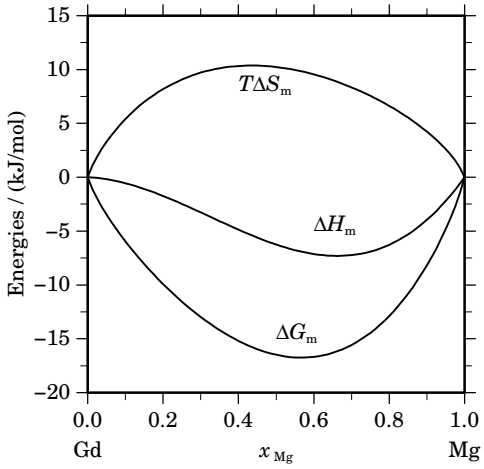

Fig. 2. Integral quantities of the liquid phase at T=1800 K.

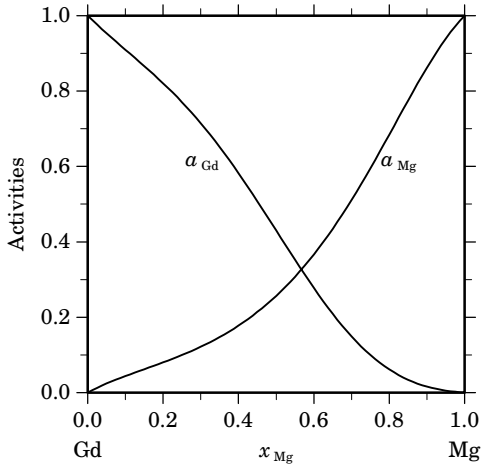

Fig. 3. Activities in the liquid phase at T=1800 K.

Table IV. Standard reaction quantities at 298.15 K for the compounds per mole of atoms.

Compound	x_{Mg}	$\Delta_{\mathrm{f}}G^{\circ}$ / (J/mol)	$\Delta_{\mathrm{f}}H^{\circ}$ / (J/mol)	$\Delta_{\mathrm{f}}S^{\circ}$ / (J/(mol·K))	$\Delta_{\mathrm{f}}C^{\circ}_{P}$ / (J/(mol·K))
$B2$	0.500	−14191	−15138	−3.176	−6.456
$C15$	0.667	−13962	−14750	−2.643	−4.322
Mg_3Gd_1	0.750	−11732	−12313	−1.949	−3.244
Mg_5Gd_1	0.833	−8274	−8659	−1.290	−2.163

References

[1965Jos] R.R. Joseph, K.A. Gschneidner jr.: Trans. Metall. Soc. AIME **233** (1965) 2063–2069.

[1978Rok] L.L. Rokhlin in: "Probl. Metalloved. Tsvetn. Splavov", N.M. Zhavoronkov (Ed.), Izd. Nauka, Moscow, 1978, pp. 59–70.

[2003Cac] G. Cacciamani, S. de Negri, A. Saccone, R. Ferro: Intermetallics **11** (2003) 1135–1151.

Gd – Mn (Gadolinium – Manganese)

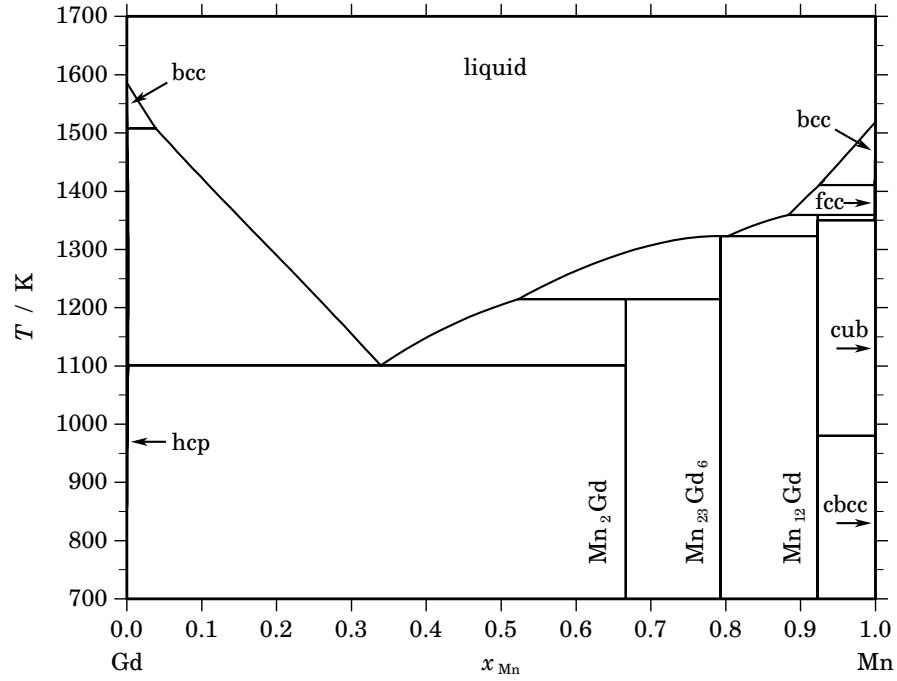

Fig. 1. Calculated phase diagram for the system Gd-Mn.

Manganese and rare earth metals are added to magnesium alloys in order to improve their creep resistance and strength. A review and a thermodynamic optimisation of the Gd-Mn system has been prepared by [2001Grö]. The phase diagram of the system Gd-Mn has been determined by Kirchmayr and Lugscheider [1967Kir]. The partial enthalpies of the components in molten Gd-Mn alloys have been measured calorimetrically by Nikolaenko and Nosova [1989Nik]. However, their data have a large range of scatter and they are not used in the optimisation [2001Grö]. Enthalpies of formation of the intermetallic compounds have been estimated from the corresponding values of the Mn-Y system which been assessed in the same publication [2001Grö].

Table I. Phases, structures and models.

Phase	Struktur-bericht	Prototype	Pearson symbol	Space group	SGTE name	Model
liquid					LIQUID	$(Gd,Mn)_1$
bcc	$A2$	W	$cI2$	$Im\bar{3}m$	BCC_A2	$(Gd,Mn)_1$
hcp	$A3$	Mg	$hP2$	$P6_3/mmc$	HCP_A3	$(Gd,Mn)_1$
Mn_2Gd	$C15$	Cu_2Mg	$cF24$	$Fd\bar{3}m$	M2R	Mn_2Gd_1
$Mn_{23}Gd_6$	$D8_a$	$Mn_{23}Th_6$	$cF116$	$Fm\bar{3}m$	M23R6	$Mn_{23}Gd_6$
$Mn_{12}Gd$	$D2_b$	$Mn_{12}Th$	$tI26$	$I4/mmm$	M12R	$Mn_{12}Gd_1$
fcc	$A1$	Cu	$cF4$	$Fm\bar{3}m$	FCC_A1	$(Gd,Mn)_1$
cbcc	$A12$	αMn	$cI58$	$I\bar{4}3m$	CBCC_A12	Mn_1
cub	$A13$	βMn	$cP20$	$P4_132$	CUB_A13	Mn_1

Table II. Invariant reactions.

Reaction	Type	T / K	Compositions / x_{Mn}			$\Delta_{\mathrm{r}}H$ / (J/mol)
bcc ⇌ hcp + liquid	metatectic	1507.9	0.001	0.001	0.039	−3502
bcc ⇌ liquid + fcc	metatectic	1410.8	0.999	0.925	0.999	−1905
liquid + fcc ⇌ $Mn_{12}Gd$	peritectic	1359.4	0.884	0.998	0.923	−15890
fcc ⇌ $Mn_{12}Gd$ + cub	eutectoid	1350.2	0.999	0.923	1.000	−2330
liquid ⇌ $Mn_{23}Gd_6$	congruent	1323.2	0.793	0.793		−21254
liquid ⇌ $Mn_{23}Gd_6$ + $Mn_{12}Gd$	eutectic	1323.0	0.803	0.793	0.923	−21198
liquid + $Mn_{23}Gd_6$ ⇌ Mn_2Gd	peritectic	1214.7	0.523	0.793	0.667	−8918
liquid ⇌ hcp + Mn_2Gd	eutectic	1100.8	0.339	0.002	0.667	−15053
cub ⇌ $Mn_{12}Gd$ + cbcc	eutectoid	980.0	1.000	0.923	1.000	−2254

Table IIIa. Integral quantities for the liquid phase at 1600 K.

x_{Mn}	ΔG_{m} [J/mol]	ΔH_{m} [J/mol]	ΔS_{m} [J/(mol·K)]	$G^{\mathrm{E}}_{\mathrm{m}}$ [J/mol]	$S^{\mathrm{E}}_{\mathrm{m}}$ [J/(mol·K)]	ΔC_P [J/(mol·K)]
0.000	0	0	0.000	0	0.000	0.000
0.100	−4044	−1159	1.803	281	−0.900	0.000
0.200	−6186	−2089	2.561	471	−1.600	0.000
0.300	−7545	−2779	2.979	581	−2.100	0.000
0.400	−8331	−3218	3.196	622	−2.400	0.000
0.500	−8617	−3396	3.263	604	−2.500	0.000
0.600	−8416	−3303	3.196	537	−2.400	0.000
0.700	−7693	−2927	2.979	433	−2.100	0.000
0.800	−6355	−2258	2.561	302	−1.600	0.000
0.900	−4171	−1286	1.803	154	−0.900	0.000
1.000	0	0	0.000	0	0.000	0.000

Reference states: Gd(liquid), Mn(liquid)

Table IIIb. Partial quantities for Gd in the liquid phase at 1600 K.

x_{Gd}	ΔG_{Gd} [J/mol]	ΔH_{Gd} [J/mol]	ΔS_{Gd} [J/(mol·K)]	$G^{\mathrm{E}}_{\mathrm{Gd}}$ [J/mol]	$S^{\mathrm{E}}_{\mathrm{Gd}}$ [J/(mol·K)]	a_{Gd}	γ_{Gd}
1.000	0	0	0.000	0	0.000	1.000	1.000
0.900	−1355	−113	0.776	47	−0.100	0.903	1.004
0.800	−2794	−466	1.455	174	−0.400	0.811	1.013
0.700	−4385	−1080	2.066	360	−0.900	0.719	1.027
0.600	−6211	−1976	2.647	584	−1.600	0.627	1.045
0.500	−8397	−3176	3.263	825	−2.500	0.532	1.064
0.400	−11130	−4700	4.019	1060	−3.600	0.433	1.083
0.300	−14747	−6570	5.110	1270	−4.900	0.330	1.100
0.200	−19978	−8807	6.982	1433	−6.400	0.223	1.114
0.100	−29105	−11433	11.045	1527	−8.100	0.112	1.122
0.000	$-\infty$	−14468	∞	1532	−10.000	0.000	1.122

Reference state: Gd(liquid)

Table IIIc. Partial quantities for Mn in the liquid phase at 1600 K.

x_{Mn}	ΔG_{Mn} [J/mol]	ΔH_{Mn} [J/mol]	ΔS_{Mn} [J/(mol·K)]	$G^{\mathrm{E}}_{\mathrm{Mn}}$ [J/mol]	$S^{\mathrm{E}}_{\mathrm{Mn}}$ [J/(mol·K)]	a_{Mn}	γ_{Mn}
0.000	$-\infty$	−12702	∞	3298	−10.000	0.000	1.281
0.100	−28247	−10575	11.045	2385	−8.100	0.120	1.196
0.200	−19752	−8581	6.982	1659	−6.400	0.227	1.133
0.300	−14920	−6743	5.110	1097	−4.900	0.326	1.086
0.400	−11511	−5081	4.019	679	−3.600	0.421	1.052
0.500	−8838	−3617	3.263	383	−2.500	0.515	1.029
0.600	−6607	−2371	2.647	189	−1.600	0.609	1.014
0.700	−4671	−1366	2.066	74	−0.900	0.704	1.006
0.800	−2950	−621	1.455	19	−0.400	0.801	1.001
0.900	−1400	−159	0.776	1	−0.100	0.900	1.000
1.000	0	0	0.000	0	0.000	1.000	1.000

Reference state: Mn(liquid)

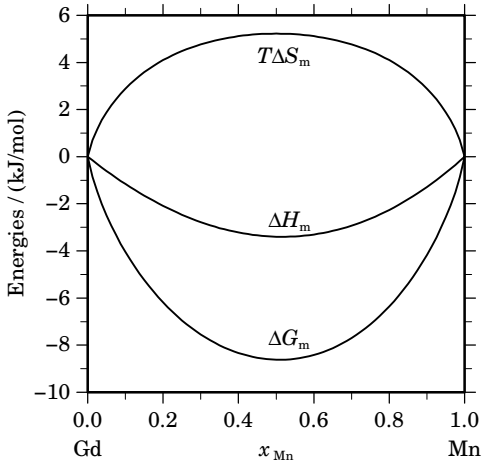

Fig. 2. Integral quantities of the liquid phase at T=1600 K.

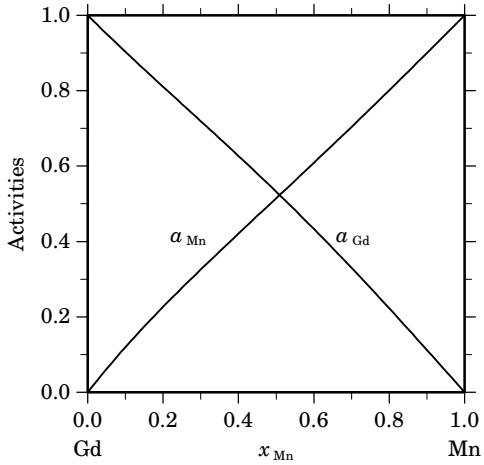

Fig. 3. Activities in the liquid phase at T=1600 K.

Table IV. Standard reaction quantities at 298.15 K for the compounds per mole of atoms.

Compound	x_{Mn}	$\Delta_{\mathrm{f}}G^{\circ}$ / (J/mol)	$\Delta_{\mathrm{f}}H^{\circ}$ / (J/mol)	$\Delta_{\mathrm{f}}S^{\circ}$ / (J/(mol·K))	$\Delta_{\mathrm{f}}C^{\circ}_{P}$ / (J/(mol·K))
Mn_2Gd_1	0.667	−6111	−6408	−0.996	−4.329
$Mn_{23}Gd_6$	0.793	−6026	−6371	−1.158	−2.689
$Mn_{12}Gd_1$	0.923	−3720	−4027	−1.031	−1.003

References

[1967Kir] H.R. Kirchmayr, W. Lugscheider: Z. Metallkd. **58** (1967) 185–188.
[1989Nik] I.V. Nikolaenko, V.V. Nosova: Ukr. Khim. Zh. **55** (1989) 1260–1262.
[2001Grö] J. Gröbner, A. Pisch, R. Schmid-Fetzer: J. Alloys Comp. **317-318** (2001) 433–437.

Gd – Mo (Gadolinium – Molybdenum)

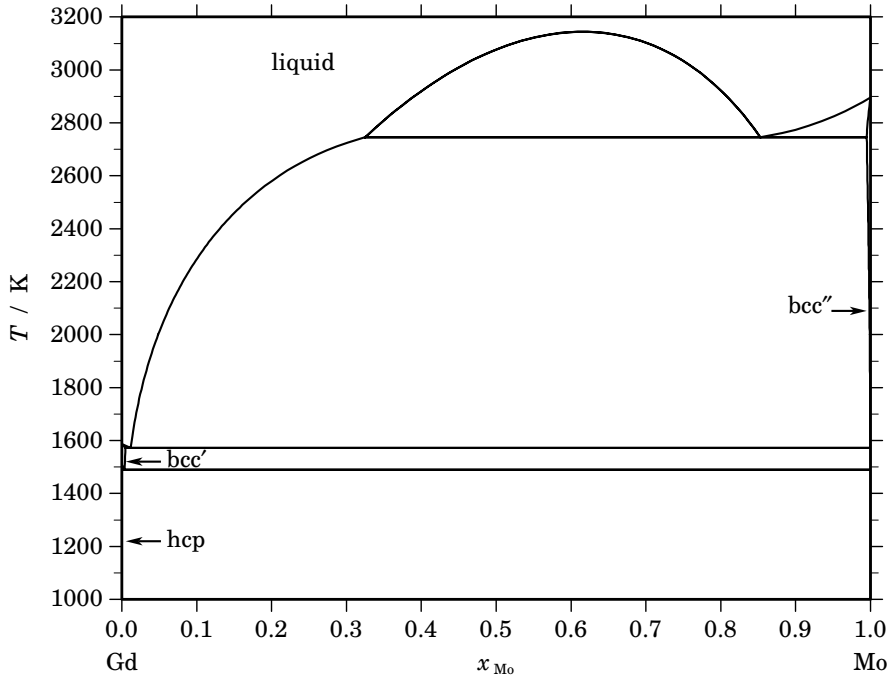

Fig. 1. Calculated phase diagram for the system Gd-Mo.

In the solid state Gd and Mo are almost insoluble in each other and no binary compounds are formed by them. The interest in this system is related to ternary and higher systems where intermetallic compounds are formed with interesting magnetic properties. The combination of gadolinium and molybdenum can also be encountered in Mo-containing stainless steel repositories for nuclear waste where Gd is added due to its high absorption cross section for thermal neutrons. The few experimental data on the Gd-Mo system consist of the temperature of the Gd-rich eutectic, the temperature and composition of the monotectic and the solubility of Gd in Mo [1966Chu]. Based on these data an optimised thermodynamic dataset of the Gd-Mo system has been reported in [2001Zin].

Table I. Phases, structures and models.

Phase	Struktur-bericht	Prototype	Pearson symbol	Space group	SGTE name	Model
liquid					LIQUID	$(Gd,Mo)_1$
bcc	$A2$	W	$cI2$	$Im\bar{3}m$	BCC_A2	$(Gd,Mo)_1$
hcp	$A3$	Mg	$hP2$	$P6_3/mmc$	HCP_A3	$(Gd,Mo)_1$

Table II. Invariant reactions.

Reaction	Type	T / K	Compositions / x_{Mo}			$\Delta_{\mathrm{r}}H$ / (J/mol)
liquid $\rightleftharpoons$ liquid′ + liquid″	critical	3142.4	0.616	0.616	0.616	0
liquid″ $\rightleftharpoons$ liquid′ + bcc″	monotectic	2745.2	0.853	0.325	0.995	−34872
liquid″ $\rightleftharpoons$ bcc′ + bcc″	eutectic	1571.8	0.012	0.005	1.000	−10174
bcc′ $\rightleftharpoons$ hcp + bcc″	eutectoid	1489.4	0.004	0.000	1.000	−3759

Table IIIa. Integral quantities for the liquid phase at 3200 K.

x_{Mo}	ΔG_{m} [J/mol]	ΔH_{m} [J/mol]	ΔS_{m} [J/(mol·K)]	$G_{\mathrm{m}}^{\mathrm{E}}$ [J/mol]	$S_{\mathrm{m}}^{\mathrm{E}}$ [J/(mol·K)]	ΔC_P [J/(mol·K)]
0.000	0	0	0.000	0	0.000	0.000
0.100	−4887	3762	2.703	3762	0.000	0.000
0.200	−6338	6976	4.161	6976	0.000	0.000
0.300	−6719	9534	5.079	9534	0.000	0.000
0.400	−6578	11328	5.596	11328	0.000	0.000
0.500	−6192	12250	5.763	12250	0.000	0.000
0.600	−5714	12192	5.596	12192	0.000	0.000
0.700	−5207	11046	5.079	11046	0.000	0.000
0.800	−4610	8704	4.161	8704	0.000	0.000
0.900	−3591	5058	2.703	5058	0.000	0.000
1.000	0	0	0.000	0	0.000	0.000

Reference states: Gd(liquid), Mo(liquid)

Table IIIb. Partial quantities for Gd in the liquid phase at 3200 K.

x_{Gd}	ΔG_{Gd} [J/mol]	ΔH_{Gd} [J/mol]	ΔS_{Gd} [J/(mol·K)]	$G_{\mathrm{Gd}}^{\mathrm{E}}$ [J/mol]	$S_{\mathrm{Gd}}^{\mathrm{E}}$ [J/(mol·K)]	a_{Gd}	γ_{Gd}
1.000	0	0	0.000	0	0.000	1.000	1.000
0.900	−2547	256	0.876	256	0.000	0.909	1.010
0.800	−4769	1168	1.855	1168	0.000	0.836	1.045
0.700	−6538	2952	2.966	2952	0.000	0.782	1.117
0.600	−7767	5824	4.247	5824	0.000	0.747	1.245
0.500	−8442	10000	5.763	10000	0.000	0.728	1.456
0.400	−8683	15696	7.619	15696	0.000	0.722	1.804
0.300	−8905	23128	10.010	23128	0.000	0.716	2.385
0.200	−10309	32512	13.382	32512	0.000	0.679	3.394
0.100	−17200	44064	19.145	44064	0.000	0.524	5.239
0.000	$-\infty$	58000	∞	58000	0.000	0.000	8.846

Reference state: Gd(liquid)

Table IIIc. Partial quantities for Mo in the liquid phase at 3200 K.

x_{Mo}	ΔG_{Mo} [J/mol]	ΔH_{Mo} [J/mol]	ΔS_{Mo} [J/(mol·K)]	$G_{\mathrm{Mo}}^{\mathrm{E}}$ [J/mol]	$S_{\mathrm{Mo}}^{\mathrm{E}}$ [J/(mol·K)]	a_{Mo}	γ_{Mo}
0.000	$-\infty$	40000	∞	40000	0.000	0.000	4.497
0.100	−25948	35316	19.145	35316	0.000	0.377	3.771
0.200	−12613	30208	13.382	30208	0.000	0.622	3.112
0.300	−7141	24892	10.010	24892	0.000	0.765	2.549
0.400	−4795	19584	7.619	19584	0.000	0.835	2.088
0.500	−3942	14500	5.763	14500	0.000	0.862	1.725
0.600	−3735	9856	4.247	9856	0.000	0.869	1.448
0.700	−3622	5868	2.966	5868	0.000	0.873	1.247
0.800	−3185	2752	1.855	2752	0.000	0.887	1.109
0.900	−2079	724	0.876	724	0.000	0.925	1.028
1.000	0	0	0.000	0	0.000	1.000	1.000

Reference state: Mo(liquid)

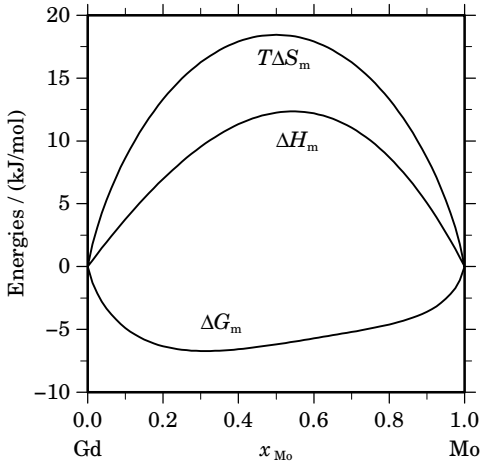

Fig. 2. Integral quantities of the liquid phase at T=3200 K.

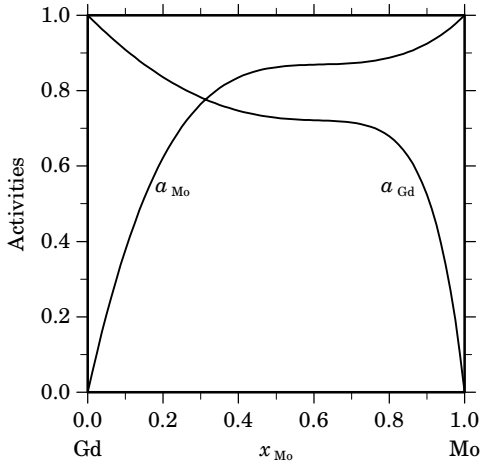

Fig. 3. Activities in the liquid phase at T=3200 K.

References

[1966Chu] Y.-C. Chuang, C.-W. Li, H.-L. Chuang, L.-M. Kao: Acta Metall. Sinica **9** (1966) 110–112.
[2001Zin] M. Zinkevich, N. Mattern, H.J. Seifert: J. Phase Equilibria **22** (2001) 43–50.

Gd – Zr (Gadolinium – Zirconium)

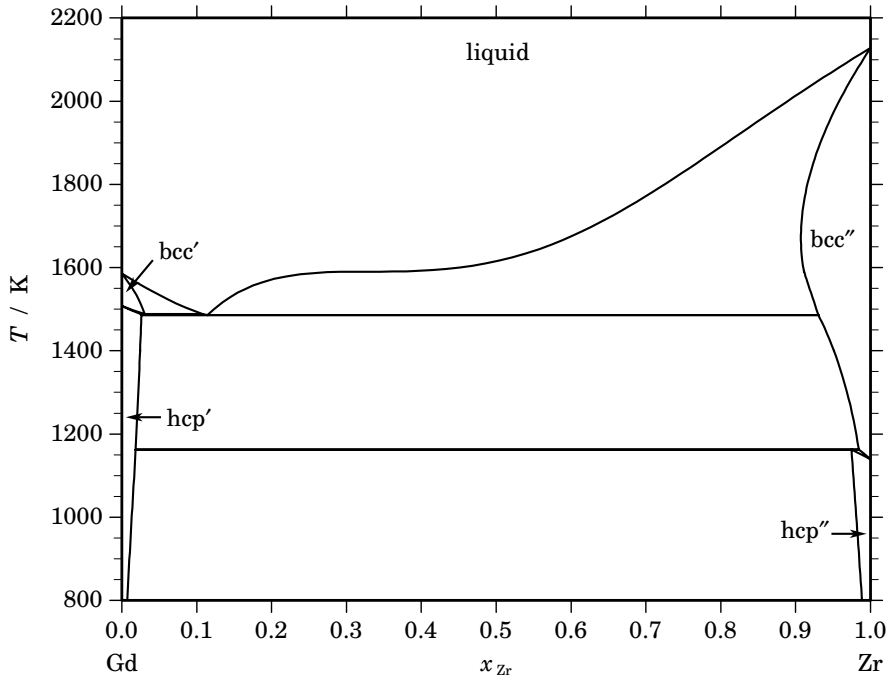

Fig. 1. Calculated phase diagram for the system Gd-Zr.

The interest in the Gd-Zr system is related to ternary and higher systems, e.g.. with iron, where intermetallic compounds with interesting magnetic properties are found. The presence of Zr enables also the formation of metallic glasses. The phase diagram of the Gd-Zr systems is of eutectic type with no intermetallic phases and limited mutual solubility in the terminal phases. The phase diagram has been investigated by Copeland and co-workers [1961Cop, 1964Cop]. No investigations of the thermodynamic mixing properties are known. Based on these limited data, a thermodynamic dataset for Gd-Zr has been optimised by [2001Zin].

Table I. Phases, structures and models.

Phase	Struktur-bericht	Prototype	Pearson symbol	Space group	SGTE name	Model
liquid					LIQUID	$(Gd,Zr)_1$
bcc	$A2$	W	$cI2$	$Im\bar{3}m$	BCC_A2	$(Gd,Zr)_1$
hcp	$A3$	Mg	$hP2$	$P6_3/mmc$	HCP_A3	$(Gd,Zr)_1$

Table II. Invariant reactions.

Reaction	Type	T / K	Compositions / x_{Zr}			$\Delta_r H$ / (J/mol)
bcc′ ⇌ hcp′ + liquid	metatectic	1488.5	0.030	0.025	0.108	−3894
liquid ⇌ hcp′ + bcc″	eutectic	1485.6	0.114	0.026	0.930	−15380
hcp′ + bcc″ ⇌ hcp″	peritectoid	1162.4	0.019	0.984	0.974	−4346

Table IIIa. Integral quantities for the liquid phase at 2200 K.

x_{Zr}	ΔG_{m} [J/mol]	ΔH_{m} [J/mol]	ΔS_{m} [J/(mol·K)]	$G^{\mathrm{E}}_{\mathrm{m}}$ [J/mol]	$S^{\mathrm{E}}_{\mathrm{m}}$ [J/(mol·K)]	ΔC_P [J/(mol·K)]
0.000	0	0	0.000	0	0.000	0.000
0.100	−3302	2265	2.531	2644	−0.172	0.000
0.200	−4695	3785	3.855	4458	−0.306	0.000
0.300	−5641	4649	4.677	5533	−0.402	0.000
0.400	−6352	4949	5.137	5959	−0.459	0.000
0.500	−6851	4777	5.285	5828	−0.478	0.000
0.600	−7079	4222	5.137	5231	−0.459	0.000
0.700	−6915	3376	4.677	4259	−0.402	0.000
0.800	−6151	2329	3.855	3002	−0.306	0.000
0.900	−4394	1174	2.531	1552	−0.172	0.000
1.000	0	0	0.000	0	0.000	0.000

Reference states: Gd(liquid), Zr(liquid)

Table IIIb. Partial quantities for Gd in the liquid phase at 2200 K.

x_{Gd}	ΔG_{Gd} [J/mol]	ΔH_{Gd} [J/mol]	ΔS_{Gd} [J/(mol·K)]	$G^{\mathrm{E}}_{\mathrm{Gd}}$ [J/mol]	$S^{\mathrm{E}}_{\mathrm{Gd}}$ [J/(mol·K)]	a_{Gd}	γ_{Gd}
1.000	0	0	0.000	0	0.000	1.000	1.000
0.900	−1497	388	0.857	430	−0.019	0.921	1.024
0.800	−2482	1431	1.779	1600	−0.076	0.873	1.091
0.700	−3198	2948	2.793	3326	−0.172	0.840	1.199
0.600	−3916	4755	3.941	5428	−0.306	0.807	1.345
0.500	−4955	6672	5.285	7724	−0.478	0.763	1.525
0.400	−6730	8516	6.930	10030	−0.688	0.692	1.730
0.300	−9856	10105	9.073	12167	−0.937	0.583	1.945
0.200	−15490	11258	12.158	13950	−1.224	0.429	2.144
0.100	−26919	11792	17.596	15199	−1.549	0.230	2.295
0.000	$-\infty$	11525	∞	15732	−1.912	0.000	2.363

Reference state: Gd(liquid)

Table IIIc. Partial quantities for Zr in the liquid phase at 2200 K.

x_{Zr}	ΔG_{Zr} [J/mol]	ΔH_{Zr} [J/mol]	ΔS_{Zr} [J/(mol·K)]	$G^{\mathrm{E}}_{\mathrm{Zr}}$ [J/mol]	$S^{\mathrm{E}}_{\mathrm{Zr}}$ [J/(mol·K)]	a_{Zr}	γ_{Zr}
0.000	$-\infty$	26688	∞	30895	−1.912	0.000	5.414
0.100	−19550	19161	17.596	22568	−1.549	0.343	3.434
0.200	−13549	13199	12.158	15891	−1.224	0.477	2.384
0.300	−11342	8619	9.073	10681	−0.937	0.538	1.793
0.400	−10006	5241	6.930	6755	−0.688	0.579	1.447
0.500	−8746	2881	5.285	3933	−0.478	0.620	1.240
0.600	−7312	1359	3.941	2032	−0.306	0.670	1.117
0.700	−5654	491	2.793	870	−0.172	0.734	1.049
0.800	−3816	97	1.779	265	−0.076	0.812	1.015
0.900	−1891	−6	0.857	36	−0.019	0.902	1.002
1.000	0	0	0.000	0	0.000	1.000	1.000

Reference state: Zr(liquid)

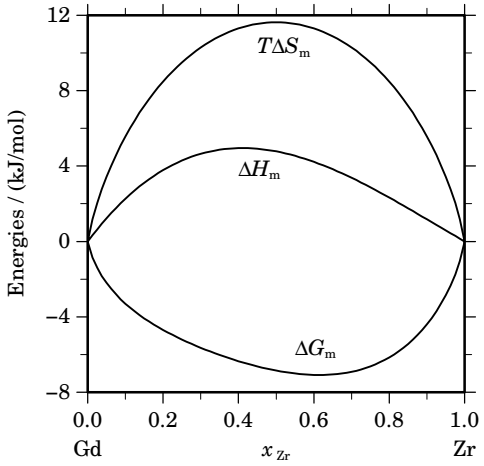

Fig. 2. Integral quantities of the liquid phase at T=2200 K.

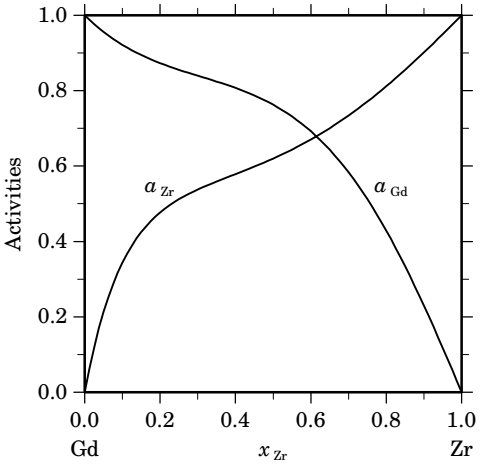

Fig. 3. Activities in the liquid phase at T=2200 K.

References

[1961Cop] M. Copeland, G. Kato, in: "Rare Earth Research", J.F. Nachman, C.E. Lundin (eds.), Plenum Press, New York, 1961, p 133.

[1964Cop] M. Copeland, H. Kato, in: "Physics and Material Problems of Reactor Control Rods", IAEA, Vienna, 1964, 295–317.

[2001Zin] M. Zinkevich, N. Mattern, H.J. Seifert: J. Phase Equilibria **22** (2001) 43–50.

Hf – Mo (Hafnium – Molybdenum)

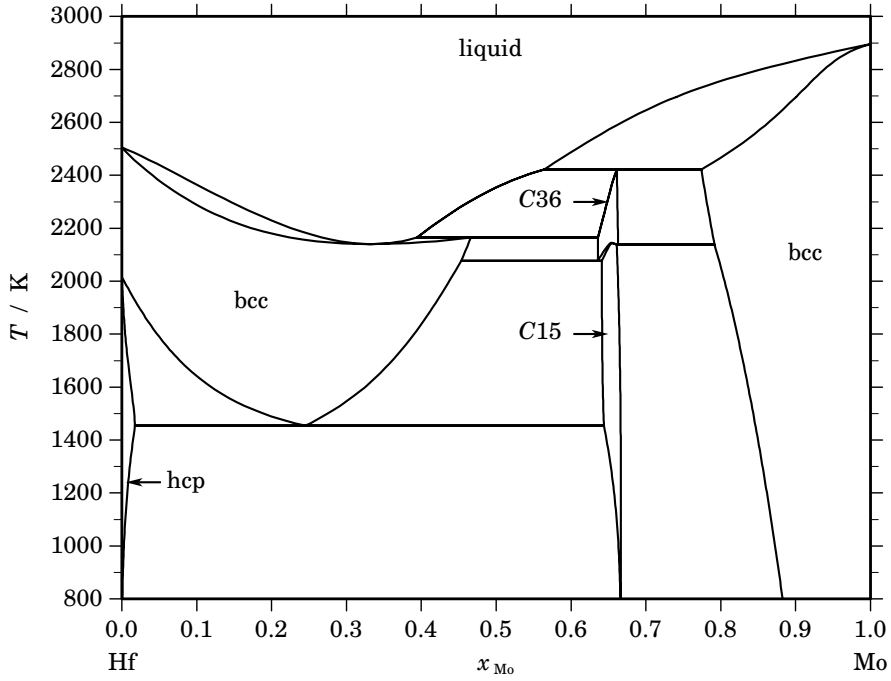

Fig. 1. Calculated phase diagram for the system Hf-Mo.

Hf, Mo and W are useful elements for developing refractory intermetallic alloys of high modulus and creep resistance at high temperatures. The experimental phase diagram of the Hf-Mo system is largely based on the early work of [1961Tay] and [1969Rud]. There was good agreement on the Mo-rich side, though discrepancy existed about phase equilibria on the Hf-rich part. [1969Rud] found a shallow minimum with congruent melting of the bcc solid solution as well as a peritectic reaction (liq + $C36 \rightleftharpoons$ bcc) instead of the eutectic reaction proposed by [1961Tay]. [1977Gar] proposed a less detailed phase diagram, obtained by gravimetric and pyrometric methods, in reasonable agreement with [1961Tay]. [1980Bre] presented a critical review of this system. The thermodynamic evaluation of the Hf-Mo system was made by [2002Sha], guided by the work of [1980Bre]. The bcc, hcp and liquid phases were described by a substitutional solution model using the Redlich-Kister equation, and the Laves phases $C15$ and $C36$ were described by a two-sublattice model. There is good overall agreement between the calculated phase diagram and experimental phase boundaries, particularly on the phase fields of the two Laves phases.

Table I. Phases, structures and models.

Phase	Struktur-bericht	Prototype	Pearson symbol	Space group	SGTE name	Model
liquid					LIQUID	$(Hf,Mo)_1$
bcc	$A2$	W	$cI2$	$Im\bar{3}m$	BCC_A2	$(Hf,Mo)_1$
hcp	$A3$	Mg	$hP2$	$P6_3/mmc$	HCP_A3	$(Hf,Mo)_1$
$C15$	$C15$	$MgCu_2$	$cF24$	$Fd\bar{3}m$	LAVES_C15	$(Hf,Mo)_2(Hf,Mo)_1$
$C36$	$C36$	$MgNi_2$	$hP24$	$P6_3/mmc$	LAVES_C36	$(Hf,Mo)_2(Hf,Mo)_1$

Table II. Invariant reactions.

Reaction	Type	T / K	Compositions / x_{Mo}			$\Delta_{\mathrm{r}}H$ / (J/mol)
liquid + bcc $\rightleftharpoons$ $C36$	peritectic	2422.2	0.564	0.774	0.661	−20551
liquid + $C36$ $\rightleftharpoons$ bcc	peritectic	2164.5	0.394	0.636	0.466	−18053
$C36$ $\rightleftharpoons$ $C15$	congruent	2149.4	0.657	0.657		−1390
liquid $\rightleftharpoons$ bcc	congruent	2140.2	0.334	0.334		−25874
$C36$ $\rightleftharpoons$ $C15$ + bcc	eutectoid	2138.4	0.663	0.661	0.792	−1427
$C36$ $\rightleftharpoons$ bcc + $C15$	eutectoid	2076.7	0.636	0.453	0.641	−1069
bcc $\rightleftharpoons$ hcp + $C15$	eutectoid	1454.1	0.245	0.018	0.644	−14023

Table IIIa. Integral quantities for the liquid phase at 2900 K.

x_{Mo}	ΔG_{m} [J/mol]	ΔH_{m} [J/mol]	ΔS_{m} [J/(mol·K)]	$G_{\mathrm{m}}^{\mathrm{E}}$ [J/mol]	$S_{\mathrm{m}}^{\mathrm{E}}$ [J/(mol·K)]	ΔC_P [J/(mol·K)]
0.000	0	0	0.000	0	0.000	0.000
0.100	−13120	1241	4.952	−5282	2.249	0.000
0.200	−20280	718	7.241	−8214	3.080	0.000
0.300	−23992	−1011	7.925	−9263	2.845	0.000
0.400	−25107	−3387	7.489	−8879	1.894	0.000
0.500	−24213	−5854	6.331	−7499	0.567	0.000
0.600	−21775	−7851	4.801	−5548	−0.794	0.000
0.700	−18163	−8823	3.221	−3433	−1.859	0.000
0.800	−13618	−8210	1.865	−1552	−2.296	0.000
0.900	−8123	−5455	0.920	−285	−1.783	0.000
1.000	0	0	0.000	0	0.000	0.000

Reference states: Hf(liquid), Mo(liquid)

Table IIIb. Partial quantities for Hf in the liquid phase at 2900 K.

x_{Hf}	ΔG_{Hf} [J/mol]	ΔH_{Hf} [J/mol]	ΔS_{Hf} [J/(mol·K)]	$G_{\mathrm{Hf}}^{\mathrm{E}}$ [J/mol]	$S_{\mathrm{Hf}}^{\mathrm{E}}$ [J/(mol·K)]	a_{Hf}	γ_{Hf}
1.000	0	0	0.000	0	0.000	1.000	1.000
0.900	−3794	975	1.644	−1253	0.768	0.854	0.949
0.800	−9766	3155	4.456	−4386	2.600	0.667	0.834
0.700	−17088	5426	7.763	−8488	4.798	0.492	0.703
0.600	−25010	6670	10.924	−12693	6.677	0.354	0.591
0.500	−32888	5772	13.331	−16174	7.568	0.256	0.511
0.400	−40242	1615	14.433	−18148	6.815	0.188	0.471
0.300	−46902	−6916	13.788	−17872	3.778	0.143	0.477
0.200	−53452	−20937	11.212	−14645	−2.170	0.109	0.545
0.100	−63329	−41564	7.505	−7809	−11.640	0.072	0.723
0.000	$-\infty$	−69914	∞	3253	−25.230	0.000	1.144

Reference state: Hf(liquid)

Table IIIc. Partial quantities for Mo in the liquid phase at 2900 K.

x_{Mo}	ΔG_{Mo} [J/mol]	ΔH_{Mo} [J/mol]	ΔS_{Mo} [J/(mol·K)]	$G^{\mathrm{E}}_{\mathrm{Mo}}$ [J/mol]	$S^{\mathrm{E}}_{\mathrm{Mo}}$ [J/(mol·K)]	a_{Mo}	γ_{Mo}
0.000	$-\infty$	23086	∞	−66147	30.770	0.000	0.064
0.100	−97058	3634	34.721	−41538	15.576	0.018	0.179
0.200	−62335	−9033	18.380	−23528	4.998	0.075	0.377
0.300	−40101	−16030	8.300	−11071	−1.710	0.190	0.632
0.400	−25251	−18473	2.337	−3158	−5.281	0.351	0.877
0.500	−15538	−17479	−0.669	1176	−6.432	0.525	1.050
0.600	−9464	−14162	−1.620	2853	−5.867	0.675	1.126
0.700	−5846	−9640	−1.309	2755	−4.274	0.785	1.121
0.800	−3659	−5029	−0.472	1721	−2.328	0.859	1.074
0.900	−1989	−1443	0.188	551	−0.688	0.921	1.023
1.000	0	0	0.000	0	0.000	1.000	1.000

Reference state: Mo(liquid)

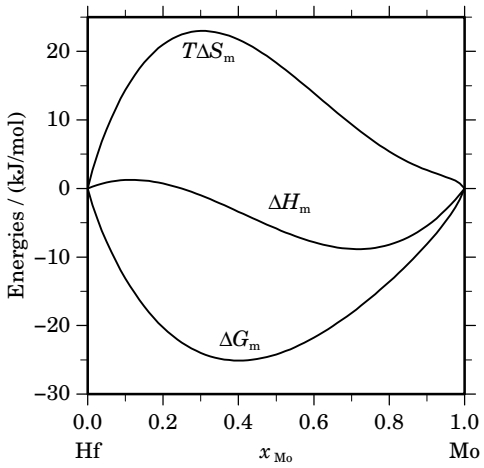

Fig. 2. Integral quantities of the liquid phase at T=2900 K.

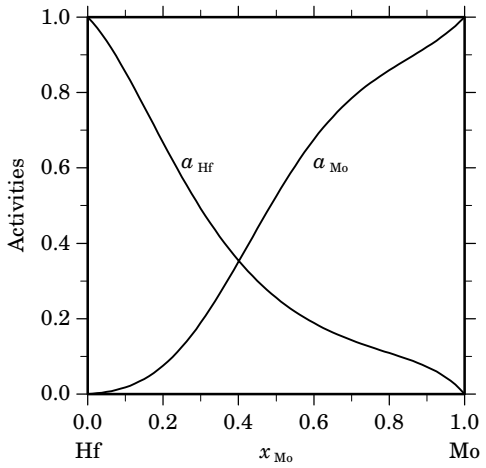

Fig. 3. Activities in the liquid phase at T=2900 K.

Table IVa. Integral quantities for the stable phases at 2050 K.

Phase	x_{Mo}	ΔG_{m} [J/mol]	ΔH_{m} [J/mol]	ΔS_{m} [J/(mol·K)]	$G^{\mathrm{E}}_{\mathrm{m}}$ [J/mol]	$S^{\mathrm{E}}_{\mathrm{m}}$ [J/(mol·K)]	ΔC_P [J/(mol·K)]
bcc	0.000	0	0	0.000	0	0.000	0.000
	0.100	−6470	3447	4.838	−929	2.135	0.000
	0.200	−9735	4259	6.826	−1205	2.666	0.000
	0.300	−11588	3112	7.171	−1176	2.092	0.000
	0.400	−12556	696	6.465	−1085	0.869	0.000
	0.448	−12787	−702	5.895	−1066	0.178	0.000
$C15$	0.641	−13451	−11144	1.125	−2325	−4.302	2.374
	0.662	−13315	−12317	0.487	−2413	−4.831	2.248
bcc	0.800	−9926	−7354	1.255	−1407	−2.901	0.000
	0.900	−6621	−5265	0.662	−1081	−2.041	0.000
	1.000	0	0	0.000	0	0.000	0.000

Reference states: Hf(bcc), Mo(bcc)

Table IVb. Partial quantities for Hf in the stable phases at 2050 K.

Phase	x_{Hf}	ΔG_{Hf} [J/mol]	ΔH_{Hf} [J/mol]	ΔS_{Hf} [J/(mol·K)]	$G^{\mathrm{E}}_{\mathrm{Hf}}$ [J/mol]	$S^{\mathrm{E}}_{\mathrm{Hf}}$ [J/(mol·K)]	a_{Hf}	γ_{Hf}
bcc	1.000	0	0	0.000	0	0.000	1.000	1.000
	0.900	−2189	1429	1.765	−393	0.889	0.879	0.977
	0.800	−4861	4822	4.723	−1058	2.868	0.752	0.940
	0.700	−7532	8806	7.970	−1453	5.004	0.643	0.918
	0.600	−10052	11965	10.740	−1345	6.493	0.554	0.924
	0.552	−11249	12759	11.711	−1128	6.774	0.517	0.936
$C15$	0.359	−11249	23863	17.128	6218	8.607	0.517	1.440
	0.338	−29545	25079	26.646	−11048	17.623	0.177	0.523
bcc	0.200	−29545	−13559	7.798	−2077	−5.601	0.177	0.885
	0.100	−46022	−37195	4.306	−6775	−14.839	0.067	0.672
	0.000	$-\infty$	−71140	∞	−16077	−26.860	0.000	0.389
	0.100	−45760	−31229	7.265	−7470	−11.880	0.064	0.638
	0.000	$-\infty$	−65174	∞	−17373	−23.900	0.000	0.352

Reference state: Hf(bcc)

Table IVc. Partial quantities for Mo in the stable phases at 2050 K.

Phase	x_{Mo}	ΔG_{Mo} [J/mol]	ΔH_{Mo} [J/mol]	ΔS_{Mo} [J/(mol·K)]	$G^{\mathrm{E}}_{\mathrm{Mo}}$ [J/mol]	$S^{\mathrm{E}}_{\mathrm{Mo}}$ [J/(mol·K)]	a_{Mo}	γ_{Mo}
bcc	0.000	$-\infty$	49860	∞	−13977	31.140	0.000	0.440
	0.100	−45001	21611	32.494	−5754	13.349	0.071	0.713
	0.200	−29228	2010	15.238	−1795	1.856	0.180	0.900
	0.300	−21051	−10172	5.306	−529	−4.704	0.291	0.969
	0.400	−16312	−16207	0.051	−694	−7.567	0.384	0.960
	0.448	−14684	−17302	−1.277	−989	−7.958	0.423	0.944
$C15$	0.641	−14684	−30739	−7.832	−7107	−11.528	0.423	0.659
	0.662	−5034	−31396	−12.860	1993	−16.287	0.744	1.124
bcc	0.800	−5034	−5806	−0.377	−1239	−2.228	0.744	0.930
	0.900	−2244	−1717	0.257	−448	−0.619	0.877	0.974
	1.000	0	0	0.000	0	0.000	1.000	1.000

Reference state: Mo(bcc)

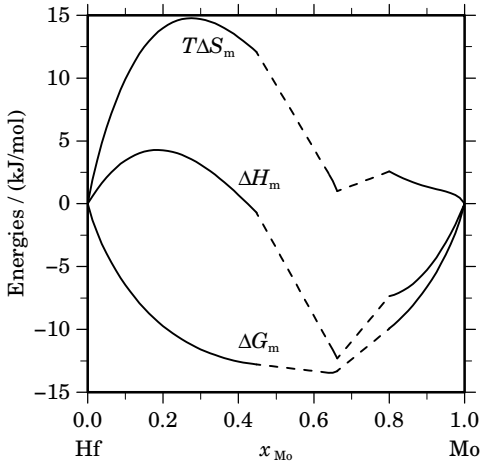

Fig. 4. Integral quantities of the stable phases at T=2050 K.

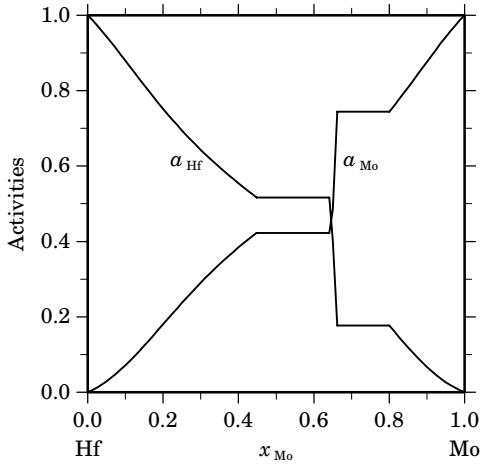

Fig. 5. Activities in the stable phases at T=2050 K.

Table V. Standard reaction quantities at 298.15 K for the compounds per mole of atoms.

Compound	x_{Mo}	$\Delta_{\mathrm{f}}G^{\circ}$ / (J/mol)	$\Delta_{\mathrm{f}}H^{\circ}$ / (J/mol)	$\Delta_{\mathrm{f}}S^{\circ}$ / (J/(mol·K))	$\Delta_{\mathrm{f}}C_P^{\circ}$ / (J/(mol·K))
$C15$	0.667	−11058	−10700	1.200	0.000

References

[1961Tay] A. Taylor, N.J. Doyle, B.J. Kagle: J. Less-Common Met. **3** (1961) 265–280.

[1969Rud] E. Rudy: Compendium of Phase Diagram Data, AFML, Wright-Patterson AFB, Ohio, Rep. No. AFML-TR-65-2, Part 5, 1969.

[1977Gar] S.P. Garg, R.J. Ackermann: Metall. Trans. A **8A** (1977) 239–244.

[1980Bre] L. Brewer, R.H. Lamoreaux in: "Molybdenum: Physico-Chemical Properties of its Compounds and Alloys", L. Brewer (ed.), Atomic Energy Rev. Spec. Issue 7, IAEA, Vienna, 1980.

[2002Sha] G. Shao: Intermetallics **10** (2002) 429–434.

Hf – Nb (Hafnium – Niobium)

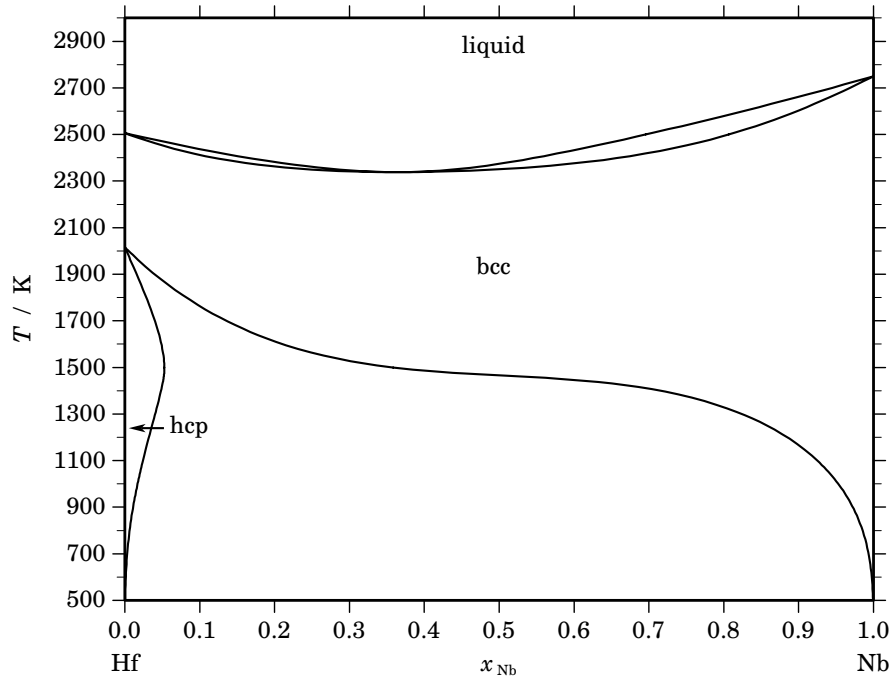

Fig. 1. Calculated phase diagram for the system Hf-Nb.

The Hf-Nb system has been reviewed and a thermodynamic dataset has been optimised in [1996Fer]. The phase diagram consists of three phases only, the liquid and bcc phases with complete miscibility and the hcp phase which has only limited solubility for Nb. The selected data for the assessment determine the melting equilibria [1964Tyl, 1969Rud] and the solid phase equilibria between bcc and hcp [1964Sie, 1964Tyl, 1971Car]. Since no experimental data for the thermodynamic mixing properties have been available various calculations and estimates from the literature have been used to approximate the mixing enthalpy for the liquid and solid alloys.

Table I. Phases, structures and models.

Phase	Struktur-bericht	Prototype	Pearson symbol	Space group	SGTE name	Model
liquid					LIQUID	$(Hf,Nb)_1$
bcc	$A2$	W	$cI2$	$Im\bar{3}m$	BCC_A2	$(Hf,Nb)_1$
hcp	$A3$	Mg	$hP2$	$P6_3/mmc$	HCP_A3	$(Hf,Nb)_1$

Table II. Invariant reactions.

Reaction	Type	T / K	Compositions / x_{Nb}		$\Delta_{\mathrm{r}}H$ / (J/mol)
liquid $\rightleftharpoons$ bcc	congruent	2338.2	0.365	0.365	-24688

Table IIIa. Integral quantities for the liquid phase at 2800 K.

x_{Nb}	ΔG_{m} [J/mol]	ΔH_{m} [J/mol]	ΔS_{m} [J/(mol·K)]	$G_{\mathrm{m}}^{\mathrm{E}}$ [J/mol]	$S_{\mathrm{m}}^{\mathrm{E}}$ [J/(mol·K)]	ΔC_P [J/(mol·K)]
0.000	0	0	0.000	0	0.000	0.000
0.100	−6640	928	2.703	928	0.000	0.000
0.200	−9969	1680	4.161	1680	0.000	0.000
0.300	−11975	2246	5.079	2246	0.000	0.000
0.400	−13055	2613	5.596	2613	0.000	0.000
0.500	−13366	2771	5.763	2771	0.000	0.000
0.600	−12962	2706	5.596	2706	0.000	0.000
0.700	−11813	2409	5.079	2409	0.000	0.000
0.800	−9784	1866	4.161	1866	0.000	0.000
0.900	−6501	1067	2.703	1067	0.000	0.000
1.000	0	0	0.000	0	0.000	0.000

Reference states: Hf(liquid), Nb(liquid)

Table IIIb. Partial quantities for Hf in the liquid phase at 2800 K.

x_{Hf}	ΔG_{Hf} [J/mol]	ΔH_{Hf} [J/mol]	ΔS_{Hf} [J/(mol·K)]	$G_{\mathrm{Hf}}^{\mathrm{E}}$ [J/mol]	$S_{\mathrm{Hf}}^{\mathrm{E}}$ [J/(mol·K)]	a_{Hf}	γ_{Hf}
1.000	0	0	0.000	0	0.000	1.000	1.000
0.900	−2367	86	0.876	86	0.000	0.903	1.004
0.800	−4837	358	1.855	358	0.000	0.812	1.016
0.700	−7463	841	2.966	841	0.000	0.726	1.037
0.600	−10336	1557	4.247	1557	0.000	0.641	1.069
0.500	−13608	2529	5.763	2529	0.000	0.557	1.115
0.400	−17551	3781	7.619	3781	0.000	0.471	1.176
0.300	−22693	5336	10.010	5336	0.000	0.377	1.258
0.200	−30252	7217	13.382	7217	0.000	0.273	1.363
0.100	−44159	9447	19.145	9447	0.000	0.150	1.500
0.000	$-\infty$	12050	∞	12050	0.000	0.000	1.678

Reference state: Hf(liquid)

Table IIIc. Partial quantities for Nb in the liquid phase at 2800 K.

x_{Nb}	ΔG_{Nb} [J/mol]	ΔH_{Nb} [J/mol]	ΔS_{Nb} [J/(mol·K)]	$G_{\mathrm{Nb}}^{\mathrm{E}}$ [J/mol]	$S_{\mathrm{Nb}}^{\mathrm{E}}$ [J/(mol·K)]	a_{Nb}	γ_{Nb}
0.000	$-\infty$	10116	∞	10116	0.000	0.000	1.544
0.100	−45098	8507	19.145	8507	0.000	0.144	1.441
0.200	−30500	6969	13.382	6969	0.000	0.270	1.349
0.300	−22504	5525	10.010	5525	0.000	0.380	1.268
0.400	−17133	4199	7.619	4199	0.000	0.479	1.198
0.500	−13125	3012	5.763	3012	0.000	0.569	1.138
0.600	−9903	1990	4.247	1990	0.000	0.654	1.089
0.700	−7150	1154	2.966	1154	0.000	0.736	1.051
0.800	−4667	528	1.855	528	0.000	0.818	1.023
0.900	−2317	136	0.876	136	0.000	0.905	1.006
1.000	0	0	0.000	0	0.000	1.000	1.000

Reference state: Nb(liquid)

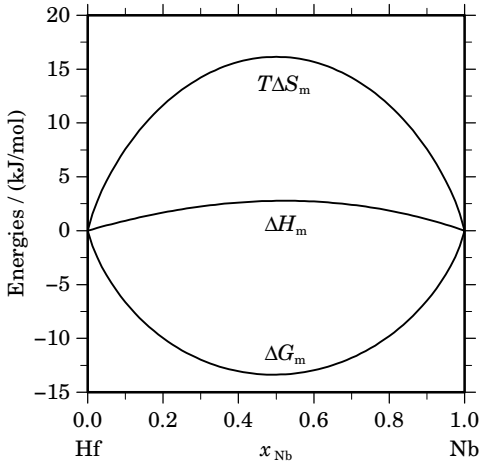

Fig. 2. Integral quantities of the liquid phase at T=2800 K.

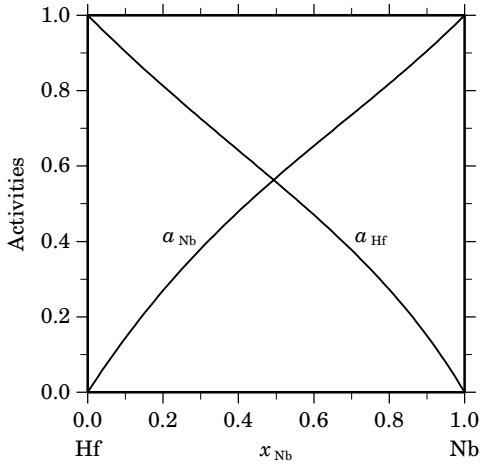

Fig. 3. Activities in the liquid phase at T=2800 K.

Table IVa. Integral quantities for the stable phases at 2200 K.

Phase	x_{Nb}	ΔG_{m} [J/mol]	ΔH_{m} [J/mol]	ΔS_{m} [J/(mol·K)]	$G_{\mathrm{m}}^{\mathrm{E}}$ [J/mol]	$S_{\mathrm{m}}^{\mathrm{E}}$ [J/(mol·K)]	ΔC_P [J/(mol·K)]
bcc	0.000	0	0	0.000	0	0.000	0.000
	0.100	−3889	2057	2.703	2057	0.000	0.000
	0.200	−5501	3652	4.161	3652	0.000	0.000
	0.300	−6389	4785	5.079	4785	0.000	0.000
	0.400	−6851	5460	5.596	5460	0.000	0.000
	0.500	−7001	5678	5.763	5678	0.000	0.000
	0.600	−6868	5442	5.596	5442	0.000	0.000
	0.700	−6420	4754	5.079	4754	0.000	0.000
	0.800	−5537	3616	4.161	3616	0.000	0.000
	0.900	−3915	2031	2.703	2031	0.000	0.000
	1.000	0	0	0.000	0	0.000	0.000

Reference states: Hf(bcc), Nb(bcc)

Table IVb. Partial quantities for Hf in the stable phases at 2200 K.

Phase	x_{Hf}	ΔG_{Hf} [J/mol]	ΔH_{Hf} [J/mol]	ΔS_{Hf} [J/(mol·K)]	$G_{\mathrm{Hf}}^{\mathrm{E}}$ [J/mol]	$S_{\mathrm{Hf}}^{\mathrm{E}}$ [J/(mol·K)]	a_{Hf}	γ_{Hf}
bcc	1.000	0	0	0.000	0	0.000	1.000	1.000
	0.900	−1695	232	0.876	232	0.000	0.911	1.013
	0.800	−3157	925	1.855	925	0.000	0.841	1.052
	0.700	−4450	2074	2.966	2074	0.000	0.784	1.120
	0.600	−5669	3675	4.247	3675	0.000	0.734	1.223
	0.500	−6955	5724	5.763	5724	0.000	0.684	1.367
	0.400	−8544	8217	7.619	8217	0.000	0.627	1.567
	0.300	−10875	11148	10.010	11148	0.000	0.552	1.839
	0.200	−14927	14513	13.382	14513	0.000	0.442	2.211
	0.100	−23810	18309	19.145	18309	0.000	0.272	2.721
	0.000	$-\infty$	22529	∞	22529	0.000	0.000	3.427

Reference state: Hf(bcc)

Table IVc. Partial quantities for Nb in the stable phases at 2200 K.

Phase	x_{Nb}	ΔG_{Nb} [J/mol]	ΔH_{Nb} [J/mol]	ΔS_{Nb} [J/(mol·K)]	$G^{\mathrm{E}}_{\mathrm{Nb}}$ [J/mol]	$S^{\mathrm{E}}_{\mathrm{Nb}}$ [J/(mol·K)]	a_{Nb}	γ_{Nb}
bcc	0.000	$-\infty$	22898	∞	22898	0.000	0.000	3.497
	0.100	−23631	18487	19.145	18487	0.000	0.275	2.747
	0.200	−14880	14560	13.382	14560	0.000	0.443	2.217
	0.300	−10911	11112	10.010	11112	0.000	0.551	1.836
	0.400	−8624	8137	7.619	8137	0.000	0.624	1.560
	0.500	−7047	5632	5.763	5632	0.000	0.680	1.361
	0.600	−5751	3593	4.247	3593	0.000	0.730	1.217
	0.700	−4510	2014	2.966	2014	0.000	0.781	1.116
	0.800	−3189	892	1.855	892	0.000	0.840	1.050
	0.900	−1705	222	0.876	222	0.000	0.911	1.012
	1.000	0	0	0.000	0	0.000	1.000	1.000

Reference state: Nb(bcc)

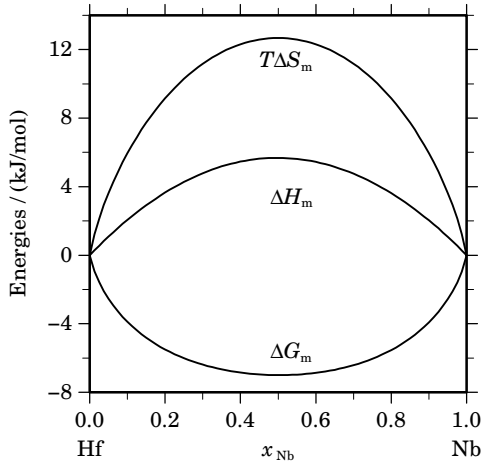

Fig. 4. Integral quantities of the stable phases at T=2200 K.

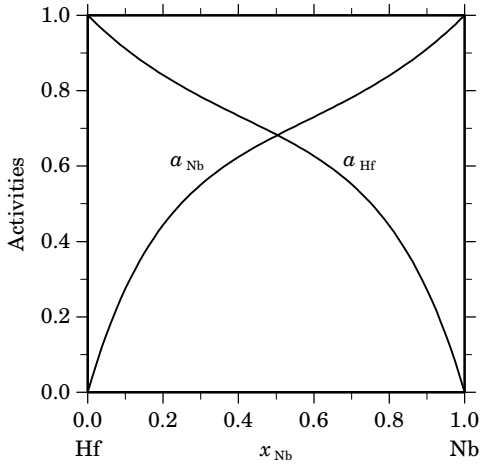

Fig. 5. Activities in the stable phases at T=2200 K.

References

[1964Sie] R.E. Siemens, H.R. Babitzke, H. Kato: U.S. Bur. Mines Rep. Invest. 6492, Washington DC., 1964

[1964Tyl] M.A. Tylkina, I.A. Tsyganova, E.M. Savitskii: Zh. Neorg. Khim. **9** (1964) 1650–1652; Russ. J. Inorg. Chem. **9** (1964) 893–895 (engl. transl.)

[1969Rud] E. Rudy: Tech. Rep. AFML-TR-65-2, Part V, Wright-Patterson AFB, OH, 1969, pp. 95–96.

[1971Car] R.W. Carpenter, C.T. Liu, P.G. Mardon: Metall. Trans. **2** (1971) 125–131.

[1996Fer] A. Fernandez Guillermet: J. Alloys Comp. **234** (1996) 111-118.

Hf – Ni (Hafnium – Nickel)

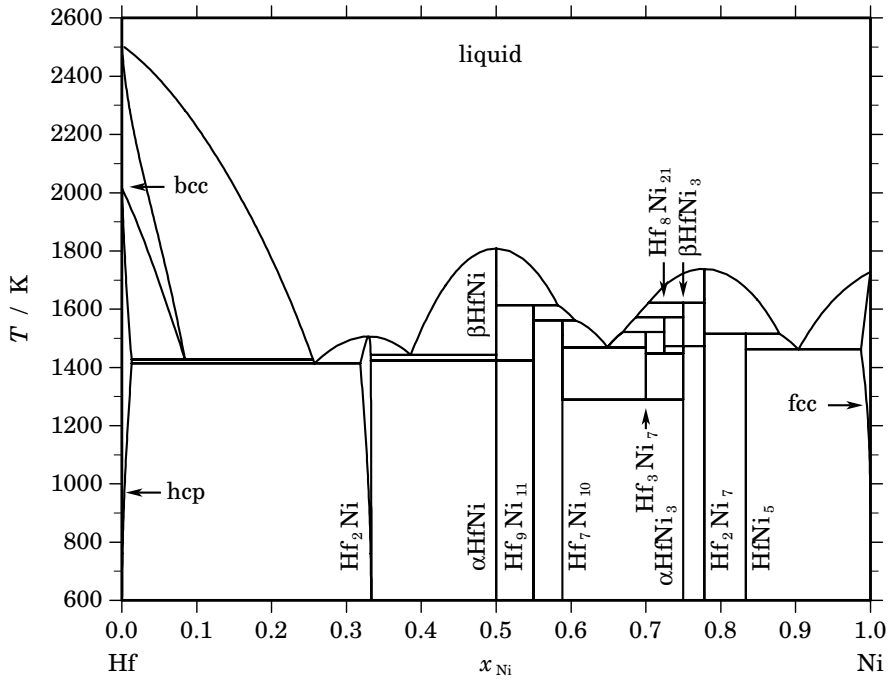

Fig. 1. Calculated phase diagram for the system Hf-Ni.

The Hf-Ni system attracts attention because Hf is a common addition to certain Ni-based superalloys where it can enhance the scale adhesion and lead to substantial gain refinement, and improve the oxidation resistance. A review on the Hf-Ni system has been given by [1983Nas] where the phase diagram has been based mainly on the results of[1967Sve, 1979Bse]. The Hf-rich part has been re-investigated by [1993Yer], the solubility of Hf in fcc-Ni has been derived from X-ray measurements of the lattice parameter [1998Haj] and sub-solidus equilibria have been investigated by [2001Wan] at two temperatures using diffusion couples which have been analysed by an electron microprobe. [1992Sel] studied the Ni-rich liquid phase by dissolution of Hf in the liquid alloy at 1743 and 1633 K, and measured the integral enthalpy of formation and the partial enthalpy of hafnium by calorimetry. Using direct reaction calorimetry, the enthalpies of formation of five compounds $HfNi_5$, Hf_2Ni_7, Hf_9Ni_{11}, HfNi, Hf_2Ni were measured [1992Sel]. [1996Ben] measured the equilibrium vapour pressure of Ni over all intermediate compounds by the Knudsen-effusion technique, and the enthalpies of formation of compounds were determined by means of the second and third law methods. [1995Guo, 1998Guo] determined the standard enthalpies of formation of Hf_2Ni_7, $HfNi_{11}$, $HfNi_3$, HfNi by high-temperature direct synthesis calorimetry. The present assessment of [2001Wan] is based mainly on the selected phase equilibrium data from [1993Yer] for the Hf-rich part and from [1967Sve] and [1979Bse] for other regions. The terminal solid solutions bcc, hcp, fcc and the liquid phase were described by substitutional solution models using the Redlich-Kister equation. The Hf_2Ni has a finite range of homogeneity and a two-sublattice model is used to described this phase with the $C16$ structure. The eight stable intermediate compounds $HfNi_5$, Hf_2Ni_7, $\alpha HfNi_3$ and $\beta HfNi_3$, Hf_8Ni_{21}, Hf_3Ni_7, Hf_7Ni_{10}, Hf_9Ni_{11}, αHfNi and βHfNi show very restricted homogeneity range and are considered as stoichiometric in this assessment. There is good agreement between the calculated phase diagram and experimental phase boundaries, although the range of the bcc phase is different from that suggested by [1983Nas]. The proposed solubility by [1983Nas] cause a very steep slope which is thermodynamically improbable [1991Oka]. The calculated quantities are consistent with most of the experimental data.

Table I. Phases, structures and models.

Phase	Struktur-bericht	Prototype	Pearson symbol	Space group	SGTE name	Model
liquid					LIQUID	$(Hf,Ni)_1$
bcc	$A2$	W	$cI2$	$Im\overline{3}m$	BCC_A2	$(Hf,Ni)_1$
hcp	$A3$	Mg	$hP2$	$P6_3/mmc$	HCP_A3	$(Hf,Ni)_1$
Hf_2Ni	$C16$	Al_2Cu	$tI12$	$I4/mcm$	HF2NI	$Hf_2(Ni,\Box)_1$
αHfNi	$B33$	CrB	$oC8$	$Cmcm$	HFNI_A	Hf_1Ni_1
βHfNi	···	···	···	···	HFNI_B	Hf_1Ni_1
Hf_9Ni_{11}	···	···	tI*	$I4/m$	HF9NI11	Hf_9Ni_{11}
Hf_7Ni_{10}	···	···	$oC68$	$C2ca$	HF7NI10	Hf_7Ni_{10}
Hf_3Ni_7	···	···	$aP20$	$P\overline{1}$	HF3NI7	Hf_3Ni_7
Hf_8Ni_{21}	···	···	$aP29$	$P\overline{1}$	HF8NI21	Hf_8Ni_{21}
$\alpha HfNi_3$	···	···	$hR12$	$R\overline{3}m$	HFNI3_A	Hf_1Ni_3
$\beta HfNi_3$	···	···	$hP40$	$P6_3/mmc$	HFNI3_B	Hf_1Ni_3
Hf_2Ni_7	···	···	$m*$*	···	HF2NI7	Hf_2Ni_7
$HfNi_5$	$C15_b$	$AuBe_5$	$cF24$	$F\overline{4}3m$	HFNI5	Hf_1Ni_5
fcc	$A1$	Cu	$cF4$	$Fm\overline{3}m$	FCC_A1	$(Hf,Ni)_1$

Table II. Invariant reactions.

Reaction	Type	T / K	Compositions / x_{Ni}			$\Delta_r H$ / (J/mol)
liquid $\rightleftharpoons$ βHfNi	congruent	1808.5	0.500	0.500		−14756
liquid $\rightleftharpoons$ Hf_2Ni_7	congruent	1738.5	0.778	0.778		−18892
liquid + Hf_2Ni_7 $\rightleftharpoons$ $\beta HfNi_3$	peritectic	1621.5	0.704	0.778	0.750	−3766
βHfNi + liquid $\rightleftharpoons$ Hf_9Ni_{11}	peritectic	1613.7	0.500	0.582	0.550	−9759
liquid + $\beta HfNi_3$ $\rightleftharpoons$ Hf_8Ni_{21}	peritectic	1573.0	0.687	0.750	0.724	−3727
Hf_9Ni_{11} + liquid $\rightleftharpoons$ Hf_7Ni_{10}	peritectic	1561.6	0.550	0.605	0.588	−9101
liquid + Hf_8Ni_{21} $\rightleftharpoons$ Hf_3Ni_7	peritectic	1521.8	0.669	0.724	0.700	−5281
Hf_2Ni_7 + liquid $\rightleftharpoons$ $HfNi_5$	peritectic	1516.1	0.778	0.878	0.833	−13605
liquid $\rightleftharpoons$ Hf_2Ni	congruent	1507.0	0.330	0.330		−14686
$\beta HfNi_3$ $\rightleftharpoons$ $\alpha HfNi_3$	polymorphic	1472.8	0.750	0.750		−3000
liquid $\rightleftharpoons$ Hf_7Ni_{10} + Hf_3Ni_7	eutectic	1468.9	0.649	0.588	0.700	−11562
liquid $\rightleftharpoons$ $HfNi_5$ + fcc	eutectic	1461.8	0.904	0.833	0.987	−16358
Hf_8Ni_{21} $\rightleftharpoons$ Hf_3Ni_7 + $\alpha HfNi_3$	eutectoid	1448.0	0.724	0.700	0.750	−2403
liquid $\rightleftharpoons$ Hf_2Ni + βHfNi	eutectic	1443.2	0.386	0.332	0.500	−13169
bcc $\rightleftharpoons$ hcp + liquid	metatectic	1427.6	0.084	0.013	0.255	−2109
βHfNi $\rightleftharpoons$ αHfNi	polymorphic	1423.1	0.500	0.500		−3000
liquid $\rightleftharpoons$ hcp + Hf_2Ni	eutectic	1414.3	0.257	0.013	0.318	−14921
Hf_3Ni_7 $\rightleftharpoons$ Hf_7Ni_{10} + $\alpha HfNi_3$	eutectoid	1289.3	0.700	0.588	0.750	−2900

Table IIIa. Integral quantities for the liquid phase at 2600 K.

x_{Ni}	ΔG_{m} [J/mol]	ΔH_{m} [J/mol]	ΔS_{m} [J/(mol·K)]	$G_{\mathrm{m}}^{\mathrm{E}}$ [J/mol]	$S_{\mathrm{m}}^{\mathrm{E}}$ [J/(mol·K)]	ΔC_P [J/(mol·K)]
0.000	0	0	0.000	0	0.000	0.000
0.100	−21408	−15537	2.258	−14380	−0.445	0.000
0.200	−36526	−30224	2.424	−25708	−1.737	0.000
0.300	−46866	−42816	1.557	−33660	−3.522	0.000
0.400	−52617	−52222	0.152	−38068	−5.444	0.000
0.500	−53899	−57503	−1.386	−38915	−7.149	0.000
0.600	−50890	−57875	−2.686	−36341	−8.282	0.000
0.700	−43845	−52710	−3.410	−30639	−8.489	0.000
0.800	−33073	−41531	−3.253	−22256	−7.414	0.000
0.900	−18819	−24017	−1.999	−11791	−4.702	0.000
1.000	0	0	0.000	0	0.000	0.000

Reference states: Hf(liquid), Ni(liquid)

Table IIIb. Partial quantities for Hf in the liquid phase at 2600 K.

x_{Hf}	ΔG_{Hf} [J/mol]	ΔH_{Hf} [J/mol]	ΔS_{Hf} [J/(mol·K)]	$G_{\mathrm{Hf}}^{\mathrm{E}}$ [J/mol]	$S_{\mathrm{Hf}}^{\mathrm{E}}$ [J/(mol·K)]	a_{Hf}	γ_{Hf}
1.000	0	0	0.000	0	0.000	1.000	1.000
0.900	−3737	−204	1.359	−1460	0.483	0.841	0.935
0.800	−11170	−2555	3.313	−6346	1.458	0.596	0.746
0.700	−22785	−9313	5.182	−15075	2.216	0.349	0.498
0.600	−38642	−22276	6.295	−27599	2.047	0.167	0.279
0.500	−58395	−42780	6.006	−43411	0.243	0.067	0.134
0.400	−81347	−71700	3.710	−61539	−3.908	0.023	0.058
0.300	−106578	−109449	−1.104	−80551	−11.115	0.007	0.024
0.200	−133345	−155976	−8.704	−98553	−22.086	0.002	0.010
0.100	−162965	−210771	−18.387	−113189	−37.532	0.001	0.005
0.000	$-\infty$	−272861	∞	−121640	−58.162	0.000	0.004

Reference state: Hf(liquid)

Table IIIc. Partial quantities for Ni in the liquid phase at 2600 K.

x_{Ni}	ΔG_{Ni} [J/mol]	ΔH_{Ni} [J/mol]	ΔS_{Ni} [J/(mol·K)]	$G_{\mathrm{Ni}}^{\mathrm{E}}$ [J/mol]	$S_{\mathrm{Ni}}^{\mathrm{E}}$ [J/(mol·K)]	a_{Ni}	γ_{Ni}
0.000	$-\infty$	−155081	∞	−157603	0.970	0.000	0.001
0.100	−180443	−153530	10.351	−130667	−8.794	0.000	0.002
0.200	−137948	−140900	−1.135	−103156	−14.517	0.002	0.008
0.300	−103053	−120991	−6.899	−77026	−16.910	0.009	0.028
0.400	−73579	−97141	−9.062	−53770	−16.681	0.033	0.083
0.500	−49404	−72225	−8.777	−34420	−14.540	0.102	0.203
0.600	−30586	−48659	−6.951	−19543	−11.198	0.243	0.405
0.700	−16959	−28393	−4.398	−9249	−7.363	0.456	0.652
0.800	−8005	−12920	−1.890	−3181	−3.746	0.691	0.863
0.900	−2802	−3267	−0.179	−525	−1.055	0.878	0.976
1.000	0	0	0.000	0	0.000	1.000	1.000

Reference state: Ni(liquid)

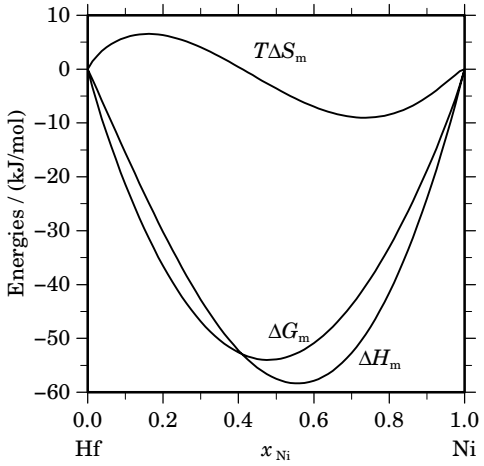

Fig. 2. Integral quantities of the liquid phase at T=2600 K.

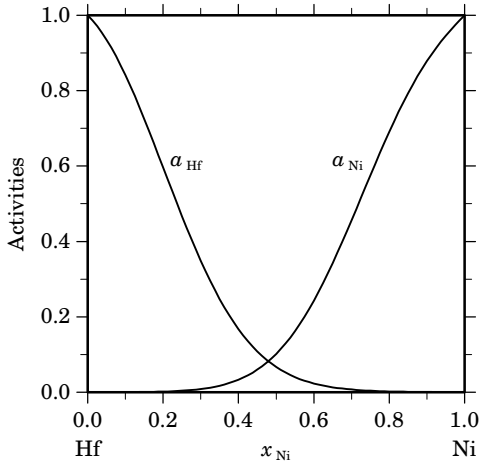

Fig. 3. Activities in the liquid phase at T=2600 K.

Table IV. Standard reaction quantities at 298.15 K for the compounds per mole of atoms.

Compound	x_{Ni}	$\Delta_f G^\circ$ / (J/mol)	$\Delta_f H^\circ$ / (J/mol)	$\Delta_f S^\circ$ / (J/(mol·K))	$\Delta_f C_P^\circ$ / (J/(mol·K))
Hf_2Ni	0.333	−37387	−36488	3.016	−0.025
αHfNi	0.500	−51478	−51198	0.939	−0.382
βHfNi	0.500	−49107	−48198	3.047	−0.382
Hf_9Ni_{11}	0.550	−50577	−50232	1.160	−0.420
Hf_7Ni_{10}	0.588	−49417	−49072	1.157	−0.450
Hf_3Ni_7	0.700	−43521	−43098	1.420	−0.535
Hf_8Ni_{21}	0.724	−41897	−41430	1.565	−0.554
$\alpha HfNi_3$	0.750	−44110	−44622	−1.718	−0.573
$\beta HfNi_3$	0.750	−41717	−41622	0.319	−0.573
Hf_2Ni_7	0.778	−41715	−42096	−1.278	−0.595
Hf_1Ni_5	0.833	−36034	−37169	−3.807	−0.637

References

[1967Sve] V.N. Svechnikov, A.K. Shurin, G.P. Dmitriyeva: Izv. Akad. Nauk SSSR, Met., No. 6 (1967) 176–179; transl.: Russ. Met. 6 (1967) 95–96.
[1979Bse] L. Bsenko: J. Less-Common Met. **63** (1979) 171–179.
[1983Nas] P. Nash, A. Nash: Bull. Alloy Phase Diagrams **4** (1983) 250–253.
[1991Oka] H. Okamoto: J. Phase Equilibria **12** (1991) 393.
[1992Sel] N. Selhaoui, J.C. Gachon, J. Hertz: Metall. Trans. B **23B** (1992) 815–819.
[1993Yer] V.N. Yeremenko, E.L. Semenova, L.A. Tretyachenko, V.M. Petyukh: J. Alloys Comp. **191** (1993) 117–119.
[1995Guo] Q. Guo, O.J. Kleppa: J. Phys. Chem. **99** (1995) 2854–2856.
[1996Ben] L. Bencze, K. Hilpert: Metall. Mater. Trans. A **27A** (1996) 3576–3590.
[1998Guo] Q. Guo, O.J. Kleppa: J. Alloys Comp. **269** (1998) 181–186.
[1998Haj] M. Hajjaji: J. Alloys Comp. **274** (1998) 185–188.
[2001Wan] T. Wang, Z. Jin, J.-C. Zhao: Z. Metallkd. **92** (2001) 441–446.

Hf – W (Hafnium – Tungsten)

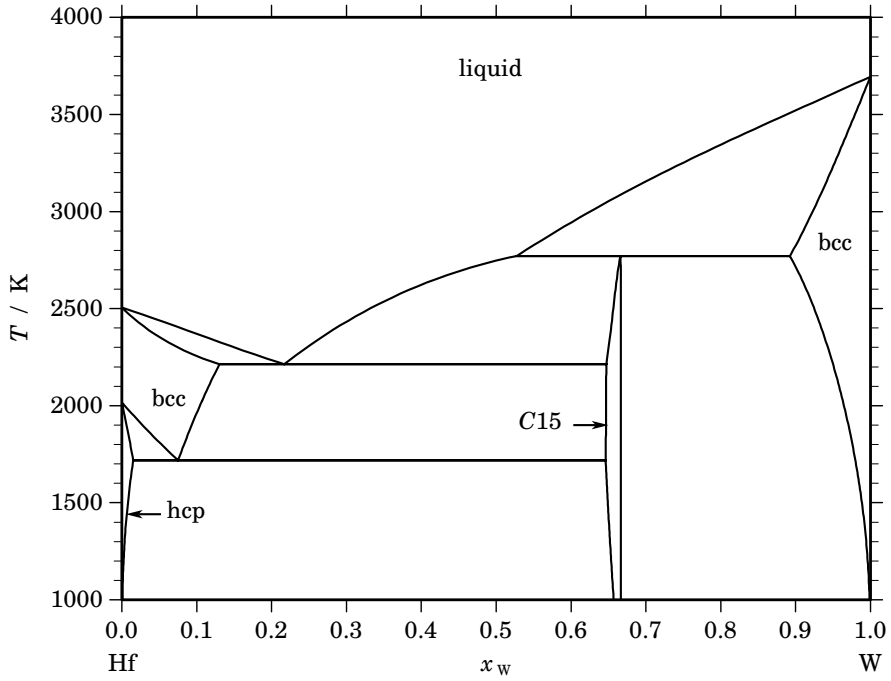

Fig. 1. Calculated phase diagram for the system Hf-W.

Hafnium and carbon are typically added in small amounts to tungsten alloys in order to improve their high-temperature creep strength. The literature on the Hf-W system has been reviewed in [1981Spe, 1991Nag] and thermodynamic optimised datasets have been reported by [1986Lee, 2002Sha]. The phase diagram is based mostly on the results of Rudy and co-workers [1960Bra, 1969Rud]. The eutectic reaction and part of the liquidus curve have been investigated by Ackermann and Rauh [1972Ack] using samples of high purity. No experimental investigations of thermodynamic mixing properties have been reported. The assessed dataset of Shao [2002Sha] is preferred over that of Lee and Lee [1986Lee] because it is based on the SGTE recommended element data. However, the calculated invariant points differ to some extent from the values which have been recommended in previous reviews [1981Spe, 1991Nag].

Table I. Phases, structures and models.

Phase	Struktur-bericht	Prototype	Pearson symbol	Space group	SGTE name	Model
liquid					LIQUID	$(Hf,W)_1$
bcc	$A2$	W	$cI2$	$Im\bar{3}m$	BCC_A2	$(Hf,W)_1$
hcp	$A3$	Mg	$hP2$	$P6_3/mmc$	HCP_A3	$(Hf,W)_1$
$C15$	$C15$	$MgCu_2$	$cF24$	$Fd\bar{3}m$	LAVES_C15	$(Hf,W)_2(Hf,W)_1$

Table II. Invariant reactions.

Reaction	Type	T / K	Compositions / x_W			$\Delta_r H$ / (J/mol)
liquid + bcc $\rightleftharpoons$ $C15$	peritectic	2771.0	0.527	0.892	0.666	−36470
liquid $\rightleftharpoons$ bcc + $C15$	eutectic	2213.7	0.217	0.130	0.647	−28411
bcc $\rightleftharpoons$ hcp + $C15$	eutectoid	1718.0	0.075	0.015	0.646	−8302

Table IIIa. Integral quantities for the liquid phase at 3700 K.

x_{W}	ΔG_{m} [J/mol]	ΔH_{m} [J/mol]	ΔS_{m} [J/(mol·K)]	$G_{\mathrm{m}}^{\mathrm{E}}$ [J/mol]	$S_{\mathrm{m}}^{\mathrm{E}}$ [J/(mol·K)]	ΔC_P [J/(mol·K)]
0.000	0	0	0.000	0	0.000	0.000
0.100	−11013	−2344	2.343	−1012	−0.360	0.000
0.200	−17002	−3976	3.521	−1608	−0.640	0.000
0.300	−20650	−4966	4.239	−1858	−0.840	0.000
0.400	−22540	−5387	4.636	−1835	−0.960	0.000
0.500	−22936	−5312	4.763	−1612	−1.000	0.000
0.600	−21964	−4811	4.636	−1259	−0.960	0.000
0.700	−19642	−3958	4.239	−850	−0.840	0.000
0.800	−15850	−2824	3.521	−456	−0.640	0.000
0.900	−10149	−1480	2.343	−148	−0.360	0.000
1.000	0	0	0.000	0	0.000	0.000

Reference states: Hf(liquid), W(liquid)

Table IIIb. Partial quantities for Hf in the liquid phase at 3700 K.

x_{Hf}	ΔG_{Hf} [J/mol]	ΔH_{Hf} [J/mol]	ΔS_{Hf} [J/(mol·K)]	$G_{\mathrm{Hf}}^{\mathrm{E}}$ [J/mol]	$S_{\mathrm{Hf}}^{\mathrm{E}}$ [J/(mol·K)]	a_{Hf}	γ_{Hf}
1.000	0	0	0.000	0	0.000	1.000	1.000
0.900	−3462	−368	0.836	−220	−0.040	0.894	0.993
0.800	−7651	−1378	1.695	−786	−0.160	0.780	0.975
0.700	−12525	−2884	2.606	−1552	−0.360	0.666	0.951
0.600	−18090	−4744	3.607	−2376	−0.640	0.555	0.926
0.500	−24436	−6812	4.763	−3112	−1.000	0.452	0.904
0.400	−31805	−8945	6.179	−3617	−1.440	0.356	0.889
0.300	−40786	−10999	8.050	−3747	−1.960	0.266	0.885
0.200	−52870	−12830	10.822	−3358	−2.560	0.179	0.897
0.100	−73142	−14294	15.905	−2306	−3.240	0.093	0.928
0.000	$-\infty$	−15247	∞	−447	−4.000	0.000	0.986

Reference state: Hf(liquid)

Table IIIc. Partial quantities for W in the liquid phase at 3700 K.

x_{W}	ΔG_{W} [J/mol]	ΔH_{W} [J/mol]	ΔS_{W} [J/(mol·K)]	$G_{\mathrm{W}}^{\mathrm{E}}$ [J/mol]	$S_{\mathrm{W}}^{\mathrm{E}}$ [J/(mol·K)]	a_{W}	γ_{W}
0.000	$-\infty$	−27247	∞	−12447	−4.000	0.000	0.667
0.100	−78974	−20126	15.905	−8138	−3.240	0.077	0.768
0.200	−54406	−14366	10.822	−4894	−2.560	0.171	0.853
0.300	−39610	−9823	8.050	−2571	−1.960	0.276	0.920
0.400	−29213	−6353	6.179	−1025	−1.440	0.387	0.967
0.500	−21436	−3812	4.763	−112	−1.000	0.498	0.996
0.600	−15402	−2056	3.607	312	−0.640	0.606	1.010
0.700	−10581	−940	2.606	392	−0.360	0.709	1.013
0.800	−6595	−322	1.695	270	−0.160	0.807	1.009
0.900	−3150	−56	0.836	92	−0.040	0.903	1.003
1.000	0	0	0.000	0	0.000	1.000	1.000

Reference state: W(liquid)

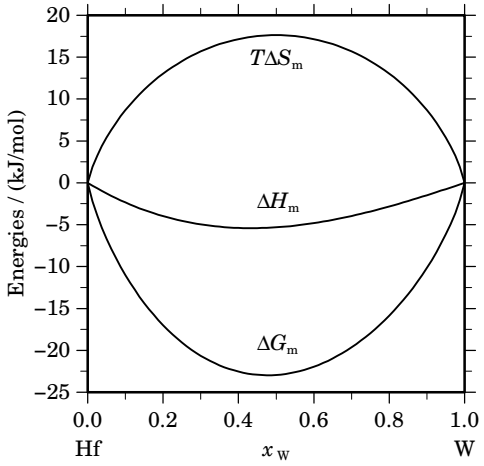

Fig. 2. Integral quantities of the liquid phase at T=3700 K.

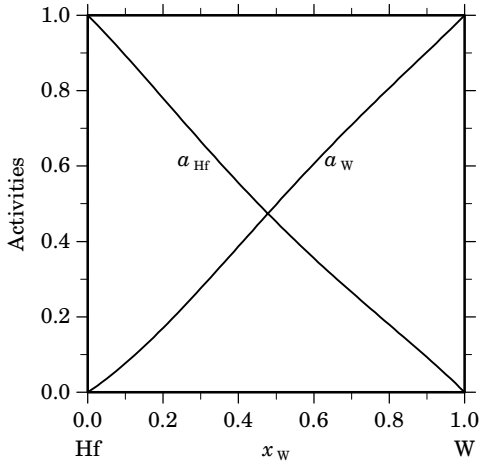

Fig. 3. Activities in the liquid phase at T=3700 K.

Table IV. Standard reaction quantities at 298.15 K for the compounds per mole of atoms.

Compound	x_W	$\Delta_f G^\circ$ / (J/mol)	$\Delta_f H^\circ$ / (J/mol)	$\Delta_f S^\circ$ / (J/(mol·K))	$\Delta_f C_P^\circ$ / (J/(mol·K))
$C15$	0.667	−13677	−14109	1.450	0.000

References

[1960Bra] H. Braun, E. Rudy: Z. Metallkd. **51** (1960) 360–363.

[1962Gie] B.C. Giessen, I. Rump, N.J. Grant: Trans. AIME **224** (1962) 60–64.

[1969Rud] E. Rudy: Compendium of Phase Diagram Data, AFML, Wright-Patterson AFB, Ohio, Rep. No. AFML-TR-65-2, Part 5, 1969.

[1972Ack] R.J. Ackermann, E.G. Rauh: High Temp. Sci. **4** (1972) 272–282.

[1981Spe] P.J. Spencer in: "Hafnium: Physico-Chemical Properties of its Compounds and Alloys", K.L. Komarek (ed.), Atomic Energy Rev. Spec. Issue 8, IAEA, Vienna, 1981, pp. 108–110.

[1986Lee] S.K. Lee, D.N. Lee: Calphad **10** (1986) 61–76.

[1991Nag] S.V. Nagender Naidu, P. Rama Rao in: "Phase Diagrams of Binary Tungsten Alloys", S.V. Nagender Naidu, P. Rama Rao, Eds., The Indian Institute of Metals, Calcutta, 1991, pp. 114–121.

[2002Sha] G. Shao: Intermetallics **10** (2002) 429–434.

Hg – Sn (Mercury – Tin)

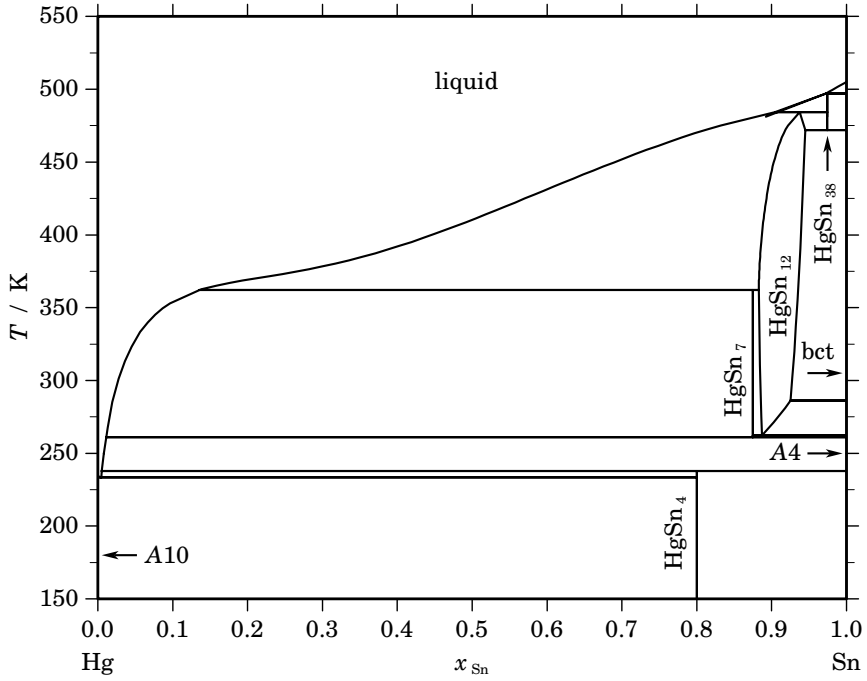

Fig. 1. Calculated phase diagram for the system Hg-Sn.

Mercury-tin alloys are of considerable interest since more than hundred years because traditional dental amalgams are based on the Ag-Hg-Sn system. More recently, tin amalgams have been developed for application in compact fluorescent lamp amalgams. According to the importance of Hg-Sn alloys many experimental investigations of the phase equilibria and their thermodynamic properties are available. The literature has been reviewed by [1993Zab, 2003Yen] and a thermodynamic dataset for Hg-Sn has been optimised in [2003Yen] which describes the phase diagram as well as the mixing properties and the vapour pressure. In the optimisation the liquidus has been optimised to fit the data of about 20 selected investigations from the literature which have been obtained by several techniques such as thermal and chemical analysis and electrochemical methods. The enthalpy of mixing has been reported in several investigations and for different temperatures. These data are mostly in agreement for Hg-rich liquids but they differ in the Sn-rich part. Within these limitations the calculations provide a good description of the experimental results. The activities of Hg and Sn have been determined in many investigations at different temperatures for the homogeneous melt as well as across 2-phase regions and again the calculations provide a good representation of the data within the range of deviation between different authors.

Table I. Phases, structures and models.

Phase	Struktur-bericht	Prototype	Pearson symbol	Space group	SGTE name	Model
liquid					LIQUID	$(Hg,Sn)_1$
$A10$	$A10$	αHg	$hR1$	$R\bar{3}m$	RHOMBO_A10	$(Hg,Sn)_1$
$HgSn_4$	···	···	···	···	HGSN4	Hg_1Sn_4
$HgSn_7$	···	$HgSn_7$	$o*^*$	···	HGSN7	Hg_1Sn_7
$HgSn_{12}$	···	$HgSn_{12}$	$hP1$	$P6_3/mmm$	HGSN12	$(Hg,\square)_1Sn_6$
$HgSn_{38}$	···	$HgSn_{38}$	$hP1$	···	HGSN38	Hg_1Sn_{38}
bct	$A5$	βSn	$tI4$	$I4_1/amd$	BCT_A5	Sn_1
$A4$	$A4$	C(diamond)	$cF8$	$Fd\bar{3}m$	DIAMOND_A4	Sn_1

Table II. Invariant reactions.

Reaction	Type	T / K	Compositions / x_{Sn}			$\Delta_r H$ / (J/mol)
liquid + bct $\rightleftharpoons$ $HgSn_{38}$	peritectic	497.1	0.973	1.000	0.974	−4761
liquid + $HgSn_{38}$ $\rightleftharpoons$ $HgSn_{12}$	peritectic	484.2	0.904	0.974	0.937	−4068
$HgSn_{38}$ $\rightleftharpoons$ $HgSn_{12}$ + bct	eutectoid	472.1	0.974	0.945	1.000	−1601
liquid + $HgSn_{12}$ $\rightleftharpoons$ $HgSn_7$	peritectic	362.1	0.136	0.883	0.875	−14
$HgSn_{12}$ + bct $\rightleftharpoons$ $A4$	peritectoid	286.2	0.925	1.000	1.000	−1967
$HgSn_{12}$ $\rightleftharpoons$ $HgSn_7$ + $A4$	eutectoid	262.2	0.887	0.875	1.000	−228
$HgSn_7$ $\rightleftharpoons$ liquid + $A4$	metatectic	261.1	0.875	0.011	1.000	−2117
liquid + $A4$ $\rightleftharpoons$ $HgSn_4$	peritectic	237.7	0.005	1.000	0.800	−1597
liquid $\rightleftharpoons$ A10 + $HgSn_4$	eutectic	233.4	0.005	0.000	0.800	−2357

Table IIIa. Integral quantities for the liquid phase at 523 K.

x_{Sn}	ΔG_m [J/mol]	ΔH_m [J/mol]	ΔS_m [J/(mol·K)]	G_m^E [J/mol]	S_m^E [J/(mol·K)]	ΔC_P [J/(mol·K)]
0.000	0	0	0.000	0	0.000	0.000
0.100	−828	451	2.446	585	−0.257	0.000
0.200	−1268	739	3.837	908	−0.324	0.000
0.300	−1612	913	4.827	1044	−0.252	0.000
0.400	−1873	1006	5.506	1053	−0.090	0.000
0.500	−2033	1040	5.876	981	0.113	0.000
0.600	−2067	1019	5.902	859	0.306	0.000
0.700	−1952	935	5.520	705	0.441	0.000
0.800	−1656	765	4.629	520	0.468	0.000
0.900	−1120	471	3.041	294	0.338	0.000
1.000	0	0	0.000	0	0.000	0.000

Reference states: Hg(liquid), Sn(liquid)

Table IIIb. Partial quantities for Hg in the liquid phase at 523 K.

x_{Hg}	ΔG_{Hg} [J/mol]	ΔH_{Hg} [J/mol]	ΔS_{Hg} [J/(mol·K)]	G^E_{Hg} [J/mol]	S^E_{Hg} [J/(mol·K)]	a_{Hg}	γ_{Hg}
1.000	0	0	0.000	0	0.000	1.000	1.000
0.900	−314	91	0.773	145	−0.103	0.930	1.034
0.800	−499	291	1.510	472	−0.345	0.892	1.115
0.700	−697	525	2.338	854	−0.628	0.852	1.217
0.600	−1016	760	3.395	1206	−0.852	0.792	1.319
0.500	−1528	1006	4.844	1487	−0.919	0.704	1.408
0.400	−2286	1317	6.890	1698	−0.729	0.591	1.478
0.300	−3350	1790	9.827	1886	−0.183	0.463	1.543
0.200	−4861	2565	14.199	2137	0.817	0.327	1.635
0.100	−7428	3825	21.516	2584	2.371	0.181	1.812
0.000	−∞	5796	∞	3402	4.578	0.000	2.186

Reference state: Hg(liquid)

Table IIIc. Partial quantities for Sn in the liquid phase at 523 K.

x_{Sn}	ΔG_{Sn} [J/mol]	ΔH_{Sn} [J/mol]	ΔS_{Sn} [J/(mol·K)]	G^E_{Sn} [J/mol]	S^E_{Sn} [J/(mol·K)]	a_{Sn}	γ_{Sn}
0.000	−∞	5524	∞	7446	−3.676	0.000	5.542
0.100	−5463	3692	17.505	4550	−1.640	0.285	2.847
0.200	−4344	2530	13.142	2655	−0.240	0.368	1.841
0.300	−3746	1817	10.636	1489	0.625	0.423	1.408
0.400	−3160	1376	8.672	825	1.054	0.484	1.209
0.500	−2539	1074	6.908	475	1.144	0.558	1.116
0.600	−1922	821	5.244	300	0.997	0.643	1.071
0.700	−1353	569	3.675	198	0.709	0.733	1.047
0.800	−855	315	2.237	116	0.381	0.822	1.027
0.900	−419	98	0.988	39	0.112	0.908	1.009
1.000	0	0	0.000	0	0.000	1.000	1.000

Reference state: Sn(liquid)

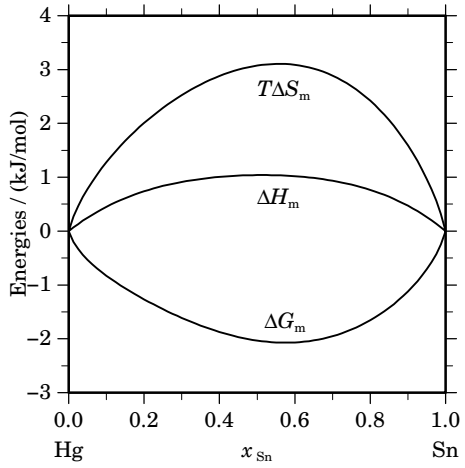

Fig. 2. Integral quantities of the liquid phase at T=523 K.

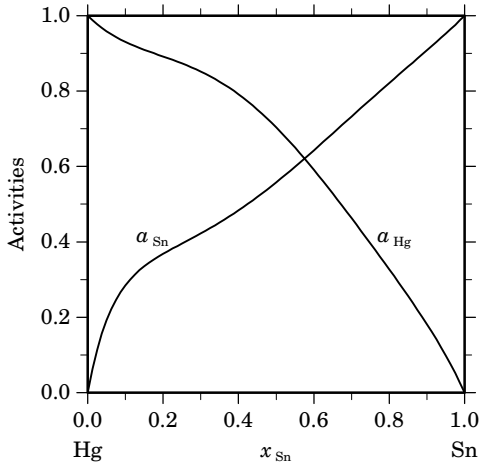

Fig. 3. Activities in the liquid phase at T=523 K.

Table IV. Standard reaction quantities at 298.15 K for the compounds per mole of atoms.

Compound	x_{Sn}	$\Delta_{\mathrm{f}}G^{\circ}$ / (J/mol)	$\Delta_{\mathrm{f}}H^{\circ}$ / (J/mol)	$\Delta_{\mathrm{f}}S^{\circ}$ / (J/(mol·K))	$\Delta_{\mathrm{f}}C_P^{\circ}$ / (J/(mol·K))
Hg_1Sn_4	0.800	459	−3109	−11.966	0.183
Hg_1Sn_7	0.875	−237	442	2.278	0.114
Hg_1Sn_{38}	0.974	530	1767	4.151	0.023

References

[1993Zab] L.A. Zabdyr, C. Guminski: J. Phase Equilibria **14** (1993) 743–752.
[2003Yen] Y.-W. Yen, J. Gröbner, S.C. Hansen, R. Schmid-Fetzer: J. Phase Equilibria **24** (2003) 151–167.

Hg – Te (Mercury – Tellurium)

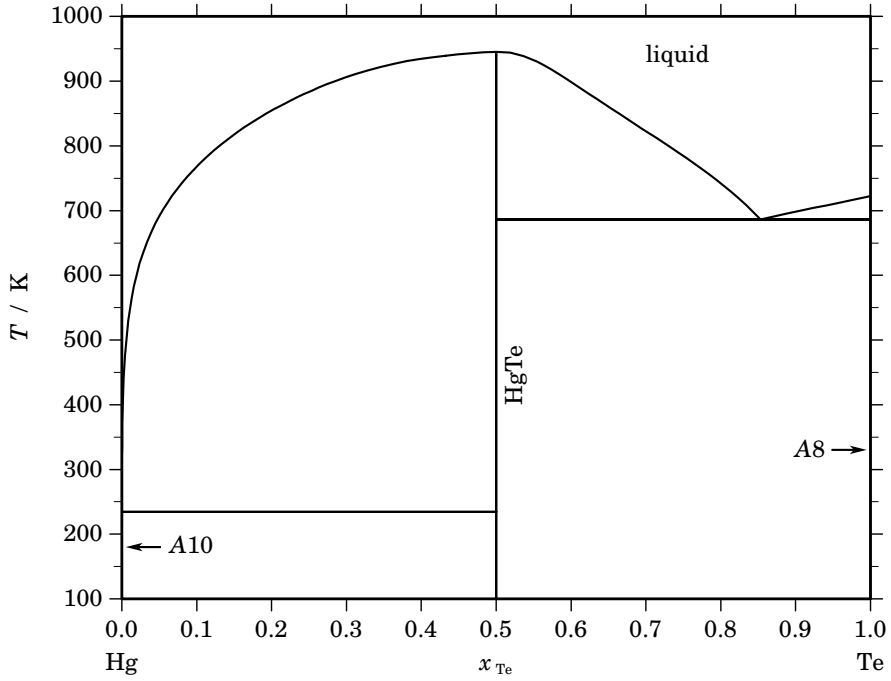

Fig. 1. Calculated phase diagram for the system Hg-Te.

The Hg-Te system is of interest because of the semimetallic compound HgTe which forms continuous solid solutions with the semiconducting compound CdTe. The resulting Cd-Hg tellurides are infrared sensitive semiconductors with wavelengths which can be tailored by means of the Cd-Hg composition ratio. Reviews and thermodynamic datasets for the Hg-Te system have been prepared by [1995Sha, 1995Yan] and the assessment of [1995Yan] is selected here because it is based on the SGTE element data. The data for the phase equilibria which have been used in the optimisation are based mainly on [1965Bre, 1967Str, 1971Dzi, 1980Har]. Partial pressure data for Hg [1963Gol, 1965Bre, 1981Su, 1989Sha] and Te [1965Bre] in the equilibrium of the liquid with the HgTe compound have been included in the assessment. Except for these partial pressure data no other thermodynamic data have been available for the liquid. The partial pressures and in addition results from EMF experiments [1964Ter] have been used to determine the Gibbs energy of formation of the HgTe compound. The terminal phases as well as the the HgTe compound have been modelled as stoichiometric since no solubility data have been available. The liquid has been described with an associate model using the species Hg, Te and HgTe.

Table I. Phases, structures and models.

Phase	Struktur-bericht	Prototype	Pearson symbol	Space group	SGTE name	Model
liquid					LIQUID	$(Hg,HgTe,Te)_1$
$A10$	$A10$	αHg	$hR1$	$R\bar{3}m$	RHOMBO_A10	$(Hg,Te)_1$
HgTe	$B3$	ZnS	$cF8$	$F\bar{4}3m$	HGTE	Hg_1Te_1
$A8$	$A8$	γSe	$hP3$	$P3_121$	TRIGONAL_A8	Te_1

Table II. Invariant reactions.

Reaction	Type	T / K	Compositions / x_{Te}			$\Delta_{\mathrm{r}}H$ / (J/mol)
liquid $\rightleftharpoons$ HgTe	congruent	945.4	0.500	0.500		−17430
liquid $\rightleftharpoons$ HgTe + $A8$	eutectic	686.3	0.853	0.500	1.000	−14214
liquid $\rightleftharpoons$ $A10$ + HgTe	eutectic	234.3	0.000	0.000	0.500	−2295

Table IIIa. Integral quantities for the liquid phase at 950 K.

x_{Te}	ΔG_{m} [J/mol]	ΔH_{m} [J/mol]	ΔS_{m} [J/(mol·K)]	$G^{\mathrm{E}}_{\mathrm{m}}$ [J/mol]	$S^{\mathrm{E}}_{\mathrm{m}}$ [J/(mol·K)]	ΔC_P [J/(mol·K)]
0.000	0	0	0.000	0	0.000	0.000
0.100	−3608	−1609	2.104	−1040	−0.599	1.807
0.200	−5954	−3441	2.645	−2002	−1.515	4.252
0.300	−7709	−5637	2.181	−2884	−2.898	7.406
0.400	−9017	−8499	0.545	−3701	−5.051	9.574
0.500	−9935	−11717	−1.875	−4460	−7.638	2.745
0.600	−9689	−12403	−2.857	−4373	−8.452	5.765
0.700	−8228	−9546	−1.387	−3403	−6.466	16.123
0.800	−6258	−5793	0.489	−2305	−3.672	13.180
0.900	−3742	−2654	1.145	−1174	−1.558	5.885
1.000	0	0	0.000	0	0.000	0.000

Reference states: Hg(liquid), Te(liquid)

Table IIIb. Partial quantities for Hg in the liquid phase at 950 K.

x_{Hg}	ΔG_{Hg} [J/mol]	ΔH_{Hg} [J/mol]	ΔS_{Hg} [J/(mol·K)]	$G^{\mathrm{E}}_{\mathrm{Hg}}$ [J/mol]	$S^{\mathrm{E}}_{\mathrm{Hg}}$ [J/(mol·K)]	a_{Hg}	γ_{Hg}
1.000	0	0	0.000	0	0.000	1.000	1.000
0.900	−871	96	1.018	−39	0.142	0.896	0.995
0.800	−1921	521	2.571	−159	0.716	0.784	0.980
0.700	−3167	1744	5.170	−350	2.204	0.670	0.957
0.600	−4543	4773	9.807	−509	5.560	0.563	0.938
0.500	−6982	276	7.640	−1507	1.877	0.413	0.826
0.400	−15978	−20129	−4.369	−8740	−11.988	0.132	0.331
0.300	−20474	−36465	−16.833	−10964	−26.843	0.075	0.250
0.200	−23917	−33459	−10.044	−11205	−23.426	0.048	0.242
0.100	−29722	−28400	1.391	−11534	−17.754	0.023	0.232
0.000	$-\infty$	−24748	∞	−11984	−13.435	0.000	0.219

Reference state: Hg(liquid)

Table IIIc. Partial quantities for Te in the liquid phase at 950 K.

x_{Te}	ΔG_{Te} [J/mol]	ΔH_{Te} [J/mol]	ΔS_{Te} [J/(mol·K)]	$G^{\mathrm{E}}_{\mathrm{Te}}$ [J/mol]	$S^{\mathrm{E}}_{\mathrm{Te}}$ [J/(mol·K)]	a_{Te}	γ_{Te}
0.000	$-\infty$	−15242	∞	−10790	−4.686	0.000	0.255
0.100	−28239	−16954	11.879	−10052	−7.266	0.028	0.280
0.200	−22086	−19290	2.943	−9373	−10.439	0.061	0.305
0.300	−18308	−22861	−4.793	−8798	−14.803	0.098	0.328
0.400	−15727	−28407	−13.348	−8489	−20.966	0.137	0.341
0.500	−12889	−23710	−11.390	−7414	−17.153	0.196	0.391
0.600	−5496	−7252	−1.848	−1461	−6.095	0.499	0.831
0.700	−2980	1991	5.232	−163	2.267	0.686	0.980
0.800	−1843	1123	3.122	−80	1.267	0.792	0.990
0.900	−855	206	1.118	−23	0.242	0.897	0.997
1.000	0	0	0.000	0	0.000	1.000	1.000

Reference state: Te(liquid)

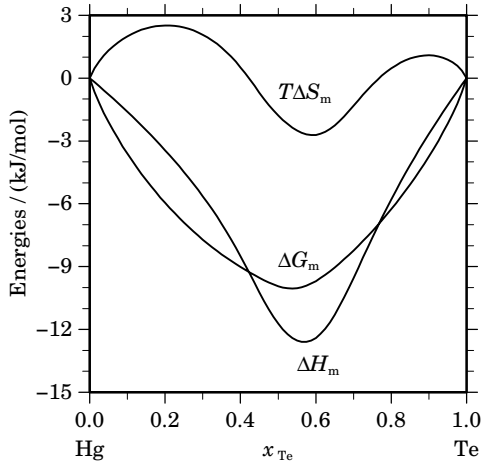

Fig. 2. Integral quantities of the liquid phase at T=950 K.

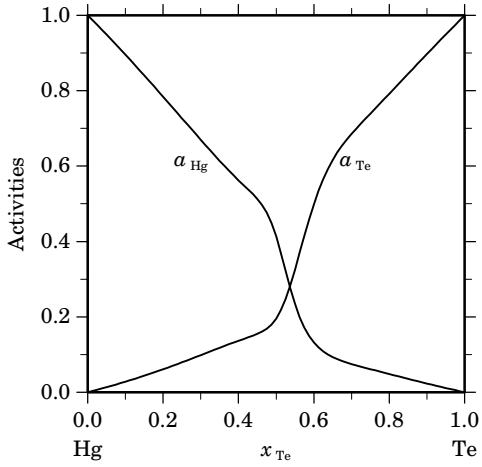

Fig. 3. Activities in the liquid phase at T=950 K.

Table IV. Standard reaction quantities at 298.15 K for the compounds per mole of atoms.

Compound	x_{Te}	$\Delta_{\mathrm{f}}G^{\circ}$ / (J/mol)	$\Delta_{\mathrm{f}}H^{\circ}$ / (J/mol)	$\Delta_{\mathrm{f}}S^{\circ}$ / (J/(mol·K))	$\Delta_{\mathrm{f}}C^{\circ}_{P}$ / (J/(mol·K))
Hg_1Te_1	0.500	−18594	−21769	−10.648	0.925

References

[1963Gol] P. Goldfinger, M. Jeunehomme: Trans. Faraday Soc. **59** (1963) 2851–2867.

[1964Ter] J. Terpilowski, E. Ratajzak: Bull. Acad. Pol. Sci. **12** (1964) 335–338.

[1965Bre] R.F. Brebrick, A.J. Strauss: J. Phys. Chem. Solids **26** (1965) 989–1002.

[1967Str] A.J. Strauss, quoted as private communication by: T.C. Harman in: "Physics and Chemistry of II/VI Compounds", M. Aven, J.S. Prener, eds, North Holland Publ. Comp., Amsterdam, 1967, p. 769.

[1971Dzi] E.Z. Dziuba: J. Cryst. Growth **8** (1971) 221–222.

[1980Har] T.C. Harman: J. Electron. Mater. **9** (1980) 945–961.

[1981Su] C. Su, P. Liao, T. Tung, R. Brebrick: High Temp. Sci. **14** (1981) 181–195.

[1989Sha] Y. Sha, K. Chen, R. Fang, R. Brebrick: J. Electrochem. Soc. **136** (1989) 3037–3041.

[1995Sha] R.C. Sharma, Y.A. Chang, C. Guminski: J. Phase Equilibria **16** (1995) 338–347.

[1995Yan] J. Yang, N.J. Silk, A. Watson, A.W. Bryant, B.B. Argent: Calphad **19** (1995) 399–414.

Hg – Zn (Mercury – Zinc)

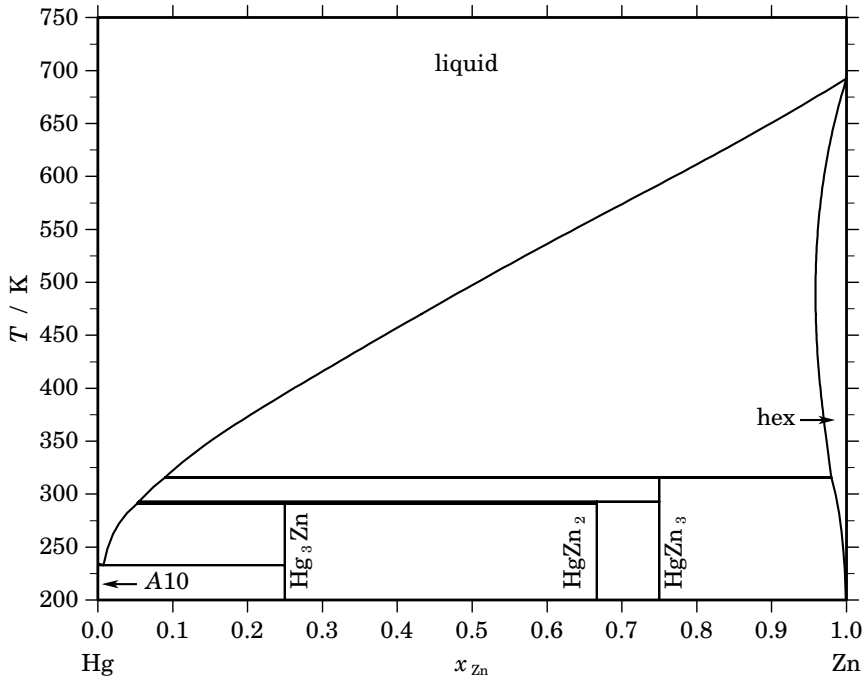

Fig. 1. Calculated phase diagram for the system Hg-Zn.

The Hg-Zn system is of interest for the semiconductor industry because of the infrared sensitive tellurides which form a continuous solid solution between HgTe and ZnTe. Reviews on the literature of the Hg-Zn system have been given in [1995Zab, 1998Han] and a thermodynamic dataset has been optimised by [1998Han] which is based on the SGTE recommended element data. The liquidus has been determined throughout the whole composition range already long ago [1903Pus]. More investigations of the liquidus in the Hg-rich region have been reported by [1910Coh] and [1946Pes] who investigated especially the eutectic close to pure mercury. Many other contributions to the liquidus have been reported in the literature and a compilation of these data can be found in the review of [1995Zab]. A wide range of scattered data has been reported in the literature for the solubility of mercury in solid zinc probably due to problems in attaining equilibrium. The most reliable data seem to be given by [1967Tan] since the samples have been equilibrated for up to one year. The solubility of Zn in solid Hg is small and not precisely known. Three intermetallic phases have been found which are all described as stoichiometric compounds in the assessment [1998Han]. Two of them , $HgZn_2$ and $HgZn_3$, seem to have a wider solubility range. From calorimetric investigations of liquid alloys enthalpies of mixing have been reported [1960Kle, 1960Wit]. The assessment takes also into account activity data for Hg in liquid alloys reported in [1912Hil, 1933Ped, 1971Koz].

Table I. Phases, structures and models.

Phase	Struktur-bericht	Prototype	Pearson symbol	Space group	SGTE name	Model
liquid					LIQUID	$(Hg,Zn)_1$
$A10$	$A10$	αHg	$hR1$	$R\bar{3}m$	RHOMBO_A10	$(Hg,Zn)_1$
Hg_3Zn	···	···	···	···	HG3ZN	Hg_3Zn_1
$HgZn_2$	···	···	···	···	HGZN2	Hg_1Zn_2
$HgZn_3$	···	β'Cu_3Ti	$oC4$	$Cmc2_1$	HGZN3	Hg_1Zn_3
hex	$A3$	Mg	$hP2$	$P6_3/mmc$	HCP_ZN	Zn_1

Table II. Invariant reactions.

Reaction	Type	T / K	Compositions / x_{Zn}			$\Delta_{\mathrm{r}}H$ / (J/mol)
liquid + hex $\rightleftharpoons$ $HgZn_3$	peritectic	315.6	0.090	0.980	0.750	−1703
liquid + $HgZn_3$ $\rightleftharpoons$ $HgZn_2$	peritectic	292.7	0.055	0.750	0.667	−330
liquid + $HgZn_2$ $\rightleftharpoons$ Hg_3Zn	peritectic	291.2	0.053	0.667	0.250	−1157
liquid $\rightleftharpoons$ $A10$ + Hg_3Zn	eutectic	233.0	0.007	0.000	0.250	−2341

Table IIIa. Integral quantities for the liquid phase at 700 K.

x_{Zn}	ΔG_{m} [J/mol]	ΔH_{m} [J/mol]	ΔS_{m} [J/(mol·K)]	$G^{\mathrm{E}}_{\mathrm{m}}$ [J/mol]	$S^{\mathrm{E}}_{\mathrm{m}}$ [J/(mol·K)]	ΔC_P [J/(mol·K)]
0.000	0	0	0.000	0	0.000	0.000
0.100	−1612	277	2.699	280	−0.004	0.000
0.200	−2413	414	4.038	500	−0.122	0.000
0.300	−2894	461	4.794	661	−0.285	0.000
0.400	−3155	456	5.157	762	−0.438	0.000
0.500	−3231	424	5.222	803	−0.542	0.000
0.600	−3136	381	5.025	781	−0.571	0.000
0.700	−2862	331	4.562	693	−0.517	0.000
0.800	−2376	266	3.774	537	−0.387	0.000
0.900	−1585	166	2.501	307	−0.202	0.000
1.000	0	0	0.000	0	0.000	0.000

Reference states: Hg(liquid), Zn(liquid)

Table IIIb. Partial quantities for Hg in the liquid phase at 700 K.

x_{Hg}	ΔG_{Hg} [J/mol]	ΔH_{Hg} [J/mol]	ΔS_{Hg} [J/(mol·K)]	$G^{\mathrm{E}}_{\mathrm{Hg}}$ [J/mol]	$S^{\mathrm{E}}_{\mathrm{Hg}}$ [J/(mol·K)]	a_{Hg}	γ_{Hg}
1.000	0	0	0.000	0	0.000	1.000	1.000
0.900	−583	79	0.946	30	0.070	0.905	1.005
0.800	−1180	245	2.036	119	0.180	0.816	1.021
0.700	−1809	415	3.178	267	0.212	0.733	1.047
0.600	−2496	544	4.342	477	0.095	0.651	1.085
0.500	−3279	617	5.566	755	−0.197	0.569	1.138
0.400	−4226	657	6.975	1107	−0.643	0.484	1.209
0.300	−5464	719	8.833	1543	−1.177	0.391	1.304
0.200	−7293	895	11.696	2075	−1.686	0.286	1.428
0.100	−10686	1308	17.134	2715	−2.011	0.159	1.594
0.000	$-\infty$	2119	∞	3482	−1.947	0.000	1.819

Reference state: Hg(liquid)

Table IIIc. Partial quantities for Zn in the liquid phase at 700 K.

x_{Zn}	ΔG_{Zn} [J/mol]	ΔH_{Zn} [J/mol]	ΔS_{Zn} [J/(mol·K)]	$G^{\mathrm{E}}_{\mathrm{Zn}}$ [J/mol]	$S^{\mathrm{E}}_{\mathrm{Zn}}$ [J/(mol·K)]	a_{Zn}	γ_{Zn}
0.000	$-\infty$	3663	∞	3096	0.810	0.000	1.702
0.100	−10873	2059	18.474	2528	−0.671	0.154	1.544
0.200	−7342	1092	12.049	2025	−1.333	0.283	1.416
0.300	−5427	568	8.563	1581	−1.447	0.394	1.312
0.400	−4143	323	6.380	1190	−1.239	0.491	1.227
0.500	−3183	231	4.877	851	−0.886	0.579	1.157
0.600	−2410	198	3.725	563	−0.522	0.661	1.102
0.700	−1747	165	2.731	329	−0.234	0.741	1.058
0.800	−1146	109	1.793	152	−0.062	0.821	1.027
0.900	−573	39	0.875	40	−0.001	0.906	1.007
1.000	0	0	0.000	0	0.000	1.000	1.000

Reference state: Zn(liquid)

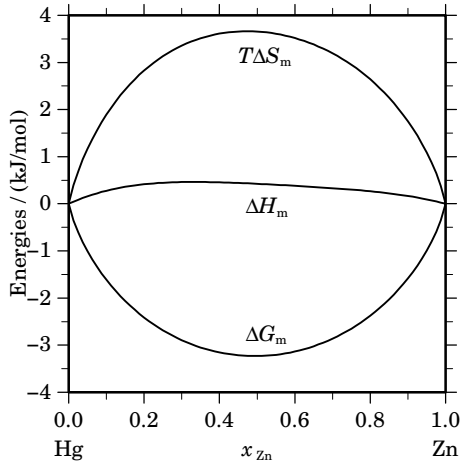

Fig. 2. Integral quantities of the liquid phase at T=700 K.

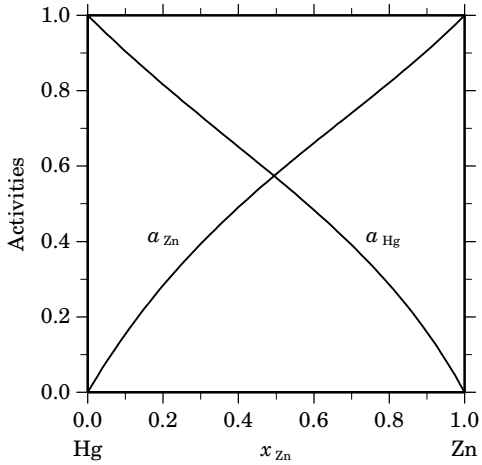

Fig. 3. Activities in the liquid phase at T=700 K.

Table IV. Standard reaction quantities at 298.15 K for the compounds per mole of atoms.

Compound	x_{Zn}	$\Delta_{\mathrm{f}}G^{\circ}$ / (J/mol)	$\Delta_{\mathrm{f}}H^{\circ}$ / (J/mol)	$\Delta_{\mathrm{f}}S^{\circ}$ / (J/(mol·K))	$\Delta_{\mathrm{f}}C^{\circ}_{P}$ / (J/(mol·K))
Hg_3Zn_1	0.250	−111	−1255	−3.835	0.003
Hg_1Zn_2	0.667	−149	−1455	−4.380	0.007
Hg_1Zn_3	0.750	−158	−1354	−4.013	0.008

References

[1903Pus] N.A. Puschin: Z. Anorg. Chem. **36** (1903) 201–254.
[1910Coh] E. Cohen, K. Inouye: Z. Phys. Chem. **71** (1910) 625–635.
[1912Hil] J. Hildebrand: Trans. Electrochem. Soc. **22** (1912) 319–324.
[1933Ped] J.S. Pedder, S. Barrat: J. Chem. Soc. (1933) 537–546.
[1946Pes] V. Peshkov: Zh. Fiz. Khim. **20** (1946) 835–851.
[1960Kle] O.J. Kleppa: Acta Metall. **8** (1960) 435–445.
[1960Wit] F.E. Wittig, P. Scheidt: Naturwiss. **47** (1960) 250–251.
[1967Tan] I. Tangerini: Metall. Ital. **59** (1968) 495–500.
[1971Koz] L.F. Kozin, R.Sh. Nigmetova, A.M. Dairova: Russ. J. Phys. Chem. **45** (1971) 1180–1182.
[1995Zab] L.A. Zabdyr, C. Guminski: J. Phase Equilibria **16** (1995) 353–360.
[1998Han] S.C. Hansen: Calphad **22** (1998) 359–373.

Ho – Mg (Holmium – Magnesium)

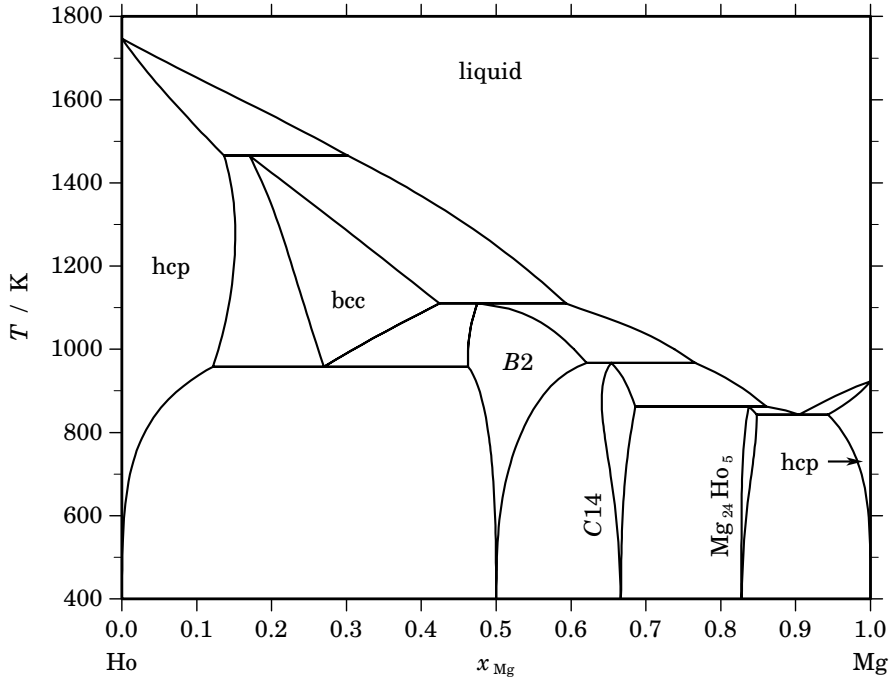

Fig. 1. Calculated phase diagram for the system Ho-Mg.

The rare earth elements have attracted some attention as additives to light metal alloys in the aerospace and automotive industry due to the improvement of mechanical properties of Al- and Mg-alloys at high temperatures. Cacciamani *et al.* [2003Cac] prepared a thermodynamic optimisation of the complete Ho-Mg system, which is primarily based on an experimental investigation of the phase equilibria at elevated temperatures throughout the whole composition range [1993Sac]. The solid solubility of Ho in magnesium has been measured by [1978Rok]. Since no thermodynamic data have been available for the Ho-Mg system the assessors estimated the values based on other systems of Mg with rare-earth metals which have been evaluated in the same publication.

Table I. Phases, structures and models.

Phase	Struktur-bericht	Prototype	Pearson symbol	Space group	SGTE name	Model
liquid					LIQUID	$(Ho,Mg)_1$
hcp	$A3$	Mg	$hP2$	$P6_3/mmc$	HCP_A3	$(Ho,Mg)_1$
bcc	$A2$	W	$cI2$	$Im\bar{3}m$	BCC_A2	$(Ho,Mg)_1$
$B2$	$B2$	CsCl	$cP2$	$Pm3m$	BCC_B2	$(Ho,Mg)_1(Ho,Mg)_1$
$C14$	$C14$	$MgZn_2$	$hP12$	$P6_3/mmc$	LAVES_C14	$(Ho,Mg)_2(Ho,Mg)_1$
$Mg_{24}Ho_5$	$A12$	αMn	$cI58$	$I\bar{4}3m$	MG24HO5	$Mg_{24}(Ho,Mg)_5$

Table II. Invariant reactions.

Reaction	Type	T / K	Compositions / x_{Mg}			$\Delta_{\mathrm{r}}H$ / (J/mol)
hcp + liquid $\rightleftharpoons$ bcc	peritectic	1465.7	0.136	0.301	0.170	−1460
bcc + liquid $\rightleftharpoons$ $B2$	peritectic	1110.2	0.424	0.593	0.475	−5711
$B2$ + liquid $\rightleftharpoons$ $C14$	peritectic	967.1	0.621	0.766	0.654	−7328
bcc $\rightleftharpoons$ hcp + $B2$	eutectoid	958.1	0.270	0.122	0.463	−4591
$C14$ + liquid $\rightleftharpoons$ $Mg_{24}Ho_5$	peritectic	862.3	0.686	0.861	0.837	−12294
liquid $\rightleftharpoons$ $Mg_{24}Ho_5$ + hcp	eutectic	842.9	0.905	0.848	0.943	−9355

Table IIIa. Integral quantities for the liquid phase at 1800 K.

x_{Mg}	ΔG_{m} [J/mol]	ΔH_{m} [J/mol]	ΔS_{m} [J/(mol·K)]	$G_{\mathrm{m}}^{\mathrm{E}}$ [J/mol]	$S_{\mathrm{m}}^{\mathrm{E}}$ [J/(mol·K)]	ΔC_P [J/(mol·K)]
0.000	0	0	0.000	0	0.000	0.000
0.100	−5705	251	3.309	−840	0.606	0.000
0.200	−9124	−396	4.849	−1635	0.688	0.000
0.300	−11474	−1626	5.471	−2332	0.392	0.000
0.400	−12950	−3123	5.459	−2878	−0.136	0.000
0.500	−13593	−4570	5.013	−3219	−0.751	0.000
0.600	−13376	−5652	4.291	−3303	−1.305	0.000
0.700	−12219	−6051	3.426	−3077	−1.653	0.000
0.800	−9975	−5453	2.512	−2486	−1.649	0.000
0.900	−6343	−3542	1.556	−1478	−1.146	0.000
1.000	0	0	0.000	0	0.000	0.000

Reference states: Ho(liquid), Mg(liquid)

Table IIIb. Partial quantities for Ho in the liquid phase at 1800 K.

x_{Ho}	ΔG_{Ho} [J/mol]	ΔH_{Ho} [J/mol]	ΔS_{Ho} [J/(mol·K)]	$G_{\mathrm{Ho}}^{\mathrm{E}}$ [J/mol]	$S_{\mathrm{Ho}}^{\mathrm{E}}$ [J/(mol·K)]	a_{Ho}	γ_{Ho}
1.000	0	0	0.000	0	0.000	1.000	1.000
0.900	−1590	502	1.162	−13	0.286	0.899	0.999
0.800	−3464	1587	2.806	−125	0.951	0.793	0.992
0.700	−5779	2622	4.667	−441	1.701	0.680	0.971
0.600	−8712	2975	6.493	−1067	2.246	0.559	0.931
0.500	−12484	2015	8.055	−2111	2.292	0.434	0.868
0.400	−17391	−891	9.167	−3678	1.548	0.313	0.782
0.300	−23894	−6376	9.732	−5875	−0.278	0.203	0.675
0.200	−32896	−15071	9.903	−8808	−3.479	0.111	0.555
0.100	−47046	−27608	10.799	−12585	−8.346	0.043	0.431
0.000	$-\infty$	−44620	∞	−17310	−15.172	0.000	0.315

Reference state: Ho(liquid)

Table IIIc. Partial quantities for Mg in the liquid phase at 1800 K.

x_{Mg}	ΔG_{Mg} [J/mol]	ΔH_{Mg} [J/mol]	ΔS_{Mg} [J/(mol·K)]	$G^{\mathrm{E}}_{\mathrm{Mg}}$ [J/mol]	$S^{\mathrm{E}}_{\mathrm{Mg}}$ [J/(mol·K)]	a_{Mg}	γ_{Mg}
0.000	$-\infty$	8060	∞	−8442	9.168	0.000	0.569
0.100	−42736	−2006	22.628	−8275	3.483	0.058	0.575
0.200	−31760	−8328	13.018	−7673	−0.364	0.120	0.599
0.300	−24763	−11539	7.347	−6744	−2.664	0.191	0.637
0.400	−19307	−12270	3.909	−5593	−3.709	0.275	0.688
0.500	−14701	−11155	1.970	−4328	−3.793	0.374	0.749
0.600	−10699	−8825	1.041	−3053	−3.206	0.489	0.815
0.700	−7215	−5912	0.724	−1877	−2.242	0.617	0.882
0.800	−4245	−3049	0.664	−905	−1.191	0.753	0.941
0.900	−1821	−868	0.530	−244	−0.346	0.885	0.984
1.000	0	0	0.000	0	0.000	1.000	1.000

Reference state: Mg(liquid)

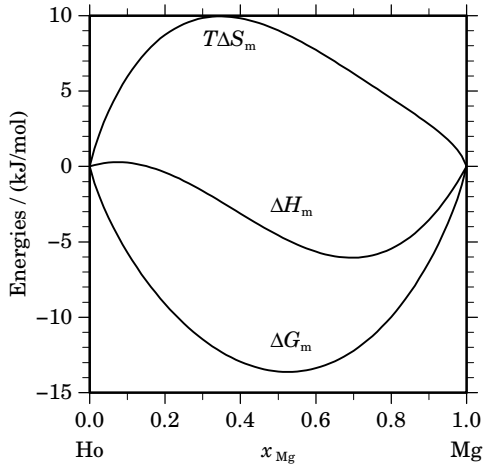

Fig. 2. Integral quantities of the liquid phase at T=1800 K.

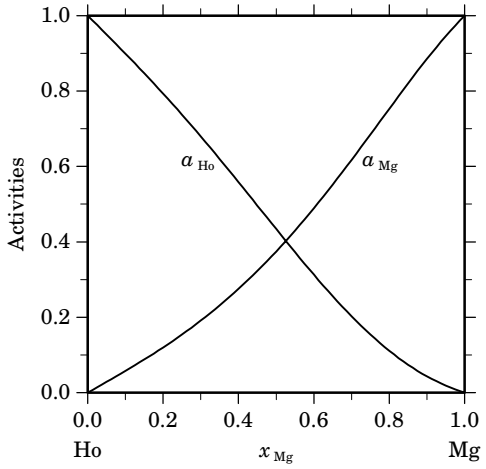

Fig. 3. Activities in the liquid phase at T=1800 K.

Table IV. Standard reaction quantities at 298.15 K for the compounds per mole of atoms.

Compound	x_{Mg}	$\Delta_{\mathrm{f}}G^{\circ}$ / (J/mol)	$\Delta_{\mathrm{f}}H^{\circ}$ / (J/mol)	$\Delta_{\mathrm{f}}S^{\circ}$ / (J/(mol·K))	$\Delta_{\mathrm{f}}C^{\circ}_{P}$ / (J/(mol·K))
$B2$	0.500	−11784	−13537	−5.882	0.000
$C14$	0.667	−11803	−13667	−6.250	0.001
$Mg_{24}Ho_5$	0.828	−8516	−10342	−6.124	0.000

References

[1978Roc] L.L. Rokhlin in: "Probl. Metalloved. Tsvetn. Splavov", N.M. Zhavoronkov (Ed.), Izd. Nauka, Moscow, 1978, pp. 59–70.

[1993Sac] A. Saccone, S. Delfino, D. Macció, R. Ferro: J. Phase Equilibria **14** (1993) 280–287.

[2003Cac] G. Cacciamani, S. de Negri, A. Saccone, R. Ferro: Intermetallics **11** (2003) 1135–1151.

In – La (Indium – Lanthanum)

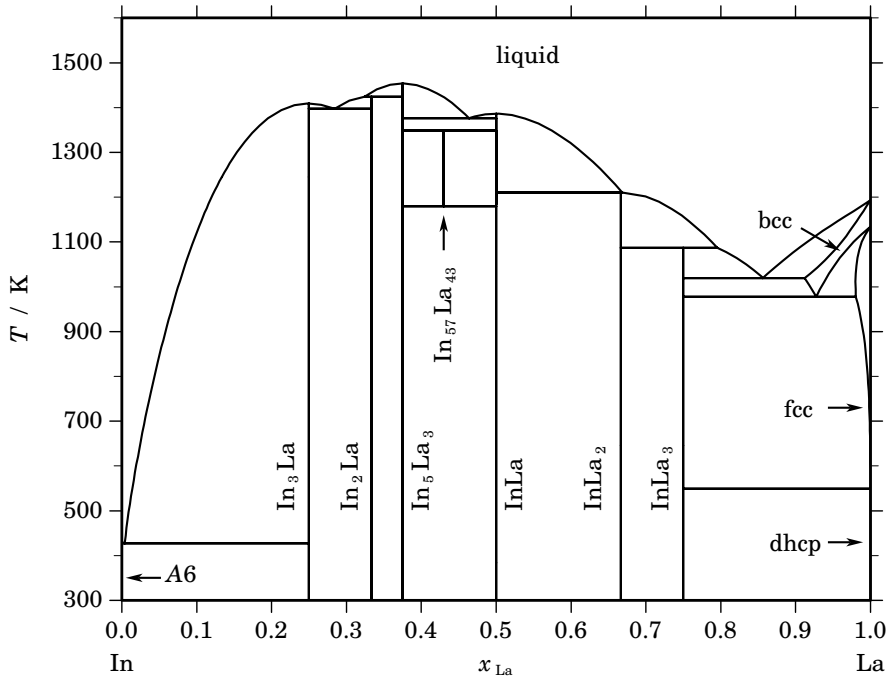

Fig. 1. Calculated phase diagram for the system In-La.

Most of the interest in the In-La system has probably been attracted by the superconducting compound $InLa_3$ which has one of the highest transition temperatures among the superconducting intermetallics of lanthanum. Variations in the reported transition temperatures between 8 and 10 K have been attributed to impurities and prompted for investigations on the solubility range and the phase diagram. The literature on the In-La system has been reviewed by [1992Pal] and a thermodynamic dataset has been optimised in [2002Wei] which is presented here. The phase diagram for the In-La system has been essentially worked out by [1974McM] and in addition the liquidus of In-rich melts with up to 10 at.% La has been investigated by [1971Deg]. Seven intermetallic compounds have been established and only for In_5La_3 a small range of solid solubility has been indicated but not quantified. Therefore, the assessment [2002Wei] describes all of them as stoichiometric. Enthalpies of formation have been measured by [1977Bor] across the whole composition range. For In_3La several other measurements of the enthalpy of formation have been reported and also EMF measurements of the Gibbs energy of formation [1971Deg].

Table I. Phases, structures and models.

Phase	Struktur-bericht	Prototype	Pearson symbol	Space group	SGTE name	Model
liquid					LIQUID	$(In,La)_1$
$A6$	$A6$	In	$tI2$	$I4/mmm$	TETRAGONAL_A6	In_1
In_3La	$L1_2$	$AuCu_3$	$cP4$	$Pm\bar{3}m$	IN3LA	In_3La_1
In_2La	···	$CeCu_2$	$oI12$	$Imma$	IN2LA	In_2La_1
In_5La_3	···	Pd_5Pu_3	$oC32$	$Cmcm$	IN5LA3	In_5La_3
$In_{57}La_{43}$	···	···	···	···	IN57LA43	$In_{57}La_{43}$
InLa	$B2$	CsCl	$cP2$	$Pm\bar{3}m$	INLA	In_1La_1
$InLa_2$	$B8_2$	$InNi_2$	$hP6$	$P6_3/mmc$	INLA2	In_1La_2
$InLa_3$	$L1_2$	$AuCu_3$	$cP4$	$Pm\bar{3}m$	INLA3	In_1La_3
bcc	$A2$	W	$cI2$	$Im\bar{3}m$	BCC_A2	$(In,La)_1$
fcc	$A1$	Cu	$cF4$	$Fm3\bar{3}m$	FCC_A1	$(In,La)_1$
dhcp	$A3'$	αLa	$hP4$	$P6_3/mmc$	DHCP	$(In,La)_1$

Table II. Invariant reactions.

Reaction	Type	T / K	Compositions / x_{La}			$\Delta_r H$ / (J/mol)
liquid $\rightleftharpoons$ In_5La_3	congruent	1453.8	0.375	0.375		−21411
liquid + In_5La_3 $\rightleftharpoons$ In_2La	peritectic	1424.3	0.324	0.375	0.333	−18701
liquid $\rightleftharpoons$ In_3La	congruent	1409.0	0.250	0.250		−26980
liquid $\rightleftharpoons$ In_3La + In_2La	eutectic	1397.4	0.284	0.250	0.333	−24731
liquid $\rightleftharpoons$ InLa	congruent	1386.6	0.500	0.500		−23309
liquid $\rightleftharpoons$ In_5La_3 + InLa	eutectic	1376.3	0.464	0.375	0.500	−22165
In_5La_3 + InLa $\rightleftharpoons$ $In_{57}La_{43}$	peritectoid	1348.9	0.375	0.500	0.430	0
InLa + liquid $\rightleftharpoons$ $InLa_2$	peritectic	1210.7	0.500	0.668	0.667	−12261
$In_{57}La_{43}$ $\rightleftharpoons$ In_5La_3 + InLa	eutectoid	1179.4	0.430	0.375	0.500	0
$InLa_2$ + liquid $\rightleftharpoons$ $InLa_3$	peritectic	1086.7	0.667	0.796	0.750	−5978
liquid $\rightleftharpoons$ $InLa_3$ + bcc	eutectic	1019.5	0.856	0.750	0.912	−6203
bcc $\rightleftharpoons$ $InLa_3$ + fcc	eutectoid	977.9	0.927	0.750	0.980	−2560
fcc $\rightleftharpoons$ $InLa_3$ + dhcp	eutectoid	549.4	1.000	0.750	1.000	−369
liquid $\rightleftharpoons$ $A6$ + In_3La	eutectic	427.4	0.004	0.000	0.250	−3377

Table IIIa. Integral quantities for the liquid phase at 1500 K.

x_{La}	ΔG_{m} [J/mol]	ΔH_{m} [J/mol]	ΔS_{m} [J/(mol·K)]	$G_{\mathrm{m}}^{\mathrm{E}}$ [J/mol]	$S_{\mathrm{m}}^{\mathrm{E}}$ [J/(mol·K)]	ΔC_P [J/(mol·K)]
0.000	0	0	0.000	0	0.000	0.000
0.100	−15954	−18215	−1.508	−11899	−4.210	0.000
0.200	−26035	−30946	−3.274	−19794	−7.435	0.000
0.300	−31814	−38732	−4.612	−24195	−9.691	0.000
0.400	−34006	−42112	−5.404	−25612	−10.999	0.000
0.500	−33200	−41623	−5.615	−24555	−11.378	0.000
0.600	−29927	−37804	−5.251	−21533	−10.847	0.000
0.700	−24676	−31194	−4.345	−17057	−9.424	0.000
0.800	−17877	−22331	−2.969	−11636	−7.130	0.000
0.900	−9835	−11753	−1.279	−5780	−3.982	0.000
1.000	0	0	0.000	0	0.000	0.000

Reference states: In(liquid), La(liquid)

Table IIIb. Partial quantities for In in the liquid phase at 1500 K.

x_{In}	ΔG_{In} [J/mol]	ΔH_{In} [J/mol]	ΔS_{In} [J/(mol·K)]	$G_{\mathrm{In}}^{\mathrm{E}}$ [J/mol]	$S_{\mathrm{In}}^{\mathrm{E}}$ [J/(mol·K)]	a_{In}	γ_{In}
1.000	0	0	0.000	0	0.000	1.000	1.000
0.900	−3401	−2832	0.380	−2087	−0.496	0.761	0.846
0.800	−10451	−10608	−0.105	−7668	−1.960	0.433	0.541
0.700	−20172	−22253	−1.388	−15723	−4.353	0.198	0.283
0.600	−31604	−36690	−3.390	−25233	−7.638	0.079	0.132
0.500	−43823	−52841	−6.012	−35178	−11.775	0.030	0.060
0.400	−55965	−69629	−9.109	−44537	−16.728	0.011	0.028
0.300	−67308	−85978	−12.447	−52292	−22.457	0.005	0.015
0.200	−77495	−100810	−15.544	−57422	−28.925	0.002	0.010
0.100	−87625	−113049	−16.950	−58908	−36.094	0.001	0.009
0.000	$-\infty$	−121618	∞	−55729	−43.926	0.000	0.011

Reference state: In(liquid)

Table IIIc. Partial quantities for La in the liquid phase at 1500 K.

x_{La}	ΔG_{La} [J/mol]	ΔH_{La} [J/mol]	ΔS_{La} [J/(mol·K)]	$G_{\mathrm{La}}^{\mathrm{E}}$ [J/mol]	$S_{\mathrm{La}}^{\mathrm{E}}$ [J/(mol·K)]	a_{La}	γ_{La}
0.000	$-\infty$	−211362	∞	−140711	−47.101	0.000	0.000
0.100	−128926	−156665	−18.492	−100209	−37.637	0.000	0.000
0.200	−88372	−112297	−15.950	−68300	−29.332	0.001	0.004
0.300	−58979	−77183	−12.136	−43964	−22.146	0.009	0.029
0.400	−37609	−50244	−8.423	−26181	−16.042	0.049	0.123
0.500	−22577	−30405	−5.218	−13932	−10.981	0.164	0.327
0.600	−12568	−16587	−2.679	−6197	−6.927	0.365	0.608
0.700	−6405	−7715	−0.873	−1956	−3.839	0.598	0.855
0.800	−2973	−2711	0.174	−190	−1.681	0.788	0.985
0.900	−1191	−498	0.462	123	−0.414	0.909	1.010
1.000	0	0	0.000	0	0.000	1.000	1.000

Reference state: La(liquid)

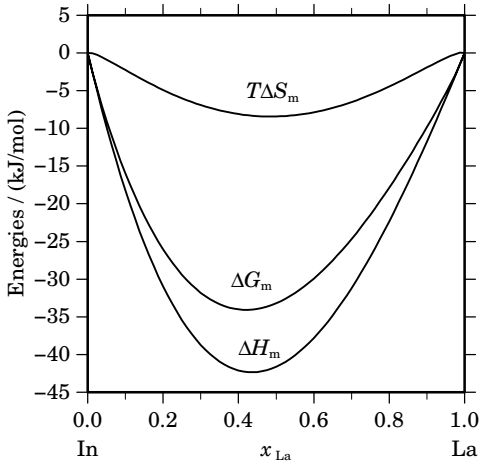

Fig. 2. Integral quantities of the liquid phase at T=1500 K.

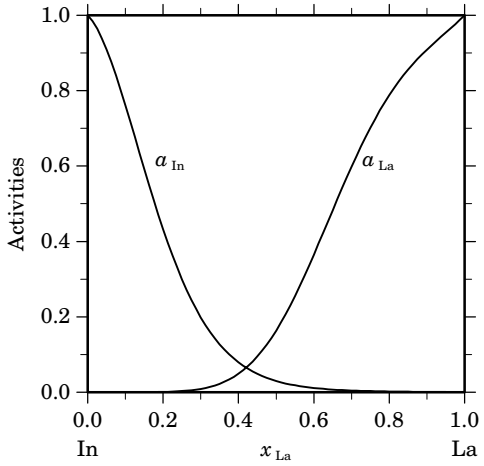

Fig. 3. Activities in the liquid phase at T=1500 K.

Table IV. Standard reaction quantities at 298.15 K for the compounds per mole of atoms.

Compound	x_{La}	$\Delta_{\mathrm{f}}G^{\circ}$ / (J/mol)	$\Delta_{\mathrm{f}}H^{\circ}$ / (J/mol)	$\Delta_{\mathrm{f}}S^{\circ}$ / (J/(mol·K))	$\Delta_{\mathrm{f}}C_P^{\circ}$ / (J/(mol·K))
In_3La_1	0.250	−52657	−57092	−14.876	0.000
In_2La_1	0.333	−53128	−56759	−12.181	0.000
In_5La_3	0.375	−53323	−56714	−11.374	0.000
$In_{57}La_{43}$	0.430	−53434	−57105	−12.314	−0.002
In_1La_1	0.500	−53577	−57607	−13.518	0.000
In_1La_2	0.667	−35950	−37692	−5.843	0.000
In_1La_3	0.750	−27021	−28087	−3.574	0.000

References

[1974McM] O.D. McMasters, K.A. Gschneidner, Jr.: J. Less-Common Met. **38** (1974) 137–148.

[1971Deg] V.A. Degtyar, A.P. Bayanov, L.A. Vnuchkova, V.V. Serebrennikov: Izv. Akad. Nauk SSSR, Met. **4** (1971) 149–153.

[1977Bor] A. Borsese, A. Calabretta, S. Delfino, R. Ferro: J. Less-Common Met. **51** (1977) 45–49.

[1992Pal] A. Palenzona, S. Cirafici in: "Phase Diagrams of Indium Alloys and Their Engineering Applications", C.E.T. White, H. Okamoto (eds.), ASM Intl., Materials Park, OH, 1992, pp. 145–151.

[2002Wei] Y. Wei, X. Su, F. Yin, Z. Li, X. Wu, C. Chen: J. Alloys Comp. **333** (2002) 118–121.

In – Pd (Indium – Palladium)

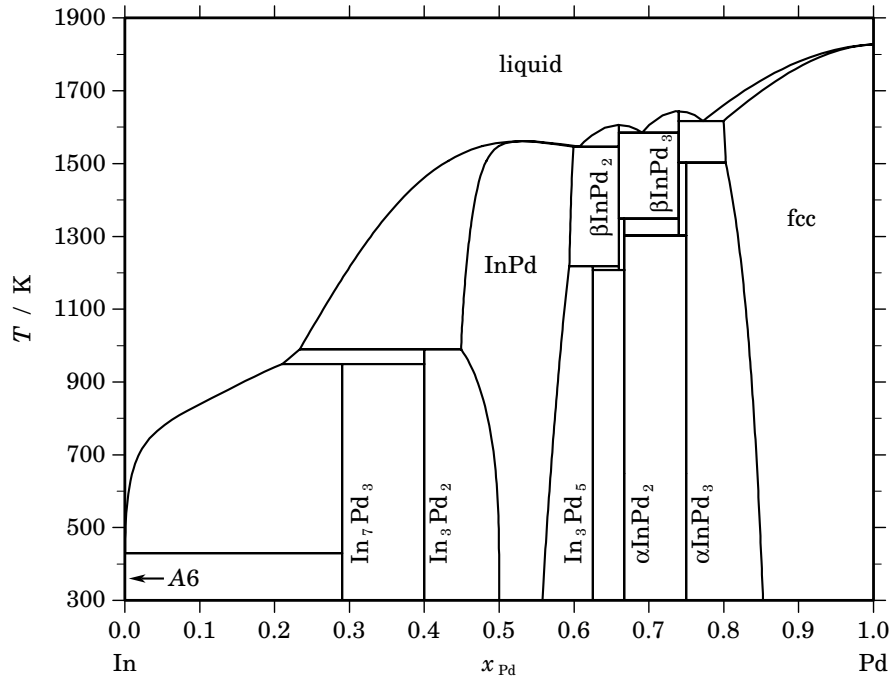

Fig. 1. Calculated phase diagram for the system In-Pd.

Palladium alloys with small amounts of indium are used for certain dental applications where In lowers the melting point of the alloys and causes the formation of an oxide layer which promotes the bonding between the alloy and ceramic materials. Furthermore, the In-Pd is of interest for the manufacturing of certain semiconductor devices when Pd-containing contacts are used on In-containing semiconductors, such as InSb or InP. The In-Pd system has been reviewed in [1992Oka] but since then new experimental work required a revision in the In-rich part. An updated review including an optimised thermodynamic dataset has been given by [2002Jia] which is presented here. The phase diagram has been determined by [1959Kni] and it has been modified later in the Pd-rich part [1988Sch] and recently in the In-rich part [2002Fla]. The enthalpy of mixing has been investigated for the melt in the range 0-65 at.% Pd at several temperatures and it has been found to be independent of temperature [1995ElA]. Enthalpies of formation for the solid phases have been determined in several investigations across the whole composition range and they are well represented by the calculation [2002Jia] within the deviations among the different datasets. Activities of In across the whole composition range have been reported from 873 K [1975Bir] up to 1273 K [1978Sch]. The heat capacities of the intermetallic compounds have been measured up to about 1000 K by [1975, 2001Per]. The dataset should not be used at too high temperatures because an artificial inverse miscibility gap opens in the liquid above 3100 K.

Table I. Phases, structures and models.

Phase	Struktur-bericht	Prototype	Pearson symbol	Space group	SGTE name	Model
liquid					LIQUID	$(In,Pd)_1$
$A6$	$A6$	In	$tI2$	$I4/mmm$	TETRAGONAL_A6	In_1
In_7Pd_3	$D8_f$	Ir_3Ge_7	$cI40$	$Im\bar{3}m$	IN7PD3	In_7Pd_3
In_3Pd_2	$D5_{13}$	Al_3Ni_2	$hP5$	$P\bar{3}m1$	IN3PD2	In_3Pd_2
InPd	$B2$	CsCl	$cP2$	$Pm\bar{3}m$	INPD	$(In,Pd)_1(Pd,\Box)_1$
In_3Pd_5	···	Ge_3Rh_5	$oP16$	$Pbam$	IN3PD5	In_3Pd_5
$\alpha InPd_2$	$C23$	Co_2Si	$oP12$	$Pnma$	INPD2_A	In_1Pd_2
$\beta InPd_2$	···	···	···	···	INPD2_B	$In_{17}Pd_{33}$
$\beta InPd_3$	···	···	···	···	INPD3_B	$In_{13}Pd_{37}$
$\alpha InPd_3$	$D0_{22}$	Al_3Ti	$tI8$	$I4/mmm$	INPD3_A	$InPd_3$
fcc	$A1$	Cu	$cF4$	$Fm\bar{3}\bar{3}m$	FCC_A1	$(In,Pd)_1$

Table II. Invariant reactions.

Reaction	Type	T / K	Compositions / x_{Pd}			$\Delta_r H$ / (J/mol)
liquid $\rightleftharpoons$ $\beta InPd_3$	congruent	1644.5	0.740	0.740		−12565
liquid $\rightleftharpoons$ $\beta InPd_3$ + fcc	eutectic	1617.2	0.772	0.740	0.800	−11246
liquid $\rightleftharpoons$ $\beta InPd_2$	congruent	1606.4	0.660	0.660		−12665
liquid $\rightleftharpoons$ $\beta InPd_2$ + $\beta InPd_3$	eutectic	1584.7	0.691	0.660	0.740	−11949
liquid $\rightleftharpoons$ InPd	congruent	1561.5	0.530	0.530		−15642
liquid $\rightleftharpoons$ InPd + $\beta InPd_2$	eutectic	1546.0	0.607	0.599	0.660	−12739
$\beta InPd_3$ + fcc $\rightleftharpoons$ $\alpha InPd_3$	peritectoid	1502.3	0.740	0.803	0.750	−2892
$\beta InPd_2$ + $\beta InPd_3$ $\rightleftharpoons$ $\alpha InPd_2$	peritectoid	1348.8	0.660	0.740	0.667	−2044
$\beta InPd_3$ $\rightleftharpoons$ $\alpha InPd_2$ + $\alpha InPd_3$	eutectoid	1302.1	0.740	0.667	0.750	−2134
InPd + $\beta InPd_2$ $\rightleftharpoons$ In_3Pd_5	peritectoid	1218.5	0.594	0.660	0.625	−767
$\beta InPd_2$ $\rightleftharpoons$ In_3Pd_5 + $\alpha InPd_2$	eutectoid	1207.5	0.660	0.625	0.667	−1588
liquid + InPd $\rightleftharpoons$ In_3Pd_2	peritectic	989.7	0.234	0.449	0.400	−6750
liquid + In_3Pd_2 $\rightleftharpoons$ In_7Pd_3	peritectic	949.2	0.210	0.400	0.290	−5932
liquid $\rightleftharpoons$ $A6$ + In_7Pd_3	eutectic	429.6	0.000	0.000	0.290	−3289

Table IIIa. Integral quantities for the liquid phase at 1900 K.

x_{Pd}	ΔG_m [J/mol]	ΔH_m [J/mol]	ΔS_m [J/(mol·K)]	G_m^E [J/mol]	S_m^E [J/(mol·K)]	ΔC_P [J/(mol·K)]
0.000	0	0	0.000	0	0.000	0.000
0.100	−10269	−12872	−1.370	−5134	−4.073	0.000
0.200	−18251	−25809	−3.978	−10346	−8.138	0.000
0.300	−24684	−37886	−6.948	−15034	−12.027	0.000
0.400	−29309	−48080	−9.879	−18677	−15.475	0.000
0.500	−31790	−55270	−12.358	−20840	−18.121	0.000
0.600	−31800	−58235	−13.913	−21168	−19.509	0.000
0.700	−29043	−55658	−14.008	−19393	−19.087	0.000
0.800	−23233	−46120	−12.046	−15328	−16.207	0.000
0.900	−14005	−28106	−7.421	−8870	−10.124	0.000
1.000	0	0	0.000	0	0.000	0.000

Reference states: In(liquid), Pd(liquid)

Table IIIb. Partial quantities for In in the liquid phase at 1900 K.

x_{In}	ΔG_{In} [J/mol]	ΔH_{In} [J/mol]	ΔS_{In} [J/(mol·K)]	$G^{\mathrm{E}}_{\mathrm{In}}$ [J/mol]	$S^{\mathrm{E}}_{\mathrm{In}}$ [J/(mol·K)]	a_{In}	γ_{In}
1.000	0	0	0.000	0	0.000	1.000	1.000
0.900	−1517	178	0.892	147	0.016	0.908	1.009
0.800	−3783	−471	1.744	−258	−0.112	0.787	0.984
0.700	−7932	−3943	2.100	−2298	−0.866	0.605	0.865
0.600	−14872	−12531	1.232	−6802	−3.015	0.390	0.650
0.500	−25304	−28823	−1.852	−14354	−7.615	0.202	0.403
0.400	−39757	−55703	−8.393	−25282	−16.011	0.081	0.202
0.300	−58687	−96351	−19.823	−39667	−29.834	0.024	0.081
0.200	−82764	−154243	−37.620	−57339	−51.002	0.005	0.027
0.100	−114252	−233150	−62.578	−77877	−81.723	0.001	0.007
0.000	−∞	−337140	∞	−100611	−124.489	0.000	0.002

Reference state: In(liquid)

Table IIIc. Partial quantities for Pd in the liquid phase at 1900 K.

x_{Pd}	ΔG_{Pd} [J/mol]	ΔH_{Pd} [J/mol]	ΔS_{Pd} [J/(mol·K)]	$G^{\mathrm{E}}_{\mathrm{Pd}}$ [J/mol]	$S^{\mathrm{E}}_{\mathrm{Pd}}$ [J/(mol·K)]	a_{Pd}	γ_{Pd}
0.000	−∞	−125562	∞	−48720	−40.443	0.000	0.046
0.100	−89034	−130323	−21.731	−52658	−40.876	0.004	0.036
0.200	−76122	−127161	−26.862	−50697	−40.244	0.008	0.040
0.300	−63772	−117085	−28.060	−44752	−38.070	0.018	0.059
0.400	−50965	−101403	−26.546	−36490	−34.165	0.040	0.099
0.500	−38276	−81717	−22.864	−27326	−28.627	0.089	0.177
0.600	−26496	−59924	−17.594	−18426	−21.841	0.187	0.311
0.700	−16339	−38218	−11.516	−10704	−14.481	0.355	0.508
0.800	−8350	−19089	−5.652	−4825	−7.508	0.589	0.737
0.900	−2867	−5323	−1.293	−1202	−2.169	0.834	0.927
1.000	0	0	0.000	0	0.000	1.000	1.000

Reference state: Pd(liquid)

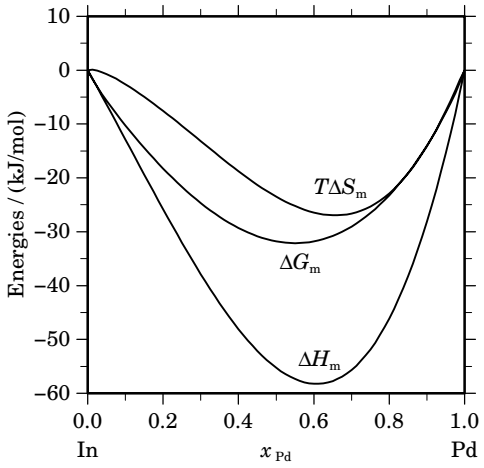

Fig. 2. Integral quantities of the liquid phase at T=1900 K.

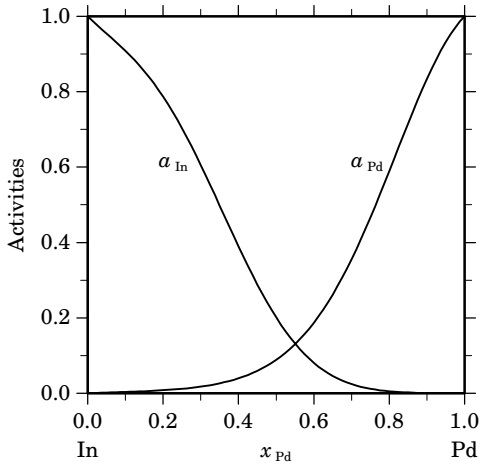

Fig. 3. Activities in the liquid phase at T=1900 K.

Table IV. Standard reaction quantities at 298.15 K for the compounds per mole of atoms.

Compound	x_{Pd}	$\Delta_{\mathrm{f}}G^{\circ}$ / (J/mol)	$\Delta_{\mathrm{f}}H^{\circ}$ / (J/mol)	$\Delta_{\mathrm{f}}S^{\circ}$ / (J/(mol·K))	$\Delta_{\mathrm{f}}C_P^{\circ}$ / (J/(mol·K))
In_7Pd_3	0.290	−38518	−41122	−8.733	−1.067
In_3Pd_2	0.400	−52041	−56456	−14.811	−2.415
In_3Pd_5	0.625	−56502	−60537	−13.534	−1.768
$\beta InPd_2$	0.660	−54590	−58730	−13.885	0.000
$\alpha InPd_2$	0.667	−55055	−58941	−13.032	−1.677
$\beta InPd_3$	0.740	−48986	−52801	−12.796	0.000
$\alpha InPd_3$	0.750	−49942	−54212	−14.320	0.000

References

[1959Kni] J.R. Knight, D.W. Rhys: J. Less-Common Met. **1** (1959) 292–303.

[1975Bir] J.M Bird, A.W. Bryant, J.N. Pratt: J. Chem. Thermodyn. **7** (1975) 577–586.

[1975Bry] A.W. Bryant, J.M. Bird, J.N. Pratt: J. Less-Common Met. **42** (1975) 249–253.

[1978Sch] H.J. Schaller, H. Borodowsky: Ber. Bunsenges. Phys. Chem. **82** (1978) 773–778.

[1988Sch] E.E. Schmid, V. Carle: Prakt. Metallogr. **25** (1988) 340–348.

[1992Oka] H. Okamoto in: "Phase Diagrams of Indium Alloys and Their Engineering Applications", C.E.T. White, H. Okamoto (eds.), ASM Intl., Materials Park, OH, 1992, pp. 207–210.

[1995ElA] D. El Allam, M. Gaune-Escard, J.P. Bros, E. Hayer: Metall. Mater. Trans. B **26B** (1995) 767–773.

[2001Per] L. Perring, J.J. Kuntz, F. Bussy, J.C. Gachon: Thermochim. Acta **366** (2001) 31–36.

[2002Fla] H. Flandorfer: J. Alloys Comp. **336** (2002) 176–180.

[2002Jia] C. Jiang, Z.-K. Liu: Metall. Mater. Trans. A **33A** (2002) 3597–3603.

Ir – Ni (Iridium – Nickel)

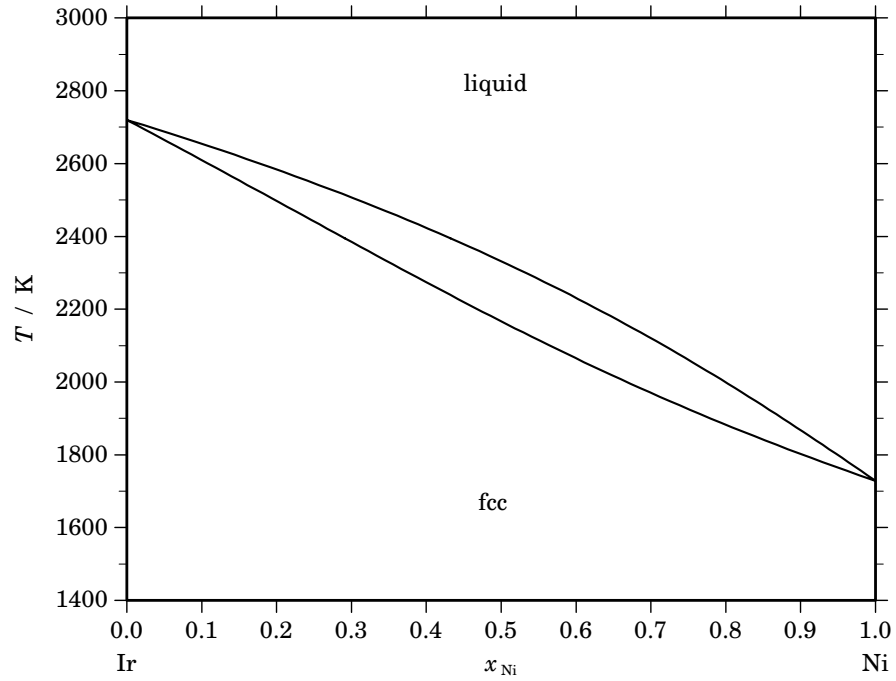

Fig. 1. Calculated phase diagram for the system Ir-Ni.

The thermodynamic description of the Ir-Ni system was established by Korb [2004Kor]. The equilibrium phases of the Ir-Ni system are the liquid and the fcc continuous solid solution. The Ir-Ni system was determined by [1970Rau] using X-ray diffraction (XRD) and optical microscopy. A continuous series of solid solutions was found, and no decomposition reaction or formation of superlattice phase was detected [1991Yan]. The same conclusion was confirmed by [1970Buc] on the basis of XRD, specific heat, magnetic susceptibility, and Debye temperature measurements. No changes in structure occurred after annealing alloys for several days in the temperature range from 773 to 1373 K [1970Buc]. The Curie temperatures of the fcc alloys were determined by [1960Cra]. The data show a linear dependence of Curie temperature on composition. The calculated phase diagram shows good agreement with published experimental data [1991Yan].

Table I. Phases, structures and models.

Phase	Struktur-bericht	Prototype	Pearson symbol	Space group	SGTE name	Model
liquid					LIQUID	$(Ir,Ni)_1$
fcc	$A1$	Cu	$cF4$	$Fm\overline{3}m$	FCC_A1	$(Ir,Ni)_1$

Table IIa. Integral quantities for the liquid phase at 2800 K.

x_{Ni}	ΔG_{m} [J/mol]	ΔH_{m} [J/mol]	ΔS_{m} [J/(mol·K)]	$G_{\mathrm{m}}^{\mathrm{E}}$ [J/mol]	$S_{\mathrm{m}}^{\mathrm{E}}$ [J/(mol·K)]	ΔC_P [J/(mol·K)]
0.000	0	0	0.000	0	0.000	0.000
0.100	−7618	−50	2.703	−50	0.000	0.000
0.200	−11739	−89	4.161	−89	0.000	0.000
0.300	−14338	−117	5.079	−117	0.000	0.000
0.400	−15802	−134	5.596	−134	0.000	0.000
0.500	−16276	−139	5.763	−139	0.000	0.000
0.600	−15802	−134	5.596	−134	0.000	0.000
0.700	−14338	−117	5.079	−117	0.000	0.000
0.800	−11739	−89	4.161	−89	0.000	0.000
0.900	−7618	−50	2.703	−50	0.000	0.000
1.000	0	0	0.000	0	0.000	0.000

Reference states: Ir(liquid), Ni(liquid)

Table IIb. Partial quantities for Ir in the liquid phase at 2800 K.

x_{Ir}	ΔG_{Ir} [J/mol]	ΔH_{Ir} [J/mol]	ΔS_{Ir} [J/(mol·K)]	$G_{\mathrm{Ir}}^{\mathrm{E}}$ [J/mol]	$S_{\mathrm{Ir}}^{\mathrm{E}}$ [J/(mol·K)]	a_{Ir}	γ_{Ir}
1.000	0	0	0.000	0	0.000	1.000	1.000
0.900	−2458	−6	0.876	−6	0.000	0.900	1.000
0.800	−5217	−22	1.855	−22	0.000	0.799	0.999
0.700	−8354	−50	2.966	−50	0.000	0.698	0.998
0.600	−11981	−89	4.247	−89	0.000	0.598	0.996
0.500	−16276	−139	5.763	−139	0.000	0.497	0.994
0.400	−21532	−200	7.619	−200	0.000	0.397	0.991
0.300	−28302	−273	10.010	−273	0.000	0.297	0.988
0.200	−37825	−356	13.382	−356	0.000	0.197	0.985
0.100	−54057	−451	19.145	−451	0.000	0.098	0.981
0.000	$-\infty$	−557	∞	−557	0.000	0.000	0.976

Reference state: Ir(liquid)

Table IIc. Partial quantities for Ni in the liquid phase at 2800 K.

x_{Ni}	ΔG_{Ni} [J/mol]	ΔH_{Ni} [J/mol]	ΔS_{Ni} [J/(mol·K)]	$G_{\mathrm{Ni}}^{\mathrm{E}}$ [J/mol]	$S_{\mathrm{Ni}}^{\mathrm{E}}$ [J/(mol·K)]	a_{Ni}	γ_{Ni}
0.000	$-\infty$	−557	∞	−557	0.000	0.000	0.976
0.100	−54057	−451	19.145	−451	0.000	0.098	0.981
0.200	−37825	−356	13.382	−356	0.000	0.197	0.985
0.300	−28302	−273	10.010	−273	0.000	0.297	0.988
0.400	−21532	−200	7.619	−200	0.000	0.397	0.991
0.500	−16276	−139	5.763	−139	0.000	0.497	0.994
0.600	−11981	−89	4.247	−89	0.000	0.598	0.996
0.700	−8354	−50	2.966	−50	0.000	0.698	0.998
0.800	−5217	−22	1.855	−22	0.000	0.799	0.999
0.900	−2458	−6	0.876	−6	0.000	0.900	1.000
1.000	0	0	0.000	0	0.000	1.000	1.000

Reference state: Ni(liquid)

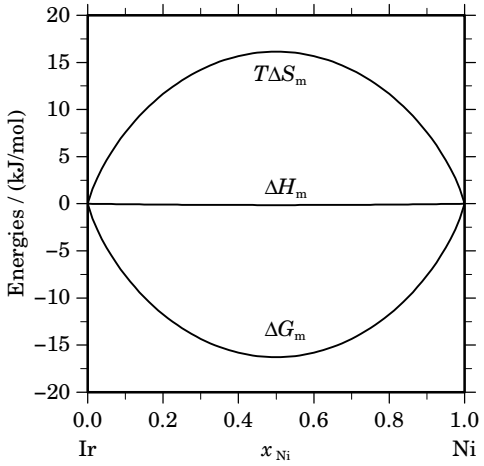

Fig. 2. Integral quantities of the liquid phase at T=2800 K.

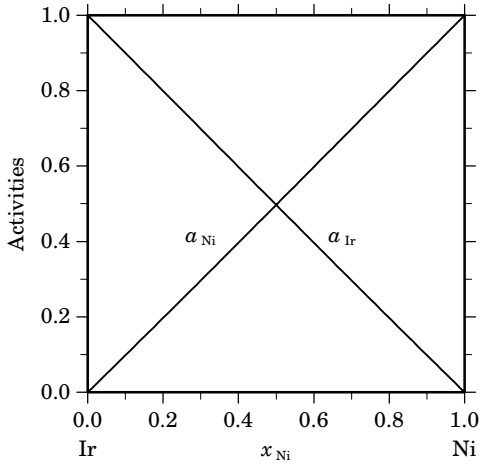

Fig. 3. Activities in the liquid phase at T=2800 K.

Table IIIa. Integral quantities for the stable phases at 1600 K.

Phase	x_{Ni}	ΔG_{m} [J/mol]	ΔH_{m} [J/mol]	ΔS_{m} [J/(mol·K)]	$G_{\mathrm{m}}^{\mathrm{E}}$ [J/mol]	$S_{\mathrm{m}}^{\mathrm{E}}$ [J/(mol·K)]	ΔC_P [J/(mol·K)]
fcc	0.000	0	0	0.000	0	0.000	0.000
	0.100	−4193	133	2.703	132	0.001	−0.003
	0.200	−6423	236	4.162	234	0.001	−0.006
	0.300	−7819	310	5.081	307	0.002	−0.009
	0.400	−8602	355	5.598	351	0.002	−0.011
	0.500	−8855	371	5.766	366	0.003	−0.014
	0.600	−8602	357	5.599	352	0.003	−0.016
	0.700	−7819	313	5.082	308	0.003	−0.017
	0.800	−6422	240	4.164	235	0.003	−0.015
	0.900	−4192	136	2.705	132	0.002	−0.010
	1.000	0	0	0.000	0	0.000	0.000

Reference states: Ir(fcc), Ni(fcc)

Table IIIb. Partial quantities for Ir in the stable phases at 1600 K.

Phase	x_{Ir}	ΔG_{Ir} [J/mol]	ΔH_{Ir} [J/mol]	ΔS_{Ir} [J/(mol·K)]	$G_{\mathrm{Ir}}^{\mathrm{E}}$ [J/mol]	$S_{\mathrm{Ir}}^{\mathrm{E}}$ [J/(mol·K)]	a_{Ir}	γ_{Ir}
fcc	1.000	0	0	0.000	0	0.000	1.000	1.000
	0.900	−1387	15	0.876	15	0.000	0.901	1.001
	0.800	−2910	58	1.855	58	0.000	0.804	1.004
	0.700	−4614	131	2.966	131	0.000	0.707	1.010
	0.600	−6562	234	4.247	234	0.000	0.611	1.018
	0.500	−8856	366	5.764	365	0.000	0.514	1.028
	0.400	−11663	528	7.620	526	0.001	0.416	1.040
	0.300	−15300	722	10.014	717	0.003	0.317	1.055
	0.200	−20473	950	13.389	937	0.008	0.215	1.073
	0.100	−29443	1213	19.160	1189	0.015	0.109	1.093
	0.000	$-\infty$	1516	∞	1471	0.028	0.000	1.117

Reference state: Ir(fcc)

Table IIIc. Partial quantities for Ni in the stable phases at 1600 K.

Phase	x_{Ni}	ΔG_{Ni} [J/mol]	ΔH_{Ni} [J/mol]	ΔS_{Ni} [J/(mol·K)]	$G^{\mathrm{E}}_{\mathrm{Ni}}$ [J/mol]	$S^{\mathrm{E}}_{\mathrm{Ni}}$ [J/(mol·K)]	a_{Ni}	γ_{Ni}
fcc	0.000	$-\infty$	1472	∞	1462	0.006	0.000	1.116
	0.100	−29447	1194	19.151	1185	0.006	0.109	1.093
	0.200	−20474	946	13.387	937	0.006	0.215	1.073
	0.300	−15299	727	10.016	718	0.006	0.317	1.055
	0.400	−11662	537	7.624	528	0.005	0.416	1.040
	0.500	−8854	375	5.768	367	0.005	0.514	1.028
	0.600	−6560	242	4.252	235	0.004	0.611	1.018
	0.700	−4612	138	2.969	133	0.003	0.707	1.010
	0.800	−2909	62	1.857	59	0.002	0.804	1.004
	0.900	−1387	16	0.877	15	0.001	0.901	1.001
	1.000	0	0	0.000	0	0.000	1.000	1.000

Reference state: Ni(fcc)

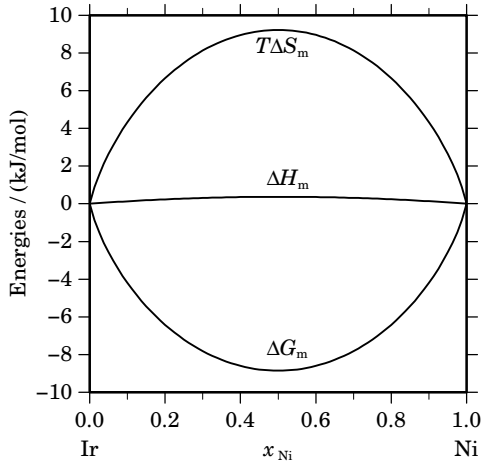

Fig. 4. Integral quantities of the stable phases at T=1600 K.

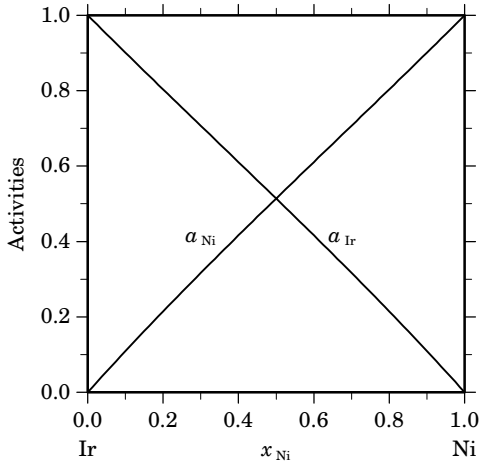

Fig. 5. Activities in the stable phases at T=1600 K.

References

[1960Cra] J. Crangle, D. Parsons: Proc. Roy. Soc. A **255A** (1960) 509–519.
[1970Buc] E. Bucher, W.F. Brinkman, J.P. Maita, A.S. Cooper: Phys. Rev. B **1B** (1970) 274–277.
[1970Rau] E. Raub, E. Röschel: Z. Metallkd. **61** (1970) 113–115.
[1991Yan] S.C. Yang, N. Chen, P. Nash in: "Phase Diagrams of Binary Nickel Alloys", P. Nash (ed.), ASM Intl., Materials Park, OH, 1991, pp. 181–182.
[2004Kor] J. Korb, unpublished assessment, GTT-Technologies, 2004.

Ir – Pt (Iridium – Platinum)

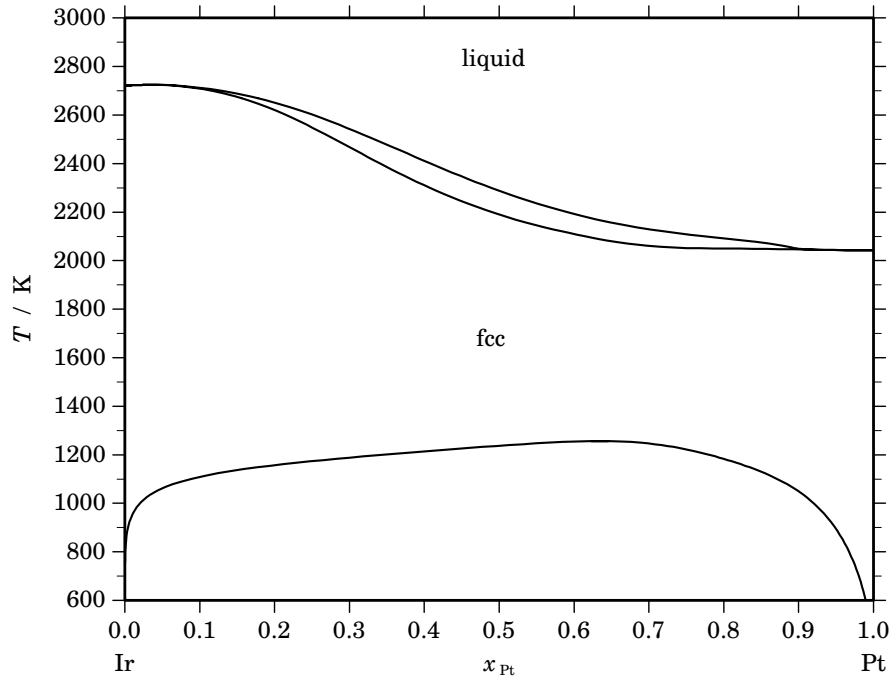

Fig. 1. Calculated phase diagram for the system Ir-Pt.

The equilibrium phases in the Ir-Pt system are the liquid phase and the fcc phase, exhibiting a miscibility gap. Experimental data on the Ir-Pt system are limited, the liquid and fcc phase boundaries were studied by [1930Mül], the miscibility gap in the fcc phase was investigated by [1956Rau]. The thermodynamic descriptions for all the stable phases in the Ir-Pt system were obtained by Korb and Jantzen [2004Kor] using available experimental data [1930Mül, 1956Rau]. The calculated phase diagram compares well with experimental data from the literature as collected in [1990Mas].

Table I. Phases, structures and models.

Phase	Struktur-bericht	Prototype	Pearson symbol	Space group	SGTE name	Model
liquid					LIQUID	$(Ir,Pt)_1$
fcc	$A1$	Cu	$cF4$	$Fm\overline{3}m$	FCC_A1	$(Ir,Pt)_1$

Table II. Invariant reactions.

Reaction	Type	T / K	Compositions / x_{Pt}			$\Delta_{\mathrm{r}}H$ / (J/mol)
liquid $\rightleftharpoons$ fcc	congruent	2724.0	0.037	0.037		−37912
fcc $\rightleftharpoons$ fcc′ + fcc″	critical	1255.6	0.634	0.634	0.634	0

Table IIIa. Integral quantities for the liquid phase at 2800 K.

x_{Pt}	ΔG_{m} [J/mol]	ΔH_{m} [J/mol]	ΔS_{m} [J/(mol·K)]	$G_{\mathrm{m}}^{\mathrm{E}}$ [J/mol]	$S_{\mathrm{m}}^{\mathrm{E}}$ [J/(mol·K)]	ΔC_P [J/(mol·K)]
0.000	0	0	0.000	0	0.000	0.000
0.100	−14600	3112	6.326	−7032	3.623	0.000
0.200	−22737	5870	10.217	−11088	6.056	0.000
0.300	−26919	8149	12.524	−12697	7.445	0.000
0.400	−28059	9821	13.528	−12391	7.933	0.000
0.500	−26835	10759	13.426	−10698	7.663	0.000
0.600	−23818	10836	12.377	−8150	6.781	0.000
0.700	−19497	9926	10.508	−5276	5.429	0.000
0.800	−14256	7901	7.913	−2606	3.752	0.000
0.900	−8239	4634	4.598	−671	1.895	0.000
1.000	0	0	0.000	0	0.000	0.000

Reference states: Ir(liquid), Pt(liquid)

Table IIIb. Partial quantities for Ir in the liquid phase at 2800 K.

x_{Ir}	ΔG_{Ir} [J/mol]	ΔH_{Ir} [J/mol]	ΔS_{Ir} [J/(mol·K)]	$G_{\mathrm{Ir}}^{\mathrm{E}}$ [J/mol]	$S_{\mathrm{Ir}}^{\mathrm{E}}$ [J/(mol·K)]	a_{Ir}	γ_{Ir}
1.000	0	0	0.000	0	0.000	1.000	1.000
0.900	−4029	155	1.495	−1576	0.619	0.841	0.935
0.800	−10794	791	4.137	−5599	2.282	0.629	0.786
0.700	−19311	2160	7.668	−11008	4.703	0.436	0.623
0.600	−28634	4517	11.840	−16742	7.592	0.292	0.487
0.500	−37879	8115	16.426	−21742	10.663	0.197	0.393
0.400	−46279	13208	21.246	−24947	13.627	0.137	0.342
0.300	−53327	20051	26.206	−25298	16.196	0.101	0.337
0.200	−59202	28896	31.464	−21734	18.082	0.079	0.393
0.100	−66800	39997	38.142	−13194	18.997	0.057	0.567
0.000	$-\infty$	53609	∞	1380	18.653	0.000	1.061

Reference state: Ir(liquid)

Table IIIc. Partial quantities for Pt in the liquid phase at 2800 K.

x_{Pt}	ΔG_{Pt} [J/mol]	ΔH_{Pt} [J/mol]	ΔS_{Pt} [J/(mol·K)]	$G_{\mathrm{Pt}}^{\mathrm{E}}$ [J/mol]	$S_{\mathrm{Pt}}^{\mathrm{E}}$ [J/(mol·K)]	a_{Pt}	γ_{Pt}
0.000	$-\infty$	32460	∞	−86968	42.653	0.000	0.024
0.100	−109737	29719	49.806	−56132	30.661	0.009	0.090
0.200	−70511	26189	34.536	−33042	21.154	0.048	0.242
0.300	−44669	22123	23.854	−16640	13.844	0.147	0.489
0.400	−27196	17777	16.062	−5864	8.443	0.311	0.777
0.500	−15792	13402	10.426	345	4.663	0.507	1.015
0.600	−8844	9254	6.464	3048	2.216	0.684	1.140
0.700	−4999	5586	3.780	3305	0.815	0.807	1.153
0.800	−3019	2652	2.025	2176	0.170	0.878	1.098
0.900	−1732	705	0.871	721	−0.005	0.928	1.031
1.000	0	0	0.000	0	0.000	1.000	1.000

Reference state: Pt(liquid)

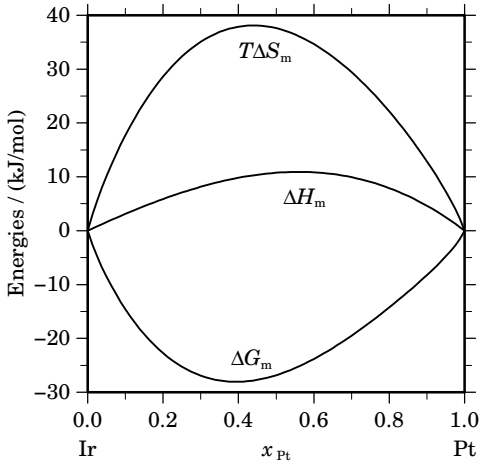

Fig. 2. Integral quantities of the liquid phase at T=2800 K.

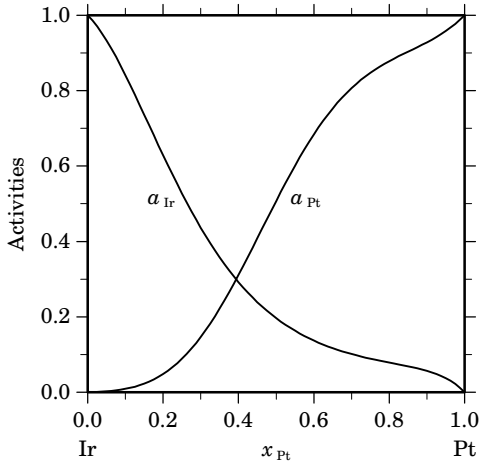

Fig. 3. Activities in the liquid phase at T=2800 K.

Table IVa. Integral quantities for the stable phases at 1400 K.

Phase	x_{Pt}	ΔG_{m} [J/mol]	ΔH_{m} [J/mol]	ΔS_{m} [J/(mol·K)]	$G^{\mathrm{E}}_{\mathrm{m}}$ [J/mol]	$S^{\mathrm{E}}_{\mathrm{m}}$ [J/(mol·K)]	ΔC_P [J/(mol·K)]
fcc	0.000	0	0	0.000	0	0.000	0.000
	0.100	−3247	8899	8.676	537	5.973	0.000
	0.200	−4557	14443	13.571	1268	9.410	0.000
	0.300	−5035	17147	15.844	2076	10.765	0.000
	0.400	−4992	17529	16.086	2842	10.491	0.000
	0.500	−4618	16106	14.803	3450	9.040	0.000
	0.600	−4052	13394	12.461	3782	6.866	0.000
	0.700	−3390	9911	9.501	3720	4.422	0.000
	0.800	−2677	6173	6.321	3148	2.160	0.000
	0.900	−1837	2697	3.239	1947	0.536	0.000
	1.000	0	0	0.000	0	0.000	0.000

Reference states: Ir(fcc), Pt(fcc)

Table IVb. Partial quantities for Ir in the stable phases at 1400 K.

Phase	x_{Ir}	ΔG_{Ir} [J/mol]	ΔH_{Ir} [J/mol]	ΔS_{Ir} [J/(mol·K)]	$G^{\mathrm{E}}_{\mathrm{Ir}}$ [J/mol]	$S^{\mathrm{E}}_{\mathrm{Ir}}$ [J/(mol·K)]	a_{Ir}	γ_{Ir}
fcc	1.000	0	0	0.000	0	0.000	1.000	1.000
	0.900	−1343	1764	2.219	−117	1.343	0.891	0.990
	0.800	−2907	6367	6.625	−309	4.769	0.779	0.974
	0.700	−4496	12776	12.337	−344	9.371	0.680	0.971
	0.600	−5931	19956	18.491	15	14.244	0.601	1.001
	0.500	−7066	26874	24.243	1003	18.480	0.545	1.090
	0.400	−7812	32496	28.792	2854	21.173	0.511	1.278
	0.300	−8212	35789	31.429	5803	21.418	0.494	1.646
	0.200	−8649	35717	31.690	10086	18.308	0.476	2.378
	0.100	−10867	31249	30.082	15936	10.938	0.393	3.932
	0.000	$-\infty$	21349	∞	23590	−1.601	0.000	7.588

Reference state: Ir(fcc)

Table IVc. Partial quantities for Pt in the stable phases at 1400 K.

Phase	x_{Pt}	ΔG_{Pt} [J/mol]	ΔH_{Pt} [J/mol]	ΔS_{Pt} [J/(mol·K)]	$G^{\mathrm{E}}_{\mathrm{Pt}}$ [J/mol]	$S^{\mathrm{E}}_{\mathrm{Pt}}$ [J/(mol·K)]	a_{Pt}	γ_{Pt}
fcc	0.000	$-\infty$	107497	∞	4011	73.919	0.000	1.411
	0.100	−20382	73117	66.785	6421	47.640	0.174	1.736
	0.200	−11155	46744	41.357	7579	27.975	0.384	1.918
	0.300	−6293	27346	24.028	7722	14.017	0.582	1.941
	0.400	−3583	13888	12.480	7083	4.861	0.735	1.838
	0.500	−2171	5337	5.363	5898	−0.400	0.830	1.660
	0.600	−1545	659	1.575	4401	−2.673	0.876	1.459
	0.700	−1324	−1180	0.103	2828	−2.863	0.893	1.275
	0.800	−1184	−1214	−0.021	1414	−1.877	0.903	1.129
	0.900	−834	−476	0.256	393	−0.620	0.931	1.034
	1.000	0	0	0.000	0	0.000	1.000	1.000

Reference state: Pt(fcc)

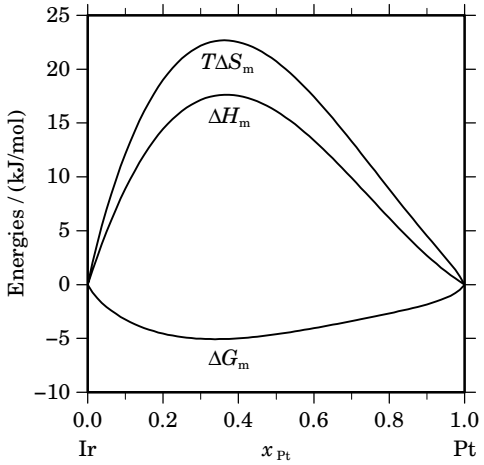

Fig. 4. Integral quantities of the stable phases at T=1400 K.

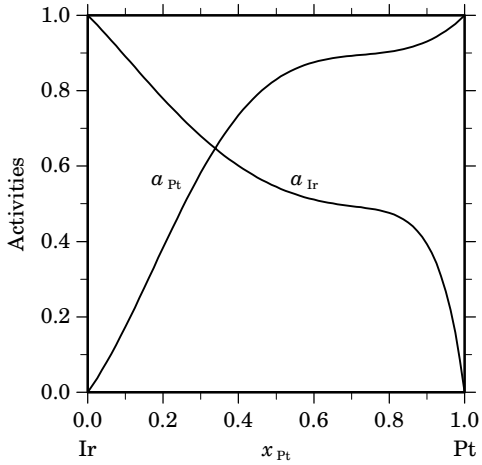

Fig. 5. Activities in the stable phases at T=1400 K.

References

[1930Mül] L. Müller: Ann. Phys. **7** (1930) 9–47.

[1956Rau] E. Raub, W. Plate: Z. Metallkd. **47** (1956) 688–693.

[1990Mas] T.B. Massalski (Ed.): "Binary Alloy Phase Diagrams", 2nd Ed., ASM Int., Materials Park, OH, 1990.

[2004Kor] J. Korb, T. Jantzen, unpublished assessment, GTT-Technologies, 2004.

Ir – Rh (Iridium – Rhodium)

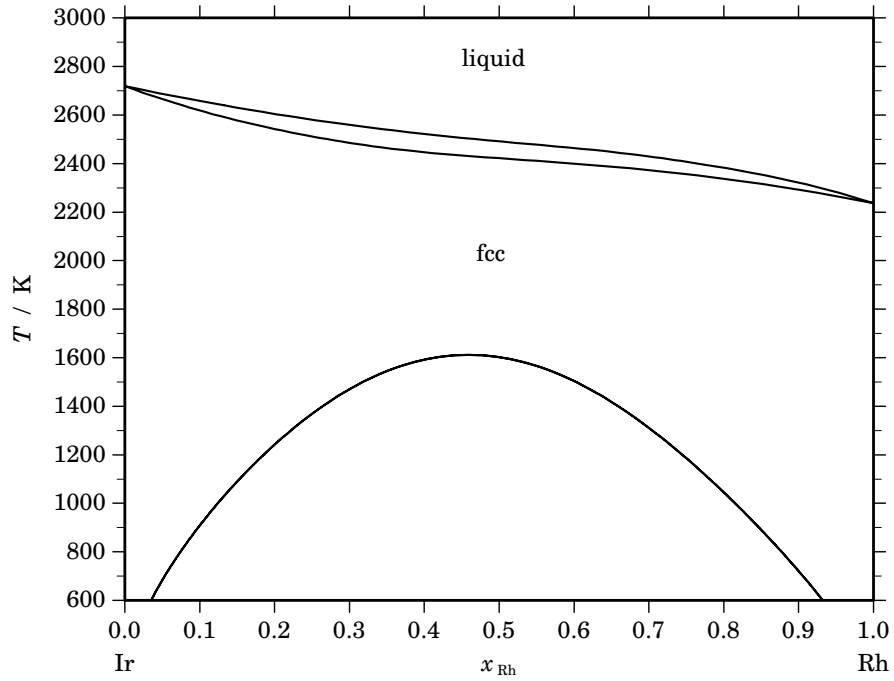

Fig. 1. Calculated phase diagram for the system Ir-Rh.

The equilibrium phases in the Ir-Rh system are the liquid phase and fcc phase, the latter exhibiting a miscibility gap at lower temperatures. [1959Rau] concluded that Ir forms a continuous series of solid solutions with Rh at high temperatures and empirically estimated the critical temperature of the miscibility gap from the difference in the melting points of the elements. The miscibility gap in the fcc phase at lower temperatures was evaluated on the basis of thermodynamic data [1983Tri]. The thermodynamic description of the Ir-Rh system was obtained by Korb and Jantzen [2004Kor] using available experimental data reported in [1991Tri]. The calculated phase diagram compares well with the diagram from the literature.

Table I. Phases, structures and models.

Phase	Struktur-bericht	Prototype	Pearson symbol	Space group	SGTE name	Model
liquid					LIQUID	$(Ir,Rh)_1$
fcc	$A1$	Cu	$cF4$	$Fm\bar{3}m$	FCC_A1	$(Ir,Rh)_1$

Table II. Invariant reactions.

Reaction	Type	T / K	Compositions / x_{Rh}			$\Delta_r H$ / (J/mol)
fcc $\rightleftharpoons$ fcc′ + fcc″	critical	1450.0	0.461	0.461	0.461	0

Table IIIa. Integral quantities for the liquid phase at 2800 K.

x_{Rh}	ΔG_{m} [J/mol]	ΔH_{m} [J/mol]	ΔS_{m} [J/(mol·K)]	$G_{\mathrm{m}}^{\mathrm{E}}$ [J/mol]	$S_{\mathrm{m}}^{\mathrm{E}}$ [J/(mol·K)]	ΔC_P [J/(mol·K)]
0.000	0	0	0.000	0	0.000	0.000
0.100	−4453	−897	1.270	3115	−1.433	0.000
0.200	−5964	−1447	1.613	5686	−2.547	0.000
0.300	−6564	−1704	1.736	7657	−3.343	0.000
0.400	−6695	−1725	1.775	8973	−3.821	0.000
0.500	−6558	−1565	1.783	9579	−3.980	0.000
0.600	−6250	−1280	1.775	9418	−3.821	0.000
0.700	−5786	−926	1.736	8436	−3.343	0.000
0.800	−5074	−557	1.613	6575	−2.547	0.000
0.900	−3786	−230	1.270	3782	−1.433	0.000
1.000	0	0	0.000	0	0.000	0.000

Reference states: Ir(liquid), Rh(liquid)

Table IIIb. Partial quantities for Ir in the liquid phase at 2800 K.

x_{Ir}	ΔG_{Ir} [J/mol]	ΔH_{Ir} [J/mol]	ΔS_{Ir} [J/(mol·K)]	$G_{\mathrm{Ir}}^{\mathrm{E}}$ [J/mol]	$S_{\mathrm{Ir}}^{\mathrm{E}}$ [J/(mol·K)]	a_{Ir}	γ_{Ir}
1.000	0	0	0.000	0	0.000	1.000	1.000
0.900	−2190	−183	0.717	263	−0.159	0.910	1.011
0.800	−4070	−658	1.219	1125	−0.637	0.840	1.049
0.700	−5606	−1314	1.533	2698	−1.433	0.786	1.123
0.600	−6800	−2040	1.700	5092	−2.547	0.747	1.245
0.500	−7717	−2724	1.783	8420	−3.980	0.718	1.436
0.400	−8539	−3255	1.887	12793	−5.731	0.693	1.732
0.300	−9709	−3522	2.209	18320	−7.801	0.659	2.197
0.200	−12354	−3414	3.193	25115	−10.189	0.588	2.941
0.100	−20318	−2819	6.249	33288	−12.896	0.418	4.178
0.000	$-\infty$	−1627	∞	42950	−15.920	0.000	6.327

Reference state: Ir(liquid)

Table IIIc. Partial quantities for Rh in the liquid phase at 2800 K.

x_{Rh}	ΔG_{Rh} [J/mol]	ΔH_{Rh} [J/mol]	ΔS_{Rh} [J/(mol·K)]	$G_{\mathrm{Rh}}^{\mathrm{E}}$ [J/mol]	$S_{\mathrm{Rh}}^{\mathrm{E}}$ [J/(mol·K)]	a_{Rh}	γ_{Rh}
0.000	$-\infty$	−10896	∞	33681	−15.920	0.000	4.249
0.100	−24823	−7324	6.249	28783	−12.896	0.344	3.443
0.200	−13540	−4601	3.193	23929	−10.189	0.559	2.795
0.300	−8801	−2614	2.209	19229	−7.801	0.685	2.284
0.400	−6537	−1253	1.887	14795	−5.731	0.755	1.888
0.500	−5399	−407	1.783	10737	−3.980	0.793	1.586
0.600	−4724	36	1.700	7169	−2.547	0.816	1.361
0.700	−4104	187	1.533	4199	−1.433	0.838	1.198
0.800	−3254	157	1.219	1940	−0.637	0.870	1.087
0.900	−1949	58	0.717	504	−0.159	0.920	1.022
1.000	0	0	0.000	0	0.000	1.000	1.000

Reference state: Rh(liquid)

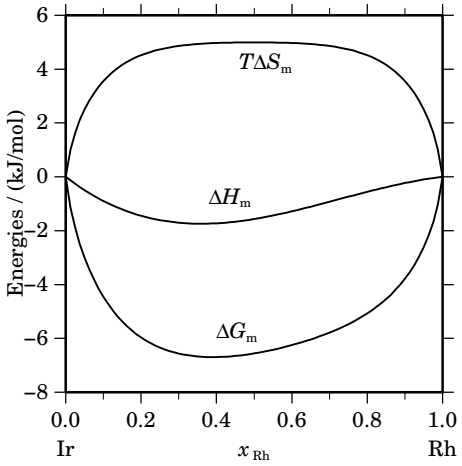

Fig. 2. Integral quantities of the liquid phase at T=2800 K.

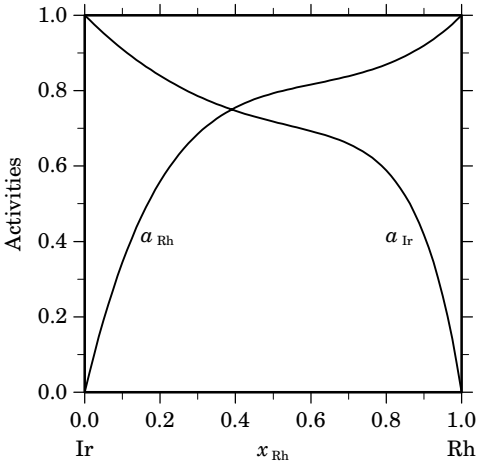

Fig. 3. Activities in the liquid phase at T=2800 K.

Table IVa. Integral quantities for the stable phases at 1800 K.

Phase	x_{Rh}	ΔG_{m} [J/mol]	ΔH_{m} [J/mol]	ΔS_{m} [J/(mol·K)]	$G_{\mathrm{m}}^{\mathrm{E}}$ [J/mol]	$S_{\mathrm{m}}^{\mathrm{E}}$ [J/(mol·K)]	ΔC_P [J/(mol·K)]
fcc	0.000	0	0	0.000	0	0.000	0.000
	0.100	−2191	1030	1.789	2675	−0.914	0.000
	0.200	−2782	1784	2.537	4707	−1.624	0.000
	0.300	−3026	2279	2.948	6116	−2.131	0.000
	0.400	−3154	2534	3.160	6919	−2.436	0.000
	0.500	−3241	2565	3.226	7133	−2.538	0.000
	0.600	−3296	2391	3.160	6776	−2.436	0.000
	0.700	−3275	2030	2.948	5867	−2.131	0.000
	0.800	−3067	1499	2.537	4422	−1.624	0.000
	0.900	−2404	817	1.789	2461	−0.913	0.000
	1.000	0	0	0.000	0	0.000	0.000

Reference states: Ir(fcc), Rh(fcc)

Table IVb. Partial quantities for Ir in the stable phases at 1800 K.

Phase	x_{Ir}	ΔG_{Ir} [J/mol]	ΔH_{Ir} [J/mol]	ΔS_{Ir} [J/(mol·K)]	$G_{\mathrm{Ir}}^{\mathrm{E}}$ [J/mol]	$S_{\mathrm{Ir}}^{\mathrm{E}}$ [J/(mol·K)]	a_{Ir}	γ_{Ir}
fcc	1.000	0	0	0.000	0	0.000	1.000	1.000
	0.900	−1253	141	0.775	324	−0.102	0.920	1.022
	0.800	−2068	541	1.449	1272	−0.406	0.871	1.089
	0.700	−2530	1164	2.052	2808	−0.914	0.844	1.206
	0.600	−2748	1974	2.623	4897	−1.624	0.832	1.387
	0.500	−2870	2936	3.226	7504	−2.538	0.825	1.651
	0.400	−3122	4014	3.965	10591	−3.654	0.812	2.029
	0.300	−3893	5173	5.037	14125	−4.973	0.771	2.570
	0.200	−6017	6377	6.886	18070	−6.496	0.669	3.345
	0.100	−12072	7590	10.923	22389	−8.222	0.446	4.464
	0.000	$-\infty$	8777	∞	27047	−10.150	0.000	6.094

Reference state: Ir(fcc)

Table IVc. Partial quantities for Rh in the stable phases at 1800 K.

Phase	x_{Rh}	ΔG_{Rh} [J/mol]	ΔH_{Rh} [J/mol]	ΔS_{Rh} [J/(mol·K)]	$G^{\mathrm{E}}_{\mathrm{Rh}}$ [J/mol]	$S^{\mathrm{E}}_{\mathrm{Rh}}$ [J/(mol·K)]	a_{Rh}	γ_{Rh}
fcc	0.000	$-\infty$	11744	∞	30014	−10.150	0.000	7.430
	0.100	−10630	9032	10.923	23831	−8.222	0.492	4.915
	0.200	−5638	6757	6.886	18450	−6.496	0.686	3.431
	0.300	−4184	4882	5.037	13835	−4.973	0.756	2.520
	0.400	−3763	3373	3.965	9951	−3.654	0.778	1.944
	0.500	−3612	2194	3.226	6762	−2.538	0.786	1.571
	0.600	−3412	1309	2.623	4233	−1.624	0.796	1.327
	0.700	−3011	683	2.052	2327	−0.913	0.818	1.168
	0.800	−2329	280	1.449	1011	−0.406	0.856	1.070
	0.900	−1330	64	0.775	247	−0.102	0.915	1.017
	1.000	0	0	0.000	0	0.000	1.000	1.000

Reference state: Rh(fcc)

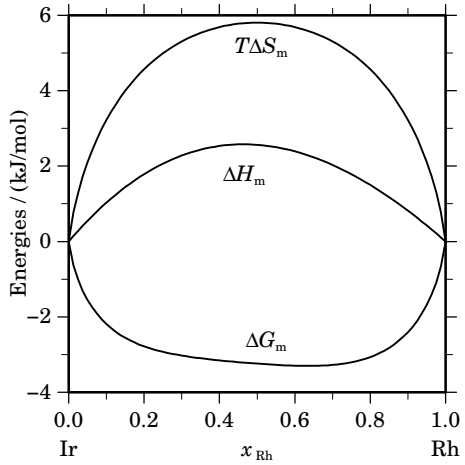

Fig. 4. Integral quantities of the stable phases at T=1800 K.

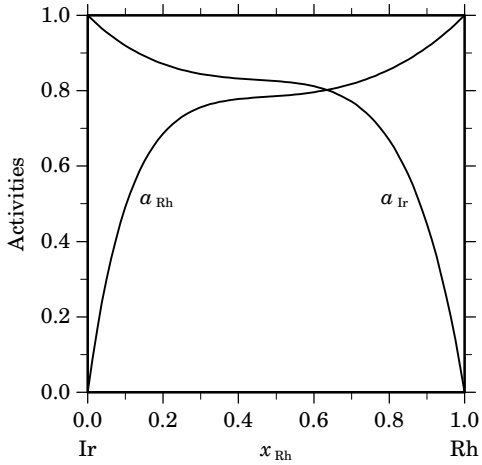

Fig. 5. Activities in the stable phases at T=1800 K.

References

[1959Rau] E. Raub: J. Less-Common Met. **1** (1959) 3–18.

[1970Kau] L. Kaufman, H. Bernstein, "Computer Calculation of Phase Diagrams", Academic Press, New York, 1970, pp. 33–91.

[1976Mof] W.G. Moffatt (ed.), "Handbook of Binary Phase Diagrams", General Electric Co., Schenectady, NY (1976).

[1983Tri] S.N. Tripathi, M.S. Chandrasekharaiah: Z. Metallkd. **74** (1983) 241–245.

[1991Tri] S.N. Tripathi, S.R. Bharadwaj, M.S. Chandrasekharaiah: J. Phase Equilibria **12** (1991) 606–608.

[2004Kor] J. Korb, T. Jantzen, unpublished assessment, GTT-Technologies, 2004.

Ir – Ru (Iridium – Ruthenium)

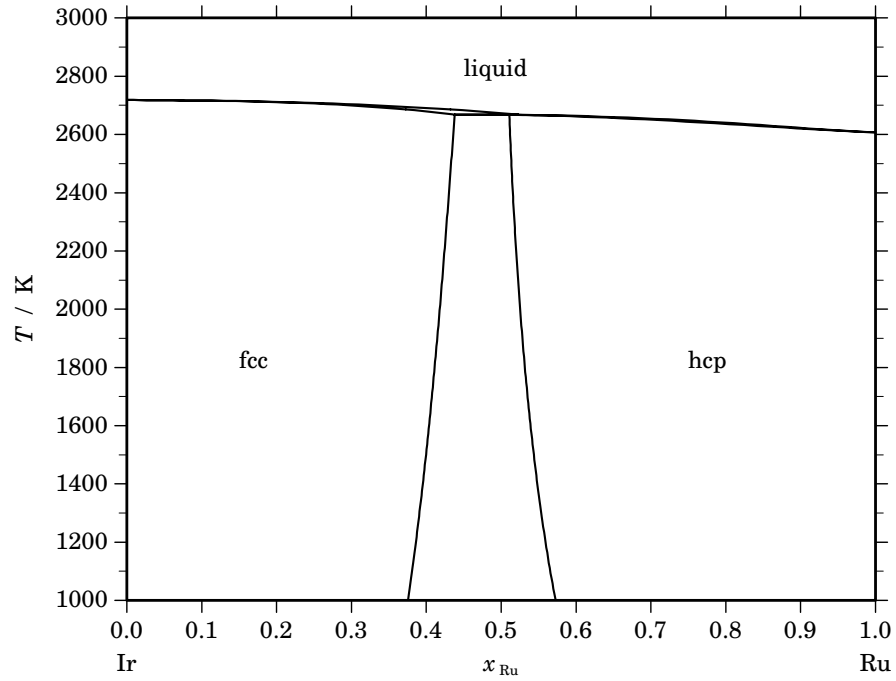

Fig. 1. Calculated phase diagram for the system Ir-Ru.

The Ir-Ru system exhibits the equilibrium phases liquid, Ir-rich fcc and Ru-rich hcp. The phase diagram was experimentally studied by [1964Rau] and [1988Ere] using thermal, X-ray, and metallographic investigations. Both studies are in good agreement. The fcc and hcp solvus boundaries as experimentally determined by Raub [1964Rau] and Eremenko *et al.* [1988Ere] are reproduced satisfactorily by the calculations. The solubility limit of Ir in hcp-Ru is 49 at.% at 2668 K [1988Ere]. The thermodynamic description of the Ir-Ru system was obtained by Korb [2004Kor]. The agreement between experimentally determined [1990Oka] and calculated phase diagrams is good for the solid-liquid range but at low temperature the two phase field between fcc and hcp appears a little wide.

Table I. Phases, structures and models.

Phase	Struktur-bericht	Prototype	Pearson symbol	Space group	SGTE name	Model
liquid					LIQUID	$(Ir,Ru)_1$
fcc	$A1$	Cu	$cF4$	$Fm\bar{3}m$	FCC_A1	$(Ir,Ru)_1$
hcp	$A3$	Mg	$hP2$	$P6_3/mmc$	HCP_A3	$(Ir,Ru)_1$

Table II. Invariant reactions.

Reaction	Type	T / K	Compositions / x_{Ru}			$\Delta_{\mathrm{r}}H$ / (J/mol)
fcc + liquid $\rightleftharpoons$ hcp	peritectic	2667.8	0.438	0.523	0.511	−73187

Table IIIa. Integral quantities for the liquid phase at 2800 K.

x_{Ru}	ΔG_{m} [J/mol]	ΔH_{m} [J/mol]	ΔS_{m} [J/(mol·K)]	$G_{\mathrm{m}}^{\mathrm{E}}$ [J/mol]	$S_{\mathrm{m}}^{\mathrm{E}}$ [J/(mol·K)]	ΔC_P [J/(mol·K)]
0.000	0	0	0.000	0	0.000	0.000
0.100	−8657	16154	8.861	−1089	6.158	0.000
0.200	−13504	28800	15.109	−1854	10.948	0.000
0.300	−16616	37839	19.448	−2395	14.369	0.000
0.400	−18439	43211	22.018	−2771	16.422	0.000
0.500	−19140	44895	22.869	−3003	17.106	0.000
0.600	−18741	42909	22.018	−3073	16.422	0.000
0.700	−17144	37311	19.448	−2923	14.369	0.000
0.800	−14108	28197	15.109	−2458	10.948	0.000
0.900	−9110	15702	8.861	−1542	6.158	0.000
1.000	0	0	0.000	0	0.000	0.000

Reference states: Ir(liquid), Ru(liquid)

Table IIIb. Partial quantities for Ir in the liquid phase at 2800 K.

x_{Ir}	ΔG_{Ir} [J/mol]	ΔH_{Ir} [J/mol]	ΔS_{Ir} [J/(mol·K)]	$G_{\mathrm{Ir}}^{\mathrm{E}}$ [J/mol]	$S_{\mathrm{Ir}}^{\mathrm{E}}$ [J/(mol·K)]	a_{Ir}	γ_{Ir}
1.000	0	0	0.000	0	0.000	1.000	1.000
0.900	−2634	1734	1.560	−182	0.684	0.893	0.992
0.800	−5770	7089	4.592	−575	2.737	0.780	0.976
0.700	−9344	16203	9.124	−1040	6.158	0.669	0.956
0.600	−13449	29098	15.195	−1556	10.948	0.561	0.935
0.500	−18354	45681	22.869	−2217	17.106	0.455	0.909
0.400	−24567	65737	32.252	−3235	24.633	0.348	0.870
0.300	−32969	88939	43.539	−4940	33.528	0.243	0.809
0.200	−45246	114841	57.174	−7777	43.792	0.143	0.716
0.100	−65917	142877	74.569	−12311	55.424	0.059	0.589
0.000	$-\infty$	172369	∞	−19221	68.425	0.000	0.438

Reference state: Ir(liquid)

Table IIIc. Partial quantities for Ru in the liquid phase at 2800 K.

x_{Ru}	ΔG_{Ru} [J/mol]	ΔH_{Ru} [J/mol]	ΔS_{Ru} [J/(mol·K)]	$G_{\mathrm{Ru}}^{\mathrm{E}}$ [J/mol]	$S_{\mathrm{Ru}}^{\mathrm{E}}$ [J/(mol·K)]	a_{Ru}	γ_{Ru}
0.000	$-\infty$	178655	∞	−12936	68.425	0.000	0.574
0.100	−62862	145932	74.569	−9256	55.424	0.067	0.672
0.200	−44442	115645	57.174	−6973	43.792	0.148	0.741
0.300	−33585	88323	43.539	−5556	33.528	0.236	0.788
0.400	−25925	64379	32.252	−4593	24.633	0.328	0.821
0.500	−19926	44109	22.869	−3789	17.106	0.425	0.850
0.600	−14857	27690	15.195	−2964	10.948	0.528	0.880
0.700	−10362	15184	9.124	−2059	6.158	0.641	0.915
0.800	−6323	6536	4.592	−1128	2.737	0.762	0.953
0.900	−2798	1571	1.560	−345	0.684	0.887	0.985
1.000	0	0	0.000	0	0.000	1.000	1.000

Reference state: Ru(liquid)

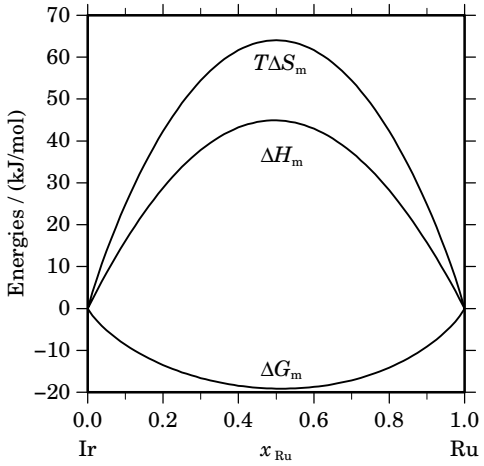

Fig. 2. Integral quantities of the liquid phase at T=2800 K.

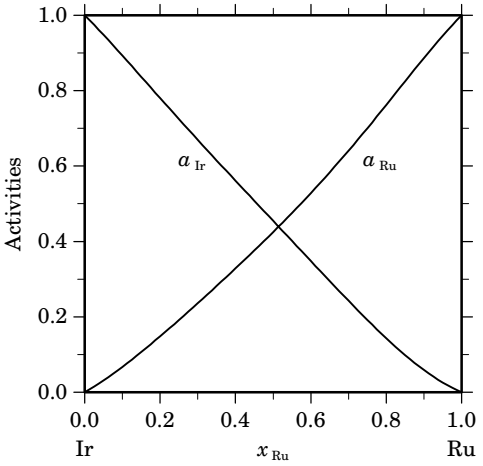

Fig. 3. Activities in the liquid phase at T=2800 K.

Table IVa. Integral quantities for the stable phases at 2000 K.

Phase	x_{Ru}	ΔG_{m} [J/mol]	ΔH_{m} [J/mol]	ΔS_{m} [J/(mol·K)]	$G_{\mathrm{m}}^{\mathrm{E}}$ [J/mol]	$S_{\mathrm{m}}^{\mathrm{E}}$ [J/(mol·K)]	ΔC_P [J/(mol·K)]
fcc	0.000	0	0	0.000	0	0.000	0.000
	0.100	−6202	−1073	2.565	−796	−0.138	0.000
	0.200	−9566	−1629	3.968	−1245	−0.192	0.000
	0.300	−11503	−1669	4.917	−1345	−0.162	0.000
	0.400	−12289	−1193	5.548	−1097	−0.048	0.000
	0.418	−12317	−1054	5.632	−1016	−0.019	0.000
hcp	0.525	−12389	−896	5.746	−884	−0.006	0.000
	0.600	−12201	−1090	5.556	−1010	−0.040	0.000
	0.700	−11182	−1154	5.014	−1024	−0.065	0.000
	0.800	−9181	−993	4.094	−860	−0.067	0.000
	0.900	−5924	−609	2.658	−519	−0.045	0.000
	1.000	0	0	0.000	0	0.000	0.000

Reference states: Ir(fcc), Ru(hcp)

Table IVb. Partial quantities for Ir in the stable phases at 2000 K.

Phase	x_{Ir}	ΔG_{Ir} [J/mol]	ΔH_{Ir} [J/mol]	ΔS_{Ir} [J/(mol·K)]	$G^{\mathrm{E}}_{\mathrm{Ir}}$ [J/mol]	$S^{\mathrm{E}}_{\mathrm{Ir}}$ [J/(mol·K)]	a_{Ir}	γ_{Ir}
fcc	1.000	0	0	0.000	0	0.000	1.000	1.000
	0.900	−1926	−258	0.834	−174	−0.042	0.891	0.990
	0.800	−4407	−1032	1.687	−696	−0.168	0.767	0.959
	0.700	−7498	−2323	2.588	−1566	−0.378	0.637	0.910
	0.600	−11279	−4129	3.575	−2785	−0.672	0.507	0.846
	0.582	−12039	−4507	3.766	−3040	−0.734	0.485	0.833
hcp	0.475	−12039	907	6.473	351	0.278	0.485	1.021
	0.400	−15632	−35	7.798	−395	0.180	0.391	0.977
	0.300	−21569	−1492	10.039	−1548	0.028	0.273	0.911
	0.200	−29643	−3173	13.235	−2879	−0.147	0.168	0.841
	0.100	−42678	−5078	18.800	−4388	−0.345	0.077	0.768
	0.000	$-\infty$	−7208	∞	−6074	−0.567	0.000	0.694

Reference state: Ir(fcc)

Table IVc. Partial quantities for Ru in the stable phases at 2000 K.

Phase	x_{Ru}	ΔG_{Ru} [J/mol]	ΔH_{Ru} [J/mol]	ΔS_{Ru} [J/(mol·K)]	$G^{\mathrm{E}}_{\mathrm{Ru}}$ [J/mol]	$S^{\mathrm{E}}_{\mathrm{Ru}}$ [J/(mol·K)]	a_{Ru}	γ_{Ru}
fcc	0.000	$-\infty$	−13306	∞	−9705	−1.801	0.000	0.558
	0.100	−44688	−8403	18.142	−6398	−1.003	0.068	0.681
	0.200	−30202	−4016	13.093	−3439	−0.288	0.163	0.813
	0.300	−20849	−145	10.352	−828	0.342	0.285	0.951
	0.400	−13803	3210	8.506	1434	0.888	0.436	1.090
	0.418	−12705	3757	8.231	1803	0.977	0.466	1.115
hcp	0.525	−12705	−2525	5.090	−2000	−0.263	0.466	0.887
	0.600	−9914	−1793	4.061	−1420	−0.187	0.551	0.918
	0.700	−6730	−1009	2.861	−799	−0.105	0.667	0.953
	0.800	−4066	−448	1.809	−355	−0.047	0.783	0.979
	0.900	−1841	−112	0.864	−89	−0.012	0.895	0.995
	1.000	0	0	0.000	0	0.000	1.000	1.000

Reference state: Ru(hcp)

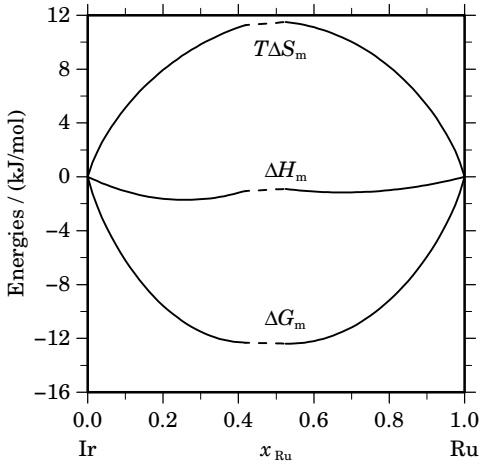

Fig. 4. Integral quantities of the stable phases at T=2000 K.

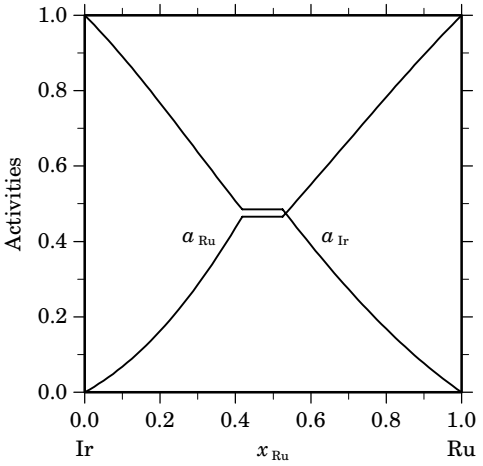

Fig. 5. Activities in the stable phases at T=2000 K.

References

[1964Rau] E. Raub: Z. Metallkd. **55** (1964) 316–319.

[1988Ere] V.N. Eremenko, V.T. Khoruzhaya, T.D. Shtepa: Izv. Akad. Nauk SSSR, Met. 1 (1988) 197–202; TR: Russ. Metall. 1 (1988) 194–198.

[1990Oka] H. Okamoto in: T.B. Massalski (Ed.), "Binary Alloy Phase Diagrams", 2nd Ed., ASM Int., Materials Park, OH, 1990.

[2004Kor] J. Korb, unpublished assessment, GTT-Technologies, 2004.

Ir – Zr (Iridium – Zirconium)

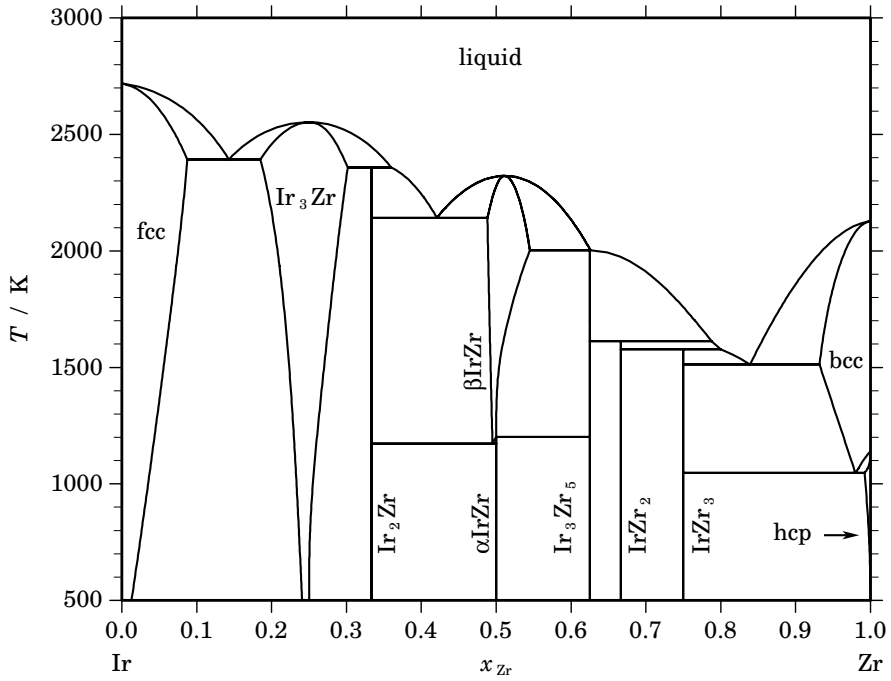

Fig. 1. Calculated phase diagram for the system Ir-Zr.

This system was assessed by Ran and Du [2006Ran], from the available experimental information on the phase diagram and thermodynamics. Iridium alloys are new materials with higher melting temperatures and superior oxidation resistance than Ni-based superalloys. The phase diagram was experimentally determined by Kuprina and Kuryachava [1974Kup], Eremenko *et al.* [1974Ere, 1978Ere1, 1978Ere2, 1980Ere]. The experimental phase diagram was assessed by Okamoto [1992Oka]. It presents four solution phases, the liquid with a complete miscibility range, the iridium based fcc phase and the zirconium rich terminal solution phases, bcc and hcp. There are three non-stoichiometric intermetallic compounds, Ir_3Zr, αIrZr and βIrZr, and four stoichiometric compounds, Ir_2Zr, Ir_3Zr_5, $IrZr_2$ and $IrZr_3$. The Ir_3Zr homogeneity range is equal to 19-30 at.% Zr at 2393 K [1980Ere]. βIrZr extends from 47 to 52 at.% Zr at 2143 K and from 49 to 50 at.% Zr below 1500 K. The crystal structures of the compounds were reported by Dwight and Beck [1959Dwi, 1961Dwi], Raman and Schubert [1964Ram], Schubert *et al.* [1964Sch], Biswas and Schubert [1967Bis], McCarthy [1971McC], Eremenko *et al.* [1978Ere2, 1980Ere], Matthias *et al.* [1961Mat], Cenzul and Parthe [1985Cen]. The enthalpy of formation of IrZr has been measured by Topor and Kleppa [1989Top].

Table I. Phases, structures and models.

Phase	Struktur-bericht	Prototype	Pearson symbol	Space group	SGTE name	Model
liquid					LIQUID	$(Ir,Zr)_1$
fcc	$A1$	Cu	$cF4$	$Fm\bar{3}m$	FCC_A1	$(Ir,Zr)_1$
Ir_3Zr	$L1_2$	$AuCu_3$	$cP4$	$Pm\bar{3}m$	IR3ZR	$(Ir,Zr)_3(Ir,Zr)_1$
Ir_2Zr	$C15$	Cu_2Mg	$cF24$	$Fd\bar{3}m$	IR2ZR	Ir_2Zr_1
αIrZr	$\cdots$	$\cdots$	$\cdots$	$\cdots$	IRZR	$(Ir,Zr)_1Zr_1$
βIrZr	$B2$	CsCl	$cP2$	$Pm\bar{3}m$	IRZR_B2	$(Ir,Zr)_1(Ir,Zr)_1$
Ir_3Zr_5	$D8_8$	Mn_5Si_3	$hP16$	$P6_3/mcm$	IR3ZR5	Ir_3Zr_5
$IrZr_2$	$C16$	Al_2Cu	$tI12$	$I4/mcm$	IRZR2	Ir_1Zr_2
$IrZr_3$	$\cdots$	αV_3S	$tI32$	$I\bar{4}2m$	IRZR3	Ir_1Zr_3
bcc	$A2$	W	$cI2$	$Im\bar{3}m$	BCC_A2	$(Ir,Zr)_1$
hcp	$A3$	Mg	$hP2$	$P6_3/mmc$	HCP_A3	$(Ir,Zr)_1$

Table II. Invariant reactions.

Reaction	Type	T / K	Compositions / x_{Zr}			$\Delta_r H$ / (J/mol)
liquid $\rightleftharpoons$ Ir_3Zr	congruent	2553.0	0.250	0.250		−36496
liquid $\rightleftharpoons$ fcc + Ir_3Zr	eutectic	2393.0	0.143	0.088	0.185	−22262
Ir_3Zr + liquid $\rightleftharpoons$ Ir_2Zr	peritectic	2358.4	0.302	0.360	0.333	−19625
liquid $\rightleftharpoons$ βIrZr	congruent	2323.0	0.511	0.511		−33162
liquid $\rightleftharpoons$ Ir_2Zr + βIrZr	eutectic	2142.6	0.421	0.333	0.488	−29582
βIrZr + liquid $\rightleftharpoons$ Ir_3Zr_5	peritectic	2003.1	0.545	0.626	0.625	−51090
Ir_3Zr_5 + liquid $\rightleftharpoons$ $IrZr_2$	peritectic	1613.0	0.625	0.788	0.667	−14992
$IrZr_2$ + liquid $\rightleftharpoons$ $IrZr_3$	peritectic	1578.2	0.667	0.800	0.750	−26785
liquid $\rightleftharpoons$ $IrZr_3$ + bcc	eutectic	1512.6	0.839	0.750	0.932	−30410
βIrZr $\rightleftharpoons$ αIrZr	congruent	1201.4	0.500	0.500		−2723
βIrZr $\rightleftharpoons$ αIrZr + Ir_3Zr_5	eutectoid	1201.4	0.500	0.500	0.625	−2723
βIrZr $\rightleftharpoons$ Ir_2Zr + αIrZr	eutectoid	1173.0	0.495	0.333	0.500	−2758
bcc $\rightleftharpoons$ $IrZr_3$ + hcp	eutectoid	1047.7	0.980	0.750	0.992	−7136

Table IIIa. Integral quantities for the liquid phase at 2800 K.

x_{Zr}	ΔG_m [J/mol]	ΔH_m [J/mol]	ΔS_m [J/(mol·K)]	G_m^E [J/mol]	S_m^E [J/(mol·K)]	ΔC_P [J/(mol·K)]
0.000	0	0	0.000	0	0.000	0.000
0.100	−40194	−40246	−0.019	−32625	−2.722	0.000
0.200	−71963	−66275	2.031	−60313	−2.129	0.000
0.300	−96417	−80063	5.841	−82196	0.762	0.000
0.400	−113075	−83589	10.531	−97407	4.935	0.000
0.500	−121215	−78831	15.137	−105078	9.374	0.000
0.600	−120012	−67766	18.659	−104344	13.063	0.000
0.700	−108557	−52373	20.066	−94336	14.987	0.000
0.800	−85837	−34629	18.288	−74187	14.128	0.000
0.900	−50599	−16512	12.174	−43031	9.471	0.000
1.000	0	0	0.000	0	0.000	0.000

Reference states: Ir(liquid), Zr(liquid)

Table IIIb. Partial quantities for Ir in the liquid phase at 2800 K.

x_{Ir}	ΔG_{Ir} [J/mol]	ΔH_{Ir} [J/mol]	ΔS_{Ir} [J/(mol·K)]	G^E_{Ir} [J/mol]	S^E_{Ir} [J/(mol·K)]	a_{Ir}	γ_{Ir}
1.000	0	0	0.000	0	0.000	1.000	1.000
0.900	−4777	−7439	−0.950	−2324	−1.827	0.814	0.905
0.800	−15648	−27117	−4.096	−10454	−5.951	0.511	0.638
0.700	−34425	−55080	−7.377	−26122	−10.342	0.228	0.326
0.600	−62956	−87372	−8.720	−51064	−12.967	0.067	0.112
0.500	−103150	−120036	−6.031	−87013	−11.794	0.012	0.024
0.400	−157036	−149118	2.828	−135704	−4.791	0.001	0.003
0.300	−226901	−170661	20.086	−198872	10.075	0.000	0.000
0.200	−315718	−180710	48.217	−278249	34.836	0.000	0.000
0.100	−429178	−175309	90.667	−375572	71.522	0.000	0.000
0.000	−∞	−150503	∞	−492574	122.168	0.000	0.000

Reference state: Ir(liquid)

Table IIIc. Partial quantities for Zr in the liquid phase at 2800 K.

x_{Zr}	ΔG_{Zr} [J/mol]	ΔH_{Zr} [J/mol]	ΔS_{Zr} [J/(mol·K)]	G^E_{Zr} [J/mol]	S^E_{Zr} [J/(mol·K)]	a_{Zr}	γ_{Zr}
0.000	−∞	−480143	∞	−348051	−47.176	0.000	0.000
0.100	−358940	−335514	8.366	−305334	−10.779	0.000	0.000
0.200	−297219	−222904	26.541	−259751	13.160	0.000	0.000
0.300	−241064	−138356	36.681	−213035	26.671	0.000	0.000
0.400	−188253	−77915	39.406	−166921	31.788	0.000	0.001
0.500	−139280	−37626	36.305	−123143	30.542	0.003	0.005
0.600	−95329	−13532	29.213	−83437	24.966	0.017	0.028
0.700	−57838	−1678	20.057	−49535	17.091	0.083	0.119
0.800	−28366	1891	10.806	−23172	8.951	0.296	0.370
0.900	−8535	1132	3.452	−6082	2.576	0.693	0.770
1.000	0	0	0.000	0	0.000	1.000	1.000

Reference state: Zr(liquid)

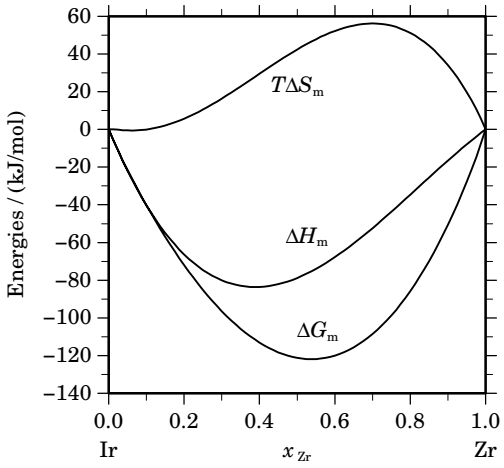

Fig. 2. Integral quantities of the liquid phase at T=2800 K.

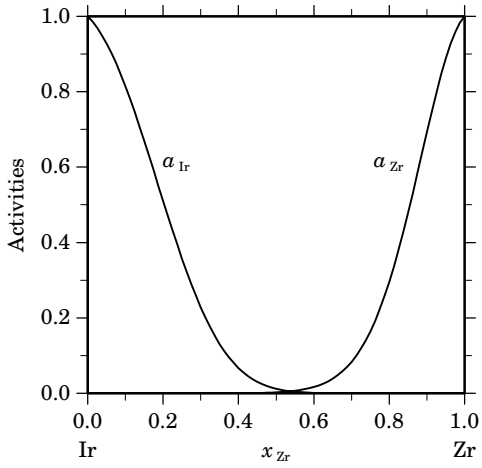

Fig. 3. Activities in the liquid phase at T=2800 K.

Table IV. Standard reaction quantities at 298.15 K for the compounds per mole of atoms.

Compound	x_{Zr}	$\Delta_{\mathrm{f}}G^{\circ}$ / (J/mol)	$\Delta_{\mathrm{f}}H^{\circ}$ / (J/mol)	$\Delta_{\mathrm{f}}S^{\circ}$ / (J/(mol·K))	$\Delta_{\mathrm{f}}C_P^{\circ}$ / (J/(mol·K))
Ir_3Zr	0.250	−81038	−80773	0.892	0.000
Ir_2Zr_1	0.333	−87313	−85827	4.982	0.000
αIrZr	0.500	−92448	−89893	8.568	0.000
βIrZr	0.500	−90393	−87162	10.837	−0.231
Ir_3Zr_5	0.625	−93849	−92893	3.207	0.000
Ir_1Zr_2	0.667	−88518	−88473	0.150	0.000
Ir_1Zr_3	0.750	−69264	−69236	0.095	0.000

References

[1959Dwi] A.E. Dwight, P.A. Beck: Trans. Metall. Soc. AIME **215** (1959) 976–979.

[1961Dwi] A.E. Dwight: Trans. ASM **53** (1961) 479–500.

[1961Mat] B.T. Matthias, V.B. Compton, E. Corenzwit: J. Phys. Chem. Solids **19** (1961) 130–133.

[1964Ram] A. Raman, K. Schubert: Z. Metallkd. **55** (1964) 704–710.

[1964Sch] K. Schubert, A. Raman, W. Rosseteutscher: Naturwiss. **51** (1964) 506–507.

[1967Bis] T.K. Biswas, K. Schubert: Z. Metallkd. **58** (1967) 558–559.

[1971McC] S.L. McCarthy: J. Low Temp. Phys. **4** (1971) 489–501.

[1974Kup] V.V. Kuprina, G.I. Kuryachaya: Vestn. MGU, Ser. 2, Khim. **15** (1974) 371–373 ;transl.: Moscow Univ. Chem. Bull. **29** (1974) 88.

[1974Ere] V.N. Eremenko, T.D. Shtepa, E.L. Semenova in: R. Rykhal, M. L'vov (Eds.), "Tezisy Dokl. Vses. Konf. Kristallokhim. Intermet. Soedin.", 2nd ed., Inst. Probl. Materialoved, Kiev, 1974, 28.

[1978Ere1] V.N. Eremenko, E.L. Semenova, T.D. Shtepa: Izv. Akad. Nauk SSSR, Met. 2 (1978) 200–203; transl.: Russ. Metall. 2 (1978) 158.

[1978Ere2] V.N. Eremenko, E.L. Semenova, T.D. Shtepa, Yu.V. Kudryavtsev: Dop. Akad. Nauk. Ukr. RSR, Ser. A, Fiz.-Mat. Tekn., No. 10 (1978) 943–945.

[1980Ere] V.N. Eremenko, E.L. Semenova, T.D. Shtepa: Izv. Akad. Nauk SSSR, Met. 5 (1980) 237–241; transl.: Russ. Metall. 5 (1978) 210.

[1985Cen] K. Cenzual, O.J. Parthe: Acta Cryst. C **41C** (1985) 820–823.

[1989Top] L. Topor, O.J. Kleppa: J. Less-Common Met. **155** (1988) 61–73.

[1992Oka] H. Okamoto: J. Phase Equilibria **13** (1992) 653–656.

[2006Ran] H. Ran, Z. Du: J. Alloys Comp. **413** (2006) 101–105.

La – Mg (Lanthanum – Magnesium)

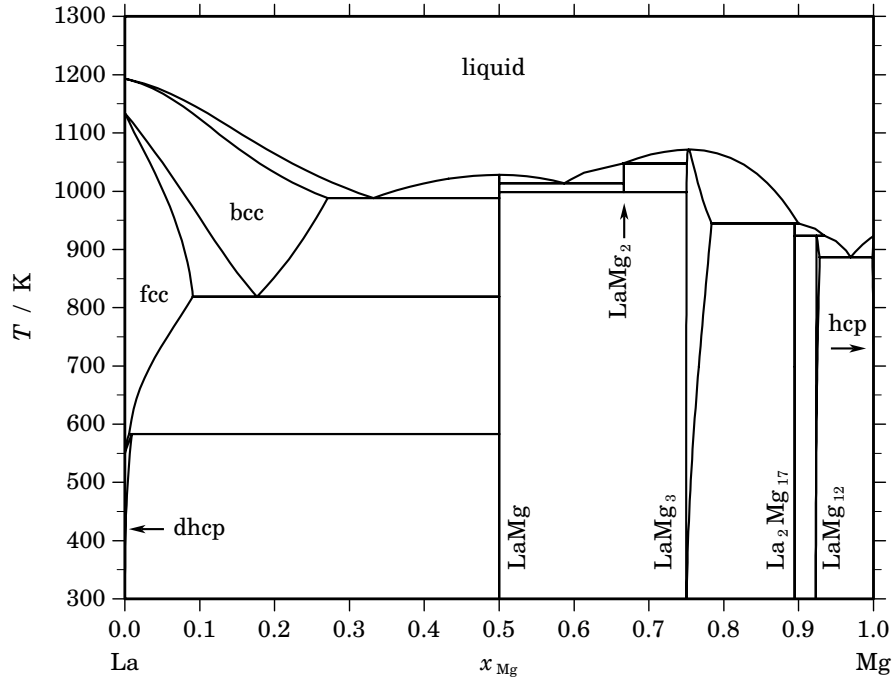

Fig. 1. Calculated phase diagram for the system La-Mg.

The addition of rare-earth metals to magnesium alloys retains their strength at elevated temperatures and improves their creep resistance over a wide range of temperature. The literature on the La-Mg system has been reviewed in [1988Nay] and a thermodynamic dataset has been optimised by [2004Guo]. For the assessment [2004Guo] have selected literature data on the phase diagram [1931Can, 1940Wei, 1947Vog, 1965Jos, 1986Man], activities of Mg in the melt at 1133 K [1973Afa], and enthapies of mixing in the melt for various temperatures and composition ranges [1995Aga]. Data for the intermetallic compounds have not been available.

Table I. Phases, structures and models.

Phase	Struktur-bericht	Prototype	Pearson symbol	Space group	SGTE name	Model
liquid					LIQUID	$(La,Mg)_1$
bcc	$A2$	W	$cI2$	$Im\bar{3}m$	BCC_A2	$(La,Mg)_1$
fcc	$A1$	Cu	$cF4$	$Fm3\bar{3}m$	FCC_A1	$(La,Mg)_1$
dhcp	$A3'$	αLa	$hP4$	$P6_3/mmc$	DHCP	$(La,Mg)_1$
LaMg	$B2$	CsCl	$cP2$	$Pm\bar{3}m$	LAMG	La_1Mg_1
$LaMg_2$	$C15$	$MgCu_2$	$cF24$	$Fd\bar{3}m$	LAMG2	La_1Mg_2
$LaMg_3$	$D0_3$	BiF_3	$cF16$	$Fm\bar{3}m$	LAMG3	$(La,Mg)_1Mg_3$
La_2Mg_{17}	···	$Ni_{17}Th_2$	$hP38$	$P6_3/mmc$	LA2MG17	La_2Mg_{17}
$LaMg_{12}$	···	$Mg_{12}Ce$	$oI338$	$Immm$	LAMG12	La_1Mg_{12}
hcp	$A3$	Mg	$hP2$	$P6_3/mmc$	HCP_A3	$(La,Mg)_1$

Table II. Invariant reactions.

Reaction	Type	T / K	Compositions / x_{Mg}			$\Delta_{\mathrm{r}}H$ / (J/mol)
liquid $\rightleftharpoons$ $LaMg_3$	congruent	1071.4	0.753	0.753		−18545
liquid + $LaMg_3$ $\rightleftharpoons$ $LaMg_2$	peritectic	1047.6	0.665	0.751	0.667	−7650
liquid $\rightleftharpoons$ LaMg	congruent	1027.9	0.500	0.500		−18136
liquid $\rightleftharpoons$ LaMg + $LaMg_2$	eutectic	1013.8	0.587	0.500	0.667	−12552
$LaMg_2$ $\rightleftharpoons$ LaMg + $LaMg_3$	eutectoid	998.2	0.667	0.500	0.750	−9747
liquid $\rightleftharpoons$ bcc + LaMg	eutectic	987.9	0.332	0.271	0.500	−10085
$LaMg_3$ + liquid $\rightleftharpoons$ La_2Mg_{17}	peritectic	944.8	0.784	0.900	0.895	−10282
La_2Mg_{17} + liquid $\rightleftharpoons$ $LaMg_{12}$	peritectic	923.3	0.895	0.935	0.924	−6900
liquid $\rightleftharpoons$ $LaMg_{12}$ + hcp	eutectic	886.5	0.970	0.928	0.999	−8589
bcc $\rightleftharpoons$ fcc + LaMg	eutectoid	818.8	0.176	0.091	0.500	−4114
fcc + LaMg $\rightleftharpoons$ dhcp	peritectoid	583.0	0.006	0.500	0.010	−357

Table IIIa. Integral quantities for the liquid phase at 1200 K.

x_{Mg}	ΔG_{m} [J/mol]	ΔH_{m} [J/mol]	ΔS_{m} [J/(mol·K)]	$G_{\mathrm{m}}^{\mathrm{E}}$ [J/mol]	$S_{\mathrm{m}}^{\mathrm{E}}$ [J/(mol·K)]	ΔC_P [J/(mol·K)]
0.000	0	0	0.000	0	0.000	0.000
0.100	−5531	−1117	3.679	−2288	0.976	0.000
0.200	−8688	−2535	5.127	−3695	0.966	0.000
0.300	−10677	−4270	5.339	−4582	0.260	0.000
0.400	−11899	−6210	4.740	−5184	−0.856	0.000
0.500	−12524	−8118	3.671	−5608	−2.092	0.000
0.600	−12551	−9629	2.435	−5836	−3.161	0.000
0.700	−11819	−10253	1.305	−5724	−3.774	0.000
0.800	−9992	−9372	0.517	−5000	−3.644	0.000
0.900	−6510	−6245	0.221	−3266	−2.482	0.000
1.000	0	0	0.000	0	0.000	0.000

Reference states: La(liquid), Mg(liquid)

Table IIIb. Partial quantities for La in the liquid phase at 1200 K.

x_{La}	ΔG_{La} [J/mol]	ΔH_{La} [J/mol]	ΔS_{La} [J/(mol·K)]	$G_{\mathrm{La}}^{\mathrm{E}}$ [J/mol]	$S_{\mathrm{La}}^{\mathrm{E}}$ [J/(mol·K)]	a_{La}	γ_{La}
1.000	0	0	0.000	0	0.000	1.000	1.000
0.900	−1562	138	1.417	−511	0.541	0.855	0.950
0.800	−3726	634	3.634	−1500	1.778	0.688	0.860
0.700	−5993	1330	6.102	−2434	3.137	0.548	0.784
0.600	−8259	1686	8.287	−3162	4.040	0.437	0.728
0.500	−10825	784	9.674	−3909	3.911	0.338	0.676
0.400	−14423	−2672	9.793	−5281	2.174	0.236	0.589
0.300	−20274	−10358	8.264	−8262	−1.747	0.131	0.437
0.200	−30273	−24330	4.953	−14215	−8.429	0.048	0.241
0.100	−47858	−47021	0.698	−24884	−18.447	0.008	0.083
0.000	$-\infty$	−81245	∞	−42390	−32.379	0.000	0.014

Reference state: La(liquid)

Table IIIc. Partial quantities for Mg in the liquid phase at 1200 K.

x_{Mg}	ΔG_{Mg} [J/mol]	ΔH_{Mg} [J/mol]	ΔS_{Mg} [J/(mol·K)]	$G^{\mathrm{E}}_{\mathrm{Mg}}$ [J/mol]	$S^{\mathrm{E}}_{\mathrm{Mg}}$ [J/(mol·K)]	a_{Mg}	γ_{Mg}
0.000	$-\infty$	−10025	∞	−28798	15.644	0.000	0.056
0.100	−41252	−12408	24.037	−18279	4.892	0.016	0.160
0.200	−28534	−15213	11.100	−12476	−2.282	0.057	0.286
0.300	−21606	−17338	3.557	−9594	−6.453	0.115	0.382
0.400	−17359	−18055	−0.580	−8217	−8.199	0.176	0.439
0.500	−14223	−17021	−2.332	−7307	−8.095	0.240	0.481
0.600	−11303	−14267	−2.470	−6206	−6.717	0.322	0.537
0.700	−8195	−10208	−1.677	−4636	−4.643	0.440	0.628
0.800	−4922	−5633	−0.592	−2696	−2.448	0.611	0.763
0.900	−1916	−1714	0.168	−864	−0.708	0.825	0.917
1.000	0	0	0.000	0	0.000	1.000	1.000

Reference state: Mg(liquid)

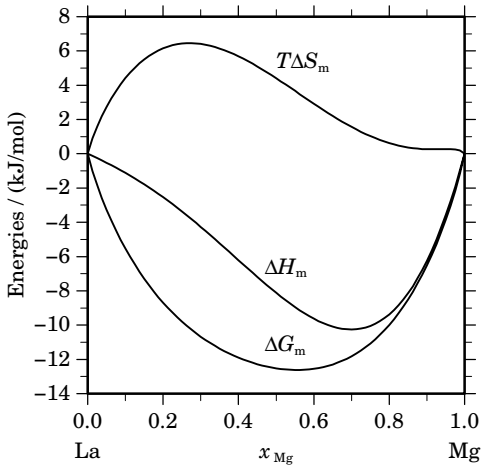

Fig. 2. Integral quantities of the liquid phase at T=1200 K.

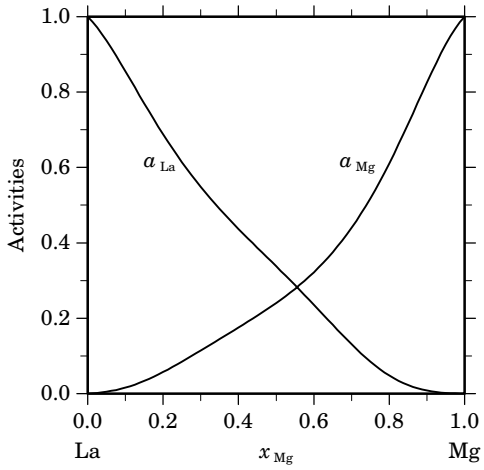

Fig. 3. Activities in the liquid phase at T=1200 K.

Table IV. Standard reaction quantities at 298.15 K for the compounds per mole of atoms.

Compound	x_{Mg}	$\Delta_{\mathrm{f}}G^{\circ}$ / (J/mol)	$\Delta_{\mathrm{f}}H^{\circ}$ / (J/mol)	$\Delta_{\mathrm{f}}S^{\circ}$ / (J/(mol·K))	$\Delta_{\mathrm{f}}C^{\circ}_{P}$ / (J/(mol·K))
La_1Mg_1	0.500	−15331	−16701	−4.594	0.000
$LaMg_3$	0.750	−17520	−19698	−7.303	0.000
La_1Mg_2	0.667	−9946	−8938	3.379	0.000
La_2Mg_{17}	0.895	−8046	−8663	−2.070	0.000
$LaMg_{12}$	0.923	−6009	−6398	−1.304	0.000

References

[1931Can] G. Canneri: Metall. Ital. **23** (1931) 803–823.
[1940Wei] F. Weibke, W. Schmidt: Z. Elektrochem. **46** (1940) 359–362.
[1947Vog] R. Vogel, T. Heumann: Z. Metallkd. **38** (1947) 1–8.
[1965Jos] R.R. Joseph, K.A. Gschneidner, Jr.: Trans. AIME **233** (1965) 2063–2069.
[1973Afa] Y.A. Afanasyev, A.P. Bayanov, Y.A. Frolov: Izv. Akad. Nauk SSSR, Met. (1973) 186–190; transl.: Russ. Metall. (1973) 155–158.
[1986Man] P. Manfrinetti, K.A. Gschneidner, Jr.: J. Less-Common Met. **123** (1986) 267–275.
[1988Nay] A.A. Nayeb-Hashemi, J.B. Clark in: "Phase Diagrams of Binary Magnesium Alloys", A.A. Nayeb-Hashemi, J.B. Clark (eds.), ASM Intl., Metals Park, OH, 1988, pp. 178–183.
[1995Aga] R. Agarwal, H. Feufel, F. Sommer: J. Alloys Comp. **217** (1995) 59–64.
[2004Guo] C. Guo, Z. Du: J. Alloys Comp. **385** (2004) 109–113.

Li – N (Lithium – Nitrogen)

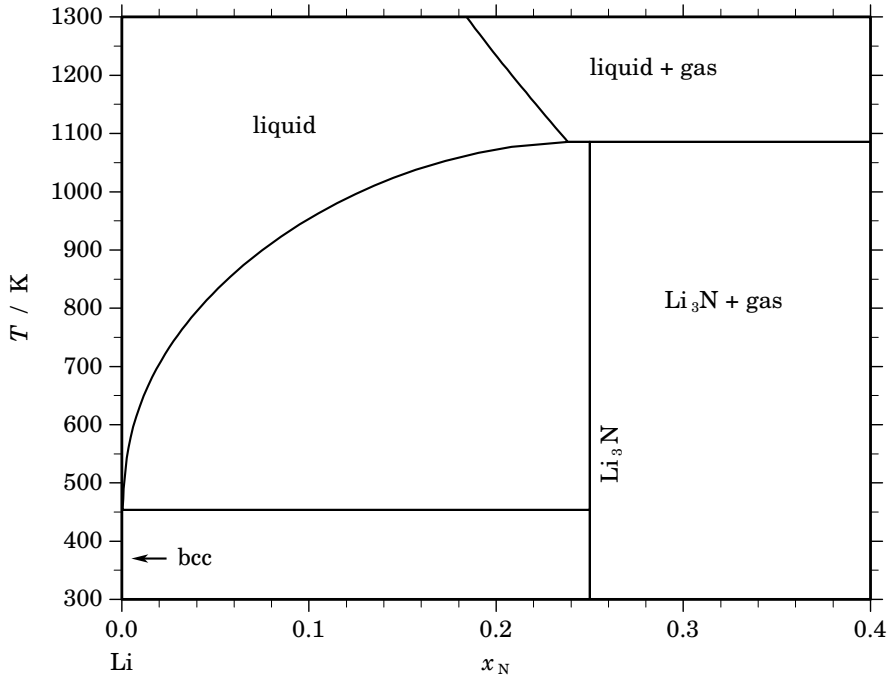

Fig. 1. Calculated phase diagram for the system Li-N.

Lithium nitride, LiN, can store more than 11% of its own weight in hydrogen which is considerably more than any other hydrogen storage material so far. Although there are still problems to solve for releasing the hydrogen from the storage the Li-N system will continue to be of high interest. The Li-N system has been reviewed by [1992San] and a thermodynamic optimisation has been reported in [2003Wan]. However the dataset of [2003Wan] leads to the formation of the liquid phase in the region where only LiN_3+gas should be stable and therefore, it has been re-assessed for the SGTE collection of binary systems [2005Fra]. The system Li-N includes 5 stable phases: gas, liquid, bcc-Li, Li_3N, and LiN_3. For the latter compound, lithium azide, no quantitative thermodynamic information seem to be available, except that under atmospheric pressure it does not melt but decomposes between 388 and 571 K. Therefore, it has not been included in the assessment. The solubility of nitrogen in solid lithium seems to be very small although no data have been reported. Therefore, bcc-Li has been treated as a pure substance. Similarly, Li_3N is described as a stoichiometric compound. The data for Li_3N are based on the SGTE substance database but with adjusted enthalpy and entropy. The solubility of nitrogen in molten Li has been measured in several investigations. A survey of these results is given in [2001Bor]. For the present optimisation a set of 3 investigations with the best agreement among them has been selected [1959Bol, 1975Ada, 1975Yon]. Since at lower temperatures the data of [1959Bol] deviate a bit too much from the other two sets the results of [1959Bol] have been used only for optimising the liquidus line above 800 K.

Table I. Phases, structures and models.

Phase	Struktur-bericht	Prototype	Pearson symbol	Space group	SGTE name	Model
liquid					LIQUID	$(Li,N)_1$
bcc	$A2$	W	$cI2$	$Im\bar{3}m$	BCC_A2	Li_1
Li_3N	$\cdots$	Li_3N	$hP4$	$P6/mmm$	LI3N	Li_3N_1

Table II. Invariant reactions.

Reaction	Type	T / K	Compositions / x_{N}			$\Delta_{\mathrm{r}}H$ / (J/mol)
liquid + gas $\rightleftharpoons$ Li_3N	gas-peritectic	1081.8	0.220	1.000	0.250	−25528
liquid $\rightleftharpoons$ bcc + Li_3N	eutectic	453.3	0.000	0.000	0.250	−3013

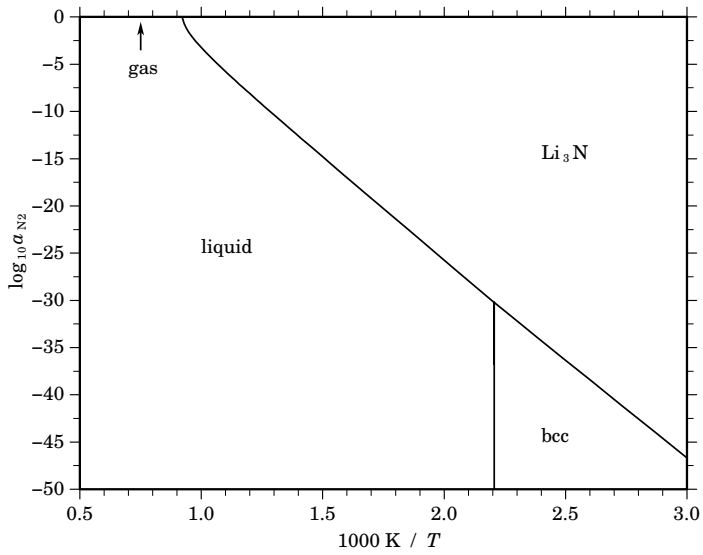

Fig. 2. Calculated temperature-activity phase diagram. Reference state: $\frac{1}{2}N_2$(gas, 0.1 MPa).

Table III. Standard reaction quantities at 298.15 K for the compounds per mole of atoms.

Compound	x_{N}	$\Delta_{\mathrm{f}}G^{\circ}$ / (J/mol)	$\Delta_{\mathrm{f}}H^{\circ}$ / (J/mol)	$\Delta_{\mathrm{f}}S^{\circ}$ / (J/(mol·K))	$\Delta_{\mathrm{f}}C_P^{\circ}$ / (J/(mol·K))
Li_3N_1	0.250	−32402	−41391	−30.149	−2.903

References

[1959Bol] K.A. Bolshakov, P.I Fedorov, L.A. Stepina: Izv. V. U. Z., Tsvet. Metall. **4** (1959) 52–53.
[1975Ada] P.F. Adams, M.G. Down, P. Hubberstey, R.J. Pulham: J. Less-Common Met. **42** (1975) 325–334.
[1975Yon] R.M. Yonco, E. Veleckis, V.A. Maroni: J. Nucl. Mater. **57** (1975) 317–324.
[1992San] J. Sangster, A.D. Pelton: J. Phase Equilibria **13** (1992) 291–296.
[2001Bor] H.U. Borgstedt, C. Guminsky: J. Phys. Chem. Ref. Data **30** (2001) 835–1158.
[2003Wan] W.J. Wang, W.X. Yuan, Y.T. Song, X.L. Chen: J. Alloys Comp. **352** (2003) 103–105.
[2005Fra] P. Franke, unpublished optimisation, 2005.

Li – Na (Lithium – Sodium)

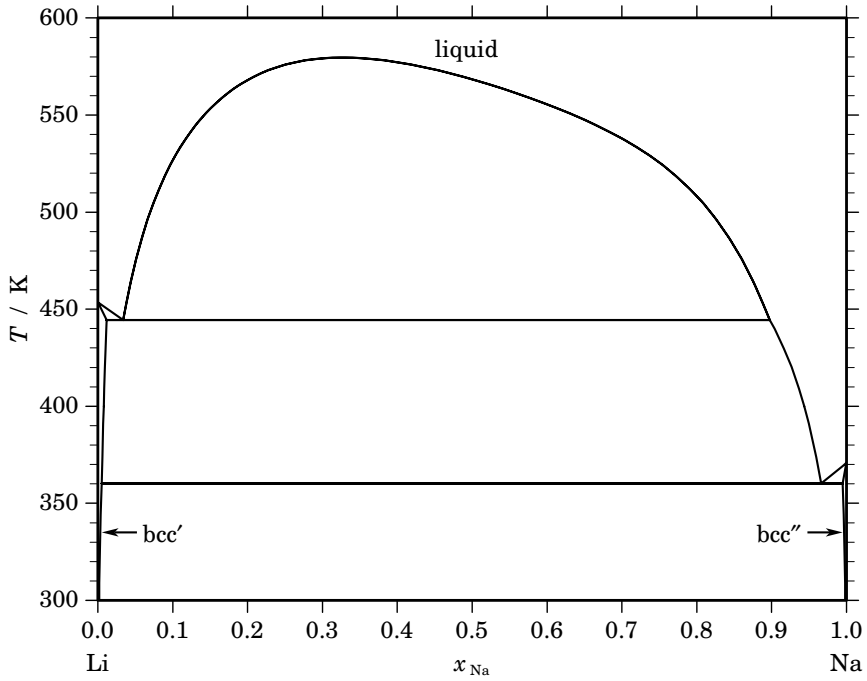

Fig. 1. Calculated phase diagram for the system Li-Na.

The literature on the Li-Na system has been reviewed by Bale [1989Bal] and a thermodynamic dataset has been optimised in [2003Zha] based on the element data recommended by SGTE. The system is characterised by dominant miscibility gaps in the liquid as well as in the solid (bcc) phase. For the optimisation Zhang *et al.* [2003Zha] have selected data for the phase equilibria from several experimental reports which are in general agreement with each other [1956Sal, 1957How, 1968Kan, 1971Sch, 1975Dow1, 1975Dow2, 1975Fei, 1975Wu, 1979End]. In most of these investigations the liquid-liquid equilibria have been determined. No data on the thermodynamics of mixing have been available.

Table I. Phases, structures and models.

Phase	Struktur-bericht	Prototype	Pearson symbol	Space group	SGTE name	Model
liquid					LIQUID	$(Li,Na)_1$
bcc	$A2$	W	$cI2$	$Im\bar{3}m$	BCC_A2	$(Li,Na)_1$

Table II. Invariant reactions.

Reaction	Type	T / K	Compositions / x_{Na}			$\Delta_r H$ / (J/mol)
liquid $\rightleftharpoons$ liquid′ + liquid″	critical	579.6	0.327	0.327	0.327	0
liquid′ $\rightleftharpoons$ bcc′ + liquid″	monotectic	444.3	0.034	0.012	0.898	−3227
liquid″ $\rightleftharpoons$ bcc′ + bcc″	eutectic	360.3	0.966	0.005	0.995	−2796

Table IIIa. Integral quantities for the liquid phase at 600 K.

x_{Na}	ΔG_{m} [J/mol]	ΔH_{m} [J/mol]	ΔS_{m} [J/(mol·K)]	$G_{\mathrm{m}}^{\mathrm{E}}$ [J/mol]	$S_{\mathrm{m}}^{\mathrm{E}}$ [J/(mol·K)]	ΔC_P [J/(mol·K)]
0.000	0	0	0.000	0	0.000	0.000
0.100	−528	1333	3.102	1094	0.399	0.000
0.200	−641	2174	4.692	1855	0.532	0.000
0.300	−703	2624	5.544	2345	0.465	0.000
0.400	−751	2766	5.862	2607	0.266	0.000
0.500	−787	2671	5.763	2671	0.000	0.000
0.600	−806	2392	5.330	2552	−0.266	0.000
0.700	−799	1969	4.614	2249	−0.465	0.000
0.800	−751	1426	3.629	1745	−0.532	0.000
0.900	−610	772	2.304	1011	−0.399	0.000
1.000	0	0	0.000	0	0.000	0.000

Reference states: Li(liquid), Na(liquid)

Table IIIb. Partial quantities for Li in the liquid phase at 600 K.

x_{Li}	ΔG_{Li} [J/mol]	ΔH_{Li} [J/mol]	ΔS_{Li} [J/(mol·K)]	$G_{\mathrm{Li}}^{\mathrm{E}}$ [J/mol]	$S_{\mathrm{Li}}^{\mathrm{E}}$ [J/(mol·K)]	a_{Li}	γ_{Li}
1.000	0	0	0.000	0	0.000	1.000	1.000
0.900	−348	264	1.020	177	0.144	0.933	1.036
0.800	−491	914	2.343	622	0.487	0.906	1.133
0.700	−543	1775	3.863	1236	0.897	0.897	1.281
0.600	−579	2714	5.488	1969	1.241	0.890	1.484
0.500	−644	3645	7.148	2814	1.385	0.879	1.758
0.400	−760	4529	8.815	3811	1.196	0.859	2.147
0.300	−963	5369	10.553	5044	0.543	0.824	2.748
0.200	−1386	6218	12.673	6643	−0.709	0.757	3.787
0.100	−2702	7170	16.453	8785	−2.692	0.582	5.818
0.000	$-\infty$	8368	∞	11691	−5.539	0.000	10.418

Reference state: Li(liquid)

Table IIIc. Partial quantities for Na in the liquid phase at 600 K.

x_{Na}	ΔG_{Na} [J/mol]	ΔH_{Na} [J/mol]	ΔS_{Na} [J/(mol·K)]	$G_{\mathrm{Na}}^{\mathrm{E}}$ [J/mol]	$S_{\mathrm{Na}}^{\mathrm{E}}$ [J/(mol·K)]	a_{Na}	γ_{Na}
0.000	$-\infty$	16160	∞	12837	5.539	0.000	13.107
0.100	−2145	10957	21.837	9342	2.692	0.651	6.505
0.200	−1239	7215	14.091	6790	0.709	0.780	3.900
0.300	−1075	4606	9.468	4931	−0.543	0.806	2.687
0.400	−1008	2845	6.422	3563	−1.196	0.817	2.043
0.500	−930	1697	4.378	2528	−1.385	0.830	1.660
0.600	−836	968	3.007	1713	−1.241	0.846	1.410
0.700	−729	512	2.068	1051	−0.897	0.864	1.234
0.800	−592	229	1.368	521	−0.487	0.888	1.110
0.900	−378	61	0.732	148	−0.144	0.927	1.030
1.000	0	0	0.000	0	0.000	1.000	1.000

Reference state: Na(liquid)

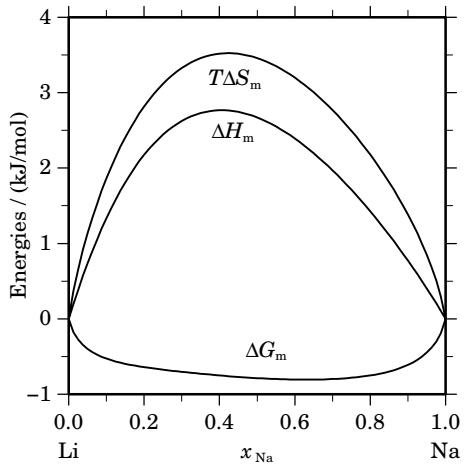

Fig. 2. Integral quantities of the liquid phase at T=600 K.

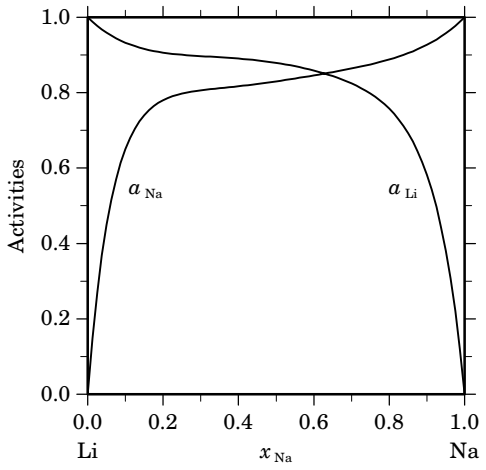

Fig. 3. Activities in the liquid phase at T=600 K.

References

[1956Sal] O.N. Salmon, D.H. Ahmann: J. Phys. Chem. **60** (1956) 13–16.
[1957How] W.H. Howland, L.F. Epstein: Adv. Chem. Ser. 19 (1957) 34–41.
[1968Kan] F.A. Kandan, R.C. Faxton, D.V. Keller: Phys. Chem. Liquids **1** (1968) 61–73.
[1971Sch] H.K. Schürmann, R.D. Parks: Phys. Rev. Lett. **27** (1971) 1790–1793.
[1975Dow1] M.G. Down, P. Hubberstey, R.J. Pulman: J. Chem. Soc. Dalton Trans. **14** (1975) 1490–1492.
[1975Dow2] M.G. Down, P. Hubberstey, R.J. Pulman: J. Chem. Soc. Faraday Trans. **71** (1975) 1387–1391.
[1975Fei] M.G. Feistma, J.J. Hallers, F.V.D. Werff, W. van der Lugt: Physica B **79B** (1975) 35–52.
[1975Wu] E.S. Wu, H. Brumberger: Phys. Lett. A **53A** (1975) 475–477.
[1979End] H. Endo, H. Hoshino, K. Tamura, M. Mushiage: Solid State Sci. **32** (1979) 1243–1246.
[1989Bal] C.W. Bale: Bull. Alloy Phase Diagrams **10** (1989) 265–268.
[2003Zha] S. Zhang, D. Shin, Z.-K. Liu: Calphad **27** (2003) 235–241.

Li – Sn (Lithium – Tin)

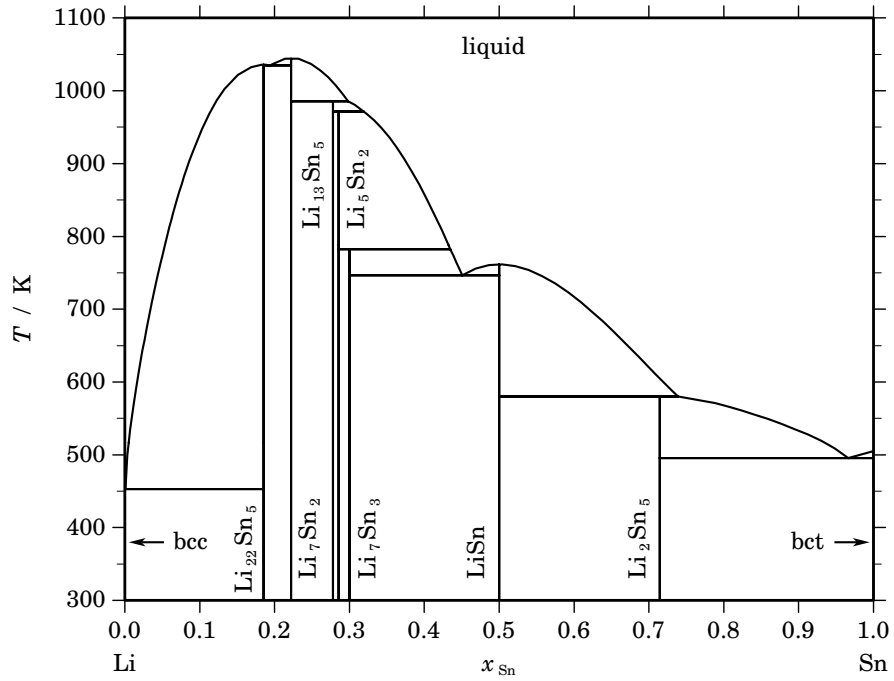

Fig. 1. Calculated phase diagram for the system Li-Sn.

Tin based materials are promising candidates for replacing conventional graphite anodes in Li-ion batteries. Compared with the intercalation compound LiC_6 which is formed with graphite the intermetallic lithium tin compounds can reach much higher storage capacities of Li per mass, especially in $Li_{22}Sn_5$. The literature on the Li-Sn system has been reviewed in [1998San] and a thermodynamic dataset has been optimised by [2005Yin]. The assessment is based on literature data on the phase diagram and on thermodynamic measurements. The selected phase equilibria have been reported by [1910Mas, 1932Bar, 1934Gru, 1964Fos, 1979Bai, 1982Dad]. Enthalpies of formation in the liquid and in two-phase regions with intermetallic compounds have been investigated at several temperatures in [1986Mos]. The activities of Li in the liquid have been measured at 1473 K by [1972Fis] and activities of Sn at 688 K have been reported in [1981Wen]. For their assessment [2005Yin] have selected enthalpies and entropies of formation for the intermetallic compounds at 688 K reported by [1981Wen] and enthalpies of formation at 298 K which have been given in [1938Kub].

Table I. Phases, structures and models.

Phase	Struktur-bericht	Prototype	Pearson symbol	Space group	SGTE name	Model
liquid					LIQUID	$(Li,Sn)_1$
bcc	$A2$	W	$cI2$	$Im\overline{3}m$	BCC_A2	$(Li,Sn)_1$
$Li_{22}Sn_5$	$\cdots$	$\cdots$	$cF432$	$F23$	LI22SN5	$Li_{22}Sn_5$
Li_7Sn_2	$\cdots$	$\cdots$	$oC36$	$Cmmm$	LI7SN2	Li_7Sn_2
$Li_{13}Sn_5$	$\cdots$	$\cdots$	$hP18$	$P\overline{3}m1$	LI13SN5	$Li_{13}Sn_5$
Li_5Sn_2	$D8_i$	Mo_2B_5	$hR7$	$R\overline{3}m$	LI5SN2	Li_5Sn_2
Li_7Sn_3	$\cdots$	$\cdots$	$mP20$	$P2_1/m$	LI7SN3	Li_7Sn_3
LiSn	$\cdots$	$\cdots$	$mP6$	$P2/m$	LISN	Li_1Sn_1
Li_2Sn_5	$\cdots$	$\cdots$	$tI14$	$P4/mbm$	LI2SN5	Li_2Sn_5
bct	$A5$	βSn	$tI4$	$I4_1/amd$	BCT_A5	Sn_1

Table II. Invariant reactions.

Reaction	Type	T / K	Compositions / x_{Sn}			$\Delta_r H$ / (J/mol)
liquid $\rightleftharpoons$ Li_7Sn_2	congruent	1044.9	0.222	0.222		−20155
liquid $\rightleftharpoons$ $Li_{22}Sn_5$	congruent	1035.9	0.185	0.185		−24056
liquid $\rightleftharpoons$ $Li_{22}Sn_5$ + Li_7Sn_2	eutectic	1035.0	0.194	0.185	0.222	−23048
Li_7Sn_2 + liquid $\rightleftharpoons$ $Li_{13}Sn_5$	peritectic	985.6	0.222	0.298	0.278	−10830
$Li_{13}Sn_5$ + liquid $\rightleftharpoons$ Li_5Sn_2	peritectic	971.5	0.278	0.319	0.286	−2660
Li_5Sn_2 + liquid $\rightleftharpoons$ Li_7Sn_3	peritectic	782.6	0.286	0.435	0.300	−1213
liquid $\rightleftharpoons$ LiSn	congruent	761.5	0.500	0.500		−13741
liquid $\rightleftharpoons$ Li_7Sn_3 + LiSn	eutectic	746.7	0.451	0.300	0.500	−12967
LiSn + liquid $\rightleftharpoons$ Li_2Sn_5	peritectic	580.0	0.500	0.739	0.714	−10446
liquid $\rightleftharpoons$ Li_2Sn_5 + bct	eutectic	495.7	0.966	0.714	1.000	−8065
liquid $\rightleftharpoons$ bcc + $Li_{22}Sn_5$	eutectic	453.1	0.001	0.000	0.185	−3049

Table IIIa. Integral quantities for the liquid phase at 1100 K.

x_{Sn}	ΔG_m [J/mol]	ΔH_m [J/mol]	ΔS_m [J/(mol·K)]	G_m^E [J/mol]	S_m^E [J/(mol·K)]	ΔC_P [J/(mol·K)]
0.000	0	0	0.000	0	0.000	0.000
0.100	−17271	−14783	2.262	−14298	−0.441	0.000
0.200	−27280	−24058	2.929	−22703	−1.231	0.000
0.300	−32274	−28656	3.290	−26687	−1.789	0.000
0.400	−33618	−29410	3.826	−27463	−1.770	0.000
0.500	−32323	−27154	4.700	−25984	−1.064	0.000
0.600	−29100	−22723	5.797	−22945	0.201	0.000
0.700	−24367	−16954	6.739	−18780	1.660	0.000
0.800	−18243	−10684	6.872	−13667	2.711	0.000
0.900	−10494	−4753	5.219	−7521	2.516	0.000
1.000	0	0	0.000	0	0.000	0.000

Reference states: Li(liquid), Sn(liquid)

Table IIIb. Partial quantities for Li in the liquid phase at 1100 K.

x_{Li}	ΔG_{Li} [J/mol]	ΔH_{Li} [J/mol]	ΔS_{Li} [J/(mol·K)]	G^E_{Li} [J/mol]	S^E_{Li} [J/(mol·K)]	a_{Li}	γ_{Li}
1.000	0	0	0.000	0	0.000	1.000	1.000
0.900	−4177	−2893	1.168	−3213	0.292	0.633	0.704
0.800	−12803	−10462	2.128	−10762	0.272	0.247	0.308
0.700	−23352	−21044	2.098	−20089	−0.868	0.078	0.111
0.600	−34091	−32970	1.019	−29419	−3.228	0.024	0.040
0.500	−44090	−44567	−0.433	−37751	−6.196	0.008	0.016
0.400	−53242	−54159	−0.834	−44862	−8.452	0.003	0.007
0.300	−62319	−60068	2.047	−51308	−7.964	0.001	0.004
0.200	−73141	−60608	11.393	−58421	−1.989	0.000	0.002
0.100	−89371	−54094	32.070	−68312	12.925	0.000	0.001
0.000	−∞	−38833	∞	−83868	40.941	0.000	0.000

Reference state: Li(liquid)

Table IIIc. Partial quantities for Sn in the liquid phase at 1100 K.

x_{Sn}	ΔG_{Sn} [J/mol]	ΔH_{Sn} [J/mol]	ΔS_{Sn} [J/(mol·K)]	G^E_{Sn} [J/mol]	S^E_{Sn} [J/(mol·K)]	a_{Sn}	γ_{Sn}
0.000	−∞	−178137	∞	−178002	−0.123	0.000	0.000
0.100	−135120	−121795	12.113	−114061	−7.032	0.000	0.000
0.200	−85190	−78439	6.137	−70470	−7.245	0.000	0.000
0.300	−53094	−46416	6.071	−42083	−3.939	0.003	0.010
0.400	−32909	−24070	8.036	−24529	0.417	0.027	0.068
0.500	−20557	−9741	9.833	−14217	4.069	0.106	0.211
0.600	−13005	−1766	10.218	−8333	5.970	0.241	0.402
0.700	−8102	1523	8.750	−4840	5.785	0.412	0.589
0.800	−4519	1797	5.741	−2478	3.886	0.610	0.763
0.900	−1730	729	2.235	−766	1.359	0.828	0.920
1.000	0	0	0.000	0	0.000	1.000	1.000

Reference state: Sn(liquid)

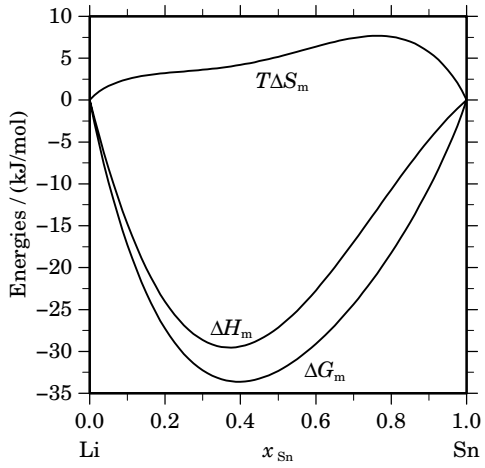

Fig. 2. Integral quantities of the liquid phase at T=1100 K.

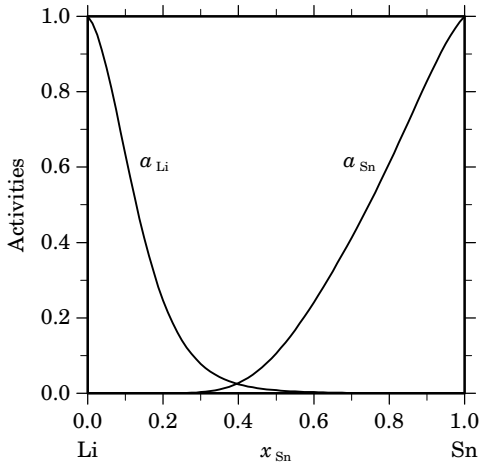

Fig. 3. Activities in the liquid phase at T=1100 K.

Table IV. Standard reaction quantities at 298.15 K for the compounds per mole of atoms.

Compound	x_{Sn}	$\Delta_{\mathrm{f}}G^{\circ}$ / (J/mol)	$\Delta_{\mathrm{f}}H^{\circ}$ / (J/mol)	$\Delta_{\mathrm{f}}S^{\circ}$ / (J/(mol·K))	$\Delta_{\mathrm{f}}C_P^{\circ}$ / (J/(mol·K))
$Li_{22}Sn_5$	0.185	−39617	−43314	−12.399	0.000
Li_7Sn_2	0.222	−39321	−41722	−8.051	0.000
$Li_{13}Sn_5$	0.278	−38604	−39897	−4.335	0.000
Li_5Sn_2	0.286	−38497	−39652	−3.875	0.000
Li_7Sn_3	0.300	−38272	−39382	−3.725	0.000
Li_1Sn_1	0.500	−34974	−35905	−3.123	0.000
Li_2Sn_5	0.714	−21424	−21834	−1.375	0.000

References

[1910Mas] G. Masing, G. Tammann: Z. Anorg. Chem. **67** (1910) 183–199.
[1932Bar] A. Baroni: Atti Rend. Accad. Lincei, Roma **16** (1932) 153–158.
[1934Gru] G. Grube, E. Meyer: Z. Elektrochem. **40** (1934) 771–777.
[1938Kub] O. Kubaschewski, W. Seith: Z. Metallkd. **30** (1938) 7–9.
[1964Fos] M.S. Foster, C.E. Crouthamel, S.E. Wood: J. Phys. Chem. **70** (1966) 3042–3045.
[1972Fis] A.K. Fischer, S.A. Johnson: J. Chem. Eng. Data **17** (1972) 280–283.
[1979Bai] D.M. Bailey, W.H. Skelton, J.F. Smith: J. Less-Common Met. **64** (1979) 233–240.
[1981Wen] C.J. Wen, R.A. Huggins: J. Electrochem. Soc. **128** (1981) 1181–1187.
[1982Dad] A.T. Dadd, P. Hubberstey, P.G. Roberts: J. Chem. Soc. Faraday Trans. I **78** (1982) 2735–2741.
[1986Mos] Z. Moser, W. Gasior, F. Sommer, G. Schwitzgebel, B. Predel: Metall. Trans. B **17** (1986) 791–796.
[1998San] J. Sangster, C.W. Bale: J. Phase Equilibria **19** (1998) 70–75.
[2005Yin] F. Yin, X. Su, Z. Li, J. Wang: J. Alloys Comp. **393** (2005) 105–108.

Mg – Tm (Magnesium – Thulium)

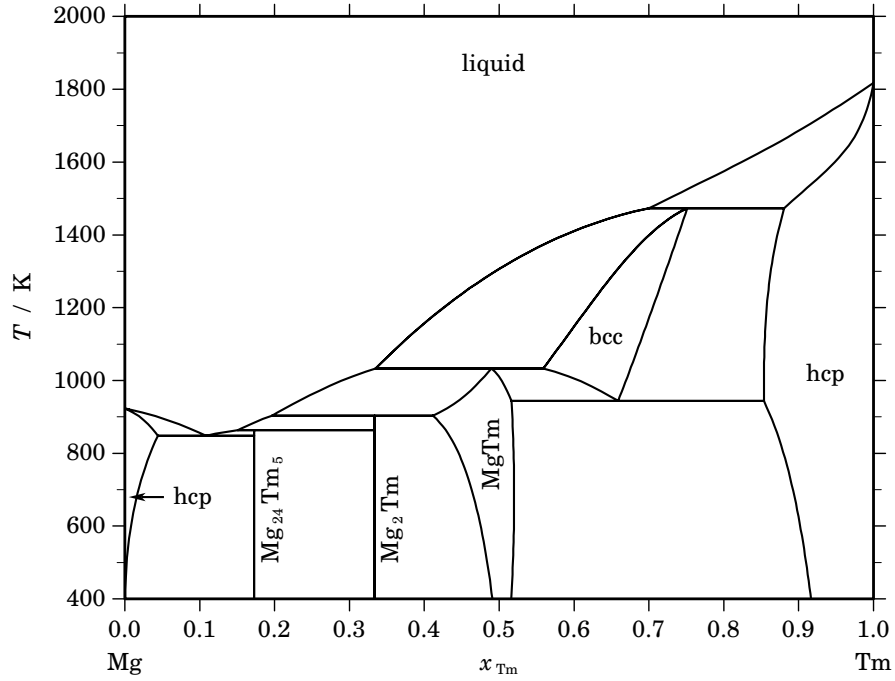

Fig. 1. Calculated phase diagram for the system Mg-Tm.

The rare earth elements have attracted some attention as additives to light metal alloys in the aerospace and automotive industry due to the improvement of mechanical properties of Al- and Mg-alloys at high temperatures. A review on the literature of the Mg-Tm system has been given by [1988Nay]. Du *et al.* [2004Du] prepared a thermodynamic optimisation of the Mg-Tm system, which is mostly based on an experimental investigation of the phase equilibria at elevated temperatures throughout the composition range from 0 to 70 at.% Tm [1995Sac]. The Mg-rich part of the phase diagram and the solubility of thulium in crystalline magnesium has been measured by [1977Rok]. No experimental reports have been available for the solubility of Mg in solid Tm and for the thermodynamic mixing properties of the melt. The thermodynamic properties of the intermetallic compounds are also not investigated experimentally except for the standard enthalpy of formation of MgTm which has been determined by [1967Ogr].

Table I. Phases, structures and models.

Phase	Struktur-bericht	Prototype	Pearson symbol	Space group	SGTE name	Model
liquid					LIQUID	$(Mg,Tm)_1$
hcp	$A3$	Mg	$hP2$	$P6_3/mmc$	HCP_A3	$(Mg,Tm)_1$
$Mg_{24}Tm_5$	$A12$	αMn	$cI58$	$I\bar{4}3m$	MG24TM5	$Mg_{24}Tm_5$
Mg_2Tm	$C14$	$MgZn_2$	$hP12$	$P6_3/mmc$	MG2TM	Mg_2Tm_1
MgTm	$B2$	CsCl	$cP2$	$Pm3m$	MGTM	$(Mg,\Box)_1(Mg,Tm)_1$
bcc	$A2$	W	$cI2$	$Im\bar{3}m$	BCC_A2	$(Mg,Tm)_1$

Table II. Invariant reactions.

Reaction	Type	T / K	Compositions / x_{Tm}			$\Delta_{\mathrm{r}}H$ / (J/mol)
liquid + hcp $\rightleftharpoons$ bcc	peritectic	1473.2	0.700	0.881	0.751	−6985
liquid + bcc $\rightleftharpoons$ MgTm	peritectic	1033.2	0.335	0.559	0.490	−11785
bcc $\rightleftharpoons$ MgTm + hcp	eutectoid	943.4	0.659	0.516	0.854	−6754
liquid + MgTm $\rightleftharpoons$ Mg_2Tm	peritectic	903.0	0.197	0.412	0.333	−6580
liquid + Mg_2Tm $\rightleftharpoons$ $Mg_{24}Tm_5$	peritectic	863.1	0.151	0.333	0.172	−9990
liquid $\rightleftharpoons$ hcp + $Mg_{24}Tm_5$	eutectic	848.0	0.109	0.044	0.172	−9407

Table IIIa. Integral quantities for the liquid phase at 1900 K.

x_{Tm}	ΔG_{m} [J/mol]	ΔH_{m} [J/mol]	ΔS_{m} [J/(mol·K)]	$G^{\mathrm{E}}_{\mathrm{m}}$ [J/mol]	$S^{\mathrm{E}}_{\mathrm{m}}$ [J/(mol·K)]	ΔC_P [J/(mol·K)]
0.000	0	0	0.000	0	0.000	0.000
0.100	−6186	−1649	2.388	−1051	−0.315	0.000
0.200	−9677	−2607	3.721	−1772	−0.439	0.000
0.300	−11850	−2994	4.661	−2200	−0.418	0.000
0.400	−13002	−2934	5.299	−2370	−0.297	0.000
0.500	−13269	−2547	5.643	−2319	−0.120	0.000
0.600	−12714	−1957	5.661	−2082	0.066	0.000
0.700	−11346	−1286	5.295	−1696	0.216	0.000
0.800	−9101	−654	4.446	−1196	0.285	0.000
0.900	−5754	−185	2.931	−619	0.228	0.000
1.000	0	0	0.000	0	0.000	0.000

Reference states: Mg(liquid), Tm(liquid)

Table IIIb. Partial quantities for Mg in the liquid phase at 1900 K.

x_{Mg}	ΔG_{Mg} [J/mol]	ΔH_{Mg} [J/mol]	ΔS_{Mg} [J/(mol·K)]	$G^{\mathrm{E}}_{\mathrm{Mg}}$ [J/mol]	$S^{\mathrm{E}}_{\mathrm{Mg}}$ [J/(mol·K)]	a_{Mg}	γ_{Mg}
1.000	0	0	0.000	0	0.000	1.000	1.000
0.900	−1835	−366	0.773	−171	−0.103	0.890	0.989
0.800	−4160	−1303	1.504	−635	−0.351	0.768	0.961
0.700	−6955	−2565	2.311	−1321	−0.655	0.644	0.920
0.600	−10226	−3909	3.325	−2156	−0.923	0.523	0.872
0.500	−14018	−5090	4.699	−3068	−1.064	0.412	0.823
0.400	−18462	−5865	6.630	−3987	−0.989	0.311	0.777
0.300	−23858	−5990	9.405	−4839	−0.606	0.221	0.736
0.200	−30977	−5220	13.557	−5552	0.175	0.141	0.704
0.100	−42430	−3311	20.589	−6055	1.444	0.068	0.682
0.000	$-\infty$	−19	∞	−6276	3.293	0.000	0.672

Reference state: Mg(liquid)

Table IIIc. Partial quantities for Tm in the liquid phase at 1900 K.

x_{Tm}	ΔG_{Tm} [J/mol]	ΔH_{Tm} [J/mol]	ΔS_{Tm} [J/(mol·K)]	$G^{\mathrm{E}}_{\mathrm{Tm}}$ [J/mol]	$S^{\mathrm{E}}_{\mathrm{Tm}}$ [J/(mol·K)]	a_{Tm}	γ_{Tm}
0.000	$-\infty$	−20361	∞	−12274	−4.256	0.000	0.460
0.100	−45345	−13197	16.920	−8970	−2.225	0.057	0.567
0.200	−31745	−7823	12.590	−6320	−0.791	0.134	0.670
0.300	−23271	−3996	10.144	−4251	0.134	0.229	0.764
0.400	−17166	−1471	8.260	−2691	0.642	0.337	0.843
0.500	−12519	−5	6.586	−1569	0.823	0.453	0.905
0.600	−8882	648	5.016	−812	0.768	0.570	0.950
0.700	−5984	731	3.534	−349	0.568	0.685	0.978
0.800	−3632	487	2.168	−107	0.313	0.795	0.993
0.900	−1679	163	0.969	−15	0.093	0.899	0.999
1.000	0	0	0.000	0	0.000	1.000	1.000

Reference state: Tm(liquid)

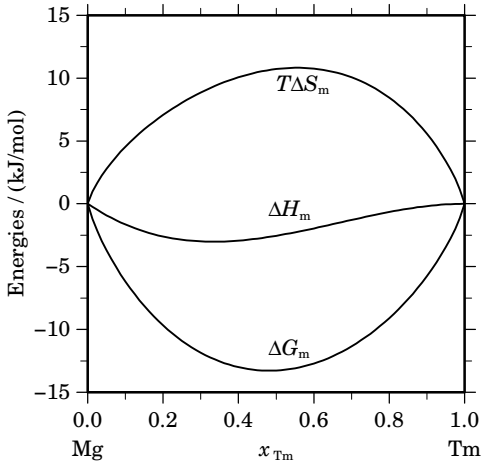

Fig. 2. Integral quantities of the liquid phase at T=1900 K.

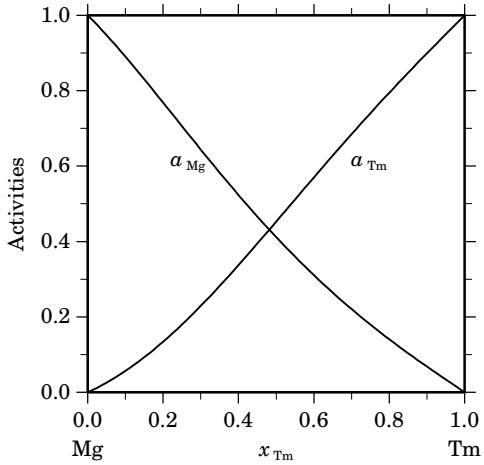

Fig. 3. Activities in the liquid phase at T=1900 K.

Table IV. Standard reaction quantities at 298.15 K for the compounds per mole of atoms.

Compound	x_{Tm}	$\Delta_{\mathrm{f}}G^{\circ}$ / (J/mol)	$\Delta_{\mathrm{f}}H^{\circ}$ / (J/mol)	$\Delta_{\mathrm{f}}S^{\circ}$ / (J/(mol·K))	$\Delta_{\mathrm{f}}C^{\circ}_{P}$ / (J/(mol·K))
$Mg_{24}Tm_5$	0.172	−4529	−5013	−1.623	0.000
Mg_2Tm_1	0.333	−8197	−9442	−4.176	0.000
MgTm	0.500	−8744	−9774	−3.454	0.343

References

[1967Ogr] J.R. Ogren, N.J. Magnani, J.F. Smith: Trans. AIME **239** (1967) 766–771.
[1977Rok] L.L. Rokhlin: Izv. Akad. Nauk SSSR, Met. (1977) 181–183; transl.: Russ. Metall. (1977) 152–154.
[1988Nay] A.A. Nayeb-Hashemi, J.B. Clark in: "Phase Diagrams of Binary Magnesium Alloys", A.A. Nayeb-Hashemi, J.B. Clark (eds.), ASM Intl., Metals Park, OH, 1988, pp. 333–336.
[1995Sac] A. Saccone, D. Macció, S. Delfino, R. Ferro: J. Alloys Comp. **220** (1995) 161–166.
[2004Du] Z. Du, H. Liu, G. Ling: J. Alloys Comp. **373** (2004) 151–155.

Mg – Yb (Magnesium – Ytterbium)

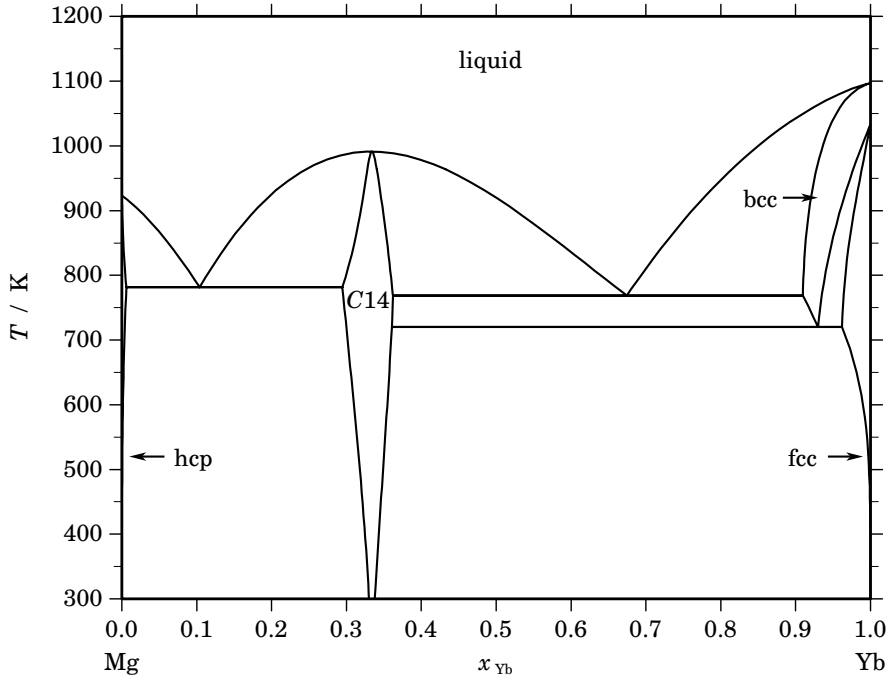

Fig. 1. Calculated phase diagram for the system Mg-Yb.

This system was assessed by Guo and Du [2006Guo], from the available experimental information on the phase diagram and thermodynamics. The interest of magnesium alloys is the potential weight saving in comparison with aluminium, and rare earth elements improve casting characteristics and enhance high temperature properties in these alloys. The phase diagram has been established by McMasters and Gschneidner [1965McM] using differential thermal analysis, metallographic methods and X-ray diffractography. It presents four solution phases, the liquid with a complete miscibility range, the magnesium rich hexagonal (hcp), and ytterbium rich bcc and fcc terminal solid solutions. There is only one non-stoichiometric intermetallic compound, Mg_2Yb, with a $C14$ structure, isotypic with $MgZn_2$, having a homogeneity range of 63.8-70.7 at.% Mg. The enthalpy of mixing of liquid alloys has been determined by Agarwal *et al.* [1995Aga] at 1013 K, 1016 K and 1018 K.

Table I. Phases, structures and models.

Phase	Struktur-bericht	Prototype	Pearson symbol	Space group	SGTE name	Model
liquid					LIQUID	$(Mg,Yb)_1$
hcp	$A3$	Mg	$hP2$	$P6_3/mmc$	HCP_A3	$(Mg,Yb)_1$
$C14$	$C14$	$MgZn_2$	$hP12$	$P6_3/mmc$	C14_LAVES	$(Mg,Yb)_2(Mg,Yb)_1$
bcc	$A2$	W	$cI2$	$Im\overline{3}m$	BCC_A2	$(Mg,Yb)_1$
fcc	$A1$	Cu	$cF4$	$Fm\overline{3}m$	FCC_A1	$(Mg,Yb)_1$

Table II. Invariant reactions.

Reaction	Type	T / K	Compositions / x_{Yb}			$\Delta_{\mathrm{r}}H$ / (J/mol)
liquid $\rightleftharpoons C14$	congruent	991.3	0.334	0.334		−16954
liquid $\rightleftharpoons$ hcp + $C14$	eutectic	781.6	0.104	0.006	0.294	−9642
liquid $\rightleftharpoons C14$ + bcc	eutectic	768.7	0.674	0.362	0.910	−9677
bcc $\rightleftharpoons C14$ + fcc	eutectoid	720.0	0.930	0.361	0.962	−1402

Table IIIa. Integral quantities for the liquid phase at 1100 K.

x_{Yb}	ΔG_{m} [J/mol]	ΔH_{m} [J/mol]	ΔS_{m} [J/(mol·K)]	$G_{\mathrm{m}}^{\mathrm{E}}$ [J/mol]	$S_{\mathrm{m}}^{\mathrm{E}}$ [J/(mol·K)]	ΔC_P [J/(mol·K)]
0.000	0	0	0.000	0	0.000	0.000
0.100	−6510	−2203	3.916	−3537	1.213	0.000
0.200	−10482	−3534	6.316	−5905	2.156	0.000
0.300	−12836	−4137	7.909	−7249	2.829	0.000
0.400	−13866	−4154	8.829	−7711	3.234	0.000
0.500	−13774	−3729	9.132	−7435	3.368	0.000
0.600	−12719	−3007	8.829	−6564	3.234	0.000
0.700	−10828	−2129	7.909	−5241	2.829	0.000
0.800	−8188	−1240	6.316	−3611	2.156	0.000
0.900	−4789	−482	3.916	−1816	1.213	0.000
1.000	0	0	0.000	0	0.000	0.000

Reference states: Mg(liquid), Yb(liquid)

Table IIIb. Partial quantities for Mg in the liquid phase at 1100 K.

x_{Mg}	ΔG_{Mg} [J/mol]	ΔH_{Mg} [J/mol]	ΔS_{Mg} [J/(mol·K)]	$G_{\mathrm{Mg}}^{\mathrm{E}}$ [J/mol]	$S_{\mathrm{Mg}}^{\mathrm{E}}$ [J/(mol·K)]	a_{Mg}	γ_{Mg}
1.000	0	0	0.000	0	0.000	1.000	1.000
0.900	−1572	−460	1.011	−608	0.135	0.842	0.936
0.800	−4282	−1648	2.394	−2241	0.539	0.626	0.783
0.700	−7875	−3279	4.178	−4613	1.213	0.423	0.604
0.600	−12107	−5064	6.403	−7435	2.156	0.266	0.444
0.500	−16762	−6717	9.132	−10422	3.368	0.160	0.320
0.400	−21668	−7952	12.469	−13287	4.851	0.094	0.234
0.300	−26755	−8481	16.613	−15743	6.602	0.054	0.179
0.200	−32223	−8017	22.005	−17503	8.623	0.030	0.148
0.100	−39340	−6275	30.059	−18280	10.914	0.014	0.136
0.000	$-\infty$	−2967	∞	−17788	13.474	0.000	0.143

Reference state: Mg(liquid)

Table IIIc. Partial quantities for Yb in the liquid phase at 1100 K.

x_{Yb}	ΔG_{Yb} [J/mol]	ΔH_{Yb} [J/mol]	ΔS_{Yb} [J/(mol·K)]	$G^{\mathrm{E}}_{\mathrm{Yb}}$ [J/mol]	$S^{\mathrm{E}}_{\mathrm{Yb}}$ [J/(mol·K)]	a_{Yb}	γ_{Yb}
0.000	$-\infty$	−26868	∞	−41690	13.474	0.000	0.010
0.100	−50956	−17891	30.059	−29896	10.914	0.004	0.038
0.200	−35282	−11077	22.005	−20562	8.623	0.021	0.106
0.300	−24412	−6138	16.613	−13401	6.602	0.069	0.231
0.400	−16505	−2789	12.469	−8124	4.851	0.165	0.411
0.500	−10786	−742	9.132	−4447	3.368	0.307	0.615
0.600	−6753	290	6.403	−2081	2.156	0.478	0.796
0.700	−4003	593	4.178	−740	1.213	0.646	0.922
0.800	−2179	455	2.394	−138	0.539	0.788	0.985
0.900	−950	162	1.011	13	0.135	0.901	1.001
1.000	0	0	0.000	0	0.000	1.000	1.000

Reference state: Yb(liquid)

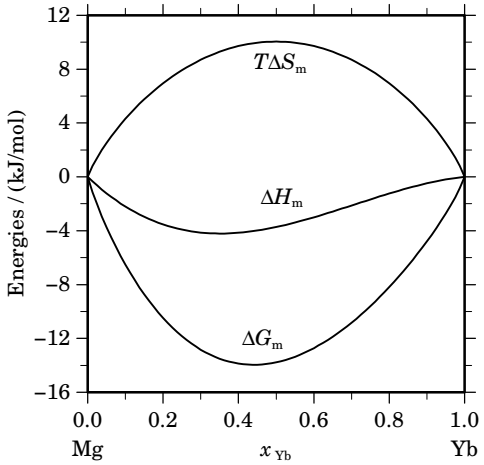

Fig. 2. Integral quantities of the liquid phase at T=1100 K.

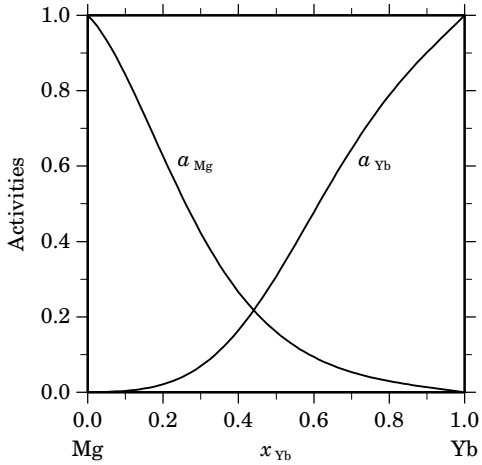

Fig. 3. Activities in the liquid phase at T=1100 K.

Table IV. Standard reaction quantities at 298.15 K for the compounds per mole of atoms.

Compound	x_{Yb}	$\Delta_{\mathrm{f}}G^{\circ}$ / (J/mol)	$\Delta_{\mathrm{f}}H^{\circ}$ / (J/mol)	$\Delta_{\mathrm{f}}S^{\circ}$ / (J/(mol·K))	$\Delta_{\mathrm{f}}C^{\circ}_{P}$ / (J/(mol·K))
$C14$	0.333	−12533	−12533	0.000	0.000

References

[1965McM] O.D. McMasters, K.A. Gschneidner Jr.: J. Less-Common Met. **8** (1965) 289–298.
[1995Aga] R. Agarwal, H. Feufel, F. Sommer: J. Alloys Comp. **217** (1995) 59–64.
[2006Guo] C. Guo, Z. Du: J. Alloys Comp. **422** (2006) 102–108.

Mn – Sc (Manganese – Scandium)

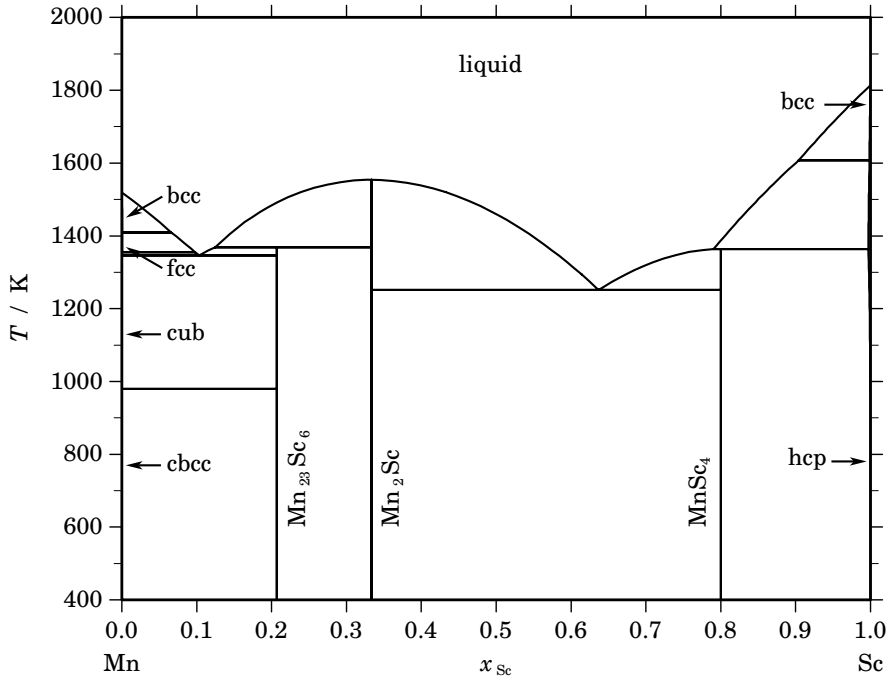

Fig. 1. Calculated phase diagram for the system Mn-Sc.

Manganese and scandium can both be encountered in light metal alloys where Sc improves the mechanical properties at higher temperatures and Mn is added for grain refining. The Mn-Sc system has been investigated by DTA and SEM/EDX across the whole composition range and an optimised thermodynamic dataset has been reported in [1998Pis]. Prior to this study the phase diagram of Mn-Sc has been largely unknown. In addition to the Laves phase Mn_2Sc [1961Dwi] two more intermetallic compounds have been found, $Mn_{23}Sc_6$ and $MnSc_4$ [1998Pis]. The available thermodynamic data have been limited to only 2 values. The enthalpy of mixing in the liquid has been measured by [1985Esi] at a composition of 15 at.% Sc and 1873 K and the enthalpy of formation of Mn_2Sc has been reported by [1983Shi]. Both values are reproduced quite well by the calculations [1998Pis]. The investigation of the phase diagram has been complicated by the sluggish formation of $MnSc_4$ and reactions of the Sc-rich alloys with the crucible in the DTA experiments [1998Pis]. Although the solubility of Sc in solid Mn has been found to be 1 at.% Sc at the eutectic temperature [1998Pis] the calculated value from the optimised dataset is much lower.

Table I. Phases, structures and models.

Phase	Struktur-bericht	Prototype	Pearson symbol	Space group	SGTE name	Model
liquid					LIQUID	$(Mn,Sc)_1$
cbcc	$A12$	αMn	$cI58$	$I\bar{4}3m$	CBCC_A12	Mn_1
cub	$A13$	βMn	$cP20$	$P4_132$	CUB_A13	Mn_1
fcc	$A1$	Cu	$cF4$	$Fm\bar{3}m$	FCC_A1	$(Mn,Sc)_1$
bcc	$A2$	W	$cI2$	$Im\bar{3}m$	BCC_A2	$(Mn,Sc)_1$
$Mn_{23}Sc_6$	···	···	$cF116$	$Fm\bar{3}m$	MN23SC6	$Mn_{23}Sc_6$
Mn_2Sc	$C14$	$MgZn_2$	$hP12$	$P6_3/mmc$	MN2SC	Mn_2Sc_1
$MnSc_4$	···	···	···	···	MNSC4	Mn_1Sc_4
hcp	$A3$	Mg	$hP2$	$P6_3/mmc$	HCP_A3	$(Mn,Sc)_1$

Table II. Invariant reactions.

Reaction	Type	T / K	Compositions / x_{Sc}			$\Delta_{\mathrm{r}}H$ / (J/mol)
bcc $\rightleftharpoons$ liquid + hcp	metatectic	1607.3	0.998	0.904	0.999	−3989
liquid $\rightleftharpoons$ Mn_2Sc	congruent	1554.1	0.333	0.333		−25592
bcc $\rightleftharpoons$ fcc + liquid	metatectic	1409.1	0.001	0.000	0.066	−1866
liquid + Mn_2Sc $\rightleftharpoons$ $Mn_{23}Sc_6$	peritectic	1368.6	0.125	0.333	0.207	−12510
liquid + hcp $\rightleftharpoons$ $MnSc_4$	peritectic	1363.6	0.790	0.997	0.800	−17729
fcc $\rightleftharpoons$ cub + liquid	metatectic	1355.3	0.001	0.000	0.098	−2096
liquid $\rightleftharpoons$ cub + $Mn_{23}Sc_6$	eutectic	1346.7	0.103	0.000	0.207	−18856
liquid $\rightleftharpoons$ Mn_2Sc + $MnSc_4$	eutectic	1251.0	0.637	0.333	0.800	−18292
cub $\rightleftharpoons$ cbcc + $Mn_{23}Sc_6$	eutectoid	980.0	0.000	0.000	0.207	−2254

Table IIIa. Integral quantities for the liquid phase at 2000 K.

x_{Sc}	ΔG_{m} [J/mol]	ΔH_{m} [J/mol]	ΔS_{m} [J/(mol·K)]	$G_{\mathrm{m}}^{\mathrm{E}}$ [J/mol]	$S_{\mathrm{m}}^{\mathrm{E}}$ [J/(mol·K)]	ΔC_P [J/(mol·K)]
0.000	0	0	0.000	0	0.000	0.000
0.100	−7982	−3298	2.342	−2576	−0.361	0.000
0.200	−12901	−5863	3.519	−4580	−0.642	0.000
0.300	−16170	−7696	4.237	−6012	−0.842	0.000
0.400	−18062	−8795	4.633	−6870	−0.962	0.000
0.500	−18683	−9162	4.761	−7157	−1.003	0.000
0.600	−18062	−8795	4.633	−6870	−0.962	0.000
0.700	−16170	−7696	4.237	−6012	−0.842	0.000
0.800	−12901	−5863	3.519	−4580	−0.642	0.000
0.900	−7982	−3298	2.342	−2576	−0.361	0.000
1.000	0	0	0.000	0	0.000	0.000

Reference states: Mn(liquid), Sc(liquid)

Table IIIb. Partial quantities for Mn in the liquid phase at 2000 K.

x_{Mn}	ΔG_{Mn} [J/mol]	ΔH_{Mn} [J/mol]	ΔS_{Mn} [J/(mol·K)]	$G_{\mathrm{Mn}}^{\mathrm{E}}$ [J/mol]	$S_{\mathrm{Mn}}^{\mathrm{E}}$ [J/(mol·K)]	a_{Mn}	γ_{Mn}
1.000	0	0	0.000	0	0.000	1.000	1.000
0.900	−2038	−366	0.836	−286	−0.040	0.885	0.983
0.800	−4856	−1466	1.695	−1145	−0.160	0.747	0.933
0.700	−8508	−3298	2.605	−2576	−0.361	0.600	0.856
0.600	−13075	−5863	3.606	−4580	−0.642	0.456	0.759
0.500	−18683	−9162	4.761	−7157	−1.003	0.325	0.650
0.400	−25543	−13193	6.175	−10306	−1.444	0.215	0.538
0.300	−34048	−17957	8.046	−14027	−1.965	0.129	0.430
0.200	−45084	−23454	10.815	−18321	−2.566	0.066	0.332
0.100	−61477	−29684	15.897	−23188	−3.248	0.025	0.248
0.000	$-\infty$	−36647	∞	−28627	−4.010	0.000	0.179

Reference state: Mn(liquid)

Table IIIc. Partial quantities for Sc in the liquid phase at 2000 K.

x_{Sc}	ΔG_{Sc} [J/mol]	ΔH_{Sc} [J/mol]	ΔS_{Sc} [J/(mol·K)]	G^E_{Sc} [J/mol]	S^E_{Sc} [J/(mol·K)]	a_{Sc}	γ_{Sc}
0.000	$-\infty$	−36647	∞	−28627	−4.010	0.000	0.179
0.100	−61477	−29684	15.897	−23188	−3.248	0.025	0.248
0.200	−45084	−23454	10.815	−18321	−2.566	0.066	0.332
0.300	−34048	−17957	8.046	−14027	−1.965	0.129	0.430
0.400	−25543	−13193	6.175	−10306	−1.444	0.215	0.538
0.500	−18683	−9162	4.761	−7157	−1.003	0.325	0.650
0.600	−13075	−5863	3.606	−4580	−0.642	0.456	0.759
0.700	−8508	−3298	2.605	−2576	−0.361	0.600	0.856
0.800	−4856	−1466	1.695	−1145	−0.160	0.747	0.933
0.900	−2038	−366	0.836	−286	−0.040	0.885	0.983
1.000	0	0	0.000	0	0.000	1.000	1.000

Reference state: Sc(liquid)

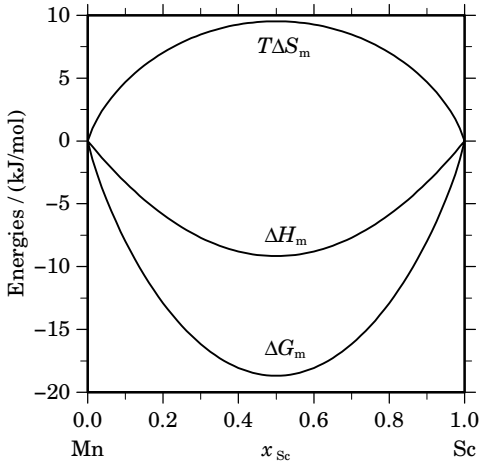

Fig. 2. Integral quantities of the liquid phase at T=2000 K.

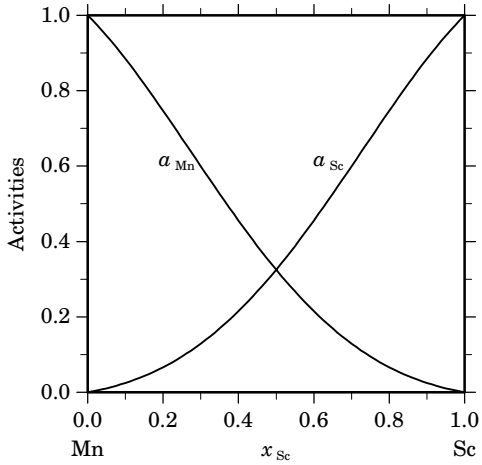

Fig. 3. Activities in the liquid phase at T=2000 K.

Table IV. Standard reaction quantities at 298.15 K for the compounds per mole of atoms.

Compound	x_{Sc}	$\Delta_f G^\circ$ / (J/mol)	$\Delta_f H^\circ$ / (J/mol)	$\Delta_f S^\circ$ / (J/(mol·K))	$\Delta_f C^\circ_P$ / (J/(mol·K))
$Mn_{23}Sc_6$	0.207	−10172	−10172	0.001	0.000
Mn_2Sc_1	0.333	−15500	−15500	0.001	0.000
Mn_1Sc_4	0.800	−7344	−7344	0.000	0.000

References

[1961Dwi] A.E. Dwight: Trans. Am. Soc. Met. **53** (1961) 479–500.
[1983Shi] A.L. Shilov, L.N. Paduretz, M.E. Kost: Zh. Fiz. Khim. **57** (1983) 255–559.
[1985Esi] Yu.O. Esin, A.F. Ermakov, S.P. Kolesnikov, P.V. Geld: Zh. Fiz. Khim. **59** (1985) 223–226.
[1998Pis] A. Pisch, R. Schmid-Fetzer: Z. Metallkd. **89** (1998) 700–703.

Mo – V (Molybdenum – Vanadium)

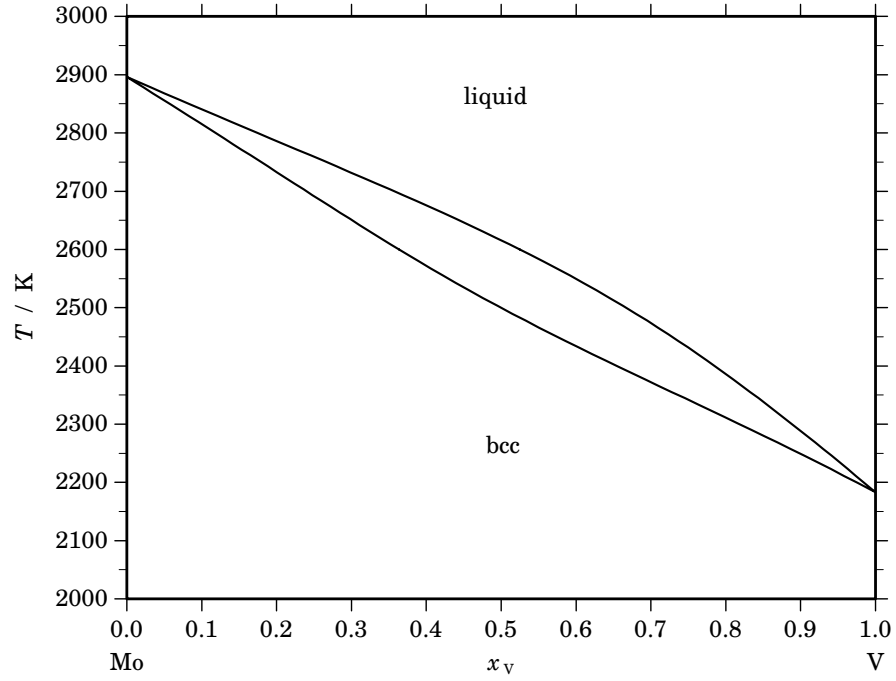

Fig. 1. Calculated phase diagram for the system Mo-V.

Molybdenum and vanadium are important alloying elements for steel and they are added both together in concentrations of some percent to certain hot work tool steels. The phase diagram of the Mo-V system is quite simple consisting of only the liquid and the solid bcc phases each with complete miscibility of the components. The literature on the Mo-V system has been reviewed by [1989Smi, 1999Zhe] and optimised thermodynamic datasets have been reported in [1999Zhe, 2002Bra]. Both reviews conclude that the most reliable data on the phase diagram have been reported by Rudy [1969Rud]. It has also been concluded that no reliable thermodynamic data of mixing have been available which are consistent with the phase diagram data. In order to estimate the thermodynamic excess quantities in the bcc solid solution, [1999Zhe] took account of theoretical considerations given in [1980Bre]. However, under these conditions the calculated two-phase region is clearly more narrow than measured by [1969Rud] although the mixing properties have been described by 4 coefficients for each phase [1999Zhe]. In view of these results [2002Bra] decided to re-assess the system using only reliable experimental data, essentially those of [1969Rud]. In the resulting optimisation these data are well reproduced using a strictly regular solution model for both phases with only one coefficient for each phase. The optimisation of [2002Bra] is recommended here because it provides a better fit to the accepted data with much less parameters. Below 1160 K a miscibility gap in the bcc phase is predicted, however, no experimental evidence is available.

Table I. Phases, structures and models.

Phase	Struktur-bericht	Prototype	Pearson symbol	Space group	SGTE name	Model
liquid					LIQUID	$(Mo,V)_1$
bcc	$A2$	W	$cI2$	$Im\overline{3}m$	BCC_A2	$(Mo,V)_1$

Table IIa. Integral quantities for the liquid phase at 2900 K.

x_{V}	ΔG_{m} [J/mol]	ΔH_{m} [J/mol]	ΔS_{m} [J/(mol·K)]	$G_{\mathrm{m}}^{\mathrm{E}}$ [J/mol]	$S_{\mathrm{m}}^{\mathrm{E}}$ [J/(mol·K)]	ΔC_P [J/(mol·K)]
0.000	0	0	0.000	0	0.000	0.000
0.100	−6238	1601	2.703	1601	0.000	0.000
0.200	−9220	2845	4.161	2845	0.000	0.000
0.300	−10995	3735	5.079	3735	0.000	0.000
0.400	−11960	4268	5.596	4268	0.000	0.000
0.500	−12267	4446	5.763	4446	0.000	0.000
0.600	−11960	4268	5.596	4268	0.000	0.000
0.700	−10995	3735	5.079	3735	0.000	0.000
0.800	−9220	2845	4.161	2845	0.000	0.000
0.900	−6238	1601	2.703	1601	0.000	0.000
1.000	0	0	0.000	0	0.000	0.000

Reference states: Mo(liquid), V(liquid)

Table IIb. Partial quantities for Mo in the liquid phase at 2900 K.

x_{Mo}	ΔG_{Mo} [J/mol]	ΔH_{Mo} [J/mol]	ΔS_{Mo} [J/(mol·K)]	$G_{\mathrm{Mo}}^{\mathrm{E}}$ [J/mol]	$S_{\mathrm{Mo}}^{\mathrm{E}}$ [J/(mol·K)]	a_{Mo}	γ_{Mo}
1.000	0	0	0.000	0	0.000	1.000	1.000
0.900	−2363	178	0.876	178	0.000	0.907	1.007
0.800	−4669	711	1.855	711	0.000	0.824	1.030
0.700	−7000	1601	2.966	1601	0.000	0.748	1.069
0.600	−9472	2845	4.247	2845	0.000	0.675	1.125
0.500	−12267	4446	5.763	4446	0.000	0.601	1.202
0.400	−15691	6402	7.619	6402	0.000	0.522	1.304
0.300	−20316	8714	10.010	8714	0.000	0.431	1.435
0.200	−27425	11382	13.382	11382	0.000	0.321	1.603
0.100	−41115	14405	19.145	14405	0.000	0.182	1.817
0.000	$-\infty$	17784	∞	17784	0.000	0.000	2.091

Reference state: Mo(liquid)

Table IIc. Partial quantities for V in the liquid phase at 2900 K.

x_{V}	ΔG_{V} [J/mol]	ΔH_{V} [J/mol]	ΔS_{V} [J/(mol·K)]	$G_{\mathrm{V}}^{\mathrm{E}}$ [J/mol]	$S_{\mathrm{V}}^{\mathrm{E}}$ [J/(mol·K)]	a_{V}	γ_{V}
0.000	$-\infty$	17784	∞	17784	0.000	0.000	2.091
0.100	−41115	14405	19.145	14405	0.000	0.182	1.817
0.200	−27425	11382	13.382	11382	0.000	0.321	1.603
0.300	−20316	8714	10.010	8714	0.000	0.431	1.435
0.400	−15691	6402	7.619	6402	0.000	0.522	1.304
0.500	−12267	4446	5.763	4446	0.000	0.601	1.202
0.600	−9472	2845	4.247	2845	0.000	0.675	1.125
0.700	−7000	1601	2.966	1601	0.000	0.748	1.069
0.800	−4669	711	1.855	711	0.000	0.824	1.030
0.900	−2363	178	0.876	178	0.000	0.907	1.007
1.000	0	0	0.000	0	0.000	1.000	1.000

Reference state: V(liquid)

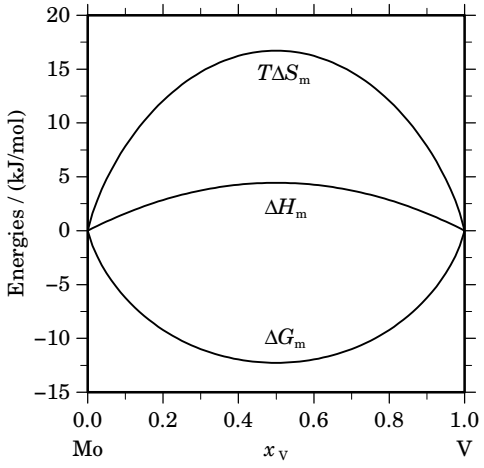

Fig. 2. Integral quantities of the liquid phase at T=2900 K.

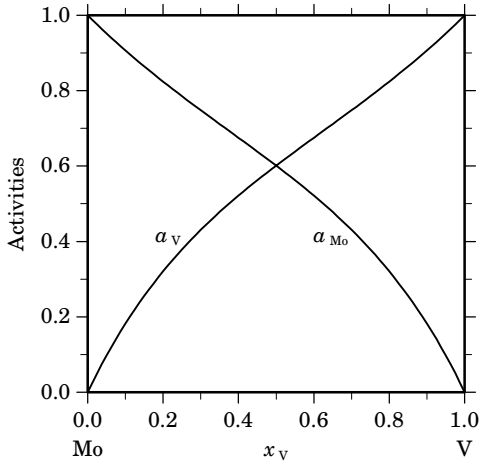

Fig. 3. Activities in the liquid phase at T=2900 K.

Table IIIa. Integral quantities for the stable phases at 2000 K.

Phase	x_V	ΔG_m [J/mol]	ΔH_m [J/mol]	ΔS_m [J/(mol·K)]	G_m^E [J/mol]	S_m^E [J/(mol·K)]	ΔC_P [J/(mol·K)]
bcc	0.000	0	0	0.000	0	0.000	0.000
	0.100	−3674	1732	2.703	1732	0.000	0.000
	0.200	−5242	3079	4.161	3079	0.000	0.000
	0.300	−6117	4041	5.079	4041	0.000	0.000
	0.400	−6573	4619	5.596	4619	0.000	0.000
	0.500	−6715	4811	5.763	4811	0.000	0.000
	0.600	−6573	4619	5.596	4619	0.000	0.000
	0.700	−6117	4041	5.079	4041	0.000	0.000
	0.800	−5242	3079	4.161	3079	0.000	0.000
	0.900	−3674	1732	2.703	1732	0.000	0.000
	1.000	0	0	0.000	0	0.000	0.000

Reference states: Mo(bcc), V(bcc)

Table IIIb. Partial quantities for Mo in the stable phases at 2000 K.

Phase	x_{Mo}	ΔG_{Mo} [J/mol]	ΔH_{Mo} [J/mol]	ΔS_{Mo} [J/(mol·K)]	G_{Mo}^E [J/mol]	S_{Mo}^E [J/(mol·K)]	a_{Mo}	γ_{Mo}
bcc	1.000	0	0	0.000	0	0.000	1.000	1.000
	0.900	−1560	192	0.876	192	0.000	0.910	1.012
	0.800	−2941	770	1.855	770	0.000	0.838	1.047
	0.700	−4199	1732	2.966	1732	0.000	0.777	1.110
	0.600	−5415	3079	4.247	3079	0.000	0.722	1.203
	0.500	−6715	4811	5.763	4811	0.000	0.668	1.336
	0.400	−8309	6928	7.619	6928	0.000	0.607	1.517
	0.300	−10591	9430	10.010	9430	0.000	0.529	1.763
	0.200	−14447	12317	13.382	12317	0.000	0.419	2.097
	0.100	−22701	15589	19.145	15589	0.000	0.255	2.553
	0.000	$-\infty$	19245	∞	19245	0.000	0.000	3.181

Reference state: Mo(bcc)

Table IIIc. Partial quantities for V in the stable phases at 2000 K.

Phase	x_V	ΔG_V [J/mol]	ΔH_V [J/mol]	ΔS_V [J/(mol·K)]	G_V^E [J/mol]	S_V^E [J/(mol·K)]	a_V	γ_V
bcc	0.000	$-\infty$	19245	∞	19245	0.000	0.000	3.181
	0.100	−22701	15588	19.145	15588	0.000	0.255	2.553
	0.200	−14447	12317	13.382	12317	0.000	0.419	2.097
	0.300	−10591	9430	10.010	9430	0.000	0.529	1.763
	0.400	−8309	6928	7.619	6928	0.000	0.607	1.517
	0.500	−6715	4811	5.763	4811	0.000	0.668	1.336
	0.600	−5415	3079	4.247	3079	0.000	0.722	1.203
	0.700	−4199	1732	2.966	1732	0.000	0.777	1.110
	0.800	−2941	770	1.855	770	0.000	0.838	1.047
	0.900	−1560	192	0.876	192	0.000	0.910	1.012
	1.000	0	0	0.000	0	0.000	1.000	1.000

Reference state: V(bcc)

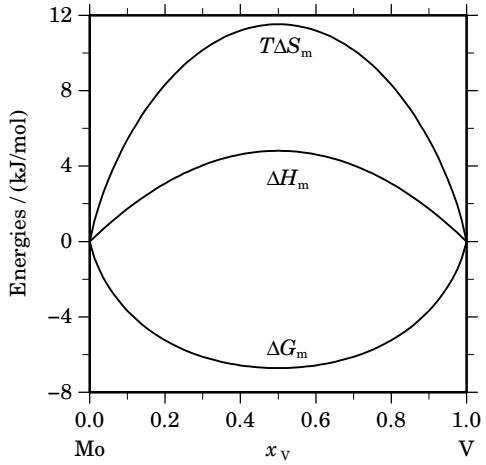

Fig. 4. Integral quantities of the stable phases at T=2000 K.

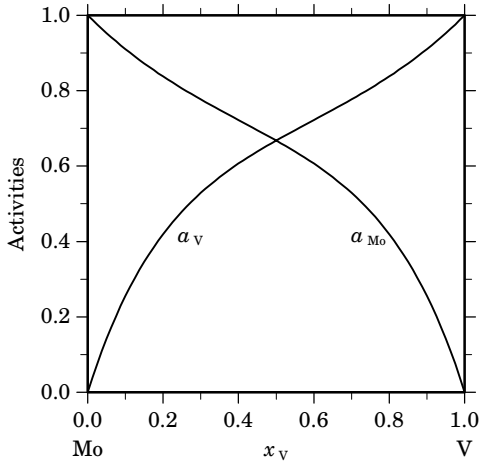

Fig. 5. Activities in the stable phases at T=2000 K.

References

[1969Rud] E. Rudy: "Compendium of Phase Diagram Data", AFML, Wright-Patterson AFB, Ohio, Rep. No. AFML-TR-65-2, Part 5, 1969, pp. 118–120.

[1980Bre] L. Brewer, R.H. Lamoreaux in: "Molybdenum: Physico-Chemical Properties of its Compounds and Alloys", L. Brewer (ed.), Atomic Energy Rev. Spec. Issue 7, IAEA, Vienna, 1980.

[1989Smi] J.F. Smith in: "Phase Diagrams of Binary Vanadium Alloys", J.F. Smith (ed.), ASM Intl., Metals Park, OH, 1989, pp. 144–147.

[1999Zhe] F. Zheng, B.B. Argent, J.F. Smith: J. Phase Equilibria **20** (1999) 370–372.

[2002Bra] J. Bratberg, K. Frisk: Calphad **26** (2002) 459–476.

Mo – Zr (Molybdenum – Zirconium)

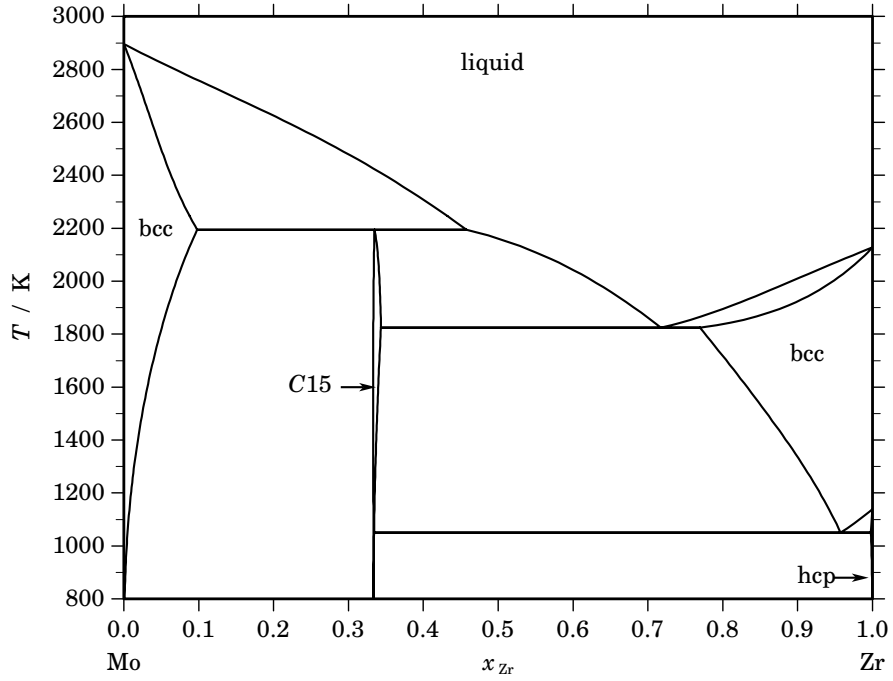

Fig. 1. Calculated phase diagram for the system Mo-Zr.

Mo is added in certain amounts to zirconium based alloys for the nuclear power industry in order to enhance their mechanical properties. Similarly, zirconium belongs to the group of alloying elements for Mo-based metals in order to further increase their strength and creep resistance at high temperatures. The literature on the Mo-Zr system has been reviewed in [1976Kub, 2002Zin, 2003Jer] and thermodynamic assessments have been reported in [2002Zin, 2003Jer]. The phase equilibria in the Mo-Zr system have been studied in several investigations but no measurements of thermodynamic data have been reported. The assessment of [2003Jer] is preferred here because in the dataset of [2002Zin] the liquid and the bcc phases are modelled with quite high excess entropies which seem to be unrealistic. This causes the slopes of the boundaries for the single-phase bcc regions to be too steep and in the liquid an artificial inverse miscibility gap opens above 4660 K. Although this is in some distance above the liquidus it indicates a certain weakness in the optimisation.

Table I. Phases, structures and models.

Phase	Struktur-bericht	Prototype	Pearson symbol	Space group	SGTE name	Model
liquid					LIQUID	$(Mo,Zr)_1$
bcc	$A2$	W	$cI2$	$Im\bar{3}m$	BCC_A2	$(Mo,Zr)_1$
hcp	$A3$	Mg	$hP2$	$P6_3/mmc$	HCP_A3	$(Mo,Zr)_1$
$C15$	$C15$	$MgCu_2$	$cF24$	$Fd\bar{3}m$	LAVES_C15	$(Mo,Zr)_2(Mo,Zr)_1$

Table II. Invariant reactions.

Reaction	Type	T / K	Compositions / x_{Zr}			$\Delta_{\mathrm{r}}H$ / (J/mol)
bcc + liquid $\rightleftharpoons C15$	peritectic	2194.2	0.098	0.457	0.335	−22868
liquid $\rightleftharpoons C15$ + bcc	eutectic	1824.9	0.717	0.343	0.769	−18826
bcc $\rightleftharpoons C15$ + hcp	eutectoid	1050.2	0.957	0.334	0.998	−5583

Table IIIa. Integral quantities for the liquid phase at 2900 K.

x_{Zr}	ΔG_{m} [J/mol]	ΔH_{m} [J/mol]	ΔS_{m} [J/(mol·K)]	$G^{\mathrm{E}}_{\mathrm{m}}$ [J/mol]	$S^{\mathrm{E}}_{\mathrm{m}}$ [J/(mol·K)]	ΔC_P [J/(mol·K)]
0.000	0	0	0.000	0	0.000	0.000
0.100	−7244	−2534	1.624	595	−1.079	0.000
0.200	−11290	−4342	2.396	776	−1.765	0.000
0.300	−14081	−5483	2.965	649	−2.114	0.000
0.400	−15909	−6020	3.410	319	−2.186	0.000
0.500	−16821	−6014	3.727	−108	−2.037	0.000
0.600	−16754	−5527	3.871	−526	−1.724	0.000
0.700	−15559	−4620	3.772	−830	−1.307	0.000
0.800	−12980	−3356	3.318	−914	−0.842	0.000
0.900	−8511	−1795	2.316	−672	−0.387	0.000
1.000	0	0	0.000	0	0.000	0.000

Reference states: Mo(liquid), Zr(liquid)

Table IIIb. Partial quantities for Mo in the liquid phase at 2900 K.

x_{Mo}	ΔG_{Mo} [J/mol]	ΔH_{Mo} [J/mol]	ΔS_{Mo} [J/(mol·K)]	$G^{\mathrm{E}}_{\mathrm{Mo}}$ [J/mol]	$S^{\mathrm{E}}_{\mathrm{Mo}}$ [J/(mol·K)]	a_{Mo}	γ_{Mo}
1.000	0	0	0.000	0	0.000	1.000	1.000
0.900	−2316	−374	0.670	224	−0.206	0.908	1.009
0.800	−4623	−1414	1.107	757	−0.749	0.826	1.032
0.700	−7213	−2996	1.454	1387	−1.511	0.741	1.059
0.600	−10415	−4998	1.868	1902	−2.380	0.649	1.082
0.500	−14621	−7297	2.526	2092	−3.238	0.545	1.091
0.400	−20348	−9768	3.648	1746	−3.970	0.430	1.075
0.300	−28379	−12290	5.548	651	−4.462	0.308	1.027
0.200	−40209	−14738	8.783	−1402	−4.599	0.189	0.943
0.100	−60146	−16990	14.881	−4626	−4.264	0.083	0.825
0.000	$-\infty$	−18923	∞	−9231	−3.342	0.000	0.682

Reference state: Mo(liquid)

Table IIIc. Partial quantities for Zr in the liquid phase at 2900 K.

x_{Zr}	ΔG_{Zr} [J/mol]	ΔH_{Zr} [J/mol]	ΔS_{Zr} [J/(mol·K)]	$G^{\mathrm{E}}_{\mathrm{Zr}}$ [J/mol]	$S^{\mathrm{E}}_{\mathrm{Zr}}$ [J/(mol·K)]	a_{Zr}	γ_{Zr}
0.000	$-\infty$	−29187	∞	8369	−12.950	0.000	1.415
0.100	−51593	−21979	10.212	3927	−8.933	0.118	1.177
0.200	−37957	−16052	7.553	850	−5.828	0.207	1.036
0.300	−30104	−11284	6.490	−1074	−3.521	0.287	0.956
0.400	−24150	−7551	5.724	−2056	−1.895	0.367	0.918
0.500	−19021	−4731	4.928	−2308	−0.836	0.454	0.909
0.600	−14357	−2699	4.020	−2040	−0.227	0.551	0.919
0.700	−10065	−1334	3.011	−1464	0.045	0.659	0.941
0.800	−6172	−511	1.952	−792	0.097	0.774	0.968
0.900	−2774	−107	0.919	−233	0.043	0.891	0.990
1.000	0	0	0.000	0	0.000	1.000	1.000

Reference state: Zr(liquid)

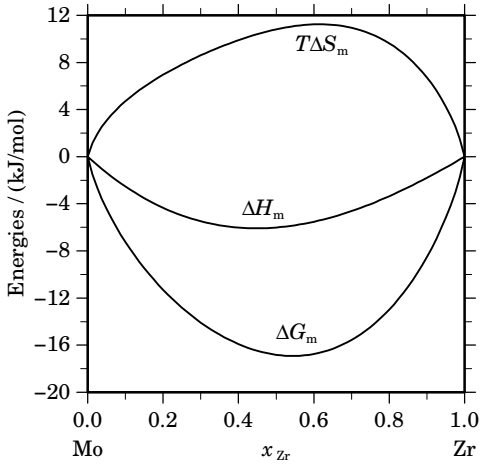

Fig. 2. Integral quantities of the liquid phase at T=2900 K.

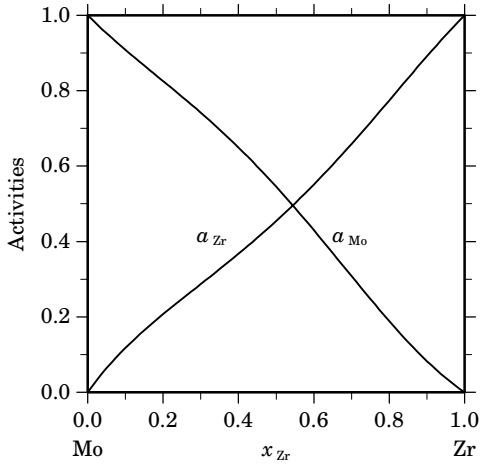

Fig. 3. Activities in the liquid phase at T=2900 K.

Table IV. Standard reaction quantities at 298.15 K for the compounds per mole of atoms.

Compound	x_{Zr}	$\Delta_{\mathrm{f}}G^{\circ}$ / (J/mol)	$\Delta_{\mathrm{f}}H^{\circ}$ / (J/mol)	$\Delta_{\mathrm{f}}S^{\circ}$ / (J/(mol·K))	$\Delta_{\mathrm{f}}C^{\circ}_{P}$ / (J/(mol·K))
$C15$	0.333	−7231	−7245	−0.048	0.000

References

[1976Kub] O. Kubaschewski, O. von Goldbeck in: "Zirconium: Physico-Chemical Properties of its Compounds and Alloys", O. Kubaschewski (ed.), Atomic Energy Rev. Spec. Issue 6, IAEA, Vienna, 1976, pp. 96–97.

[2002Zin] M. Zinkevich, N. Mattern: J. Phase Equilibria **23** (2002) 156–161.

[2003Jer] R. Jerlerud Pérez, B. Sundman: Calphad **27** (2003) 253–262.

N – Si (Nitrogen – Silicon)

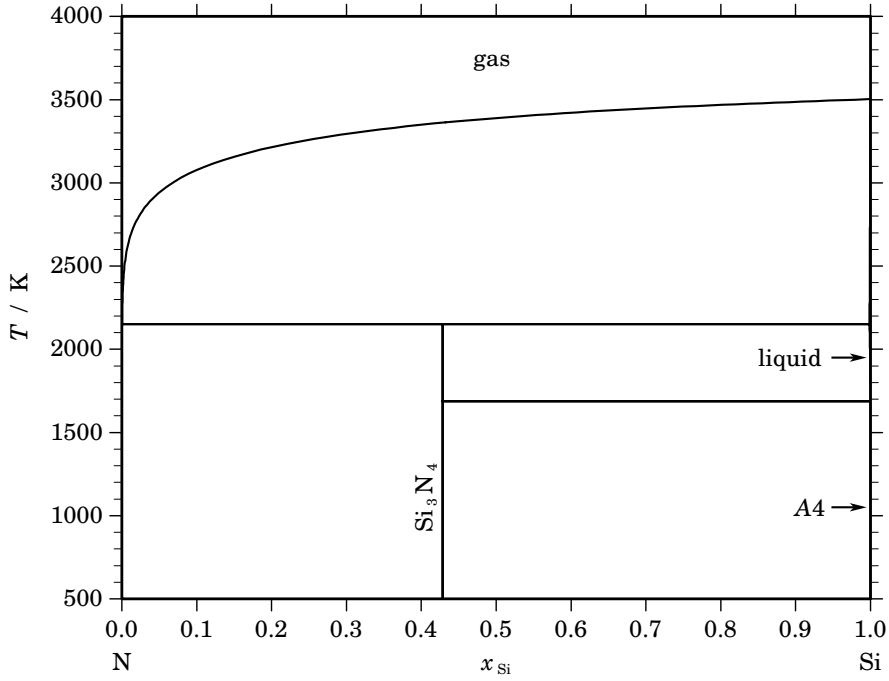

Fig. 1. Calculated phase diagram for the system N-Si.

Silicon nitride, Si_3N_4 is a lightweight, strong and tough ceramic material which is of broad technical interest, e.g.. for structural and wear-resistant applications up to high temperatures. A survey of the literature and a thermodynamic optimisation of the binary Si-N system has been given by [2003Ma]. The phase diagram of the Si-N system consists of a few phases only: solid Si ($A4$), the liquid, silicon nitride (Si_3N_4), and the gas phase. In the assessment [2003Ma] the solid phases have been treated as pure Si and Si_3N_4, respectively. The very small solubility of nitrogen in solid Si which is known experimentally [1959Kai, 1973Yat] has been omitted from the assessment. The liquid has been modelled as a substitutional solution with the species Si and N and the gas phase has been modelled with the species N, N_2, N_3, SiN, Si_2N, Si, Si_2, and Si_3 which have been taken from the SGTE substance database. The description for Si_3N_4 has been optimised based on the heat capacity values of [1976Guz] and on enthalpies of formation and entropies of formation mainly from [1959Peh]. Data for the eutectic have been selected from [1973Yat] and data for the decomposition of Si_3N_4 into liquid and gas are from [1981Dör]. Calculated partial pressures of nitrogen in the equilibrium of Si_3N_4 with Si-rich melt are in good agreement with the experimental data of [1930Hin].

Table I. Phases, structures and models.

Phase	Struktur-bericht	Prototype	Pearson symbol	Space group	SGTE name	Model
liquid					LIQUID	$(N,Si)_1$
Si_3N_4	···	···	$hP14$	$P6_3$	SI3N4	Si_3N_4
$A4$	$A4$	C(diamond)	$cF8$	$Fd\bar{3}m$	DIAMOND_A4	Si_1

Table II. Invariant reactions.

Reaction	Type	T / K	Compositions / x_{Si}			$\Delta_{\mathrm{r}}H$ / (J/mol)
gas + liquid $\rightleftharpoons$ Si_3N_4	gas-peritectic	2152.0	0.000	0.999	0.429	−123303
liquid $\rightleftharpoons$ Si_3N_4 + $A4$	eutectic	1686.9	1.000	0.429	1.000	−50217

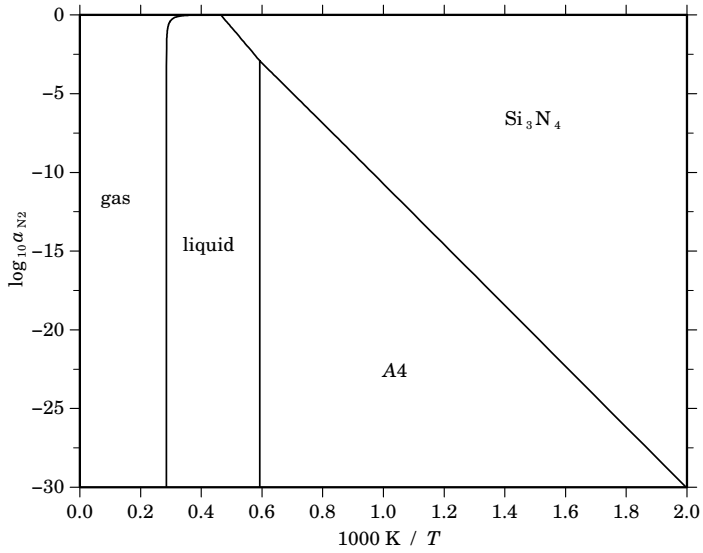

Fig. 2. Calculated temperature-activity phase diagram. Reference state: $\frac{1}{2}N_2$(gas, 0.1 MPa).

Table III. Standard reaction quantities at 298.15 K for the compounds per mole of atoms.

Compound	x_{Si}	$\Delta_{\mathrm{f}}G^\circ$ / (J/mol)	$\Delta_{\mathrm{f}}H^\circ$ / (J/mol)	$\Delta_{\mathrm{f}}S^\circ$ / (J/(mol·K))	$\Delta_{\mathrm{f}}C_P^\circ$ / (J/(mol·K))
Si_3N_4	0.429	−91714	−105603	−46.583	−3.146

References

[1930Hin] W.B. Hincke, L.R. Brantley: J. Am. Chem. Soc. **52** (1930) 48–52.
[1959Peh] R.D. Pehlke, J.F. Elliott: Trans. Metall. Soc. AIME **215** (1959) 781–785.
[1959Kai] W. Kaiser, C.K. Thurmond: J. Appl. Phys. **30** (1959) 427–431.
[1973Yat] Y. Yatsurugi, N. Akiyama, Y. Endo: J. Electrochem. Soc. **120** (1973) 975–979.
[1976Guz] I. Ya. Guzman, A.F. Demidenko, V.I. Koshchenko, M.S. Fraifel'd, Yu.V. Egner: Izv. Aked. Nauk SSSR, Neorg. Mater. **12** (1976) 1879–1881; transl.: Inorg. Mater. **12** (1976) 1546–1548.
[1981Dör] P. Dörner, L.J. Gauckler, H. Krieg, H.L. Lukas, G. Petzow, J. Weiss: J. Mater. Sci. **16** (1981) 935–943.
[2003Ma] X. Ma, C. Li, F. Wang, W. Zhang: Calphad **27** (2003) 383–388.

Nb – Ta (Niobium – Tantalum)

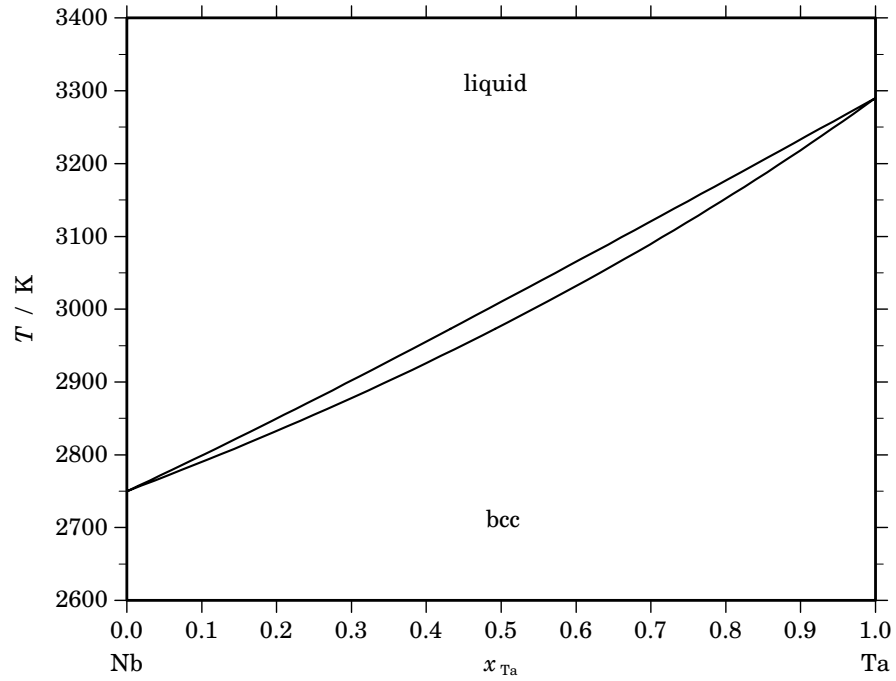

Fig. 1. Calculated phase diagram for the system Nb-Ta.

The phase diagram of the Nb-Ta system is very simple consisting only of the liquid and the bcc phases with complete miscibility for both components. The literature on the Nb-Ta has been reviewed in [1996Kris, 2004Xio] and a thermodynamic dataset has been optimised by [2004Xio] using the element data recommended by SGTE. From the few available investigations on the phase diagram only the data of [1969Rud] are considered to be reliable [1996Kris, 2004Xio] since they are compatible with the currently accepted melting temperatures of the elements. No data for the thermodynamics of Nb-Ta mixtures have been reported in the literature. Based on these limited information the system has been described as an ideal solution in the liquid and as a regular solution in the bcc phase [2004Xio].

Table I. Phases, structures and models.

Phase	Struktur-bericht	Prototype	Pearson symbol	Space group	SGTE name	Model
liquid					LIQUID	$(Nb,Ta)_1$
bcc	$A2$	W	$cI2$	$Im\overline{3}m$	BCC_A2	$(Nb,Ta)_1$

Table IIa. Integral quantities for the liquid phase at 3300 K.

x_{Ta}	ΔG_{m} [J/mol]	ΔH_{m} [J/mol]	ΔS_{m} [J/(mol·K)]	$G_{\mathrm{m}}^{\mathrm{E}}$ [J/mol]	$S_{\mathrm{m}}^{\mathrm{E}}$ [J/(mol·K)]	ΔC_P [J/(mol·K)]
0.000	0	0	0.000	0	0.000	0.000
0.100	−8920	0	2.703	0	0.000	0.000
0.200	−13730	0	4.161	0	0.000	0.000
0.300	−16761	0	5.079	0	0.000	0.000
0.400	−18466	0	5.596	0	0.000	0.000
0.500	−19019	0	5.763	0	0.000	0.000
0.600	−18466	0	5.596	0	0.000	0.000
0.700	−16761	0	5.079	0	0.000	0.000
0.800	−13730	0	4.161	0	0.000	0.000
0.900	−8920	0	2.703	0	0.000	0.000
1.000	0	0	0.000	0	0.000	0.000

Reference states: Nb(liquid), Ta(liquid)

Table IIb. Partial quantities for Nb in the liquid phase at 3300 K.

x_{Nb}	ΔG_{Nb} [J/mol]	ΔH_{Nb} [J/mol]	ΔS_{Nb} [J/(mol·K)]	$G_{\mathrm{Nb}}^{\mathrm{E}}$ [J/mol]	$S_{\mathrm{Nb}}^{\mathrm{E}}$ [J/(mol·K)]	a_{Nb}	γ_{Nb}
1.000	0	0	0.000	0	0.000	1.000	1.000
0.900	−2891	0	0.876	0	0.000	0.900	1.000
0.800	−6123	0	1.855	0	0.000	0.800	1.000
0.700	−9786	0	2.966	0	0.000	0.700	1.000
0.600	−14016	0	4.247	0	0.000	0.600	1.000
0.500	−19019	0	5.763	0	0.000	0.500	1.000
0.400	−25141	0	7.619	0	0.000	0.400	1.000
0.300	−33035	0	10.010	0	0.000	0.300	1.000
0.200	−44160	0	13.382	0	0.000	0.200	1.000
0.100	−63178	0	19.145	0	0.000	0.100	1.000
0.000	$-\infty$	0	∞	0	0.000	0.000	1.000

Reference state: Nb(liquid)

Table IIc. Partial quantities for Ta in the liquid phase at 3300 K.

x_{Ta}	ΔG_{Ta} [J/mol]	ΔH_{Ta} [J/mol]	ΔS_{Ta} [J/(mol·K)]	$G_{\mathrm{Ta}}^{\mathrm{E}}$ [J/mol]	$S_{\mathrm{Ta}}^{\mathrm{E}}$ [J/(mol·K)]	a_{Ta}	γ_{Ta}
0.000	$-\infty$	0	∞	0	0.000	0.000	1.000
0.100	−63178	0	19.145	0	0.000	0.100	1.000
0.200	−44160	0	13.382	0	0.000	0.200	1.000
0.300	−33035	0	10.010	0	0.000	0.300	1.000
0.400	−25141	0	7.619	0	0.000	0.400	1.000
0.500	−19019	0	5.763	0	0.000	0.500	1.000
0.600	−14016	0	4.247	0	0.000	0.600	1.000
0.700	−9786	0	2.966	0	0.000	0.700	1.000
0.800	−6123	0	1.855	0	0.000	0.800	1.000
0.900	−2891	0	0.876	0	0.000	0.900	1.000
1.000	0	0	0.000	0	0.000	1.000	1.000

Reference state: Ta(liquid)

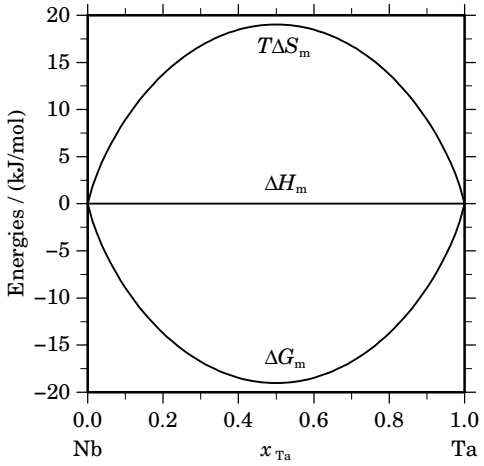

Fig. 2. Integral quantities of the liquid phase at T=3300 K.

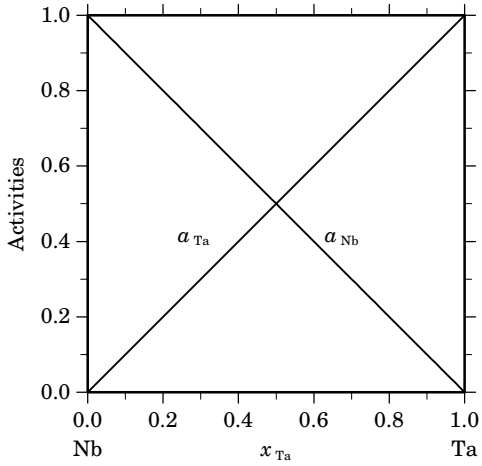

Fig. 3. Activities in the liquid phase at T=3300 K.

Table IIIa. Integral quantities for the stable phases at 2600 K.

Phase	x_{Ta}	ΔG_{m} [J/mol]	ΔH_{m} [J/mol]	ΔS_{m} [J/(mol·K)]	$G^{\mathrm{E}}_{\mathrm{m}}$ [J/mol]	$S^{\mathrm{E}}_{\mathrm{m}}$ [J/(mol·K)]	ΔC_P [J/(mol·K)]
bcc	0.000	0	0	0.000	0	0.000	0.000
	0.100	−6911	117	2.703	117	0.000	0.000
	0.200	−10610	208	4.161	208	0.000	0.000
	0.300	−12933	273	5.079	273	0.000	0.000
	0.400	−14238	312	5.596	312	0.000	0.000
	0.500	−14660	325	5.763	325	0.000	0.000
	0.600	−14238	312	5.596	312	0.000	0.000
	0.700	−12933	273	5.079	273	0.000	0.000
	0.800	−10610	208	4.161	208	0.000	0.000
	0.900	−6911	117	2.703	117	0.000	0.000
	1.000	0	0	0.000	0	0.000	0.000

Reference states: Nb(bcc), Ta(bcc)

Table IIIb. Partial quantities for Nb in the stable phases at 2600 K.

Phase	x_{Nb}	ΔG_{Nb} [J/mol]	ΔH_{Nb} [J/mol]	ΔS_{Nb} [J/(mol·K)]	$G^{\mathrm{E}}_{\mathrm{Nb}}$ [J/mol]	$S^{\mathrm{E}}_{\mathrm{Nb}}$ [J/(mol·K)]	a_{Nb}	γ_{Nb}
bcc	1.000	0	0	0.000	0	0.000	1.000	1.000
	0.900	−2265	13	0.876	13	0.000	0.901	1.001
	0.800	−4772	52	1.855	52	0.000	0.802	1.002
	0.700	−7594	117	2.966	117	0.000	0.704	1.005
	0.600	−10835	208	4.247	208	0.000	0.606	1.010
	0.500	−14660	325	5.763	325	0.000	0.508	1.015
	0.400	−19341	467	7.619	467	0.000	0.409	1.022
	0.300	−25391	636	10.010	636	0.000	0.309	1.030
	0.200	−33962	831	13.382	831	0.000	0.208	1.039
	0.100	−48725	1051	19.145	1051	0.000	0.105	1.050
	0.000	$-\infty$	1298	∞	1298	0.000	0.000	1.062

Reference state: Nb(bcc)

Table IIIc. Partial quantities for Ta in the stable phases at 2600 K.

Phase	x_{Ta}	ΔG_{Ta} [J/mol]	ΔH_{Ta} [J/mol]	ΔS_{Ta} [J/(mol·K)]	$G^{\mathrm{E}}_{\mathrm{Ta}}$ [J/mol]	$S^{\mathrm{E}}_{\mathrm{Ta}}$ [J/(mol·K)]	a_{Ta}	γ_{Ta}
bcc	0.000	$-\infty$	1298	∞	1298	0.000	0.000	1.062
	0.100	−48725	1051	19.145	1051	0.000	0.105	1.050
	0.200	−33962	831	13.382	831	0.000	0.208	1.039
	0.300	−25391	636	10.010	636	0.000	0.309	1.030
	0.400	−19341	467	7.619	467	0.000	0.409	1.022
	0.500	−14660	325	5.763	325	0.000	0.508	1.015
	0.600	−10835	208	4.247	208	0.000	0.606	1.010
	0.700	−7594	117	2.966	117	0.000	0.704	1.005
	0.800	−4772	52	1.855	52	0.000	0.802	1.002
	0.900	−2265	13	0.876	13	0.000	0.901	1.001
	1.000	0	0	0.000	0	0.000	1.000	1.000

Reference state: Ta(bcc)

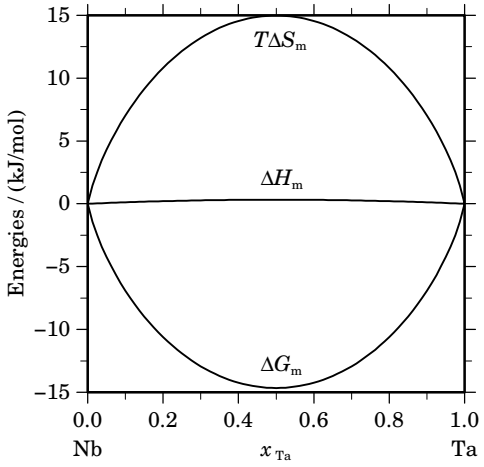

Fig. 4. Integral quantities of the stable phases at T=2600 K.

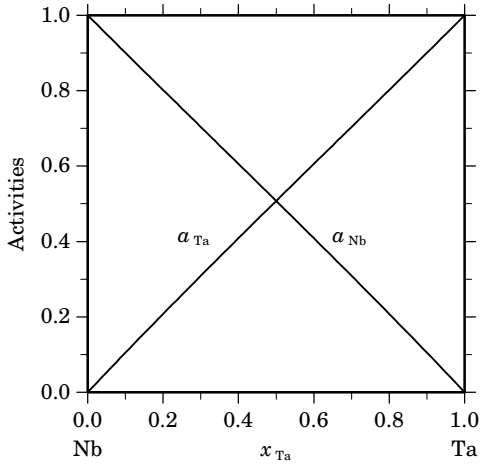

Fig. 5. Activities in the stable phases at T=2600 K.

References

[1969Rud] E. Rudy: "Compendium of Phase Diagram Data", AFML, Wright-Patterson AFB, Ohio, Rep. No. AFML-TR-65-2, Part 5, 1969.

[1996Kris] R. Krishnan, S.P. Garg, N. Krishnamurthy, E. Paul in: "Phase Diagrams of Binary Tantalum Alloys", S.P. Garg, M. Venkatraman, N. Krishnamurthy, R. Krishnan (eds.), The Indian Institute of Metals, Calcutta, 1996, pp. 118–120.

[2004Xio] W. Xiong, Y. Du, Y. Li, B.Y. Huang, H.H. Xu, H.L. Chen, Z. Pan: Calphad **28** (2004) 133–140.

Ni – Pb (Nickel – Lead)

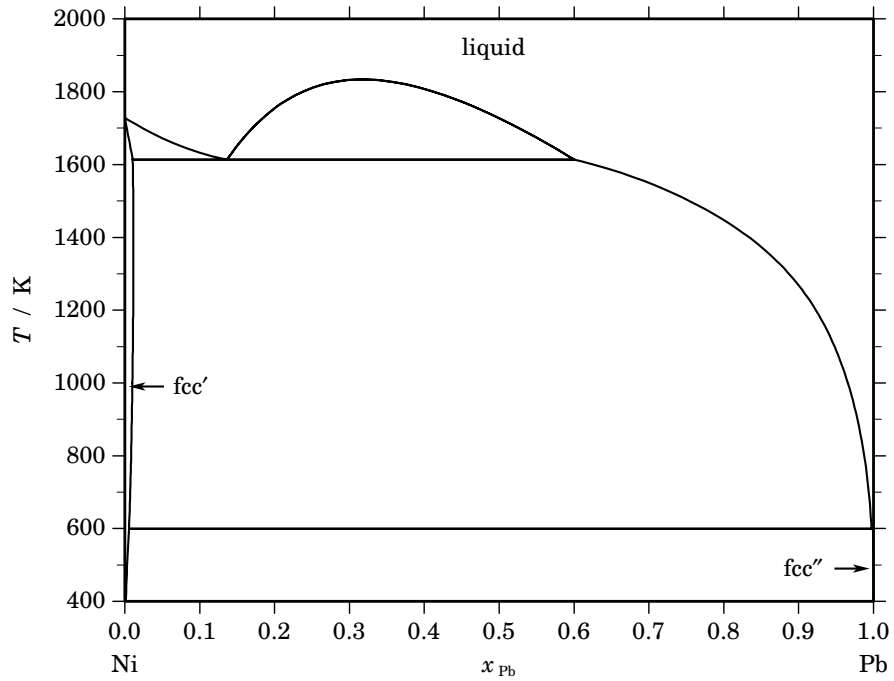

Fig. 1. Calculated phase diagram for the system Ni-Pb.

Alloys based on Ni-Pb or Cu-Ni-Pb are used as bearings in heavy-duty diesel engines. The literature on the Ni-Pb system has been reviewed in [1991Nas, 1999Gho, 2000Wan] and optimised thermodynamic datasets have been reported in [1999Gho, 2000Wan]. The Ni-Pb system has been been investigated repeatedly with various techniques. The liquidus has been determined by thermal analysis [1907Por, 1908Vos], chemical analysis [1955Pel, 1958Ald, 1959Fle, 1961Dav], and EMF measurements [1964Cav, 1981Tas]. The temperatures given in [1908Vos] had to be corrected due to a deviation in the melting point of pure Ni [1991Nas]. The activities of Ni in Pb-rich melts have been determined in EMF experiments [1964Cav] and activities of Pb in Ni-rich melts have been obtained by an isopiestic technique [1986Pom]. The location of the consolute point on the miscibility gap in the liquid has been estimated by [1960Mil] by extrapolating data from the Fe-Ni-Pb system. Both assessments [1999Gho, 2000Wan] provide good descriptions of the experimental data and they may be considered to be equivalent. The present tables and diagrams have been calculated with the data of [2000Wan] but that does not mean that those of [1999Gho] have been rejected.

Table I. Phases, structures and models.

Phase	Struktur-bericht	Prototype	Pearson symbol	Space group	SGTE name	Model
liquid					LIQUID	$(Ni,Pb)_1$
fcc	$A1$	Cu	$cF4$	$Fm\overline{3}m$	FCC_A1	$(Ni,Pb)_1$

Table II. Invariant reactions.

Reaction	Type	T / K	Compositions / x_{Pb}			$\Delta_r H$ / (J/mol)
liquid $\rightleftharpoons$ liquid′ + liquid″	critical	1832.1	0.318	0.318	0.318	0
liquid′ $\rightleftharpoons$ fcc′ + liquid″	monotectic	1613.3	0.136	0.010	0.601	−15523
liquid″ $\rightleftharpoons$ fcc′ + fcc″	eutectic	599.5	0.997	0.005	0.999	−4799

Table IIIa. Integral quantities for the liquid phase at 1900 K.

x_{Pb}	ΔG_{m} [J/mol]	ΔH_{m} [J/mol]	ΔS_{m} [J/(mol·K)]	$G_{\mathrm{m}}^{\mathrm{E}}$ [J/mol]	$S_{\mathrm{m}}^{\mathrm{E}}$ [J/(mol·K)]	ΔC_P [J/(mol·K)]
0.000	0	0	0.000	0	0.000	0.000
0.100	−2242	2790	2.648	2894	−0.055	0.000
0.200	−2944	5291	4.334	4961	0.174	0.000
0.300	−3428	7083	5.532	6222	0.453	0.000
0.400	−3863	7958	6.222	6769	0.626	0.000
0.500	−4219	7883	6.369	6731	0.606	0.000
0.600	−4397	6968	5.981	6235	0.386	0.000
0.700	−4282	5426	5.110	5368	0.031	0.000
0.800	−3769	3541	3.847	4136	−0.314	0.000
0.900	−2701	1627	2.278	2434	−0.425	0.000
1.000	0	0	0.000	0	0.000	0.000

Reference states: Ni(liquid), Pb(liquid)

Table IIIb. Partial quantities for Ni in the liquid phase at 1900 K.

x_{Ni}	ΔG_{Ni} [J/mol]	ΔH_{Ni} [J/mol]	ΔS_{Ni} [J/(mol·K)]	$G_{\mathrm{Ni}}^{\mathrm{E}}$ [J/mol]	$S_{\mathrm{Ni}}^{\mathrm{E}}$ [J/(mol·K)]	a_{Ni}	γ_{Ni}
1.000	0	0	0.000	0	0.000	1.000	1.000
0.900	−1256	55	0.690	409	−0.186	0.924	1.026
0.800	−1870	895	1.455	1655	−0.400	0.888	1.110
0.700	−2065	3026	2.680	3570	−0.286	0.877	1.254
0.600	−2230	6388	4.536	5840	0.289	0.868	1.447
0.500	−2790	10498	6.994	8160	1.231	0.838	1.676
0.400	−4094	14594	9.836	10381	2.218	0.772	1.929
0.300	−6355	17780	12.702	12665	2.692	0.669	2.229
0.200	−9790	19165	15.240	15635	1.858	0.538	2.690
0.100	−15851	18012	17.823	20525	−1.322	0.367	3.666
0.000	$-\infty$	13878	∞	29332	−8.134	0.000	6.403

Reference state: Ni(liquid)

Table IIIc. Partial quantities for Pb in the liquid phase at 1900 K.

x_{Pb}	ΔG_{Pb} [J/mol]	ΔH_{Pb} [J/mol]	ΔS_{Pb} [J/(mol·K)]	$G_{\mathrm{Pb}}^{\mathrm{E}}$ [J/mol]	$S_{\mathrm{Pb}}^{\mathrm{E}}$ [J/(mol·K)]	a_{Pb}	γ_{Pb}
0.000	$-\infty$	27333	∞	32881	−2.920	0.000	8.015
0.100	−11114	27405	20.273	25261	1.128	0.495	4.948
0.200	−7239	22875	15.849	18187	2.467	0.632	3.162
0.300	−6610	16549	12.189	12410	2.178	0.658	2.194
0.400	−6313	10312	8.750	8162	1.132	0.671	1.676
0.500	−5647	5268	5.745	5303	−0.018	0.699	1.399
0.600	−4598	1884	3.411	3472	−0.836	0.747	1.246
0.700	−3394	132	1.856	2240	−1.110	0.807	1.152
0.800	−2263	−366	0.999	1262	−0.857	0.867	1.083
0.900	−1240	−193	0.551	424	−0.325	0.924	1.027
1.000	0	0	0.000	0	0.000	1.000	1.000

Reference state: Pb(liquid)

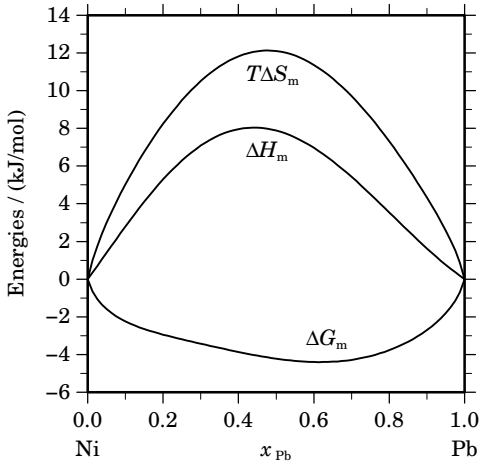

Fig. 2. Integral quantities of the liquid phase at T=1900 K.

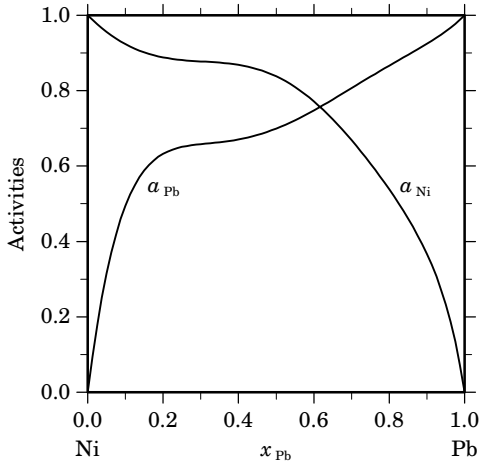

Fig. 3. Activities in the liquid phase at T=1900 K.

References

[1907Por] M.A. Portevin: Rev. Métall. **4** (1907) 814–818.

[1908Vos] G. Voss: Z. Anorg. Allg. Chem. **57** (1908) 45–48.

[1955Pel] E. Pelzel: Metall **9** (1955) 692–694.

[1958Ald] T. Alden, D.A. Stevenson, J. Wulff: Trans. Metall. Soc. AIME **212** (1958) 15–17.

[1959Fle] B. Fleischer, J.F. Elliot in: "The Physical Chemistry of Metallic Solutions & Intermetallic Compounds", Natl. Phys. Lab., U.K., Proc. Symp. No. 9, Vol. 1, Paper 2F (1959).

[1960Mil] K.O. Miller, J.F. Elliot: Trans. Metall. Soc. AIME **218** (1960) 900-910.

[1961Dav] T.R.A. Davey in: "Physical Chemistry of Process Metallurgy", AIME-TMS Conf., Vol. 7, (1961) 581–600.

[1964Cav] C.R. Cavanaugh, J.F. Elliot: Trans. Metall. Soc. AIME **230** (1964) 633–638.

[1981Tas] A. Taskinen: Scand. J. Metall. **10** (1981) 185–188.

[1986Pom] T. Pomianek: Z. Metallkd. **77** (1986) 388–392.

[1991Nas] P. Nash in: "Phase Diagrams of Binary Nickel Alloys", P. Nash (ed.), ASM Intl., Materials Park, OH, 1991, pp. 247–251.

[1999Gho] G. Ghosh: Metall. Mater. Trans. A **30A** (1999) 1481–1494.

[2000Wan] C.P. Wang, X.J. Liu, I. Ohnuma, R. Kainuma, K. Ishida: Calphad **24** (2000) 149–167.

Ni – Ru (Nickel – Ruthenium)

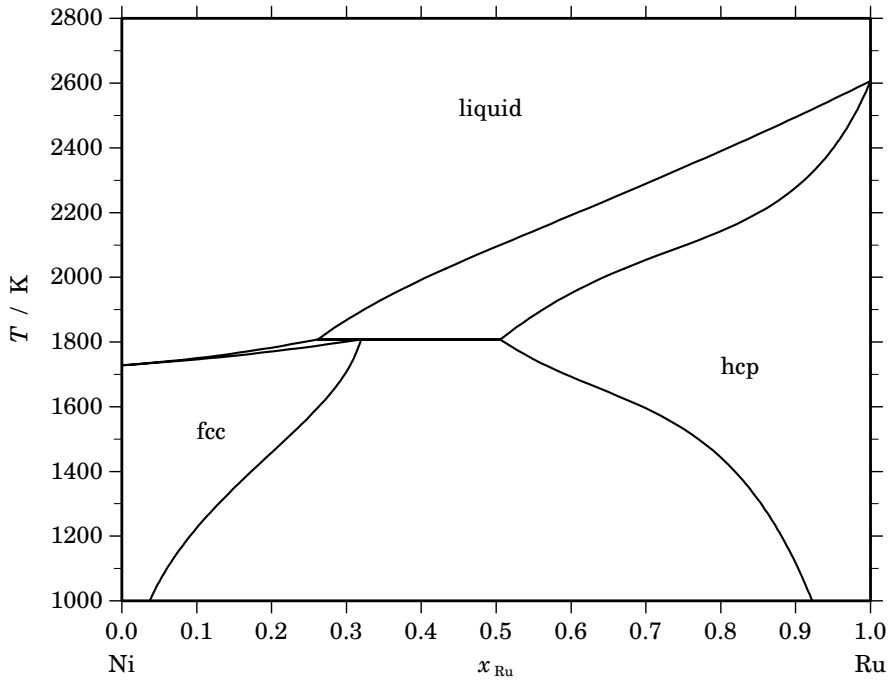

Fig. 1. Calculated phase diagram for the system Ni-Ru.

The Ni-Ru binary system contains two components interesting in the nuclear field, nickel being a major component of stainless steel structures of the vessel, and ruthenium being selected as representative of a family of non-volatile fission products. Experimental information on the phase diagram has been reported in the compilations of Hansen and Anderko [1958Han], Elliott [1965Ell] and Shunk [1969Shu]. It is based on the investigations of Raub and Menzel [1961Rau], and Kornilov and Myasnikova [1964Kor]. There is complete solubility of the components in the liquid state and a limited mutual solubility of Ni and Ru in the solid state, being maximal at the peritectic temperature. No thermodynamic data are available for the binary system. The system was assessed by Chevalier and Fischer [2001Che], and by Hallström [2004Hal]. The excess Gibbs energy of the liquid, fcc and hcp solution phases was optimised from the selected phase diagram information. A regular substitution model was used for the first two phases, and a sub-regular description for the hcp phase. The agreement with the experimental information [1961Rau, 1964Kor] is quite satisfactory.

Table I. Phases, structures and models.

Phase	Struktur-bericht	Prototype	Pearson symbol	Space group	SGTE name	Model
liquid					LIQUID	$(Ni,Ru)_1$
fcc	$A1$	Cu	$cF4$	$Fm\overline{3}m$	FCC_A1	$(Ni,Ru)_1$
hcp	$A3$	Mg	$hP2$	$P6_3/mmc$	HCP_A3	$(Ni,Ru)_1$

Table II. Invariant reactions.

Reaction	Type	T / K	Compositions / x_{Ru}			$\Delta_{\mathrm{r}}H$ / (J/mol)
liquid + hcp $\rightleftharpoons$ fcc	peritectic	1807.8	0.261	0.505	0.319	−10683

Table IIIa. Integral quantities for the liquid phase at 2700 K.

x_{Ru}	ΔG_{m} [J/mol]	ΔH_{m} [J/mol]	ΔS_{m} [J/(mol·K)]	$G_{\mathrm{m}}^{\mathrm{E}}$ [J/mol]	$S_{\mathrm{m}}^{\mathrm{E}}$ [J/(mol·K)]	ΔC_P [J/(mol·K)]
0.000	0	0	0.000	0	0.000	0.000
0.100	−6511	786	2.703	786	0.000	0.000
0.200	−9836	1398	4.161	1398	0.000	0.000
0.300	−11878	1835	5.079	1835	0.000	0.000
0.400	−13011	2097	5.596	2097	0.000	0.000
0.500	−13376	2185	5.763	2185	0.000	0.000
0.600	−13011	2097	5.596	2097	0.000	0.000
0.700	−11878	1835	5.079	1835	0.000	0.000
0.800	−9836	1398	4.161	1398	0.000	0.000
0.900	−6511	786	2.703	786	0.000	0.000
1.000	0	0	0.000	0	0.000	0.000

Reference states: Ni(liquid), Ru(liquid)

Table IIIb. Partial quantities for Ni in the liquid phase at 2700 K.

x_{Ni}	ΔG_{Ni} [J/mol]	ΔH_{Ni} [J/mol]	ΔS_{Ni} [J/(mol·K)]	$G_{\mathrm{Ni}}^{\mathrm{E}}$ [J/mol]	$S_{\mathrm{Ni}}^{\mathrm{E}}$ [J/(mol·K)]	a_{Ni}	γ_{Ni}
1.000	0	0	0.000	0	0.000	1.000	1.000
0.900	−2278	87	0.876	87	0.000	0.904	1.004
0.800	−4660	350	1.855	350	0.000	0.813	1.016
0.700	−7221	786	2.966	786	0.000	0.725	1.036
0.600	−10070	1398	4.247	1398	0.000	0.639	1.064
0.500	−13376	2185	5.763	2185	0.000	0.551	1.102
0.400	−17424	3146	7.619	3146	0.000	0.460	1.150
0.300	−22747	4282	10.010	4282	0.000	0.363	1.210
0.200	−30538	5592	13.382	5592	0.000	0.257	1.283
0.100	−44613	7078	19.145	7078	0.000	0.137	1.371
0.000	$-\infty$	8738	∞	8738	0.000	0.000	1.476

Reference state: Ni(liquid)

Table IIIc. Partial quantities for Ru in the liquid phase at 2700 K.

x_{Ru}	ΔG_{Ru} [J/mol]	ΔH_{Ru} [J/mol]	ΔS_{Ru} [J/(mol·K)]	$G_{\mathrm{Ru}}^{\mathrm{E}}$ [J/mol]	$S_{\mathrm{Ru}}^{\mathrm{E}}$ [J/(mol·K)]	a_{Ru}	γ_{Ru}
0.000	$-\infty$	8738	∞	8738	0.000	0.000	1.476
0.100	−44613	7078	19.145	7078	0.000	0.137	1.371
0.200	−30538	5592	13.382	5592	0.000	0.257	1.283
0.300	−22747	4282	10.010	4282	0.000	0.363	1.210
0.400	−17424	3146	7.619	3146	0.000	0.460	1.150
0.500	−13376	2185	5.763	2185	0.000	0.551	1.102
0.600	−10070	1398	4.247	1398	0.000	0.639	1.064
0.700	−7221	786	2.966	786	0.000	0.725	1.036
0.800	−4660	350	1.855	350	0.000	0.813	1.016
0.900	−2278	87	0.876	87	0.000	0.904	1.004
1.000	0	0	0.000	0	0.000	1.000	1.000

Reference state: Ru(liquid)

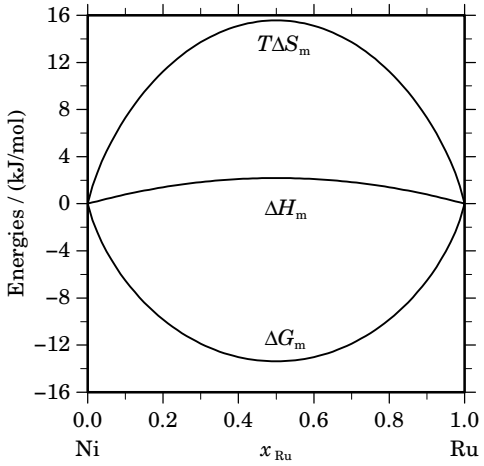

Fig. 2. Integral quantities of the liquid phase at T=2700 K.

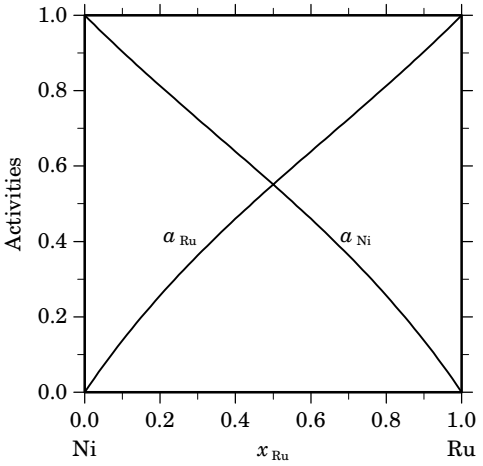

Fig. 3. Activities in the liquid phase at T=2700 K.

Table IVa. Integral quantities for the stable phases at 1700 K.

Phase	x_{Ru}	ΔG_{m} [J/mol]	ΔH_{m} [J/mol]	ΔS_{m} [J/(mol·K)]	$G_{\mathrm{m}}^{\mathrm{E}}$ [J/mol]	$S_{\mathrm{m}}^{\mathrm{E}}$ [J/(mol·K)]	ΔC_P [J/(mol·K)]
fcc	0.000	0	0	0.000	0	0.000	0.000
	0.100	−2763	3743	3.827	1832	1.124	−0.008
	0.200	−3629	6932	6.212	3444	2.052	−0.011
	0.298	−3801	9510	7.830	4806	2.767	−0.012
hcp	0.593	−3584	10118	8.060	5969	2.440	−0.009
	0.600	−3578	9930	7.946	5935	2.350	−0.008
	0.700	−3409	7141	6.206	5226	1.127	−0.006
	0.800	−3036	4272	4.299	4037	0.139	−0.004
	0.900	−2282	1750	2.372	2313	−0.331	−0.002
	1.000	0	0	0.000	0	0.000	0.000

Reference states: Ni(fcc), Ru(hcp)

Table IVb. Partial quantities for Ni in the stable phases at 1700 K.

Phase	x_{Ni}	ΔG_{Ni} [J/mol]	ΔH_{Ni} [J/mol]	ΔS_{Ni} [J/(mol·K)]	$G_{\mathrm{Ni}}^{\mathrm{E}}$ [J/mol]	$S_{\mathrm{Ni}}^{\mathrm{E}}$ [J/(mol·K)]	a_{Ni}	γ_{Ni}
fcc	1.000	0	0	0.000	0	0.000	1.000	1.000
	0.900	−1379	278	0.975	110	0.099	0.907	1.008
	0.800	−2714	1110	2.249	440	0.394	0.825	1.032
	0.702	−4019	2457	3.810	975	0.872	0.752	1.071
hcp	0.407	−4019	25335	17.267	8677	9.799	0.752	1.848
	0.400	−4091	25562	17.443	8861	9.824	0.749	1.872
	0.300	−5212	27439	19.206	11806	9.196	0.692	2.305
	0.200	−7134	26409	19.731	15615	6.349	0.604	3.018
	0.100	−12151	21616	19.863	20396	0.718	0.423	4.233
	0.000	$-\infty$	12208	∞	26259	−8.265	0.000	6.409

Reference state: Ni(fcc)

Table IVc. Partial quantities for Ru in the stable phases at 1700 K.

Phase	x_{Ru}	ΔG_{Ru} [J/mol]	ΔH_{Ru} [J/mol]	ΔS_{Ru} [J/(mol·K)]	$G^{\mathrm{E}}_{\mathrm{Ru}}$ [J/mol]	$S^{\mathrm{E}}_{\mathrm{Ru}}$ [J/(mol·K)]	a_{Ru}	γ_{Ru}
fcc	0.000	$-\infty$	40211	∞	19422	12.229	0.000	3.951
	0.100	−15217	34935	29.501	17329	10.356	0.341	3.408
	0.200	−7291	30219	22.065	15458	8.683	0.597	2.985
	0.298	−3284	26153	17.316	13844	7.241	0.793	2.663
hcp	0.593	−3284	−338	1.733	4109	−2.616	0.793	1.337
	0.600	−3236	−492	1.614	3985	−2.633	0.795	1.326
	0.700	−2636	−1558	0.634	2406	−2.331	0.830	1.186
	0.800	−2012	−1262	0.441	1142	−1.414	0.867	1.084
	0.900	−1185	−458	0.428	304	−0.448	0.920	1.022
	1.000	0	0	0.000	0	0.000	1.000	1.000

Reference state: Ru(hcp)

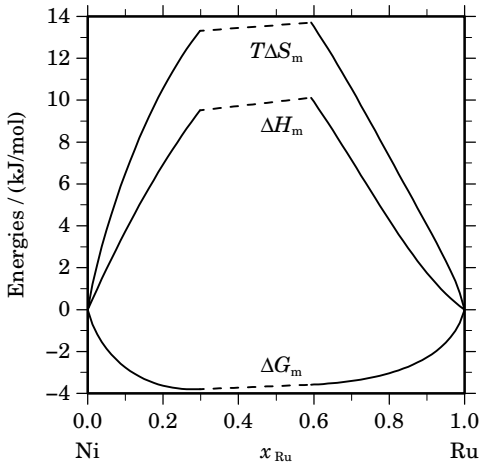

Fig. 4. Integral quantities of the stable phases at T=1700 K.

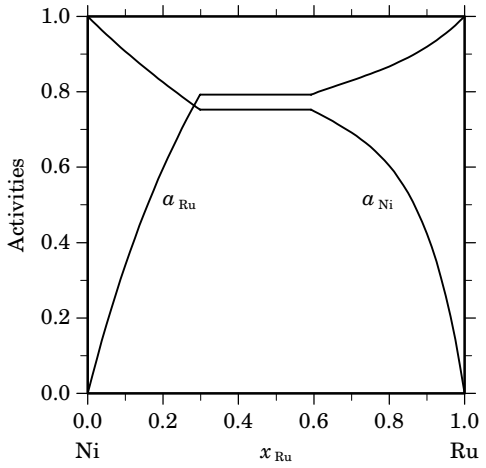

Fig. 5. Activities in the stable phases at T=1700 K.

References

[1958Han] M. Hansen, K. Anderko, “Constitution of Binary Alloys”, McGraw-Hill, New-York, 1958.
[1961Rau] E. Raub, D. Menzel: Z. Metallkd. **52** (1961) 831–833.
[1964Kor] I.I. Kornilov, K.P. Myasnikova: Russ. Metall. Min. **4** (1964) 95–101.
[1965Ell] R.P. Elliott, “Constitution of Binary Alloys”, 1st Suppl., McGraw-Hill, New-York, 1965.
[1969Shu] F.A. Shunk, “Constitution of Binary Alloys”, 2nd Suppl., McGraw-Hill, New-York, 1969.
[2001Che] P.-Y. Chevalier, E. Fischer, unpublished work, 2001.
[2004Hal] S. Hallström: J. Phase Equilibria **25** (2004) 252–254.

Ni – Zn (Nickel – Zinc)

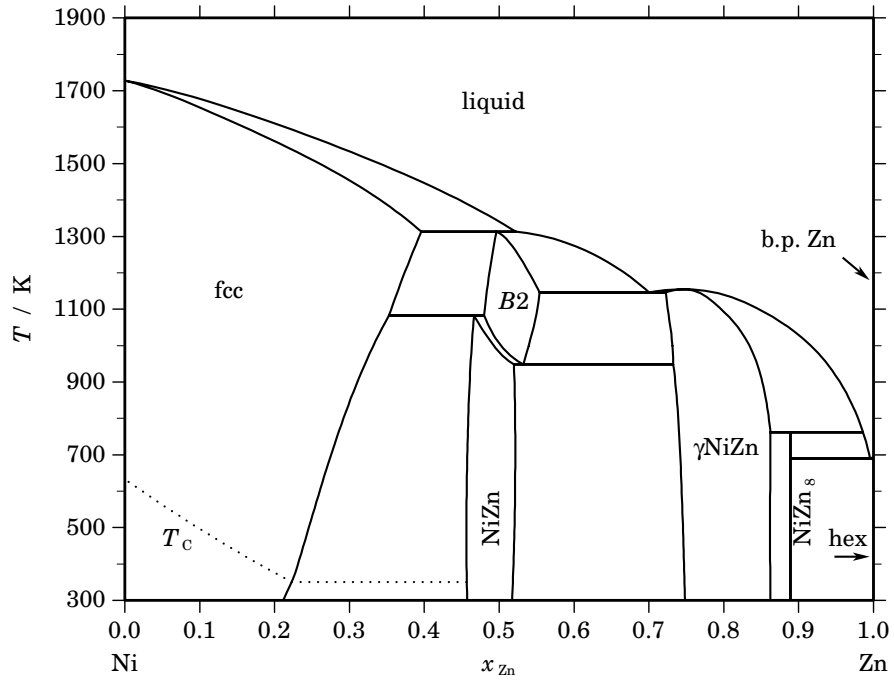

Fig. 1. Calculated phase diagram for the system Ni-Zn.

The Ni-Zn system is of interest for galvanising of high silicon steels where Ni is added to the bath in order to reduce coating thickness and to improve the coating adhesion and its appearance. The Ni-Zn system has been reviewed in [1991Nas] as well as by [2000Vas, 2002Su, 2003Mie] who also reported optimised thermodynamic datasets. Over the years, numerous studies of the Ni-Zn have been published and the optimisations [2000Vas, 2002Su, 2003Mie] are based essentially on the same experimental data but they differ in the thermodynamic modelling, especially the description of the non-stoichiometric intermetallic phases.

Data on the phase equilibria have been measured over the complete composition range and temperatures from the liquidus down into the subsolidus regions. Furthermore there are numerous studies of the zinc activity in the liquid as well as in the solid solution phases and enthalpies of formation have been determined at several temperatures.

In [2000Vas] the deviation from stoichiometry on the Zn-deficient side of the $B2$ and NiZn phases and on the Ni-poor side of γNiZn has been modelled by introducing vacancies into one of the sublattices. In [2002Su] it has been criticised that these phases contain unphysically high vacancy concentrations even at low temperatures and alternative modelling of these phases has been presented. However, the overall fit of the phase diagram and the thermodynamic data is still best in the assessment of [2000Vas] and therefore, this dataset is presented here.

Table I. Phases, structures and models.

Phase	Struktur-bericht	Prototype	Pearson symbol	Space group	SGTE name	Model
liquid					LIQUID	$(Ni,Zn)_1$
fcc	$A1$	Cu	$cF4$	$Fm\bar{3}m$	FCC_A1	$(Ni,Zn)_1$
$B2$	$B2$	CsCl	$cP2$	$Pm\bar{3}m$	NIZN_B2	$(Ni,Zn)_1(Zn,\Box)_1$
NiZn	$L1_0$	AuCu	$tP2$	$P4/mmm$	NIZN_L10	$(Ni,Zn)_1(Zn,\Box)_1$
γNiZn	$D8_2$	Cu_5Zn_8	$cI52$	$I4\bar{3}m$	NIZN_GAMMA	$(Ni,\Box)_2(Ni,Zn)_{11}Ni_2Zn_{11}$
$NiZn_8$	⋯	⋯	$mC28$	$C2/m$	NIZN8	Ni_1Zn_8
hex	$A3$	Mg	$hP2$	$P6_3/mmc$	HCP_ZN	Zn_1

Table II. Invariant reactions.

Reaction	Type	T / K	Compositions / x_{Zn}			$\Delta_r H$ / (J/mol)
fcc + liquid ⇌ $B2$	peritectic	1313.2	0.396	0.522	0.496	−14481
liquid ⇌ γNiZn	congruent	1154.6	0.747	0.747		−11420
liquid ⇌ $B2$ + γNiZn	eutectic	1146.2	0.700	0.554	0.723	−11825
fcc + $B2$ ⇌ NiZn	peritectoid	1082.5	0.353	0.480	0.466	−2068
$B2$ ⇌ NiZn + γNiZn	eutectoid	947.9	0.532	0.520	0.733	−2896
γNiZn + liquid ⇌ $NiZn_8$	peritectic	762.0	0.862	0.986	0.889	−1686
liquid ⇌ $NiZn_8$ + hex	eutectic	689.7	0.995	0.889	1.000	−7411

Table IIIa. Integral quantities for the liquid phase at 1800 K.

x_{Zn}	ΔG_m [J/mol]	ΔH_m [J/mol]	ΔS_m [J/(mol·K)]	G_m^E [J/mol]	S_m^E [J/(mol·K)]	ΔC_P [J/(mol·K)]
0.000	0	0	0.000	0	0.000	0.000
0.100	−7603	−5405	1.221	−2738	−1.482	0.000
0.200	−12565	−8753	2.117	−5076	−2.043	0.000
0.300	−16143	−10788	2.975	−7001	−2.104	0.000
0.400	−18536	−12010	3.626	−8464	−1.970	0.000
0.500	−19750	−12680	3.928	−9377	−1.835	0.000
0.600	−19687	−12819	3.815	−9614	−1.781	0.000
0.700	−18157	−12205	3.307	−9015	−1.772	0.000
0.800	−14866	−10373	2.496	−7377	−1.665	0.000
0.900	−9329	−6620	1.505	−4464	−1.198	0.000
1.000	0	0	0.000	0	0.000	0.000

Reference states: Ni(liquid), Zn(liquid)

Table IIIb. Partial quantities for Ni in the liquid phase at 1800 K.

x_{Ni}	ΔG_{Ni} [J/mol]	ΔH_{Ni} [J/mol]	ΔS_{Ni} [J/(mol·K)]	G^E_{Ni} [J/mol]	S^E_{Ni} [J/(mol·K)]	a_{Ni}	γ_{Ni}
1.000	0	0	0.000	0	0.000	1.000	1.000
0.900	−1778	−1173	0.336	−201	−0.540	0.888	0.987
0.800	−4142	−3579	0.313	−802	−1.543	0.758	0.948
0.700	−7223	−6094	0.627	−1885	−2.339	0.617	0.882
0.600	−11287	−8317	1.650	−3642	−2.597	0.470	0.784
0.500	−16754	−10571	3.435	−6380	−2.328	0.326	0.653
0.400	−24232	−13904	5.738	−10519	−1.881	0.198	0.495
0.300	−34609	−20086	8.068	−16590	−1.942	0.099	0.330
0.200	−49325	−31611	9.841	−25238	−3.541	0.037	0.185
0.100	−71680	−51700	11.100	−37220	−8.045	0.008	0.083
0.000	−∞	−84294	∞	−53405	−17.160	0.000	0.028

Reference state: Ni(liquid)

Table IIIc. Partial quantities for Zn in the liquid phase at 1800 K.

x_{Zn}	ΔG_{Zn} [J/mol]	ΔH_{Zn} [J/mol]	ΔS_{Zn} [J/(mol·K)]	G^E_{Zn} [J/mol]	S^E_{Zn} [J/(mol·K)]	a_{Zn}	γ_{Zn}
0.000	−∞	−67421	∞	−29433	−21.105	0.000	0.140
0.100	−60030	−43500	9.183	−25569	−9.961	0.018	0.181
0.200	−46256	−29452	9.336	−22169	−4.046	0.045	0.227
0.300	−36958	−21739	8.455	−18939	−1.555	0.085	0.282
0.400	−29410	−17548	6.590	−15697	−1.029	0.140	0.350
0.500	−22747	−14790	4.421	−12373	−1.342	0.219	0.437
0.600	−16657	−12097	2.533	−9011	−1.714	0.329	0.548
0.700	−11106	−8827	1.266	−5768	−1.700	0.476	0.680
0.800	−6251	−5064	0.660	−2912	−1.195	0.659	0.823
0.900	−2401	−1611	0.439	−824	−0.437	0.852	0.946
1.000	0	0	0.000	0	0.000	1.000	1.000

Reference state: Zn(liquid)

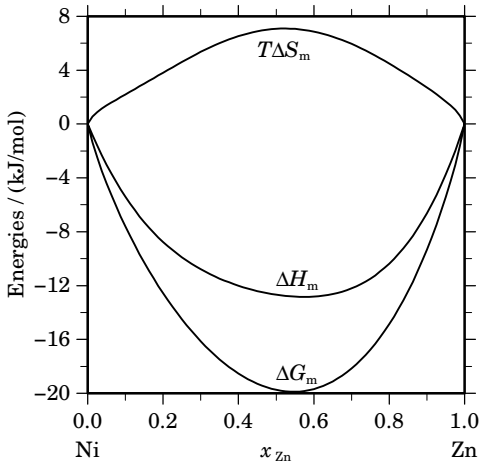

Fig. 2. Integral quantities of the liquid phase at T=1800 K.

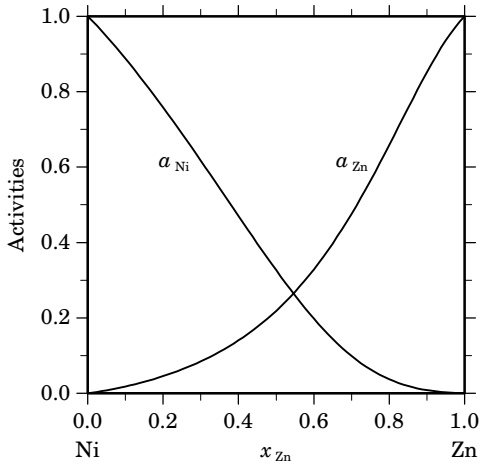

Fig. 3. Activities in the liquid phase at T=1800 K.

Table IV. Standard reaction quantities at 298.15 K for the compounds per mole of atoms.

Compound	x_{Zn}	$\Delta_{\mathrm{f}}G^{\circ}$ / (J/mol)	$\Delta_{\mathrm{f}}H^{\circ}$ / (J/mol)	$\Delta_{\mathrm{f}}S^{\circ}$ / (J/(mol·K))	$\Delta_{\mathrm{f}}C_P^{\circ}$ / (J/(mol·K))
$NiZn_8$	0.889	−10220	−10215	0.015	−0.085

References

[1991Nas] P. Nash, Y.Y. Pan in: "Phase Diagrams of Binary Nickel Alloys", P. Nash (ed.), ASM Intl., Materials Park, OH, 1991, pp. 382–390.
[2000Vas] G.P. Vassiliev, T. Gomez-Acebo, J.-C. Tedenac: J. Phase Equilibria **21** (2000) 287–301.
[2002Su] X. Su, N.-Y. Tang, J.M. Toguri: J. Phase Equilibria **23** (2002) 140–148.
[2003Mie] J. Miettinen: Calphad **27** (2003) 263–274.

Os – Si (Osmium – Silicon)

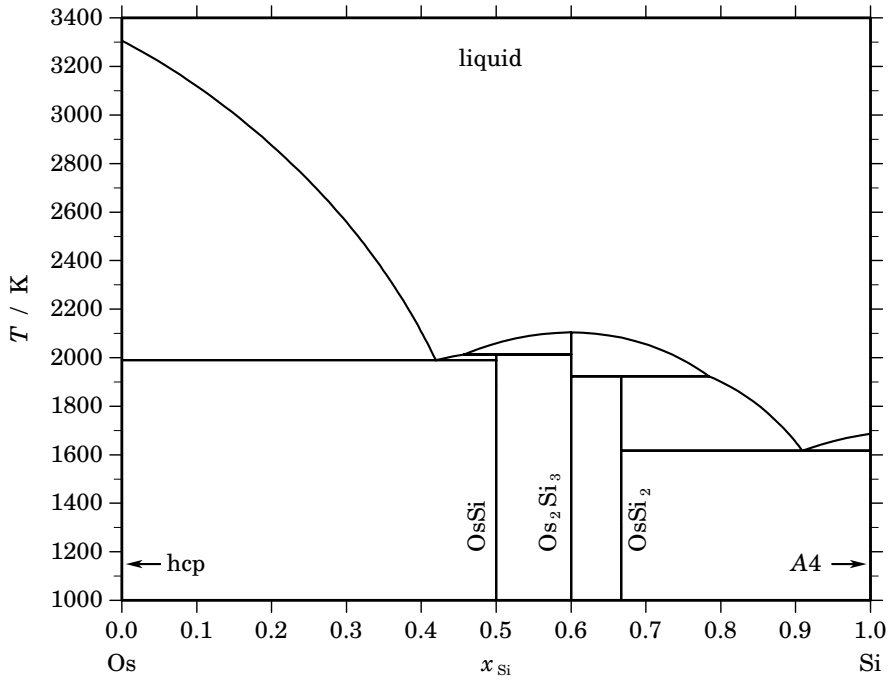

Fig. 1. Calculated phase diagram for the system Os-Si.

A survey on the literature of the Os-Si system and a thermodynamic assessment has been reported in [2001Liu]. The complete phase diagram of the system has been investigated by [1988Sch]. In addition to these data [2001Liu] have selected results from [1962Fin, 1983Mas]. Except for the enthalpy of formation of Os_2Si_3 [1998Mes] no other thermodynamic data have been determined experimentally.

Table I. Phases, structures and models.

Phase	Strukturbericht	Prototype	Pearson symbol	Space group	SGTE name	Model
liquid					LIQUID	$(Os,Si)_1$
hcp	$A3$	Mg	$hP2$	$P6_3/mmc$	HCP_A3	$(Os,Si)_1$
OsSi	$B20$	FeSi	$cP8$	$P2_13$	OSSI	Os_1Si_1
Os_2Si_3	···	···	$oP40$	$Pbcn$	OS2SI3	Os_2Si_3
$OsSi_2$	···	$FeSi_2$	$oC48$	$Cmca$	OSSI2	Os_1Si_2
$A4$	$A4$	C(diamond)	$cF8$	$Fd\bar{3}m$	DIAMOND_A4	Si_1

Table II. Invariant reactions.

Reaction	Type	T / K	Compositions / x_{Si}			$\Delta_r H$ / (J/mol)
liquid $\rightleftharpoons$ Os_2Si_3	congruent	2103.9	0.600	0.600		−45530
liquid + Os_2Si_3 $\rightleftharpoons$ OsSi	peritectic	2013.0	0.457	0.600	0.500	−26309
liquid $\rightleftharpoons$ hcp + OsSi	eutectic	1990.3	0.419	0.000	0.500	−36247
Os_2Si_3 + liquid $\rightleftharpoons$ $OsSi_2$	peritectic	1923.2	0.600	0.784	0.667	−18032
liquid $\rightleftharpoons$ $OsSi_2$ + $A4$	eutectic	1616.3	0.909	0.667	1.000	−44778

Table IIIa. Integral quantities for the liquid phase at 3400 K.

x_{Si}	ΔG_{m} [J/mol]	ΔH_{m} [J/mol]	ΔS_{m} [J/(mol·K)]	$G_{\mathrm{m}}^{\mathrm{E}}$ [J/mol]	$S_{\mathrm{m}}^{\mathrm{E}}$ [J/(mol·K)]	ΔC_P [J/(mol·K)]
0.000	0	0	0.000	0	0.000	0.000
0.100	−11585	−9343	0.659	−2395	−2.043	0.000
0.200	−18082	−17492	0.174	−3936	−3.987	0.000
0.300	−22012	−24116	−0.619	−4743	−5.698	0.000
0.400	−23963	−28884	−1.447	−4938	−7.043	0.000
0.500	−24235	−31466	−2.127	−4640	−7.890	0.000
0.600	−22997	−31531	−2.510	−3972	−8.106	0.000
0.700	−20321	−28747	−2.478	−3053	−7.557	0.000
0.800	−16150	−22785	−1.952	−2004	−6.112	0.000
0.900	−10136	−13313	−0.934	−946	−3.637	0.000
1.000	0	0	0.000	0	0.000	0.000

Reference states: Os(liquid), Si(liquid)

Table IIIb. Partial quantities for Os in the liquid phase at 3400 K.

x_{Os}	ΔG_{Os} [J/mol]	ΔH_{Os} [J/mol]	ΔS_{Os} [J/(mol·K)]	$G_{\mathrm{Os}}^{\mathrm{E}}$ [J/mol]	$S_{\mathrm{Os}}^{\mathrm{E}}$ [J/(mol·K)]	a_{Os}	γ_{Os}
1.000	0	0	0.000	0	0.000	1.000	1.000
0.900	−3426	−542	0.848	−447	−0.028	0.886	0.984
0.800	−7936	−2609	1.567	−1628	−0.288	0.755	0.944
0.700	−13384	−6862	1.918	−3301	−1.047	0.623	0.890
0.600	−19664	−13963	1.677	−5224	−2.570	0.499	0.831
0.500	−26751	−24574	0.640	−7156	−5.123	0.388	0.776
0.400	−34758	−39357	−1.352	−8855	−8.971	0.292	0.731
0.300	−44117	−58972	−4.369	−10081	−14.380	0.210	0.700
0.200	−56089	−84082	−8.233	−10591	−21.615	0.138	0.688
0.100	−75237	−115349	−11.798	−10144	−30.943	0.070	0.698
0.000	$-\infty$	−153434	∞	−8499	−42.628	0.000	0.740

Reference state: Os(liquid)

Table IIIc. Partial quantities for Si in the liquid phase at 3400 K.

x_{Si}	ΔG_{Si} [J/mol]	ΔH_{Si} [J/mol]	ΔS_{Si} [J/(mol·K)]	$G_{\mathrm{Si}}^{\mathrm{E}}$ [J/mol]	$S_{\mathrm{Si}}^{\mathrm{E}}$ [J/(mol·K)]	a_{Si}	γ_{Si}
0.000	$-\infty$	−98296	∞	−28623	−20.492	0.000	0.363
0.100	−85017	−88552	−1.040	−19925	−20.185	0.049	0.494
0.200	−58665	−77025	−5.400	−13167	−18.782	0.126	0.628
0.300	−42144	−64376	−6.539	−8109	−16.549	0.225	0.751
0.400	−30412	−51266	−6.134	−4509	−13.752	0.341	0.853
0.500	−21720	−38359	−4.894	−2125	−10.657	0.464	0.928
0.600	−15157	−26314	−3.282	−716	−7.529	0.585	0.975
0.700	−10123	−15794	−1.668	−40	−4.633	0.699	0.999
0.800	−6165	−7461	−0.381	143	−2.236	0.804	1.005
0.900	−2902	−1975	0.273	76	−0.603	0.902	1.003
1.000	0	0	0.000	0	0.000	1.000	1.000

Reference state: Si(liquid)

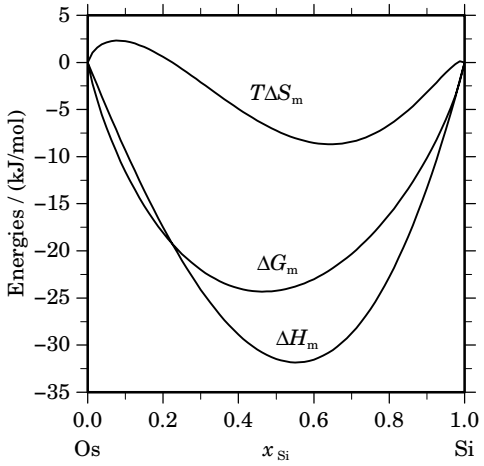

Fig. 2. Integral quantities of the liquid phase at T=3400 K.

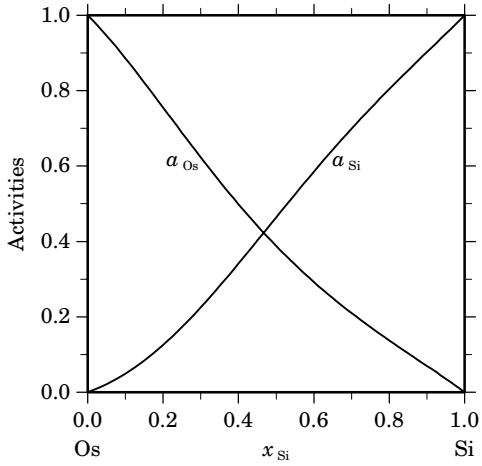

Fig. 3. Activities in the liquid phase at T=3400 K.

Table IV. Standard reaction quantities at 298.15 K for the compounds per mole of atoms.

Compound	x_{Si}	$\Delta_f G^\circ$ / (J/mol)	$\Delta_f H^\circ$ / (J/mol)	$\Delta_f S^\circ$ / (J/(mol·K))	$\Delta_f C_P^\circ$ / (J/(mol·K))
Os_1Si_1	0.500	−25045	−25415	−1.242	0.000
Os_2Si_3	0.600	−29912	−30450	−1.805	0.000
Os_1Si_2	0.667	−28148	−28745	−2.001	0.000

References

[1962Fin] L.N. Finnie: J. Less-Common Met. **4** (1962) 24–34.
[1983Mas] K. Mason, G. Müller-Vogt: J. Cryst. Growth **63** (1983) 34–38.
[1988Sch] L. Schellenberg, H.F. Braun, J. Muller: J. Less-Common Met. **144** (1988) 341–350.
[1998Mes] S.V. Meschel, O.J. Kleppa: J. Alloys Comp. **280** (1998) 231–239.
[2001Liu] Y.Q. Liu, G. Shao, K.P. Homewood: J. Alloys Comp. **320** (2001) 72–79.

Pd – Rh (Palladium – Rhodium)

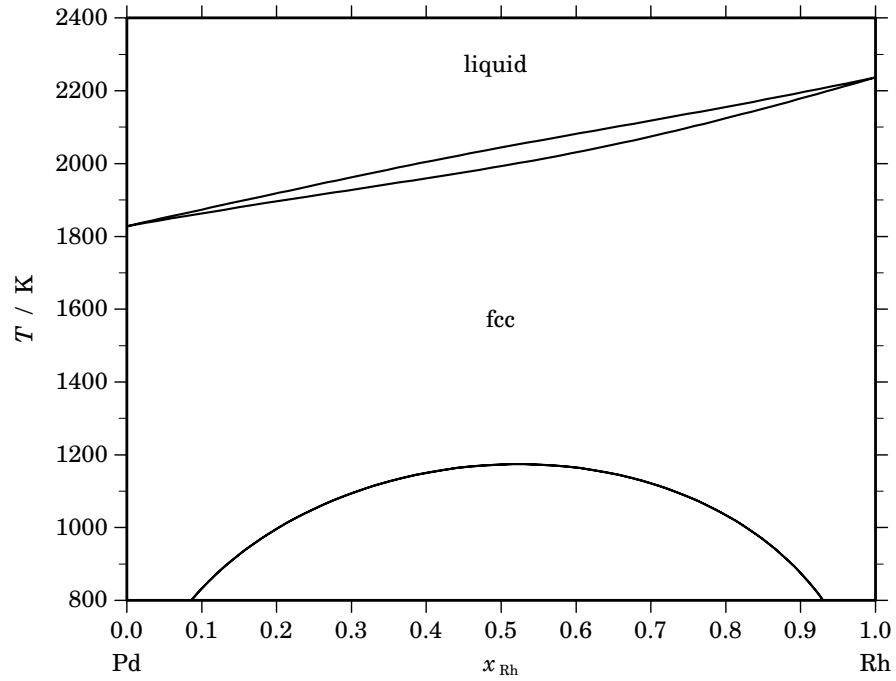

Fig. 1. Calculated phase diagram for the system Pd-Rh.

The system Pd-Rh is characterised by two solution phases, liquid and fcc with continuous miscibility at higher temperatures and a broad miscibility gap opening in the fcc phase at lower temperatures [1959Rau2, 1987Shi]. The melting range is experimentally ill defined [1994Oka]. The thermodynamic assessment of the Pd-Rh system was carried out by Korb [2004Kor]. The calculated miscibility gap agrees well with [1959Rau2] and [1959Rau1] in the Pd-rich region and with [1987Shi] near the critical point. The calculated liquidus and solidus must be seen as a result of the thermodynamic calculations, see [1994Oka].

Table I. Phases, structures and models.

Phase	Struktur-bericht	Prototype	Pearson symbol	Space group	SGTE name	Model
liquid					LIQUID	$(Pd,Rh)_1$
fcc	$A1$	Cu	$cF4$	$Fm\overline{3}m$	FCC_A1	$(Pd,Rh)_1$

Table II. Invariant reactions.

Reaction	Type	T / K	Compositions / x_{Rh}			$\Delta_{\mathrm{r}}H$ / (J/mol)
fcc $\rightleftharpoons$ fcc′ + fcc″	critical	1173.6	0.523	0.523	0.523	0

Table IIIa. Integral quantities for the liquid phase at 2250 K.

x_{Rh}	ΔG_{m} [J/mol]	ΔH_{m} [J/mol]	ΔS_{m} [J/(mol·K)]	$G_{\mathrm{m}}^{\mathrm{E}}$ [J/mol]	$S_{\mathrm{m}}^{\mathrm{E}}$ [J/(mol·K)]	ΔC_P [J/(mol·K)]
0.000	0	0	0.000	0	0.000	0.000
0.100	−4468	1613	2.703	1613	0.000	0.000
0.200	−6493	2868	4.161	2868	0.000	0.000
0.300	−7663	3765	5.079	3765	0.000	0.000
0.400	−8288	4303	5.596	4303	0.000	0.000
0.500	−8485	4482	5.763	4482	0.000	0.000
0.600	−8288	4303	5.596	4303	0.000	0.000
0.700	−7663	3765	5.079	3765	0.000	0.000
0.800	−6493	2868	4.161	2868	0.000	0.000
0.900	−4468	1613	2.703	1613	0.000	0.000
1.000	0	0	0.000	0	0.000	0.000

Reference states: Pd(liquid), Rh(liquid)

Table IIIb. Partial quantities for Pd in the liquid phase at 2250 K.

x_{Pd}	ΔG_{Pd} [J/mol]	ΔH_{Pd} [J/mol]	ΔS_{Pd} [J/(mol·K)]	$G_{\mathrm{Pd}}^{\mathrm{E}}$ [J/mol]	$S_{\mathrm{Pd}}^{\mathrm{E}}$ [J/(mol·K)]	a_{Pd}	γ_{Pd}
1.000	0	0	0.000	0	0.000	1.000	1.000
0.900	−1792	179	0.876	179	0.000	0.909	1.010
0.800	−3457	717	1.855	717	0.000	0.831	1.039
0.700	−5059	1613	2.966	1613	0.000	0.763	1.090
0.600	−6688	2868	4.247	2868	0.000	0.699	1.166
0.500	−8485	4482	5.763	4482	0.000	0.635	1.271
0.400	−10688	6454	7.619	6454	0.000	0.565	1.412
0.300	−13739	8784	10.010	8784	0.000	0.480	1.599
0.200	−18635	11474	13.382	11474	0.000	0.369	1.847
0.100	−28555	14521	19.145	14521	0.000	0.217	2.173
0.000	$-\infty$	17928	∞	17928	0.000	0.000	2.607

Reference state: Pd(liquid)

Table IIIc. Partial quantities for Rh in the liquid phase at 2250 K.

x_{Rh}	ΔG_{Rh} [J/mol]	ΔH_{Rh} [J/mol]	ΔS_{Rh} [J/(mol·K)]	$G_{\mathrm{Rh}}^{\mathrm{E}}$ [J/mol]	$S_{\mathrm{Rh}}^{\mathrm{E}}$ [J/(mol·K)]	a_{Rh}	γ_{Rh}
0.000	$-\infty$	17928	∞	17928	0.000	0.000	2.607
0.100	−28555	14521	19.145	14521	0.000	0.217	2.173
0.200	−18635	11474	13.382	11474	0.000	0.369	1.847
0.300	−13739	8784	10.010	8784	0.000	0.480	1.599
0.400	−10688	6454	7.619	6454	0.000	0.565	1.412
0.500	−8485	4482	5.763	4482	0.000	0.635	1.271
0.600	−6688	2868	4.247	2868	0.000	0.699	1.166
0.700	−5059	1613	2.966	1613	0.000	0.763	1.090
0.800	−3457	717	1.855	717	0.000	0.831	1.039
0.900	−1792	179	0.876	179	0.000	0.909	1.010
1.000	0	0	0.000	0	0.000	1.000	1.000

Reference state: Rh(liquid)

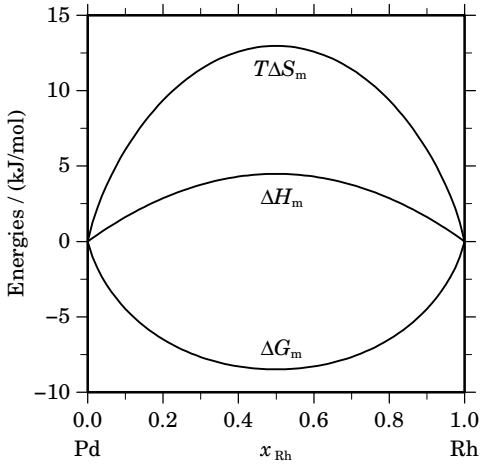

Fig. 2. Integral quantities of the liquid phase at T=2250 K.

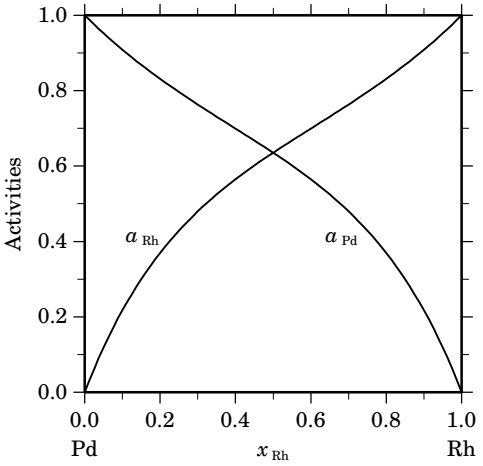

Fig. 3. Activities in the liquid phase at T=2250 K.

Table IVa. Integral quantities for the stable phases at 1575 K.

Phase	x_{Rh}	ΔG_{m} [J/mol]	ΔH_{m} [J/mol]	ΔS_{m} [J/(mol·K)]	$G^{\mathrm{E}}_{\mathrm{m}}$ [J/mol]	$S^{\mathrm{E}}_{\mathrm{m}}$ [J/(mol·K)]	ΔC_P [J/(mol·K)]
fcc	0.000	0	0	0.000	0	0.000	0.000
	0.100	−2547	1710	2.703	1710	0.000	0.000
	0.200	−3494	3059	4.161	3059	0.000	0.000
	0.300	−3959	4041	5.079	4041	0.000	0.000
	0.400	−4166	4647	5.596	4647	0.000	0.000
	0.500	−4206	4871	5.763	4871	0.000	0.000
	0.600	−4108	4705	5.596	4705	0.000	0.000
	0.700	−3857	4142	5.079	4142	0.000	0.000
	0.800	−3377	3176	4.161	3176	0.000	0.000
	0.900	−2460	1797	2.703	1797	0.000	0.000
	1.000	0	0	0.000	0	0.000	0.000

Reference states: Pd(fcc), Rh(fcc)

Table IVb. Partial quantities for Pd in the stable phases at 1575 K.

Phase	x_{Pd}	ΔG_{Pd} [J/mol]	ΔH_{Pd} [J/mol]	ΔS_{Pd} [J/(mol·K)]	$G^{\mathrm{E}}_{\mathrm{Pd}}$ [J/mol]	$S^{\mathrm{E}}_{\mathrm{Pd}}$ [J/(mol·K)]	a_{Pd}	γ_{Pd}
fcc	1.000	0	0	0.000	0	0.000	1.000	1.000
	0.900	−1201	179	0.876	179	0.000	0.912	1.014
	0.800	−2196	726	1.855	726	0.000	0.846	1.057
	0.700	−3015	1656	2.966	1656	0.000	0.794	1.135
	0.600	−3707	2982	4.247	2982	0.000	0.753	1.256
	0.500	−4357	4720	5.763	4720	0.000	0.717	1.434
	0.400	−5115	6884	7.619	6884	0.000	0.677	1.692
	0.300	−6278	9488	10.010	9488	0.000	0.619	2.064
	0.200	−8529	12547	13.382	12547	0.000	0.521	2.607
	0.100	−14077	16076	19.145	16076	0.000	0.341	3.413
	0.000	$-\infty$	20089	∞	20089	0.000	0.000	4.637

Reference state: Pd(fcc)

Table IVc. Partial quantities for Rh in the stable phases at 1575 K.

Phase	x_{Rh}	ΔG_{Rh} [J/mol]	ΔH_{Rh} [J/mol]	ΔS_{Rh} [J/(mol·K)]	$G^{\mathrm{E}}_{\mathrm{Rh}}$ [J/mol]	$S^{\mathrm{E}}_{\mathrm{Rh}}$ [J/(mol·K)]	a_{Rh}	γ_{Rh}
fcc	0.000	$-\infty$	18879	∞	18879	0.000	0.000	4.228
	0.100	−14665	15488	19.145	15488	0.000	0.326	3.263
	0.200	−8684	12393	13.382	12393	0.000	0.515	2.576
	0.300	−6160	9607	10.010	9607	0.000	0.625	2.083
	0.400	−4854	7145	7.619	7145	0.000	0.690	1.726
	0.500	−4055	5022	5.763	5022	0.000	0.734	1.467
	0.600	−3436	3253	4.247	3253	0.000	0.769	1.282
	0.700	−2819	1852	2.966	1852	0.000	0.806	1.152
	0.800	−2090	833	1.855	833	0.000	0.853	1.066
	0.900	−1169	211	0.876	211	0.000	0.915	1.016
	1.000	0	0	0.000	0	0.000	1.000	1.000

Reference state: Rh(fcc)

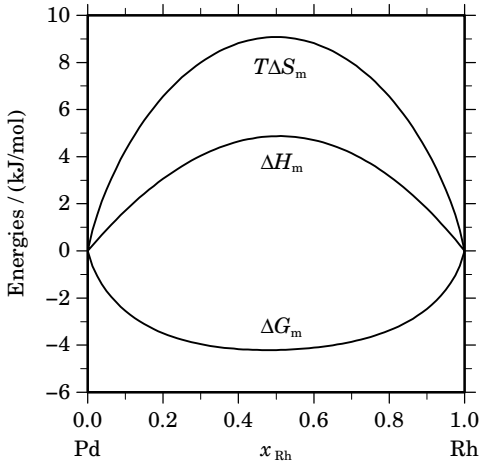

Fig. 4. Integral quantities of the stable phases at T=1575 K.

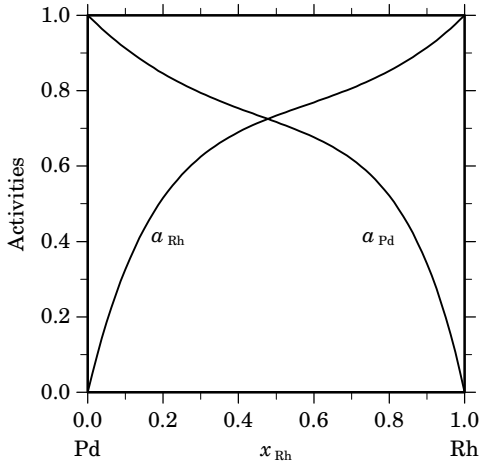

Fig. 5. Activities in the stable phases at T=1575 K.

References

[1931Tam] G. Tammann, H.J. Rocha in: "Festschrift zum 50-jährigen Bestehen der Platinschmelze G. Siebert GmbH", Hanau, (1931) pp. 317–320.
[1959Rau1] E. Raub: J. Less-Common Met. **1** (1959) 3–18.
[1959Rau2] E. Raub, H. Beeskow, D. Menzel: Z. Metallkd. **50** (1959) 428–431.
[1987Shi] J.E. Shield, R.K. Williams: Scr. Metall. **21** (1987) 1475–1479.
[1994Oka] H. Okamoto: J. Phase Equilibria **15** (1994) 208–212 and 369.
[2004Kor] J. Korb, unpublished assessment, GTT-Technologies, 2004.

Pd – Sm (Palladium – Samarium)

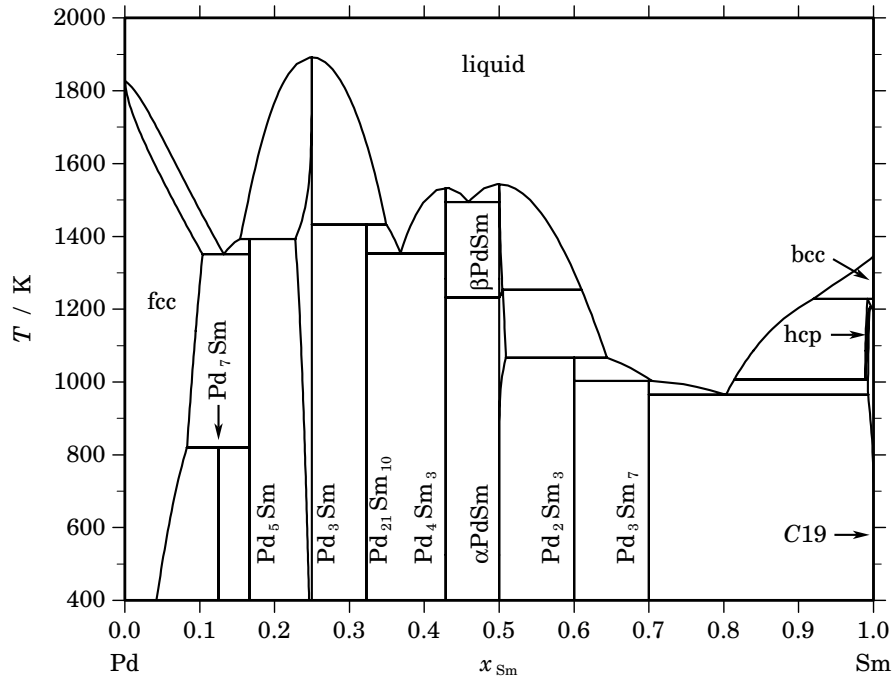

Fig. 1. Calculated phase diagram for the system Pd-Sm.

Intermetallic compounds of palladium with rare earth metals are of interest due to their potential use in hydrogen diffusion membranes for purification and isotope enrichment. A review on the Pd-Sm system and a thermodynamic assessment has been given by [2000Du]. The optimisation is based on the phase diagram data which have been reported in [1973Loe] across the whole composition range with additional investigations in Pd-rich alloys by [1989Sak]. Enthalpies of formation have been reported for PdSm [1975Pal, 1998Guo] and for Pd_3Sm and Pd_4Sm_3 [1998Guo]. Data for the other intermetallic compounds have been estimated. For the liquid no thermodynamic data have been available. From the dataset [2000Du] a rather unusual transformation behaviour is calculated for the Sm-phases having dissolved small amounts of Pd, as shown in the enlarged part of the phase diagram, Fig. 2. However, it should be noted that the only investigation in this region of the system [1973Loe] does not provide any quantitative data for the solubility of Pd in either of the phases of Sm. It has only been stated that the solubility of Pd in Sm is certainly below 1 at.% and that dissolution of Pd in Sm results in a peritectic reaction at 1228 K.

References

[1973Loe] O. Loebich, Jr., E. Raub: J. Less-Common Met. **30** (1973) 47–62.
[1975Pal] A. Palenzona, S. Cirafici: Thermochim. Acta **12** (1975) 267–275.
[1989Sak] Y. Sakamoto, K. Takao, S. Takeda, T. Takeda: J. Less-Common Met. **152** (1989) 127–138.
[1998Guo] Q. Guo, O.J. Kleppa: Metall. Mater. Trans. B **29B** (1998) 815–820.
[2000Du] Z. Du, H. Yang: Z. Metallkd. **91** (2000) 455–459.

Table I. Phases, structures and models.

Phase	Struktur-bericht	Prototype	Pearson symbol	Space group	SGTE name	Model
liquid					LIQUID	$(Pd,Sm)_1$
fcc	$A1$	Cu	$cF4$	$Fm\overline{3}m$	FCC_A1	$(Pd,Sm)_1$
Pd_7Sm	⋯	⋯	$c*^*$	⋯	PD7SM	Pd_7Sm_1
Pd_5Sm	⋯	⋯	$o*72$	⋯	PD5SM	Pd_5Sm_1
Pd_3Sm	$L1_2$	$AuCu_3$	$cP4$	$Pm\overline{3}m$	MPD3	$Pd_3(Pd,Sm)_1$
$Pd_{21}Sm_{10}$	⋯	⋯	$mC124$	$C2/m$	PD21SM10	$Pd_{21}Sm_{10}$
Pd_4Sm_3	⋯	⋯	$hR14$	$R\overline{3}$	PD4SM3	Pd_4Sm_3
βPdSm	⋯	⋯	⋯	⋯	MSM_B	$(Pd,Sm)_1Sm_1$
αPdSm	$B33$	CrB	$oC8$	$Cmcm$	MSM_A	$(Pd,Sm)_1Sm_1$
Pd_2Sm_3	⋯	⋯	⋯	⋯	PD2SM3	Pd_2Sm_3
Pd_3Sm_7	$D10_2$	Fe_3Th_7	$hP20$	$P6_3mc$	PD3SM7	Pd_3Sm_7
bcc	$A2$	W	$cI2$	$Im\overline{3}m$	BCC_A2	$(Pd,Sm)_1$
hcp	$A3$	Mg	$hP2$	$P6_3/mmc$	HCP_A3	$(Pd,Sm)_1$
$C19$	$C19$	αSm	$hR3$	$R\overline{3}m$	RHOMB_C19	$(Pd,Sm)_1$

Table II. Invariant reactions.

Reaction	Type	T / K	Compositions / x_{Sm}			$\Delta_r H$ / (J/mol)
liquid $\rightleftharpoons$ Pd_3Sm	congruent	1892.6	0.250	0.250		−17371
liquid $\rightleftharpoons$ βPdSm	congruent	1543.4	0.500	0.500		−16078
liquid $\rightleftharpoons$ Pd_4Sm_3	congruent	1533.7	0.429	0.429		−11538
liquid $\rightleftharpoons$ Pd_4Sm_3 + βPdSm	eutectic	1494.4	0.459	0.429	0.500	−12868
Pd_3Sm + liquid $\rightleftharpoons$ $Pd_{21}Sm_{10}$	peritectic	1432.8	0.250	0.349	0.323	−6860
liquid + Pd_3Sm $\rightleftharpoons$ Pd_5Sm	peritectic	1392.8	0.154	0.228	0.167	−16571
liquid $\rightleftharpoons$ $Pd_{21}Sm_{10}$ + Pd_4Sm_3	eutectic	1353.5	0.368	0.323	0.429	−8983
liquid $\rightleftharpoons$ fcc + Pd_5Sm	eutectic	1350.8	0.132	0.104	0.167	−14236
βPdSm + liquid $\rightleftharpoons$ αPdSm	peritectic	1253.6	0.504	0.610	0.505	−373
βPdSm $\rightleftharpoons$ Pd_4Sm_3 + αPdSm	eutectoid	1231.8	0.500	0.429	0.500	−500
liquid + bcc $\rightleftharpoons$ hcp	peritectic	1228.0	0.920	0.999	0.992	−3329
hcp $\rightleftharpoons$ $C19$	congruent	1206.9	0.996	0.996		−83
αPdSm + liquid $\rightleftharpoons$ Pd_2Sm_3	peritectic	1067.0	0.509	0.644	0.600	−24025
hcp $\rightleftharpoons$ liquid + $C19$	metatectic	1007.0	0.989	0.814	0.993	−85
Pd_2Sm_3 + liquid $\rightleftharpoons$ Pd_3Sm_7	peritectic	1002.9	0.600	0.704	0.700	−33524
liquid $\rightleftharpoons$ Pd_3Sm_7 + $C19$	eutectic	965.0	0.803	0.700	0.993	−24810
fcc + Pd_5Sm $\rightleftharpoons$ Pd_7Sm	peritectoid	820.1	0.083	0.167	0.125	−4864

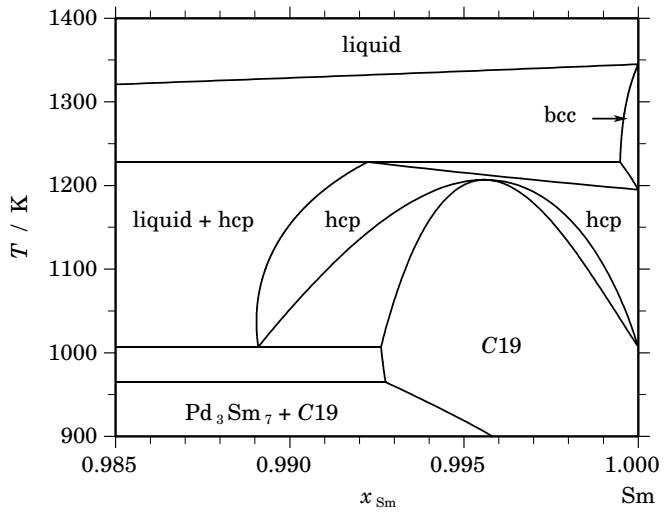

Fig. 2. Partial phase diagram for the system Pd-Sm.

Table IIIa. Integral quantities for the liquid phase at 1900 K.

x_{Sm}	ΔG_{m} [J/mol]	ΔH_{m} [J/mol]	ΔS_{m} [J/(mol·K)]	$G_{\mathrm{m}}^{\mathrm{E}}$ [J/mol]	$S_{\mathrm{m}}^{\mathrm{E}}$ [J/(mol·K)]	ΔC_P [J/(mol·K)]
0.000	0	0	0.000	0	0.000	0.000
0.100	−33174	−40773	−3.999	−28038	−6.702	0.000
0.200	−54865	−67889	−6.855	−46960	−11.016	0.000
0.300	−67497	−83073	−8.198	−57847	−13.277	0.000
0.400	−72413	−88047	−8.228	−61782	−13.824	0.000
0.500	−70796	−84535	−7.231	−59846	−12.994	0.000
0.600	−63755	−74260	−5.529	−53123	−11.125	0.000
0.700	−52345	−58946	−3.474	−42695	−8.553	0.000
0.800	−37548	−40315	−1.456	−29643	−5.617	0.000
0.900	−20186	−20092	0.050	−15051	−2.653	0.000
1.000	0	0	0.000	0	0.000	0.000

Reference states: Pd(liquid), Sm(liquid)

Table IIIb. Partial quantities for Pd in the liquid phase at 1900 K.

x_{Pd}	ΔG_{Pd} [J/mol]	ΔH_{Pd} [J/mol]	ΔS_{Pd} [J/(mol·K)]	$G_{\mathrm{Pd}}^{\mathrm{E}}$ [J/mol]	$S_{\mathrm{Pd}}^{\mathrm{E}}$ [J/(mol·K)]	a_{Pd}	γ_{Pd}
1.000	0	0	0.000	0	0.000	1.000	1.000
0.900	−6403	−7115	−0.375	−4739	−1.251	0.667	0.741
0.800	−21037	−26164	−2.698	−17512	−4.553	0.264	0.330
0.700	−41790	−53698	−6.267	−36156	−9.233	0.071	0.101
0.600	−66574	−86272	−10.367	−58504	−14.615	0.015	0.025
0.500	−93344	−120439	−14.260	−82394	−20.024	0.003	0.005
0.400	−120135	−152751	−17.166	−105660	−24.785	0.000	0.001
0.300	−145157	−179762	−18.213	−126137	−28.224	0.000	0.000
0.200	−167087	−198026	−16.284	−141662	−29.666	0.000	0.000
0.100	−186444	−204096	−9.290	−150069	−28.435	0.000	0.000
0.000	$-\infty$	−194524	∞	−149194	−23.858	0.000	0.000

Reference state: Pd(liquid)

Table IIIc. Partial quantities for Sm in the liquid phase at 1900 K.

x_{Sm}	ΔG_{Sm} [J/mol]	ΔH_{Sm} [J/mol]	ΔS_{Sm} [J/(mol·K)]	$G^{\mathrm{E}}_{\mathrm{Sm}}$ [J/mol]	$S^{\mathrm{E}}_{\mathrm{Sm}}$ [J/(mol·K)]	a_{Sm}	γ_{Sm}
0.000	$-\infty$	−481754	∞	−329575	−80.094	0.000	0.000
0.100	−274109	−343689	−36.621	−237734	−55.766	0.000	0.000
0.200	−190176	−234792	−23.482	−164751	−36.864	0.000	0.000
0.300	−127480	−151614	−12.702	−108460	−22.713	0.000	0.001
0.400	−81172	−90709	−5.019	−66697	−12.638	0.006	0.015
0.500	−48249	−48631	−0.201	−37298	−5.964	0.047	0.094
0.600	−26169	−21933	2.230	−18099	−2.018	0.191	0.318
0.700	−12568	−7167	2.843	−6934	−0.123	0.451	0.645
0.800	−5164	−887	2.251	−1639	0.395	0.721	0.901
0.900	−1713	353	1.087	−49	0.211	0.897	0.997
1.000	0	0	0.000	0	0.000	1.000	1.000

Reference state: Sm(liquid)

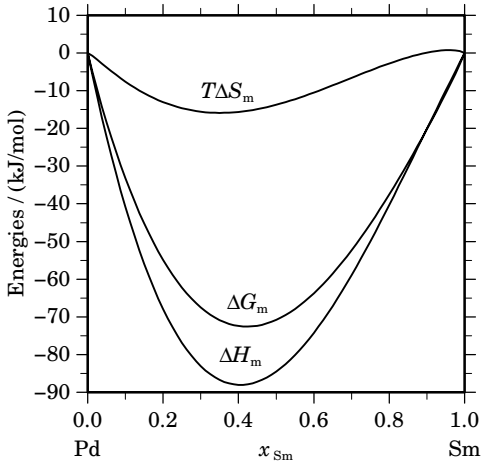

Fig. 3. Integral quantities of the liquid phase at T=1900 K.

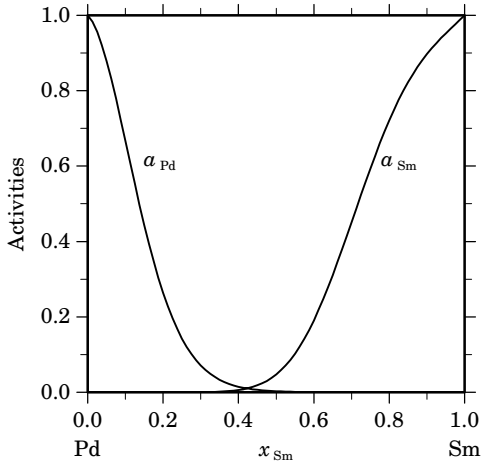

Fig. 4. Activities in the liquid phase at T=1900 K.

Table IV. Standard reaction quantities at 298.15 K for the compounds per mole of atoms.

Compound	x_{Sm}	$\Delta_{\mathrm{f}}G^{\circ}$ / (J/mol)	$\Delta_{\mathrm{f}}H^{\circ}$ / (J/mol)	$\Delta_{\mathrm{f}}S^{\circ}$ / (J/(mol·K))	$\Delta_{\mathrm{f}}C^{\circ}_{P}$ / (J/(mol·K))
Pd_7Sm_1	0.125	−50065	−54184	−13.816	0.000
Pd_5Sm_1	0.167	−61735	−65216	−11.673	0.000
Pd_3Sm	0.250	−76326	−78630	−7.730	0.000
$Pd_{21}Sm_{10}$	0.323	−79495	−81600	−7.059	0.000
Pd_4Sm_3	0.429	−83754	−85887	−7.153	0.000
αPdSm	0.500	−85011	−87873	−9.596	0.000
βPdSm	0.500	−84633	−87373	−9.191	0.000
Pd_2Sm_3	0.600	−83287	−90298	−23.516	0.000
Pd_3Sm_7	0.700	−73285	−82372	−30.477	0.000

Pd – Tb (Palladium – Terbium)

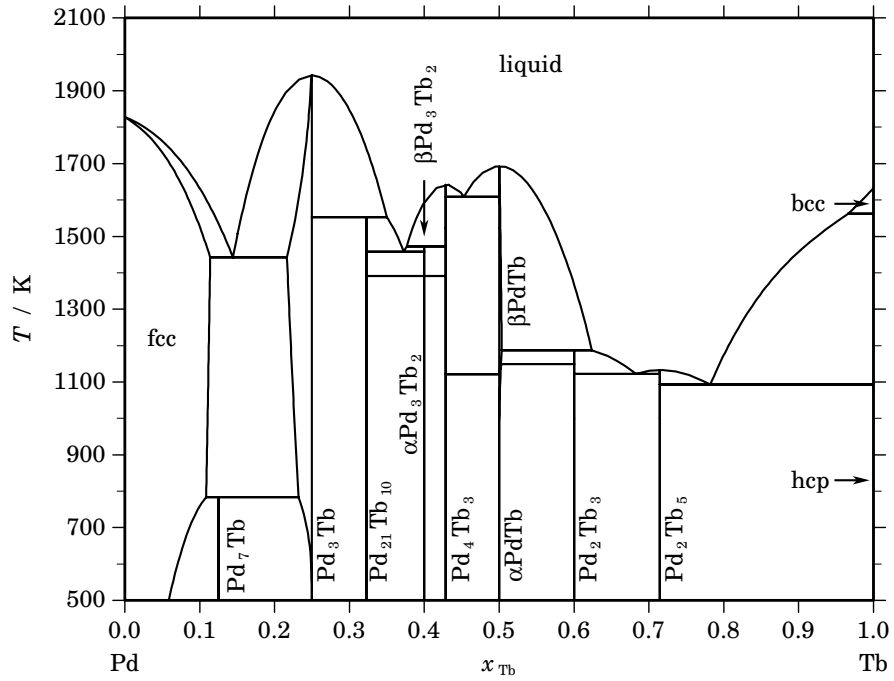

Fig. 1. Calculated phase diagram for the system Pd-Tb.

Intermetallic compounds of palladium with rare earth metals are of interest due to their potential use in hydrogen diffusion membranes for purification and isotope enrichment. Only few and insufficient experimental data are known of the Pd-Tb system. After comparing the phase diagrams of palladium with some of the heavier rare earth metals (Gd, Dy, Ho,Er) a phase diagram of Pd-Tb has been proposed by [1990Bor]. The melting temperatures of the intermetallic Pd-Tb compounds have been interpolated from series of known values for Pd-compounds with adjacent rare earth elements. The melting point of PdTb which has been measured by [1975Pal] is in agreement with the interpolation. The region of the phase diagram around the compound Pd_7Tb has been experimentally investigated by [1993Tak]. Enthalpies of formation have been determined for PdTb [1974Pal, 1995Guo] and Pd_2Tb_5 [1974Pal]. Based on these investigations a thermodynamic assessment has been prepared by [2000Du]. However, in view of the scarce available data it is much desired to verify the phase diagram and further thermodynamic properties by selected key experiments.

Table I. Phases, structures and models.

Phase	Struktur-bericht	Prototype	Pearson symbol	Space group	SGTE name	Model
liquid					LIQUID	$(Pd,Tb)_1$
fcc	$A1$	Cu	$cF4$	$Fm\overline{3}m$	FCC_A1	$(Pd,Tb)_1$
Pd_7Tb	⋯	⋯	⋯	⋯	PD7TB	Pd_7Tb_1
Pd_3Tb	$L1_2$	$AuCu_3$	$cP4$	$Pm\overline{3}m$	PD3TB	$Pd_3(Pd,Tb)_1$
$Pd_{21}Tb_{10}$	⋯	⋯	⋯	⋯	PD21TB10	$Pd_{21}Tb_{10}$
αPd_3Tb_2	⋯	⋯	⋯	⋯	PD3TB2_A	Pd_3Tb_2
βPd_3Tb_2	⋯	⋯	⋯	⋯	PD3TB2_B	Pd_3Tb_2
Pd_4Tb_3	⋯	⋯	$hR14$	$R\overline{3}$	PD4TB3	Pd_4Tb_3
αPdTb	$B33$	CrB	$oC8$	$Cmcm$	PDTB_A	$(Pd,Tb)_1Tb_1$
βPdTb	$B27$	FeB	$oP8$	$Pnma$	PDTB_B	$(Pd,Tb)_1Tb_1$
Pd_2Tb_3	$D5_a$	U_3Si_2	$tP10$	$P4/mbm$	PD2TB3	Pd_2Tb_5
Pd_2Tb_5	⋯	⋯	$cF144$	$Fd\overline{3}m$	PD2TB5	Pd_2Tb_5
bcc	$A2$	W	$cI2$	$Im\overline{3}m$	BCC_A2	$(Pd,Tb)_1$
hcp	$A3$	Mg	$hP2$	$P6_3/mmc$	HCP_A3	$(Pd,Tb)_1$

Table II. Invariant reactions.

Reaction	Type	T / K	Compositions / x_{Tb}			$\Delta_r H$ / (J/mol)
liquid ⇌ Pd_3Tb	congruent	1942.6	0.250	0.250		−20035
liquid ⇌ βPdTb	congruent	1693.3	0.500	0.500		−13376
liquid ⇌ Pd_4Tb_3	congruent	1642.3	0.429	0.429		−9365
liquid ⇌ Pd_4Tb_3 + βPdTb	eutectic	1609.1	0.453	0.429	0.500	−10202
liquid + bcc ⇌ hcp	peritectic	1562.0	0.966	1.000	1.000	−4381
Pd_3Tb + liquid ⇌ $Pd_{21}Tb_{10}$	peritectic	1552.5	0.250	0.350	0.323	−6964
liquid + Pd_4Tb_3 ⇌ βPd_3Tb_2	peritectic	1472.7	0.377	0.429	0.400	−4516
liquid ⇌ $Pd_{21}Tb_{10}$ + βPd_3Tb_2	eutectic	1457.5	0.372	0.323	0.400	−8381
liquid ⇌ fcc + Pd_3Tb	eutectic	1442.6	0.144	0.114	0.217	−9155
βPd_3Tb_2 ⇌ αPd_3Tb_2	polymorphic	1391.5	0.400	0.400		−156
βPdTb + liquid ⇌ Pd_2Tb_3	peritectic	1187.5	0.503	0.624	0.600	−21422
βPdTb + Pd_2Tb_3 ⇌ αPdTb	peritectoid	1148.9	0.502	0.600	0.503	−90
liquid ⇌ Pd_2Tb_5	congruent	1133.3	0.714	0.714		−17632
liquid ⇌ Pd_2Tb_3 + Pd_2Tb_5	eutectic	1122.2	0.683	0.600	0.714	−18458
Pd_4Tb_3 + βPdTb ⇌ αPdTb	peritectoid	1120.9	0.429	0.500	0.500	−153
liquid ⇌ Pd_2Tb_5 + hcp	eutectic	1093.1	0.782	0.714	1.000	−15719
fcc + Pd_3Tb ⇌ Pd_7Tb	peritectoid	783.0	0.109	0.232	0.125	−7586

Table IIIa. Integral quantities for the liquid phase at 2000 K.

x_{Tb}	ΔG_{m} [J/mol]	ΔH_{m} [J/mol]	ΔS_{m} [J/(mol·K)]	$G_{\mathrm{m}}^{\mathrm{E}}$ [J/mol]	$S_{\mathrm{m}}^{\mathrm{E}}$ [J/(mol·K)]	ΔC_P [J/(mol·K)]
0.000	0	0	0.000	0	0.000	0.000
0.100	−32168	−41630	−4.731	−26763	−7.434	0.000
0.200	−53410	−69164	−7.877	−45089	−12.037	0.000
0.300	−66070	−84418	−9.174	−55912	−14.253	0.000
0.400	−71357	−89209	−8.926	−60166	−14.522	0.000
0.500	−70310	−85355	−7.523	−58783	−13.286	0.000
0.600	−63890	−74672	−5.391	−52698	−10.987	0.000
0.700	−53002	−58979	−2.988	−42844	−8.067	0.000
0.800	−38475	−40090	−0.808	−30154	−4.968	0.000
0.900	−20967	−19825	0.571	−15561	−2.132	0.000
1.000	0	0	0.000	0	0.000	0.000

Reference states: Pd(liquid), Tb(liquid)

Table IIIb. Partial quantities for Pd in the liquid phase at 2000 K.

x_{Pd}	ΔG_{Pd} [J/mol]	ΔH_{Pd} [J/mol]	ΔS_{Pd} [J/(mol·K)]	$G_{\mathrm{Pd}}^{\mathrm{E}}$ [J/mol]	$S_{\mathrm{Pd}}^{\mathrm{E}}$ [J/(mol·K)]	a_{Pd}	γ_{Pd}
1.000	0	0	0.000	0	0.000	1.000	1.000
0.900	−6126	−7351	−0.613	−4374	−1.489	0.692	0.769
0.800	−19961	−26982	−3.510	−16251	−5.366	0.301	0.376
0.700	−39695	−55258	−7.782	−33764	−10.747	0.092	0.131
0.600	−63540	−88546	−12.503	−55046	−16.750	0.022	0.037
0.500	−89756	−123211	−16.727	−78230	−22.490	0.005	0.009
0.400	−116687	−155618	−19.466	−101450	−27.084	0.001	0.002
0.300	−142859	−182135	−19.638	−122838	−29.648	0.000	0.001
0.200	−167292	−199126	−15.917	−140528	−29.299	0.000	0.000
0.100	−190943	−202958	−6.007	−152653	−25.152	0.000	0.000
0.000	$-\infty$	−189996	∞	−157346	−16.325	0.000	0.000

Reference state: Pd(liquid)

Table IIIc. Partial quantities for Tb in the liquid phase at 2000 K.

x_{Tb}	ΔG_{Tb} [J/mol]	ΔH_{Tb} [J/mol]	ΔS_{Tb} [J/(mol·K)]	$G_{\mathrm{Tb}}^{\mathrm{E}}$ [J/mol]	$S_{\mathrm{Tb}}^{\mathrm{E}}$ [J/(mol·K)]	a_{Tb}	γ_{Tb}
0.000	$-\infty$	−492842	∞	−312920	−89.961	0.000	0.000
0.100	−266552	−350141	−41.794	−228262	−60.939	0.000	0.000
0.200	−187205	−237890	−25.343	−160442	−38.724	0.000	0.000
0.300	−127613	−152456	−12.422	−107592	−22.432	0.000	0.002
0.400	−83083	−90204	−3.560	−67846	−11.179	0.007	0.017
0.500	−50863	−47499	1.682	−39337	−4.081	0.047	0.094
0.600	−28692	−20708	3.992	−20197	−0.256	0.178	0.297
0.700	−14492	−6197	4.147	−8560	1.182	0.418	0.598
0.800	−6271	−332	2.970	−2560	1.114	0.686	0.857
0.900	−2081	523	1.302	−329	0.426	0.882	0.980
1.000	0	0	0.000	0	0.000	1.000	1.000

Reference state: Tb(liquid)

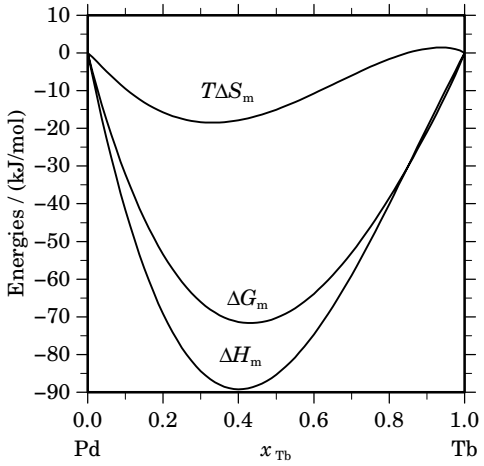

Fig. 2. Integral quantities of the liquid phase at T=2000 K.

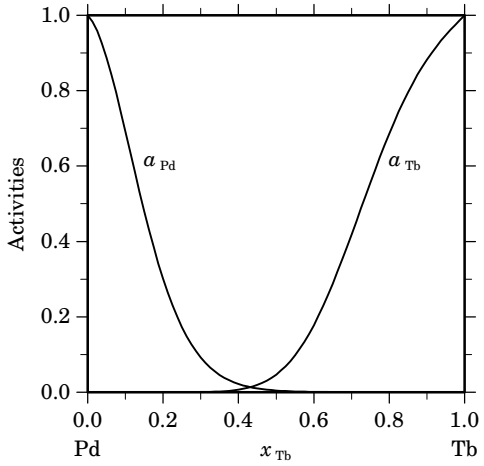

Fig. 3. Activities in the liquid phase at T=2000 K.

Table IV. Standard reaction quantities at 298.15 K for the compounds per mole of atoms.

Compound	x_{Tb}	$\Delta_{\mathrm{f}}G^{\circ}$ / (J/mol)	$\Delta_{\mathrm{f}}H^{\circ}$ / (J/mol)	$\Delta_{\mathrm{f}}S^{\circ}$ / (J/(mol·K))	$\Delta_{\mathrm{f}}C_P^{\circ}$ / (J/(mol·K))
Pd_7Tb_1	0.125	−47937	−52022	−13.703	0.000
Pd_3Tb	0.250	−79090	−82053	−9.937	0.000
$Pd_{21}Tb_{10}$	0.323	−80159	−82457	−7.710	0.000
αPd_3Tb_2	0.400	−81089	−82910	−6.105	0.000
βPd_3Tb_2	0.400	−80966	−82753	−5.993	0.000
Pd_4Tb_3	0.429	−81420	−83082	−5.575	0.000
αPdTb	0.500	−81709	−83719	−6.742	0.000
βPdTb	0.500	−81597	−83566	−6.606	0.000
Pd_2Tb_3	0.600	−79334	−84434	−17.105	0.000
Pd_2Tb_5	0.714	−57901	−61113	−10.771	0.000

References

[1974Pal] A. Palenzona, S. Cirafici: Thermochim. Acta **10** (1974) 313–317.
[1975Pal] A. Palenzona, S. Cirafici: Thermochim. Acta **12** (1975) 267–275.
[1990Bor] G. Borzone, G. Cacciamani, R. Ferro: Calphad **14** (1990) 139–149.
[1993Tak] K. Takao, Y. Sakamoto, T. Araki, H. Kohzuma: J. Alloys Comp. **193** (1993) 41–43.
[1995Guo] Q. Guo, O.J. Kleppa: J. Alloys Comp. **221** (1995) 50–55.
[2000Du] Z. Du, H. Yang, K. Han: Z. Metallkd. **91** (2000) 988–991.

Ru – Si (Ruthenium – Silicon)

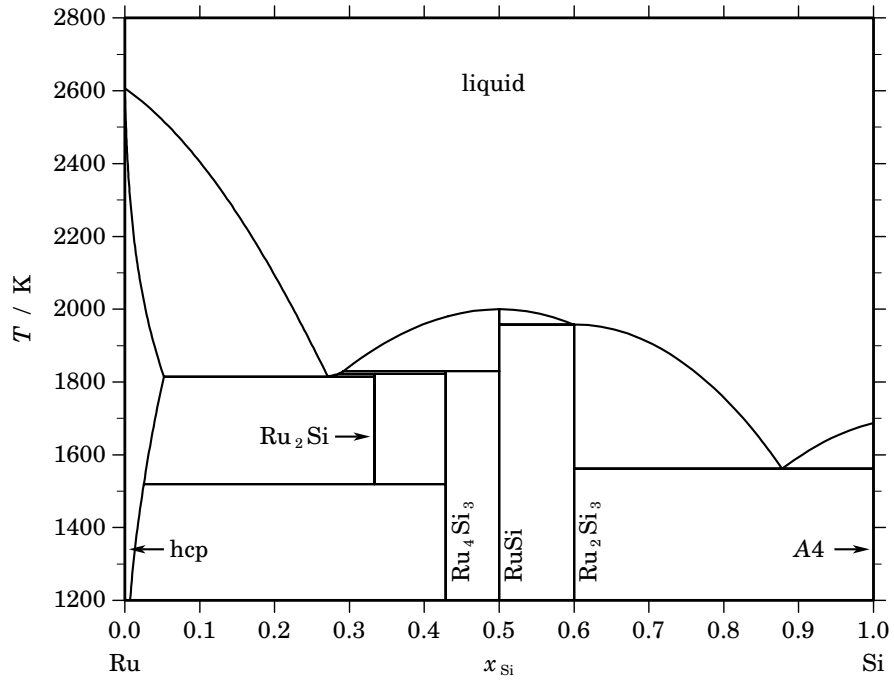

Fig. 1. Calculated phase diagram for the system Ru-Si.

Ruthenium silicides are of interest for manufacturing high-density integrated circuit devices since they have a very good lattice match with silicon and relatively low electrical resistance. Other potential applications are in light emitting diodes and thermoelectrical devices.

Assessed thermodynamic datasets for the Ru-Si system have been reported by [2001Du, 2001Liu] which are based on essentially the same experimental data from the literature. Here, the assessment of [2001Du] has been selected for presentation. The phase diagram data have been selected mainly from [1999Per] with additional information from [1965Obr]. The system contains seven stable phases: the liquid with a continuous miscibility range, the Ru-based hcp phase with limited solubility of Si, the terminal Si-phase with practically no solubility for Ru and 4 ruthenium silicides with narrow homogeneity ranges. The compound Ru_5Si_3 which has been reported in [1970Eng, 1988Wei] has not been confirmed in the redetermination of the phase diagram by [1999Per]. For the thermodynamic modelling of RuSi and Ru_2Si_3 heat capacity measurements have been available [1997Kun, 1998Per]. The specific heat of the remaining two compounds has been approximated according to the Neumann-Kopp rule. Enthalpies of formation have been determined experimentally for Ru_4Si_3 [1997Per], RuSi [1988Top, 1997Per, 1998Cic] and Ru_2Si_3 [1997Per, 1998Cic, 1998Mes]. Since the transformation temperatures of the polymorphic forms of both RuSi and Ru_2Si_3 are not known in both cases only a single compound is used in the modelling. No thermodynamic data have been reported for the liquid. More recently, a new compound, $RuSi_2$, has been observed by DTA to form peritectoidally at 1235 K [2002Iva].

Table I. Phases, structures and models.

Phase	Struktur-bericht	Prototype	Pearson symbol	Space group	SGTE name	Model
liquid					LIQUID	$(Ru,Si)_1$
hcp	$A3$	Mg	$hP2$	$P6_3/mmc$	HCP_A3	$(Ru,Si)_1$
Ru_2Si	$C23$	Co_2Si	$oP12$	$Pnma$	RU2SI	Ru_2Si_1
Ru_4Si_3	⋯	⋯	$oP28$	$Pnma$	RU4SI3	Ru_4Si_3
αRuSi	$B20$	FeSi	$cP8$	$P2_13$	RUSI	Ru_1Si_1
βRuSi	$B2$	CsCl	$cP2$	$Pm\overline{3}m$	RUSI	Ru_1Si_1
αRu_2Si_3	⋯	⋯	$oP40$	$Pbcn$	RU2SI3	Ru_2Si_3
βRu_2Si_3	⋯	⋯	$tI80$	$P\overline{4}c2$	RU2SI3	Ru_2Si_3
$A4$	$A4$	C(diamond)	$cF8$	$Fd\overline{3}m$	DIAMOND_A4	$(Ru,Si)_1$

Table II. Invariant reactions.

Reaction	Type	T / K	Compositions / x_{Si}			$\Delta_r H$ / (J/mol)
liquid ⇌ RuSi	congruent	1999.8	0.500	0.500		−72028
liquid ⇌ Ru_2Si_3	congruent	1957.9	0.600	0.600		−63893
liquid ⇌ RuSi + Ru_2Si_3	eutectic	1957.9	0.599	0.500	0.600	−63939
liquid + RuSi ⇌ Ru_4Si_3	peritectic	1830.0	0.292	0.500	0.429	−17095
liquid + Ru_4Si_3 ⇌ Ru_2Si	peritectic	1822.4	0.286	0.429	0.333	−30723
liquid ⇌ hcp + Ru_2Si	eutectic	1814.5	0.271	0.052	0.333	−45476
liquid ⇌ Ru_2Si_3 + $A4$	eutectic	1561.7	0.878	0.600	1.000	−50965
Ru_2Si ⇌ hcp + Ru_4Si_3	eutectoid	1519.7	0.333	0.025	0.429	−1559

Table IIIa. Integral quantities for the liquid phase at 2700 K.

x_{Si}	ΔG_m [J/mol]	ΔH_m [J/mol]	ΔS_m [J/(mol·K)]	G_m^E [J/mol]	S_m^E [J/(mol·K)]	ΔC_P [J/(mol·K)]
0.000	0	0	0.000	0	0.000	0.000
0.100	−17380	−8782	3.185	−10082	0.482	0.000
0.200	−29461	−15915	5.017	−18227	0.856	0.000
0.300	−38035	−21287	6.203	−24322	1.124	0.000
0.400	−43360	−24783	6.880	−28251	1.285	0.000
0.500	−45463	−26290	7.101	−29902	1.338	0.000
0.600	−44270	−25693	6.880	−29162	1.285	0.000
0.700	−39628	−22880	6.203	−25915	1.124	0.000
0.800	−31282	−17736	5.017	−20048	0.856	0.000
0.900	−18745	−10147	3.185	−11448	0.482	0.000
1.000	0	0	0.000	0	0.000	0.000

Reference states: Ru(liquid), Si(liquid)

Table IIIb. Partial quantities for Ru in the liquid phase at 2700 K.

x_{Ru}	ΔG_{Ru} [J/mol]	ΔH_{Ru} [J/mol]	ΔS_{Ru} [J/(mol·K)]	$G^{\mathrm{E}}_{\mathrm{Ru}}$ [J/mol]	$S^{\mathrm{E}}_{\mathrm{Ru}}$ [J/(mol·K)]	a_{Ru}	γ_{Ru}
1.000	0	0	0.000	0	0.000	1.000	1.000
0.900	−3315	−805	0.930	−950	0.054	0.863	0.959
0.800	−8959	−3372	2.069	−3950	0.214	0.671	0.839
0.700	−17236	−7928	3.447	−9229	0.482	0.464	0.663
0.600	−28481	−14701	5.104	−17014	0.856	0.281	0.469
0.500	−43093	−23919	7.101	−27532	1.338	0.147	0.293
0.400	−61581	−35809	9.545	−41011	1.927	0.064	0.161
0.300	−84708	−50599	12.633	−57680	2.623	0.023	0.077
0.200	−113895	−68516	16.807	−77764	3.425	0.006	0.031
0.100	−153183	−89787	23.480	−101492	4.335	0.001	0.011
0.000	−∞	−114641	∞	−129092	5.352	0.000	0.003

Reference state: Ru(liquid)

Table IIIc. Partial quantities for Si in the liquid phase at 2700 K.

x_{Si}	ΔG_{Si} [J/mol]	ΔH_{Si} [J/mol]	ΔS_{Si} [J/(mol·K)]	$G^{\mathrm{E}}_{\mathrm{Si}}$ [J/mol]	$S^{\mathrm{E}}_{\mathrm{Si}}$ [J/(mol·K)]	a_{Si}	γ_{Si}
0.000	−∞	−95677	∞	−110128	5.352	0.000	0.007
0.100	−143967	−80570	23.480	−92276	4.335	0.002	0.016
0.200	−111467	−66088	16.807	−75337	3.425	0.007	0.035
0.300	−86566	−52457	12.633	−59538	2.623	0.021	0.071
0.400	−65678	−39905	9.545	−45108	1.927	0.054	0.134
0.500	−47834	−28660	7.101	−32273	1.338	0.119	0.237
0.600	−32729	−18950	5.104	−21262	0.856	0.233	0.388
0.700	−20308	−11000	3.447	−12301	0.482	0.405	0.578
0.800	−10628	−5041	2.069	−5619	0.214	0.623	0.779
0.900	−3808	−1298	0.930	−1443	0.054	0.844	0.938
1.000	0	0	0.000	0	0.000	1.000	1.000

Reference state: Si(liquid)

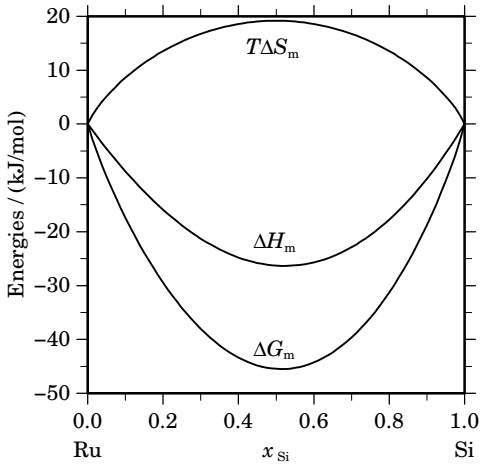

Fig. 2. Integral quantities of the liquid phase at T=2700 K.

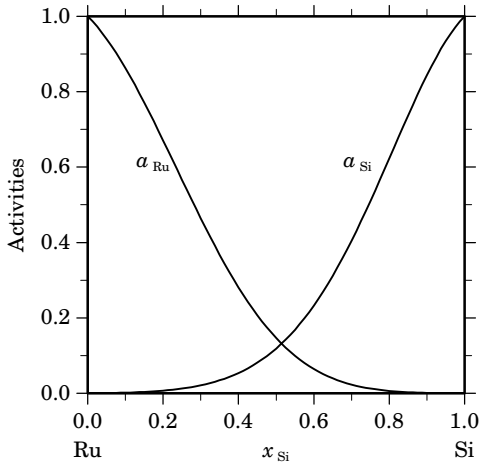

Fig. 3. Activities in the liquid phase at T=2700 K.

Table IV. Standard reaction quantities at 298.15 K for the compounds per mole of atoms.

Compound	x_{Si}	$\Delta_{\mathrm{f}}G^{\circ}$ / (J/mol)	$\Delta_{\mathrm{f}}H^{\circ}$ / (J/mol)	$\Delta_{\mathrm{f}}S^{\circ}$ / (J/(mol·K))	$\Delta_{\mathrm{f}}C_P^{\circ}$ / (J/(mol·K))
Ru_2Si_1	0.333	−34167	−35195	−3.446	0.000
Ru_4Si_3	0.429	−45949	−47788	−6.169	0.000
Ru_1Si_1	0.500	−51627	−52988	−4.562	−0.315
Ru_2Si_3	0.600	−47019	−47723	−2.360	−0.149

References

[1965Obr] W. Obrowski: Metallwiss. Tech. (Berlin) **19** (1965) 741–742.

[1970Eng] I. Engstrom: Acta Chem. Scand. **24** (1970) 1466–1468.

[1988Top] L. Topor, O.J. Kleppa: Z. Metallkd. **79** (1988) 623–628.

[1988Wei] F. Weitzer, P. Rogl, J.C. Schuster: Z. Metallkd. **79** (1988) 154–156.

[1997Kun] J.J. Kuntz, L. Perring, P. Feschotte, J.C. Gachon: J. Solid State Chem. **133** (1997) 439–444.

[1997Per] L. Perring, P. Feschotte, J.C. Gachon: Thermochim. Acta **293** (1997) 101–108.

[1998Cic] A. Ciccioli, G. Balducci, G. Gigli, L. Perring, J.J. Kuntz, J.C. Gachon: Ber. Bunsenges. Phys. Chem. **102** (1998) 1275–1278.

[1998Per] L. Perring, F. Bussy, J.J. Kuntz, J.C. Gachon: Ber. Bunsenges. Phys. Chem. **102** (1998) 1211–1216.

[1998Mes] S.V. Meschel, O.J. Kleppa: J. Alloys Comp. **274** (1998) 193–200.

[1999Per] L. Perring, F. Bussy, J.C. Gachon, P. Feschotte: J. Alloys Comp. **284** (1999) 198–205.

[2001Du] Y. Du, K.H. Chen, J.C. Schuster, L. Perring, B.Y. Huang, Z.H. Yua, J.C. Gachon: Z. Metallkd. **92** (2001) 323–327.

[2001Liu] Y.Q. Liu, G. Shao, K.P. Homewood: J. Alloys Comp. **320** (2001) 72–79.

[2002Iva] L. Ivanenko, G. Behr, C.R. Spinella, V.E. Borisenko: J. Cryst. Growth **236** (2002) 572–576.

Ru – Zr (Ruthenium – Zirconium)

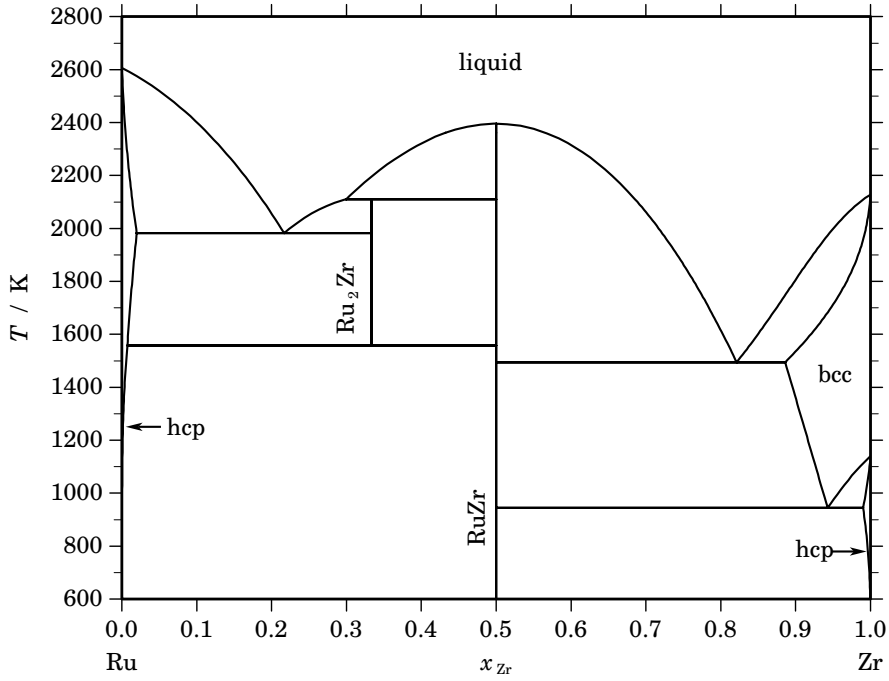

Fig. 1. Calculated phase diagram for the system Ru-Zr.

The Ru-Zr binary system contains two components interesting for the nuclear field, ruthenium being selected as representative of a family of non-volatile fission products, and zirconium being a major component of the zircalloy cladding. Experimental information on the phase diagram has been reported in the compilations of Hansen and Anderko [1958Han], Elliott [1965Ell] and Shunk [1969Shu], and more recently by Okamoto [1993Oka]. The phase diagram is based on the investigations of Raub and Röschel [1963Rau], and Eremenko *et al.* [1980Ere, 1988Ere]. There is complete solubility in the liquid, and a limited one in the solid state: 2 at.% Zr in hcp-Ru at 1983 K, 1 at.% Ru in hcp-Zr at 940 K, 11.4 at.% Ru in bcc-Zr at 1494 K. Two intermetallic compounds were identified, Ru_2Zr and RuZr, with a limited non-stoichiometry range. The enthalpy of formation of RuZr has been measured calorimetrically [1988Top]. The system was assessed by Chevalier and Fischer [1995Che]. The excess Gibbs energy of the liquid, hcp and bcc solution phases was optimised from the selected experimental information. A sub-regular substitution model was used for the first two phases, and a regular one for the third one. The heat capacity of the compounds which have been considered to be stoichiometric, Ru_2Zr and RuZr, was estimated from the pure components by the Neumann-Kopp rule. The enthalpy of formation and entropy at room temperature were estimated in consistency with the available experimental information. The agreement with the experimental information [1963Rau, 1988Ere, 1988Kle] is quite satisfactory.

Table I. Phases, structures and models.

Phase	Struktur-bericht	Prototype	Pearson symbol	Space group	SGTE name	Model
liquid					LIQUID	$(Ru,Zr)_1$
hcp	$A3$	Mg	$hP2$	$P6_3/mmc$	HCP_A3	$(Ru,Zr)_1$
Ru_2Zr	$C14$	$MgZn_2$	$hP12$	$P6_3/mmc$	RU2ZR	Ru_2Zr_1
RuZr	$B2$	CsCl	$cP2$	$Pm\bar{3}m$	RUZR	Ru_1Zr_1
bcc	$A2$	W	$cI2$	$Im\bar{3}m$	BCC_A2	$(Ru,Zr)_1$

Table II. Invariant reactions.

Reaction	Type	T / K	Compositions / x_{Zr}			$\Delta_{\mathrm{r}}H$ / (J/mol)
liquid ⇌ RuZr	congruent	2395.8	0.500	0.500		−58741
liquid + RuZr ⇌ Ru_2Zr	peritectic	2109.9	0.299	0.500	0.333	−25761
liquid ⇌ hcp + Ru_2Zr	eutectic	1982.6	0.217	0.020	0.333	−30867
Ru_2Zr ⇌ hcp + RuZr	eutectoid	1558.5	0.333	0.007	0.500	−8594
liquid ⇌ RuZr + bcc	eutectic	1494.4	0.821	0.500	0.886	−16778
bcc ⇌ RuZr + hcp	eutectoid	944.2	0.943	0.500	0.990	−5799

Table IIIa. Integral quantities for the liquid phase at 2700 K.

x_{Zr}	ΔG_{m} [J/mol]	ΔH_{m} [J/mol]	ΔS_{m} [J/(mol·K)]	$G_{\mathrm{m}}^{\mathrm{E}}$ [J/mol]	$S_{\mathrm{m}}^{\mathrm{E}}$ [J/(mol·K)]	ΔC_P [J/(mol·K)]
0.000	0	0	0.000	0	0.000	0.000
0.100	−19446	−12148	2.703	−12148	0.000	0.000
0.200	−33445	−22211	4.161	−22211	0.000	0.000
0.300	−43674	−29960	5.079	−29960	0.000	0.000
0.400	−50272	−35164	5.596	−35164	0.000	0.000
0.500	−53151	−37591	5.763	−37591	0.000	0.000
0.600	−52119	−37010	5.596	−37010	0.000	0.000
0.700	−46905	−33192	5.079	−33192	0.000	0.000
0.800	−37138	−25904	4.161	−25904	0.000	0.000
0.900	−22215	−14918	2.703	−14918	0.000	0.000
1.000	0	0	0.000	0	0.000	0.000

Reference states: Ru(liquid), Zr(liquid)

Table IIIb. Partial quantities for Ru in the liquid phase at 2700 K.

x_{Ru}	ΔG_{Ru} [J/mol]	ΔH_{Ru} [J/mol]	ΔS_{Ru} [J/(mol·K)]	$G_{\mathrm{Ru}}^{\mathrm{E}}$ [J/mol]	$S_{\mathrm{Ru}}^{\mathrm{E}}$ [J/(mol·K)]	a_{Ru}	γ_{Ru}
1.000	0	0	0.000	0	0.000	1.000	1.000
0.900	−3369	−1004	0.876	−1004	0.000	0.861	0.956
0.800	−9331	−4322	1.855	−4322	0.000	0.660	0.825
0.700	−18424	−10417	2.966	−10417	0.000	0.440	0.629
0.600	−31217	−19749	4.247	−19749	0.000	0.249	0.415
0.500	−48343	−32782	5.763	−32782	0.000	0.116	0.232
0.400	−70546	−49976	7.619	−49976	0.000	0.043	0.108
0.300	−98821	−71792	10.010	−71792	0.000	0.012	0.041
0.200	−134824	−98694	13.382	−98694	0.000	0.002	0.012
0.100	−182832	−131141	19.145	−131141	0.000	0.000	0.003
0.000	$-\infty$	−169596	∞	−169596	0.000	0.000	0.001

Reference state: Ru(liquid)

Table IIIc. Partial quantities for Zr in the liquid phase at 2700 K.

x_{Zr}	ΔG_{Zr} [J/mol]	ΔH_{Zr} [J/mol]	ΔS_{Zr} [J/(mol·K)]	$G^{\mathrm{E}}_{\mathrm{Zr}}$ [J/mol]	$S^{\mathrm{E}}_{\mathrm{Zr}}$ [J/(mol·K)]	a_{Zr}	γ_{Zr}
0.000	$-\infty$	−131127	∞	−131127	0.000	0.000	0.003
0.100	−164136	−112445	19.145	−112445	0.000	0.001	0.007
0.200	−129900	−93770	13.382	−93770	0.000	0.003	0.015
0.300	−102591	−75562	10.010	−75562	0.000	0.010	0.035
0.400	−78855	−58285	7.619	−58285	0.000	0.030	0.075
0.500	−57960	−42399	5.763	−42399	0.000	0.076	0.151
0.600	−39834	−28366	4.247	−28366	0.000	0.170	0.283
0.700	−24656	−16649	2.966	−16649	0.000	0.333	0.476
0.800	−12717	−7707	1.855	−7707	0.000	0.568	0.709
0.900	−4369	−2004	0.876	−2004	0.000	0.823	0.915
1.000	0	0	0.000	0	0.000	1.000	1.000

Reference state: Zr(liquid)

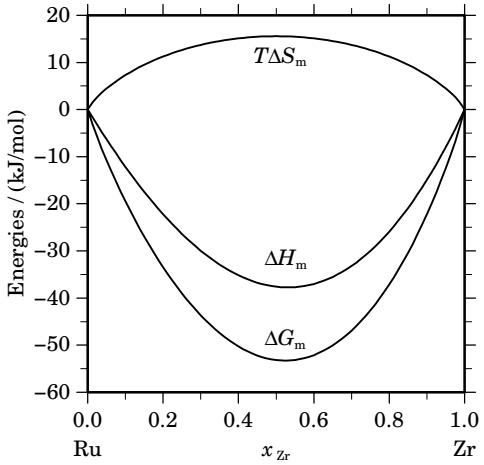

Fig. 2. Integral quantities of the liquid phase at T=2700 K.

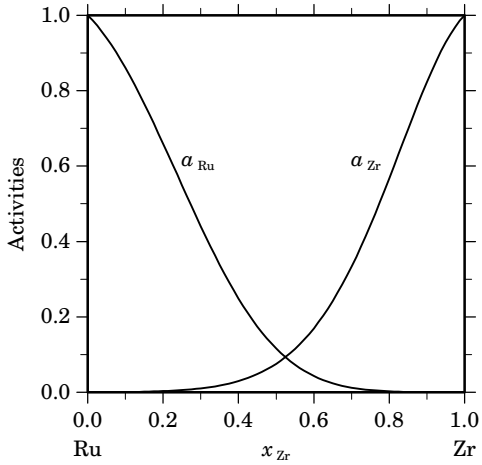

Fig. 3. Activities in the liquid phase at T=2700 K.

Table IV. Standard reaction quantities at 298.15 K for the compounds per mole of atoms.

Compound	x_{Zr}	$\Delta_{\mathrm{f}}G^{\circ}$ / (J/mol)	$\Delta_{\mathrm{f}}H^{\circ}$ / (J/mol)	$\Delta_{\mathrm{f}}S^{\circ}$ / (J/(mol·K))	$\Delta_{\mathrm{f}}C^{\circ}_{P}$ / (J/(mol·K))
$\mathrm{Ru_2Zr_1}$	0.333	−37235	−36957	0.932	0.000
$\mathrm{Ru_1Zr_1}$	0.500	−66529	−68650	−7.113	0.000

References

[1958Han] M. Hansen, K. Anderko, “Constitution of Binary Alloys”, McGraw-Hill, New-York, 1958.
[1963Rau] E. Raub, E. Röschel: Z. Metallkd. **54** (1963) 455–462.
[1965Ell] R.P. Elliott, “Constitution of Binary Alloys”, 1st Suppl., McGraw-Hill, New-York, 1965.
[1969Shu] F.A. Shunk, “Constitution of Binary Alloys”, 2nd Suppl., McGraw-Hill, New-York, 1969.
[1980Ere] V.N. Eremenko, E.L. Semenova, T.D. Shtepa: Russ. Metall. 2 (1980) 177-180.
[1988Ere] V.N. Eremenko, V.G. Khoruzhaya, T.D. Shtepa: Russ. Metall. 1 (1988) 194-198.
[1988Top] L. Topor, O.J. Kleppa: Metall. Trans. A **19A** (1988) 1061–1066.
[1993Oka] H. Okamoto: J. Phase Equilibria **14** (1993) 225–227.
[1995Che] P.Y. Chevalier, E. Fischer, unpublished work, 1995.

Sn – V (Tin – Vanadium)

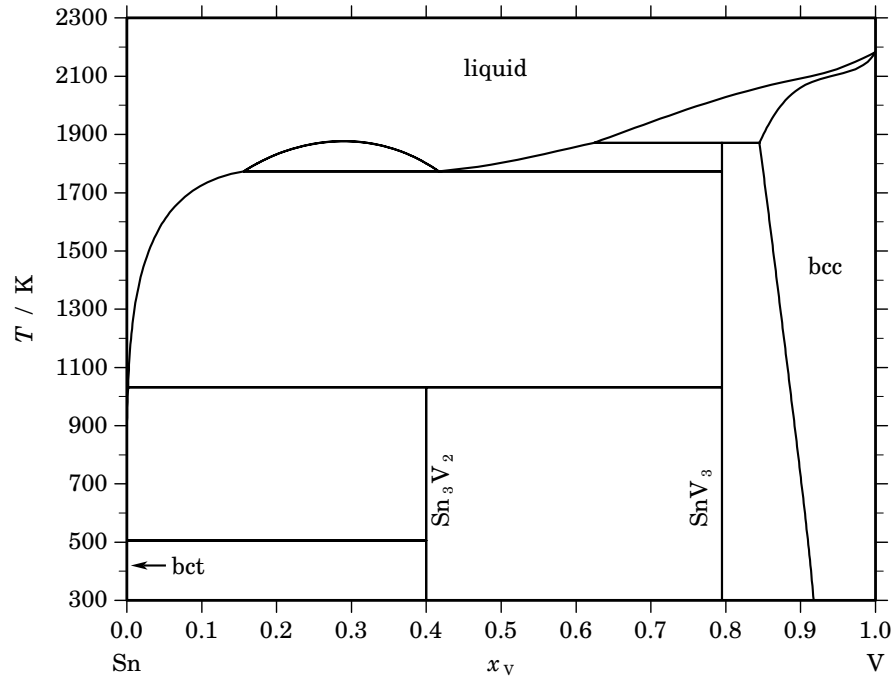

Fig. 1. Calculated phase diagram for the system Sn-V.

The literature on the Sn-V system has been reviewed in [1989Smi, 2002Stu] and a thermodynamic dataset has been optimised by [2002Stu] using the element data recommended by SGTE. In the assessment the selected data for the phase diagram have been taken from the literature [1969Dar, 1973Mar, 1979Gon] as well as from new experiments done by the assessors [2002Stu]. The heat capacity of SnV_3 has been adjusted to the experimental data of [1975Kna]. The partial enthalpy of solution of V in the melt at 1783 K from 0-67 at.% V has been determined by Esin *et al.* [1977Esi] and it has been used in the optimisation of the liquid. However, in a more recent calorimetric investigation of liquid Sn-V alloys [2000Bou] a much higher value of the partial enthalpy of V in the limit of pure Sn has been reported than by [1977Esi]. The dataset should not be used at too high temperatures because an artificial inverse miscibility gap opens in the liquid above 3300 K.

Table I. Phases, structures and models.

Phase	Struktur-bericht	Prototype	Pearson symbol	Space group	SGTE name	Model
liquid					LIQUID	$(Sn,V)_1$
bct	$A5$	βSn	$tI4$	$I4_1/amd$	BCT_A5	Sn_1
Sn_3V_2	C_b	$CuMg_2$	$oF48$	$Fddd$	SN3V2	Sn_3V_2
SnV_3	$A15$	Cr_3Si	$cP8$	$Pm\bar{3}n$	SNV3	$Sn_{41}V_{159}$
bcc	$A2$	W	$cI2$	$Im\bar{3}m$	BCC_A2	$(Sn,V)_1$

Table II. Invariant reactions.

Reaction	Type	T / K	Compositions / x_{V}			$\Delta_{\mathrm{r}}H$ / (J/mol)
liquid $\rightleftharpoons$ liquid′ + liquid″	critical	1874.5	0.290	0.290	0.290	0
liquid″ + bcc $\rightleftharpoons$ SnV_3	peritectic	1871.3	0.624	0.845	0.795	−10090
liquid″ $\rightleftharpoons$ liquid′ + SnV_3	monotectic	1773.4	0.417	0.156	0.795	−10786
liquid′ + SnV_3 $\rightleftharpoons$ Sn_3V_2	peritectic	1032.2	0.002	0.795	0.400	−21282
liquid′ $\rightleftharpoons$ bct + Sn_3V_2	eutectic	505.1	0.000	0.000	0.400	−7029

Table IIIa. Integral quantities for the liquid phase at 2200 K.

x_{V}	ΔG_{m} [J/mol]	ΔH_{m} [J/mol]	ΔS_{m} [J/(mol·K)]	$G^{\mathrm{E}}_{\mathrm{m}}$ [J/mol]	$S^{\mathrm{E}}_{\mathrm{m}}$ [J/(mol·K)]	ΔC_P [J/(mol·K)]
0.000	0	0	0.000	0	0.000	0.000
0.100	−2953	1611	2.075	2994	−0.628	0.000
0.200	−4073	1409	2.492	5080	−1.669	0.000
0.300	−4835	−71	2.165	6339	−2.914	0.000
0.400	−5456	−2290	1.439	6855	−4.157	0.000
0.500	−5958	−4701	0.571	6721	−5.192	0.000
0.600	−6275	−6749	−0.215	6036	−5.811	0.000
0.700	−6268	−7873	−0.729	4905	−5.808	0.000
0.800	−5711	−7507	−0.816	3442	−4.977	0.000
0.900	−4181	−5076	−0.407	1765	−3.110	0.000
1.000	0	0	0.000	0	0.000	0.000

Reference states: Sn(liquid), V(liquid)

Table IIIb. Partial quantities for Sn in the liquid phase at 2200 K.

x_{Sn}	ΔG_{Sn} [J/mol]	ΔH_{Sn} [J/mol]	ΔS_{Sn} [J/(mol·K)]	$G^{\mathrm{E}}_{\mathrm{Sn}}$ [J/mol]	$S^{\mathrm{E}}_{\mathrm{Sn}}$ [J/(mol·K)]	a_{Sn}	γ_{Sn}
1.000	0	0	0.000	0	0.000	1.000	1.000
0.900	−1461	995	1.116	466	0.240	0.923	1.026
0.800	−2319	3271	2.541	1762	0.686	0.881	1.101
0.700	−2803	5750	3.888	3721	0.922	0.858	1.226
0.600	−3190	7336	4.784	6154	0.537	0.840	1.400
0.500	−3825	6909	4.879	8854	−0.884	0.811	1.623
0.400	−5169	3332	3.864	11592	−3.754	0.754	1.885
0.300	−7904	−4553	1.523	14119	−8.487	0.649	2.164
0.200	−13272	−17925	−2.115	16167	−15.497	0.484	2.420
0.100	−24671	−37982	−6.051	17448	−25.196	0.260	2.596
0.000	$-\infty$	−65944	∞	17652	−37.998	0.000	2.625

Reference state: Sn(liquid)

Table IIIc. Partial quantities for V in the liquid phase at 2200 K.

x_V	ΔG_V [J/mol]	ΔH_V [J/mol]	ΔS_V [J/(mol·K)]	G_V^E [J/mol]	S_V^E [J/(mol·K)]	a_V	γ_V
0.000	$-\infty$	26937	∞	34716	−3.536	0.000	6.672
0.100	−16378	7158	10.698	25741	−8.447	0.408	4.085
0.200	−11088	−6036	2.296	18352	−11.085	0.545	2.727
0.300	−9576	−13655	−1.854	12447	−11.865	0.592	1.975
0.400	−8855	−16730	−3.580	7906	−11.198	0.616	1.541
0.500	−8091	−16311	−3.736	4588	−9.500	0.643	1.285
0.600	−7012	−13470	−2.935	2332	−7.183	0.682	1.136
0.700	−5568	−9296	−1.695	957	−4.661	0.738	1.054
0.800	−3821	−4903	−0.492	261	−2.347	0.811	1.014
0.900	−1905	−1420	0.220	22	−0.656	0.901	1.001
1.000	0	0	0.000	0	0.000	1.000	1.000

Reference state: V(liquid)

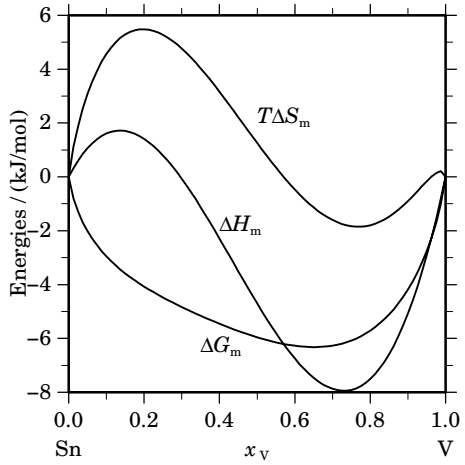

Fig. 2. Integral quantities of the liquid phase at T=2200 K.

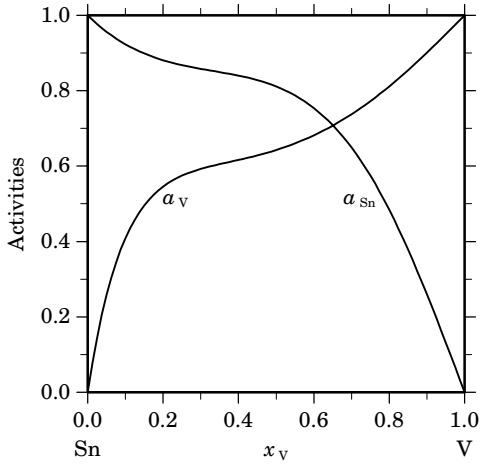

Fig. 3. Activities in the liquid phase at T=2200 K.

Table IV. Standard reaction quantities at 298.15 K for the compounds per mole of atoms.

Compound	x_V	$\Delta_f G^\circ$ / (J/mol)	$\Delta_f H^\circ$ / (J/mol)	$\Delta_f S^\circ$ / (J/(mol·K))	$\Delta_f C_P^\circ$ / (J/(mol·K))
Sn_3V_2	0.400	−21588	−26353	−15.984	0.000
SnV_3	0.795	−15538	−16710	−3.932	−0.504

References

[1969Dar] J.B. Darby, Jr,. D.B. Jugle: Trans. Metall. Soc. AIME **245** (1969) 2515–2518.
[1973Mar] L.V. Marchukova, N.M. Matveeva, I.I. Kornilov: Russ. Metall. 2 (1973) 157–159.
[1975Kna] G.S. Knapp, S.D. Bader, H.V. Culbert, F.Y. Fradin, T.E. Klippert: Phys. Rev. B **11B** (1975) 4331–4338.
[1977Esi] Yu.O. Esin, M.G. Valishev, P.V. Gel'd: Russ. J. Phys. Chem. **51** (1977) 273. Fradin, T.E. Klippert: Phys. Rev. B **11B** (1975) 4331–4338.
[1979Gon] L.V. Goncharuk, V.N. Eremenko, G.M. Lukashenko, V.R. Sidorko: Dokl. Akad. Nauk SSSR **245** (1979) 865–867.
[1989Smi] J.F. Smith in: "Phase Diagrams of Binary Vanadium Alloys", J.F. Smith (ed.), ASM Intl., Metals Park, OH, 1989, pp. 270–274.
[2000Bou] A. Bouhajib, A. Nadiri, Y. Yacoubi, R. Castanet: Phys. Chem. Liq. **38** (2000) 261–268.
[2002Stu] T. Studnitzky, B. Onderka, R. Schmid-Fetzer: Z. Metallkd. **93** (2002) 48–57.

V – W (Vanadium – Tungsten)

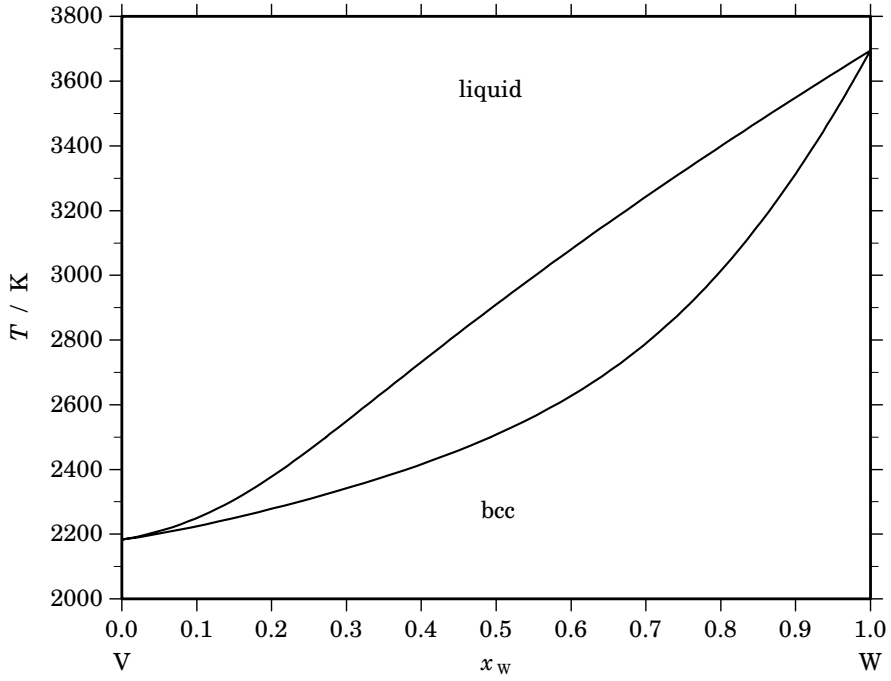

Fig. 1. Calculated phase diagram for the system V-W.

The literature on the V-W system has been reviewed in [1991Nag] and thermodynamic datasets have been optimised by [2005Bra, 2005Hua]. The phase diagram consists only of the liquid and the bcc phases with continuous solubility for the components. The phase diagram has been investigated several times with some conflicting results especially in the V-rich part where older investigations found a minimum in the solidus line. Later investigations [1969Rud, 1975Kol] found that the solidus increases monotonically when W is added to vanadium alloys. Therefore, the previous minimum was attributed to higher levels of impurity in the samples of the older investigations. No data on the thermodynamics of mixing have been available. For the optimisation of the thermodynamic dataset [2005Bra] have selected the solidus data of [1969Rud] and the liquidus data of [1960Bar] for samples with more than 30 at.% W. The evaluation of [2005Bra] is preferred here over that of [2005Hua] because the latter authors propose excess entropies for the liquid and bcc phases which are quite high. The dataset of [2005Bra] predicts a miscibility gap in the bcc phase below 1070 K, however, no experimental evidence is available.

Table I. Phases, structures and models.

Phase	Struktur-bericht	Prototype	Pearson symbol	Space group	SGTE name	Model
liquid					LIQUID	$(V,W)_1$
bcc	$A2$	W	$cI2$	$Im\overline{3}m$	BCC_A2	$(V,W)_1$

Table IIa. Integral quantities for the liquid phase at 3700 K.

x_{W}	ΔG_{m} [J/mol]	ΔH_{m} [J/mol]	ΔS_{m} [J/(mol·K)]	$G_{\mathrm{m}}^{\mathrm{E}}$ [J/mol]	$S_{\mathrm{m}}^{\mathrm{E}}$ [J/(mol·K)]	ΔC_P [J/(mol·K)]
0.000	0	0	0.000	0	0.000	0.000
0.100	−10001	0	2.703	0	0.000	0.000
0.200	−15394	0	4.161	0	0.000	0.000
0.300	−18792	0	5.079	0	0.000	0.000
0.400	−20704	0	5.596	0	0.000	0.000
0.500	−21324	0	5.763	0	0.000	0.000
0.600	−20704	0	5.596	0	0.000	0.000
0.700	−18792	0	5.079	0	0.000	0.000
0.800	−15394	0	4.161	0	0.000	0.000
0.900	−10001	0	2.703	0	0.000	0.000
1.000	0	0	0.000	0	0.000	0.000

Reference states: V(liquid), W(liquid)

Table IIb. Partial quantities for V in the liquid phase at 3700 K.

x_{V}	ΔG_{V} [J/mol]	ΔH_{V} [J/mol]	ΔS_{V} [J/(mol·K)]	$G_{\mathrm{V}}^{\mathrm{E}}$ [J/mol]	$S_{\mathrm{V}}^{\mathrm{E}}$ [J/(mol·K)]	a_{V}	γ_{V}
1.000	0	0	0.000	0	0.000	1.000	1.000
0.900	−3241	0	0.876	0	0.000	0.900	1.000
0.800	−6865	0	1.855	0	0.000	0.800	1.000
0.700	−10973	0	2.966	0	0.000	0.700	1.000
0.600	−15715	0	4.247	0	0.000	0.600	1.000
0.500	−21324	0	5.763	0	0.000	0.500	1.000
0.400	−28189	0	7.619	0	0.000	0.400	1.000
0.300	−37039	0	10.010	0	0.000	0.300	1.000
0.200	−49512	0	13.382	0	0.000	0.200	1.000
0.100	−70836	0	19.145	0	0.000	0.100	1.000
0.000	$-\infty$	0	∞	0	0.000	0.000	1.000

Reference state: V(liquid)

Table IIc. Partial quantities for W in the liquid phase at 3700 K.

x_{W}	ΔG_{W} [J/mol]	ΔH_{W} [J/mol]	ΔS_{W} [J/(mol·K)]	$G_{\mathrm{W}}^{\mathrm{E}}$ [J/mol]	$S_{\mathrm{W}}^{\mathrm{E}}$ [J/(mol·K)]	a_{W}	γ_{W}
0.000	$-\infty$	0	∞	0	0.000	0.000	1.000
0.100	−70836	0	19.145	0	0.000	0.100	1.000
0.200	−49512	0	13.382	0	0.000	0.200	1.000
0.300	−37039	0	10.010	0	0.000	0.300	1.000
0.400	−28189	0	7.619	0	0.000	0.400	1.000
0.500	−21324	0	5.763	0	0.000	0.500	1.000
0.600	−15715	0	4.247	0	0.000	0.600	1.000
0.700	−10973	0	2.966	0	0.000	0.700	1.000
0.800	−6865	0	1.855	0	0.000	0.800	1.000
0.900	−3241	0	0.876	0	0.000	0.900	1.000
1.000	0	0	0.000	0	0.000	1.000	1.000

Reference state: W(liquid)

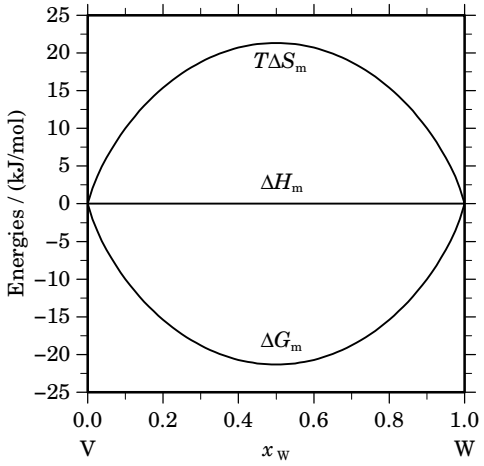

Fig. 2. Integral quantities of the liquid phase at T=3700 K.

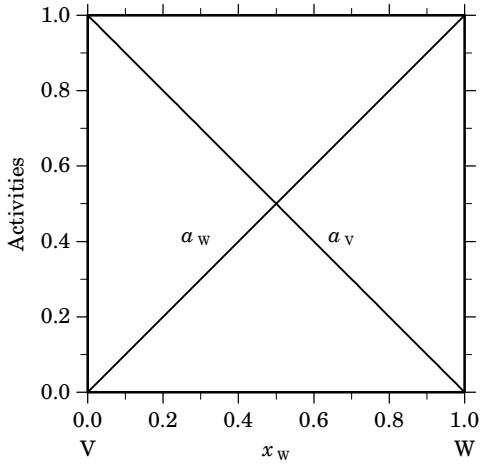

Fig. 3. Activities in the liquid phase at T=3700 K.

Table IIIa. Integral quantities for the stable phases at 2000 K.

Phase	x_W	ΔG_m [J/mol]	ΔH_m [J/mol]	ΔS_m [J/(mol·K)]	G_m^E [J/mol]	S_m^E [J/(mol·K)]	ΔC_P [J/(mol·K)]
bcc	0.000	0	0	0.000	0	0.000	0.000
	0.100	−3801	1605	2.703	1605	0.000	0.000
	0.200	−5469	2852	4.161	2852	0.000	0.000
	0.300	−6414	3744	5.079	3744	0.000	0.000
	0.400	−6913	4279	5.596	4279	0.000	0.000
	0.500	−7069	4457	5.763	4457	0.000	0.000
	0.600	−6913	4279	5.596	4279	0.000	0.000
	0.700	−6414	3744	5.079	3744	0.000	0.000
	0.800	−5469	2852	4.161	2852	0.000	0.000
	0.900	−3801	1605	2.703	1605	0.000	0.000
	1.000	0	0	0.000	0	0.000	0.000

Reference states: V(bcc), W(bcc)

Table IIIb. Partial quantities for V in the stable phases at 2000 K.

Phase	x_V	ΔG_V [J/mol]	ΔH_V [J/mol]	ΔS_V [J/(mol·K)]	G_V^E [J/mol]	S_V^E [J/(mol·K)]	a_V	γ_V
bcc	1.000	0	0	0.000	0	0.000	1.000	1.000
	0.900	−1574	178	0.876	178	0.000	0.910	1.011
	0.800	−2998	713	1.855	713	0.000	0.835	1.044
	0.700	−4327	1605	2.966	1605	0.000	0.771	1.101
	0.600	−5642	2852	4.247	2852	0.000	0.712	1.187
	0.500	−7069	4457	5.763	4457	0.000	0.654	1.307
	0.400	−8819	6418	7.619	6418	0.000	0.588	1.471
	0.300	−11285	8736	10.010	8736	0.000	0.507	1.691
	0.200	−15354	11410	13.382	11410	0.000	0.397	1.986
	0.100	−23849	14441	19.145	14441	0.000	0.238	2.383
	0.000	$-\infty$	17828	∞	17828	0.000	0.000	2.922

Reference state: V(bcc)

Table IIIc. Partial quantities for W in the stable phases at 2000 K.

Phase	x_W	ΔG_W [J/mol]	ΔH_W [J/mol]	ΔS_W [J/(mol·K)]	G_W^E [J/mol]	S_W^E [J/(mol·K)]	a_W	γ_W
bcc	0.000	$-\infty$	17828	∞	17828	0.000	0.000	2.922
	0.100	−23849	14441	19.145	14441	0.000	0.238	2.383
	0.200	−15353	11410	13.382	11410	0.000	0.397	1.986
	0.300	−11285	8736	10.010	8736	0.000	0.507	1.691
	0.400	−8819	6418	7.619	6418	0.000	0.588	1.471
	0.500	−7069	4457	5.763	4457	0.000	0.654	1.307
	0.600	−5642	2852	4.247	2852	0.000	0.712	1.187
	0.700	−4327	1605	2.966	1605	0.000	0.771	1.101
	0.800	−2998	713	1.855	713	0.000	0.835	1.044
	0.900	−1574	178	0.876	178	0.000	0.910	1.011
	1.000	0	0	0.000	0	0.000	1.000	1.000

Reference state: W(bcc)

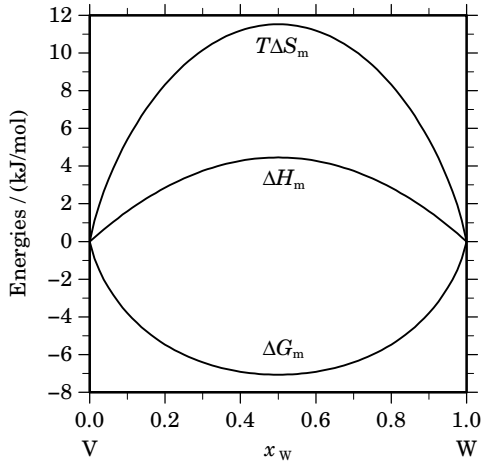

Fig. 4. Integral quantities of the stable phases at T=2000 K.

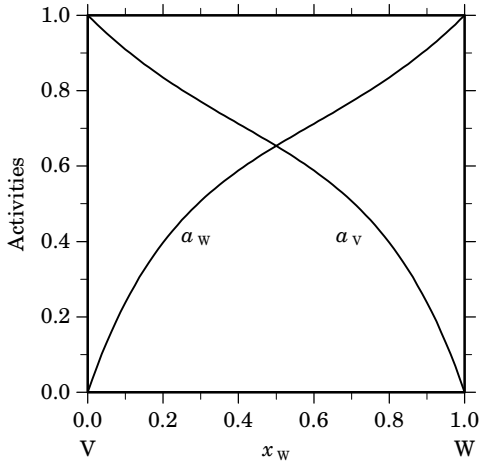

Fig. 5. Activities in the stable phases at T=2000 K.

References

[1960Bar] V.V. Baron, Yu.V. Efimov, E.M. Savitskii: Izv. Akad. Nauk SSSR, Otd. Tekh. Nauk, Metall. Top. 1 (1960) 70–74; transl.: Russ. Met. Fuels 1 (1960) 45–49.

[1969Rud] E. Rudy: Compendium of Phase Diagram Data, AFML, Wright-Patterson AFB, Ohio, Rep. No. AFML-TR-65-2, Part 5, 1969.

[1975Kol] V.M. Koltygin, M.V. Pikunov, A.S. Petukhova: Izv. Vyssh. Uchebn. Zaved. Tsvetn. Metall. 6 (1975) 126–129.

[1991Nag] S.V. Nagender Naidu, A.M. Sriramamurthy, M. Vijayakumar, P. Rama Rao in: "Phase Diagrams of Binary Tungsten Alloys", S.V. Nagender Naidu, P. Rama Rao, Eds., The Indian Institute of Metals, Calcutta, 1991, pp. 295–300.

[2005Bra] J. Bratberg: Z. Metallkd. **96** (2005) 335–344.

[2005Hua] S. Huang, J. Vleugels, L. Li, O. Van der Biest: J. Alloys Comp. **395** (2005) 68–74.

W – Zr (Tungsten – Zirconium)

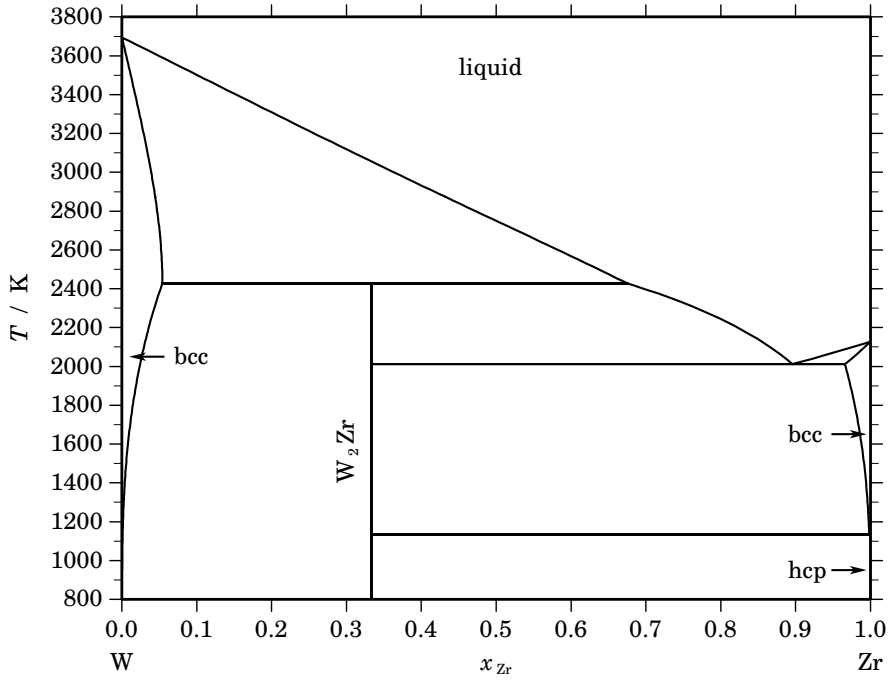

Fig. 1. Calculated phase diagram for the system W-Zr.

The W-Zr binary system contains two components, tungsten and zirconium, interesting for many application fields. The selected phase diagram, originates from the assessment of Nagender Naidu and Rama Rao [1987Nag]. It is based on metallographic analysis, incipient-melting data, X-ray diffraction [1953Dom, 1953Gea], dilatometry, liquidus measurements [1953Gea], and on invariant temperatures reported by Savitskii and Zakharov [1962Sav]. The intermetallic phase W_2Zr was identified with a narrow non-stoichiometry range (33 - 35 at%.Zr) and decomposes peritectically. The mutual solid solubility of Zr in bcc-W and W in bcc-Zr is limited. The solubility of W in hcp-Zr is negligible, and equal to 0.25 at.% [1953Dom] at the eutectoid temperature. A solubility of Zr in (W) equal to 1.5 at.% at 1922 K was reported by Elliott [1965Ell]. There is a complete miscibility in the liquid state. There are no experimental data available for the solution thermodynamics of the W-Zr system. This system was assessed by Chevalier [2005Che]. A sub-regular substitution model was used for the liquid and a regular one for the bcc solid solution. The heat capacity of W_2Zr was estimated from the pure elements by using the Neumann-Kopp rule. The enthalpy and entropy of formation of W_2Zr were optimised in consistency with the temperatures of the invariant reactions. The calculated phase diagram and the invariant reactions are in very satisfactory agreement with the experimental data. However, there is a need for further experimental determinations of thermodynamic properties of W_2Zr and liquid.

Table I. Phases, structures and models.

Phase	Struktur-bericht	Prototype	Pearson symbol	Space group	SGTE name	Model
liquid					LIQUID	$(W,Zr)_1$
bcc	$A2$	W	$cI2$	$Im\bar{3}m$	BCC_A2	$(W,Zr)_1$
hcp	$A3$	Mg	$hP2$	$P6_3/mmc$	HCP_A3	$(W,Zr)_1$
W_2Zr	$C15$	$MgCu_2$	$cF24$	$Fd\bar{3}m$	W2ZR	W_2Zr_1

Table II. Invariant reactions.

Reaction	Type	T / K	Compositions / x_{Zr}			$\Delta_{\mathrm{r}}H$ / (J/mol)
bcc + liquid $\rightleftharpoons$ W_2Zr	peritectic	2426.9	0.054	0.675	0.333	−18328
liquid $\rightleftharpoons$ W_2Zr + bcc	eutectic	2012.0	0.896	0.333	0.966	−23335
bcc $\rightleftharpoons$ W_2Zr + hcp	eutectoid	1134.7	0.998	0.333	1.000	−4227

Table IIIa. Integral quantities for the liquid phase at 3700 K.

x_{Zr}	ΔG_{m} [J/mol]	ΔH_{m} [J/mol]	ΔS_{m} [J/(mol·K)]	$G^{\mathrm{E}}_{\mathrm{m}}$ [J/mol]	$S^{\mathrm{E}}_{\mathrm{m}}$ [J/(mol·K)]	ΔC_P [J/(mol·K)]
0.000	0	0	0.000	0	0.000	0.000
0.100	−9406	595	2.703	595	0.000	0.000
0.200	−14224	1170	4.161	1170	0.000	0.000
0.300	−17110	1682	5.079	1682	0.000	0.000
0.400	−18614	2091	5.596	2091	0.000	0.000
0.500	−18971	2352	5.763	2352	0.000	0.000
0.600	−18278	2426	5.596	2426	0.000	0.000
0.700	−16523	2270	5.079	2270	0.000	0.000
0.800	−13553	1841	4.161	1841	0.000	0.000
0.900	−8902	1099	2.703	1099	0.000	0.000
1.000	0	0	0.000	0	0.000	0.000

Reference states: W(liquid), Zr(liquid)

Table IIIb. Partial quantities for W in the liquid phase at 3700 K.

x_{W}	ΔG_{W} [J/mol]	ΔH_{W} [J/mol]	ΔS_{W} [J/(mol·K)]	$G^{\mathrm{E}}_{\mathrm{W}}$ [J/mol]	$S^{\mathrm{E}}_{\mathrm{W}}$ [J/(mol·K)]	a_{W}	γ_{W}
1.000	0	0	0.000	0	0.000	1.000	1.000
0.900	−3238	3	0.876	3	0.000	0.900	1.000
0.800	−6796	69	1.855	69	0.000	0.802	1.002
0.700	−10692	281	2.966	281	0.000	0.706	1.009
0.600	−14992	723	4.247	723	0.000	0.614	1.024
0.500	−19845	1479	5.763	1479	0.000	0.525	1.049
0.400	−25556	2633	7.619	2633	0.000	0.436	1.089
0.300	−32770	4268	10.010	4268	0.000	0.345	1.149
0.200	−43043	6470	13.382	6470	0.000	0.247	1.234
0.100	−61515	9321	19.145	9321	0.000	0.135	1.354
0.000	$-\infty$	12905	∞	12905	0.000	0.000	1.521

Reference state: W(liquid)

Table IIIc. Partial quantities for Zr in the liquid phase at 3700 K.

x_{Zr}	ΔG_{Zr} [J/mol]	ΔH_{Zr} [J/mol]	ΔS_{Zr} [J/(mol·K)]	G^E_{Zr} [J/mol]	S^E_{Zr} [J/(mol·K)]	a_{Zr}	γ_{Zr}
0.000	$-\infty$	5914	∞	5914	0.000	0.000	1.212
0.100	−64913	5923	19.145	5923	0.000	0.121	1.212
0.200	−43937	5575	13.382	5575	0.000	0.240	1.199
0.300	−32085	4953	10.010	4953	0.000	0.352	1.175
0.400	−24046	4143	7.619	4143	0.000	0.458	1.144
0.500	−18098	3226	5.763	3226	0.000	0.555	1.111
0.600	−13426	2289	4.247	2289	0.000	0.646	1.077
0.700	−9560	1413	2.966	1413	0.000	0.733	1.047
0.800	−6181	684	1.855	684	0.000	0.818	1.022
0.900	−3056	185	0.876	185	0.000	0.905	1.006
1.000	0	0	0.000	0	0.000	1.000	1.000

Reference state: Zr(liquid)

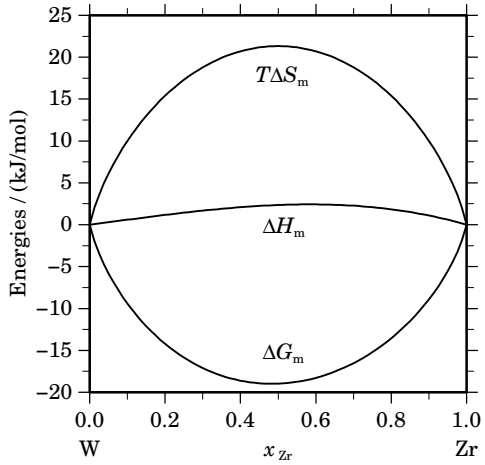

Fig. 2. Integral quantities of the liquid phase at T=3700 K.

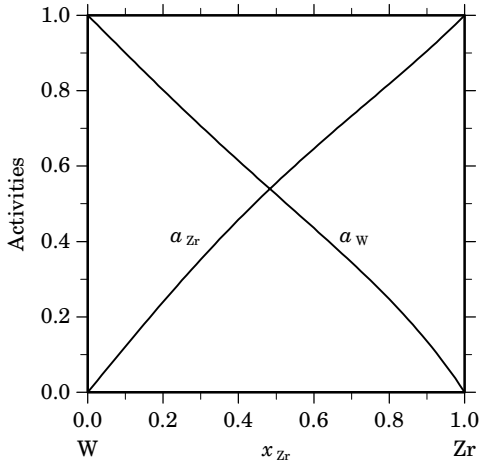

Fig. 3. Activities in the liquid phase at T=3700 K.

Table IV. Standard reaction quantities at 298.15 K for the compounds per mole of atoms.

Compound	x_{Zr}	$\Delta_f G^\circ$ / (J/mol)	$\Delta_f H^\circ$ / (J/mol)	$\Delta_f S^\circ$ / (J/(mol·K))	$\Delta_f C^\circ_P$ / (J/(mol·K))
W_2Zr_1	0.333	−3033	−2892	0.471	−0.028

References

[1953Dom] R.F. Domagala, D.J. McPherson, M. Hansen: Trans. AIME **197** (1953) 73–79.

[1953Gea] G.A. Geach, G.F. Slattery: Trans. AIME **197** (1953) 747–748.

[1962Sav] E.M. Savitskii, A.M. Zakharov: Russ. J. Inorg. Chem. **7** (1962) 1337–1340.

[1965Ell] R.P. Elliott, "Constitution of Binary Alloys", First supplement, McGraw-Hill Book Company, New-York, Saint Louis, San Francisco, Toronto, London, Sydney, 1965.

[1987Nag] S.V. Nagender Naidu, P. Rama Rao: J. Alloy Phase Diagrams **3** (1987) 47–56.

[2005Che] P.-Y. Chevalier, Unpublished work, July 2005.